Furthering Our Understanding of Tumour Budding in Oestrogen Receptor Negative Breast Cancer.

Francesca Savioli

MBChB, BSc (Hons), MRCS

Submitted in fulfilment of the requirements for the degree of Doctor of Medicine

Institute of Cancer Sciences

College of Medical, Veterinary and Life Sciences

October 2023

Summary

Every year, 55,900 people are diagnosed with breast cancer in the UK alone(1). Treatment modalities for this heterogeneous disease should be individualised and tailored to each case according to an increasing number of molecular, clinical, and personal factors. Molecular subtypes have been classified into Luminal A/B, HER-2 enriched, and basal-like cancers, which overlap significantly with Triple Negative Breast Cancers (TNBC). These cancers are difficult to treat have a poorer prognostic profile(3-5).

Tumour budding, most extensively described in colorectal cancer, represents an isolated group of up to four cancer cells found at the invasive tumour front, separate from the tumour mass(6). Tumour budding in high levels is associated is a marker of poor prognosis in numerous cancers including breast(6-13).

Tumour budding denotes one of the fundamental behaviours of solid tumours in the transition towards metastasis. This finding is felt to be a histopathological depiction of a process belonging under the umbrella term of epithelial-mesenchymal transition (EMT) in which tumour cells adopt new characteristics to facilitate the migration from the solid tumour mass and tumour micro-environment to allow seeding to distant sites(14). Tumour budding has been associated with reduced survival in intraductal breast carcinomas when a value of 20 tumour buds/0.385mm^2 was used as a threshold to denote “low tumour budding” versus “high tumour budding” phenotype (10). Nonetheless, different thresholds and methods of counting tumour buds have been documented in the literature as having prognostic power, and therefore standardisation has yet to be reached for tumour budding as a prognostic marker in breast cancer(11-13).

A cohort of ER-negative surplus specimens from patients who underwent surgery for primary operable breast cancer was examined and tumour buds scored. A threshold of 28 was identified to have prognostic significance, with “high tumour budding” phenotype associated with reduced cancer-specific survival. Based on this population, 50 patient specimens (25 high tumour budding, 25 low tumour budding) were analysed using TempoSEQ for to evaluate RNA expression and evaluate differential expression. Four highly differential expressed genes were identified as JUNB, ODAM, RFX5 and TBX22.

This thesis aimed to examine JUNB, ODAM, RFX5 and TBX22 histologically, using immunohistochemistry to validate these findings at the protein expression level.

The hypothesis was that differential gene expression at the transcriptional level should be reflected in protein expression in the high vs low tumour budding specimens, and that this would be reflected in a prognostic effect on cancer-specific survival.

Protein expression for JUNB, ODAM, RFX5 and TBX22 was assessed using immunohistochemistry in the Glasgow Breast Cancer Cohort (n=850), composed of surplus specimens of breast cancers from patients operated for primary operable breast cancers in Glasgow between 1995-1998. The cohort was validated using full section specimens, where protein expression was compared between tumour mass and tumour buds to confirm that expression was comparable before tissue microarray (TMA) cores were utilised for higher-throughput examination of the entire cohort. Only ductal cancers were included in the final analysis (n=736).

Comparisons between quantitative expression of JUNB, ODAM, RFX5 and TBX22 to clinicopathological factors and outcome were made, and molecular subgroups examined in turn to establish whether transcriptional differences in gene expression was comparable to protein expression at the tumour level. Quantitative analysis was manually made using weighted histoscores, and thresholds created by using R to establish prognostic group thresholds for each protein expression in the different cellular compartments: membrane, cytoplasm, and nucleus.

High cytoplasmic JUNB expression was associated with increased cancer-specific survival (CSS) in TNBC and ER-negative cancer. High nuclear expression of JUNB was associated with improved CSS across all patients within this cohort and in the ER+ patients in particular. Membrane expression amongst this cohort was low and could not be analysed. Combined nuclear and cytoplasmic scores suggested that when comparing the high nuclear, high cytoplasmic versus high nuclear, low cytoplasmic JUNB phenotypes, the latter group had poorer CSS.

High cytoplasmic ODAM expression was associated with worse CSS for HER-2 enriched patients in this cohort. Low nuclear ODAM expression was associated with worse CSS across the entire cohort. Combined scoring suggested that low nuclear and high cytoplasmic (combined) expression of ODAM was associated with reduced survival compared to all high expression. Membrane ODAM was not assessed due to low scores throughout the cohort.

Across the whole cohort, low RFX5 cytoplasmic expression was shown to be associated with reduced CSS. Membrane RFX5 WHS did not predict survival across the cohort, but correlated with grade, molecular subtype and Klintrup Makinen score. No effect was observed between nuclear RFX5 expression and survival or clinicopathological factors. Combined membrane, cytoplasmic and nuclear scores allowed the observation that an “all low” phenotype was associated with worse survival, particularly in the Luminal A and HER2-enriched subgroups.

Cytoplasmic TBX22 expression was not associated with prognosis but was found to be particularly high in the HER-2 enriched cohort. Nuclear TBX22 also did not have a prognostic effect on this breast cancer cohort. Membrane scoring was once again low across the whole cohort.

Subsequently, a fresh cohort of TNBCs (n=207) from patients who underwent surgical resection for primary operable invasive cancer at two Glasgow hospitals from 1995-2010 were evaluated. A selection of 50 specimens from this cohort (25 high tumour budding, 25 low tumour budding) from this cohort was examined using GeoMx Digital Spacer Profiling. The GeoMX DSP technology allowed the spatial analysis and exploration of RNA transcription within different portions of the tumour and tumour microenvironment. By examining the differential gene expression in “high tumour budding” versus “low tumour budding” phenotype TNBC specimens, several differentially expressed genes were identified. Amongst the differentially expressed genes identified using GeoMX DSP technology, HIF-1alpha, Bcl-2 and CD3 expression was noted to be significantly different between high and low tumour budding TNBC specimens. HIF-1alpha was most differentially expressed in tumour cells in low budding group, together with CD4 expression. When examining the tumour microenvironment (i.e., stroma rich portions of the specimen), Bcl-2 was amongst the most differentially expressed genes. HIF-1alpha, associated with hypoxia, led to the additional examination of CAIX, another well-documented marker of tissue hypoxia, to be examined using immunohistochemistry, and CD4, which had a more stable antibody available for immunohistochemistry, was used as a proxy for CD3, to validate these findings at the protein expression level. Thresholds based on literature search and individual prognostic power were utilised for each protein weighted histoscore. This study suggested that for HIF-1alpha, recurrence-free survival (RFS) was

worse in high cytoplasmic HIF-1alpha expressing tumours, and disease-free survival (DFS) was worse in high nuclear HIF-1alpha expressing tumours. High CAIX cytoplasmic expression was associated with poorer RFS, while low Bcl-2 was associated with poorer RFS and DFS. Low stromal and tumoural CD3 expression were each associated with worse RFS, and low combined stromal and tumoral CD3 expression was associated with worse RFS.

In summary, the result from this thesis suggests that both at the transcriptional level and protein expression level, tumour budding may affect prognosis, and that this effect may be more pronounced in certain subgroups, including TNBC. Identification of differential gene and protein expression may therefore allow further targets for therapy to be identified, and subsequently become an additional element in the arsenal of prognostication and treatment of breast cancer.

Table of Contents

List of Tables

List of Figures

Acknowledgments

Firstly, thank you Prof. Joanne Edwards, for your unending support. Any fears I had about embarking on a lab-based thesis proposal were assuaged by your kind, approachable and expert input at all stages of this work. Thank you to Dr Jean Quinn, who tutored me through all the elements of the lab-based practice, and who was always available for troubleshooting and support. To Mr Laszlo Romics, who during my years of research, and to this day, provides ideas, support, and suggestions for both research and career decision-making.

To Ms Liz Morrow, thank you for leading the way into this project with your own work. Thank you also to Prof. Donald McMillan for his expert insight into inflammation and cancer and to Professors Paul Horgan and Campbell Roxburgh for allowing me to join the excellent team of clinical research fellows at Glasgow Royal Infirmary. I also would like to acknowledge Ms Alison Lannigan, without whom I'd never have applied for this position. I thank all the members of the Edwards lab, but particularly would like to acknowledge Dr Kathryn Pennel, who was my expert to turn to about all things lab-based, Sara Albadran, my statistics, western blotting and RStudio expert (and moral support!), Molly McKenzie's enduring and tolerant support with DEPMAP and RStudio. Thank you to Dr Gerard Lynch for his help with understanding TempoSEQ and to Dr Hester van Wyk, who taught me how to count tumour buds(!), Alan Whittingham and Dr Warapan Numprasit for your help in counterscoring and to Dr Suad Shamis for her work with the TNBC cohort. Thank you to Phimmada Hathakarnkul for her help with GeoMx and Dr Jennifer Hay and Hannah Morgan, who patiently dealt with all my slides, as well as the Glasgow Biorepository for allowing me to use their specimens. I am grateful to Dr Liz Mallon, for her expert teaching on histopathology and to Colin Nixon for his help in staining a portion of these specimens. Thank you to all the patients who allowed their surplus specimens to be utilised for research, and to whom I hope I have done justice to by producing this work.

Thank you to my mum Arafa, dad Lorenzo and sister Giulia for their support over the years. Finally, none of the last few years' work would have been possible without the tolerant, generous, and motivating support of my husband Hikmat. When one day this thesis sits gathering dust on a shelf somewhere, you, and the family we have created with our two boys, will remain my greatest achievement of all.

Author's Declaration

The work presented in this thesis was performed by the author except where acknowledged. This thesis has not been submitted for a degree or diploma at this or any other institution.

Francesca Savioli

October 2023

Definitions/Abbreviations

ADC Antibody drug conjugates

AKT Protein kinase B

AR Androgen receptor

ARE Androgen responsive element

Bcl2 B cell lymphoma 2

C TC Circulating tumour cell

CAIX Carbonic anhydrase IX

CCL Chemokine C-C motif ligand

CD3/4 Cluster of differentiation 3/4

CK Cytokeratin

CMS Consensus molecular subtypes

CRP c-reactive protein

CXCL Chemokine C-X-C motif ligand

EDTA Ethylenediaminetetraacetic acid

EGFR Epidermal growth factor receptor

EMT Epithelial mesenchymal transition

ER Oestrogen Receptor

FFPE Formalin-fixed paraffin-embedded

FGFR2 Fibroblast growth factor receptor 2

FOX01 FOrkhead boX Other 1

GMCSF Granulocyte macrophage-stimulating factor

GPS Glasgow prognostic score

GSK-3 Glycogen synthase kinase 3

GTRF Glasgow tissue research facility

H&E Haematoxylin and Eosin

HeLa Henrietta Lacks

HER2 Human epidermal growth factor 2

HIER Heat induced epitope retrieval

HIF-1α Hypoxia Inducible factor 1α

ICCC Intra class correlation coefficient

IDC-NST Intraductal carcinoma of no special type

IL Interleukin

ITB Intratumoural budding

ITBCC International Tumour Budding Consensus Conference

KM Klintrup Makinen

MAPK Mitogen activated protein kinase

MMP Matrix metalloproteinase

mTOR mammalian Target Of Rapamycin

NFκB Nuclear Factor Kappa B

NLR Neutrophil to Lymphocyte ratio

ODAM Odontogenic ameloblast-associated protein

PI3K phosphatidylinositol (3,4,5)-triphosphate kinase

PARP poly(adenosine diphosphate-ribose) polymerase

PDK1 Pyruvate dehydrogenase Kinase 1

PDL1 Programmed cell death 1 ligand 1

PIP Phosphatidylinositol (4,5)-bisphosphate

PR Progesterone Receptor

PTB Peritumoural budding

PTEN phosphatase and tensin homolog

RFX5 Regulatory factor X5

RNA ribonucleic acid

SEB1 SEven Binding 1

SLUG Snail Family Transcription Repressor 2

SNAIL Snail Family Transcription Repressor 1

STAT3 Signal transducer and activator of transcription 3

TBST Tris buffer saline solution plus tween

TBX22 T-box transcription factor 22

TGFβ Transforming growth factor Beta

TIL tumour infiltrating lymphocyte

TMA Tissue microarray

TME Tumour microenvironment

TNBC Triple negative breast cancer

TNM Tissue node metastasis

TOE Tumour organismal environment

TSP Tumour Stroma percentage

TWIST Twist related protein

VEGF vascular endothelial growth factor

Wnt Wingless-related integration site

Chapter 1 Introduction

1.1 Introduction

This chapter introduces the reader to the epidemiology and clinical features of breast cancer, assessment of disease as well as the various treatment modalities currently available. In the following chapters, the classification of breast cancer subtypes is explored in further detail, as well as challenges in treatment and prognosis. These will create a background for the further development of this study, which considers the role of tumour budding and how knowledge and evaluation of budding has led to the assessment of differential gene expression within different breast cancer phenotypes. Finally, the differentially expressed genes identified through this process are described, and validation of their respective protein expression in relation to prognosis in different breast cancer subgroups is addressed to propose a hypothesis and research aim for the remaining chapters in this study, with potential significance for further research in therapeutic and prognostic tools for treatment of breast cancer.

1.1.1 Breast Cancer

Our understanding of the pathophysiology and therapeutic options for breast cancer has evolved significantly since Halstead first documented his theories on the surgical management of breast disease in the 1800s through radical mastectomy(15). We now understand that breast cancer is a heterogeneous disease, and in accordance with this, treatment modalities should be individualised and tailored to each case according to an increasing number of molecular, clinical, and personal factors.

1.1.2 Epidemiology

Every year, approximately 56,000 people are diagnosed with breast cancer in the UK alone, of which 23% are thought to be preventable. Despite improvement in detection and treatment modalities this disease still leads to around 11,500 deaths every year (1). Trends suggest that incidence is increasing, with rates increasing by 18% in the UK(1). However, annual mortality rates have been projected to fall to 11,400 by 2038-2040(1). Although this demonstrates an improvement in prognosis overall, there remains a significant proportion of patients who would benefit from early detection, a broader spectrum of treatment options, and the identification of biomarkers which may provide prognostic and therapeutic targets.

1.1.3 Pathogenesis

Breast carcinoma, which results from neoplastic changes to the breast epithelial cells, can be subclassified into subtypes pertaining to the cellular origins. It is now accepted that a pre-neoplastic stage of carcinoma in situ (CIS) is the precursor to the two common invasive and therefore malignant carcinoma types, with recent work highlighting this considered to be encompassed within the eight hallmarks of cancer(16). These hallmarks include the cellular changes which lead to proliferative signalling, evasion of growth suppression, resistance to cell death, replicative immortality, vascular induction/access, invasive and metastatic activity, the reprogramming of cellular metabolism and evasion from immune destruction(16). Elucidating the cellular and molecular processes which underlie each of these principles that we may be able to harness and understand cancer pathology, and potential targets for prevention and treatment of malignant disease.

1.1.4 Risk Factors

Several environmental and genetic factors have been implicated in the lifetime risk of developing breast cancer. These are summarised in the table adapted from Veronesi et al. (*Table* 1-1*)*(17).

Table 1-1 Risk Factors for the Development of Breast Cancer. Environmental and intrinsic factors associated with increased risk of developing breast cancer - from Veronesi et al.(17)

Factor	Relative Risk (RR)	High-risk characteristic
Age	>10	Elderly individual
Geographical Location	5	Developed country
Breast Density	>5	Extensive dense breast tissue on mammography
Age at menarche	3	Before age 11
Age at menopause	2	After age 54
Age at first full pregnancy	3	First child after 40
Family History	≥2	Breast cancer in first-degree relative
Previous benign breast disease	4-5	Atypical hyperplasia
Cancer in other breast	>4	Previous breast cancer

Socioeconomic group	2	Groups I and II
Body-Mass Index (BMI) Pre-menopause Post-menopause	 0-7 2	 High BMI High BMI
Alcohol use	1.07	7% increase with each daily drink
Exposure to ionising radiation	3	Abnormal exposure to young girls after age 10
Breastfeeding and parity	RR falls by 4.3% every 12 months of breastfeeding in addition to a 7% reduction for every birth	Not breastfeeding
Use of exogenous hormones Oral contraceptive Hormone-replacement therapy Diethylstilbestrol	 1.2 1.66 2	 Current users Current users Use during pregnancy

Environmental factors include alcohol consumption, raised body-mass index and reduced exercise which have all been associated with increased risk of breast cancer.

Increasing age has been identified as a risk factor for breast cancer, as well as geographical location, with developed countries seeing a higher incidence of disease.

Hormonal exposure, whether intrinsic such as early menarche, late menopause, late first full-term pregnancy or nulliparity, or extrinsic such as exposure through hormonal contraceptive or replacement methods, has also been identified to increase the relative risk of developing breast cancer. Reduced breastfeeding rates, and shorter breastfeeding terms have also been implicated in an increased propensity to developing breast cancer, particularly in the West.

Family history (i.e., disease in a first-degree relative) has been shown to increase risk of breast cancer, although these pertain in particular to early-life cancers before 50 years. In addition, gene mutations such as those pertaining to the BRCA-1 and BRCA-2 mutations, are associated with increased incidence of

breast cancer, particularly certain molecular types such as triple-negative breast cancer, and male breast cancers.

It is clear therefore that although some risks are non-modifiable, namely family history and age of menarche/menopause, there are several interventions which may reduce the relative risk of disease for patients, particularly those who are known to already have increased intrinsic risk.

1.1.5 Diagnosis & Role of Multi-Disciplinary Team

The two most common routes for identifying breast cancers in the UK is either through the presentation of a symptomatic patient, or via the Breast Screening Programme. Most symptomatic patients will present with a lump, change in breast contour, or skin change, with the occasional presentation due to axillary changes. In Scotland, and the wider UK, such patients can obtain what is commonly known as a “Triple assessment” through the National Health Service (NHS), in the form of 1) History and examination, 2) Radiological investigation and 3) Tissue sampling. Often these are available within the same setting, through a specialised service. Within the UK, women between the age of 50 and 70 years are offered mammography at 3-yearly intervals. This initiative has led to a significant increase in identification, and early treatment of subclinical disease, identifying 9 new cases for every 1000 patients screened(1). Patients out-with this age group can self-refer for screening after 70 years, and if younger, may be identified through other routes, such as through the family history or genetic screening service, although other modalities may be employed for screening and surveillance, due to variations in breast tissue quality in younger patients. Patients identified through the screening programme are then also sent to the “Triple assessment” service for full assessment and diagnosis. Radiological assessment will usually involve either one or a combination of mammography, ultrasonography (including of the axilla if appropriate), or referral for magnetic resonance imaging (MRI). Tissue sampling can be either low volume cytological sampling, although most recently this has been largely replaced by core-biopsy, and in some cases, large volume sampling by other methods, ideally under radiological guidance. These can usually be carried out in the outpatient clinic setting under local anaesthetic, to allow prompt diagnosis as part of a “62-day pathway”. This condition demands that patients with a suspicion of breast cancer are assessed, diagnosed, and if indicated, commenced

on treatment within a 62-day period. Triple assessment allows staging and treatment planning, based on several clinicopathological factors.

1.1.6 Breast Cancer Staging and Treatment Planning

Like many other cancers, staging is characterised using the American Joint Committee on Cancer (AJCC) Tumour, Nodal, Metastasis (TNM) staging system, although prognosis and treatment planning also relies on additional criteria(18). TNM staging can be subdivided based on the level at which the staging has been assessed, being at clinical diagnosis (cTNM), at surgical resection/pathological assessment (pTNM) or in the post-therapy setting (ypTNM)(18). These are then subdivided based on tumour features as Tis-4, regional lymph node features as N0-3 and according to the presence of metastases as M0-1, each with prognostic implications(19). Staging therefore often relies on additional imaging, such as CT or MRI to establish metastatic spread, or localised tumour appearances to help address decision-making questions in treatment planning. It is important to note that the diagnosis of breast cancer is often a two -stage process, often not completed until after surgery, when further histopathological features can be fully established, such as nodal status. In some cases, additional gene expression signature predictive assays such as Oncotype DX Recurrence Score, Mammaprint, or scoring tools such as the PREDICT scoring system can be utilised to further inform decision making with regards to adjuvant therapies(20-23).

Additional prognostic indicators include the presence (or absence) of nuclear oestrogen receptor (ER) and progesterone receptor (PR), Human epidermal growth factor 2 (HER2) membrane receptor as well as Nottingham Prognostic Index (NPI) which considers tumour size, lymph node status and histological grade in order to give a prognostic score (excellent to poor)(24). Other factors, such as lymphovascular invasion, necrosis and tumour-stroma percentage have also shown prognostic influence, and are useful biomarkers, as discussed later in this chapter.

Although surgical resection remains the mainstay of treatment for breast cancer with curative intent, current practice dictates that each patient is considered on a case-by-case basis through the input of a multidisciplinary team (MDT). This usually involves but is not solely composed of a surgeon, radiologist, pathologist, and oncologist, with input from an MDT coordinator, as well as allied health professionals including cancer nurse specialists, amongst others. A final

consensus based on clinicopathological, and patient factors can then be reached to allow progression to treatment, often requiring multiple modalities.

1.1.7 Therapeutic Options

Surgery remains, at present, the mainstay of curative therapy for breast cancer. This now extends to a spectrum of breast-conservation (Breast Conservation Surgery, BCS) options which include oncoplastic surgery (OPS), as well as more radical mastectomy techniques. BCS has allowed patients to undergo operations which may avoid significant morbidity and psychological effect associated with mastectomy, with similar oncological outcomes(25-28). For patients undergoing mastectomy, nipple-sparing versus nipple-sacrificing techniques can be utilised depending on tumour and patient factors, with autologous replacement of tissue being favoured over implant reconstruction when possible(29). In cases of invasive disease, the axilla is also assessed, either through sentinel node biopsy or if previous evidence of axillary spread, with more extensive dissection. As a general rule, patients with more than 2 positive sentinel nodes are considered for axillary node dissection(29). More recently however, evidence of similar outcomes for surgical versus non-operative therapy directed towards the axilla has once again, broadened the spectrum of options available for patients(28-30). Decisions regarding each option is made on a patient-to-patient basis, and relies on histopathology, tumour biology and patient clinical factors.

To support the use of BCS, radiotherapy has taken a significant role in the adjuvant therapy against breast cancer. In addition to this, systemic adjuvant chemotherapeutic agents may be used, either in the neoadjuvant (i.e. pre-operative) or adjuvant setting, as well as hormonal therapy. The use of adjuncts such as these is based on the knowledge that even in early disease, micro-metastatic spread may already have occurred, and therefore systemic therapy can provide additional probability of cure(31). These systemic adjuncts were first introduced in the 1970’s, with the advent of aromatase inhibitors and Tamoxifen in the 1980’s and 90’s marking a significant shift in options for both operable and palliative breast cancer(32-34). Hormone therapies, used predominantly in ER+ cancers, are of particular use considering the natural history of recurrent ER+ disease favours long-term, late relapse(35).

With regards to systemic chemotherapy, Anthracyclines are regularly used for patients with breast cancer and are considered to be the standard of care in

most cases(36, 37). Additional treatments have been included to help reduce treatment side effects and toxicity, such as docetaxel(38, 39). Current evidence has suggested that escalation of dose-dense chemotherapy may be valuable in cases of high-risk disease in patients in both ER+ and ER- disease, although this is yet to be fully adopted into daily practice via the St-Gallen consensus(40, 41). Several studies have looked at non-anthracycline regimens, and in some cases of early, low risk disease, have shown evidence of good prognosis, using agents which are combined with anthracyclines on their own or in different combinations. These include the use of paclitaxel, docetaxel, and cyclophosphamide, with the use of trastuzumab in HER2-enriched cancers. These may be of particular use in older patients, or those withe comorbidities raising the stakes with regards to toxicity associated with anthracyclines(42, 43). Certain subsets of cancer, such as in TNBCs, the use of capecitabine has been the topic of discussion amongst oncologists, with recent adoption for use in younger, less comorbid patients who may benefit from treatment escalation in the neo-adjuvant setting, thanks in part to the evidence from the CREATE-X trial(44, 45). The use of bisphosphonates in postmenopausal patients has also been recommended in both hormone-positive and non-hormone-positive breast cancer patients who are candidates for adjuvant therapies(46).

At present, neoadjuvant therapy is offered mainly for Stage II and III breast cancers, or HER2-enriched and TNBC tumours(29). A more recent development in our knowledge of HER2-enriched tumours, and the development of drugs such as Trastuzumab (Herceptin) and other anti-HER2 agents has also improved prognosis for this subset of cancers. More recent work has been done looking at the use of HER2-blocking agents in dual-therapy setting, or in extended therapy duration, with some suggestion that in specific groups, the use of these agents may be tailored according to pre-treatment prognostic factors(47-49).

The length of therapy is therefore often tailored to patient pathological characteristics, and tolerance of side-effects related to treatment. It may therefore be useful to identify biomarkers associated with cancers with late-recurrence tendency to allow those patients to make informed decisions regarding the length of hormonal adjuvant treatment or provide longer follow up after primary treatment(50). In younger patients on the other hand, disease recurrence often follows a different course. In this case, difficulties in decision-

making with regards to using combined or single agent hormone therapies can lead to tailor-made regimens which again, increase the need for biomarkers to help stratify risk. This would allow informed decisions to be made amongst younger women, particularly those who may plan for a break in therapy to allow conception to take place within family-planning(31, 51, 52).

Recently, targeted therapies have been considered as an adjunct in these situations, such as Cyclin-dependent kinases (CDK), mTOR inhibitors and PI3K inhibitors being used with hormonal therapy in early-stage breast cancer(53, 54). These drugs, some of which are in Phase 3 trials, have been identified thanks to a deeper understanding of breast cancer molecular and signalling pathways involved in disease progression. The PI3K/AKT/mTOR signalling pathway has been shown to play a role in cell metabolism, growth, proliferation, apoptosis, and angiogenesis and provides an attractive target for therapies(55, 56). The pathway is summarised below (*Figure 1-1)*. This pathway involves the activation of cell membrane receptors by ligands such as insulin, which then activate phosphatidylinositol (3,4,5)-triphosphate kinase (PI3K), resulting in a phosphorylation cascade starting with PIP2. Consequently, protein kinase B (PKB), more commonly known as AKT, and PDK1 are recruited to the cell membrane and together, allow the phosphorylation of AKT to activate cytoplasmic and nuclear targets, such as FOXO1 (Forkhead box Other 1) and mTOR (mammalian Target of Rapamycin), with resultant downstream effects on cell survival, growth and proliferation(55, 56). AKT, a serine-threonine protein kinase, exists in three isoforms (AKT1, AKT2 and AKT3) with varied locations and numerous substrates, which include those relating to important pathways involved in Wnt signalling, for example, involved in embryonic development, or mTOR protein, which can stimulate cellular growth through increased protein synthesis and ribosome production in response to increased extracellular levels of nutrients such as glucose(57). mTOR and FOXO1 are two downstream targets, with the latter belonging to the Fox family, and with a role in glucose and lipid metabolism, particularly with regards to proliferation, apoptosis and differentiation, as well as resistance to oxidative stress(58, 59).

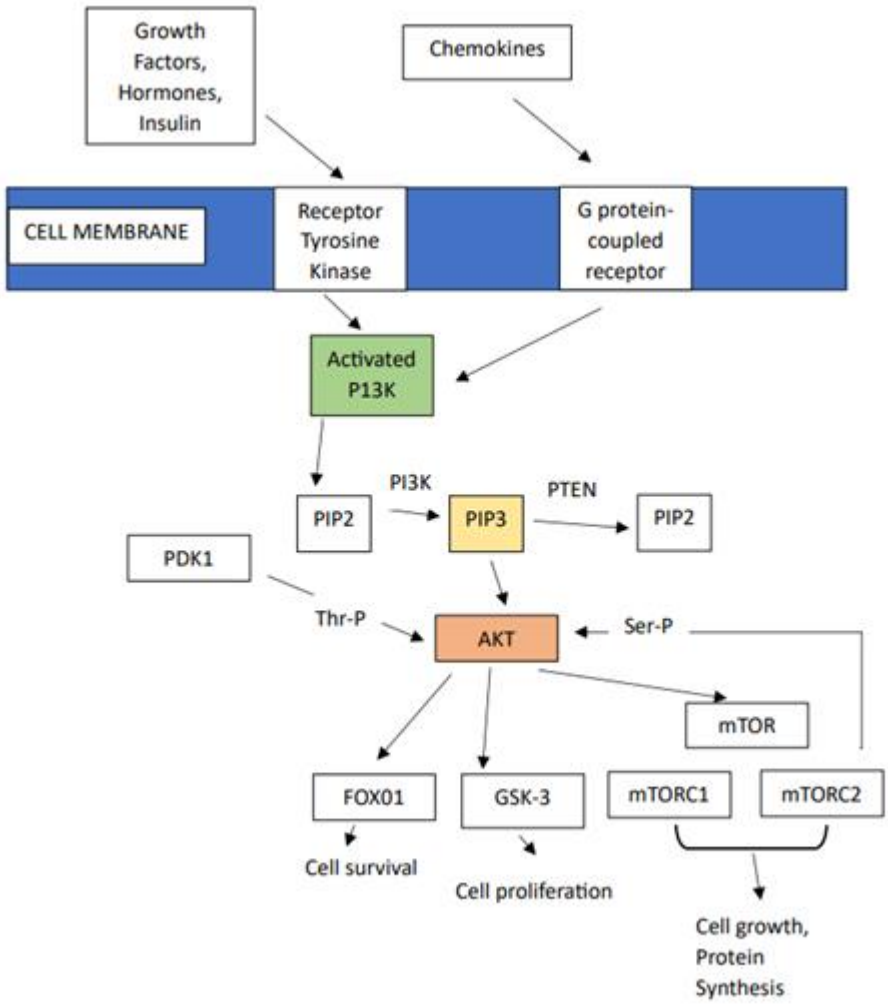

Figure 1-1 The PI3K/AKT/mTOR Pathway The presence of extracellular chemokine and growth factors activates the recruitment and phosphorylation of AKT through PI3K, leading to downstream activation of endpoints leading to increased cell survival, proliferation and growth. Cancers, including breast, have been demonstrated to harness this signalling pathway as a method to increase growth. This pathway has provided targets for chemotherapy, such as mTOR inhibitors everolimus and temsirolimus, which may propose additional benefit in different subtypes of breast cancer. mTOR: mammalian Target Of Rapamycin, FOX01: FOrkhead boX Other 1, PI3K: phosphatidylinositol (3,4,5)-triphosphate kinase, AKT: protein kinase, PIP: phosphatidylinositol lipid , PTEN: phosphatase and tensin homolog, PDK1: phosphoinositide-dependent protein kinase 1, GSK3: Glycogen synthase kinase 3. Adapted from Miriescu et al.(56).

Within this pathway, the role of phosphatase and tensin homolog (PTEN) has been of particular interest. PTEN has been shown to act as a tumour-suppressor by dephosphorylating PIP3 to PIP2 which then inhibits AKT activity at the cell membrane (56, 60, 61). It is through our understanding of how mutations in elements of this pathway, particularly PI3K, AKT and PTEN, which have been found to have mutations within their subunits in breast cancer, that potential

targets for chemotherapy may become available(62-64). The loss of PTEN, or increased activation of AKT and PI3K via mutational change, results in poorer outcomes, both through increased disease progression as well as through resistance to endocrine therapy, as shown through phase III trials(56, 62, 64, 65). It appears that within certain molecular subtypes of breast cancer, different mutational signatures can be found, for example with PTEN and PIK3CA mutations being more often associated with Luminal breast cancers with different mutational combinations attributed to other luminal subtypes(64, 66, 67). This may act as a prognostic tool as well as a chemotherapeutic target for other breast cancer subtypes.

Androgen receptors (AR) have also emerged as a potential target for therapy and prognostic indicator in breast cancer. Apart from the known hormone receptors, ER and PR, ARs have been identified in more than 70% of breast cancers at both early and later stage of disease and have been shown to play differing roles in molecular breast cancer subtypes(68, 69). AR, a cytoplasmic type 1 nuclear receptor is activated by androgens (such as testosterone) in the cytosol with downstream effect on nuclear androgen-responsive elements (AREs). Additional activity through cross-signalling with other pathways, including the mTOR, FOXO1 and wnt/beta-catenin pathways has been identified(70). As expected, a relationship between ER and PR to AR has been identified, with combinations of absent/present receptors being linked with different prognoses in molecular subtypes of cancer. For example, ER+ and AR+ tumour subtypes have been shown to have improved prognosis compared to those with ER- and AR+ profiles(71-73). However, it remains uncertain whether ARs also work independently from ER/PR as a disease stratification tool(74). In TNBCs, which have 50% prevalence of AR+ status, recent evidence suggests that AR- status may provide a useful risk stratification tool to identify those at higher risk of relapse(75).

AR inhibitor agents, commonly used in treatment of prostate cancer, are currently in phase II trials, with specific trials aimed at ER+/PR+ cancers (NCT00755885, NCT02463032), HER2-enriched (NCT02091960), and Metastatic/non-metastatic TNBC cancer types(NCT02689427, NCT02580448, NCT01842321)(68). The latter subsets are of interest to this thesis, due to lack of targeted therapeutic options for TNBC. It remains to be seen however, whether there may be enough evidence for their use, in view of the systemic side effects

which can already be perceived in patients receiving these for other cancer subtypes and their acceptability.
Finally, more recent developments have identified antibody drug conjugates (ADC), CDK4/6 inhibitors, and PARP-inhibitors, particularly in the hormone-positive breast cancers, which once again open the arsenal for anticancer therapies(32). With regards to HER2-negative patients with BRCA1 and BRCA2 germline mutations, recent results from the OlympiA trial suggest that poly(adenosine diphosphate-ribose) polymerase (PARP-) inhibitors improved disease-free survival in phase 3, double-blind randomized controlled trial(76).

Further developments have also come from our improved understanding of the immune landscape of breast cancer. For example, in TNBCs, there is strong evidence that this subtype has a high degree of immune-cell infiltration, both within the tumour and TME, leading to further progress in our understanding of targets for immunotherapy. Immune-checkpoint inhibition, which has been adopted into other cancers such as that of the lung, are now being examined for their use in breast cancer(77-79). Programmed cell death 1 (PD-1) ligand 1 (PD-L1) expression has been one such biomarker which has reached Phase 3 trials in the neo-adjuvant and adjuvant setting for TNBC disease (80). These may reveal themselves to be of additional use as part of a dual/combined approach with other agents(81, 82). Once again, the value of increasing our understanding of the tumour immune landscape and interaction will allow the identification of biomarkers which will help address gaps in the therapeutic arsenal against breast cancer.

However, patient factors and cancer biology will impact the efficacy and applicability of these therapies, therefore, further understanding of the role of biomarkers in prognosis and as targets remains of interest. This is of particular use for patients who could be identified as lower risk, to avoid the toxicity associated with adjuvant therapy in favour of an expectant or “watch and wait” approach.

1.1.8 Breast Cancer Subtypes – Histology Versus Molecular Subtyping

When considering the histology of breast cancer, the vast majority of breast cancers fall into the category of ductal carcinoma of no special type (IDC-NST) (70-75%)(83), with lobular carcinoma as the next largest group, identified according to their histological structure within their tissue area of origin, the

breast ductal-lobular unit. In clinical practice, lobular cancers are usually identified by the lack of E-Cadherin expression at biopsy analysis. A smaller series of cellular types have also been described, including invasive mucinous, cribriform, tubular or medullary cancers(84). However, more recent work to establish the cytopathological and molecular characteristics of breast cancer has allowed breast cancers to be classified according to other criteria, with clinical and prognostic significance. These are described later in this chapter.

In clinical practice, breast cancer is subdivided into three common subtypes depending on the presence of surface and nuclear receptors on immunohistochemical assessment, typically as ER/PR+, Human-epidermal growth factor 2- (ERBB2 or HER2-) enriched (a combination of these) or Triple-negative (TNBCs). These are usually described as 1) hormone-positive, HER2-negative, 2) hormone positive, HER2 positive, or 3) triple-negative breast cancers(85). In the literature and research setting however, and over the course of this thesis, molecular subtypes have more recently been employed to subdivide breast cancers, with four main groups having been described, which have considerable overlap with their clinical subgroup counterparts(86). These were elucidated thanks to the advent of gene assay techniques, which in future will allow treatment to be tailored more closely to patient's individual gene signature by allowing risk stratification and prediction of response to adjuvant therapies(87). First discussed by Perou et al. in 2000, the use of cDNA microarray of 38 breast cancers allowed them to examine and cluster this series of cancer into four molecular subtypes: Luminal, HER2-enriched, basal-like cancers, and normal breast cells. Since then, more subgroups have been added, although currently 5 main groups are considered valid, regardless of their prognosis. Later work has suggested that these groups not only differ in their genetic signature, but also in their prognosis(88). The four main subgroups which are described in this thesis are Luminal A, Luminal B, Triple-Negative and Her2-enriched breast cancers.

Luminal A cancers, characterised by hormone-receptor positive status, differs from Luminal B due to the presence of HER2-negative status(89). Luminal A cancers make up to 60% of total breast cancers and are identified by a gene signature suggesting expression of genes activated by the ER transcription factor, and a low expression of cell proliferation genes. This translates into a histology in which ER and PR is positive, Bcl2 and cytokeratin are richly expressed, and

Ki67, a marker of proliferation is low. In addition, invasive histological grade is low, and as such, these cancers have a tendency towards improved prognosis. (90)

Luminal B breast cancers, accounting for up to 20% of cancers, have higher markers of proliferation in their gene signature, including MK16, cyclin B1 and are most often shown to be (but not always) HER2, KI67 and EGFR positive at immunohistochemistry analysis(89). As expected, Luminal B cancers often have poorer prognosis than their A counterparts, although certain subgroups demonstrate good response to neoadjuvant chemotherapy(87). The St-Gallen consensus has since allowed the categorisation of Luminal B into two main groups, ER+/HER2- and ER+/HER2+ types, differing from Luminal A cancers with regards to having higher proliferative index markers, such as Ki67, although currently, a standardised threshold remains to be upheld across the board(91).

HER2-enriched cancers (15%) are so called due to their high expression of HER2, or associated genes. This group, although there is overlap with Luminal B cancers, does not correspond directly to the formerly described group, as often genomic expression does not match the protein expression profile at immunohistochemical analysis(92, 93). Current consensus therefore considers this group to be appropriate in the absence of ER/PR(91). Although associated with poorer prognosis, the advent of Trastuzumab and other anti-HER2 agents in the neoadjuvant setting has improved outcomes significantly in this group(92).

The fourth group, known as Basal-like subtype, make up approximately 10% of all breast cancers. The gene signature of this group resembles that of normal breast myoepithelial cells (hence the term “basal”) such as CK5, CK17, P-cadherin, CD44, EGFR, caveolin 1 and 2, nestin and lower luminal epithelial markers (CK8/18, Kit, etc.)(87, 94). These cancers are known for their poor prognostic profile and have significant (but incomplete) overlap with the TNBC subtype(95). Basal-like breast cancers exhibit features such as high mitoses, high levels of tumour necrosis, significant stromal lymphocyte infiltration, and are often found to have poor clinical prognostic features such as large tumour size and high grade, with regional node invasion at diagnosis(94). As described later in this thesis, basal-like cancers and TNBCs are associated with high levels of p53 mutation, and associated with BRCA1 germline mutations(87). TNBC has a median survival of 65% at 5-years in primary regional disease(96-98).

Interestingly, this subgroup also exhibits a greater response (in some cases) to chemotherapy in early disease (99). It is through our understanding of the role of BRCA1 mutation and the effect on DNA-repair promoting error accumulation which has led to our understanding of how PARP-1 inhibitors may, through their role in the blockade of PARP1 (which has a role in DNA repair) lead to improved response to this chemotherapeutic agent in this poor prognostic subgroup(100). TNBCs run a more aggressive clinical course. Often chemotherapy is offered (particularly in higher stage disease at diagnosis) as neoadjuvant therapy before the mainstay of therapy for most breast cancers, surgery, comes into play(86).

Two additional molecular subgroups, known as “Normal Breast” and “Claudin-low” cancers, have also been described, but are not considered in the following thesis. Normal breast subgroup tumours (5%) are poorly understood, of uncertain significance, but are described by their similarity in gene signature to adipose tissue, although there is overlap with TNBCs due to their lack of ER/PR/HER2 expression(101). Claudin-low cancers exhibit low expression of genes associated with inter-cellular attachment such as those relating to tight-junctions, or genes for claudin-3,4,7 and e-cadherin, and have overlap with TNBC and basal-like cancers(102).

Overall, the 4 main subgroups (with Luminal B representing two “sub-subgroups”) can be summarised as described below,(*Table* 1-2) although it is important to note the significant overlap and progress of current research may delineate further methods of stratifying these groups further.

Table 1-2 Characteristics of the four described molecular subtypes of breast cancer. Adapted from Eroles et al. and from the St-Gallen International Expert Consensus of primary therapy of Early Breast cancer, 2013 (87, 103).

Molecular Subtype	Proportion of breast cancers (%)	ER/PR/HER2 profile	Ki67/ Proliferative index	Histological grade	Prognosis
Luminal A	50-60	ER+/PR+/HER2-	Low	Low	Excellent
Luminal B	10-20	ER+/PR+ and HER2+ OR HER2-	High	Intermediate	Intermediate/poor

Basal-like / TNBC	10-20	ER-/PR-/HER2-	High	High	Poor
HER2-enriched	10-15	ER-/PR-/HER2+	High	High	Poor

The role of Ki67, although recognised as an important marker of proliferation, has yet to be fully absorbed into clinical practice. Ki67 encodes two protein isoforms first described in the 1980's and known to be expressed in active cell cycle stages, compared to resting cells, within the nucleus(104, 105). It has now been well-established as a marker of proliferation, with high levels suggesting high levels of mitosis and which has been related to p53 activity(106). Prognosis has been shown to be poorer in cancers with high levels of Ki67 expression, although the threshold or prognostic subgroups divisions have yet to be determined (107). However, recent work suggests that despite variation in assays amongst laboratories, Ki67 is a reliable prognostic indicator, calling for a consensus to be reached in the preparation of specimens, validation and scoring techniques using immunohistochemistry and manual scoring, and allow the use of Ki67 into common practice as a way to predict which patients may benefit from more aggressive therapy, earlier follow up, or even as a target for therapy(107, 108). Within this thesis, Ki67$\leq$14 has been utilized as the cut-off for high versus low expression, as supported by the literature(87). To support the role of Ki67 as a prognostic biomarker, two major trials, the IMPACT study (Immediate Preoperative Anastrozole, Tamoxifen, or Combined with Tamoxifen) and the PO24 study of neoadjuvant letrozole vs tamoxifen have seen the levels of Ki67 to correlate with recurrence rates, and in other cases, to relate to lack of response/effect of pre-operative therapies (108-110). These have since led to our understanding that Ki67 may allow patients with low-risk disease to avoid potentially toxic chemotherapeutic agents, based on low Ki67 levels at post-treatment pathology results(110).

1.1.9 Challenges in Treatment and Prognosis

As our understanding of breast cancer deepens and the availability of chemotherapeutic and surgical techniques broadens, creating reproducible and reliable algorithms for the management of this heterogeneous group of cancers becomes more complex. Two patients with the same histological findings may

not be suitable for the same therapeutic options, as these can be affected by comorbidity, patient wishes and surgical local practice. Having robust prognostic tools to stratify risk can therefore be of extreme importance in individualizing therapy for patients, and this will include identifying prognostic biomarkers. Additionally, biomarkers which may predict the likely response to therapies will be essential in helping form post-treatment follow up regimen for patients with breast cancer. Systemic and local tumour factors have been examined with regards to many solid tumours, starting with host-level changes in circulating factors, as well as tumour and micro-environment changes, described below.

1.1.10 Systemic Inflammation

Recent work has shifted our viewpoint on cancer to focus not only on the tumour itself, but on the tumour microenvironment (TME) as well as what has been coined by the "tumour-organismal environment" or TOE(111). This theory suggests that beyond the immediate tumour and surrounding tissue, systemic changes in physiology may in turn be affected by the tumour, as well as promoting tumourigenic progression. When considering the physiological effects of cancer upon the patient on a more systemic level, there is clear evidence that inflammation plays a significant role in cancer at all stages of disease, with the immune system playing a significant enabling role both locally, and distant to the tumour site(16). The role of the TME, including the role of immune cells within this landscape will be discussed later in this chapter. When considering systemic inflammation, this can be clinically seen in patients with cancer-derived syndromes presenting with night-sweats, pyrexia, or metabolic rate changes leading to weight loss and fatigue, but on a molecular and cellular level, there is clear evidence that systemic inflammation may create a pro-tumorigenic environment and promote disease progression(112).

Systemic inflammation can be subdivided according to several established factors which are known to be affected/affect cancer progression, namely neutrophil count, white cell count, Glasgow prognostic score, albumin and CRP (C-reactive protein), cancer cachexia, B symptoms and circulating myeloid-derived suppressor cell count(112). Acute phase proteins such as CRP, LDH, and subsequent changes in albumin due to re-direction of liver synthesis, have been combined into scoring systems. A recent systematic review by the author of this thesis has identified a role for markers of pre-operative systemic inflammation

to be associated with poorer prognosis in specific cases of breast cancer, as well as after surgical intervention, when postoperative complications may play a role in determining recurrence risks(113, 114). The detection and assay of serum levels of biomarkers such acute phase proteins, as well as the relative levels of immune cells in the host serum, have been determined to have prognostic influence on cancer progression, most notably in colorectal cancers. This includes neutrophil-to-lymphocyte ratio (NLR), as well as acute phase proteins such as CRP(113). In other cancer types including colorectal malignancy, the Glasgow Prognostic Score (GPS), a prediction tool involving CRP and serum albumin has been utilised as a measure of risk of recurrence although this has yet to become more common in research relating to breast disease(115, 116). Circulating macrophages (or their systemic predecessors, monocytes), have also been shown to provide a prognostic indicator of poorer survival in colorectal cancer(117). Other cell types, including platelets, eosinophils and NK cells have been implicated in cancer prognosis, particularly when combining this to their ratio to lymphocytes, but ongoing work is required with regards to their effect in breast cancer(113, 118). Nonetheless, it is evident that the immune system has both far-reaching and tumour-specific effects which may improve our understanding of tumour progression, as well as provide targets for therapy(112).

1.1.11 Tumour Microenvironment and the Role of Hypoxia, Apoptosis, and Immune cells

There is now established evidence that the tumour does not function as a single, independent entity within a cancer patient, but that the tumour microenvironment, and to some degree, the overall physiological conditions within a patient, all play a part in establishing conditions which lead to cancer(16, 111, 119, 120). Cancers affect and in turn, are affected by local cytokine, chemokine and cellular effects from local tissue stroma and immune cells, and vascular endothelium(112). Characteristics such as necrosis, Klintrup Makinen score, and tumour stroma percentage (TSP) can be helpful indicators of prognosis and are considered to be characteristics of TME-related inflammation(112).

1.1.12 Tumour Necrosis

Tumour necrosis is a well-established marker of poor prognosis in a number of solid cancers and has been shown to be independent from other clinicopathological factors in determining disease progression(121, 122). Within breast cancers, there are two main types of described necrosis, one being of the intraductal architecture (known as “comedo-necrosis”), and one found within the invasive tumour mass. The latter is a significant prognostic indicator (when in high levels) and is considered as the necrosis of interest in this thesis. Necrosis is thought to represent the imbalance between tissue proliferation, and the ability for vascular supply to match this growth, leading to hypoxia and cell necrosis within the central portions of tumour mass, as well as the immune effect of local inflammatory response to the tumour itself(112, 121).

1.1.13 Tumour Stroma Percentage

Tumour stroma, which has gained interest in recent decades, describes the tumour micro-environment, which influences both tumour cell behaviour as well as local endothelial and distant metastatic potential(123). TSP (high stroma to tumour percentage) is known to be associated with poorer cancer-specific survival in node-negative ductal breast cancer and has been associated with lower levels of tumour inflammatory infiltrate(123-125). The relationship between TSP and TNBC is however, thought to be more complex, with reports suggesting that in some cases, prognostic measurements related to high TSP are not always associated with poor outcomes(126). Finally, TSP has also been found to correlate to efficacy of adjuvant chemotherapy, with high levels of TSP being related to poorer outcomes, suggesting that it may be used as a biomarker to inform decision-making with regards to which patients are likely to benefit from chemotherapy, whilst avoiding potential toxicity in those unlikely to gain improved survival outcomes(127).

1.1.14 Klintrup Makinen Score

Decreasing Klintrup-Makinen score, considered an indicator of peritumoural inflammatory infiltrate, has been associated with poorer prognosis in cancers including colorectal cancer, and therefore may be another element of the TME which should be considered when assessing the role of TME in cancer pathology(128). A low score is used to describe low peritumoural immune cell infiltrate, increasing to a band-like infiltrate, and finally more extensive

infiltrate forming a “cup”-like zone at the invasive margin with evidence of tumour destruction by immune cells (0-3)(129). Tumour-infiltrating lymphocytes (TILs) have been shown to be associated with prognosis in breast cancer, with CD3+ T cells forming a large subset of the overall cell types involved(130, 131). Within this group, CD4+ helper T cells and regulatory cells have also been identified to have roles in prognosis for ovarian, lung and other cancer types, although these are sometimes protective, at other times they have been associated with reduced survival (132-135). TILs are discussed in more detail in a later chapter, particularly in the context of TNBCs. Other elements of the immune response, including tumour associated macrophages (TAMS), have also been associated with poor prognosis in TNBCs, but are beyond the scope of this study(136). Other biomarkers which are associated with the tumour environment, such as hypoxia and acid-base controlling elements, are discussed in more detail later in this thesis.

1.1.15 Local Cellular Immune Response

Immune cell recruitment to the TME has been examined and noted to vary according to levels of disease progress. Acute inflammatory cells such as T-lymphocytes have been associated with reduced levels of necrosis, and improved outcomes, suggesting that these may represent anti-cancer immunity, as seen in colorectal cancer(137-139). The shift from acute inflammatory cells to those of the innate response, such as macrophages, neutrophils and myeloid-derived suppressor cells (MDSC) has been described in cases of more advanced cancer and cancers with poorer prognosis, suggesting that these may inform or be influenced by more advanced disease stage and participate in progression(140).

1.1.16 Other Markers of Local Inflammation – Inflammasomes, Cytokines, Chemokines, and Transcription Factors

As our understanding of the TME and systemic host landscape increases, numerous other influences on tumour progression and incidence have been identified. Inflammasomes is the term used to describe large protein complexes which contribute to tumour proliferation through their induction of interleukin-ß and interleukin-18, as well as encouraging inflammatory-mediated cell death(141). It is therefore unclear whether these protein complexes have a pro-tumorigenic or anti-tumorigenic property, although it is suspected that they may oscillate between these two functions depending on the level of disease(141).

Inflammatory cytokines such as vascular endothelial growth factor (VEGF), granulocyte macrophage stimulating factor (GMCSF), Interleukins (IL)-1β, IL-6 and Transforming Growth Factor- Beta (TGFβ) amongst others, have been implicated in cancer(112, 142, 143). One well known cytokine, IL-6, has been demonstrated to participate in local and systemic inflammation, particularly the role of macrophages, discussed later in this chapter(112, 137, 138, 142). Chemokines such as Chemokine C-C MOTIF LIGAND (CCL)2, 17 and 22 and Chemokine C-X-C motif ligand (CXCL) 1, 8, 12, 13 have been identified at high levels in tumour cells, as have several transcription factors which relate to immune cell recruitment and activity. STAT3 (Signal Transducer and Activator of Transcription 3), a transcription factor with roles in anti-apoptosis and immune cell proliferation, has been associated with IL-6 cytokine, while NF-κB (Nuclear Factor Kappa-B) has been described as an upstream regulator of the immune response at multiple levels, as well as being associated with the development of cancer. NF-κB activation occurs through two main pathways (with significant cross-talk), described as the canonical and non-canonical signalling pathways(144). Due to its far-reaching effects within the normal and cancer-related tissue environment, the NF-κB transcription factor family has garnered significant interest, and recently been identified as a feature in the development of resistance to hormonal therapy in breast cancers. This suggests the effects of NF-κB are complex and multiple, implying its role as an important biomarker within the TME(144, 145).

1.1.17 EMT & Tumour Budding

Thanks in part to changes within the tumour cells, TME, and within the wider systemic environment several invasive properties have been identified which tumour cells adopt in order to metastasize. This relies in part on the breaching of the extracellular membrane, (particularly the basement membrane) which normally provides a junction between cellular planes and facilitates communication between tissue types to maintain homeostasis(119). When the normal boundary between tissue types is breached, several mechanisms are in place to repair these, through both cytokine and migratory cellular behaviours. These include response to hypoxia, apoptotic mechanisms and growth arrest or differentiation (146). Numerous mechanisms are in place within the basement membrane itself to maintain its integrity, including the presence of Cadherins, which provide integrity, and which are commonly lost in many cancers(147). It is

the loss of these, in particular E-Cadherin, weakening of adherens junctions, as well as reduced levels of membrane and cytoplasmic levels of ß-catenin (together with additional changes in local transcription factors) which constitutes evidence of the development of a state known as Epithelial-mesenchymal transition (EMT)(148). As a well-established hallmark of cancer, the study of EMT has revealed that tumour budding is closely associated with a number of changes also seen in tumour cells which adopt a tumour budding phenotype, although this is not a consistent finding, and therefore suggests a more complex relationship between tumour budding and the process of EMT(149). Recent summary by Lugli has been described below, (*Figure 1-2)*.

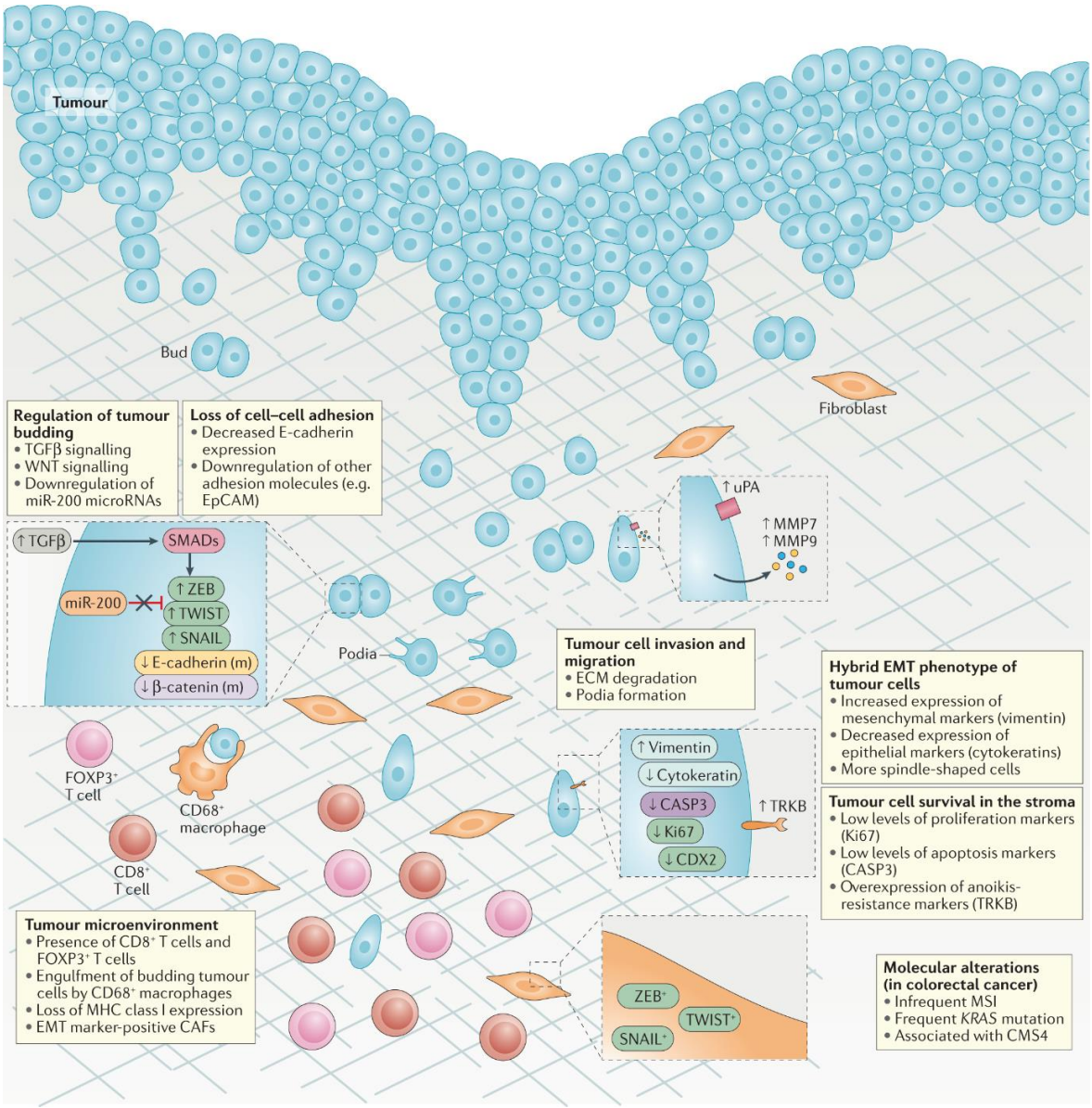

Figure 1-2 The extracellular, intracellular and molecular factors associated with tumour budding.Taken from Lugli et al.(149)

Tumour budding, a feature exhibited by solid cancers, is increasing in interest as an emerging, and in some cases established, prognostic biomarker. Most extensively described in colorectal cancer, a tumour bud is an isolated group of up to four cancer cells found at the invasive tumour front, separate from the tumour mass(7). Tumour budding (TB) can be considered to be one of the bridging elements between tumour and TME, with two main subsets of budding having been defined. Intra-tumoural budding (ITB), as the name suggests, consists of clusters of cells within the tumour mass, whereas peritumoural budding (PTB), is seen at the interface between the invasive tumour front and TME(149). When compared to tumour mass cells, TB cells have reduced levels of E-cadherin, as well as low nuclear Ki-67, whereas vimentin is more highly expressed(150). In 2016, the International Tumour Budding Consensus Conference (ITBCC) published a scoring system when it became apparent that TB score was associated with the risk of lymph node metastasis in patients with early invasive disease and survival in patients with more advanced stages of colorectal cancer(6-8, 151). Since then, recommendations by a number of bodies, including the College of American Pathologists and International Collaboration on Cancer Reporting protocols for Colorectal Cancer Pathology, as well as within the WHO and TNM staging recommendations have supported its use in regular clinical practice(149). This morphological biomarker has consequently been studied in numerous other cancers, including breast cancer, where emerging evidence to its role in outcome stratification have been proposed(10-13, 152).

TB denotes one of the fundamental behaviours of solid tumours in the transition towards metastasis. This finding is suspected to be a histopathological depiction of a process belonging under the umbrella term of epithelial-mesenchymal transition (EMT) in which tumour cells adopt new characteristics to facilitate the migration from the solid tumour mass and tumour micro-environment to allow seeding at distant sites(14). However, the exact way in which tumour buds exist with respect to EMT is uncertain, partly due to our emerging understanding of the signalling pathways and protein expression which characterise these processes. When examining the transcriptional profile of EMT cells versus TB, similar patterns in cytoskeletal changes, such as changes brought on by increased levels of nuclear ß-catenin expression have been identified(153). However, cells undergoing EMT, and TBs are not identical. One example of

differing transcription factor profiles is in examining the level of expression of SEB1 (SEven Binding 1), SLUG (Snail Family Transcription Repressor 2), SNAIL (Snail Family Transcription Repressor 1), TWIST1 (Twist related protein 1) and TWIST2, which are absent in TB compared to their overexpression in cells undergoing EMT(154). However, more in-depth examination of breast cancer molecular subtypes, has suggested that some of these biomarkers, including SNAIL and TWIST, have been found to have significantly increased (former) or decreased (the latter) expression in the stroma of TNBCs, while ZEB1 was more highly expressed in hormone-positive cancer stroma, although these were not identified within the tumour buds themselves(148). Stromal cells such as interstitial and cancer-associated fibroblasts (also described as cancer-associated myofibroblasts) may be associated with changes in the TME which promote or respond to the presence of TBs and are associated with their progression to fully fledged circulating tumour cells (CTCs)(148). Tumour budding in the cancer periphery (peripheral tumour budding, PTB) and intratumoural budding, ITB, may have different roles within the biology and natural history of the cancer(13). Understanding the natural history and difference between ITB and PTB will be of use in assessing whether prognosis can be determined only on full section of cancer, or whether core biopsies at the pre-diagnostic stage may already allow stratification for treatment planning(13). This is particularly important in patients with TNBC who often qualify for neoadjuvant therapy before a surgical specimen is available for analysis. It can be therefore surmised that TB is a “snapshot” of a dynamic process, immortalised for analysis during immunohistochemical examination, but which may bridge the process of solid tumour to EMT and metastasis(153).

With regards to tumour budding and breast cancer, previous work has shown that tumour budding was associated with reduced cancer-specific survival (CSS), amongst other markers of disease progression at diagnosis(10). These are looking specifically at intraductal carcinoma of no specific type (IDC-NOS). Gujam et al., using a cut-off value of 20 buds/0.385mm^2 found that patients with higher budding counts had poorer CSS. Liang et al. for example established that in patients with a higher tumour bud count (using a cut off-of $\geq$8 buds/0.950mm^2) TB count was independently associated with poorer overall survival(12). Sun et al. have reported that poorly differentiated clusters of 5 or more cells were prognostically associated with lymphovascular invasion, tumour budding grade,

rate of relapse and disease-free survival as well as overall survival(11). Salhia et al., used a slightly different cut-off of 1-5 cells, and counted buds across a 10 HPF area of more than 4 buds, and examined PTB versus ITB scores(155). “Poorly differentiated clusters” (made up of larger numbers than 5 cells) have also gained interest for breast cancers, although remain outside the scope of this thesis/study(11). It is clear therefore that although this area is promising, a standardised approach is required to establish the use of TB as a prognostic indicator.

The molecular characteristics of TB have recently been of interest, and some studies in colorectal and pancreatic cancers have demonstrated how TBs can vary in their presence amongst molecular subgroups of colorectal cancer, as stratified by their Consensus Molecular Subtypes (CMS) classification(156, 157). Suggested mechanisms for this variation has been through evidence of the role of varying microRNA (miRNA) regulation on TB development, which are also known to have effects on EMT phenotype(149, 158). It therefore stands that tumour budding phenotype will vary amongst breast cancer molecular subtypes, and that further examination of the variation in the transcriptomic landscape of tumour buds in breast cancer is warranted. Emerging evidence of the immune infiltrates associated with tumour budding also suggest that a switch from innate to adaptive immunity in areas of proximity to TB may also be associated with poor prognosis, suggesting this may be of value with regards to understanding how harnessing the inflammatory infiltrate of cancer TME may provide solutions in prevention of metastasis(159). However, as Lugli et al. suggest in their recent work, several issues need to be addressed to allow tumour budding to be utilised in our common clinical parlance, namely the knowledge of TB in relation to clinicopathological factors as well as robust, easily reproducible techniques for the preparation, processing, scoring of specimens, and subsequent analysis of tumour budding results.

1.1.18 Tumour Budding and TempO-Seq Analysis to Assess Differential Gene Expression

Previously in our lab, Elizabeth Morrow used TempO-Seq, a bulk RNA-seq method to assess the transcriptomic landscape of ER-negative cancers in relation to tumour budding(2). This study forms the basis for a large part of the following thesis and is explained in more detail below. TempO-Seq for 25 highest budding

patients and 25 lowest budding ER-negative patients within the Glasgow Breast Cancer Cohort known as the "1800 Cohort" was performed. This cohort, made of 850 surplus cancer specimens, was established using retrospectively collected data from patients who underwent breast cancer surgery for operable primary breast cancer in two Glasgow Hospitals between 1995 and 1998. This cohort, and the TempO-Seq process is described in more detail in Materials and Methods Chapter. TempO-Seq analysis allowed the most differentially expressed genes to be identified and form the basis for further validation studies. Any gene with a log2-fold or more change in expression (high or low) was of interest. The heat map which resulted from the analysis is described in below, (*Figure 1-4)*(2). The 20 most differentially expressed genes in this cohort are shown.

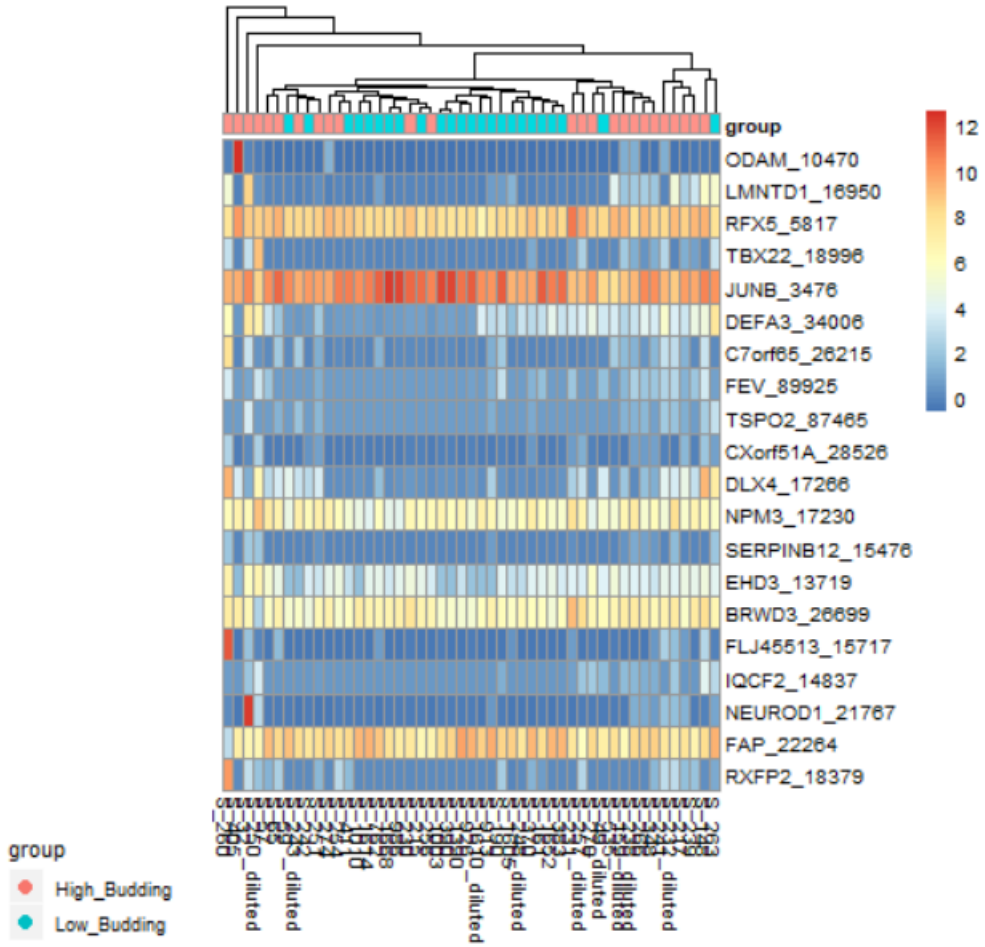

Figure 1-3 Heat map of the top 20 differentially expressed genes when comparing low to high tumour budding phenotype ER-negative tumours in the Glasgow Breast Cancer (1800) Cohort. Adapted from data provided by Bioclavis and E Morrow(2)

The top five differentially expressed genes were chosen as the basis for this study. These were then reduced to 4, after LMNTD1 was found not to have a

readily available antibody and protocol for further validation at the time of study. The remaining 4 were identified as ODAM, RFX5, JUNB and TBX22. JUNB was over-expressed in high-budding tumours, while the remaining 3 are under-expressed, particularly ODAM, (*Figure 1-3)*. Each gene and respective protein will form the basis of a separate individual chapter in this thesis as the protein expression and its relation to clinicopathological characteristics is explored in greater detail.

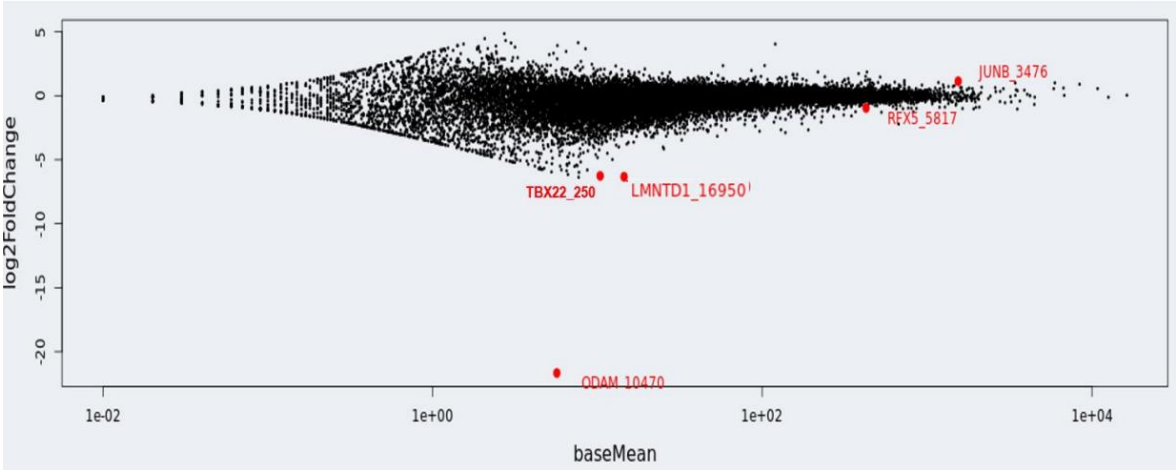

Figure 1-4 MA plot showing 5 most differentially expressed genes in high tumour-budding phenotype ER-negative tumours in the Glasgow Breast Cancer Cohort. Adapted from data provided by TempO-seq Bioclavis and E.Morrow(2).

1.1.19 Tumour budding and Triple Negative Breast Cancers

Taking the above results one step further, an additional element of this study explores the transcriptomic landscape of TNBCs in relation to tumour budding. In this particular subset of cancers with poor prognosis and often with early recurrence, tumour budding was considered a valuable asset in understanding some of the factors which may affect outcome. The digital spatial profile of gene expression was examined using GeoMX Digital Spatial Profiler, to establish how the tumour, and TME may differ with regards to gene expression between high tumour budding and low tumour budding cancers. This was then followed by immunohistochemical analysis to establish how this relates to protein expression, and clinicopathological findings relating to outcome. GeoMX DSP is a novel technology which allows specimens to be analysed for differential gene expression based on comparison of different regions of interest, and relating to whether these represent TME or tumour itself. This is described later in the chapter 7.

1.1.20 Research Aims & Hypothesis

Breast cancer is common, and heterogeneous. Thanks to advances in surgical and oncological practices, diagnosis and survival have improved, despite increasing incidence. However, due to ongoing cases of recurrence, and in cases of advanced disease, it is imperative to identify biomarkers which not only provide prognostic information but may also represent targets for therapy. A deeper understanding of the transcriptomic landscape of breast cancers, and particularly those with poorer outcomes such as ER-negative, HER2-enriched and TNBCs can aid in this effort. TNBC cancers, some of the breast cancers with poorest outcomes and relative dearth of options for adjuvant therapies, pose a particular concern, and are considered to be of particular interest in this study. Thanks to information provided by transcriptome analysis via TempO-Seq (bulk RNA-seq), this study aims to achieve the following:

- Validate if the differentially expressed genes identified using bulk RNA-seq (JUNB, ODAM, RFX5 and TBX22) are associated with changes in protein expression in relation to tumour budding.
- Describe how JUNB, ODAM, RFX5 and TBX22 are expressed within the tumour cell and establish associations with clinicopathological characteristics across all molecular subtypes.
- Explore the digital spatial profile of gene expression in TNBCs and how differential gene expression relates to tumour budding.
- Compare how differential gene expression relates to protein expression in TNBC and the relationship between protein expression and prognosis in TNBC.

It was hypothesised that protein expression would relate to prognosis and provide potential biomarkers to allow risk stratification, as well as relating to tumour budding phenotype, validating the results of previous work, and providing further information on the role of these proteins in breast cancer pathology.

Chapter 2 Materials and Methods

2.1 Patient cohorts

Studies described in this thesis used data and tissue from two patient cohorts. These are described below in more detail and have ethical approval by the Research Ethics Committee of the West Glasgow University Hospitals NHS Trust. The first cohort is known as the 1800 Breast array but will be described henceforth as the Glasgow Breast Cancer Cohort (SafeHaven database number GSH/18/0Noo8), and the second is known as the Triple Negative Breast Cancer Cohort (TNBC Cohort, SafeHaven database number GSH/21/ON/oo8). The two cohorts are geographically similar, although the second was selected purely on the basis of patients being TNBC for inclusion, and therefore may differ in age and clinicopathological characteristics as a result. The portions of this research that were based on either one or both cohorts will be indicated respectively within the course of this thesis.

2.1.1 The Glasgow Breast Cancer Cohort

The Glasgow Breast Cancer Cohort consists of 850 breast cancer patients with primary operable breast cancer retrospectively identified from West Glasgow hospitals between 1995 and 2001. These patients underwent curative surgical resection according to local contemporary standards of care at either Glasgow Royal Infirmary, Western Infirmary or Stobhill hospitals, and any surplus primary tumour tissue was formalin-fixed, paraffin embedded (FFPE) and prepared as part of a Tissue micro-array (TMA). Clinicopathological data, such as age, tumour size, grade and ER, PR and HER2 expression status as well as any adjuvant treatment courses had been previously recorded and were available together with data regarding previously examined protein expression studies. ER, PR and HER2 profiling was carried out retrospectively to ensure standardisation, as some cancer diagnosis dates preceded the use of routine HER2 testing. The cohort micro-array was constructed by the Glasgow Tissue Research Facility (GTRF) using full sections cut from FFPE blocks, which Dr Elizabeth Mallon (Pathologist, Queen Elizabeth University Hospital) identified and marked out for tumour-rich areas. Three cores were lifted from each block and deposited into recipient paraffin blocks. The TMA slides were also equipped with other tissue type cores to act as positive controls during staining, and TMA maps drawn up to allow identification of each core with a TMA-ID linking this to an anonymised database containing clinicopathological information. Clinicopathological data follow up was completed 15 April 2019. A sub-group of 50 patients with known ER-negative

status were also identified, and full section slides were cut from surplus tissue, and used for tumour-bud characterisation, quantification, and analysis, as will be indicated in the results section. Details of this cohort is described below, (*Table 2-1)*. As noted in following chapters, several cores were lost or were not assessable, and therefore total numbers utilised for the protein expression analyses are indicated in each chapter. For analysis, non-ductal cancers were excluded (n=68).

Table 2-1 The Glasgow Breast Cancer Cohort, Population clinicopathological characteristics. *ATAC trial: Arimidex, Tamoxifen, Alone or Combination Trial

	n (%)
Number of patients	850
Median follow up time	162 months
Events	
Breast Cancer Death	174 (20.5)
Non-breast Cancer Death	158 (18.6)
Age	
<50	248 (29.2)
≥50	602 (70.8)
Tumour Type	
Ductal	736 (86.6)
Lobular	68 (8.0)
Other	46 (5.4)
Invasive Tumour Size (mm)	
≤20	496 (58.4)
21-49	309 (36.4)
≥50	44 (5.2)
Missing	1 (0.1)
Tumour Grade	
I	161 (18.9)
II	382 (44.9)
III	305 (35.9)
Missing	2 (0.2)
Nodal Status	
Negative	490 (57.6)
Positive	348 (40.9)
Missing	12 (1.4)
ER status	
Negative	570 (67.1)
Positive	276 (32.5)
Missing	4 (0.5)
PR Status	
Negative	396 (46.6)
Positive	448 (52.7)
Missing	6 (0.7)
HER2 status	
Negative	699 (82.2)
Positive	128 (15.1)

Missing	23 (2.7)
Type of breast surgery	
Breast conservation surgery (BCS)	328 (38.6)
Mastectomy	521 (61.3)
Missing	1 (0.1)
Type of Axillary Surgery	
Sentinel lymph node biopsy	0 (0)
Axillary sampling	27 (3.2)
Axillary clearance	808 (95.1)
None	0 (0)
Missing	1 (0.1)
Adjuvant therapy:	
Endocrine	
Tamoxifen	528 (62.1)
ATAC Trial*	32 (3.8)
No	141 (16.6)
Missing	149 (17.5)
Chemotherapy	
Yes	331 (38.9)
No	516 (60.7)
Missing	3 (0.4)
Radiotherapy	
Yes	401 (47.2)
No	446 (52.5)
Missing	3 (0.4)

2.1.2 Triple Negative Breast Cancer Cohort

The TNBC database consists of 207 patients with triple negative breast cancer who underwent curative surgical resection for primary operable invasive breast cancer at two Glasgow Hospitals between 2011 and 2019. Clinicopathological characteristics including age, nodal status, grade was collected, together with survival and recurrence events. FFPE blocks of surplus tissue were cut by the GTRF as part of a TMA microarray as described above. Data analysis was performed after patients who received neoadjuvant chemotherapy were excluded (n=50). Details of this cohort is described in the table below, (*Table 2-2*). These were subsequently used for GeoMx digital spatial profiling of differential gene expression and immunohistochemistry, described later in this chapter.

Table 2-2 Clinicopathological characteristics of the TNBC Cohort.

Clinicopathological Characteristics	Patients n (%)
Number of patients	
Entire cohort	207 (100)
Included for analysis	157 (75.8)
Median Follow up	73 months
Age (n=157)	
≤50	37 (23.6)
>50	120 (76.4)
Tumour Size (n=154)	
<20mm	66 (42.9)
20-49mm	79 (51.3)
>50mm	9 (5.8)
Invasive Grade (n=154)	
I	1(0.6)
II	8(5.2)
III	145(94.2)
Nodal Status (n=154)	
Negative	122(65)
Positive	32(35)
Received adjuvant (n=157)	
Chemotherapy	102(65)
Radiotherapy	55(35)
Identified via (n=157)	
Screening	38(24.2)
Symptomatic	117(74.5)
At surgery	2(1.3)
Re-excision required after primary surgery (n=157)	
No	146(93)
Yes	11(7)

2.2 Haematoxylin and Eosin Staining

Full section slides from the TNBC cohort (described above), and the entire TMA microarray available from the TNBC and Glasgow Breast Cancer cohorts were

stained using Haematoxylin and eosin standard protocol prior to further immunohistochemistry staining. Once stained, the slides were scanned using the Hamamatsu NanoZoomer (Welwyn Garden City, UK) into the NanoZoomer Digital Pathology (NDP) Server (NDP serve 3.3.47, Hamamatsu Photonics K.K., 2020) digital slide viewer by the GTRF.

2.3 Pan-cytokeratin Anti-human Antibody Staining

Full section slides from the TNBC cohort were stained by Colin Nixon (Histopathology, Beatson Institute for Cancer Research). An anti-human pan-cytokeratin (CK) antibody (M3515, Agilent) was stained on an Agilent AutostainerLink48. Sections for investigation were loaded into an Agilent pre-treatment module to be dewaxed and undergo heat induced epitope retrieval (HIER,UltraVision Quanto) with high pH target retrieval solution (TRS) (K8004, Agilent). Sections were heated to 97^{0}C for 20 minutes in high TRS. After HIER all sections were rinsed in flex wash buffer (K8007, Agilent) prior to being loaded onto the autostainer. The sections underwent peroxidase blocking (S2024, Agilent) for 5 minutes and washed with flex buffer. CK antibody was diluted in antibody diluent (S2022, Agilent) and applied at a 1/350 dilution for 35 minutes. The sections were washed with flex wash buffer before application of mouse secondary antibody (K4001, Agilent) for 30 minutes. Sections were rinsed with flex wash buffer. All sections had Liquid DAB (K3468, Agilent) for 10 minutes. The sections were then washed in water and counterstained with haematoxylin z (RBA-4201-00A, CellPath) then rinsed in tap water, dehydrated through graded ethanol's and placed in xylene. The stained sections were coverslipped in xylene using DPX mountant (SEA-1300-00A, CellPath). Once stained, the sections were scanned onto NDPServe as described above by the Glasgow Tissue Research Facility (GTRF).

2.4 Tumour Budding Scoring

Tumour budding scoring was performed by Fadia Gujam in the Glasgow Breast Cancer Cohort. In the TNBC cohort, tumour bud scoring was performed by FS. During optimisation, it was noted that tumour buds were difficult to visualise on exclusively H&E-stained slides, and pancytokeratin staining was performed according to routine protocol described above. Once stained, the buds were counted as previously described(10), whereby 5 areas of interest of 0.385μm were identified on the tumour margin. The total number of tumour buds,

defined as a group of up to 5 tumour cells, was recorded for each of the 5 areas of interest. The highest of the counts for these 5 areas of interest was used for analysis. Patients in the Glasgow Breast Cancer Cohort were divided into low budding (≤28 buds) and high budding (>28 buds) after a threshold for high and low budding scores was set using log rank statistics performed in R Studio (RStudio, Boston, MA, USA) using survminer, survival, tidyverse and maxtstat packages. In the TNBC cohort, a threshold of 20 was identified using log rank statistics performed in R Studio (RStudio, Boston, MA, USA) using survminer, survival, tidyverse and maxtstat packages.

Further analysis was then completed using SPSS 28 (IBM, New York, USA). Kaplan Meier log rank survival curves were used to examine association between tumour budding and recurrence-free survival (RFS) and cancer-specific survival (CSS) in the TNBC cohort. In the Glasgow Breast Cancer Cohort, population was then stratified according to ER-receptor status and/or clinical subtype (Luminal A, Luminal B, TNBC or HER2-enriched) during analysis. Cox-regression univariate and, when statistically significant ($p<0.05$), multivariate analyses was performed to establish the association between tumour budding and other clinicopathological characteristics, and Chi-squared test was used to establish the association between tumour budding and other prognostic indicators. A result was considered statistically significant when $p=<0.05$. SPSS was utilised for all statistical analysis (SPSS Version 28, IBM, New York, USA).

2.5 Assessment of Necrosis, Tumour Stroma Percentage and Klintrup Makinen

Assessment of Necrosis, Tumour stroma percentage and Klintrup Makinen scoring was performed on the Glasgow Breast Cancer Cohort by Fadia Gujam, using Slidepath software to visualise the slides. On a high-definition computer at 10x magnification factor, a representative area was selected based on the presence of tumour cells at all 4 corners of the visual field. TSP was graded as a percentage, with patients with a T:S ratio ≤50% being “low TSP”, and above 50% being “high TSP”. Klintrup Makinen was similarly assessed at 10x magnification, where the invasive tumour edge was assessed for peritumoural inflammatory infiltrate at the tumour edge, and scored as 0 (no infiltrate), 1 (patchy infiltrate), 2 (continuous layer of infiltrate), or 3 (“cup” of inflammatory infiltrate”). Necrosis scoring (limited to necrosis within the tumour only) was assessed at 10% magnification to look for areas of necrosis, following which a 20x

magnification was used to assess the proportion of the visual field occupied by necrosis: 0 indicating none/single necrotic cells, 1 indicating mild (<25%), 2 indicating moderate (>25%).

2.6 Transcriptomics

Whole-genome RNA-seq was performed, initially on a subset of patients from the Glasgow Breast Cancer cohort, and subsequently on the entire cohort. The initial subset of 50 patients, of which 25 were the highest budding, and 25 lowest budding counts, consisted of ER- patients, as described in E Morrow's thesis(2). This allowed the identification of differentially expressed genes which form the basis of this thesis. During the study period, the remaining Glasgow Breast Cancer cohort was analysed using the same technique, and subsequently stratified according to molecular subgroups. RNA sequencing performed using TempO-Seq was utilised for gene expression profiling and expression analysis (Biospyder Technologies, Carlsbad, CA, USA). The technique can be briefly described as follows: FFPE slides were examined for areas of interest, and these portions excised and added to 80µ BioSpyder 1 x FFPE TempO-Seq lysis buffer in wells of a PCR plate. The samples were then overlaid with mineral oil and deparaffinized by heating at 95°C for 5 minutes. The samples were then lysed in TempO-Seq protease mix, and then combined with annealing buffer and detector oligonucleotides (DO) and incubated overnight at 45°C. The unbound DOs (which would eventually pair with another DO to allow sequence analysis) were subsequently degraded, ligated into complete probe sequence, then amplified in a PCR step before purification. Finally, the combined probes were entered into an indexed multiplex library for sequencing to count the relative amount of each target DO pair, thus indicating the expression level of each gene. Statistical analysis was performed by Bioclavis (Bioclavis, Glasgow, UK), initially allowing the identification of the most highly differentially expressed genes, and subsequently to examine the gene expression across different molecular subtypes within the Glasgow Breast Cancer Cohort. Differential expression analysis results were transferred to the author (FS) in the form of heatmaps to identify any clustering of samples, and differential expression analysis was carried out using MA plots, as well as principal component analyses.

2.7 Antibody Validation – Specificity

Western Blotting was utilised to validate the antibody sensitivity for the antibodies utilised in this study. The results of WB for HIF-1α, CAIX, Bcl-2 and CD3 are described by S Shamis but were performed as below for JUNB, ODAM, RFX5 and TBX22(160).

Precast gradient protein gels (4-20% Mini-PROTEAN TGX) were utilised and assembled within the gel tanks. Running buffer (Bio Rad #1610732) was utilised to fill the tanks. Ladder (Precision Plus Protein Dual Xtra Standards, Anti-ladder Precision Protein StrepTactin – HRP Conjugate 5000, BioRad) was loaded into the first lane, after which an empty lane was left, and then following lanes reserved for the cell lysates. Cell lysates (as described in each chapter) were loaded into the lanes and run for 90 minutes at 120V.

Subsequently, the gels were removed, applied to transfer membrane (polyvinylidene fluoride membrane, Amesham Pharmacia Biotech, Buckinghamshire, UK) as part of a "sandwich" cassette composed of sponges and filter paper and soaked in transfer buffer (Bio Rad#1610734), after compression rolling to remove air bubbles. The assembly order for the cassette is described in below, (*Figure 2-1*).

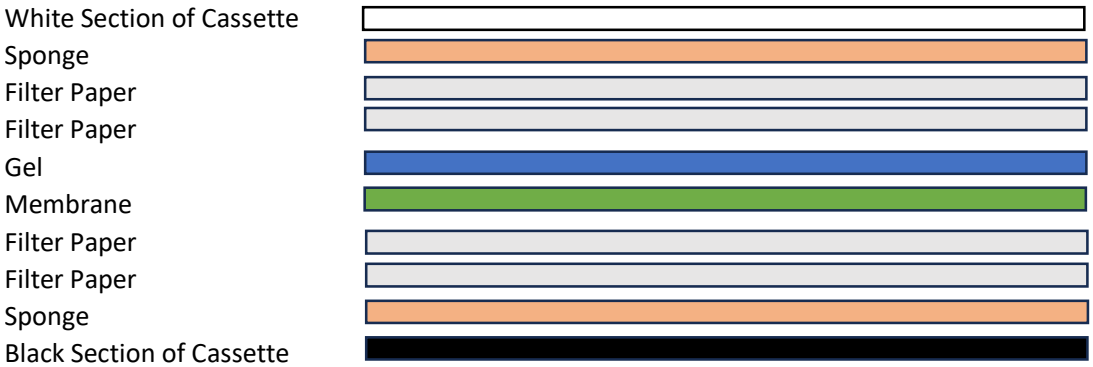

Figure 2-1 Western Blot Transfer Casette. Diagrammatic representation of the order of application of elements within the transfer cassette.

Once assembled, the cassette was inserted into the tank, immersed in transfer buffer and current run at 300mA for 90 minutes. Once transfer was completed, the membrane was extracted from the disassembled cassette, blocked with a blocking buffer as described below (*Table 2-3*) for 1 hour on a platform shaker, and incubated in primary antibody overnight. Once incubated, the membranes were washed three times with TBST for 10minutes, and secondary antibody (either mouse, or rabbit, according to the antibody, as described below) and anti-ladder at 1:50000 for 90 minutes at room temperature, before three further

washes for 10minutes with TBST. Finally, membranes were incubated in HRP substrate enhanced chemiluminescence reagent for 5 minutes, before blotting with ECL (Pierce ECL Western) Blotting substrate (ThermoScientific 32106) and imaging was performed using Sungene Gene Sys. For each antibody, this process was repeated 3 times to ensure reproducibility. Results from the most visually clear WB was included within the results section of each protein chapter.

Table 2-3 Antibodies Used for Western Blot and Optimal Conditions for Use

Primary Antibody	Cat. Number	Manufacturer	Origin	Blocking solution	Secondary antibody	Secondary antibody	Clone	Incubating conditions
JUNB 1:4000	Ab245500	Abcam	Rabbit	1:5000 0.3% BSA, 90min	1:5000 0.3% BSA, 90min	(IgG HRP linked antibody – Cell signalling)	Polyclonal	overnight in cold room 4^0
ODAM 1:4000	16509-1-AP	ProteinTech	Rabbit	3% BSA in TBST, 60 min	1:5000 0.3% BSA, 90min	(IgG HRP linked antibody – Cell signalling)	Polyclonal	overnight in cold room 4^0
RFX5 1:7500	Ab239038	Abcam	Rabbit	3% BSA in TBST, 60 min	1:5000 0.3% BSA, 90min	(IgG HRP linked antibody – Cell signalling)	Polyclonal	1 hour at room temperature
TBX22 1:10000	Ab140345	AbCam	Mouse	3% BSA in TBST, 60 min	1:10000 0.3% BSA, 90min		Monoclonal	overnight in cold room 4^0

2.8 Immunohistochemistry

Immunohistochemistry (IHC) was used to examine protein expression for genes identified to be differentially expressed when analysed via TempO-Seq. The Glasgow Breast Cancer cohort (both full section slides and TMA microarrays) were stained for JUNB, ODAM, RFX5 and TBX22 by FS apart from TMAs for TBX22 by JQ and AW.

The TNBC cohort was stained for CAIX, HIF-1α, Bcl2 and CD3 by Jean Quinn and Suad Shamis. Antibody optimisation was performed using surplus breast tissue (full section and TMAs).

TMA sections were acquired from the NHS GTRF and were stored at 4ºC until use. The slides were baked at 55ºC for 1 hour prior to use to minimise the loss of cores. The RFX5 and TBX22 TMA microarrays, which were stained after the advent of the Coronavirus-19 pandemic, were stored in wax to preserve the integrity of the tissue whilst restrictions in accessing the laboratory were in place. These slides required additional de-waxing for 2 hours at 55ºC to soften the wax, and subsequently dipped in Xylene for 20 minutes, following which the slides were then dipped in Histoclear (National Diagnostics HS-200) and rehydration steps were taken as described below, for all slides. A negative control slide was included in each set of staining slides, and negative isotype controls on the TMAs were included in the microarray.

2.8.1 Dewaxing and Rehydration

Sections were dewaxed in Histoclear (2 x 5 minutes) and rehydrated in graded alcohols; 100% ethanol (5 minutes), 90% ethanol (5 minutes), 70% ethanol (5 minutes) and then rinsed in running water for 5 minutes.

2.8.2 Antigen Retrieval

Antigen retrieval was performed using Citrate buffer pH6, HIER (Heat-induced epitope retrieval) buffer, or TRIS-EDTA buffer pH9 depending on the antibody utilised. The required buffer and antibody incubation process is summarised below, (*Table 2-4*).

Table 2-4 Antibodies Used for Immunohistochemistry and Optimal Conditions for Use

Antibody	Manufacturer	Dilution	Origin	Blocking solution	Clone	Antigen-retrieval Buffer	Incubating conditions	Expected staining location
JUNB	Abcam (Ab245500)	1:400	Rabbit	10% Casein 60 min	Polyclonal	Citrate Buffer (pH6)	overnight in cold room 4^0	Unknown
ODAM	ProteinTech (16509-1-AP)	1:400	Rabbit	10% Casein 60 min	Polyclonal	Tris-EDTA buffer (pH9)	overnight in cold room 4^0	Unknown
RFX5	Abcam (Ab239038)	1:750	Rabbit	10% Casein 60 min	Polyclonal	Tris-EDTA buffer (pH9)	1 hour at room temperature	Unknown
TBX22	AbCam (Ab140345)	1:1000	Mouse	10% Casein 60 min	Monoclonal	Tris-EDTA buffer (pH9)	overnight in cold room 4^0	Unknown
HIF1-A	Novus Biologicals (NB 100-122)	1:150	Mouse	1.5% horse serum 60 min	Monoclonal	Tris-EDTA buffer (pH9)	Overnight in cold room 4^0	Cytoplasmic & Nuclear
Bcl-2	Agilent (#M0887)	1:150	Mouse	3% BSA in TBST 60 min	Monoclonal	Tris-EDTA buffer (pH9)	Overnight in cold room 4^0	Cytoplasmic
CAIX	Bioscience (Slovakia M75 antibody (clone 75 antibody)	1:500	Mouse	10% casein 60 min	Monoclonal	Citrate Buffer (pH6)	Overnight in cold room 4^0	Cytoplasmic & Membrane
CD3	Leica (#565-L-CE)	1:100	Mouse	200µl UVQ protein, 5 min	Monoclonal	HIER Buffer	Overnight in cold room 4^0	Cytoplasmic

Antigen retrieval in either citrate (pH6) or Tris-EDTA (pH9) was performed under pressure and the slides allowed to cool in the buffer before being rinsed in water.

2.8.3 Blocking Endogenous Peroxidase Activity

The slides were bathed in 3% H_2O_2 for 20minutes, before rinsing in running water.

2.8.4 Blocking Non-specific Antigen Binding

The slide specimen was circled with Dako Pen (S2002, Dako, Agilent Technologies, UK) and were incubated with a 10% casein blocking solution (diluted in Dako antibody diluent, S0809 Dako, Agilent Technologies, UK) for 1 hour at room temperature.

2.8.5 Primary Antibody Incubation

Antibodies JUNB, ODAM, RFX5 and TBX22 were diluted as described (*Table 2-4*) in antibody diluent (Dako, Agilent Technologies, UK). Prior to adding the antibodies, blocking solution was gently tapped off, and then once the antibody was added, the slides were incubated in a humidified tray for 1 hour at room temperature, or at 4^{o}C overnight, as indicated.

2.8.6 Secondary Antibody Incubation / Signal Detection

The slides were washed in TBS (2 x 10 minutes), incubated in ImmPRESS™ reagent (Vector Lab. Inc., USA, Vector #MP-7800), for 30 minutes at room temperature, then washed in TBS (2 x 5 minutes).

DAB ImPACT™ chromogen substate (Vector Lab Inc., USA, #SK-4105) was added to the slides and these were incubated for 5 minutes at room temperature, prior to rinsing for 10 minutes in running water.

2.8.7 Counter-staining, Dehydration, and Mounting

Slides were stained in Harris haematoxylin (Gill lll Leica#3801540) for 30 sec, rinsed in running water for 2 minutes, then dipped in 1% acid alcohol (Leica #3803651E) for 20sec before rinsing in running water for a further 2 minutes. Finally, the slides were bathed in Scott's Tap Water Substitute (Leica#380290E) for 2 minutes, prior to rehydration in sequentially higher concentrations of ethanol (70%, 90%, 100%, 100%) for 30 seconds each time. The slides were finally dipped in Histoclear (20 seconds, then 2 minutes in a second bath) and mounted using Pertex mounting fluid (Histolab Products AB, Gothenburg, Sweden).

2.8.8 Weighted Histoscore of IHC Staining

Stained slides were digitally scanned using a Hamamatsu NanoZoomer Digital Slide Scanner (Hamamatsu Photonics K.K. Shizuoka, Japan) and scoring was performed by a single observer, FS unless indicated otherwise. The images were viewed using NDPServe 3 image viewer platform. For the Glasgow Breast Cancer Cohort, membrane, nuclear and cytoplasmic scoring was performed manually, intraclass correlation coefficient (ICCC) and were calculated, deeming an ICCC>0.7 as an indicator of score reliability. The individual score correlation was compared visually using Scatter plots and Bland Altman plots. At the time of scoring, the proportion of cells with no (0) staining, weak (1), moderate (2) or strong (3) staining was recorded, and calculated as follows:

Equation 2-1 Formula for Calculation of Weighted Histoscore (WHS)

$$\textbf{Weighted histoscore} = (0 \times \text{No staining}) + (1 \times \text{mild staining}) + (2 \times \text{moderate staining}) + (3 \times \text{heavy staining})$$

Where more than one core per specimen was available, scores were averaged. Due to the relative age of the specimens, single core/specimen samples were still included in the final analysis, with the single score utilised as the final score for each protein and cellular location (membrane/cytoplasm/nucleus). Due to these novel biomarkers being of uncertain location within the cell structure, all three of membrane, nucleus and cytoplasm were scored in turn, and the results are described in the results section of this thesis.

QuPath digital scoring (QuPath, Edinburgh, UK) was utilised to score the TNBC cohort for HIF-1α, CAIX, Bcl2 and CD3. This was performed by a single observer, Suad Shamis. This technique relies on computerised artificial intelligence whereby TMAs were assessed according to a standardised cell detection method and according to manual annotations for AI memorisation, prior to setting three intensity thresholds for weak/mod/strong staining. 10% of the cores were scored manually to ensure reliability by a second observer, Sara Albadran. Briefly, QuPath scoring is performed as follows: The TMA de-arrayer function allows the creation of a TMA grid which is then checked for correct core positioning, following which stain vectors are estimated using a visual stain editor to optimise stain quality. Following cell detection, annotations were made to allow learning software to identify tumour cells (versus stroma, necrosis, immune cells etc.), before intensity thresholds for weak/mod/strong staining were selected using examples within the specimen. These thresholds were applied to create a

re-validated threshold classifier, which could then be applied to all the slides. Similarly to manual scores, three cores from each specimen were scored, with an average score being used as the final WHS, unless only one core was available, in which case this score was utilized. For JUNB, ODAM, RFX5 and TBX22 at the time of analysis using Qupath, it was not possible to gain reproducible results for expression. The scoring with QuPath for the TNBC cohort occurred later, after successful troubleshooting with the help of advisors from the software prociders/programmers.

2.9 Statistical analysis of weighted histoscore analysis of IHC studies

Each protein underwent log rank statistical test to determine a threshold for high and low expression. This test was performed using R Studio (RStudio, MA, USA) using survminer, survival, tidyverse and maxstat packages. The results of these threshold analyses are described in the results section of this thesis. The histoscore results for each patient were subsequently coded into high or low protein expression and used to assess correlation with survival and other clinicopathological characteristics.

Kaplan Meier log rank survival curves were utilised to assess the correlation between protein expression and CSS and stratified according to patient subgroups: ER-status and molecular subgroup. Subsequently, Cox regression analysis was used to derive hazard ratio and perform multivariate analyses whenever log rank $p<0.05$. A result was considered statistically significant when $p<0.05$.

2.10 GeoMx

This study utilised the GeoMx digital spatial profiler (DSP) to explore the role of potential biomarkers in the TNBC cohort. This technology allowed the spatial analysis of RNA transcription within the TNBC samples, providing further information on expression within different portions of the tumour micro-environment.

As described earlier in the chapter, 50 TNBC archival TMA sections (25 highest budding phenotype, 25 lowest budding phenotype) from specimens resected from patients in Glasgow were positioned on glass slides, dewaxed, and prepared by target retrieval, digestion with proteinase K, post-fixed, and subsequently incubated with GeoMx RNA detection probes. The latter process required an overnight incubation and was followed by washes with in-situ hybridization

probes for RNA using an ultraviolet photocleavable linker. Slides were then stained with fluorescently labelled antibodies to allow spatial analysis to be performed, the slides were stained with fluorescent labelled antibodies to pan-cytokeratin (PanCK), considered to be a tumour-cell marker, and CD45, considered a leukocyte marker and allowing regions of interest to be limited to tumour tissue (the former), or stroma (the latter). Once successful 3-plex immunofluorescence staining was possible, TMA cores were manually selected, and circular region of interest (ROIs) selected, according to the presence of fluorescently labelled anti-PanCK.

Once ROIs were selected, the GeoMX platform was utilised to locally collect information regarding each region. This was performed by the GeoMx platform cleaving barcodes within the ROI after automatically examining each region with controlled UV laser, following which these barcodes were then processed by plating onto an individual well on a mictrotitre plate, before further processing was possible, and allowing comparison of quantified RNA expression in between tumour-rich and stroma-rich portions of the ROIs. This portion of the analysis was possible thanks to the use of NanoString nCounter Instrument, which allowed GeoMx to count the unique indexing oligos assigned to each target gene.

To allow comparison of tumour-rich areas to stroma-rich areas, Linear Mixed Models (LMM) statistical testing was used and allowed difference in expression between high tumour budding and low tumour budding expressing tumours to be analysed. In total, 84 genes were assessed in the RNA panel, with differential gene expression assessed using the GeoMxTools R package tool (‘mixedModelDE’ in R package ‘lmerTest’). Differentially expressed genes with a log2 fold change $\geq$1 and p=<0.05 were considered statistically significant. Volcano plots were created using a plugin script (https://github.com/NanostringBiostats?DSPPlugins/tree/master/DSPPlugVolcanoPlot), and Heatmaps comparing low to high tumour budding groups were performed using R (Complexheatmap, RStudio, Boston, MA, USA).

To validate results of GeoMX DSP analyses, TMA specimens were processed and stained using IHC as described in previous sections, to allow protein-level validation of expression. IHC staining of HIF-1αCAIX, BLC2 and CD3 was used to evaluate each specimen for macrophage, lymphocyte, apoptosis, and hypoxia. A negative control slide was performed each time to check for non-specific staining.

Chapter 3 JUNB

3.1 Introduction

JUNB is a member of the JUN group of Activating-Protein-1 (AP-1) transcription factors, which have been shown to play a part in the Transforming Growth Factor Beta (TGFß)/SMAD pathway(161-163). The AP1 transcription factors are involved in the regulation of gene activity within the cell cycle, as well as in controlling the development and progression of cancer(164). Within the cell cycle, JUNB has been shown to promote cell migration, with in-vitro studies using embryonic fibroblast cells suggesting a role in activating cyclin A to positively regulate transition from S to G2/M stage(164). Although the AP-1 family components can be found in homodimeric (Jun/Jun) or heterodimeric (Jun/Fos) forms, current evidence suggests that the heterodimeric form of Jun, Jun/Fos (Fos is another member of the AP-1 family), may be the true functional state of these transcription factors *in-vivo(164-166)*. JUNB has also been demonstrated to play an important role in Th cell programming and differentiation, lymphovascular proliferation, inhibits apoptosis, and EMT (164, 167-169). JUNB has been shown to have a role in angiogenesis, particularly through effects on cell morphology, motility and leading to neovascularisation and branching(164, 170). Evidence suggests that hypoxia can induce JUNB, with a bi-directional effect on VEGF, which also in turn promotes JUNB phosphorylation and translation(171, 172). Overall, JUNB roles in endothelial cells by influencing angiogenesis, neurovascular alignment, branching and formation of filopodia, as well as specifically in retinal vascular development(164, 170, 173-177).

3.1.1 JUNB and Cancer

Current evidence suggests that the role of JUNB may have dual effects, both as a promoter of invasion and migration(178), as well as a suppressor of metastasis(167). JUNB has been demonstrated to promote progression through the cell cycle via cyclin E1 and repression of TGFß2 genes, resulting in a pro-invasive phenotype(179). Subsequently, JUNB has been shown to reduce activity of TGFß2 expression, although in cases of over-expression, JUNB may promote the effects of TGFß2 on cell proliferation and pro-EMT behaviour, such as that seen during advanced cancers, during which environmental TGFß2 levels are higher than usual(179). JUNB is therefore proposed to promote invasion, with recent mouse model studies suggest that JUNB-knock-down and knock-out mice with metastatic head and neck squamous cell carcinoma saw reduced cell invasion and migration, with significantly reduced lung metastasis and prolonged

survival(180). In *in vitro* studies of gall-bladder cancer and prostate cancer, high JUNB levels appeared to predict poorer survival, promoted by the upregulatory role of PDK-1 through its action on EMT, when PDK-1 is over-expressed, (often co-expressed with JUNB) in IHC studies(181, 182).

3.1.2 The Study cohorts

The following chapter describes how JUNB was identified as one of the most differentially expressed genes on TempO-Seq analysis of the Glasgow Breast Cancer Cohort surplus biorepository tissue, and how this compares to JUNB in the same cohort using immunohistochemistry. Prior to commencing the immunohistochemistry for the Glasgow Breast Cancer Cohort, the staining protocol was optimized, and specificity analysis was performed. The process for the results therefore can be represented below, (Figure 3-1).

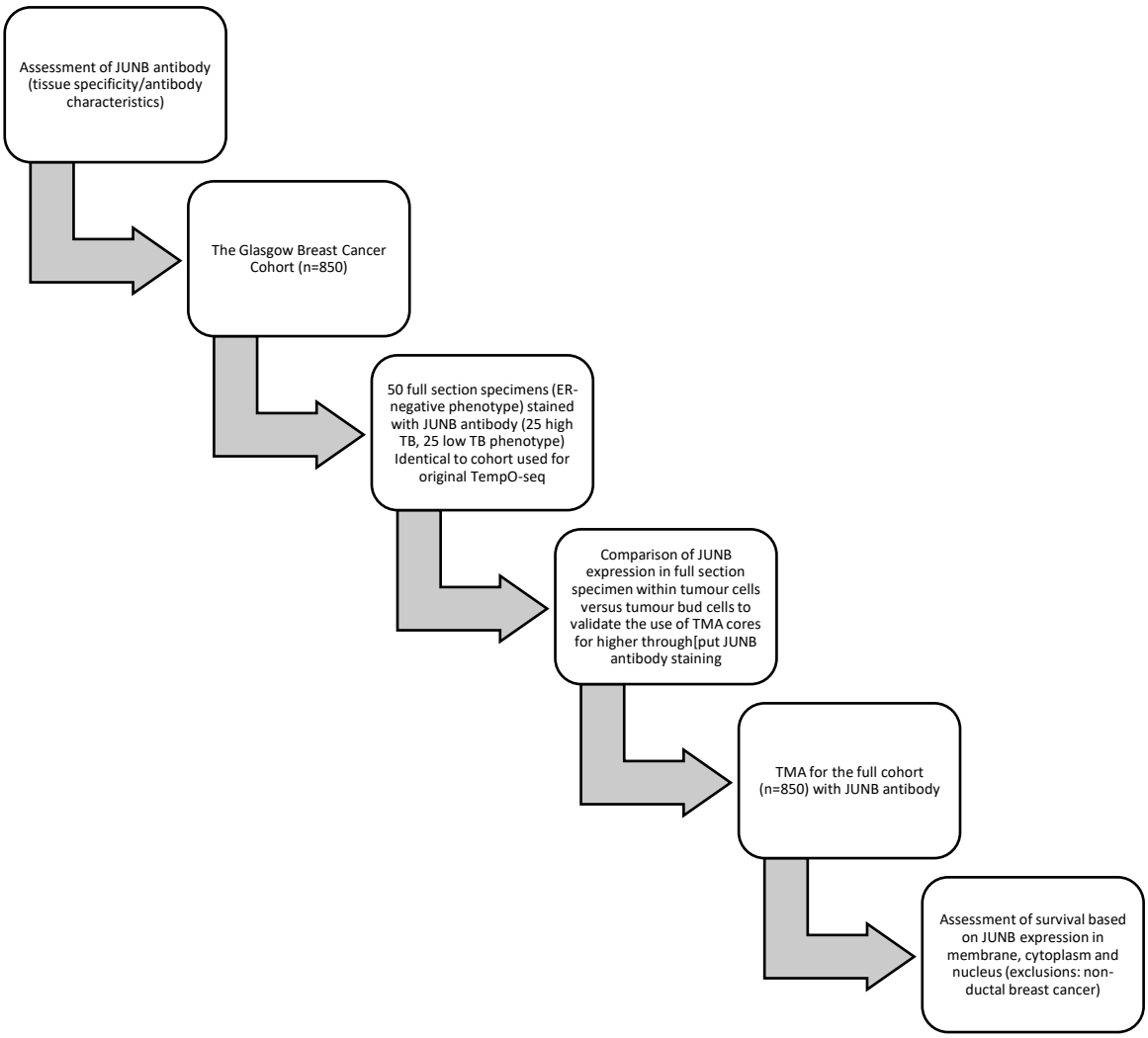

Figure 3-1 Study process flowchart for JUNB protein expression analysis.

The 50 full section ER-negative specimens used for TempoSEQ, selected by virtue of being either of highest tumour budding (n=25) or lowest tumour budding

(n=25) phenotype were stained, scored, and analysed for JUNB. JUNB expression within the tumour compared to that within the peritumoural buds was compared. TMAs that contained 3 tumour cores for each patient from the Glasgow Breast Cancer Cohort were stained, scored, and analysed. Weighted histoscores for this JUNB expression in the cellular, membrane and nuclear portions of breast tumour cells were manually assessed and analysed in relation to clinicopathological characteristics, including tumour budding, and cancer-specific survival. It was hypothesised that JUNB expression would correlate with worse prognosis, although in patients with poorer prognostic indicators (higher disease stage, higher tumour budding status) this effect may be more pronounced.

3.2 Results

3.2.1 JUNB Expression Within Cell Lineages

An exploratory search was performed using DEPMAP, a freely accessible cancer dependency map online database which compiles the information from genomic data and large-scale cancer cell line datasets. A search was performed for differential JUNB protein expression (versus knockdown), and a list of cancer cell lines with different levels of JUNB expression compiled. Breast had a high transcript per million (TPM) compared to lineages originating from other organs, such as skin, bone and eye, (*Figure 3-2*).

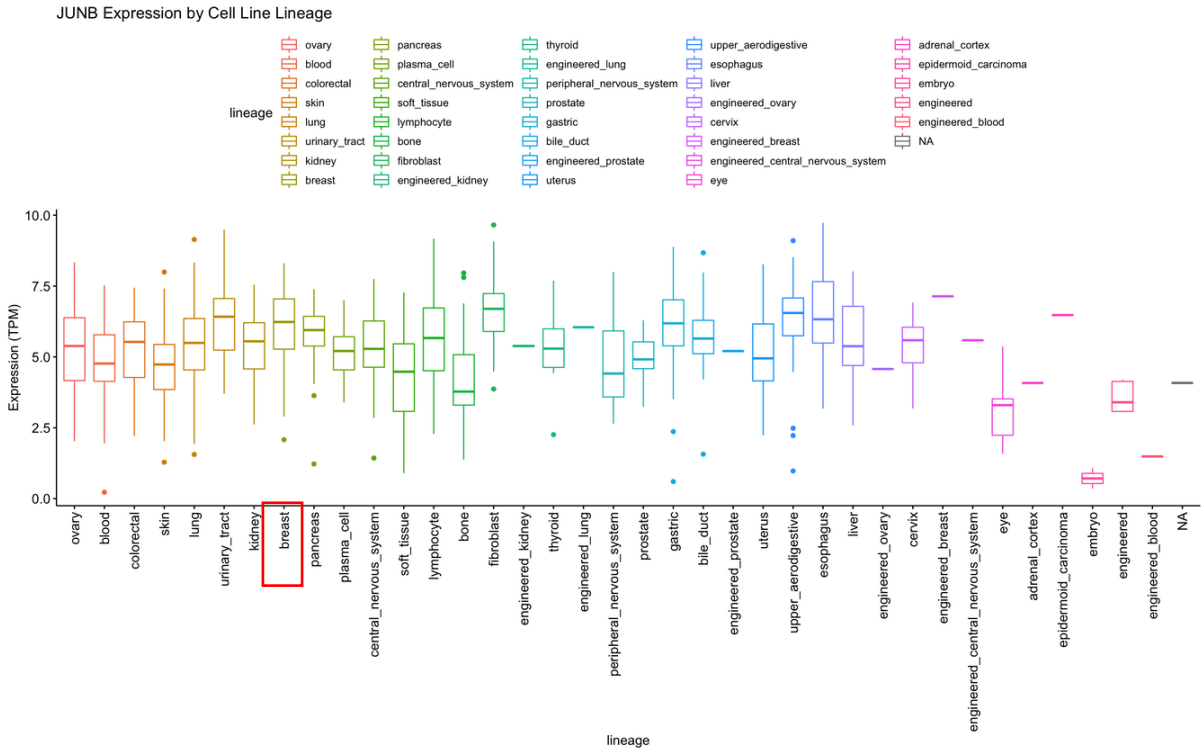

Figure 3-2 DEPMAP JUNB expression by cell lineage. (Transcripts per million, TPM: for every 1,000,000 RNA molecules in the RNA-seq sample, x came from this gene/transcript.)

When exclusively examining breast cancer cell lines known to express JUNB, most cell lines for which JUNB expression levels have been recorded appear high, (*Figure 3-3*). Within our laboratory, the cell lines MDAMB453, MCF7 and MDAMB231 were available, all of which had high expression of JUNB. This is confirmed later in the chapter using Western Blotting. However, colorectal and prostate cancer cell lines were also available for further analysis that expressed higher levels of JUNB expression, (*Figure 3-4*,*Figure 3-5*).

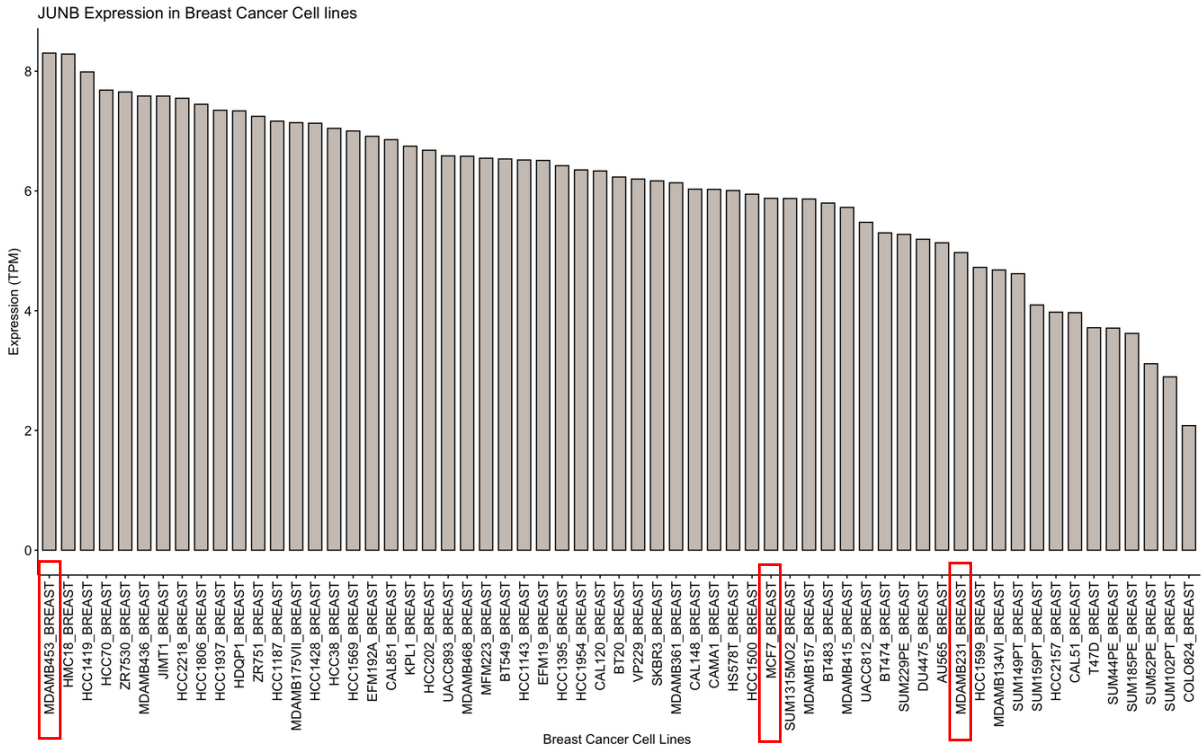

Figure 3-3 DEPMAP JUNB Expression in Breast Cancer Cell lines. (Transcripts per million, TPM: for every 1,000,000 RNA molecules in the RNA-seq sample, x came from this gene/transcript). The cell lines highlighted were utilised for specificity assays.

When DEPMAP was explored with regards to colorectal cancer cell lines, it appeared that all the available cell lines on the database had some evidence of JUNB RNA expression, (*Figure 3-4*). T84, HT29 and DLD1 colorectal cancer cell lines had relatively high levels of expression, confirmed later by Western

Blotting.

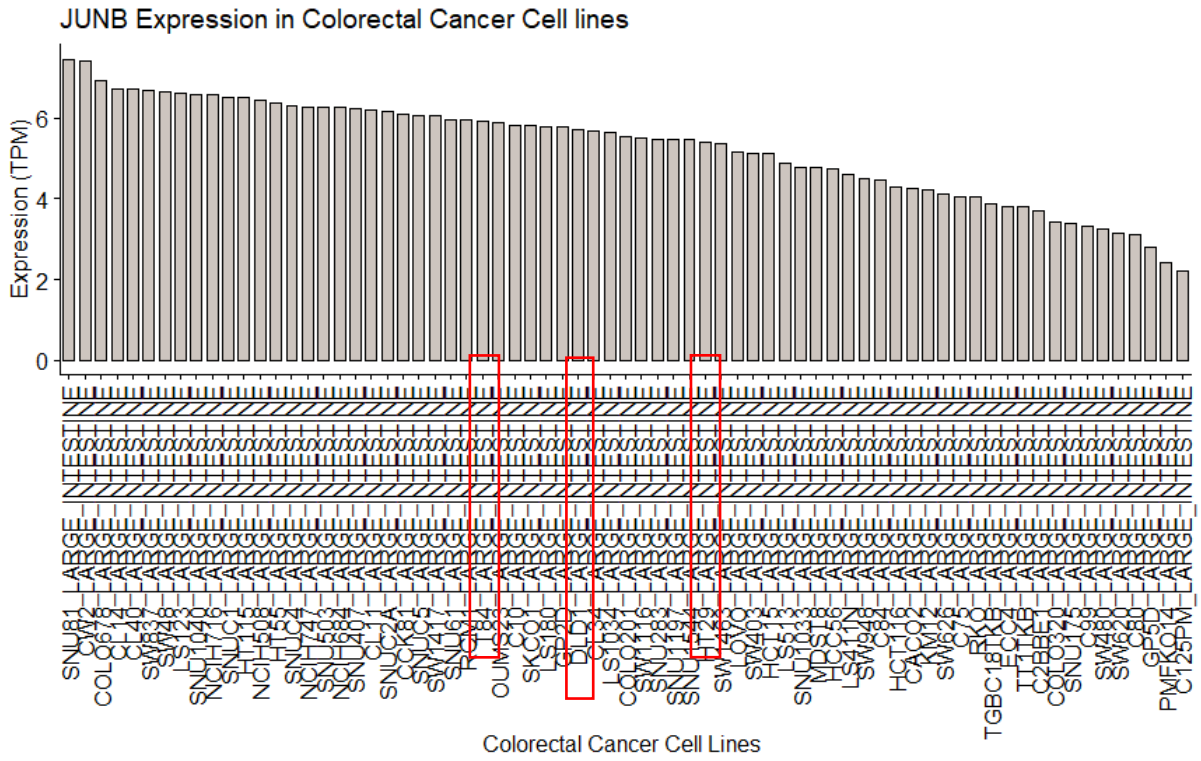

Figure 3-4 DEPMAP JUNB Expression in Colorectal Cancer Cell lines. (Transcripts per million, TPM: for every 1,000,000 RNA molecules in the RNA-seq sample, x came from this gene/transcript. The cell line highlighted were utilised for specificity assays.)

When DEPMAP was probed for prostate cancer cell lines expressing JUNB, fewer cell lines (11) had available data, (*Figure 3-5*). LNCaP cell line lysates were available within our laboratory, with relatively high expression levels, confirmed

later Western Blotting.

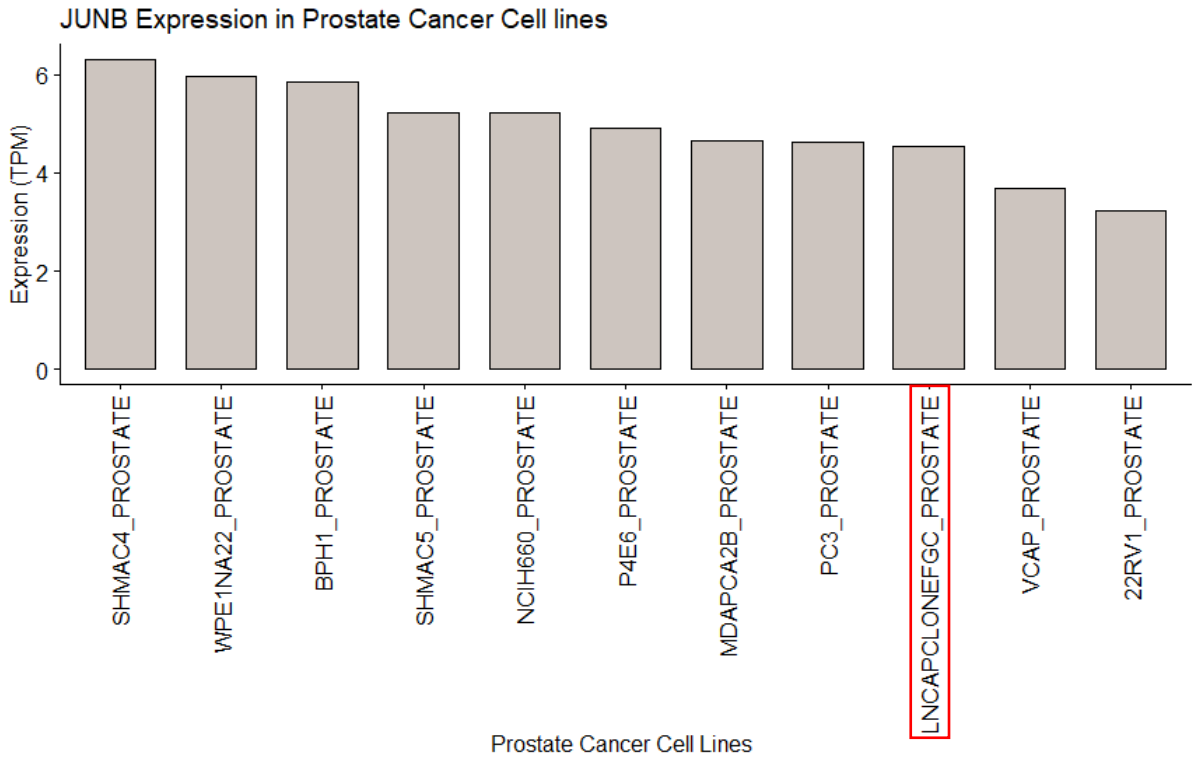

Figure 3-5 DEPMAP JUNB Expression in Prostate Cancer Cell lines. Transcripts per million, TPM: for every 1,000,000 RNA molecules in the RNA-seq sample, x came from this gene/transcript). The cell line highlighted was utilised for specificity assays.

3.2.2 JUNB Antibody Specificity

Examples of weak, moderate, and strong staining are shown in their respective sections within this chapter, together with a true positive and negative control tissue. Antibody specificity was validated using western blotting. A single band (reproduced in triplicate) was observed at 33kDa in breast MCF7 cell lysate, and ß-actin was seen at strong intensity at 45 kDa, (*Figure 3-6*).

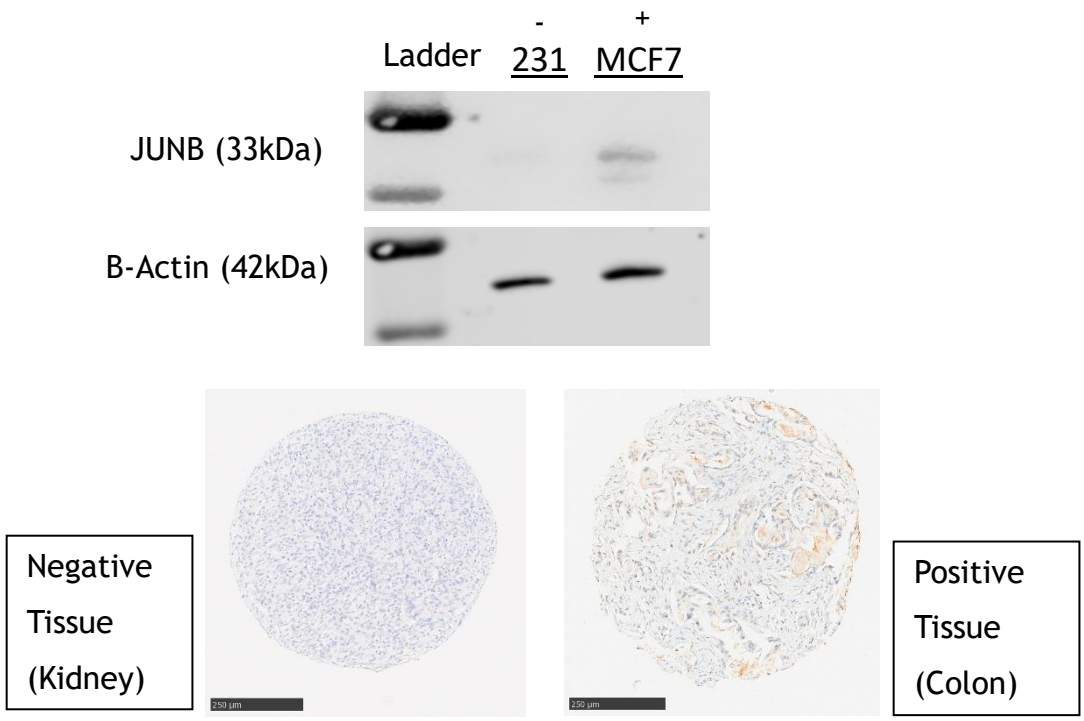

Figure 3-6 JUNB expression antibody specificity on Western Blotting. Examples of positive and negative tissue types used for analysis are included.

3.2.3 JUNB Expression in Full Section Specimens

JUNB expression was first assessed using full section surplus breast cancer tissue in a selected cohort of the Glasgow Breast Cancer Cohort. The sub-cohort of 50 patients had previously been used for TempO-Seq analysis and allowed identification of the most differentially expressed genes, of which one was JUNB. As described previously, 50 patient sections with ER-negative phenotype were selected, 25 with high tumour budding and 25 with low tumour budding characteristics. These were stained for JUNB protein expression. Manual weighted histoscores were produced for nuclear, cytoplasmic and membrane expression of JUNB by a single observer (FS). 45 specimens were included for analysis, as 5 patients had missing/damaged section slides. Cytoplasmic, nuclear and membrane expression of JUNB were manually scored for validation by Alan Whittingham using 10% of this sub-cohort. Scores were 0 for membrane, 0-30 for cytoplasm, and 0-240 for nucleus. Each cellular location will be discussed in turn in the subsections below.

3.2.4 Membrane JUNB Expression in Full Section Specimens

JUNB expression in membrane in the full section and then in the full Glasgow Cohort was 0, therefore this portion of cellular JUNB expression was not assessed further.

3.2.5 Cytoplasmic JUNB Expression in Full Section Specimens

After selecting the original 50 ER- patients with ductal cancer from the Glasgow Breast Cohort and stained using JUNB-specific antibody. Weighted histoscores were generated by manual evaluation by a single observer (FS). Examples of light, moderate and strong cytoplasmic staining, together with positive and negative control tissue are shown below, (*Figure 3-7*).

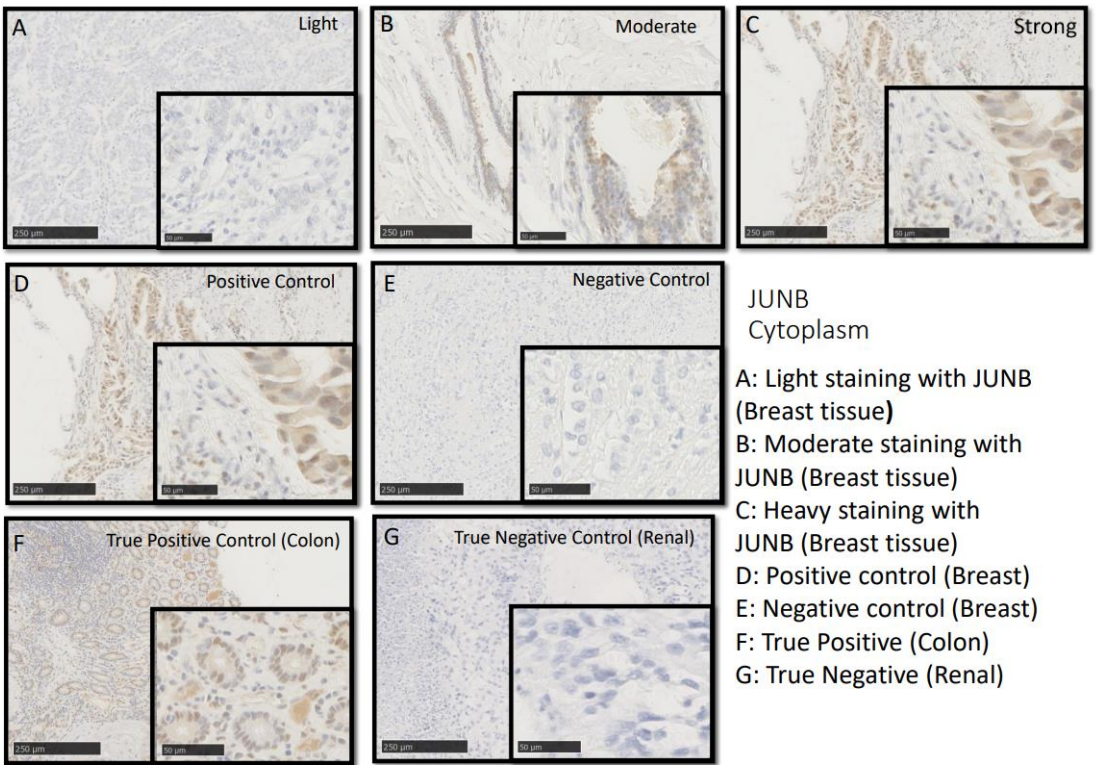

Figure 3-7 JUNB cytoplasm staining representative images.

Cytoplasmic expression of JUNB was manually scored by a single assessor (FS), and scores varied from 0-240, (*Figure 3-8*).

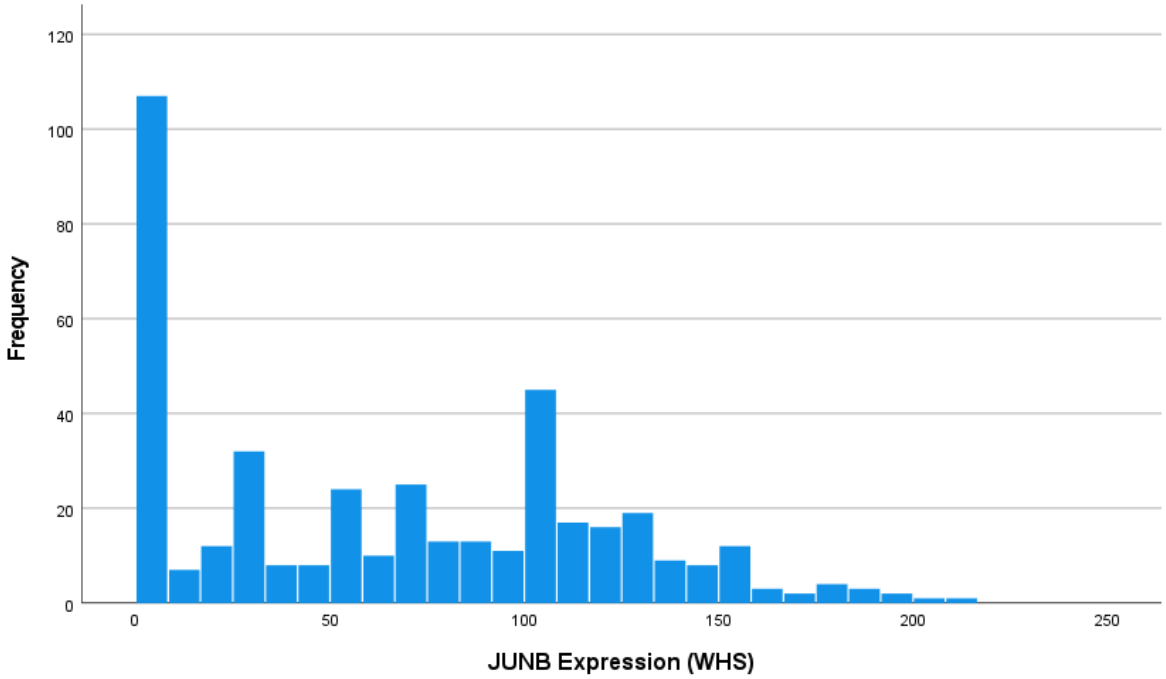

Figure 3-8 JUNB Cytoplasm expression in full section specimens. (WHS, weighted histoscores)

Manual assessment for validation by Alan Whittingham using 10% of this sub-cohort is described using the scatter plot below, (*Figure 3-9*). An intraclass correlation coefficient (ICCC) of 0.991 suggests a strong correlation between validation and primary assessors' scores.

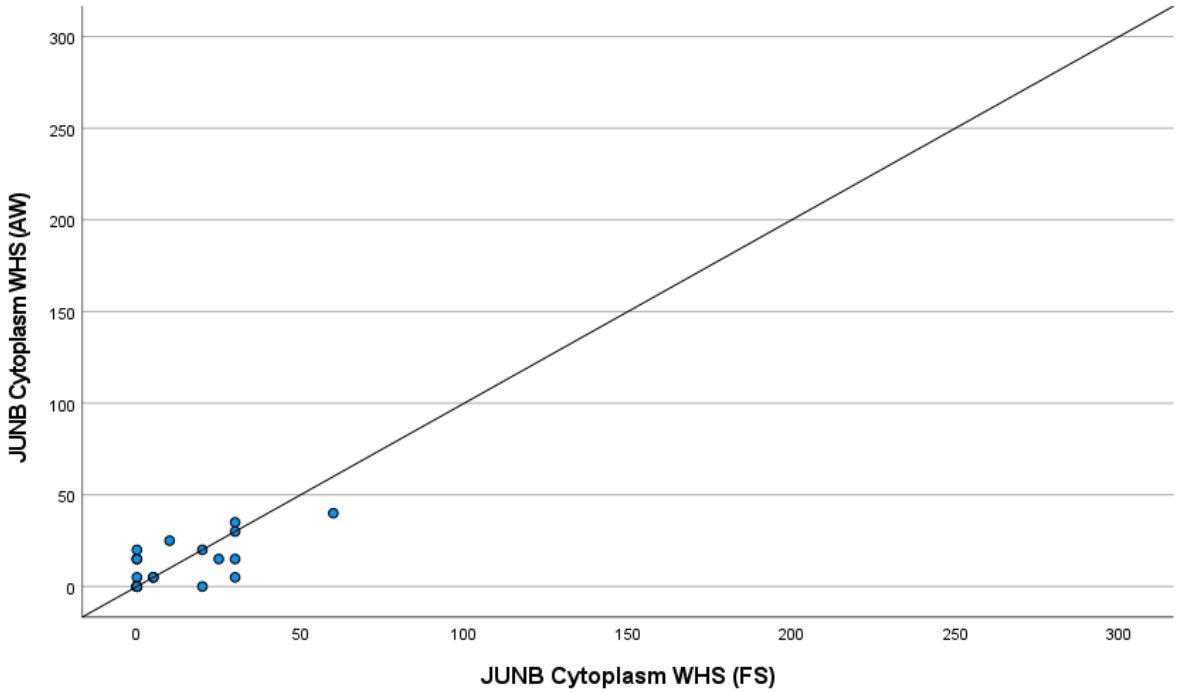

Figure 3-9 Correlation between FS and AW manual weighted histoscore (WHS) for cytoplasm JUNB staining. Scatter plot showing correlation between FS and AW for cytoplasmic JUNB scores. Intraclass correlation coefficient 0.991 for 10% specimens.

A subsequent comparison of averages and differences in scores was plotted as an Bland-Altman plot and demonstrated no bias between observers, (*Figure 3-10)*.

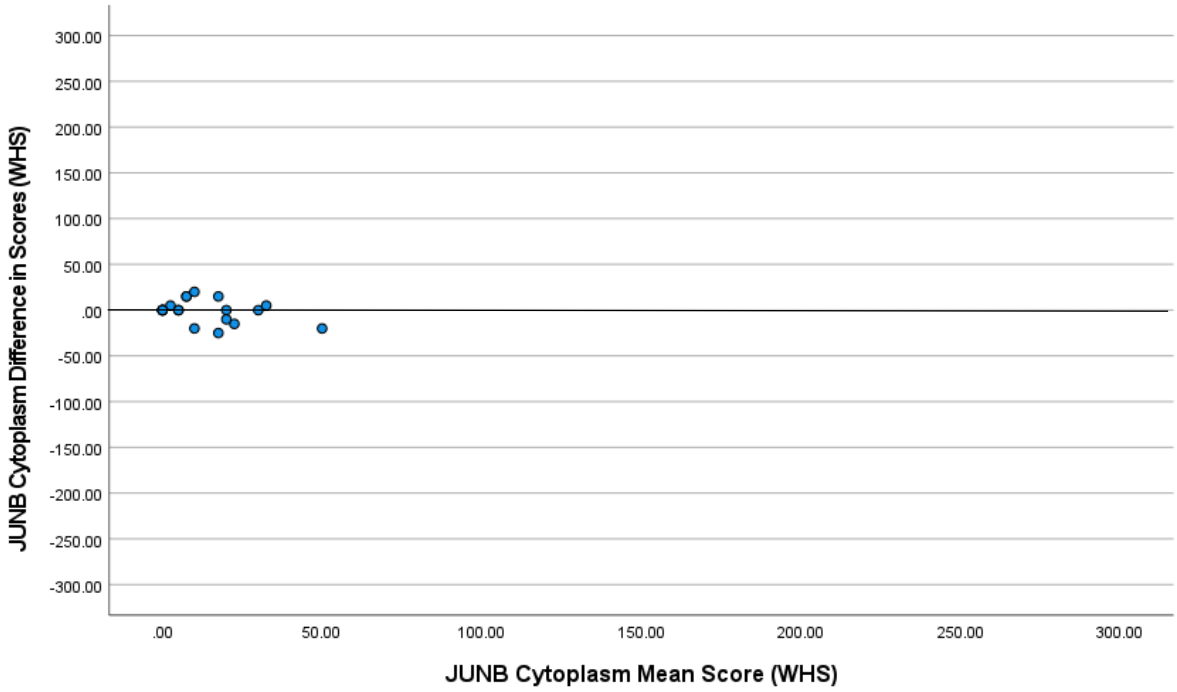

Figure 3-10 Bland Altman Plot comparing difference in scores to mean scores for JUNB expression in cytoplasm.

3.2.6 JUNB Cytoplasm Expression in Tumour Cells Versus Tumour Buds

JUNB cytoplasmic expression was compared between tumour buds (where present) and intratumoural cells. A scatter plot was used to visualise the correlation between cytoplasmic JUNB expression in intratumoral cells and tumour buds, (*Figure 3-11*). Only 45 full sections stained had tumour buds present, in these specimens the WHS of the buds were comparable to that of the

tumour core. The intraclass correlation coefficient (ICCC) was 0.997.

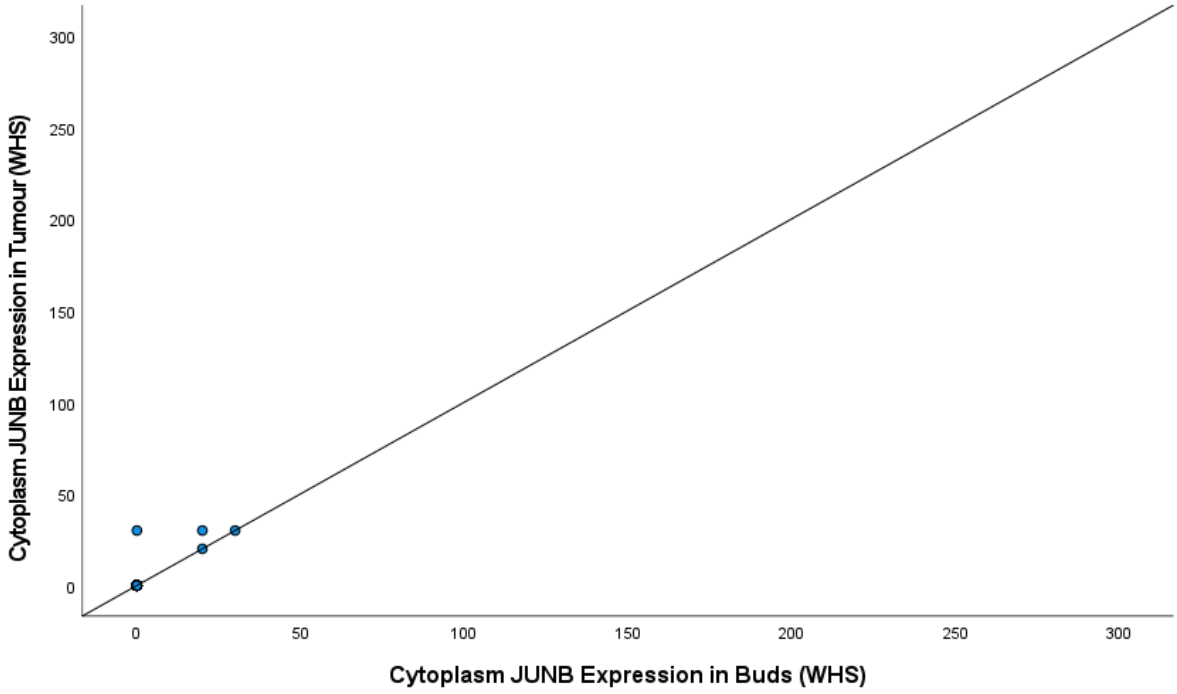

Figure 3-11 Cytoplasm JUNB expression in tumour versus tumour buds. ICCC 0.997.

A subsequent comparison of averages and differences in scores was plotted as a Bland-Altman plot and demonstrated no bias between observers, (*Figure 3-12*).

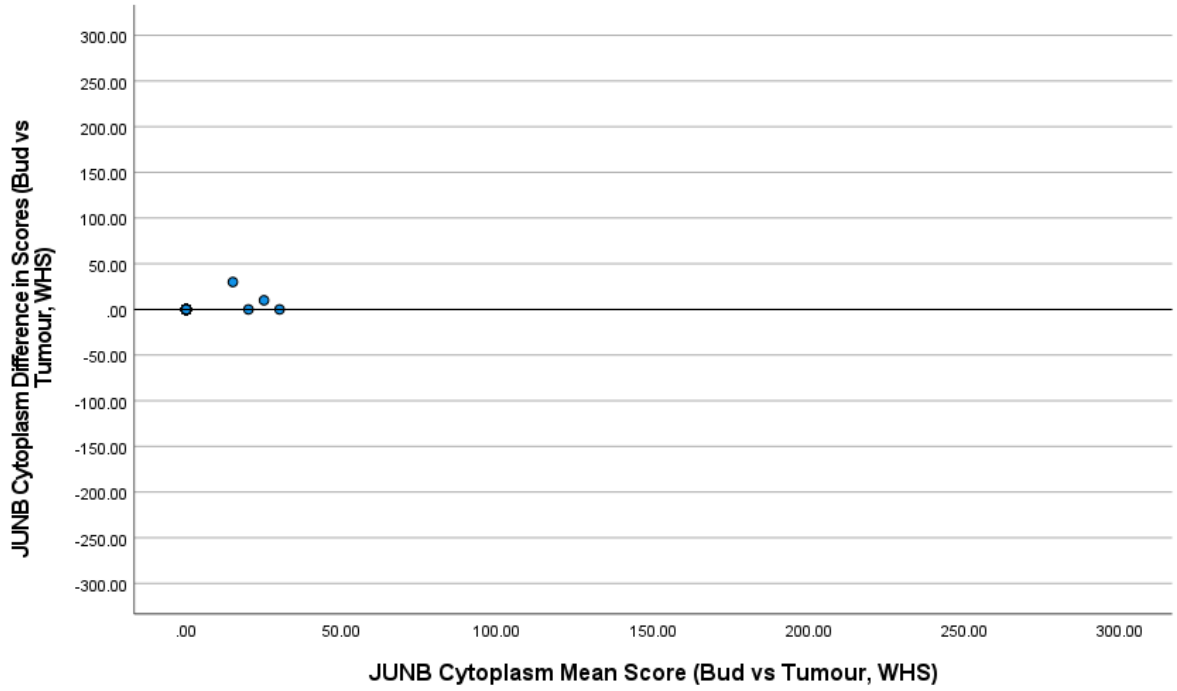

Figure 3-12 A Bland Altman Plot comparing the difference in scores to mean scores for JUNB expression in cytoplasm in Bud vs Tumour cells.

Based on these findings, it was possible to infer that further analysis of protein expression could be expanded to the full cohort of the Glasgow Breast Cancer

Cohort in the form of a tissue microarray and remain representative of expression both within the tumour buds as in within the intratumoural environment, (*Figure 3-13*).

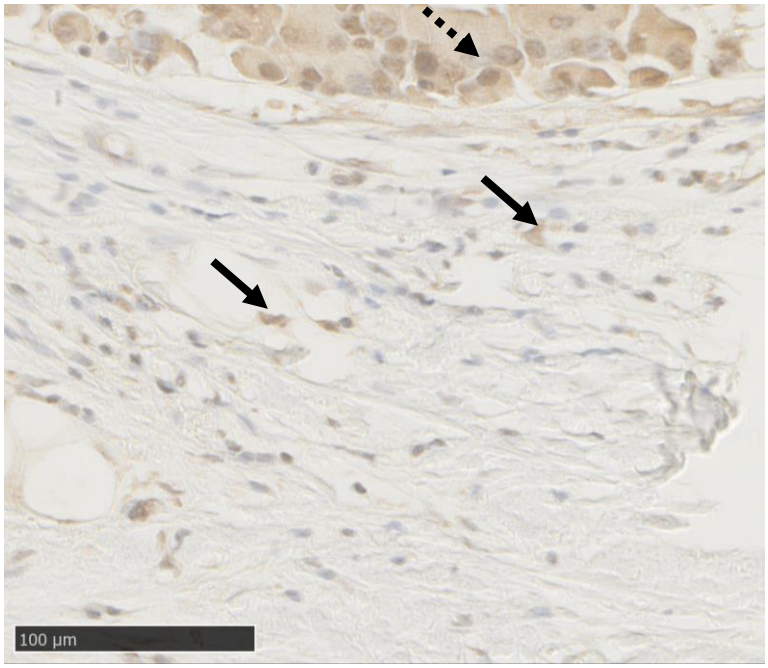

Figure 3-13 Cytoplasmic JUNB Staining in tumour mass (dotted arrow) correlated closely with staining in tumour buds (black arrow)

3.2.7 Nuclear JUNB Expression in Full Section Specimens

Using JUNB-specific antibody, weighted histoscores were generated by manual evaluation by a single observer (FS). Examples of light, moderate and strong nuclear staining, together with positive and negative control tissue are shown

below, (*Figure 3-14*)

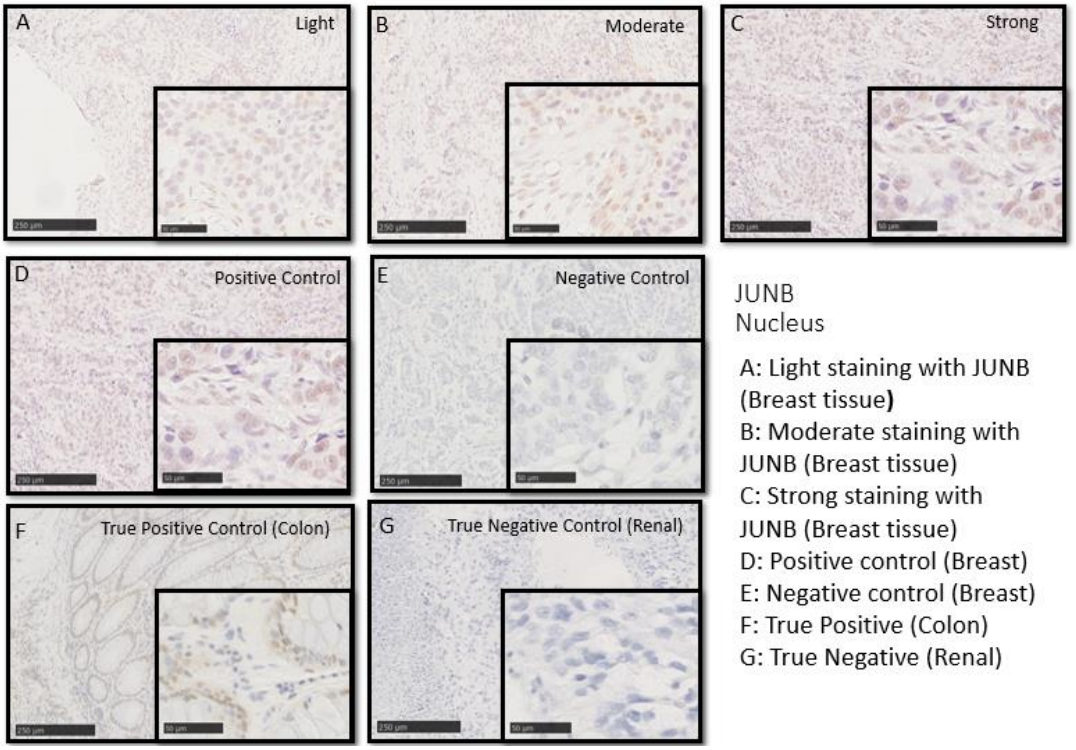

Figure 3-14 JUNB Nuclear staining representative images

Nuclear expression of JUNB was manually scored by a single assessor (FS), and scores varied from 0-240, (*Figure 3-15*).

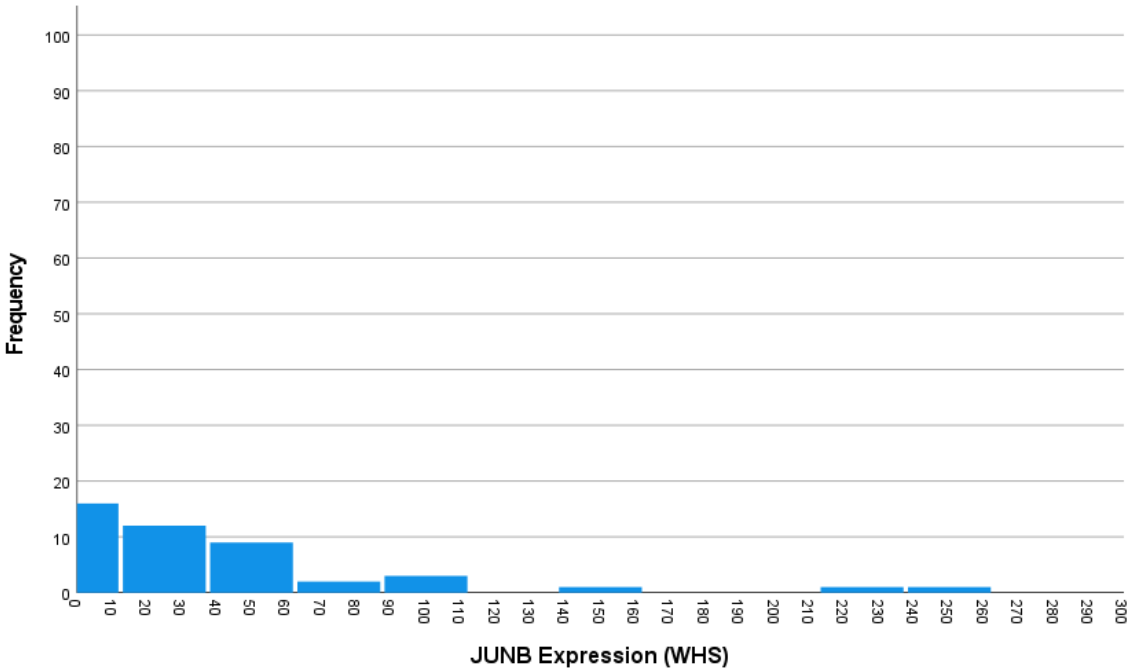

Figure 3-15 JUNB nuclear expression. (WHS, weighted histoscores)

Manual assessment for validation by Alan Whittingham using 10% of this sub-cohort is described using the scatter plot below, (*Figure 3-16*). An intraclass correlation coefficient (ICCC) of 0.992 suggests a strong correlation between

validation and primary assessors' scores.

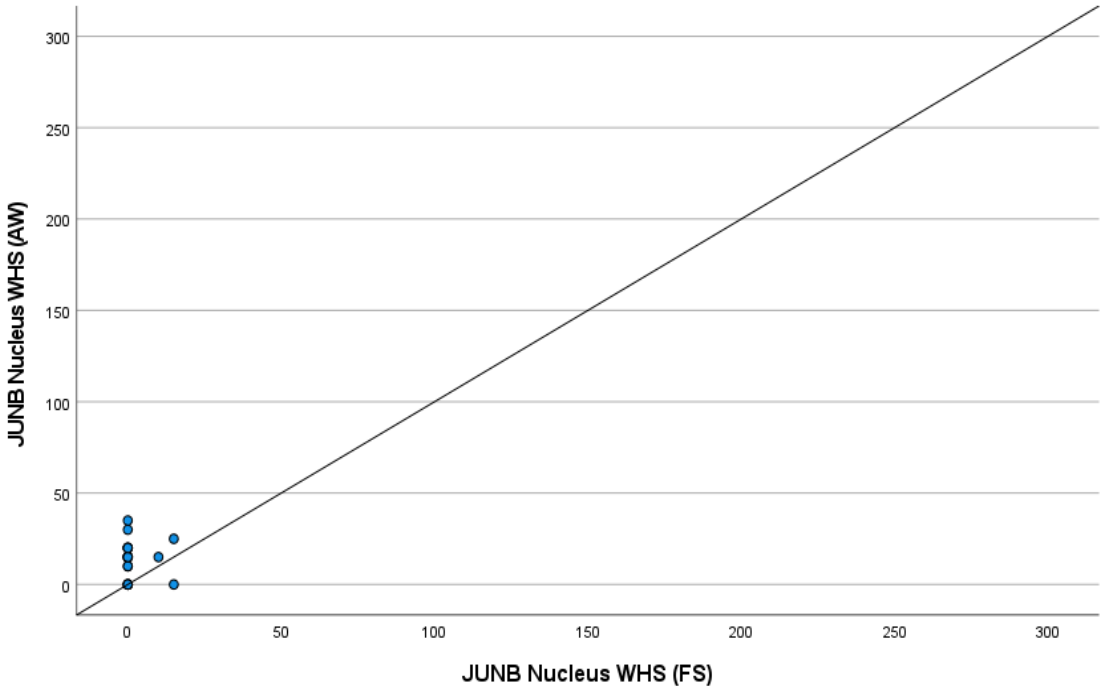

Figure 3-16 Correlation between FS and AW manual weighted histoscore (WHS) for nuclear JUNB staining. Scatter plot showing correlation between FS and AW for nuclear JUNB scores. Intraclass correlation coefficient 0.992 for 10% specimens.

A subsequent comparison of averages and differences in scores was plotted as an Bland-Altman plot and demonstrated no bias between observers, (*Figure 3-17*).

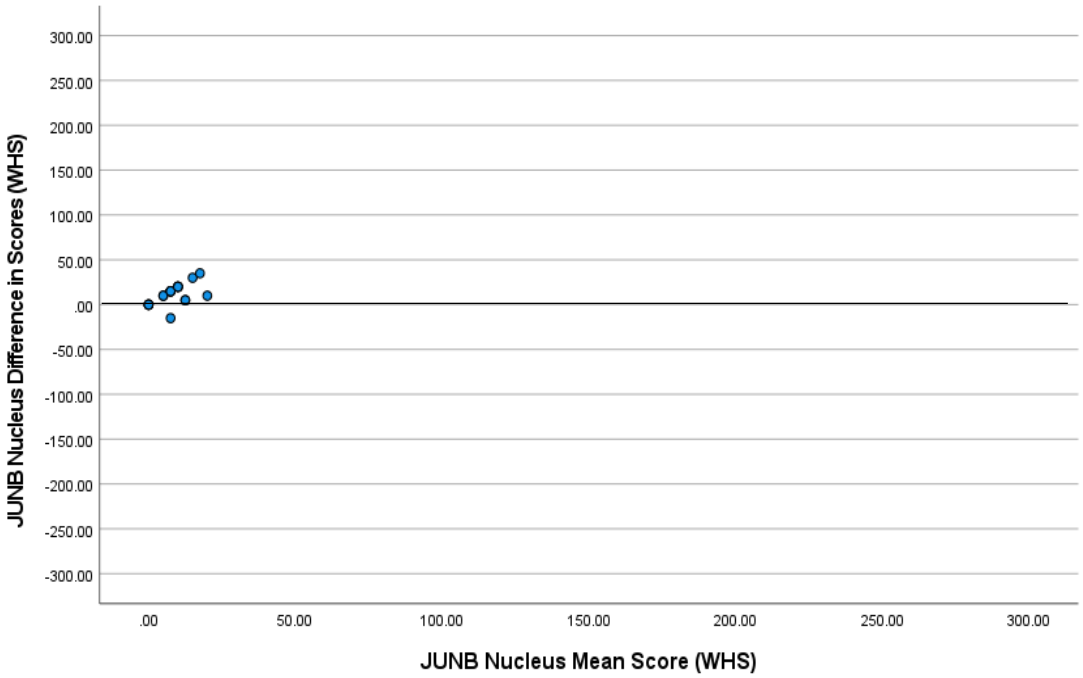

Figure 3-17 Bland Altman Plot comparing the difference in scores to mean scores for JUNB expression in Nucleus.

3.2.8 JUNB Nucleus Expression in Tumour Cells Versus Tumour Buds

JUNB nuclear expression was compared between tumour buds (where present) and intratumoural cells. A scatter plot was used to visualise the correlation between nuclear JUNB expression in intratumoral cells and tumour buds, (*Figure 3-18*). Only 43 full sections stained had tumour buds present, in these the WHS of the bud were comparable to that of the tumour core. The intraclass correlation coefficient (ICCC) was 0.999.

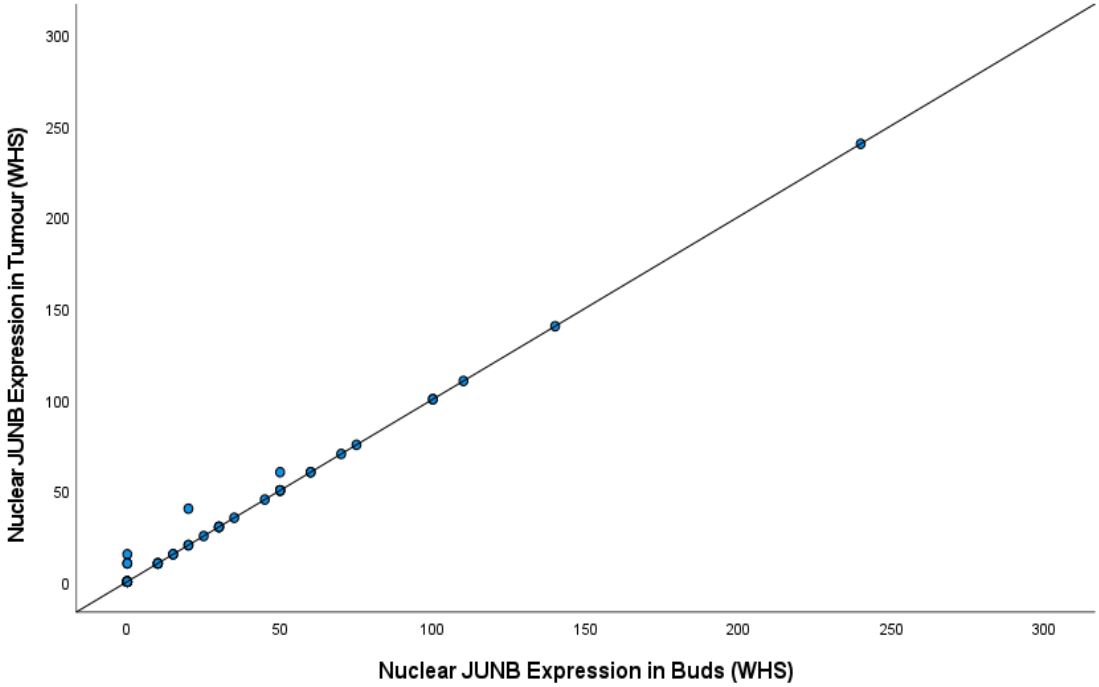

Figure 3-18 Nucleus JUNB expression in tumour versus tumour buds. ICCC 0.999.

A subsequent comparison of averages and differences in scores was plotted as a Bland-Altman plot and demonstrated no bias between observers, (Figure 3-19).

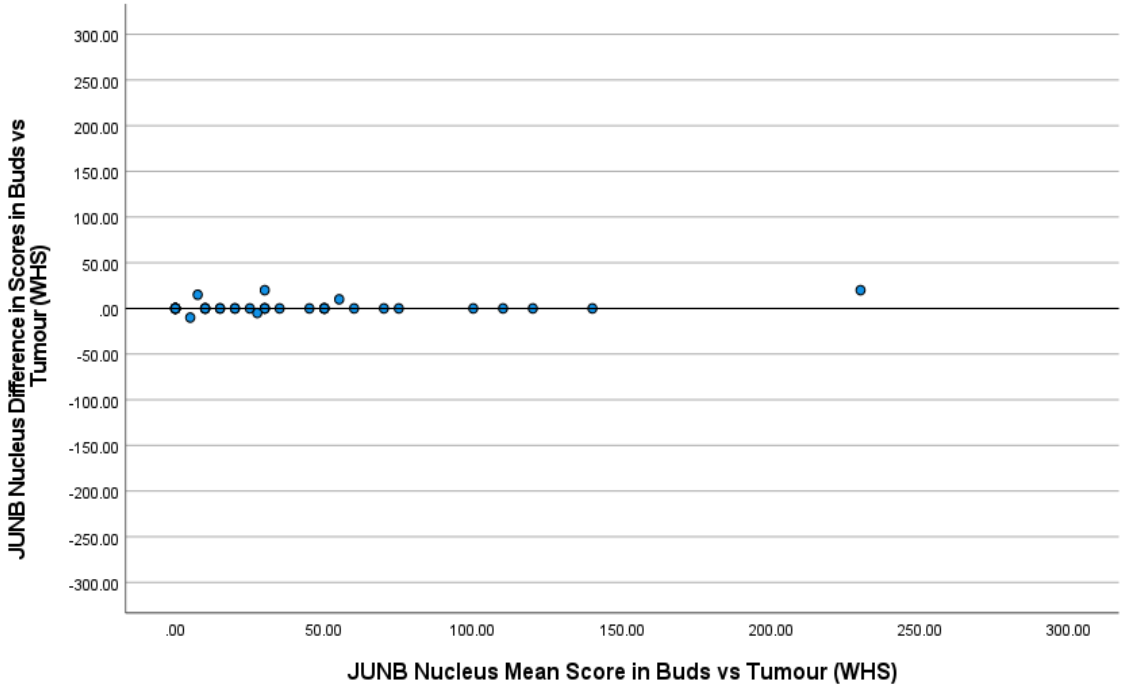

Figure 3-19 A Bland Altman plot comparing the difference in scores to mean scores for JUNB expression in the nucleus in Bud vs Tumour cells.

Based on these findings, it was possible to infer that further analysis of protein expression could be expanded to the full cohort of the Glasgow Breast Cancer Cohort in the form of a tissue microarray and remain representative of expression both within the tumour buds as in within the intratumoural environment, (*Figure 3-20*)

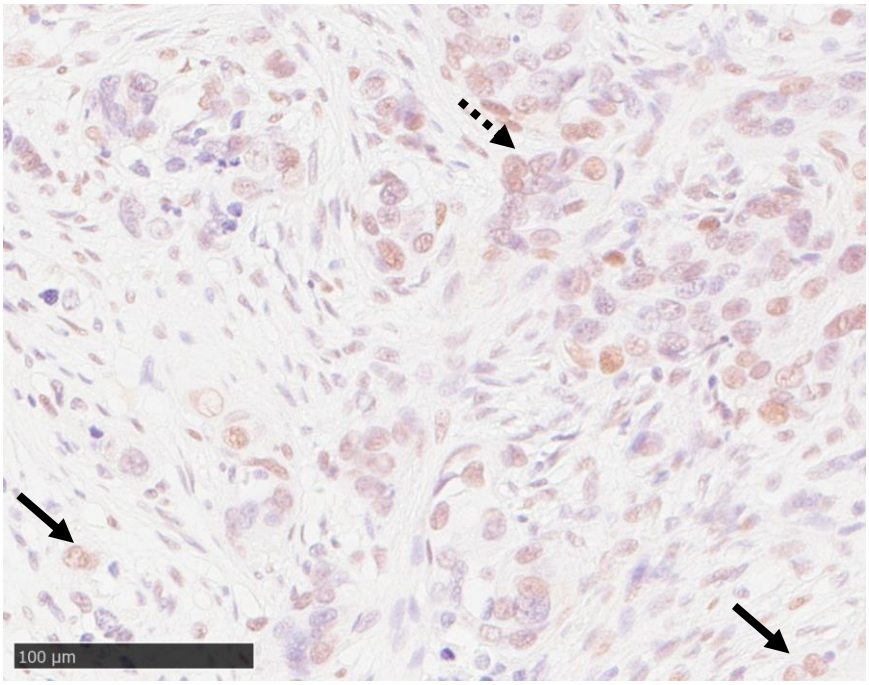

Figure 3-20 Nuclear JUNB staining in tumour mass (dotted arrow) correlated closely with staining in tumour buds (black arrow)

3.2.9 JUNB Expression in the Glasgow Breast Cancer Cohort

TMA slides composed of specimens from the Glasgow Breast Cancer Cohort were used to assess JUNB expression. Slides were stained with JUNB antibody, and manually assessed using the weighted histoscore method. Included patients had ductal cancer only, resulting in 736 specimens being included in the overall cohort. There were 3 TMA cores per specimen assessed and an average WHS was calculated, unless only one specimen was available, in which case this was used as the final WHS. 412 cases were included in the final analysis as out of the total 736 cases, 324 did not have assessable cores, (*Figure 3-21*).

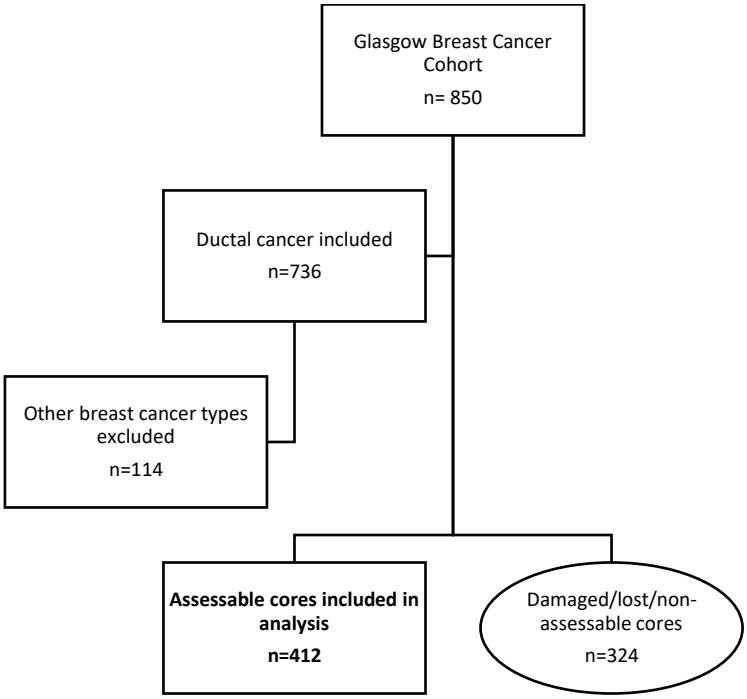

Figure 3-21 CONSORT diagram of cases included in analysis from the Glasgow Breast Cancer Cohort

Manual weighted histoscores of JUNB expression were performed by FS. Validation of the scores (minimum 10%) was performed by Hester van Wyk.

3.2.10 JUNB Membrane Expression in the Glasgow Breast Cancer Cohort

As discussed previously, membrane expression of JUNB was zero across the cohort, and therefore no analysis of expression and survival was performed.

3.2.11 JUNB Cytoplasmic Expression in the Glasgow Breast Cancer Cohort

Manual weighted histoscores of cytoplasmic JUNB expression were performed by FS. Scores by FS varied between 0 and 220, with a mean of 64.5. 104 patient

cores had a WHS of 0, (*Figure 3-22*).

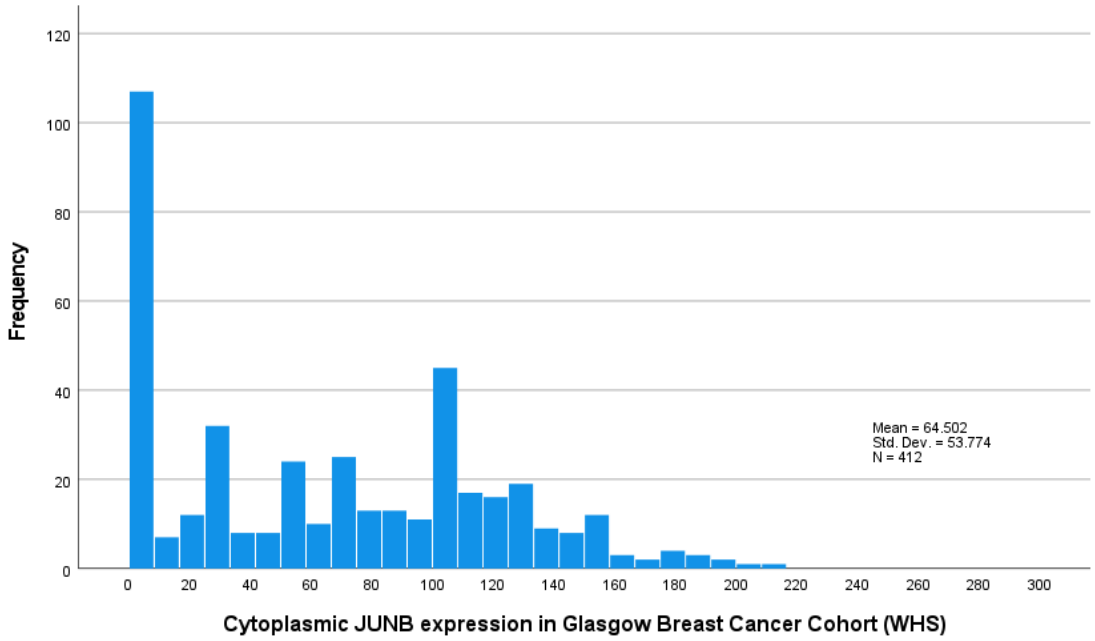

Figure 3-22 Figure 3-23 Distribution of JUNB Cytoplasmic expression (weighted histoscores) in the Glasgow Breast Cancer Cohort. Mean Score 64.5, SD 53.8.

Counter-scores were performed manually by Hester van Wyk for a minimum of 10% of cores, (n=66) and are shown below for comparison, (*Figure 3-24*). WHS were reproducible between the two scorers for 66 cores. An intraclass correlation coefficient (ICCC) of 0.718 suggested a strong positive correlation between validation and primary assessor's scores.

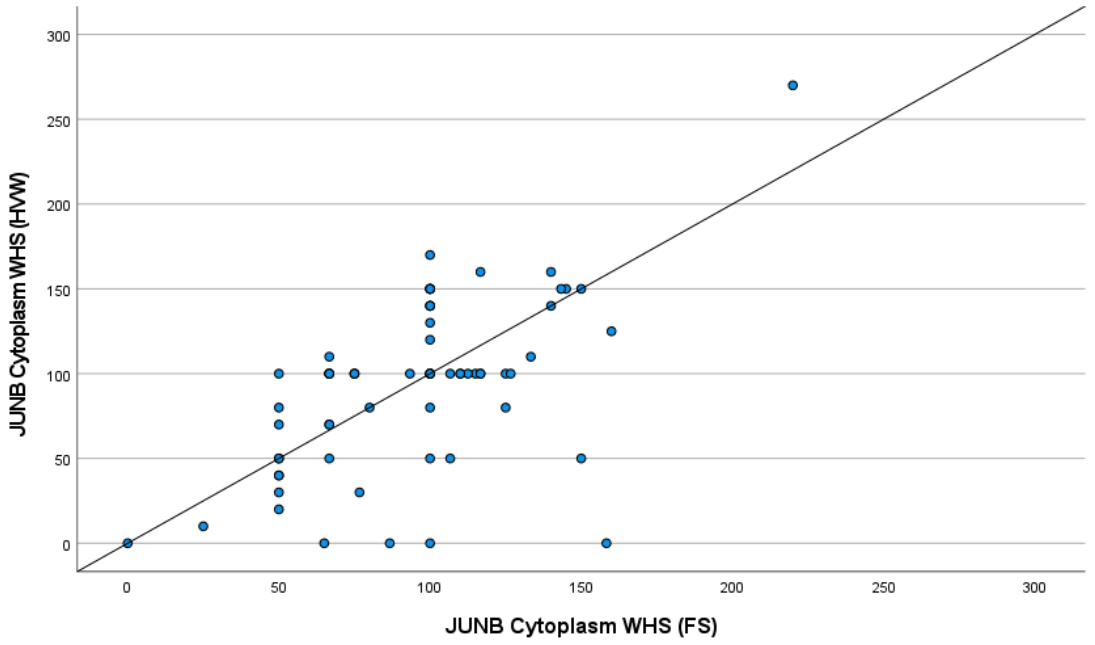

Figure 3-24 Correlation between FS and HVW manual weighted histoscore (WHS) for JUNB cytoplasm staining. Scatter plot showing correlation between FS and HVW for cytoplasm JUNB scores. Intraclass correlation coefficient 0.718 for >10% specimens.

A subsequent comparison of averages and differences in scores was produced as a Bland-Altman plot and suggested the scores correlated satisfactorily, (*Figure 3-25*).

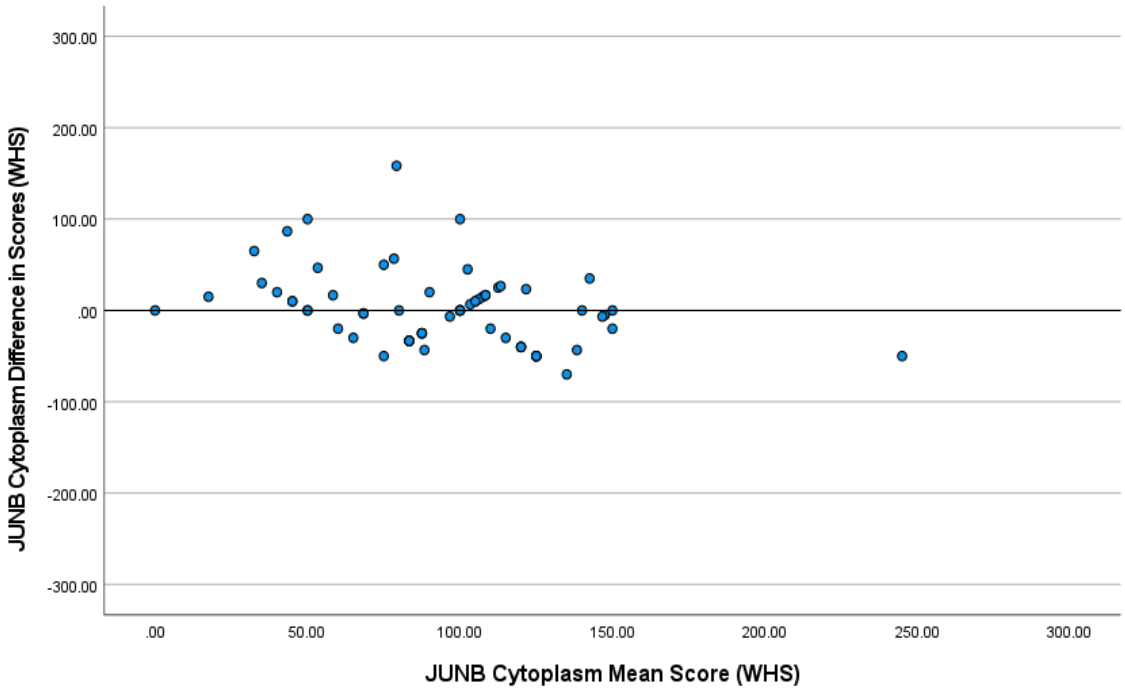

Figure 3-25 Bland-Altman Plot comparing difference in scores to mean scores for JUNB cytoplasmic expression.

A threshold for high and low JUNB cytoplasm expression was delineated using R Studio to compare high versus low JUNB cytoplasmic expression according to survival. The threshold was identified as 112.5 as described below, (*Figure 3-26*).

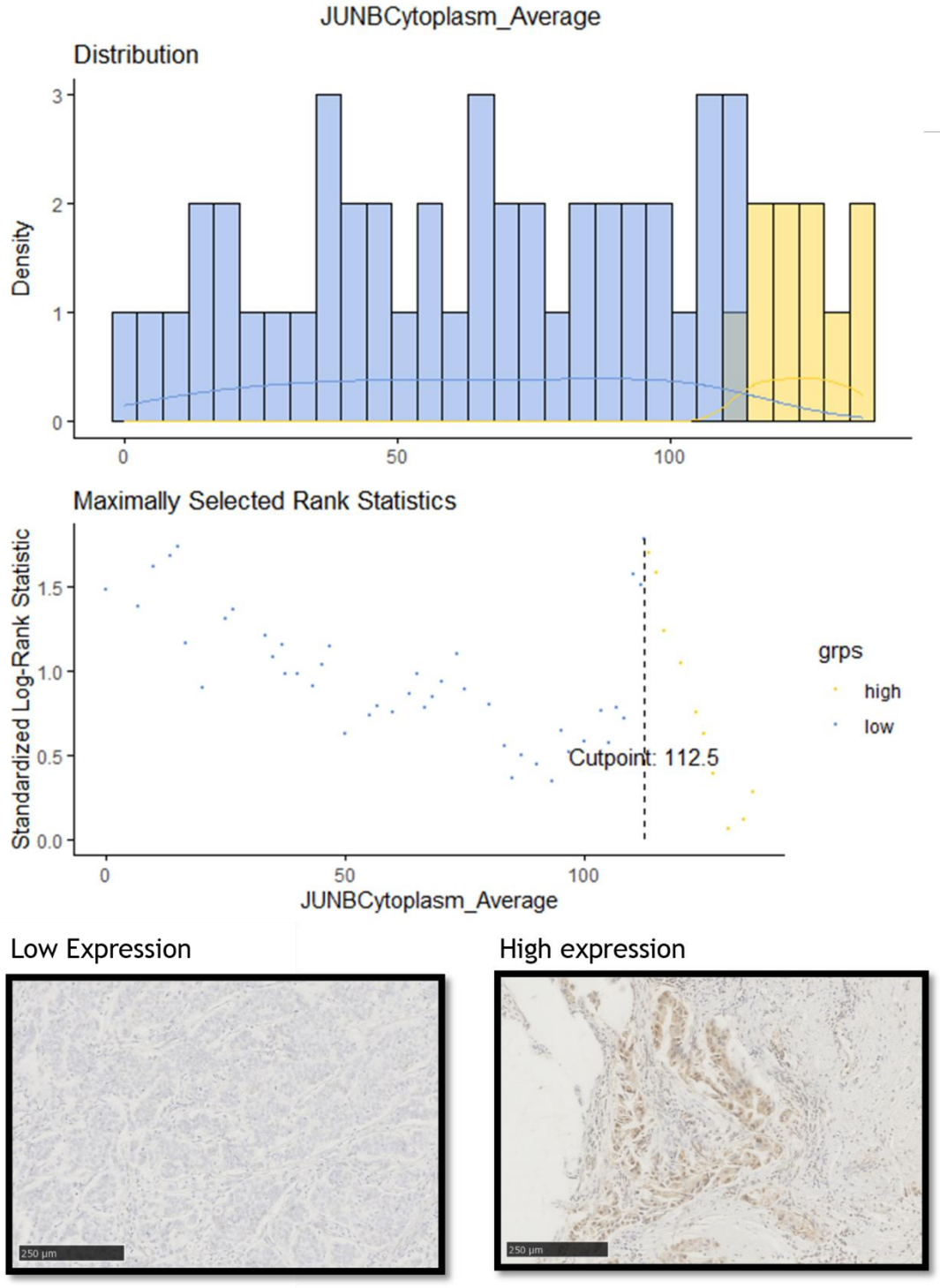

Figure 3-26 JUNB cytoplasm expression threshold for high and low expression in the Glasgow Breast Cancer Cohort. The threshold was identified as 112.5, with patients with weighted histoscores above 112.5 considered to have high JUNB cytoplasmic expression. Examples of protein expression (high/low) on breast cancer specimens are described below the graphical representation.

3.2.12 Cytoplasmic JUNB and Survival in the Glasgow Breast Cancer Cohort

850 patients had TMAs produced from the Glasgow Breast Cancer Cohort, of which 736 had ductal cancer and were included in the cohort for analysis. Of these, 722 of 736 had valid cancer-specific survival data and 411 patients had viable cores, leading to 403 patients with both viable cores and survival data. 319 patients had low JUNB cytoplasm expression and had 72 events, while 84 had high expression and saw 12 events. Survival in the low JUNB group was 86% at 5 years, and 72% at 10 years, while in the high JUNB group survival was 87% at 5 years, and 85% at 10 years. Using Kaplan Meier survival analysis, mean cancer-specific survival (CSS) time for low JUNB cytoplasm expression was 151.2 months compared to high JUNB expression survival of 160.8 months, (HR 0.625, 95% C.I.; 0.340-1.156, log rank p=0.135), (*Figure 3-27*)

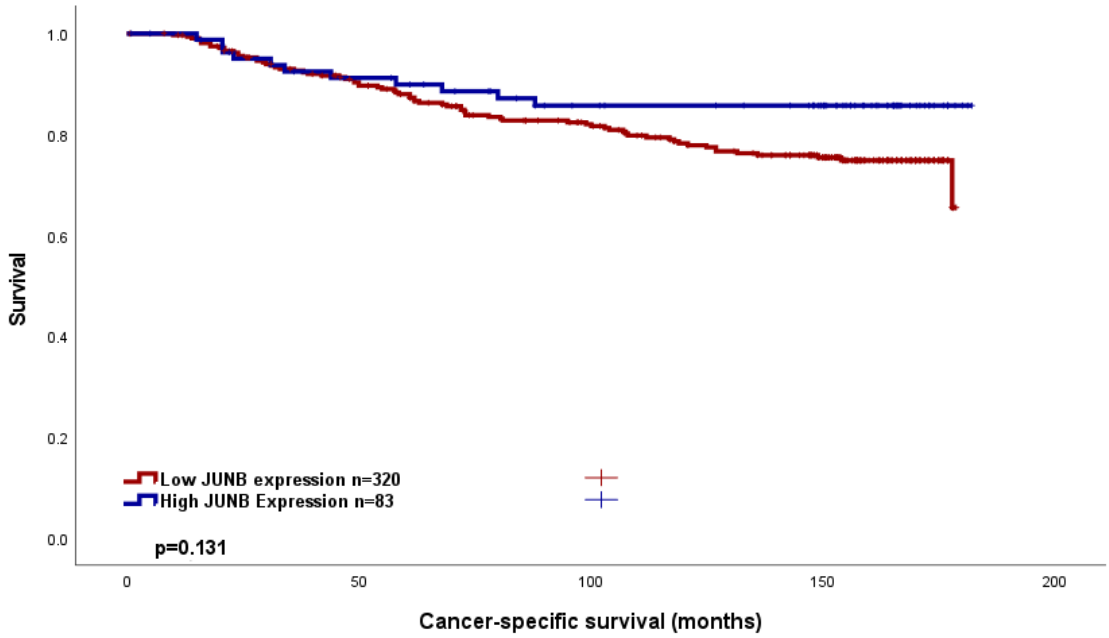

Figure 3-27 Cancer-specific survival in the Glasgow Breast Cancer Cohort according to JUNB Cytoplasmic expression. Kaplan Meier Curve showing the association between JUNB cytoplasm expression and survival (months). HR 0.625, 95% C.I.; 0.340-1.156, log rank p=0.135. 10-year survival noted at each key.

Within the entire Glasgow Breast Cancer Cohort, inter-factor correlation was assessed between the high and low JUNB cytoplasmic expressors (*Table* 3-1).

Table 3-1 Clinicopathological factors and their relation to JUNB cytoplasmic expression in the Glasgow Breast Cancer Cohort. **Chi-squared analysis.**

Clinicopathological factor	**JUNB Cytoplasmic staining (%)**		**p**
	Low	**High**	
Age (years)			
≤50	99(75.6)	32(24.4)	0.122
>50	228(81.1)	53(18.9)	
Tumour Size			
≤20mm	**196(83.8)**	**38(16.2)**	**0.036**
21-49mm	**120(74.1)**	**42(25.9)**	
≥50mm	**11(68.8)**	**5(31.2)**	
Grade			
I	68(82.9)	14(17.1)	0.501
II	148(80)	37(20)	
III	111(76.6)	34(23.4)	
Molecular Subtype			
Luminal A	**163(83.2)**	**33(16.8)**	**<0.001**
Luminal B	**98(85.2)**	**17(14.8)**	
TNBC	**37(66.1)**	**19(33.9)**	
HER2 enriched	**18(52.9))**	**16(47.1)**	
Nodal Status			
N_0	**183(75.9)**	**58(24.1)**	**<0.001**
N_1	**142(86.1)**	**23(13.9)**	
Lymphatic Invasion			
Absent	108(81.2)	25(18.8)	1.000
Present	58(80.6)	14(19.4)	
Vascular Invasion			
Absent	145(80.1)	36(19.9)	0.580
Present	21(87.5)	3(12.5)	
Necrosis			
Absent	**169(82.8)**	**35(17.2)**	**0.050**
Present	**146(74.5)**	**50(25.5)**	
Klintrup Makinen			
0	42(85.7)	7(14.3)	
1	177(80.5)	43(19.5)	0.406
2	76(75.2)	25(24.8)	
3	23(74.2)	8(25.8)	
Ki67			
Low (<15%)	201(79.8)	51(20.2)	0.798
High (>15%)	114(78.6)	31(21.4)	
Tumour Bud			
-Low	211(78.1)	59(21.9)	0.606
-High	109(80.7)	26(19.3)	
Tissue Stroma Percentage			
Low	225(79.5)	58(20.5)	0.693
High	95(76.6)	27(23.4)	

The cohort was subsequently stratified according to Oestrogen receptor status (ER-negative; ER- and ER-positive; ER+). 403 patients had valid ER-status data available.

In the ER- patient group (n=92), 57 patients had low JUNB cytoplasmic expression and had 23 events, while 35 had high JUNB expression and had 5 events. Survival in the low JUNB group was 69% at 5 years, and 51% at 10 years, while in the high JUNB group survival was 86% at 5 and at 10 years (HR 0.300, 96% C.I. 0.114-0.790, p=0.015) (*Figure 3-28*).

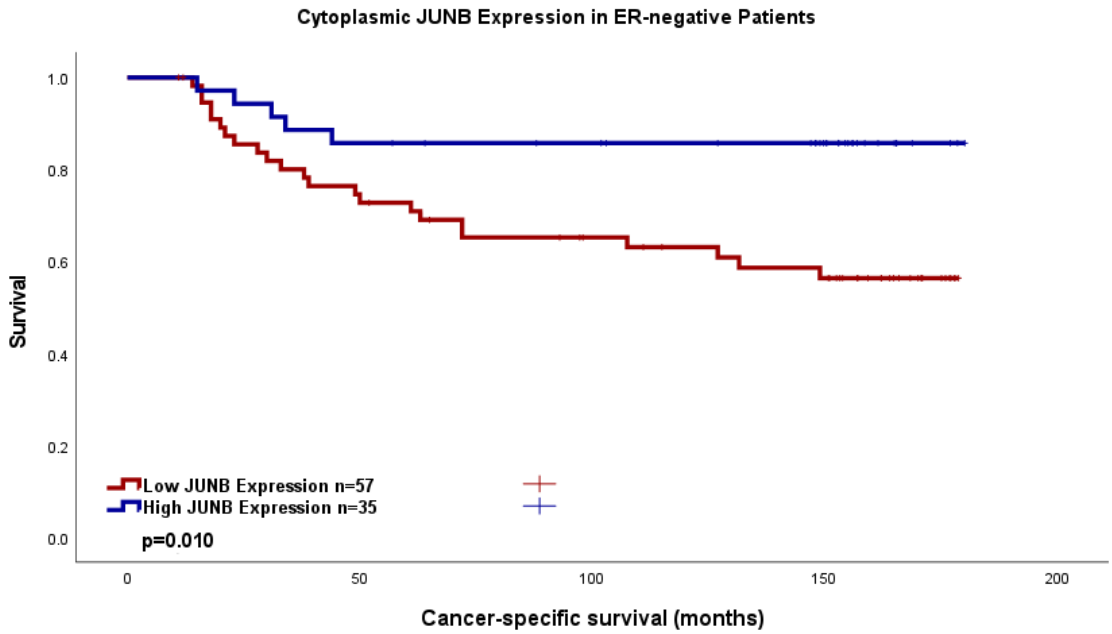

Figure 3-28 Cancer-specific survival in the Glasgow Breast Cancer Cohort according to JUNB Cytoplasmic expression in ER-negative patients. Kaplan Meier Curve showing the association between JUNB cytoplasm expression and survival (months). HR 0.300, 96% C.I. 0.114-0.790, p=0.015.

To further assess the effect of clinicopathological factors on survival in the ER- patients with the Glasgow Breast Cancer cohort, a Cox regression analysis was performed. Here, no factor was identified to be statistically significant on multivariate analysis, (Table 3-2).

Table 3-2 Clinicopathological factors and their prognostic significance within ER-negative patients in the Glasgow Breast Cancer Cohort. univariate and multivariate Cox regression analysis.

Clinicopathological Factor	Univariate analysis (HR, 95% C.I.)	p	Multivariate analysis (HR, 95% C.I.)	p
Age	1.154(0.725-1.837)	0.546		

Tumour Size		**0.002**		
<20mm		**<0.001**		1.000
20-49mm	**1.808(1.110-2.947)**	**0.017**	1.000(0.137-7.290)	1.000
>50mm	**4.276(1.947-9.391)**	**<0.001**	1.000(0.001-760.243)	1.000
Invasive Grade		**0.007**		
I		**0.978**		1.000
II	**23701.260(0-4.431^{E+63})**	**0.885**	1.000(0.006-162.641)	1.000
III	**24714.988(0-4.618^{E+63})**	**0.885**	1.000(0.007-138.941)	1.000
Nodal Status	**2.957(1.819-4.809)**	**<0.001**	1.000(0.107-9.331)	1.000
Lymphatic Invasion	**5.240(2.864-9.585)**	**<0.001**	1.000(0.114-8.779)	1.000
Vascular Invasion	**4.270(2.282-7.992)**	**<0.001**	1.000(0.016-60.646)	1.000
Necrosis	**4.495(1.950-10.360)**	**<0.001**	1.000(0.103-9.689)	1.000
Klintrup-Makinen		0.206		
0		0.746		
1	8202.926(o-6.729E+64)	0.900		
2	9480.490(0-7.777^{E+64})	0.898		
3	5943.584(0-4.885^{E+64})	0.903		
Ki67	1.212(0.735-2.000)	0.451		
Tumour budding	**2.881(1.809-4.589)**	**<0.001**	1.000(0.103-9.707)	1.000
Tumour stroma percentage	**1.961(1.237-3.107)**	**0.004**	1.000(0.103-9.403)	1.000
JUNB expression	**0.300(0.114-0.790)**	**0.015**	1.000(0.173-5.769)	1.000

Within the ER-negative group, inter-factor correlation was assessed when comparing the high and low JUNB cytoplasmic expressors, (*Table 3-3*). Here, nodal status appeared significantly associated with JUNB cytoplasmic expression.

Table 3-3 Clinicopathological factors and their prognostic significance within ER-negative patients in the Glasgow Breast Cancer Cohort, Chi-squared analysis.

Clinicopathological factor	**JUNB Cytoplasmic staining (%)**		**p**
	Low	**High**	
Age (years)			
≤50	24(60)	16(40)	0.829
>50	34(64.2)	19(35.8)	

Tumour Size			
≤20mm	28(62.2)	17(37.8)	0.530
21-49mm	25(59.5)	17(40.5)	
≥50mm	5(83.3)	1(16.7)	
Grade			
I	2	0	0.431
II	14(56)	11(44)	
III	42(63.6)	24(36.4)	
Nodal Status			
N_0	**30(52.6)**	**27(47.4)**	**0.017**
N_1	**28(77.8)**	**8(22.2)**	
Lymphatic Invasion			
Absent	8(44.4)	10(55.6)	0.710
Present	6(54.5)	5(45.5)	
Vascular Invasion			
Absent	12(48)	13(52)	1.000
Present	2(50)	2(50)	
Necrosis			
Absent	18(78.3)	5(21.7)	0.083
Present	39(56.5)	30(43.5)	
Klintrup Makinen			
	4(100)	0	
1	22(62.9)	13(37.1)	0.457
2	24(60)	16(40)	
3	7(58.3)	5(41.7)	
Ki67			
Low (<15%)	24(60)	16(40)	0.660
High (>15%)	30(65.2)	16(34.8)	
Tumour Bud			
-Low	44(59.5)	30(40.5)	0.420
-High	13(72.2)	5(27.8)	
Tissue Stroma Percentage			
Low	40(63.5)	23(36.5)	0.653
High	17(58.6)	12(41.4)	

In the ER-positive patient group, 262 patients had low JUNB nuclear expression and had 49 events, while 49 had high JUNB expression and saw 7 events. Survival in the low JUNB group was 89% at 5 years, and 76% at 10 years, while in the high JUNB group survival was 89% at 5 and 84% at 10 years (HR 0.801 , 96% C.I. 0.363-

1.771, p=0.584) (*Figure 3-29*).

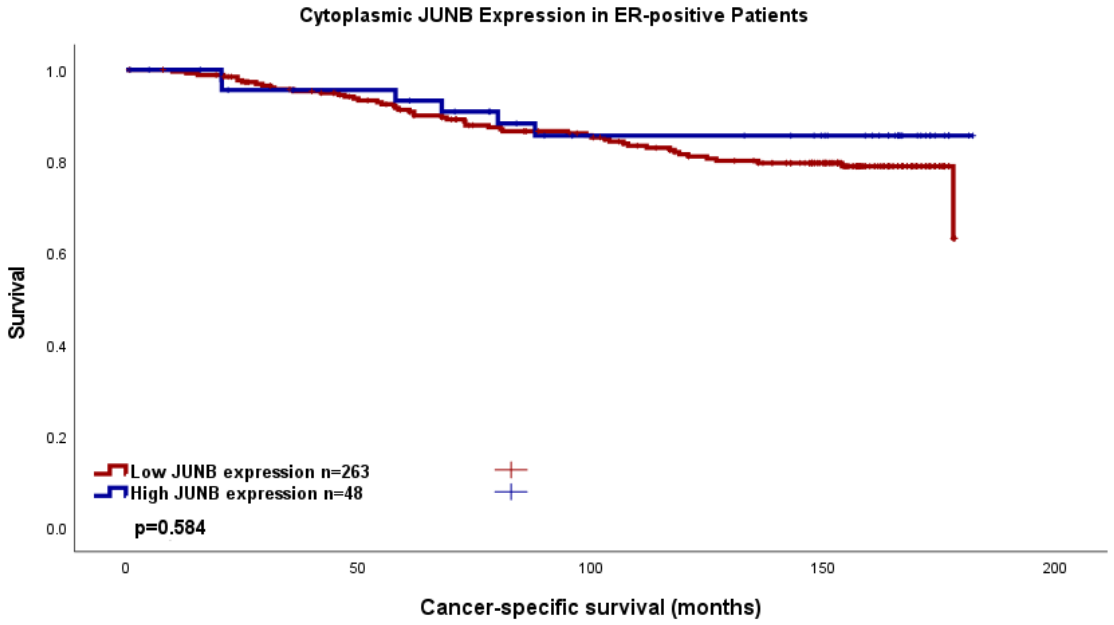

Figure 3-29 Cancer-specific survival in the Glasgow Breast Cancer Cohort according to JUNB Cytoplasmic expression in ER-positive patients. Kaplan Meier Curve showing the association between JUNB cytoplasm expression and survival (months). HR 0.801, 96% C.I. 0.363-1.771, p=0.584.

Within the ER-positive group, inter-factor correlation was assessed when comparing the high and low JUNB cytoplasmic expressors, (Table *3-4*). Here, tumour size and nodal status appeared significantly associated with JUNB cytoplasmic expression.

Table 3-4 Clinicopathological factors and their prognostic significance within ER-positive patients in the Glasgow Breast Cancer Cohort, Chi-squared analysis.

Clinicopathological factor	**JUNB Cytoplasmic staining (%)**		**p**
	Low	**High**	
Age (years)			
≤50	75(82.4)	16(17.6)	0.609
>50	194(85.1)	34(14.69)	
Tumour Size			
≤20mm	**168(88.9)**	**21(11.1)**	**0.007**
21-49mm	**95(79.2)**	**25(20.8)**	
≥50mm	**6(60)**	**4(40)**	
Grade			
I	66(82.5)	14(17.5)	0.675
II	134(83.8)	26(16.2)	
III	69(87.3)	10(12.7)	
Nodal Status			
N_0	**153(83.2)**	**31(16.8)**	**0.001**

N_1	**114(88.4)**	**15(11.6)**	
Lymphatic Invasion			
Absent	100(87)	15(13)	0.819
Present	52(85.2)	9(14.8)	
Vascular Invasion			
Absent	133(85.3)	23(14.7)	0.318
Present	19(95)	1(5)	
Necrosis			
Absent	151(83.4)	30(16.6)	0.877
Present	107(84.3)	20(15.7)	
Klintrup Makinen			
0	38(84.4)	7(15.6)	
1	155(83.8)	30(16.2)	0.995
2	52(85.2)	9(14.8)	
3	16(84.2)	3(15.8)	
Ki67			
Low (<15%)	177(83.5)	35(16.5)	0.869
High (>15%)	84(84.8)	15(15.2)	
Tumour Bud			
-Low	167(85.2)	29(14.8)	0.524
-High	96(82.1)	21(17.9)	
Tissue Stroma Percentage			
Low	185(84.1)	35(15.9)	1.000
High	78(83.9)	15(16.1)	

Further stratification according to molecular subtype was then performed. These subtypes were divided into Luminal A, Luminal B, Triple-negative and HER-2 enriched groups. For 10 patients, molecular subgroup was not available. For the remaining patients, there were 189 Luminal A, 114 Luminal B, 56 TNBC and 34 HER-2 enriched cases. Luminal A patients had 157 low nuclear JUNB expressors with 21 events, and 32 high-JUNB expressors with 2 events. Luminal B patients had 97 low JUNB expressors with 27 events, and 17 high JUNB expressors with 5 events. The TNBC patients had 37 low JUNB expressors with 15 events, and 19 patients with high JUNB with 2 events. Finally, HER-2 enriched patients consisted of 18 low JUNB cases with 7 events, and 16 high JUNB cases with 3 events. Kaplan Meier curves are shown for each subgroup below.

Luminal A patients had a 5-year survival of 91% at 5 years and 84% at 10 years for low JUNB expressors, compared to 93% at 5 years and at 10 years for high JUNB expressors. (HR 0.494 95% C.I. 0.116-2.106, p=0.340). Mean survival for low JUNB nuclear expressors was 162.9 months, while for high JUNB expressors it was

172.5 months, (p=0.330), (*Figure 3-30*).

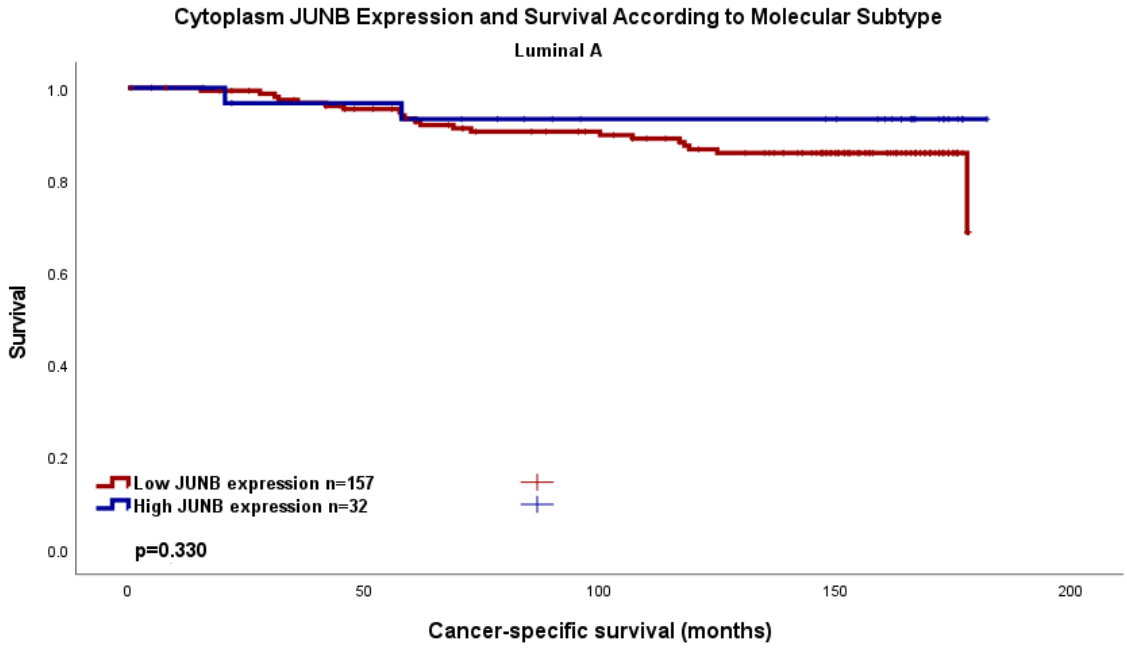

Figure 3-30 Cancer-specific survival in Luminal A patients in the Glasgow Breast Cancer Cohort according to JUNB cytoplasmic expression. Kaplan Meier Curve showing the association between JUNB nuclear expression and survival (months). HR 0.494 95% C.I. 0.116-2.106, p=0.340

Within the Luminal A group, inter-factor correlation was assessed when comparing the high and low JUNB cytoplasmic expressors, (Table 3-5). Here, no statistically significant association was seen with JUNB cytoplasmic expression.

Table 3-5 Clinicopathological factors and their relation to JUNB Cytoplasmic expression in Luminal A patients in the Glasgow Breast Cancer Cohort. Chi-squared analysis.

Clinicopathological factor	JUNB Cytoplasmic staining (%)		p
	Low	High	
Age (years)			
≤50	43(79.6)	11(20.4)	0.402
>50	120(84.5)	22(15.5)	
Tumour Size			
20mm	106(87.6)	15(12.4)	0.105
21-49mm	53(75.7)	17(24.3)	
≥50mm	4(80)	1(20)	
Grade			
I	51(79.7)	13(20.3)	0.430
II	84(83.2)	17(16.8)	
III	28(90.3)	3(9.7)	
Nodal Status			
N_0	94(81)	22(19)	0.241
N_1	68(87.2)	10(12.8)	
Lymphatic Invasion			

Absent	70(85.4)	12(14.6)	0.413
Present	26(78.8)	7(21.2)	
Vascular Invasion			
Absent	84(81.6)	19(18.4)	0.212
Present	12	0	
Necrosis			
Absent	98(79.7)	25(20.3)	0.227
Present	57(87.7)	8(12.3)	
Klintrup Makinen			
0	23(85.2)	4(14.8)	0.794
1	98(81)	23(19)	
2	29(87.9)	4(12.1)	
3	6(85.7)	1(14.3)	
Ki67			
Low (<15%)	0	0	n/a
High (>15%)	163(83.2)	33(16.8)	
Tumour Bud			
-Low	101(85.6)	17(14.4)	0.237
-High	57(78.1)	16(21.9)	
Tissue Stroma Percentage			
Low	105(81.4)	24(18.6)	0.545
High	53(85.5)	9(14.5)	

Luminal B patients had a 5-year survival of 86% At 5 years, and 64% at 10 years for low JUNB expressors, compared to 81% at 5 years and 66% at 10 years for high JUNB nuclear expressors. (HR 1.196, 95% C.I. 0.461-3.107, p=0.713). Mean survival for low JUNB nuclear expressors was 145.4 months, while for high JUNB expressors it was 139.3 months, (p=0.712), (*Figure 3-31*).

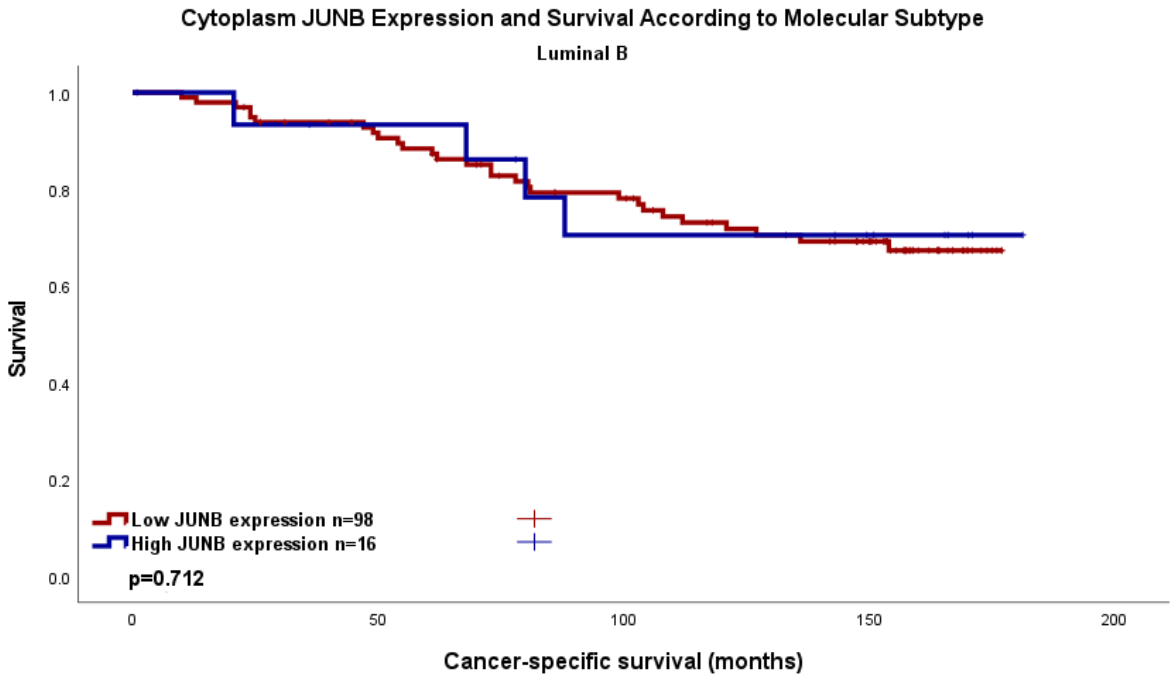

Figure 3-31 Cancer-specific survival in Luminal B patients in the Glasgow Breast Cancer Cohort according to JUNB cytoplasmic expression. Kaplan Meier Curve showing the

association between JUNB cytoplasmic expression and survival (months). HR 1.196, 95% C.I. 0.461-3.107, p=0.713.

Within the Luminal B group, inter-factor correlation was assessed when comparing the high and low JUNB cytoplasmic expressors, (Table 3-6). Here, tumour size and nodal status were associated with JUNB cytoplasmic staining.

Table 3-6 Clinicopathological factors and their relation to JUNB Cytoplasmic expression in Luminal B patients in the Glasgow Breast Cancer Cohort. **Chi-squared analysis.**

Clinicopathological factor	**JUNB Cytoplasmic staining (%)**		**p**
	Low	**High**	
Age (years)			
≤50	33(86.8)	5(13.2)	1.000
>50	65(84.4)	12(15.6)	
Tumour Size			
≤20mm	**55(90.2)**	**6(9.8)**	**0.027**
21-49mm	**40(83.3)**	**8(16.7)**	
≥50mm	**3(50)**	**3(50)**	
Grade			
I	13(92.9)	1(7.1)	0.670
II	45(70.3)	9(29.7)	
III	40(85.1)	7(14.9)	
Nodal Status			
N_0	**52(85.2)**	**9(14.8)**	**<0.001**
N_1	**46(90.2)**	**5(9.8)**	
Lymphatic Invasion			
Absent	27(90)	3(10)	1.000
Present	26(92.9)	2(7.1)	
Vascular Invasion			
Absent	46(92)	4(8)	0.536
Present	7(87.5)	1(12.5)	
Necrosis			
Absent	49(90.7)	5(9.3)	0.119
Present	47(79.7)	12(20.3)	
Klintrup Makinen			
0	13(86.7)	3(13.3)	
1	53(88.3)	7(11.7)	0.802
2	22(81.5)	5(18.5)	
3	10(83.3)	2(16.7)	
Ki67			
Low (<15%)	13(86.7)	2(13.3)	1.000
High (>15%)	85(85)	15(15)	
Tumour Bud			
-Low	60(83.3)	12(16.7)	0.591
-High	38(88.4)	5(16.6)	
Tissue Stroma Percentage			
Low	74(87.1)	11(12.9)	0.376

High	24(80)	6(20)	

TNBC patients had a 5-year survival of 72% At 5 years, and 50% at 10 years for low JUNB expressors, compared to 89% at 5 years and 89% at 10 years for high JUNB nuclear expressors. (HR 0.222, 95% C.I. 0.051-0.971, p=0.046). Mean survival for low JUNB nuclear expressors was 125.7 months, while for high JUNB expressors it was 164.3 months, (p=0.028), (*Figure 3-32*).

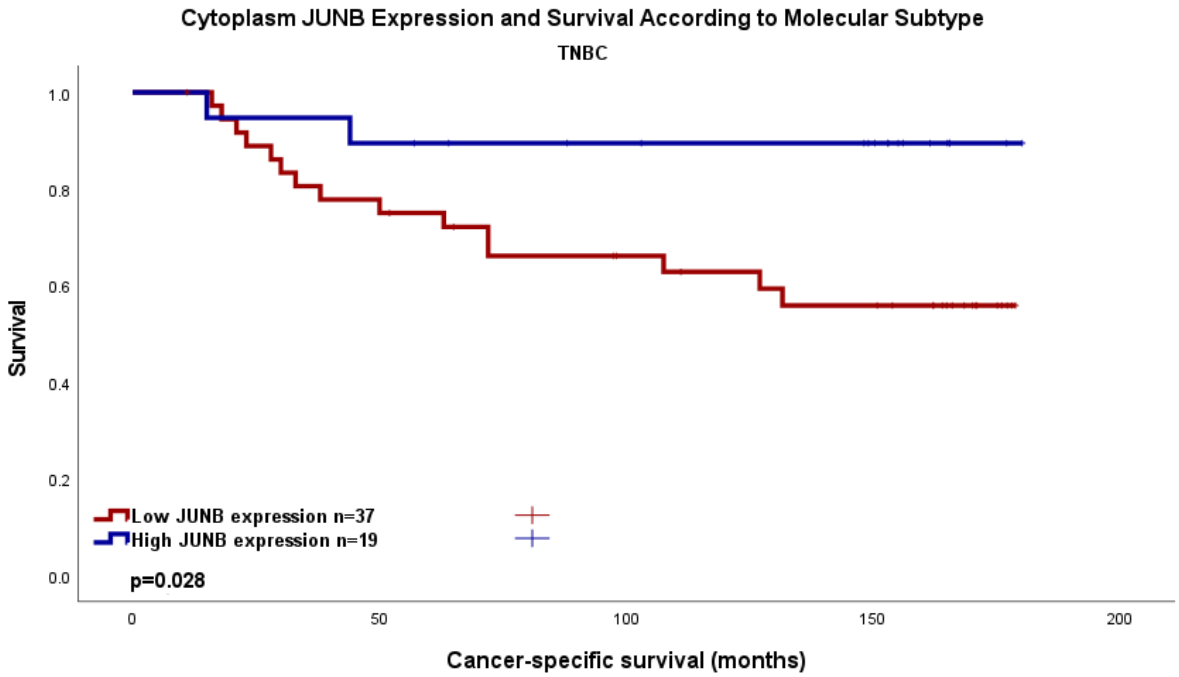

Figure 3-32 Cancer-specific survival in TNBC patients in the Glasgow Breast Cancer Cohort according to JUNB cytoplasmic expression. Kaplan Meier Curve showing the association between JUNB cytoplasmic expression and survival (months). HR 0.222, 95% C.I. 0.051-0.971, p=0.046.

To further assess the effect of clinicopathological factors in TNBC cancers on survival in the Glasgow Breast Cancer cohort, a Cox regression analysis was performed, (

Table 3-7). On univariate analysis, tumour size, lymphatic invasion, vascular invasion, necrosis, tumour stroma percentage and JUNB cytoplasmic expression were significantly associated with survival, but this effect was lost on multivariate analysis.

Table 3-7 Clinicopathological factors and their prognostic significance within TNBC patients in the Glasgow Breast Cancer Cohort. Univariate and multivariate Cox regression analysis.

Clinicopathological Factor	Univariate analysis (HR, 95% C.I.)	p	Multivariate analysis (HR, 95% C.I.)	p

Age	1.379(0.771-2.466)	0.278		
Tumour Size		**<0.001**		
<20mm		**<0.001**		0.988
20-49mm	**2.706(1.424-5.143)**	**0.002**	0.431(0-2.081E+112)	0.995
>50mm	**13.077(4.946-34.573)**	**<0.001**	1.118E+11(0-1.332E+194)	0.906
Invasive Grade		0.066		
I		0.596		
II	11318.331(0-8.64^{E+56})	0.881		
III	8169.349(0-6.465^{E+56})	0.885		
Nodal Status	**3.795(2.064-6.980)**	**<0.001**	0.003(0-2.147E+27)	0.865
Lymphatic Invasion	**6.343(2.811-14.315)**	**<0.001**	1.588(0-2.694E+13)	0.976
Vascular Invasion	**5.727(2.761-11.879)**	**<0.001**	0.095(0-1.638E+29)	0.947
Necrosis	**4.867(1.748-13.557)**	**0.002**	14778.635(0-2.403E+117)	0.942
Klintrup-Makinen		0.323		
0		0.917		
1	8351.396(0-1.126E+68)	0.905		
2	9387.727(0-1.265E+68)	0.903		
3	6708.822(0-9.062E+67)	0.907		
Ki67	0.819(0.414-1.620)	0.565		
Tumour budding	**2.466(1.373-4.429)**	**0.003**	0.030(0-4.771E+25)	0.912
Tumour stroma percentage	**1.812(1.003-3.276)**	**0.049**	1.244(0-3.300E+14)	0.990
JUNB expression	**0.222(0.051-0.971)**	**0.046**	0(0-765017914.4)	0.502

When different clinicopathological factors were compared for inter-factor correlation within the TNBC portion of the Glasgow Breast Cancer cohort, none of the factors correlated significantly with JUNB cytoplasmic expression, (*Table 3-8*).

Table 3-8 Clinicopathological factors and their relation to JUNB cytoplasmic expression in TNBC patients in the Glasgow Breast Cancer Cohort. Chi-squared analysis.

Clinicopathological factor	**JUNB Nuclear staining (%)**		**p**
	Low	**High**	

Age (years)			
≤50	16(59.3)	11(40.7)	0.399
>50	21(72.4)	8(27.6)	
Tumour Size			
≤20mm	18(66.7)	9(33.3)	0.887
21-49mm	18(66.7)	9(33.3)	
≥50mm	1(50)	1(50)	
Grade			
I	2	0	0.527
II	9(60)	6(40)	
III	26(66.7)	13(33.3)	
Nodal Status			
N_0	20(57.1)	15(42.9)	0.086
N_1	17(81)	4(19)	
Lymphatic Invasion			
Absent	4(36.4)	7(63.6)	0.596
Present	3(60)	2(40)	
Vascular Invasion			
Absent	6(42.9)	8(57.1)	1.000
Present	1(50)	1(50)	
Necrosis			
Absent	15(78.9)	4(21.1)	0.149
Present	21(58.3)	15(41.7)	
Klintrup Makinen			
0	4(100)	0	
1	16(66.7)	8(33.3)	0.428
2	12(57.1)	9(42.9)	
3	4(66.7)	2(33.3)	
Ki67			
Low (<15%)	17(65.4)	9(34.6)	1.000
High (>15%)	16(66.7)	8(33.3)	
Tumour Bud			
-Low	26(61.9)	16(38.1)	0.506
-High	10(76.9)	3(23.1)	
Tissue Stroma Percentage			
Low	29(87.9)	14(12.1)	0.733
High	7(58.3)	5(41.7)	

HER-2 enriched patients had a 5-year survival of 65% at 5 years and 52% at 10 years for low JUNB expressors, compared to 81% at 5 years and 81% at 10 years for high JUNB nuclear expressors. (HR 0.401, 95% C.I. 0.104-1.554, p=0.186). Mean survival for low JUNB nuclear expressors was 122.3 months, while for high

JUNB expressors it was 150.6 months, (p=0.171), (*Figure 3-33*).

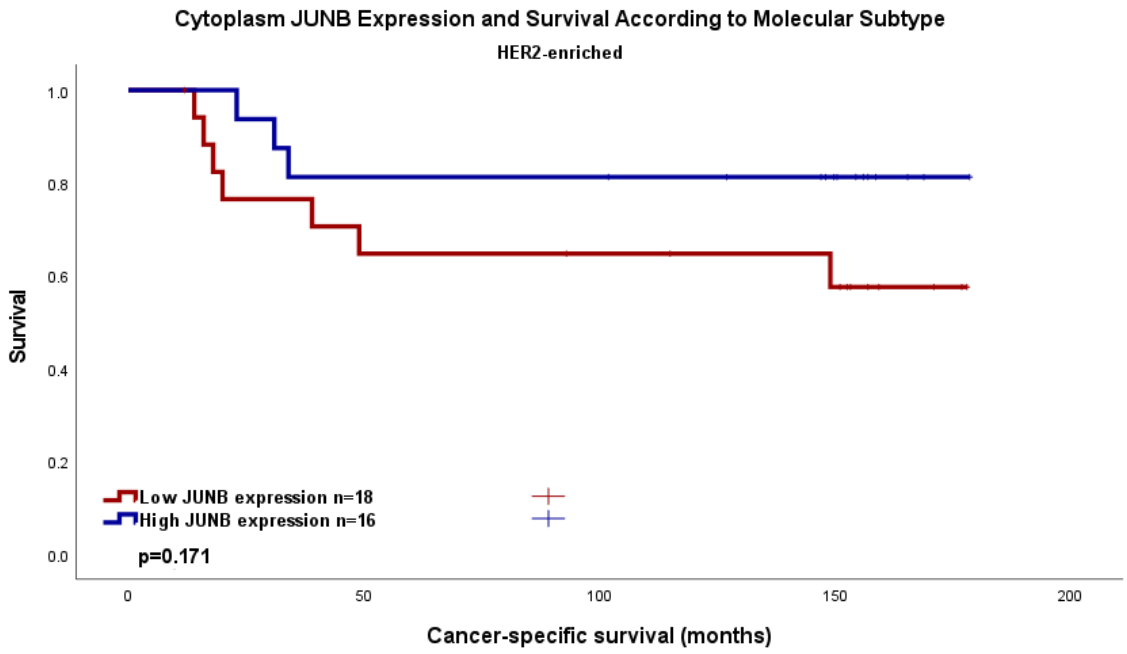

Figure 3-33 Cancer-specific survival in HER2-enriched patients in the Glasgow Breast Cancer Cohort according to JUNB cytoplasmic expression. Kaplan Meier Curve showing the association between JUNB cytoplasmic expression and survival (months). HR 0.401, 95% C.I. 0.104-1.554, p=0.186.

Within the HER2-enriched group, inter-factor correlation was assessed when comparing the high and low JUNB cytoplasmic expressors, (Table 3-9). Here no statistically significant association was seen with JUNB cytoplasmic staining.

Table 3-9 Clinicopathological factors and their relation to JUNB Cytoplasmic expression in HER2-enriched patients in the Glasgow Breast Cancer Cohort. Chi-squared analysis.

Clinicopathological factor	**JUNB Nuclear staining (%)**		**p**
	Low	**High**	
Age (years)			
≤50	6(54.5)	5(45.5)	1.000
>50	12(52.2)	11(47.8)	
Tumour Size			
≤20mm	9(52.9)	8(47.1)	0.198
21-49mm	6(42.9)	8(57.1)	
≥50mm	3	0	
Grade			
I	0	0	1.000
II	5(50)	5(50)	
III	13(54.2)	11(45.8)	
Nodal Status			
N_0	10(45.5)	12(54.5)	0.297
N_1	8(66.7)	4(33.3)	

Lymphatic Invasion			
Absent	4(57.1)	3(42.9)	1.000
Present	2(40)	3(60)	
Vascular Invasion			
Absent	6(54.5)	5(45.5)	1.000
Present	0	1	
Necrosis			
Absent	2(66.7)	1(33.3)	1.000
Present	16(51.6)	15(48.4)	
Klintrup Makinen			
0	4(44.4)	5(55.6)	
1	4(44.4)	5(55.6)	0.693
2	11(61.1)	7(38.9)	
3	3(50)	3(50)	
Ki67			
Low (<15%)	6(46.2)	7(53.8)	0.493
High (>15%)	12(60)	8(20)	
Tumour Bud			
-Low	15(51.7)	14(48.3)	1.000
-High	3(60)	2(40)	
Tissue Stroma Percentage			
Low	9(50)	9(50)	0.744
High	9(56.3)	7(43.7)	

3.2.13 JUNB Nuclear Expression in the Glasgow Breast Cancer Cohort

Manual weighted histoscores of nuclear expression of JUNB were performed by FS. Scores varied from 0 to 260 with a mean of 79.2. 48 patient cores had a WHS of 0, (*Figure 3-34*).

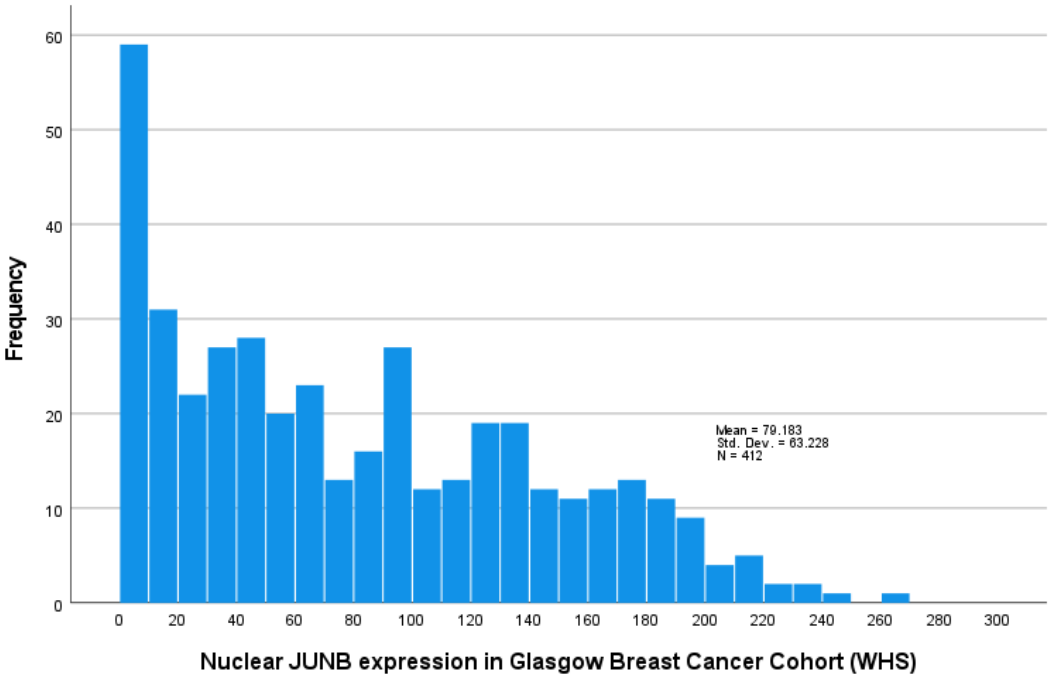

Figure 3-34 Distribution of JUNB Nuclear expression (weighted histoscores) in the Glasgow Breast Cancer Cohort. Mean Score 79.18, SD 62.23.

Counter-scores were performed manually by HVW for a minimum of 10% of cores, (n=67) and are shown below for comparison, (Figure 3-35). WHS were reproducible between the two scorers for 67 cores. An intraclass correlation coefficient (ICCC) of 0.907 suggested a strong positive correlation between validation and primary assessor's scores.

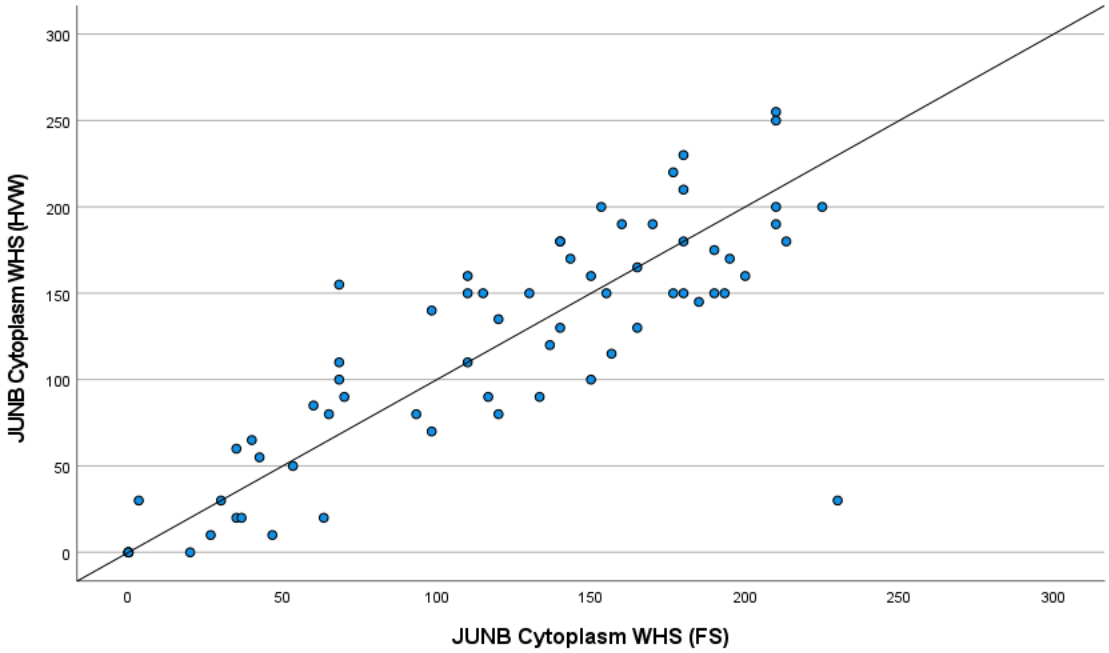

Figure 3-35 Correlation between FS and HVW manual weighted histoscore (WHS) for JUNB nucleus staining. Scatter plot showing correlation between FS and HVW for nucleus JUNB scores. Intraclass correlation coefficient 0.907 for 10% specimens.

A subsequent comparison of averages and differences in scores was produced as a Bland-Altman plot and suggested the scores correlated satisfactorily (*Figure 3-36*).

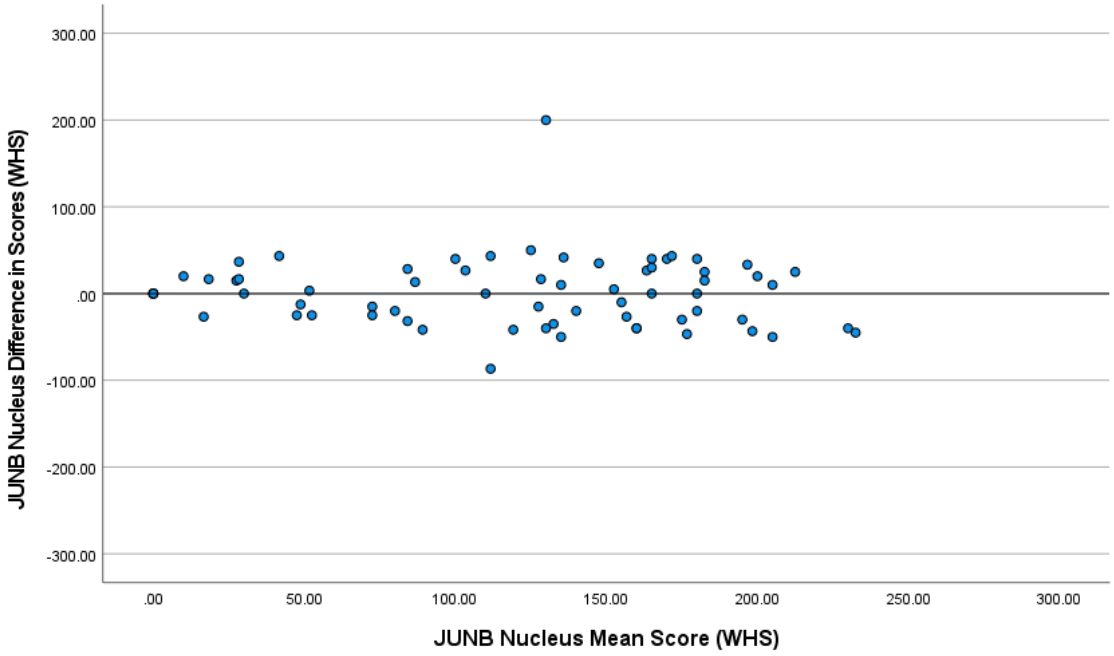

Figure 3-36 Bland-Altman Plot comparing difference in scores to mean scores for JUNB nuclear expression.

A threshold for high and low JUNB nuclear expression was delineated using R Studio to compare high versus low JUNB nuclear expression according to survival. The threshold was identified as 115 (*Figure 3-37*).

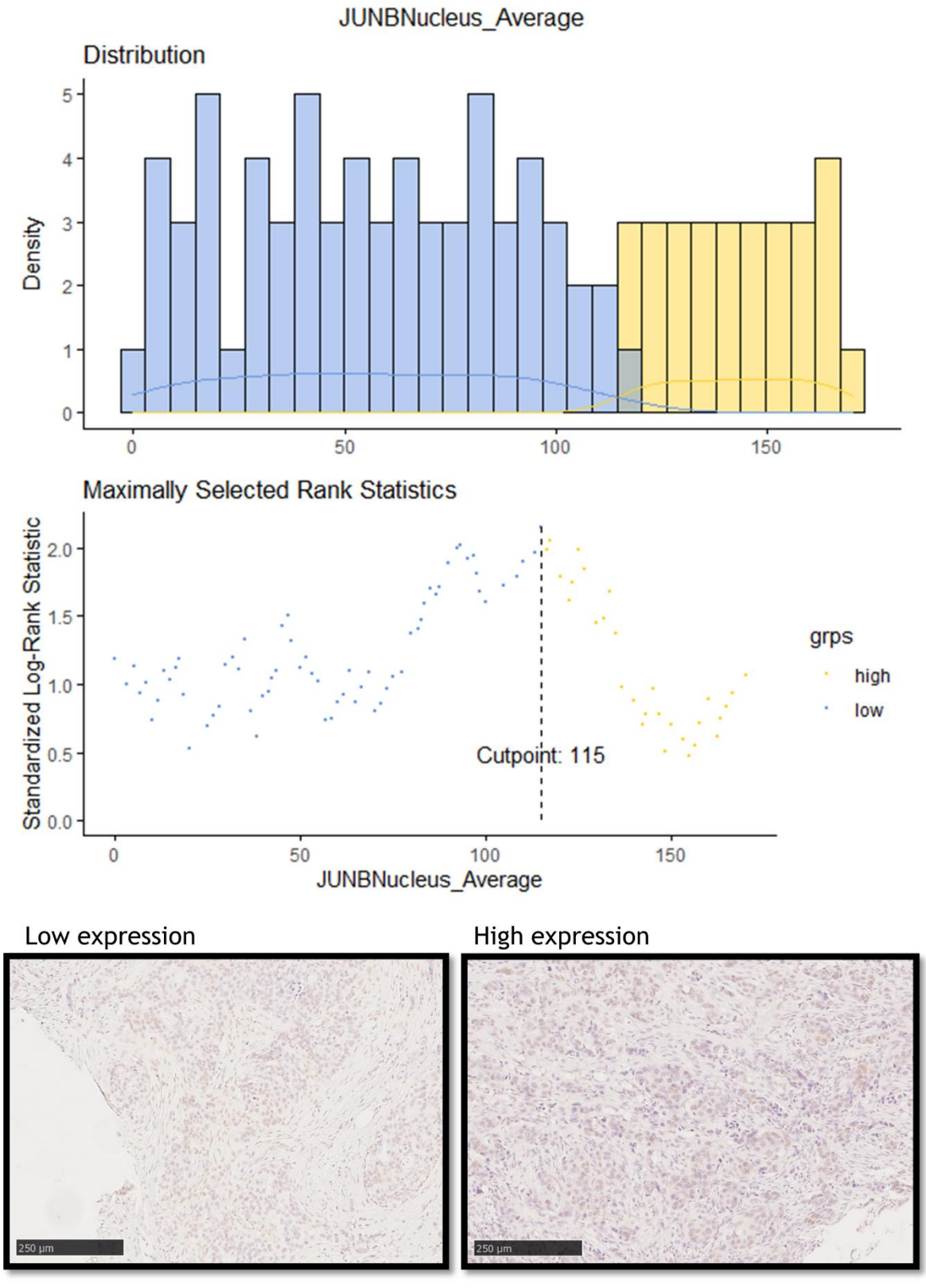

Figure 3-37 JUNB Nuclear expression - threshold for high and low expression of JUNB in the nucleus of the Glasgow Breast Cancer Cohort was identified as 115, with patients with weighted scores above 115 considered to have high JUNB nuclear expression. Examples of protein expression as seen on specimens are also described below the graphical representation.

3.2.14 Nuclear JUNB and Survival in the Glasgow Breast Cancer Cohort

850 patients had TMAs produced from the Glasgow Breast Cancer Cohort, of which 736 had ductal cancer and were included in the cohort for analysis. Of these, 722 of 736 had valid cancer-specific survival data and 414 had viable cores, leading to a final 412 patients with both viable cores and valid survival data. 280 patients had low JUNB nuclear expression and had 51 events, while 123 had high expression and saw 33 events. Survival in the low JUNB group was 88% at 5 years, and 77% at 10 years, while in the high JUNB group survival was 81% at 5 years, and 67% at 10 years. Using Kaplan Meier survival analysis, mean cancer-specific survival (CSS) time for low JUNB nuclear expression was 158.4 months compared to high JUNB expression survival of 145.5 months, suggesting that high JUNB nuclear expression was associated with reduced survival (HR 1.623, 95% C.I.; 1.048-2.516, log rank p=0.030), (*Figure 3-38*).

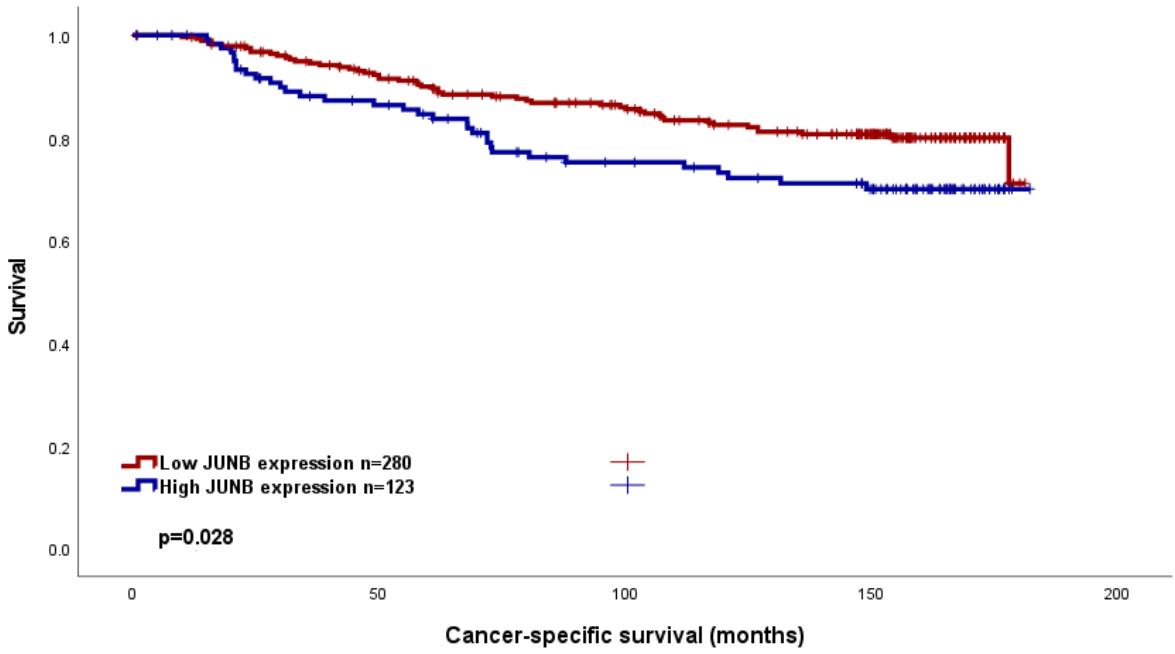

Figure 3-38 Cancer-specific survival in the Glasgow Breast Cancer Cohort according to JUNB Nuclear expression. Kaplan Meier Curve showing the association between JUNB nuclear expression and survival (months). HR 1.623 (95% C.I. 1.048-2.516), p=0.030.

To further assess the effect of clinicopathological factors on survival in the Glasgow Breast Cancer cohort, a Cox regression analysis was performed, (*Table 3-10*). On multivariate analysis, tumour size, molecular subtype, necrosis, tumour budding, and Klintrup Makinen Score remained significant, while JUNB nuclear expression lost its statistical significance.

Table 3-10 Clinicopathological factors and their prognostic significance within the Glasgow Breast Cancer Cohort. Univariate and multivariate Cox regression analysis.

Clinicopathological Factor	Univariate analysis (HR, 95% C.I.)	p	Multivariate analysis (HR, 95% C.I.)	p
Age	0.947(0.680-1.318)	0.746		
Tumour Size		**<0.001**		
<20mm		**<0.001**		**0.033**
20-49mm	**2.117(1.525-2.939)**	**<0.001**	**2.699(1.055-6.906)**	**0.038**
>50mm	**4.528(2.579-7.951)**	**<0.001**	**7.655(1.260-46.501)**	**0.027**
Invasive Grade		**<0.001**		
I		**<0.001**		0.980
II	**2.332(1.226-4.436)**	**0.010**	0.872(0.219-3.475)	0.846
III	**4.043(2.162-7.563)**	**<0.001**	0.867(0.198-3.795)	0.850
Molecular Subtype		**<0.001**		
Luminal A		**<0.001**		**0.033**
Luminal B	**2.343(1.525-3.599)**	**<0.001**	**4.989(0.920-27.044)**	**0.062**
TNBC	**2.710(1.779-4.128)**	**<0.001**	**8.653(1.397-53.595)**	**0.020**
HER2-enriched	**2.946(1.771-4.900)**	**<0.001**	**22.0744(2.368-205.766)**	**0.007**
Nodal Status	**3.258(2.339-4.537)**	**<0.001**	1.322(0.545-3.209)	0.537
Lymphatic Invasion	**4.255(2.813-6.435)**	**<0.001**	2.461(0.927-6.535)	0.071
Vascular Invasion	**3.440(2.163-5.470)**	**<0.001**	1.705(0.627-4.635)	0.296
Necrosis	**3.288(2.290-4.722)**	**<0.001**	**3.298(1.129-9.631)**	**0.029**
Klintrup-Makinen		**0.033**		
0		**0.030**		**<0.001**
1	**0.812(0.481-1.372)**	**0.437**	**0.027(0.007-0.105)**	**<0.001**
2	**1.310(0.757-2.265)**	**0.334**	**0.008(0.001-0.062)**	**<0.001**
3	**0.621(0.277-1.395)**	**0.249**	**0.024(0.001-0.403)**	**0.010**
Ki67	**1.658(1.199-2.294)**	**0.002**	2.547(0.581-11.168)	0.215
Tumour budding	**1.755(1.282-2.403)**	**<0.001**	**2.789(1.004-7.744)**	**0.049**

Tumour stroma percentage	**1.884(1.374-2.582)**	**<0.001**	**1.706(0.714-4.077)**	0.229
JUNB expression	**1.623(1.048-2.516)**	**0.030**	1.149(0.437-3.021)	0.778

When different clinicopathological factors were compared for inter-factor correlation, age, tumour size, grade Klintrup Makinen and necrosis were found to be significantly associated with JUNB nuclear expression, (Table 3-11).

Table 3-11 Clinicopathological factors and their relation to JUNB nuclear expression in the Glasgow Breast Cancer Cohort. Chi-squared analysis.

Clinicopathological factor	**JUNB Nuclear staining (%)**		**p**
	Low	**High**	
Age (years)			
≤50	**81(61.8)**	**50(38.2)**	**0.016**
>50	**207(73.7)**	**74(26.3)**	
Tumour Size			
≤20mm	**175(74.8)**	**59(25.2)**	**0.009**
21-49mm	**106(40.5)**	**56(59.5)**	
≥50mm	**7(43.6)**	**9(56.3)**	
Grade			
I	**59(71.9)**	**23(28.1)**	**0.017**
II	**140(75.7)**	**45(24.3)**	
III	**89(61.4)**	**56(38.6)**	
Nodal Status			
N_0	170(70.5)	71(29.5)	0.144
N_1	116(70.3)	49(29.7)	
Lymphatic Invasion			
Absent	103(77.4)	30(22.6)	0.496
Present	52(72.2)	20(27.8)	
Vascular Invasion			
Absent	138(76.2)	43(23.8)	0.614
Present	17(70.8)	7(29.2)	
Necrosis			
Absent	**152(74.5)**	**52(25.5)**	**0.017**
Present	**124(14.3)**	**72(85.7)**	
Klintrup Makinen			
0	**38(77.6)**	**11(22.4)**	**0.023**
1	**159(72.3)**	**61(27.7)**	
2	**58(57.4)**	**43(42.6)**	
3	**23(74.2)**	**8(25.8)**	
Ki67			
Low (<15%)	181(71.8)	71(28.2)	0.257
High (>15%)	96(66.2)	49(33.8)	
Tumour Bud			
-Low	184(68.1)	86(31.9)	0.493
-High	97(71.9)	38(28.1)	
Tissue Stroma Percentage			
Low	200(70.7)	83(29.3)	0.412

High	81(66.4)	41(33.6)	

Stratification of the cohort to compare patients according to ER status was performed. 403 had valid ER-status data available. In the ER-negative patient group (n=92), 46 patients had low JUNB nuclear expression and had 14 events, while 46 had high JUNB expression and saw 14 events. Survival in the low JUNB group was 73% at 5 years, and 64% at 10 years, while in the high JUNB group survival was 78% at 5 and 64% at 10 years (HR 0.963 95% C.I. 0.459-2.022, p=0.920), (*Figure 3-39*).

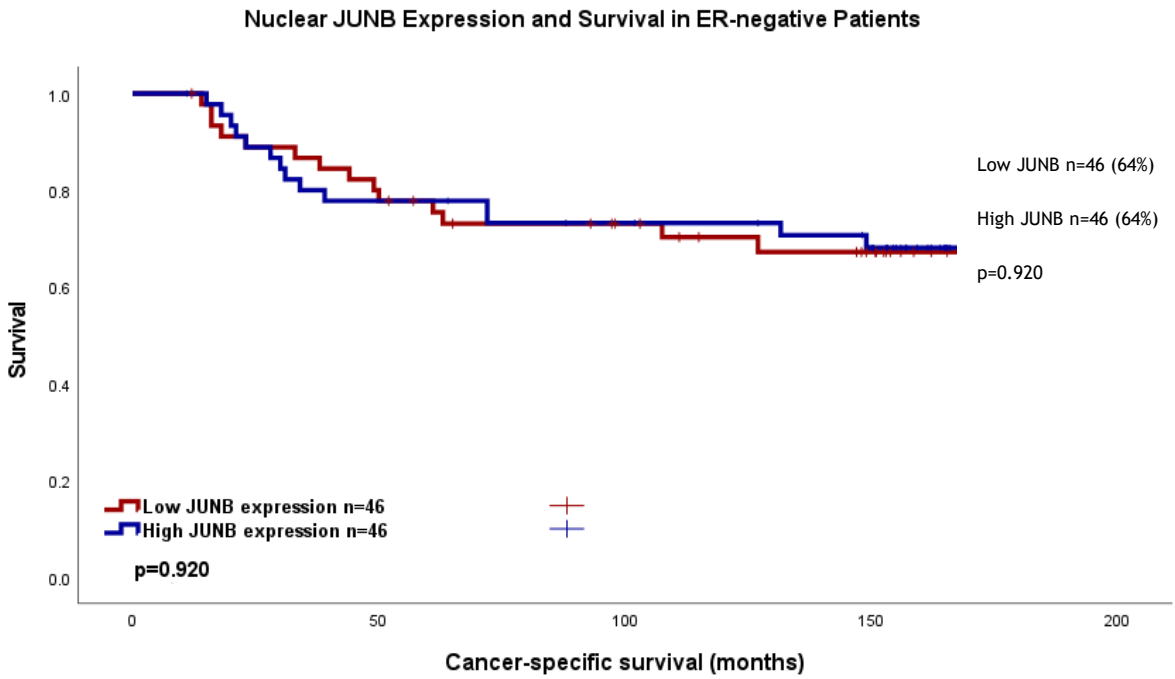

Figure 3-39 Cancer-specific survival in ER-negative patients in the Glasgow Breast Cancer Cohort according to JUNB nuclear expression. Kaplan Meier Curve showing the association between JUNB nuclear expression and survival (months). HR 0.963 95% C.I. 0.459-2.022, p=0.920.

Within the ER-negative group, inter-factor correlation was assessed when comparing the high and low JUNB nuclear expressors, (*Table 3-3*). Here, no association was identified with JUNB nuclear expression.

Table 3-12 Clinicopathological factors and their relation to JUNB nuclear expression in ER-negative patients in the Glasgow Breast Cancer Cohort. Chi-squared analysis.

Clinicopathological factor	JUNB Nuclear staining (%)		p
	Low	High	
Age (years)			
≤50	19(47.5)	21(52.5)	0.678
>50	28(52.8)	25(47.2)	
Tumour Size			
≤20mm	23(51.1)	22(48.9)	0.679

21-49mm	20(47.6)	22(52.4)	
≥50mm	4(66.7)	2(33.3)	
Grade			
I	2(100)	0	0.274
II	14(56)	11(44)	
III	31(47)	35(53)	
Nodal Status			
N_0	25(43.9)	32(56.1)	0.137
N_1	22(61.1)	14(38.9)	
Lymphatic Invasion			
Absent	10(55.6)	8(44.4)	0.710
Present	5(45.5)	6(54.5)	
Vascular Invasion			
Absent	14(56)	11(44)	0.330
Present	1(25)	3(75)	
Necrosis			
Absent	14(60.9)	9(39.1)	0.336
Present	32(46.4)	37(53.6)	
Klintrup Makinen			
0	3(75)	1(25)	
1	17(48.6)	18(51.4)	0.432
2	18(45)	22(55)	
3	8(66.7)	4(33.3)	
Ki67			
Low (<15%)	22(55)	18(45)	0.517
High (>15%)	21(45.7)	25(54.3)	
Tumour Bud			
-Low	36(48.6)	38(51.4)	0.793
-High	10(55.6)	8(44.4)	
Tissue Stroma Percentage			
Low	32(50.8)	31(49.2)	1.000
High	14(48.3)	15(51.7)	

In the ER-positive group (n=311), 234 had low nuclear JUNB expression, with 37 events, and 77 high JUNB expression, with 19 events. Survival in the low nuclear JUNB ER-positive group was 91% at 5 years and 80% at 10 years, and in the high JUNB group was 83% at 5 years and 69% at 10 years (HR 1.801, 95% C.I. 1.035-3.133, p=0.037), (*Figure 3-40*).

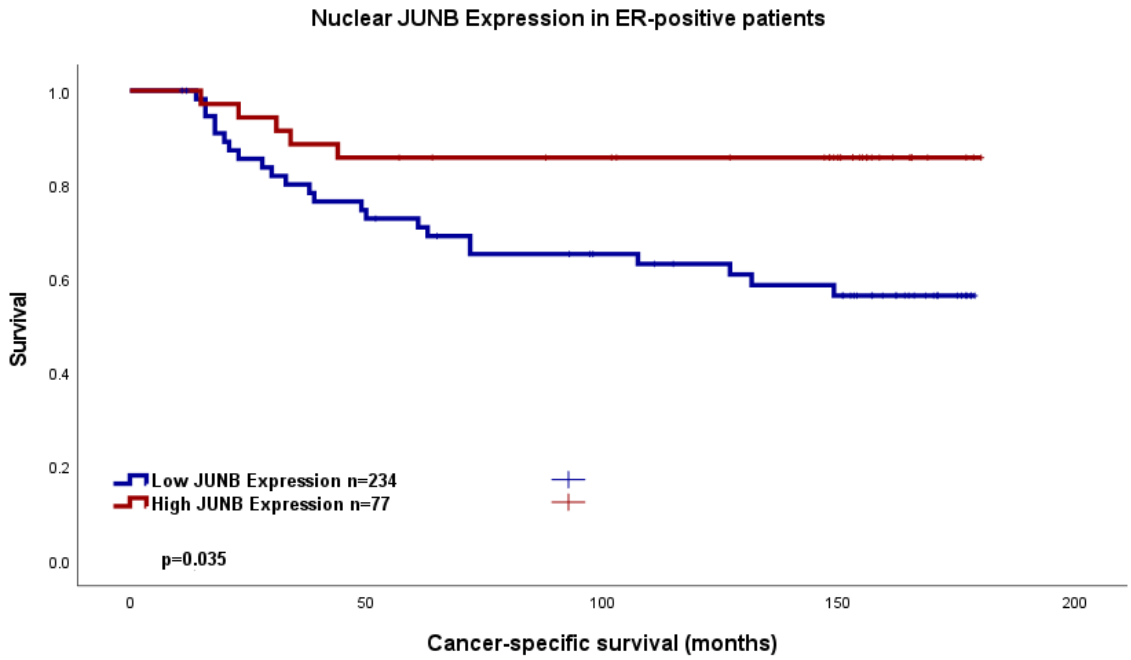

Figure 3-40 Cancer-specific survival in ER-positive patients in the Glasgow Breast Cancer Cohort according to JUNB nuclear expression. Kaplan Meier Curve showing the association between JUNB nuclear expression and survival (months). HR 1.801, 95% C.I. 1.035-3.133, p=0.037.

To further assess the effect of clinicopathological factors on survival in the ER-positive patients with the Glasgow Breast Cancer cohort, a Cox regression analysis was performed. (Table *3-13*). On multivariate analysis, only nodal status and Ki67, remained independently significant.

Table 3-13 Clinicopathological factors and their prognostic significance in the ER-positive patients within the Glasgow Breast Cancer Cohort. Univariate and multivariate Cox regression analysis

Clinicopathological Factor	Univariate analysis (HR, 95% C.I.)	p	Multivariate analysis (HR, 95% C.I.)	p
Age	0.951 (0.590-1.534)	0.838		
Tumour Size <20mm		**<0.001**		0.248
20-49mm	**2.283(1.465-3.558)**	**<0.001**	1.428(0.790-2.583)	0.239
>50mm	**4.371(1.939-9.854)**	**<0.001**	2.367(0.763-7.344)	0.136
Invasive Grade I		0.978		
II	23701(0-4.431^{E+63})	0.885		
III		0.885		

	24714.988(0-4.618^{E+63})			
Nodal Status	**3.427(2.179-5.390)**	**<0.001**	**2.647(1.454-4.820)**	**0.001**
Lymphatic Invasion	**3.331(1.872-5.926)**	**<0.001**	0.542(0.155-1.891)	0.336
Vascular Invasion	**2.599(1.292-5.228)**	**0.007**	0.800(0.287-2.225)	0.669
Necrosis	**2.720(1.754-4.216)**	**<0.001**	1.659(0.924-2.978)	0.090
Klintrup-Makinen 0 1 2 3	 0.579(0.331-1.010) 0.960(0.495-1.863) 0.336(0.098-1.148)	 0.066 0.054 0.903 0.082		
Ki67	**2.151(1.395-3.315)**	**<0.001**	**0.165(0.034-0.787)**	**0.024**
Tumour budding	1.468(0.957-2.252)	0.079	1.528(0.840-2.780)	0.165
Tumour stroma percentage	**1.812(1.174-2.796)**	**0.007**	1.317(0.723-2.401)	0.368
JUNB expression	**1.801(1.035-3.133)**	**0.037**	1.580 (0.874-2.854)	0.130

Within the ER-positive group, inter-factor correlation was assessed when comparing the high and low JUNB nuclear expressors, (*Table 3-14*Table 3-3). Here, tumour size and nodal status were associated with JUNB nuclear expression.

Table 3-14 Clinicopathological factors and their relation to JUNB nuclear expression in ER-positive patients in the Glasgow Breast Cancer Cohort. Chi-squared analysis.

Clinicopathological factor	**JUNB Nuclear staining (%)**		**p**
	Low	**High**	
Age (years)			
≤50	62(68.1)	29(31.9)	0.061
>50	179(78.5)	49(21.5)	
Tumour Size			
≤20mm	**152(80.4)**	**37(19.6)**	**<0.001**
21-49mm	**86(71.7)**	**34(28.3)**	
≥50mm	**3(30)**	**7(70)**	
Grade			
I	57(71.3)	23(28.8)	0.390
II	126(78.8)	34(21.3)	
III	58(73.4)	21(26.6)	

Nodal Status			
N_0	**145(78.8)**	**39(21.2)**	**0.025**
N_1	**94(72.9)**	**35(27.1)**	
Lymphatic Invasion			
Absent	93(70.9)	22(19.1)	0.561
Present	47(77)	14(23)	
Vascular Invasion			
Absent	124(79.5)	32(20.5)	1.000
Present	16(80)	4(20)	
Necrosis			
Absent	138(76.2)	43(23.8)	0.506
Present	92(72.4)	35(27.6)	
Klintrup Makinen			
0	35(77.8)	10(22.2)	0.318
1	142(76.8)	43(23.2)	
2	40(65.6)	21(34.4)	
3	15(78.9)	4(21.1)	
Ki67			
Low (<15%)	159(75)	53(25)	1.000
High (>15%)	75(75.8)	24(24.2)	
Tumour Bud			
-Low	148(75.5)	48(24.5)	0.893
-High	87(74.4)	30(25.6)	
Tissue Stroma Percentage			
Low	168(76.4)	52(23.6)	0.475
High	67(72)	26(28)	

Further stratification according to molecular subtype was then performed. These subtypes were divided into Luminal A, Luminal B, Triple-negative and HER-2 enriched groups. For 10 patients, molecular subgroup was not available. For the remaining patients, there were 189 Luminal A, 94 Luminal B, 97 TNBC and 48 HER-2 enriched cases. Luminal A patients had 142 low nuclear JUNB expressors with 16 events, and 47 high-JUNB expressors with 7 events. Luminal B patients had 84 low JUNB expressors with 20 events, and 30 high JUNB expressors with 12 events. The TNBC patients had 31 low JUNB expressors with 10 events, and 25 patients with high JUNB with 7 events. Finally, HER-2 enriched patients consisted of 14 low JUNB cases with 3 events, and 20 high JUNB cases with 7 events. Kaplan Meier curves are shown for each subgroup below.

Luminal A patients had a 5-year survival of 93% at 5 years and 86% at 10 years for low JUNB expressors, compared to 88% at 5 years and 83% at 10 years for high JUNB expressors. (HR 1.432, 95% C.I. 0.588-3.485, p=0.429). Mean survival for low JUNB nuclear expressors was 165.6 months, while for high JUNB expressors it was 161.4 months, with no survival benefit according to nuclear JUNB status (p=0.427), (*Figure 3-41*).

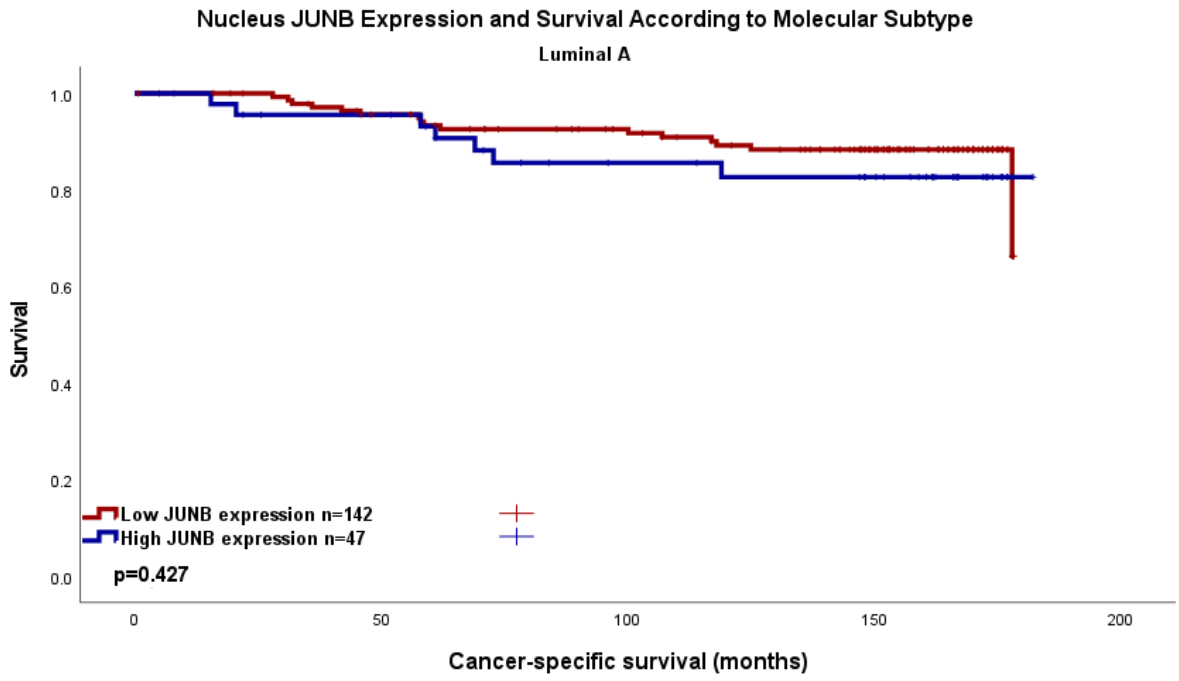

Figure 3-41 Cancer-specific survival in Luminal A patients in the Glasgow Breast Cancer Cohort according to JUNB nuclear expression. Kaplan Meier Curve showing the association between JUNB nuclear expression and survival (months). HR 1.432, 95% C.I. 0.588-3.485, p=0.429.

Within the Luminal A group, inter-factor correlation was assessed when comparing the high and low JUNB nuclear expressors, (*Table 3-15*). Here, tumour size and nodal status were associated with JUNB nuclear staining.

Table 3-15 Clinicopathological factors and their relation to JUNB nuclear expression in Luminal A patients in the Glasgow Breast Cancer Cohort. Chi-squared analysis.

Clinicopathological factor	JUNB Nuclear staining (%)		p
	Low	High	
Age (years)			
≤50	37(68.5)	17(31.5)	0.193
>50	111(111)	31(21.8)	
Tumour Size			
≤20mm	**98(81)**	**23(19)**	**0.027**
21-49mm	**48(68.6)**	**22(31.4)**	
≥50mm	**2(40)**	**3(60)**	
Grade			
I	45(70.3)	19(29.7)	0.425
II	80(79.2)	21(20.8)	
III	23(74.2)	8(25.8)	
Nodal Status			
N_0	**90(77.6)**	**26(22.4)**	**0.039**
N_1	**58(74.4)**	**20(25.6)**	
Lymphatic Invasion			

Absent	65(79.3)	17(20.7)	0.605
Present	28(84.8)	5(15.2)	
Vascular Invasion			
Absent	83(80.6)	20(19.4)	1.000
Present	10(83.3)	2(16.7)	
Necrosis			
Absent	91(74)	32(26)	0.862
Present	49(85.4)	16(24.6)	
Klintrup Makinen			
0	20(74.1)	7(25.9)	
1	92(76)	29(24)	0.641
2	22(66.7)	11(33.3)	
3	6(85.7)	1(14.3)	
Ki67			
Low (<15%)	148(75.5)	48(24.5)	n/a
High (>15%)	0	0	
Tumour Bud			
-Low	92(78)	26(22)	0.232
-High	51(69.9)	22(30.1)	
Tissue Stroma Percentage			
Low	98(76)	31(24)	0.722
High	45(72.6)	17(27.4)	

Luminal B patients had a 5-year survival of 89% At 5 years, and 69% at 10 years for low JUNB expressors, compared to 74% at 5 years and 49% at 10 years for high JUNB nuclear expressors. (HR 2.115, 95% C.I.; 1.032-4.334, p=0.041). Mean survival for low JUNB nuclear expressors was 153.5 months, while for high JUNB expressors it was 124.5 months, suggesting a survival benefit for low nuclear JUNB expressors (p=0.036), (*Figure 3-42*).

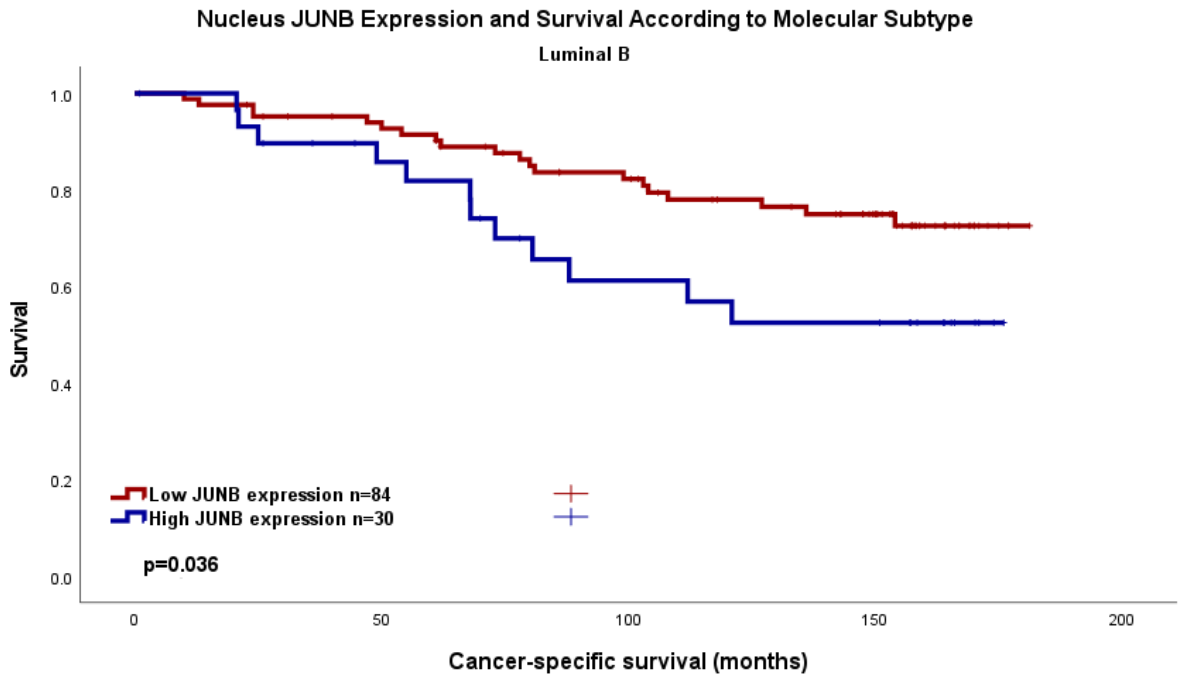

Figure 3-42 Cancer-specific survival in Luminal B patients in the Glasgow Breast Cancer Cohort according to JUNB nuclear expression. Kaplan Meier Curve showing the association between JUNB nuclear expression and survival (months). HR 2.115, 95% C.I.; 1.032-4.334, p=0.041.

To further assess the effect of clinicopathological factors on survival in the Luminal B patients with the Glasgow Breast Cancer cohort, a Cox regression analysis was performed. (Table 3-16). On multivariate analysis however, no factor was independently significant.

Table 3-16 Clinicopathological factors and their prognostic significance in the Luminal B patients within the Glasgow Breast Cancer Cohort. Univariate and multivariate Cox regression analysis.

Clinicopathological Factor	Univariate analysis (HR, 95% C.I.)	p	Multivariate analysis (HR, 95% C.I.)	p
Age	1.077(0.565-2.052)	0.823		
Tumour Size <20mm 20-49mm >50mm	 1.590(0.858-2.946) 2.908(0.983-8.601)	0.122 0.103 0.141 0.054		
Invasive Grade I II		0.191 0.194 0.744		

III	1.199(0.403-3.565) 1.972(0.684-5.688)	0.209		
Nodal Status	**3.062(1.645-5.700)**	**<0.001**	**2.886(1.045-7.970)**	**0.041**
Lymphatic Invasion	**3.901(1.711-8.897)**	**0.001**	2.369(0.800-7.014)	0.120
Vascular Invasion	1.643(0.666-4.054)	0.281		
Necrosis	**2.456(1.287-4.685)**	**0.006**	0.927(0.348-2.468)	0.880
Klintrup-Makinen 0 1 2 3	 0.645(0.287-1.449) 0.994(0.287-2.399) 0.269(0.057-1.267)	0.169 0.232 0.288 0.989 0.097		
Ki67	0.977(0.418-2.335)	0.979		
Tumour budding	1.461(0.811-2.630)	0.207		
Tumour stroma percentage	1.771(0.960-3.266)	0.067		
JUNB expression	**2.115(1.032-4.334)**	**0.041**	1.172(0.409-3.353)	0.768

Within the Luminal B group, inter-factor correlation was assessed when comparing the high and low JUNB nuclear expressors, (*Table 3-17*). Here, tumour size and nodal status were associated with JUNB nuclear staining.

Table 3-17 Clinicopathological factors and their relation to JUNB nuclear expression in Luminal B patients in the Glasgow Breast Cancer Cohort. Chi-squared analysis.

Clinicopathological factor	**JUNB Nuclear staining (%)**		**p**
	Low	**High**	
Age (years)			
≤50	25(65.8)	13(34.2)	0.122
>50	60(77.9)	17(22.1)	
Tumour Size			
≤20mm	**48(78.7)**	**13(21.3)**	**0.004**
21-49mm	**36(75)**	**12(25)**	
≥50mm	**1(16.7)**	**5(83.3)**	
Grade			
I	10(71.4)	4(28.6)	0.671
II	42(77.8)	12(22.2)	
III	33(70.2)	14(29.8)	
Nodal Status			
N_0	49(80.3)	12(19.7)	0.097

N_1	35(68.6)	16(31.4)	
Lymphatic Invasion			
Absent	25(83.3)	5(16.7)	0.143
Present	19(67.9)	9(32.1)	
Vascular Invasion			
Absent	38(76)	12(24)	0.628
Present	6(75)	2(25)	
Necrosis			
Absent	43(79.6)	11(20.4)	0.113
Present	40(67.8)	19(32.2)	
Klintrup Makinen			
0	13(81.3)	3(18.7)	
1	13(81.2)	3(18.8)	0.254
2	47(78.3)	13(21.7)	
3	16(59.3)	11(40.7)	
Ki67			
Low (<15%)	10(66.7)	5(33.3)	0.344
High (>15%)	75(75)	25(25)	
Tumour Bud			
-Low	50(69.4)	22(30.6)	0.116
-High	35(81.4)	8(18.6)	
Tissue Stroma Percentage			
Low	64(75.3)	21(24.7)	0.366
High	21(70)	9(30)	

TNBC patients had a 5-year survival of 74% At 5 years, and 61% at 10 years for low JUNB expressors, compared to 83% at 5 years and 66% at 10 years for high JUNB nuclear expressors. (HR 0.836, 95% C.I.; 0.317-2.201, p=0.717). Mean survival for low JUNB nuclear expressors was 136.9 months, while for high JUNB expressors it was 140.1 months, (p=0.716), (*Figure 3-43*).

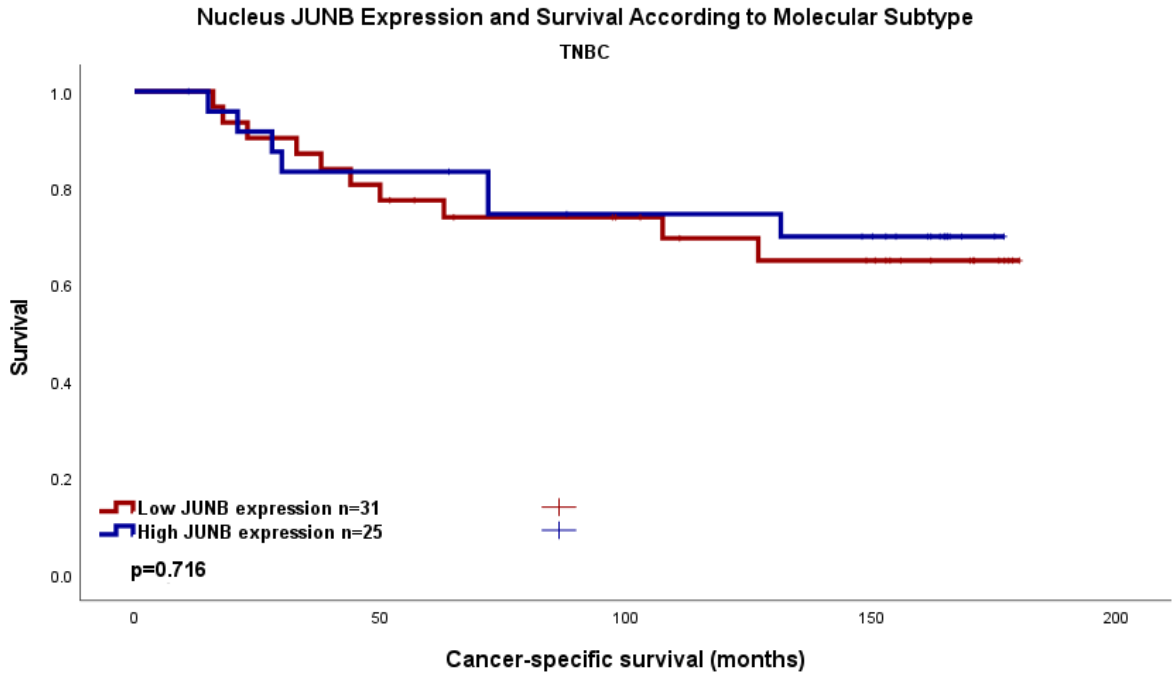

Figure 3-43 Cancer-specific survival in TNBC patients in the Glasgow Breast Cancer Cohort according to JUNB nuclear expression. Kaplan Meier Curve showing the association between JUNB nuclear expression and survival (months). HR 0.836, 95% C.I.; 0.317-2.201, p=0.717.

Within the TNBC group, inter-factor correlation was assessed when comparing the high and low JUNB nuclear expressors, (*Table 3-17*). Here, no association with JUNB nuclear staining was identified.

Table 3-18 Clinicopathological factors and their relation to JUNB nuclear expression in TNBC patients in the Glasgow Breast Cancer Cohort. Chi-squared analysis.

Clinicopathological factor	JUNB Nuclear staining (%)		p
	Low	High	
Age (years)			
≤50	14(51.9)	13(48.1)	0.788
>50	17(58.6)	12(41.4)	
Tumour Size			
≤20mm	16(59.3)	11(40.7)	0.851
21-49mm	14(51.9)	13(48.1)	
≥50mm	1(50)	1(50)	
Grade			
I	2(100)	0	0.367
II	9(60)	6(40)	
III	20(51.3)	19(48.7)	
Nodal Status			
N_0	18(51.4)	17(48.6)	0.580
N_1	13(61.9)	8(38.1)	
Lymphatic Invasion			
Absent	6(545)	5(45.5)	1.000
Present	3(60)	2(40)	

Vascular Invasion			
Absent	9(64.3)	5(35.7)	0.175
Present	0	2(100)	
Necrosis			
Absent	11(57.9)	8(42.1)	0.781
Present	19(52.8)	17(47.2)	
Klintrup Makinen			
0	3(75)	1(25)	
1	12(50)	12(50)	0.736
2	11(52.4)	10(47.6)	
3	4(66.7)	2(33.3)	
Ki67			
Low (<15%)	15(57.7)	11(42.3)	1.000
High (>15%)	13(54.2)	11(45.8)	
Tumour Bud			
-Low	23(54.8)	19(45.2)	1.000
-High	7(53.8)	6(46.2)	
Tissue Stroma Percentage			
Low	24(55.8)	19(44.2)	0.753
High	6(50)	6(50)	

HER-2 enriched patients had a 5-year survival of 77% At 5 years and 10 years for low JUNB expressors, compared to 70% at 5 years and 60% at 10 years for high JUNB nuclear expressors. (HR 1.473, 95% C.I.; 0.380-5.709, p=0.575). Mean survival for low JUNB nuclear expressors was 143 months, while for high JUNB expressors it was 131.5 months, (p=0.573), (*Figure 3-44*).

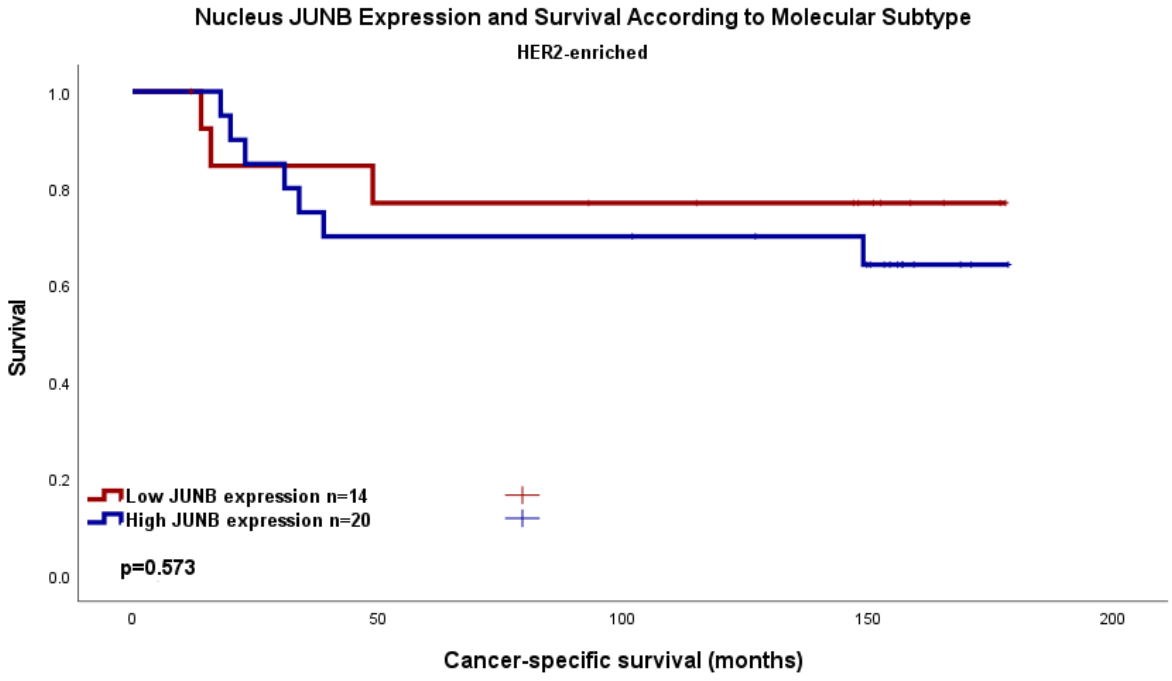

Figure 3-44 Cancer-specific survival in HER-2 enriched patients in the Glasgow Breast Cancer Cohort according to JUNB nuclear expression. Kaplan Meier Curve showing the association

between JUNB nuclear expression and survival (months). HR 1.473, 95% C.I.; 0.380-5.709, p=0.575.

Within the HER2-enriched group, inter-factor correlation was assessed when comparing the high and low JUNB nuclear expressors, (Table 3-19). Here, no association with JUNB nuclear staining was identified.

Table 3-19 Clinicopathological factors and their relation to JUNB nuclear expression in HER2-enriched patients in the Glasgow Breast Cancer Cohort. Chi-squared analysis.

Clinicopathological factor	JUNB Nuclear staining (%)		p
	Low	High	
Age (years)			
≤50	4(36.4)	7(63.6)	1.000
>50	10(43.5)	13(56.5)	
Tumour Size			
≤20mm	6(35.3)	11(64.7)	0.095
21-49mm	5(35.7)	9(64.3)	
≥50mm	3(100)	0	
Grade			
I	0	0	0.704
II	5(50)	5(50)	
III	9(37.5)	15(62.5)	
Nodal Status			
N_0	7(31.8)	15(68.2)	0.163
N_1	7(58.3)	5(41.7)	
Lymphatic Invasion			
Absent	4(57.1)	3(42.9)	0.293
Present	1(20)	4(80)	
Vascular Invasion			
Absent	5(45.5)	6(54.5)	1.000
Present	0	1(100)	
Necrosis			
Absent	2(66.7)	1(54.5)	0.555
Present	12(38.7)	19(61.3)	
Klintrup Makinen			
0	0	0	0.398
1	3(33.3)	6(66.7)	
2	7(38.9)	11(61.1)	
3	4(66.7)	2(33.3)	
Ki67			
Low (<15%)	6(46.2)	7(53.8)	0.717
High (>15%)	7(35)	13(65)	
Tumour Bud			
-Low	11(37.9)	18(62.1)	0.627
-High	3(60)	2(40)	
Tissue Stroma Percentage			
Low	7(38.9)	11(61.1)	1.000
High	7(43.8)	9(56.3)	

3.2.15 JUNB Expression in the Glasgow Breast Cancer Cohort - Combined Scoring

Weighted histoscores for nuclear and cytoplasm expression of JUNB were combined to create four categories: JUNB high nuclear:high cytoplasm (HNHC, All High), JUNB high nuclear:low cytoplasm (HNLC), JUNB low nuclear: high cytoplasm(LNHC), and JUNB low nuclear: low cytoplasm(LNLC, All-Low), to assess whether more prognostic power could be conferred to JUNB protein expression on cancer-specific survival. 403 patients had valid survival data. 57 patients had All High phenotype with 9 events, 66 had HNLC and 24 events, and 26 had LNHC with 2 events, while 254 had All Low with 49 events.

In the All-High group 5-year survival was 85%- and 10-year survival 83%. The HNLC group had a 5-year survival of 77% and 10-year survival of 54%. The LNHC group had a 5-year survival of 96% and 10-year survival of 91%. The All-Low group had a 5-year survival of 88%, with 10-year survival at 76%, (Figure 3-45).

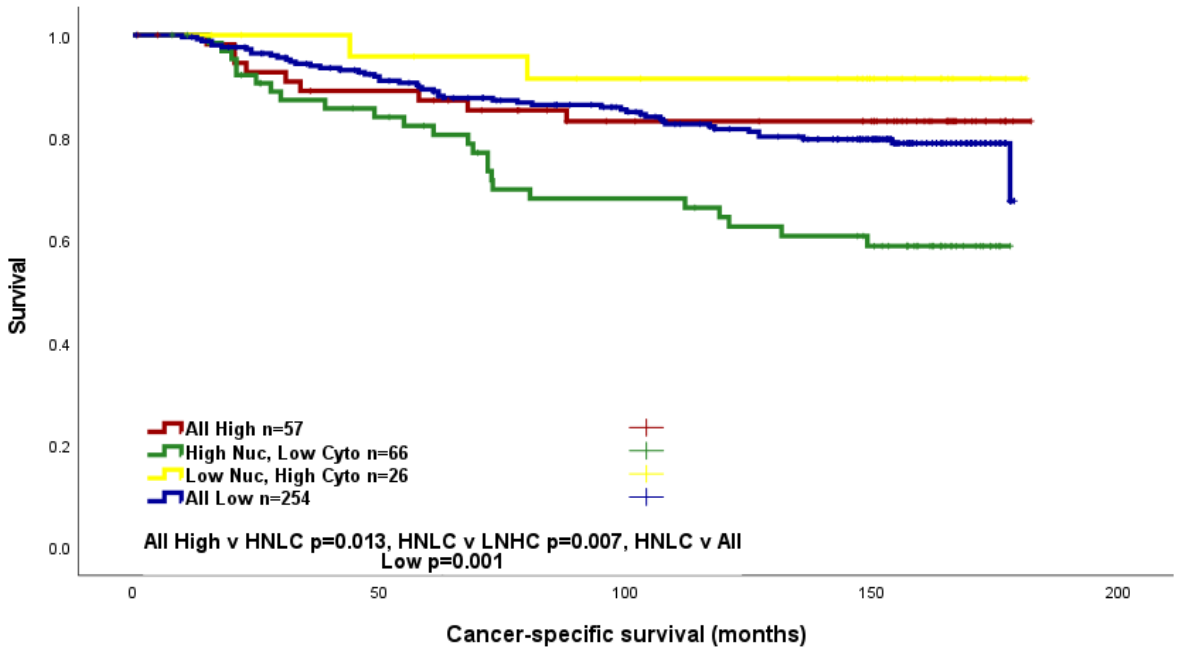

Figure 3-45 Combined Nuclear and Cytoplasmic JUNB expression and survival in the Glasgow Breast Cancer Cohort. Pairwise comparisons are described in the graph.

Pairwise comparison demonstrated that HNLC had statistically significant worse survival than the other three groups, (*Table 3-20*).

Table 3-20 Pairwise comparisons on Kaplan Meier survival analysis for combined nuclear and cytoplasmic JUNB expression

Pairwise Comparison p=	1 HNHC	2 HNLC	3 LNHC	4 LNLC
1 HNHC		**0.013**	0.307	0.646
2 HNLC	**0.013**		**0.007**	**0.001**
3 LNHC	0.307	**0.007**		0.155
4 LNLC	0.646	**0.001**	0.155	

On multivariate analysis however, JUNB combined scoring did not remain statistically significant, (*Table 3-21*).

Table 3-21 Clinicopathological factors and their prognostic significance in the Glasgow Breast Cancer Cohort with regards to combined nuclear and cytoplasmic JUNB scoring. Univariate and multivariate Cox regression analysis.

Clinicopathological Factor	**Univariate analysis (HR, 95% C.I.)**	**p**	**Multivariate analysis (HR, 95% C.I.)**	**p**
Age	0.951 (0.590-1.534)	0.838		
Tumour Size <20mm 20-49mm >50mm	**2.170 (1.552-3.033)**	**<0.001**	 1.164(0.523-2.588) 1.759(0.314-9.862)	 0.799 0.710 0.521
Invasive Grade I II III	**1.862(1.352-2.564)**	**<0.001**	 1.489(0.389-5.702) 1.160(0.294-4.569)	 0.777 0.561 0.832
Nodal Status	1.009 (0.991-1.027)	0.329		
Molecular Subtype Luminal A Luminal B TNBC HER2-enriched	**2.116 (1.193-3.751)**	**0.010**	 **3.567(0.720-17.680)** **4.373(0.826-23.153)** **13.810(2.463-77.424)**	 **0.024** **0.119** **0.083** **0.003**

Lymphatic Invasion	**3.331 (1.872-5.926)**	**<0.001**	3.251(1.227-8.611)	**0.018**
Vascular Invasion	**2.599 (1.292-5.228)**	**0.007**	1.282(0.485-3.386)	0.617
Necrosis	**2.720 (1.754-4.216)**	**<0.001**	1.480(0.642-3.415)	0.358
Klintrup-Makinen 0 1 2 3	0.869 (0.644-1.174)	0.361		
Ki67	**2.151 (1.395-3.315)**	**<0.001**	1.344(0.327-5.528)	0.682
Tumour budding	**2.320 (1.506-3.575)**	**<0.001**	**2.772(1.115-6.893)**	**0.028**
Tumour stroma percentage	1.468 (0.957-2.252)	0.079	1.860(0.809-4.276)	0.144
JUNB combined score HNLC HNLC v All High HNLC v LNHC HNLC v All Low	 **2.571(1.195-5.534)** **0.445(0.096-2.059)** **1.180(0.580-2.402)**	**0.004** **0.003** **0.016** **0.300** **0.648**	 3.397(0.706-16.354) 0(0) 1.625(0.382-6.921)	 0.439 0.127 0.978 0.511

Examining the relationship between clinicopathological factors and patients in the different combined score groups, tumour size, grade, nodal status, molecular subtype, necrosis, and KM score appeared significantly correlated to combined score, (Table 3-22).

Table 3-22 Clinicopathological factors and their relation to JUNB combined nuclear and cytoplasmic expression in the Glasgow Breast Cancer Cohort. Chi-squared analysis.

Clinicopathological factor	**JUNB Combined Cytoplasmic and Nuclear staining (%)**				**p**
	HNHC	**HNLC**	**LNHC**	**LNLC**	
Age (years)					0.086
≤50	23(17.6)	27(20.6)	9(6.9)	72(55)	
>50	36(12.8)	38(13.5)	17(6)	190(67.6)	

Tumour Size					**0.041**
≤20mm	**25(10.7)**	**34(14.5)**	**13(5.6)**	**162(69.2)**	
21-49mm	**29(17.9)**	**27(16.7)**	**13(8)**	**93(57.4)**	
≥50mm	**5(31.3)**	**4(25)**	**0**	**7(43.8)**	
Grade					**0.017**
I	**12(14.6)**	**11(13.4)**	**2(2.4)**	**57(69.5)**	
II	**25(13.5)**	**20(10.8)**	**12(6.5)**	**128(69.2)**	
III	**22(15.2)**	**34(23.4)**	**12(8.3)**	**77(53.1)**	
Nodal Status					**0.011**
N_0	**38(15.8)**	**33(13.7)**	**20(8.3)**	**150(62.2)**	
N_1	**18(10.9)**	**31(18.8)**	**5(3.0)**	**111(67.3)**	
Molecular Subtype					**<0.001**
Luminal A	**23(11.7)**	**25(12.8)**	**10(5.1)**	**138(70.4)**	
Luminal B	**12(10.4)**	**18(15.7)**	**5(4.3)**	**80(69.6)**	
TNBC	**12(21.4)**	**13(23.2)**	**7(12.5)**	**24(42.9)**	
HER-2 enriched	**12(35.3)**	**8(23.5)**	**4(12.5)**	**10(29.4)**	
Lymphatic Invasion					0.851
Absent	16(13.3)	14(13.2)	9(4.9)	94(6.8)	
Present	10(13.9)	10(13.9)	4(5.6)	48(66.7)	
Vascular Invasion					0.463
Absent	24(13.3)	19(10.5)	12(6.6)	126(69.6)	
Present	2(8.3)	5(20.8)	1(4.2)	16(66.7)	
Necrosis					**0.028**
Absent	**25(12.3)**	**27(13.2)**	**10(4.9)**	**142(69.6)**	
Present	**34(17.3)**	**38(19.4)**	**16(8.2)**	**108(55.1)**	
Klintrup Makinen					**0.026**
0	**3(6.1)**	**8(16.3)**	**4(8.2)**	**34(69.4)**	
1	**33(15.0)**	**28(12.7)**	**10(4.5)**	**149(67.7)**	
2	**19(18.8)**	**24(23.8)**	**6(5.9)**	**52(51.5)**	
3	**3(9.7)**	**5(16.1)**	**5(16.1)**	**18(58.1)**	
Ki67					0.689
Low (<15%)	34(13.5)	37(14.7)	17(6.7)	164(65.1)	
High (>15%)	23(15.9)	26(17.9)	8(5.5)	88(60.7)	
Tumour Bud					0.694

-Low	40(14.8)	46(17.0)	19(7.0)	165(61.1)	
-High	19(14.1)	19(14.1)	7(5.2)	90(66.7)	
Tissue Stroma Percentage					0.397
Low	42(14.8)	41(14.5)	16(5.7)	184(65.0)	
High	17(13.9)	24(19.7)	10(8.2)	71(58.2)	

When stratifying according to molecular subtype, Luminal A patients had a 5-year survival of 90%- and 10-year survival of 90% for the All High group , 5-year survival of 86% and 10-year survival of 75% for the HNLC group, a 5-year survival of 100%- and 10-year survival of 100% for the LNHC group and a 5-year survival of 92% and 10 year survival of 85% for the All Low group, (*Figure 3-46*).

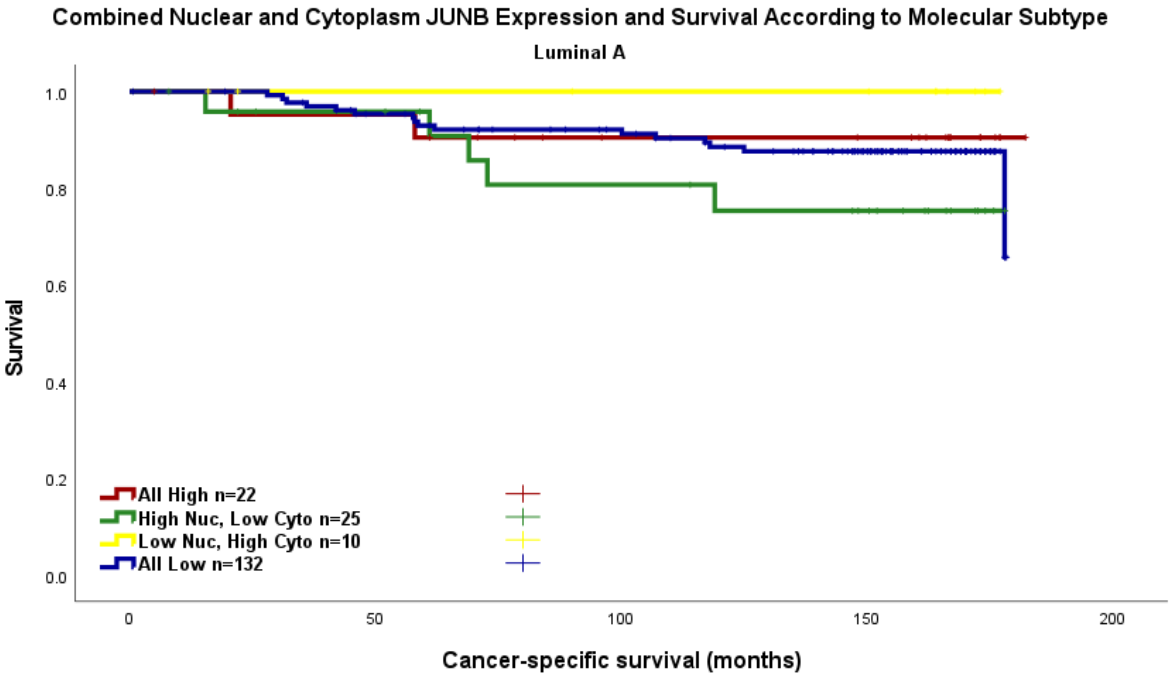

Figure 3-46 Combined Nuclear and Cytoplasm JUNB expression and survival in the Luminal A patients within the Glasgow Breast Cancer Cohort. Pairwise comparisons are described in the graph.

Pairwise comparison demonstrated no significant difference in survival between the combined score subgroups in the luminal A patients,(Table 3-23).

Table 3-23 Pairwise comparisons on Kaplan Meier survival analysis for combined nuclear and cytoplasmic JUNB expression in Luminal A patients.

Pairwise Comparison p=	1 HNHC	2 HNLC	3 LNHC	4 LNLC
1 HNHC		0.281	0.363	0.740

2 HNLC	0.281		0.136	0.208
3 LNHC	0.363	0.136		0.316
4 LNLC	0.740	0.208	0.316	

Examining the relationship between clinicopathological factors and patients in the different combined score groups in the Luminal A patients, none of the other factors correlated significantly with combined score, (Table 3-24).

Table 3-24 Clinicopathological factors and their relation to JUNB combined nuclear and cytoplasmic expression in the Luminal A patients in the Glasgow Breast Cancer Cohort. Chi-squared analysis.

Clinicopathological factor	JUNB Combined Cytoplasmic and Nuclear staining (%)				p
	HNHC	HNLC	LNHC	LNLC	
Age (years)					
≤50	10(18.5)	7(13.0)	1(1.9)	36(66.7)	0.202
>50	13(9.2)	18(12.7)	9(6.3)	102(71.8)	
Tumour Size					
≤20mm	11(9.1)	12(9.9)	4(3.3)	94(77.7)	0.076
21-49mm	11(15.7)	11(15.7)	6(8.6)	42(60.0)	
≥50mm	1(20.0)	2(40.0)	0	2(40.0)	
Grade					
I	11(17.2)	8(12.5)	2(3.1)	43(67.2)	0.271
II	11(10.9)	10(9.9)	6(5.9)	74(73.3)	
III	1(3.2)	7(22.6)	2(6.5)	21(67.7)	
Nodal Status					
N_0	14(12.1)	12(10.3)	8(6.9)	82(70.7)	0.172
N_1	8(10.3)	12(15.4)	2(2.6)	56(71.8)	
Lymphatic Invasion					
Absent	9(11.0)	8(9.8)	3(3.7)	62(75.6)	0.437
Present	4(12.1)	1(3.0)	3(9.1)	25(75.8)	
Vascular Invasion					
Absent	13(12.6)	7(6.8)	6(5.8)	77(74.8)	0.301
Present	0	2(16.7)	0	10(83.3)	
Necrosis					
Absent	17(13.8)	15(12.2)	8(6.5)	83(67.5)	0.544
Present	6(9.2)	10(15.4)	2(3.1)	47(72.3)	
Klintrup Makinen					
0	2(7.4)	5(18.5)	2(7.4)	18(66.7)	0.508
1	17(13.8)	12(12.2)	6(6.5)	86(71.1)	
2	4(12.1)	7(21.2)	0	22(66.7)	
3	0	1(14.3)	1(14.3)	5(71.4)	
Ki67					
Low (<15%)	23(11.7)	25(12.8)	10(5.1)	138(70.4)	n/a
High (>15%)	0	0	0	0	
Tumour Bud					
-Low	12(10.2)	14(11.9)	5(4.2)	87(73.7)	0.460
-High	11(15.1)	11(15.1)	5(6.8)	46(63.0)	
Tissue Stroma Percentage					

Low	17(13.2)	14(10.9)	7(5.4)	91(70.5)	0.568
High	6(9.7)	11(17.7)	3(4.8)	42(67.7)	

When stratifying according to molecular subtype, Luminal B patients had a 5-year survival of 79- and 10-year survival of 66% for the All High group, 5-year survival of 71% and 10-year survival of 52% for the HNLC group, a 5-year survival of 100%- and 10-year survival of 80% for the LNHC group and a 5-year survival of 88% and 10 year survival of 69% for the LNLC group, (*Figure 3-47*).

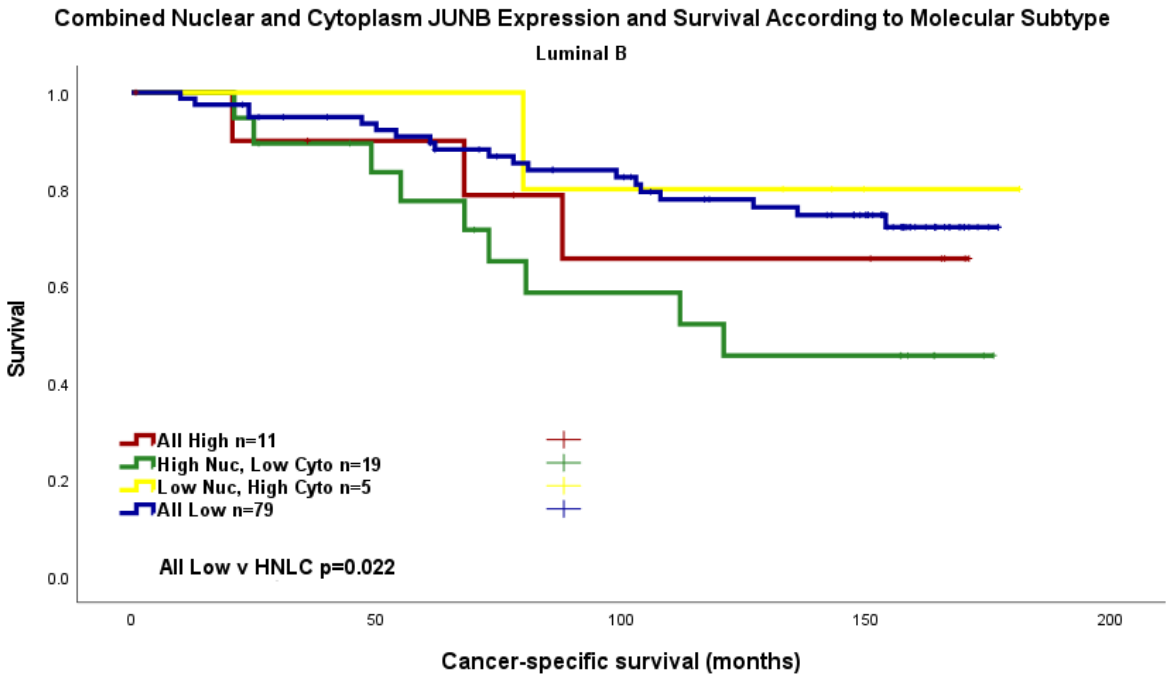

Figure 3-47 Combined nuclear and cytoplasm JUNB expression and survival in the Luminal B patients within the Glasgow Breast Cancer Cohort Pairwise comparisons are described in the graph.

Pairwise comparison demonstrated that the HNLC group had significantly worse survival than the All-Low group in the luminal B patients, (*Table 3-25*).

Table 3-25 Pairwise comparisons on Kaplan Meier survival analysis for combined nuclear and cytoplasmic JUNB expression in Luminal B patients.

Pairwise Comparison p=	1 HNHC	2 HNLC	3 LNHC	4 LNLC
1 HNHC		0.418	0.556	0.582
2 HNLC	0.418		0.205	**0.022**
3 LNHC	0.556	0.205		0.774
4 LNLC	0.582	**0.022**	0.774	

On multivariate analysis however, JUNB combined scoring did not remain statistically significant, (Table 3-26).

Table 3-26 Clinicopathological factors and their prognostic significance in the Luminal B patients within the Glasgow Breast Cancer Cohort with regards to combined nuclear and cytoplasmic JUNB scoring. Univariate and multivariate Cox regression analysis.

Clinicopathological Factor	Univariate analysis (HR, 95% C.I.)	p	Multivariate analysis (HR, 95% C.I.)	p
Age	1.077(0.565-2.052)	0.823		
Tumour Size		0.122		
<20mm		0.103		
20-49mm	1.590(0.858-2.946)	0.141		
>50mm	2.908(0.983-8.601)	0.054		
Invasive Grade		0.191		
I		0.194		
II	1.199(0.403-3.565)	0.744		
III	1.972(0.684-5.688)	0.209		
Nodal Status	**3.062(1.645-5.700)**	**<0.001**	2.548(0.913-7.111)	0.074
Lymphatic Invasion	**3.901(1.711-8.897)**	**0.001**	2.404(0.822-7.032)	0.109
Vascular Invasion	1.643(0.666-4.054)	0.281		
Necrosis	**2.456(1.287-4.685)**	**0.006**	1.100(0.410-2.955)	0.850
Klintrup-Makinen		0.169		
0		0.232		
1	0.645(0.287-1.449)	0.288		
2	0.994(0.287-2.399)	0.989		
3	0.269(0.057-1.267)	0.097		
Ki67	0.977(0.418-2.335)	0.979		
Tumour budding	1.461(0.811-2.630)	0.207		
Tumour stroma percentage	1.771(0.960-3.266)	0.067		
JUNB combined score		**0.195**		
All Low		**0.153**		0.906
All Low v All High	**1.421(0.420-4.805)**	**0.572**	0(0)	0.988
All Low v HNLC	**2.457(1.109-5.442)**	**0.027**	1.496(0.519-4.309)	0.456

All Low v LNHC	**0.733(0.098-5.478)**	**0.762**	0(0)	0.989

Examining the relationship between clinicopathological factors and patients in the different combined score groups in the Luminal B patients, tumour size and nodal status correlated with combined score, (Table 3-27).

Table 3-27 Clinicopathological factors and their relation to JUNB combined nuclear and cytoplasmic expression in the Luminal B patients in the Glasgow Breast Cancer Cohort. Chi-squared analysis.

Clinicopathological factor	**JUNB Combined Cytoplasmic and Nuclear staining (%)**				**p**
	HNHC	**HNLC**	**LNHC**	**LNLC**	
Age (years)					
≤50	3(7.9)	10(26.3)	2(5.3)	23(60.5)	0.154
>50	9(11.7)	8(10.4)	3(3.9)	57(74.0)	
Tumour Size					
≤20mm	**3(4.9)**	**10(16.4)**	**3(4.9)**	**45(73.8)**	**0.017**
21-49mm	**6(12.5)**	**6(12.5)**	**2(4.2)**	**34(70.8)**	
≥50mm	**3(50.0)**	**2(33.3)**	**0**	**1(16.7)**	
Grade					
I	1(7.1)	3(21.4)	0	10(71.4)	0.870
II	6(11.1)	6(11.1)	3(5.6)	39(72.2)	
III	5(10.6)	9(19.1)	2(4.3)	31(66.0)	
Nodal Status					
N_0	**5(8.2)**	**7(11.5)**	**4(6.6)**	**45(73.8)**	**<0.001**
N_1	**5(9.8)**	**11(21.6)**	**0**	**35(68.6)**	
Lymphatic Invasion					
Absent	1(3.3)	4(13.3)	2(6.7)	23(76.7)	0.325
Present	2(7.1)	7(25.0)	0	19(67.9)	
Vascular Invasion					
Absent	3(6.0)	9(13.0)	1(1.9)	37(74)	0.393
Present	0	2(25.0)	1(12.5)	5(62.5)	
Necrosis					
Absent	4(7.4)	7(13.0)	1(1.9)	42(77.8)	0.234
Present	8(13.6)	11(18.6)	4(6.8)	36(61.0)	
Klintrup Makinen					
0	1(6.2)	2(12.5)	2(12.5)	11(68.8)	
1	6(10.0)	7(11.7)	1(1.7)	46(76.7)	0.487
2	4(14.8)	7(25.9)	1(3.7)	15(55.6)	
3	1(8.3)	2(16.7)	1(8.3)	8(66.7)	
Ki67					
Low (<15%)	1(6.7)	4(26.7)	1(6.7)	9(60)	0.570
High (>15%)	11(11.0)	14(14.0)	4(4.0)	71(71.0)	
Tumour Bud					
-Low	9(12.5)	13(18.1)	3(4.2)	47(65.3)	0.568
-High	3(7.0)	5(11.6)	2(4.7)	33(76.7)	
Tissue Stroma Percentage					

Low	7(8.2)	14(16.5)	4(4.7)	60(70.6)	0.616
High	5(16.7)	4(13.3)	1(3.3)	20(66.7)	

TNBC patients had a 5-year survival of 92%- and 10-year survival of 92% for the All High group, a 5-year survival of 75% and 10-year survival of 44% for the HNLC group, a 5-year survival of 86% and 10-year survival of 86% for the LNHC group and a 5-year survival of 70% and 10 year survival of 54% for the All Low group, (Figure 3-48).

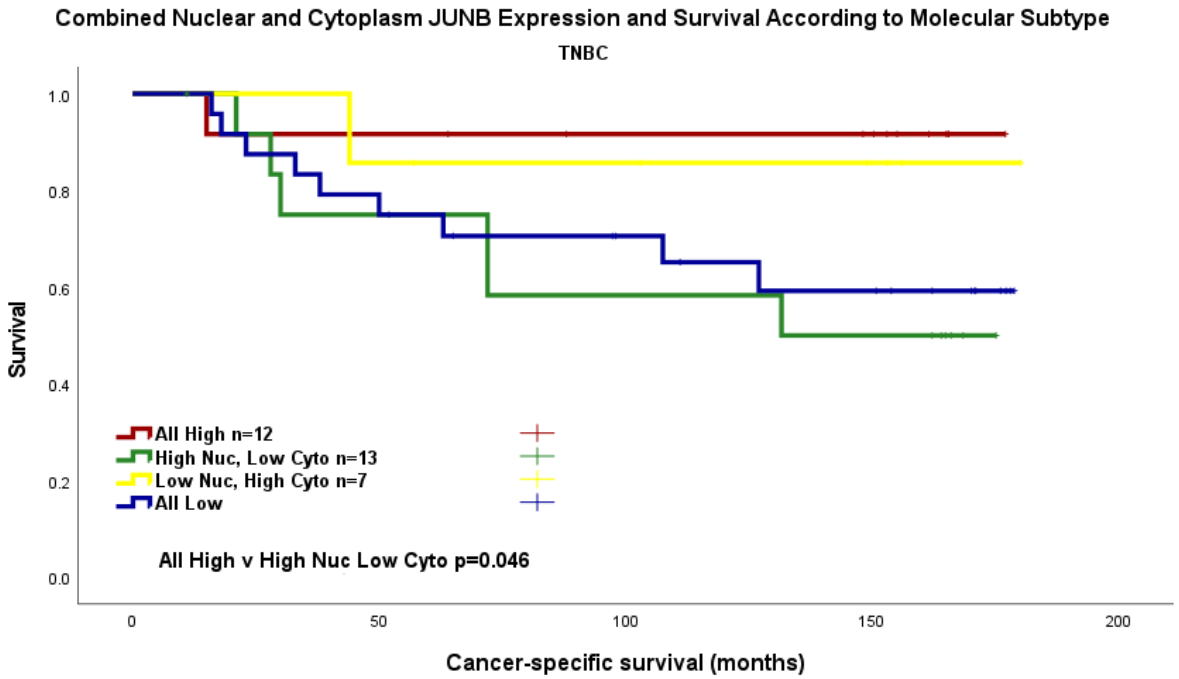

Figure 3-48 Combined nuclear and cytoplasm JUNB expression and survival in the TNBC patients within the Glasgow Breast Cancer Cohort Pairwise comparisons are described in the graph.

Pairwise comparison demonstrated that the HNLC group had significantly worse survival than the All-High group in the TNBC patients, (*Table 3-28*).

Table 3-28 Pairwise comparisons on Kaplan Meier survival analysis for combined nuclear and cytoplasmic JUNB expression in TNBC patients.

Pairwise Comparison p=	1 HNHC	2 HNLC	3 LNHC	4 LNLC
1 HNHC		**0.046**	0.723	0.083
2 HNLC	**0.046**		0.185	0.287
3 LNHC	0.723	0.185		0.666
4 LNLC	0.083	0.287	0.666	

On Cox regression analysis, All High vs HNLC survival was no longer statistically significant however (HR 6.721(95% C.I. 0.809-55.872), p=0.078) therefore no multivariate analysis was performed.

Within the TBNC group, inter-factor correlation was assessed when comparing the different combined score groups, (*Table 3-29*). Here, no association was identified.

Table 3-29 Clinicopathological factors and their relation to JUNB combined nuclear and cytoplasmic expression in the TNBC patients in the Glasgow Breast Cancer Cohort. Chi-squared analysis.

Clinicopathological factor	JUNB Combined Cytoplasmic and Nuclear staining (%)				p
	HNHC	HNLC	LNHC	LNLC	
Age (years)					
≤50	6(22.2)	7(25.9)	5(18.5)	9(33.3)	0.424
>50	6(20.7)	6(20.7)	2(6.9)	15(51.7)	
Tumour Size					
≤20mm	6(22.2)	5(18.50	3(11.1)	13(48.1)	0.822
21-49mm	5(18.5)	8(29.6)	4(14.8)	10(37.0)	
≥50mm	1(50.0)	0	0	1(50.0)	
Grade					
I	0	0	0	2(100)	0.231
II	5(33.3)	1(6.7)	1(6.7)	8(53.3)	
III	7(17.9)	12(30.8)	6(15.4)	14(35.9)	
Nodal Status					
N_0	11(31.40	6(17.1)	4(11.4)	14(40.0)	0.107
N_1	1(4.8)	7(33.3)	3(14.3)	10(47.6)	
Lymphatic Invasion					
Absent	4(36.4)	1(9.1)	3(27.3)	3(27.3)	0.832
Present	1(20.0)	1(20.0)	1(20.0)	2(40.0)	
Vascular Invasion					
Absent	4(28.6)	1(7.1)	4(28.6)	5(35.7)	0.249
Present	1(50.0)	1(50.0)	0	0	
Necrosis					
Absent	3(15.8)	5(26.3)	1(5.3)	10(52.6)	0.448
Present	9(25.0)	8(22.2)	6(16.7)	13(36.1)	
Klintrup Makinen					
0	0	6(50)	5(41.7)	1(8.3)	0.886
1	6(25.0)	6(25.0)	2(5.3)	10(52.6)	
2	5(23.8)	5(23.8)	4(19.0)	7(33.3)	
3	1(16.7)	1(16.7)	1(16.7)	3(50.0)	
Ki67					
Low (<15%)	5(19.2)	6(23.1)	4(15.4)	11(41.7)	0.991
High (>15%)	5(20.8)	6(25.0)	3(12.5)	10(41.7)	
Tumour Bud					
-Low	9(21.4)	10(23.8)	7(16.7)	16(38.1)	0.428
-High	3(23.1)	3(23.1)	0	7(53.8)	

Tissue Stroma Percentage					
Low	10(23.3)	20.9)	4(9.3)	20(46.5)	0.302
High	2(16.7)	4(33.3)	3(25.0)	3(25.0)	

HER-2 enriched patients had a 5-year survival of 75%- and 10-year survival of 75% for the All High group, a 5-year survival of 63% and 10-year survival of 42% for the HNLC group, a 5-year survival of 100% and 10-year survival of 100% for the LNHC group and a 5-year survival of 68% and 10 year survival of 68% for the All Low group, (*Figure 3-49*).

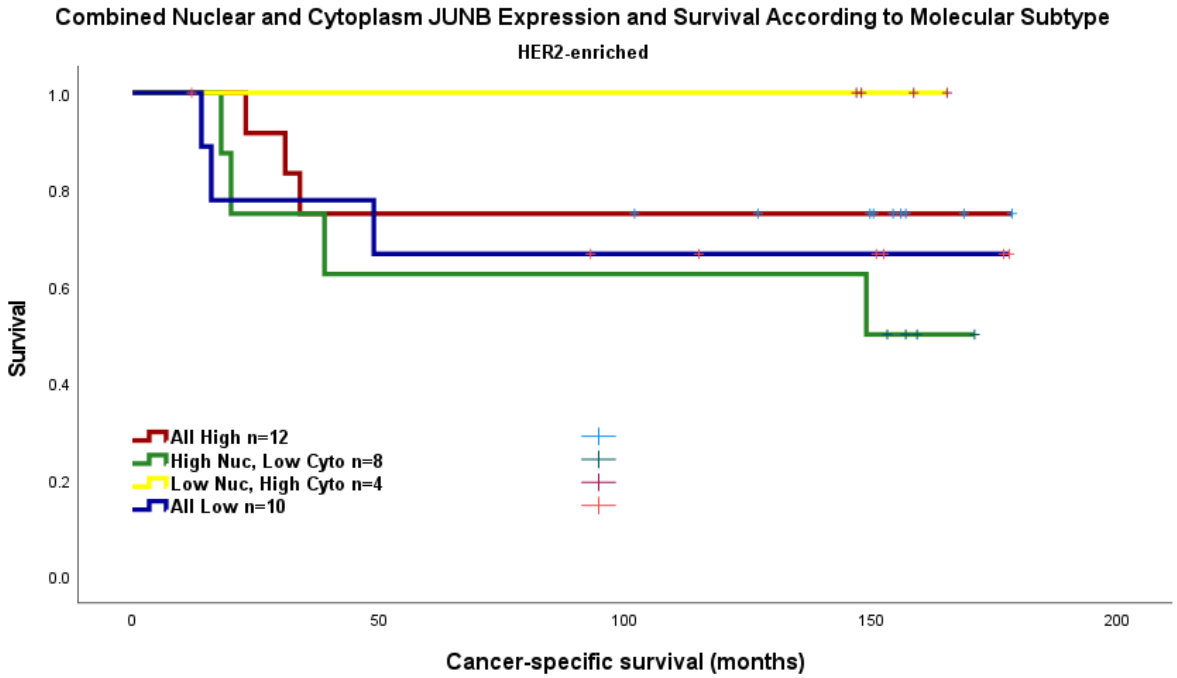

Figure 3-49 Combined nuclear and cytoplasm JUNB expression and survival in the TNBC patients within the Glasgow Breast Cancer Cohort. Pairwise comparisons are described in the graph.

Pairwise comparison failed to demonstrate a difference in survival in the combined scoring subgroups in the HER2-enriched patients, (*Table 3-30*).

Table 3-30 Pairwise comparisons on Kaplan Meier survival analysis for combined nuclear and cytoplasmic JUNB expression in HER2-enriched patients.

Pairwise Comparison p=	1 HNHC	2 HNLC	3 LNHC	4 LNLC
1 HNHC		0.291	0.295	0.638
2 HNLC	0.291		0.144	0.219
3 LNHC	0.295	0.144		0.670
4 LNLC	0.638	0.219	0.670	

Within the HER-2 enriched group, inter-factor correlation was assessed when comparing the combined score groups, (Table 3-31). Here, an association between nodal status and combined nuclear and cytoplasmic score was seen.

Table 3-31 Clinicopathological factors and their relation to JUNB combined nuclear and cytoplasmic expression in the HER2-enriched patients in the Glasgow Breast Cancer Cohort. Chi-squared analysis.

Clinicopathological factor	JUNB Combined Cytoplasmic and Nuclear staining (%)				p
	HNHC	HNLC	LNHC	LNLC	
Age (years)					
≤50	4(36.4)	3(27.3)	1(9.1)	3(27.3)	0.973
>50	8(34.8)	5(21.7)	3(13.0)	7(30.4)	
Tumour Size					
≤20mm	5(19.2)	6(23.1)	4(15.4)	11(42.3)	0.991
21-49mm	5(20.8)	6(25.0)	3(12.5)	10(41.7)	
≥50mm	5(19.2)	6(23.1)	4(15.4)	11(42.3)	0.991
Grade					
I	0	0	0	0	0.800
II	3(30.0)	2(20.0)	2(20.0)	3(30.0)	
III	9(37.5)	6(25.0)	2(8.3)	7(29.2)	
Nodal Status					
N_0	**8(36.4)**	**7(31.8)**	**4(18.2)**	**3(13.6)**	**0.026**
N_1	**4(33.3)**	**1(8.3)**	**0**	**7(58.3)**	
Lymphatic Invasion					
Absent	2(28.6)	1(14.3)	1(14.3)	3(42.9)	0.589
Present	3(60.0)	1(8.3)	0	1(58.3)	
Vascular Invasion					
Absent	4(36.4)	2(18.2)	1(9.1)	4(36.4)	0.676
Present	1(100)	0	0	0	
Necrosis					
Absent	1(33.3)	0	0	2(66.7)	0.437
Present	11(35.5)	8(25.8)	4(12.9)	8(25.8)	
Klintrup Makinen					
0	4(44.4)	2(22.2)	1(11.2)	2(22.2)	0.646
1	4(44.4)	2(22.2)	1(11.1)	2(22.2)	
2	6(33.3)	5(27.8)	1(5.6)	6(33.3)	
3	1(16.7)	1(16.7)	2(33.3)	2(33.3)	
Ki67					
Low (<15%)	5(38.5)	2(15.4)	2(15.4)	4(30.8)	0.647
High (>15%)	7(35.0)	6(30.0)	1(5.0)	6(30.0)	
Tumour Bud					
-Low	10(34.5)	8(27.6)	4(13.8)	7(24.1)	0.265
-High	2(40.0)	0	0	3(60.0)	
Tissue Stroma Percentage					
Low	8(44.4)	3(16.7)	1(5.6)	6(33.3)	0.373
High	4(25.0)	5(31.3)	3(18.8)	4(25.0)	

3.3 Discussion

In BRCA1 variant cells, JUNB was found to play a role in transcriptional activation of the AD1 domain on BRCA-1 gene, particularly in the homodimeric form, suggesting a role in tumour suppression in susceptible ovarian and breast cells(183). Recently, a proposed mechanism of the involvement of JUNB in fibroblast growth factor receptor 2 FGF7/FGFR2 signalling was put forward, for hormone-dependent breast cancer in premenopausal women, suggesting that the presence of high JUNB levels may lead to promotion of transcription of gene sets leading to poor prognosis (184).

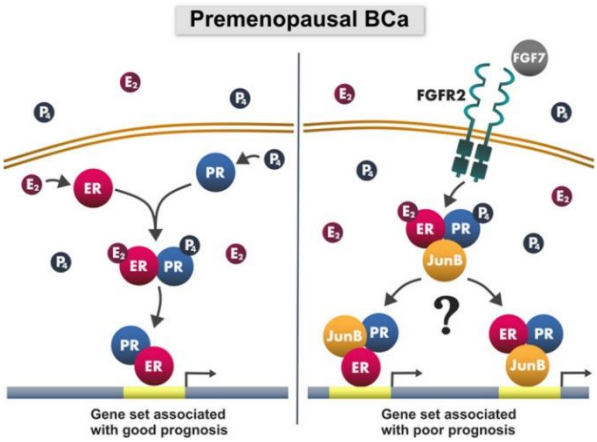

Figure 3-50 Proposed mechanism of the involvement of JUNB in FGF7/FGFR2 signalling in hormone-dependent (premenopausal) breast cancer. Taken from Mieczkowski K et al. (184).

TGFβ plays a dual role in the natural history of tumourigenesis, initially acting as a tumour-suppressor, and in the later stages of cancer, enhancing migration, invasion and survival of tumour cells, and promoting EMT(185). Induction of JUNB by TGFβ is thought to play a role in redirecting SMAD2/3 to different target sites, playing a role in activating late TGFβ target genes and participating in a feed-forward pathway(186). Some of these later pathways are in crosstalk with components of the WNT signalling pathway, particularly leading to a more "migratory and mesenchymal cell phenotype(186-188). This role appears to be of particular importance in Basal type/TNBC type breast cancers(162).

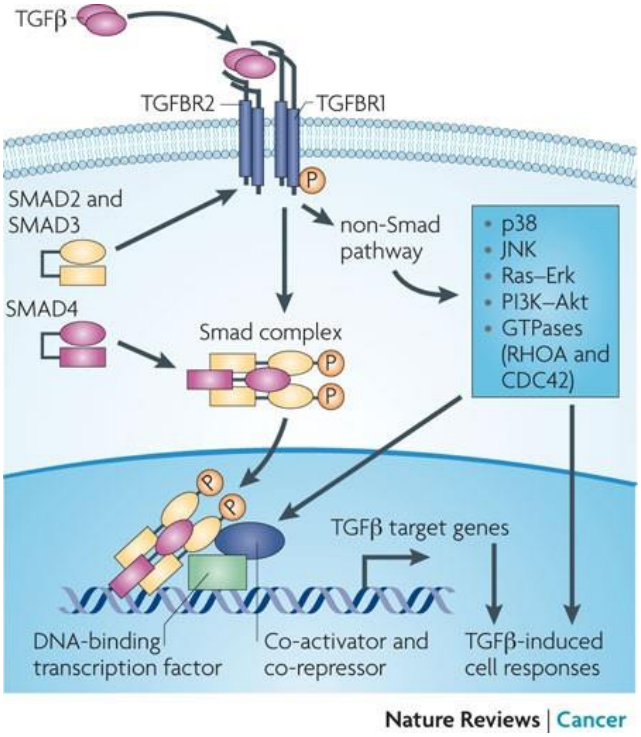

Figure 3-51 The TGF-Beta / SMAD complex pathway. Taken from Ikushima et al., (185)

Finally, there is additional evidence that JUNB may play a role in resistance against flavopiridol, a cyclin-dependent kinase inhibitor treatment in breast cancer in in-vitro cell-studies (189). Recent work suggests that circulating or disseminated tumour cells (DTCs) identified in the bone marrow of breast cancer patients with raised JUNB allowed the identification of patients with higher risk of recurrence of disease following treatment for breast cancer(178, 190).

Cytoplasmic expression of JUNB, using a threshold of 112.5 to demarcate high versus low expression, suggested that there was no significant difference in survival across the 403 patients within the Glasgow Breast Cohort with valid data. In this group, molecular subtype, nodal status, tumour size and necrosis correlated with JUNB expression, and further stratification according to ER status suggested a survival benefit in ER-negative patients for those with high cytoplasmic JUNB expression (p=0.010), with nodal status remaining associated with cytoplasmic JUNB expression. In the ER-negative subgroup, this difference was lost on multivariate regression analysis when compared with other clinicopathological factors. The same effect was not seen in ER-positive patients. However, on closer examination of the molecular subgroups, high JUNB cytoplasmic expression was associated with increased survival in TNBC (p=0.028). This significance was lost on multivariate regression analysis when

examined against tumour stroma percentage, necrosis, lymphovascular invasion and tumour size.

Nuclear expression of JUNB, using a threshold of 115 to demarcate high versus low expression, was associated with a survival benefit for high JUNB expression in across the cohort (p=0.028), and associated with age, size, grade, necrosis and KM score. However, when held against tumour size, invasive grade, lymphovascular invasion, necrosis, Ki67, molecular subtype, TSP and tumour budding in multivariate regression analysis, the statistically significant effect was lost. This was also seen in ER-positive patients within this group, who had increased survival when nuclear JUNB expression was high (p=0.035), and in which nodal status, and tumour size were associated with JUNB expression. On further stratification into molecular subgroups, however, low nuclear JUNB expression was associated with improved survival in Luminal B patients (p=0.036), although once again tumour size appeared associated to JUNB expression.

When nuclear and cytoplasmic JUNB expression was combined into form a score, the groups with a survival difference seen with HNLC having overall poor survival compared to other subgroups within the whole Glasgow Breast Cancer cohort, and again seen to associate with size, grade, nodal status and KM score. However, this effect was lost on multivariate regression analysis. When stratifying according to molecular subgroups, Luminal B and TNBC groups appeared to have worse survival in their HNLC groups on univariate analysis, and in Luminal B, association between nodal status and tumour size were seen once again.

Previous work by Kharman-Biz et al. suggested that JunB levels were expressed more highly in tumour cells compared to adjacent tissues, particularly when compared to other members of the AP-1 family(191). In addition, JUNB mRNA expression was associated with reduced tumour size and stage of disease, which would be consistent with our current findings of improved survival in high JUNB expression within the cytoplasm(191). This is an effect which overall is also seen in JUNB nuclear expression. This would agree with previous evidence of the action of JUNB as a tumour suppressor versus pro-invasion factor at different points in a cancer’s natural history. The association between JUNB expression, and clinicopathological findings such as tumour size and nodal status in

particular, may provide an inside into where JUNB is most likely to contribute to some protective qualities against cancer progression, particularly when expressed in the cytoplasm versus nucleus. Overall, JUNB expression appears to confer an effect on survival in breast cancer in this particular cohort and may therefore indicate a promising route for prognostic and therapeutic study.

Chapter 4 ODAM

4.1 Introduction

Odontogenic ameloblast-associated protein (ODAM) has been identified in multiple types of epithelial cells, including the human adrenal gland, cerebral cortex, colon, epididymis, kidney, lung, mammary gland, prostate, salivary gland, duodenum, ileum, stomach, thyroid and trachea(192). ODAM is encoded by the EO-009 gene, consisting of ten coding exons located within chromosome 4q13 as part of the secretory calcium-binding phosphoprotein (SCPP) cluster(193, 194). This cluster (of which ODAM is encoded for by a ~800 kpb region), gives rise to elements which have been found to participate in bone and tooth development and mineralization, in part through the regulation of matrix metalloproteinase-20 (MMP-20)(193-195). Evidence supports the hypothesis that ODAM originates from a protein formed of 279 amino acids, of which shorter peptides may play additional roles within the cell(196, 197). Previously named *APin*, ODAM was first described by the Japanese NEDO human cDNA-sequencing project using KATO III cell line, but has since been fully characterized within ameloblasts, and has since been found to form part of the basal lamina(198, 199). ODAM is expressed at higher levels during the stages associated with odontogeneic maturation and mineralization, as well as in response to disruption of periodontal integrity(196, 198, 200-202). ODAM appears to also play a role not just as a matrix protein within cellular junctions, but also in cell signalling and gene activation when actively secreted(203). Evidence therefore supports localisation of ODAM in the cytoplasmic, nuclear, and extracellular environment to carry out its functions(204).

4.1.1 ODAM and cancer

ODAM is highly expressed in the cell membrane and nucleus of lung, mammary gland, prostate, salivary gland, stomach, thyroid, and tracheal tissues(192). The expression of ODAM has been identified in highly invasive MDA-MB231 breast cancer cells (where expression appears reduced compared to other less-invasive cell lines), along with other cancer cells, including calcifying epithelial odontogenic tumours (CEOT), and those of the colon, lung, stomach and melanoma(204-208). When transfected with cytomegalovirus promoter-based b-plasmids encoding for ODAM, ODAM-negative MDA-MB231 breast cancer cells exhibited a reduction in growth rate and lung metastatic properties in SCID-beige mice(197). ODAM expression correlates with adoption of invasive behaviours(192). However, some findings have provided equivocal information regarding the role of

ODAM, as nuclear expression of ODAM in melanomas appears to correlate with increased risk of sentinel lymph node metastasis and therefore poorer prognosis, and ODAM expression appears to correlate with reduced OS in lung adenocarcinoma(208, 209).

ODAM expression relates directly to expression of RhoA and Rho-associated kinase (ROCK) resulting in increased adhesion signalling (as evidenced by increased beta-catenin and e-cadherin expression in cases of increased ODAM expression) and reduced cellular migration via suppressive activity on PTEN signalling and down-regulation of AKT phosphorylation, as suggested by ROCK suppression studies(192). In addition, ODAM-mediated RhoA signalling results in actin filament rearrangement in breast cancer cell line MCF-7, and promotes cell adhesion(192). Additionally, ODAM is thought to have an inhibitory effect on Runx2-mediated transcriptional activation of genes which have an antiproliferative effect in MDA-MB-231 breast cancer cell lines, suggesting a role in proliferative control, and a broad role for ODAM and its derivative proteins(197, 210, 211). ODAM expression has been shown to be essential for inhibiting breast cancer (and lung cancer) cellular migration and invasion *in vitro*, as supported by *in vivo* mouse model studies(192, 208). Finally, reduced ODAM expression in bone tissue in mouse models was associated with breast cancer metastasis, suggesting that ODAM may also play a role in the establishment of bony metastases in breast cancer(192). The role of ODAM on MMP-20 may also play a role in metastasis formation, as MMP-20 was found in greater levels in advanced breast cancers (compared to early stage), potentially through a role relating to basement membrane and extracellular matrix remodelling which plays a part in metastatic spread(212, 213). Moreover, overexpression of ODAM was found to suppress invasion and migration in prostate cancers, correlating with a reduction in protein levels of MMP-20(214). ODAM expression was an independent predictor of recurrence, and cases with low ODAM expression were significantly more likely to have lymph node metastasis, higher preoperative PSA levels, and Gleason scores(214).ODAM therefore appears to be a promising cancer biomarker for several neoplasms, including breast cancer.

4.1.2 The Study Cohorts

The following chapter describes how ODAM was identified as one of the most differentially expressed genes on TempO-Seq analysis of the Glasgow Breast

Cancer Cohort surplus biorepository tissue, and how this compares to ODAM expression in the same cohort using immunohistochemistry. Prior to commencing the immunohistochemistry for the Glasgow Breast Cancer Cohort, the staining protocol was optimized, and specificity analysis was performed. The process for the results therefore can be represented below, (*Figure 4-1*).

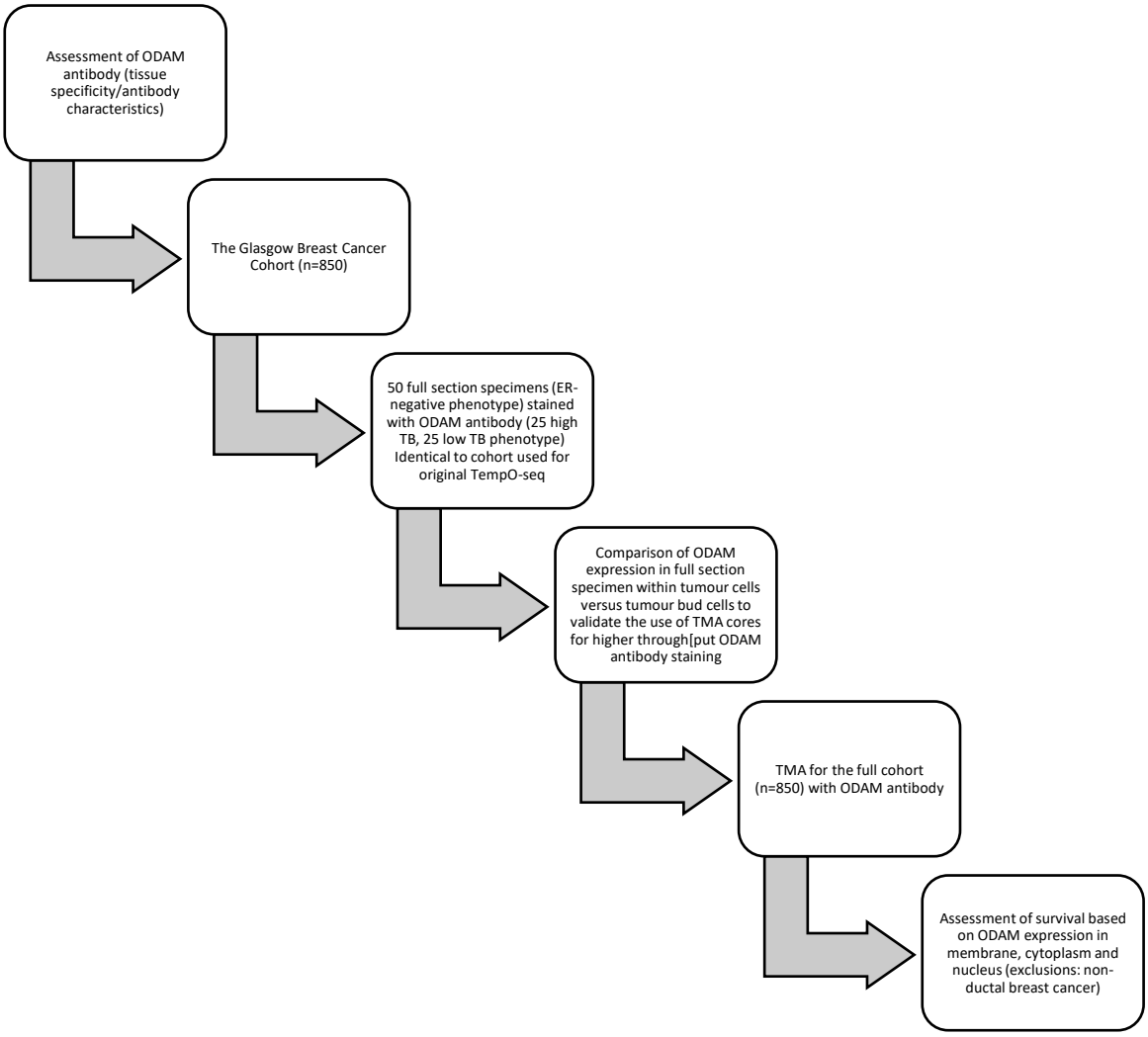

Figure 4-1 Study process flowchart for ODAM protein expression analysis

The cohort was initially stained in part using the 50 full section ER-negative specimens used for TempO-Seq, originally selected by virtue of being either of high tumour budding (n=25) or low tumour budding (n=25) phenotype. ODAM expression within the tumour was compared to that within the peritumoural buds following which breast tissue microarrays were produced from the entire Glasgow Breast Cancer Cohort were analysed to produce the results discussed later in this chapter. Weighted histoscores (WHS) for this ODAM expression in the cellular, membrane and nuclear compartments of breast tumour cells were manually assessed and analysed in relation to clinicopathological characteristics,

including tumour budding, and cancer-specific survival. It was hypothesised that ODAM expression may correlate inversely with survival, and that in patients with poorer prognostic indicators (higher disease stage, higher tumour budding status) this effect may be more pronounced.

4.2 Results

4.2.1 ODAM Expression Within Cell Lineages

To identify cell lines suitable for antibody specificity, an exploratory search was performed using DEPMAP, a freely accessible cancer dependency map online database which compiles the information from genomic data and large-scale cancer cell line datasets. When a search was performed for ODAM protein expression (versus knockdown) and compiling the cancer cell line lineage data information with regards to ODAM's expression, Breast appeared to have comparatively high transcripts per million (TPM) compared to other lineages (Figure 1).

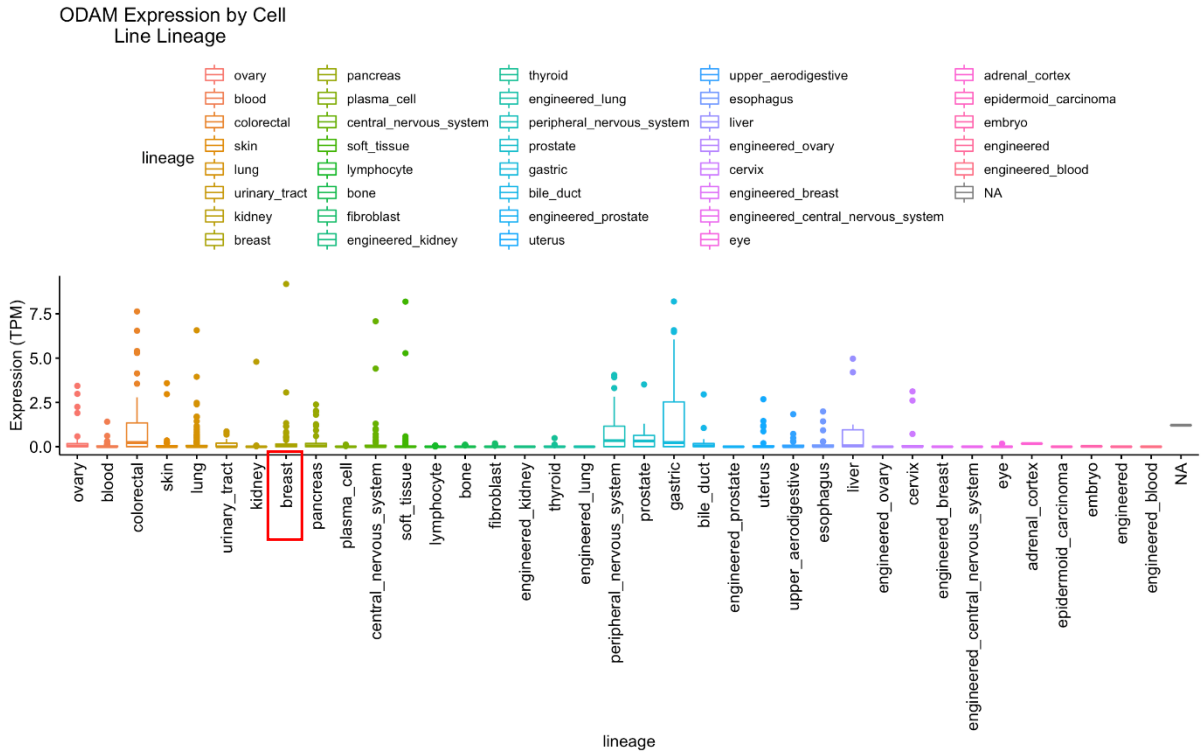

Figure 4-2 DEPMAP ODAM expression by cell lineage (Transcripts per million, TPM: for every 1,000,000 RNA molecules in the RNA-seq sample, x came from this gene/transcript.)

When exclusively examining breast cancer cell lines known to express ODAM, there is considerable variability in expression, (*Figure 4-3*). ODAM expression varies in expression within different types of Breast cell lines and appears to be in low levels of expression in approximately half of the overall lines for which

information is available. In the breast cancer cell lines with ODAM expression, this is mostly low-level (less than 2.5 TPM) apart from two lines, HCC1187 and HCC1500. Within our laboratory, the available cell lines were MDAMB453 and MDAMB231, the former of which had some, albeit low expression, while the latter had little/no expression of ODAM. However, colorectal and prostate cancer cell lines were also available for further analysis that expressed higher levels of ODAM expression, described later in this chapter

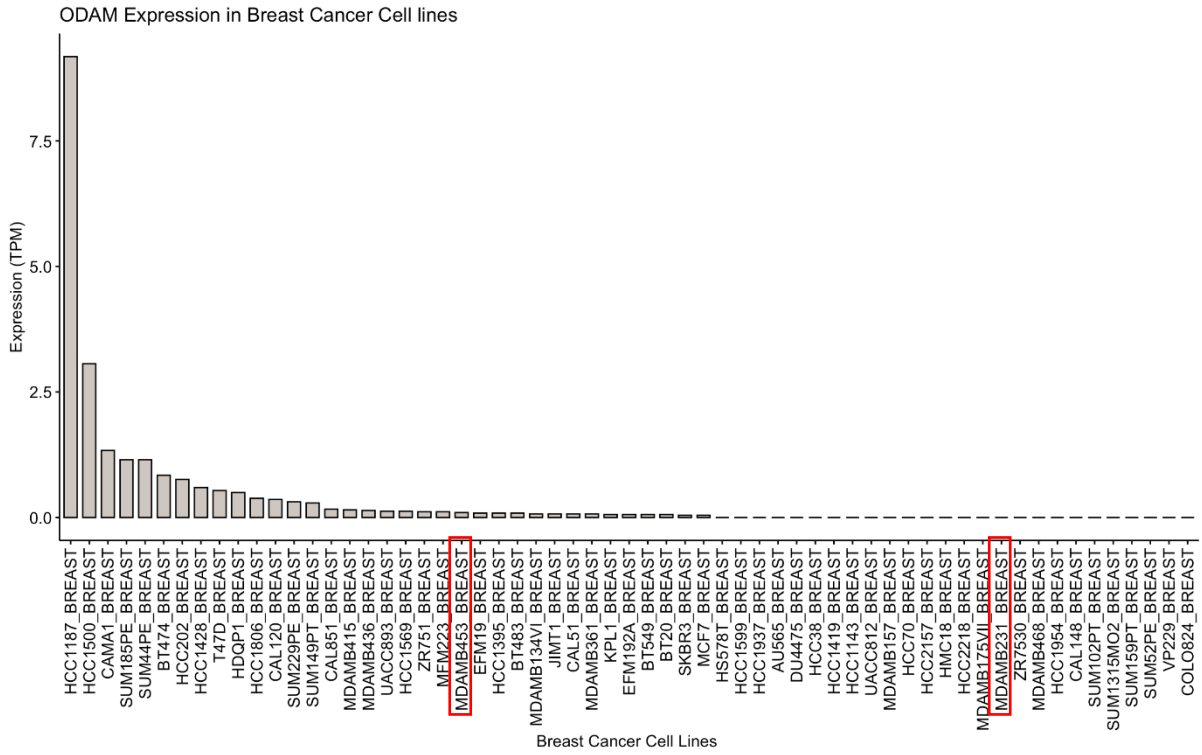

Figure 4-3 DEPMAP ODAM Expression in Breast Cancer Cell lines (Transcripts per million, TPM: for every 1,000,000 RNA molecules in the RNA-seq sample, x came from this gene/transcript.)

When DEPMAP was explored with regards to colorectal cancer cell lines, it appeared that almost 2/3 of the available cell lines on the database had some evidence of ODAM RNA expression, of which three were available in our laboratory, namely HT29, DLD1 and T84, (*Figure 4-4*).

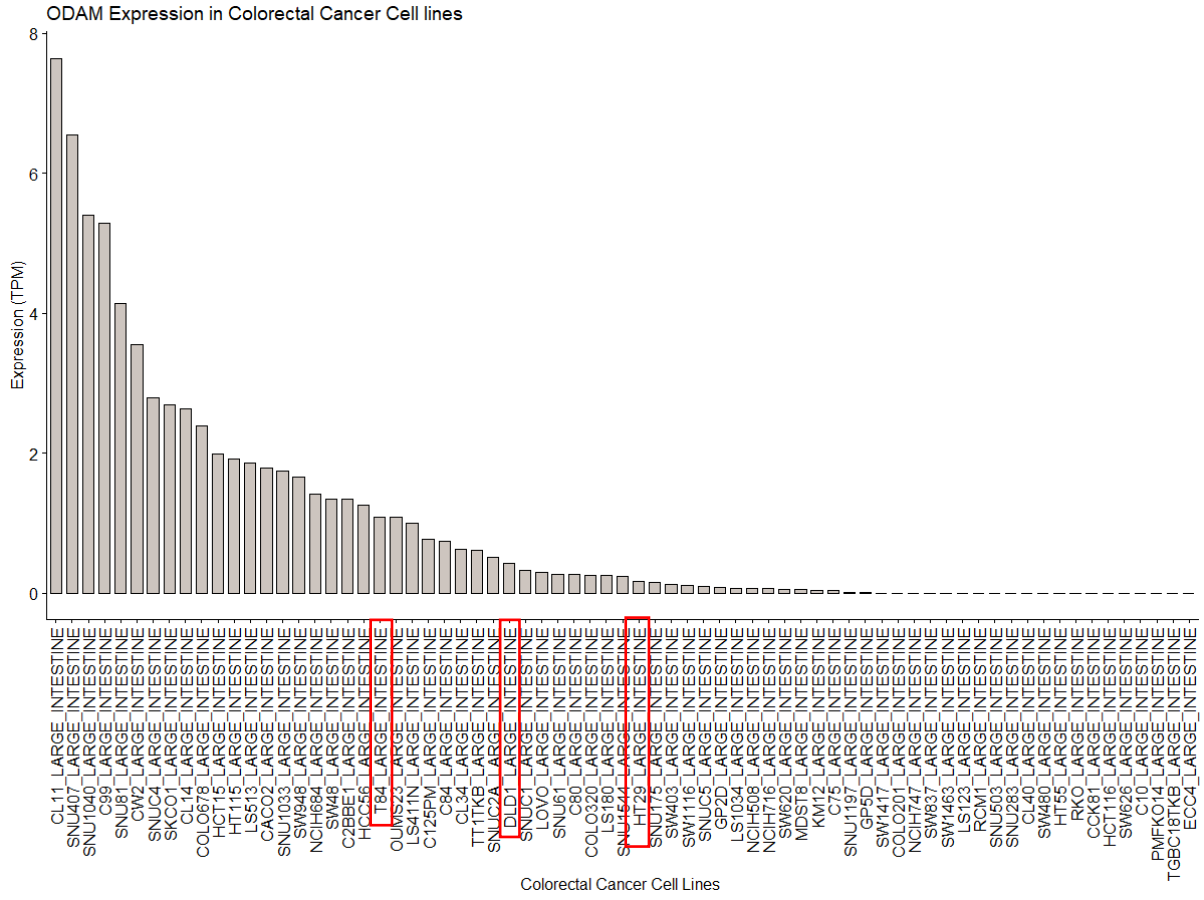

Figure 4-4 DEPMAP ODAM Expression in Colorectal Cancer Cell lines (Transcripts per million, TPM: for every 1,000,000 RNA molecules in the RNA-seq sample, x came from this gene/transcript.)

When DEPMAP was probed for prostate cancer cell lines, fewer cell lines had available data, although LNCAP cell lines figured here, and were available within our laboratory, (*Figure 4-5*).

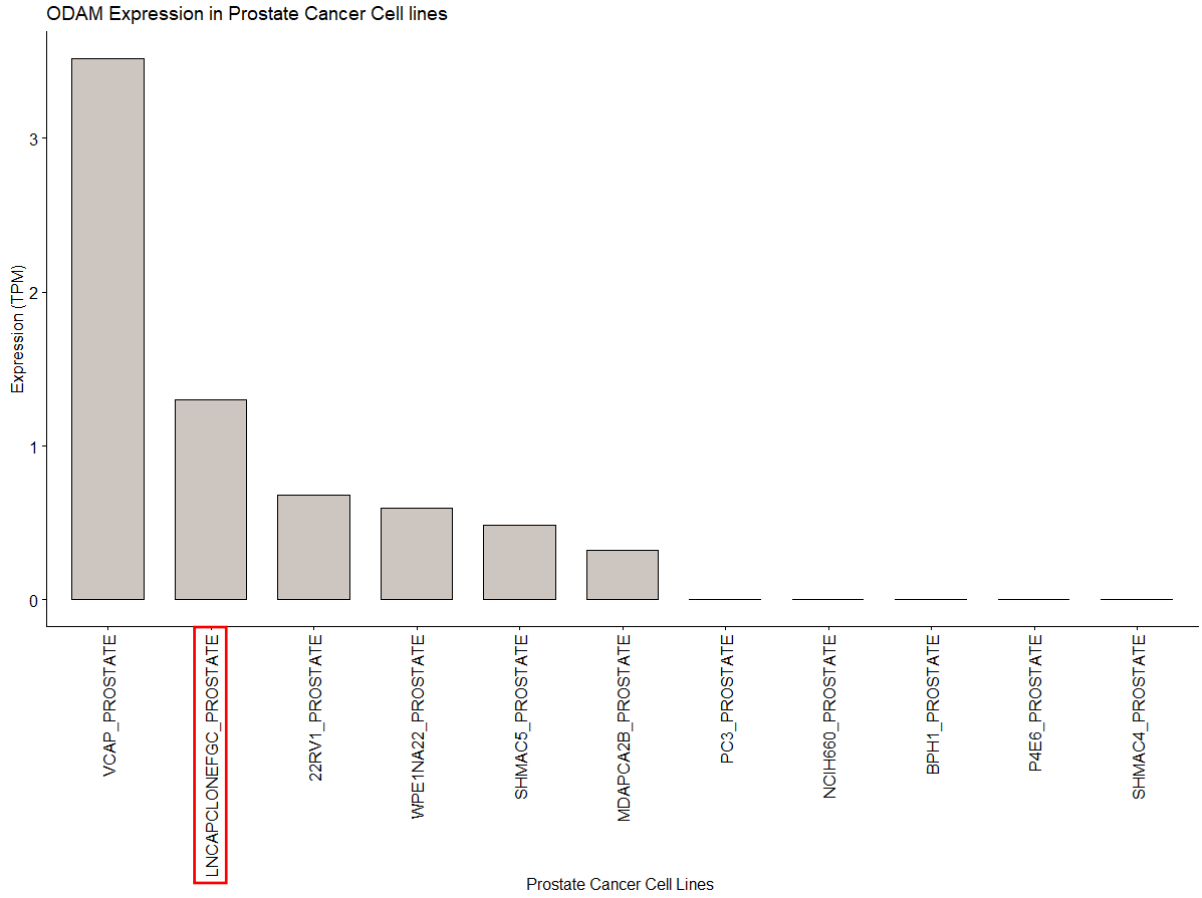

Figure 4-5 DEPMAP ODAM Expression in Prostate Cancer Cell lines (Transcripts per million, TPM: for every 1,000,000 RNA molecules in the RNA-seq sample, x came from this gene/transcript.)

4.2.2 ODAM Antibody Specificity

Examples of weak, moderate, and strong staining are shown in their respective sections within this chapter, together with a true positive and negative control tissue. Antibody specificity was validated using western blotting (Figure 5). A single band (reproduced in triplicate) was observed at 17kDa in breast 231 (weakly) and colorectal DLD1 cell lysate, and ß-actin was seen at strong

intensity at 45kDa, (*Figure 4-6*).

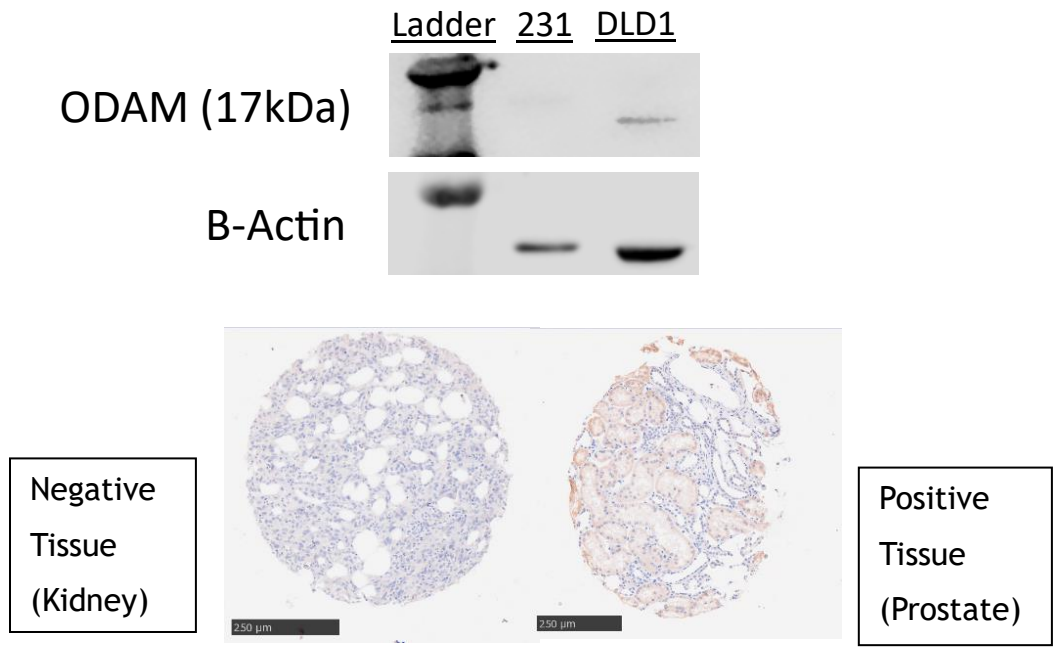

Figure 4-6 ODAM expression and antibody specificity on Western Blotting. Examples of positive and negative tissue types used for analysis are included.

4.2.3 ODAM Expression in Full Section Specimens

ODAM expression was first assessed using full section breast cancer tissue in a selected cohort of the Glasgow Breast Cancer Cohort. The sub-cohort of 50 patients had previously been used for TempO-Seq analysis and allowed identification of the most differentially expressed RNA, of which ODAM was one. As described previously, 50 patient sections with ER-negative phenotype were selected, 25 with high tumour budding and 25 with low tumour budding characteristics. These were prepared, optimised, and stained for ODAM (see methods). Manual weighted histoscores were produced for nuclear, cytoplasmic and membrane expression of ODAM by a single observer (FS). 41 specimens were included for analysis, as 9 patients had missing/damaged section slides. Cytoplasmic, nuclear and membrane expression of ODAM were manually scored for validation by Alan Whittingham using 10% of this sub-cohort. Scores varied from 0 to 130 for membrane, 0-210 for cytoplasm and 0-110 for nucleus. Each cellular location will be discussed in turn in the subsections below.

4.2.4 Membrane ODAM Expression in Full Section Specimens

ODAM expression in membrane in the full section and then in the full Glasgow cohort was 0, therefore this portion of cellular ODAM expression was not assessed further.

4.2.5 Cytoplasmic ODAM Expression in Full section specimens

After selecting the original 50 patients ER- patients with ductal cancer selected from the Glasgow Breast Cohort and used for TempO-Seq, these were stained using ODAM-specific antibody. Weighted histoscores were generated by manual evaluation by a single observer (FS). Examples of light, moderate and strong cytoplasmic staining, together with positive and negative control tissue are shown in below, (*Figure 4-7*).

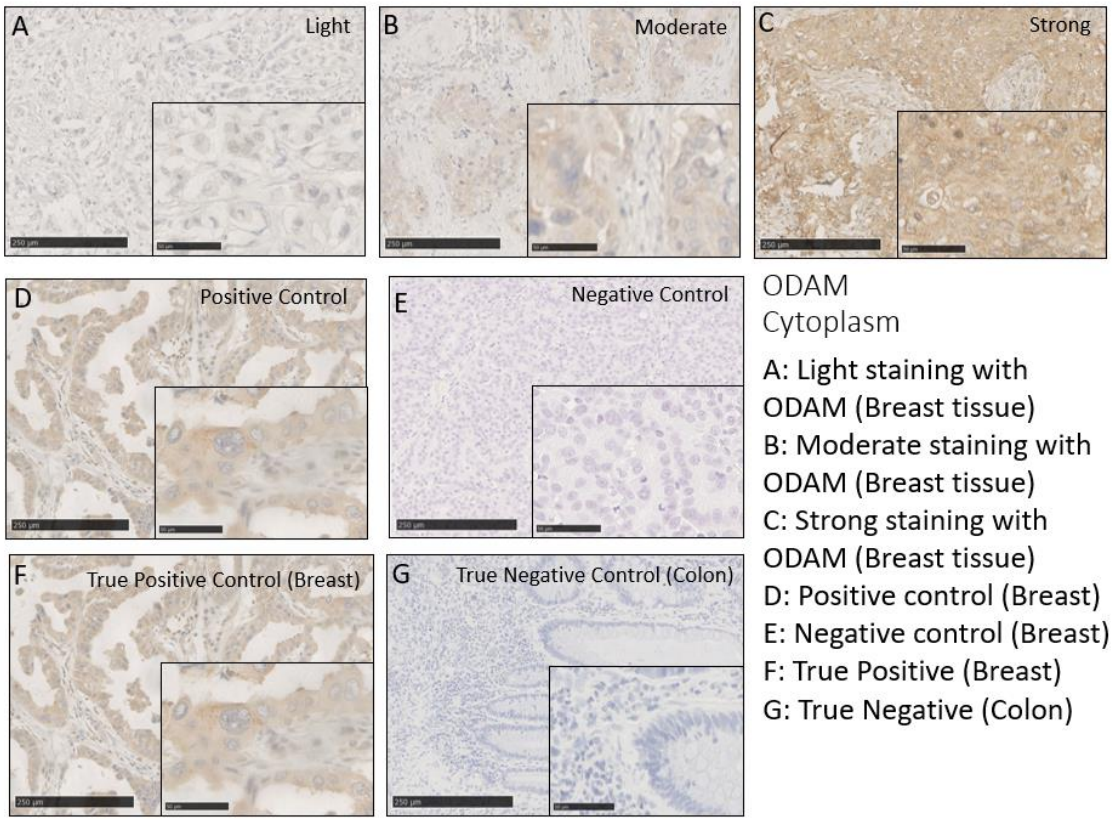

Figure 4-7 ODAM cytoplasm staining representative images.

Cytoplasm expression of ODAM was manually scored by a single assessor (FS), and scores varied from 0-210, (*Figure 4-8*).

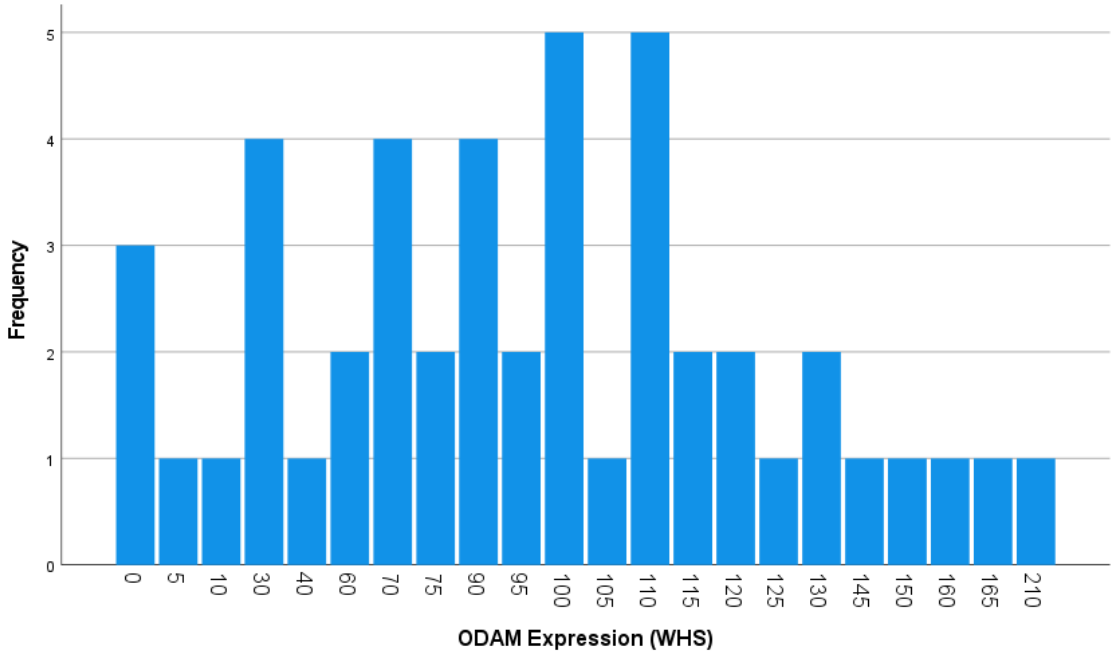

Figure 4-8 ODAM Cytoplasm expression in full section specimens (WHS, weighted histoscores)

Manual assessment for validation by Alan Whittingham using 10% of this sub-cohort is described using a scatter plot, (*Figure 4-9*). An intraclass correlation coefficient (ICCC) of 0.933 suggested a strong positive correlation between validation and primary assessors' scores.

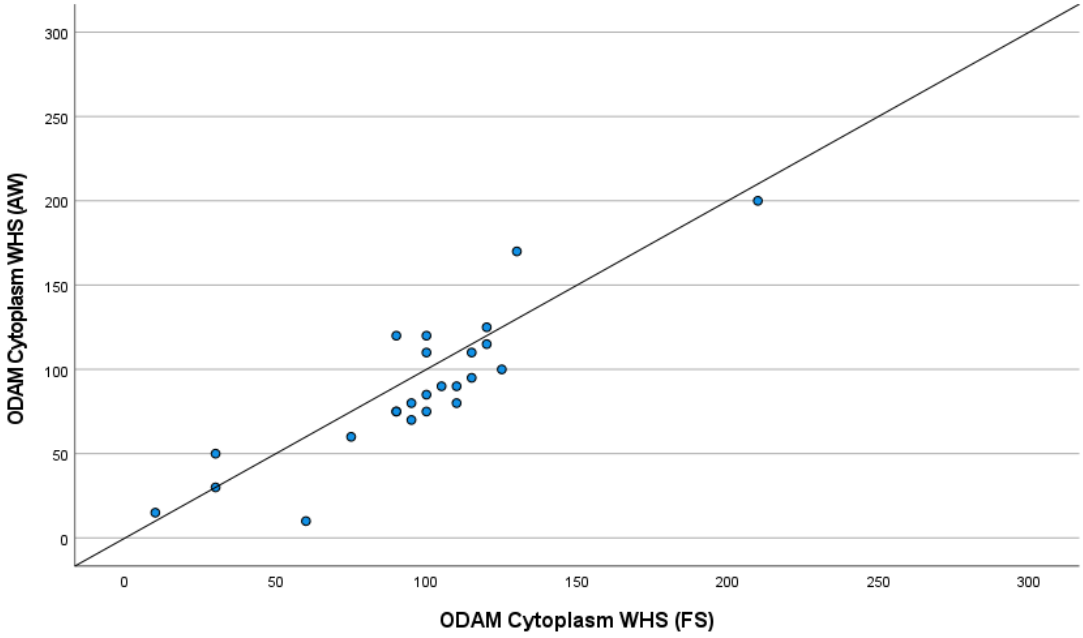

Figure 4-9 Correlation between FS and AW manual weighted histoscore (WHS) for ODAM cytoplasm staining. Scatter plot showing correlation between FS and AW for cytoplasm ODAM scores. Intraclass correlation coefficient 0.933 for 10% specimens.

A subsequent comparison of averages and differences in scores was produced as a Bland-Altman plot and suggested the scores correlated satisfactorily, (*Figure 4-10*).

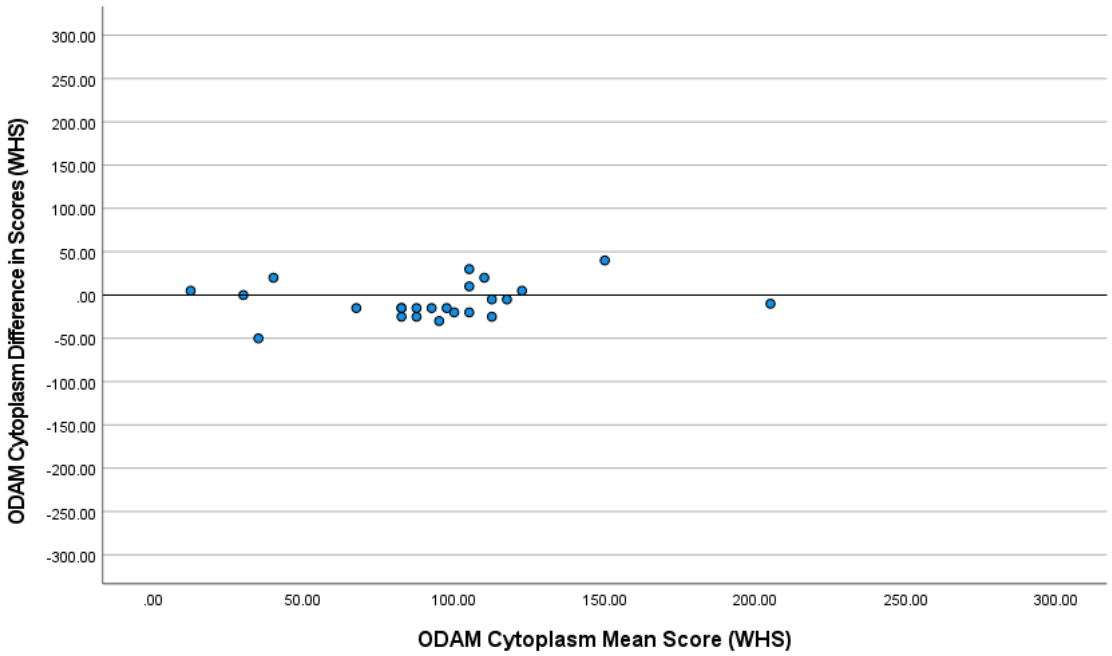

Figure 4-10 Bland Altman Plot comparing difference in scores to mean scores for ODAM expression in cytoplasm.

4.2.6 ODAM Cytoplasmic Expression in Tumour Cells Versus Tumour Buds

ODAM expression was compared between tumour buds (where present) and intratumoural cells. A scatter plot was used to visualise the correlation between cytoplasmic ODAM expression in intratumoral cells and tumour buds, (*Figure 4-11)*. Only 16 full sections stained had tumour buds present, in these specimens the WHS of the buds were comparable to that of the tumour core. The intraclass

correlation coefficient (ICCC) was 1.

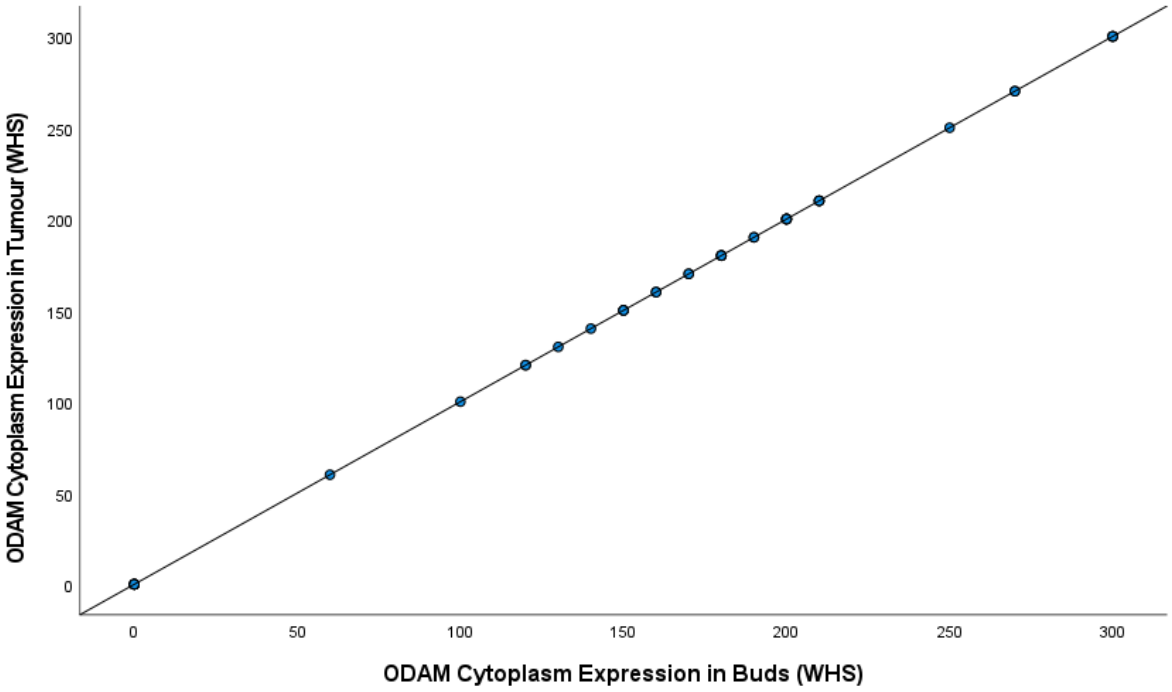

Figure 4-11 Cytoplasm ODAM expression in tumour versus tumour buds, ICCC 1

A subsequent comparison of averages and differences in scores was plotted as a Bland-Altman plot and demonstrated no bias between observers, (*Figure 4-12*).

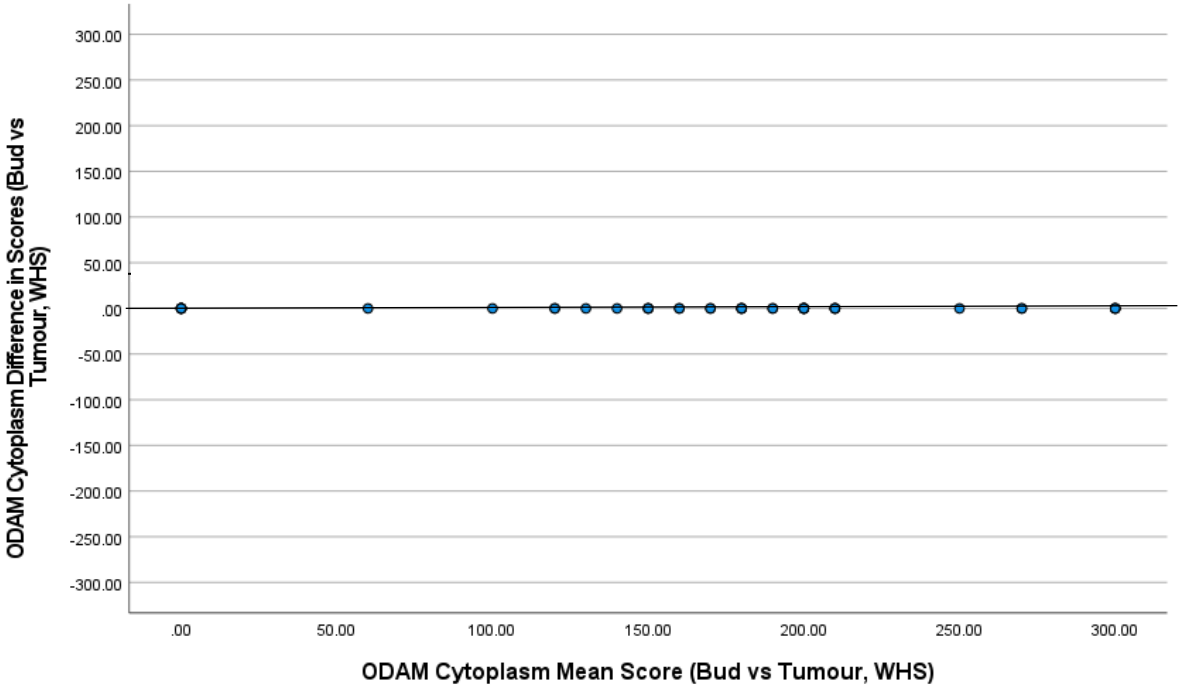

Figure 4-12 Bland Altman Plot comparing the difference in scores to mean scores for ODAM expression in cytoplasm in buds and tumour cells.

Based on these findings, it was possible to infer that further analysis of protein expression could be expanded to the full cohort of the Glasgow Breast Cancer

Cohort in the form of a tissue microarray and remain representative of expression both within the tumour buds as in within the intratumoural environment,(*Figure 4-13*).

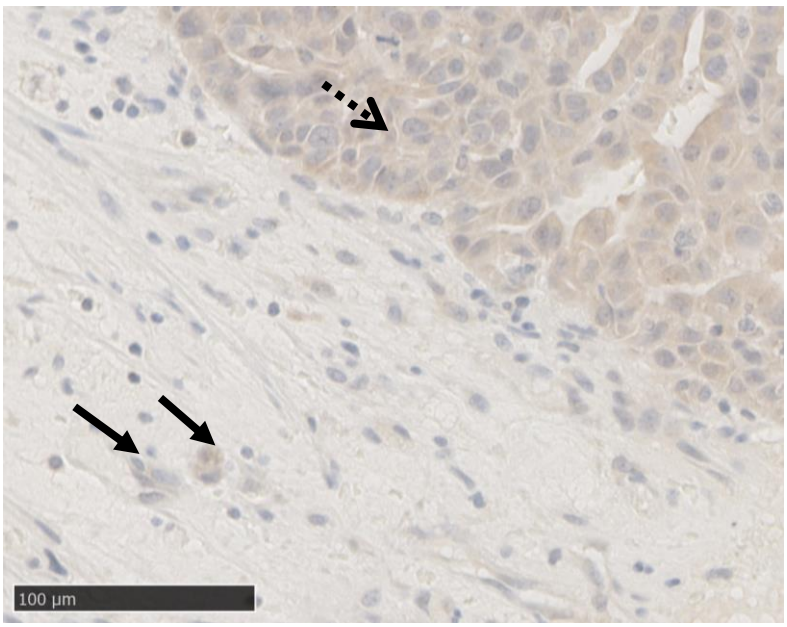

Figure 4-13 Cytoplasmic ODAM staining in tumour mass (dotted arrow) correlated closely with staining in tumour buds (black arrow)

4.2.7 Nuclear ODAM Expression in Full Section Specimens

Using ODAM-specific antibody, weighted histoscores were generated by manual evaluation by a single observer (FS). Examples of light, moderate and strong nuclear staining, together with positive and negative control tissue are shown below, (*Figure 4-14*).

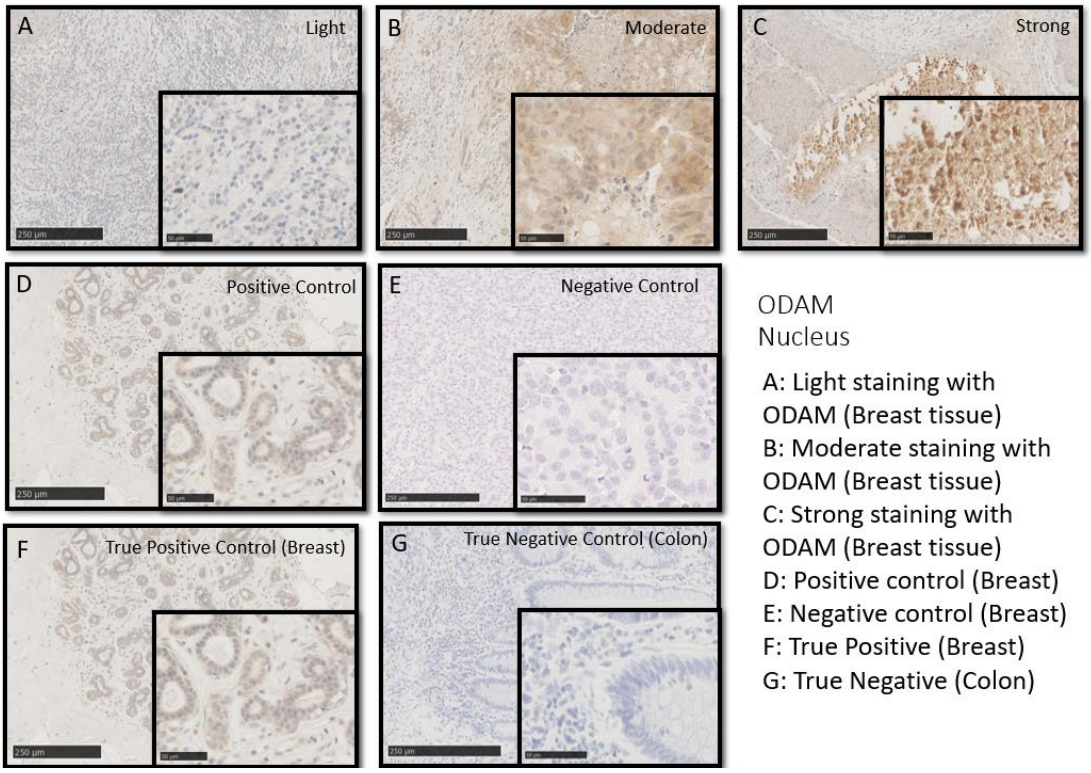

Figure 4-14 ODAM nuclear staining representative images

Nuclear expression of ODAM was manually scored by a single assessor (FS), and scores varied from 0-250 (*Figure 4-15*Figure 4-16).

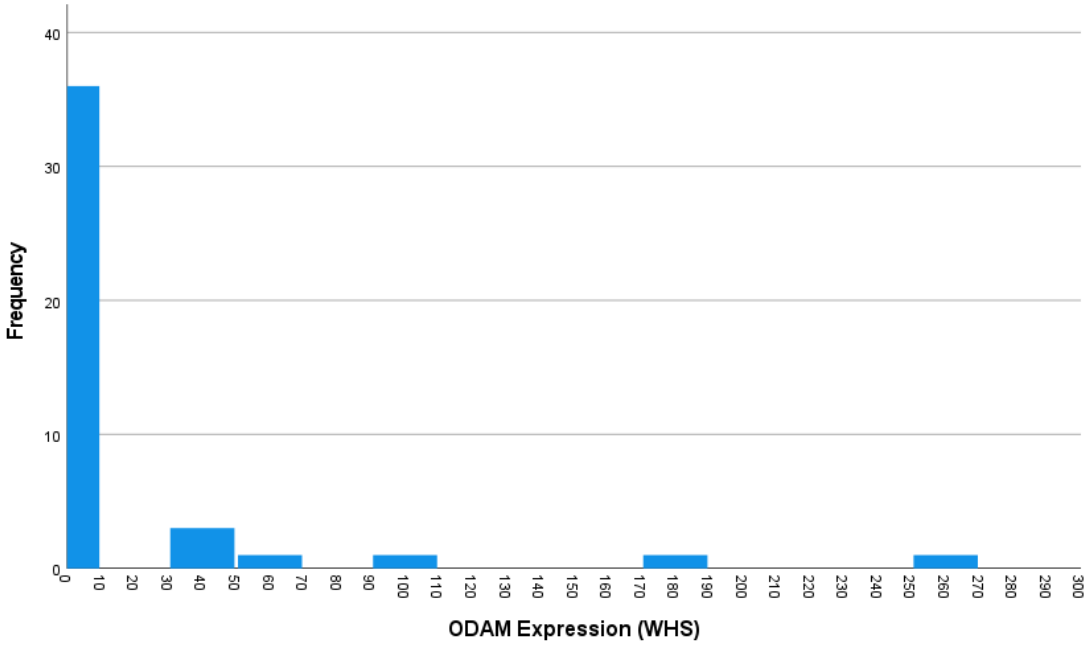

Figure 4-15 ODAM nuclear expression (WHS, weighted histoscores).

Manual assessment for validation by AN using 10% of this sub-cohort is described using the scatter plot in below, (Figure 4-16). An intraclass correlation coefficient (ICCC) of 0.992 suggesting a strong correlation between validation

and primary assessors' scores.

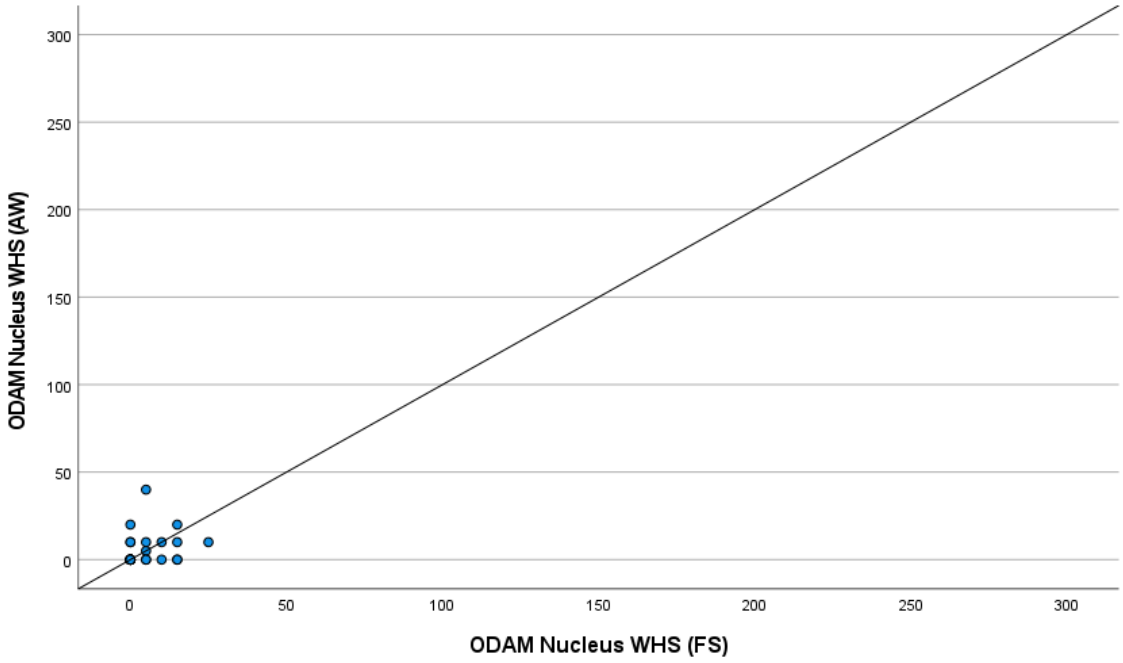

Figure 4-16 Correlation between FS and AW manual weighted histoscore (WHS) for nuclear ODAM staining. Scatter plot showing correlation between FS and AW nuclear scores. Intraclass correlation coefficient 0.992 for 10% specimens.

A subsequent comparison of averages and differences in scores was produced as a Bland-Altman plot suggested the scores correlated satisfactorily (Figure 4-17).

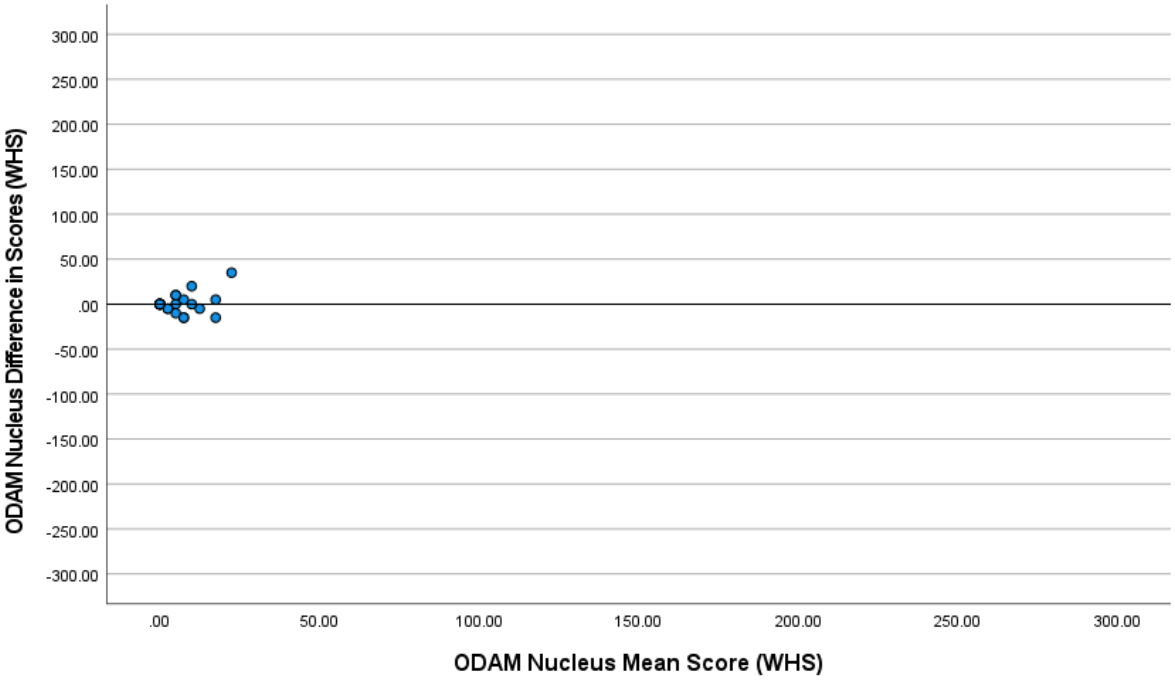

Figure 4-17 Bland Altman Plot comparing difference in scores to mean scores for ODAM expression in nucleus.

4.2.8 ODAM Nuclear Expression in Tumour cells Versus Tumour Buds

ODAM nuclear expression was compared between tumour buds (where present) and intratumoural cells. A scatter plot was used to visualise the correlation between nuclear ODAM expression in intratumoral cells and tumour buds (*Figure 4-18*). Only 7 full sections stained had tumour buds present, in these the WHS of the bud were comparable to that of the tumour core. The intraclass correlation coefficient (ICCC) was 1.

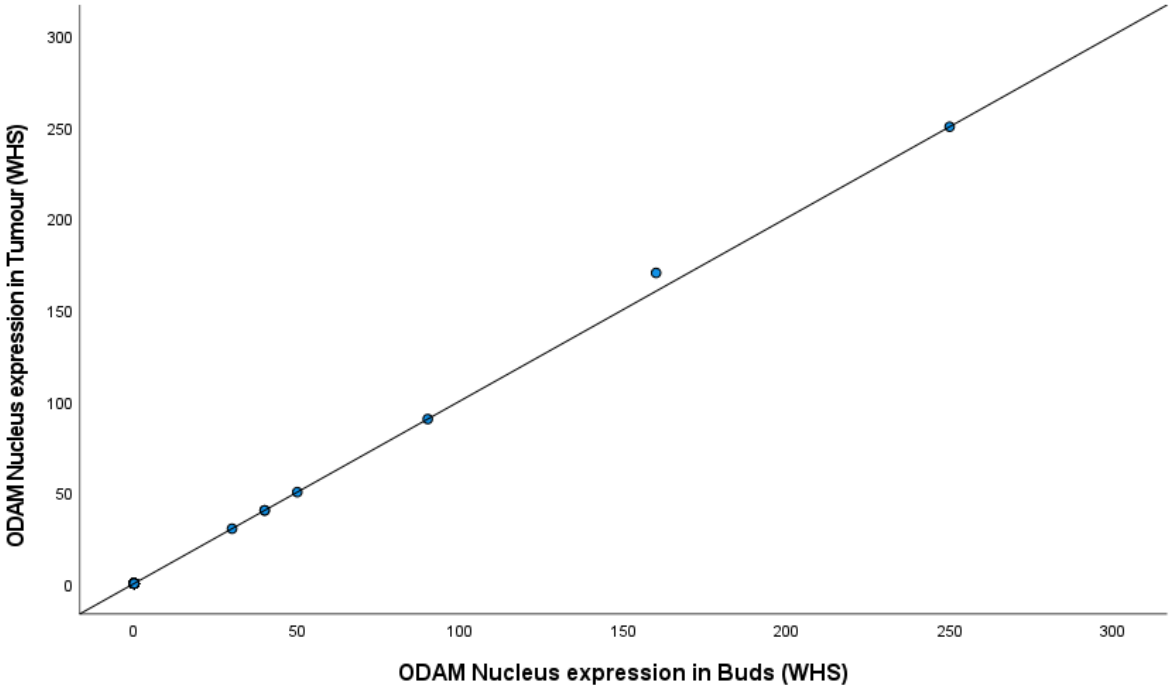

Figure 4-18 Nucleus ODAM expression in tumour versus tumour buds, ICCC 1.

A subsequent comparison of averages and differences in scores was plotted as a Bland-Altman plot and demonstrated no bias between observers, (*Figure 4-19*).

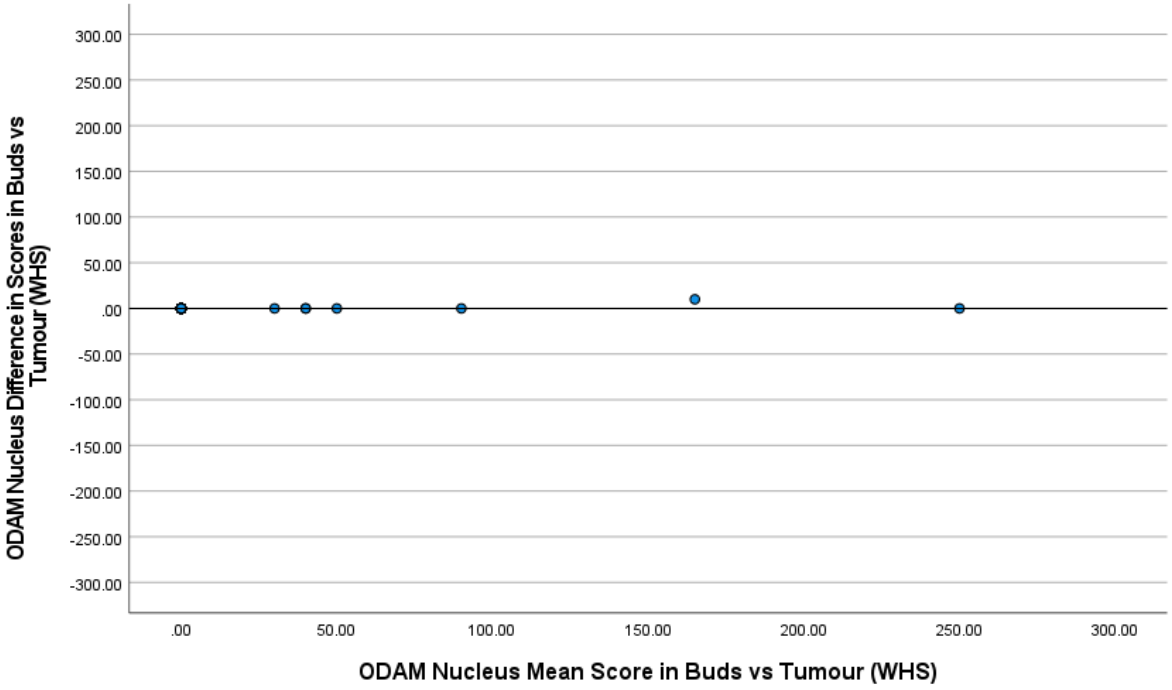

Figure 4-19 Bland Altman Plot comparing the difference in scores to mean scores for ODAM expression in nucleus in Bud vs Tumour cells.

Based on these findings, it was possible to infer that further analysis of protein expression could be expanded to the full cohort of the Glasgow Breast Cancer Cohort in the form of a tissue microarray and remain representative of expression both within the tumour buds as in within the intratumoural environment,(*Figure 4-20*).

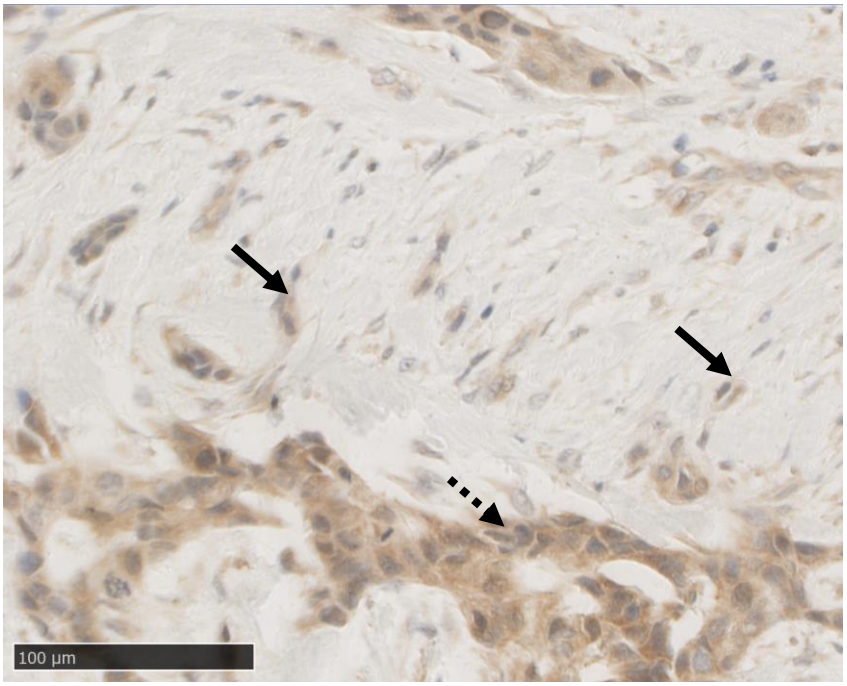

Figure 4-20 Nuclear ODAM staining in tumour mass (dotted arrow) correlated closely with staining in tumour buds (black arrow)

4.2.9 ODAM Expression in the Glasgow Breast Cancer Cohort

TMA slides composed of specimens from the Glasgow Breast Cancer Cohort were used to assess ODAM expression. Slides were stained with ODAM antibody, and manually assessed to achieve a weighted histoscore. Included patients had ductal cancer only, resulting in 736 specimens being included in the overall cohort. Each specimen was assessed on 3 different TMA slides, and an average WHS was calculated, unless only one specimen was available, in which case this was used as the final WHS. 411 cases were included in the final analysis as out of the total 736 cases, 325 did not have assessable cores, (*Figure 4-21*).

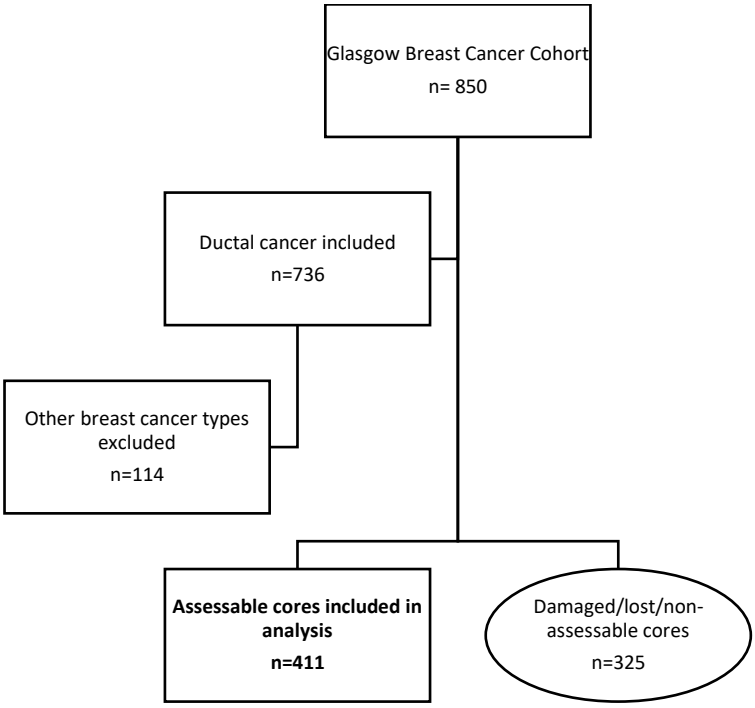

Figure 4-21 CONSORT diagram of cases included in analysis from the Glasgow Breast Cancer Cohort.

Manual weighted histoscores of ODAM expression were performed by FS. Validation of the scores (minimum 10%) was performed by Hester van Wyk.

4.2.10 ODAM Membrane Expression in the Glasgow Breast Cancer Cohort

As discussed previously, membrane expression of ODAM was zero across the cohort, and therefore no analysis of expression and survival was performed.

4.2.11 ODAM Cytoplasmic Expression in the Glasgow Breast Cancer Cohort

Manual weighted histoscores of cytoplasmic ODAM expression were performed by FS. Scores by FS varied between 0 and 300 with a mean of 171.4,(*Figure 4-22*).

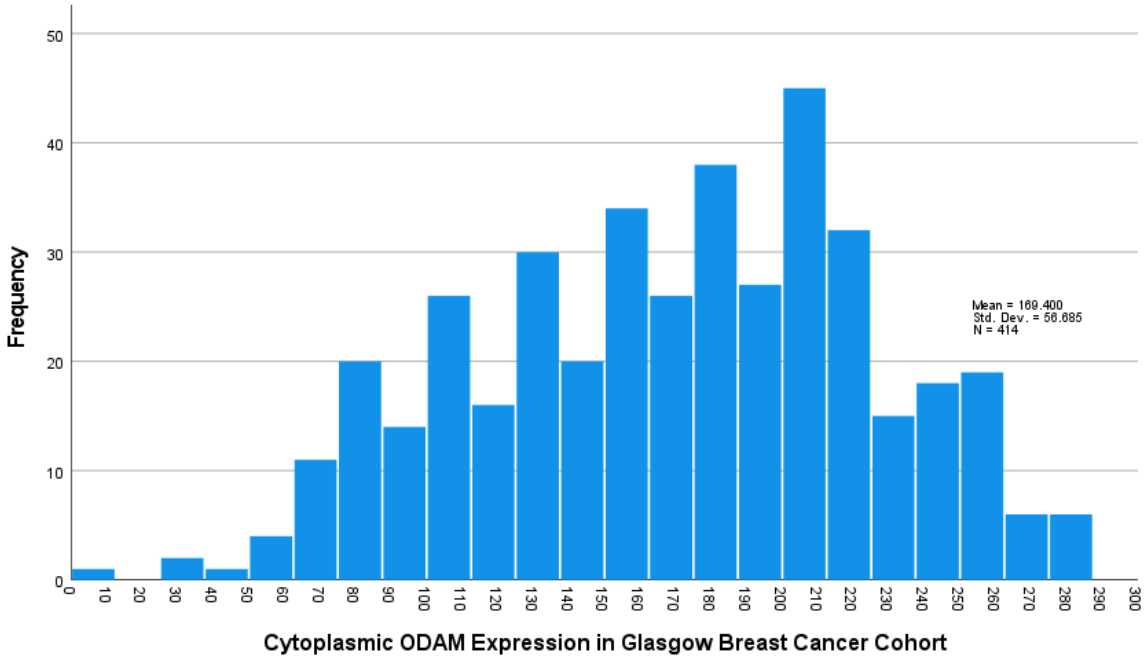

Figure 4-22 Distribution of ODAM cytoplasm expression (weighted histoscores) in the Glasgow Breast Cancer Cohort. Mean score 169.27, SD 56.4.

Counter-scores were performed manually by Hester van Wyk for a minimum of 10% of cores, (n=90) and are shown below for comparison, (*Figure 4-23*). WHS were reproducible between the two scorers for 90 cores. An intraclass correlation coefficient (ICCC) of 0.992 suggested a strong positive correlation between validation and primary assessor's scores.

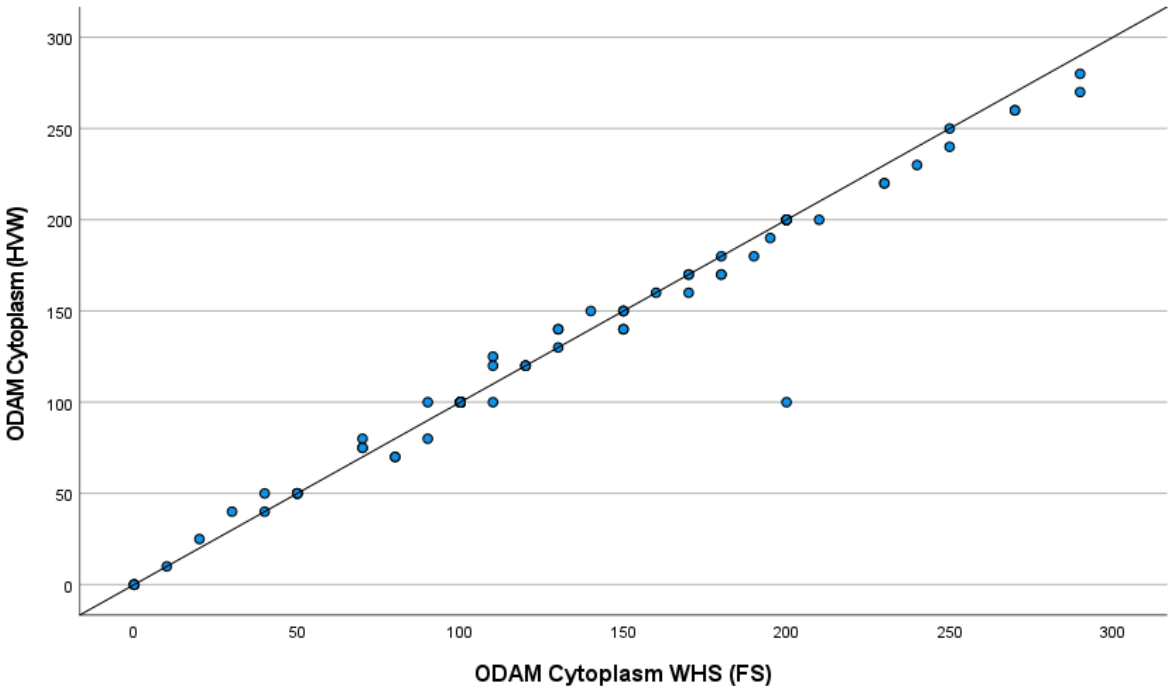

Figure 4-23 Correlation between FS and HVW manual weighted histoscore (WHS) for ODAM cytoplasm staining. Scatter plot showing correlation between FS and HVW for ODAM scores. Intraclass correlation coefficient 0.992 for >10% specimens.

A subsequent comparison of averages and differences in scores was produced as a Bland-Altman plot and suggested the scores correlated satisfactorily (*Figure 4-24*).

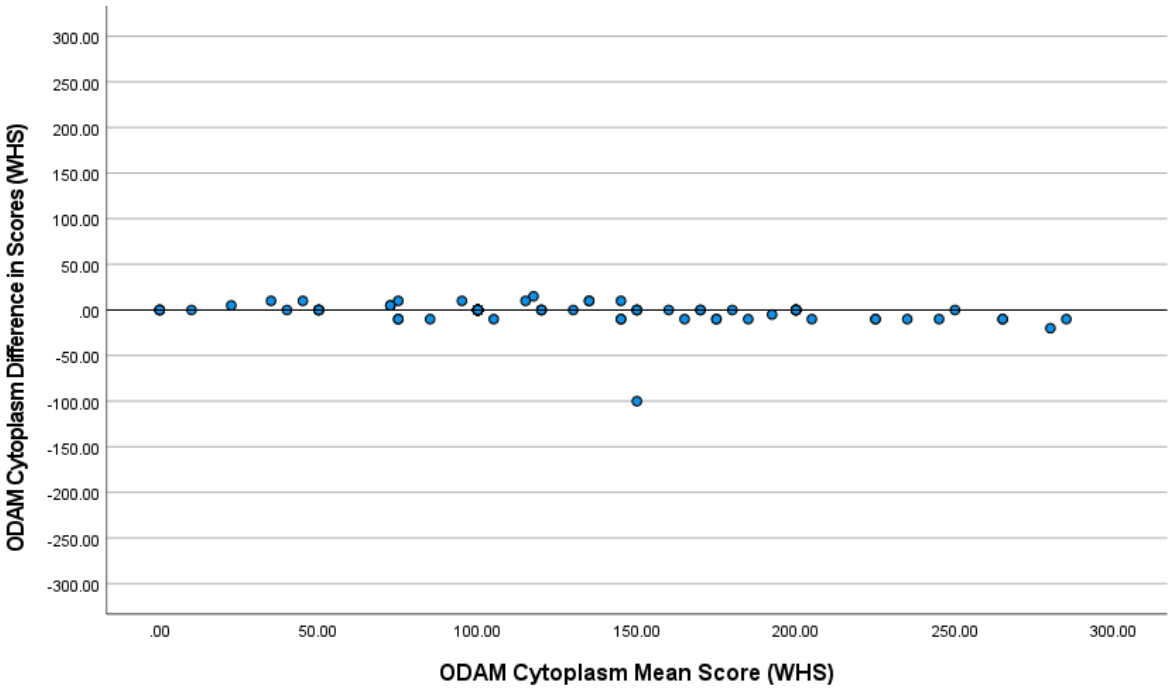

Figure 4-24 Bland-Altman Plot comparing difference in scores to mean scores for ODAM cytoplasmic expression.

A threshold for high and low ODAM cytoplasm expression were delineated using R Studio to compare high versus low ODAM expression according to survival. The threshold was identified as 153.3 as described below, (*Figure 4-25*).

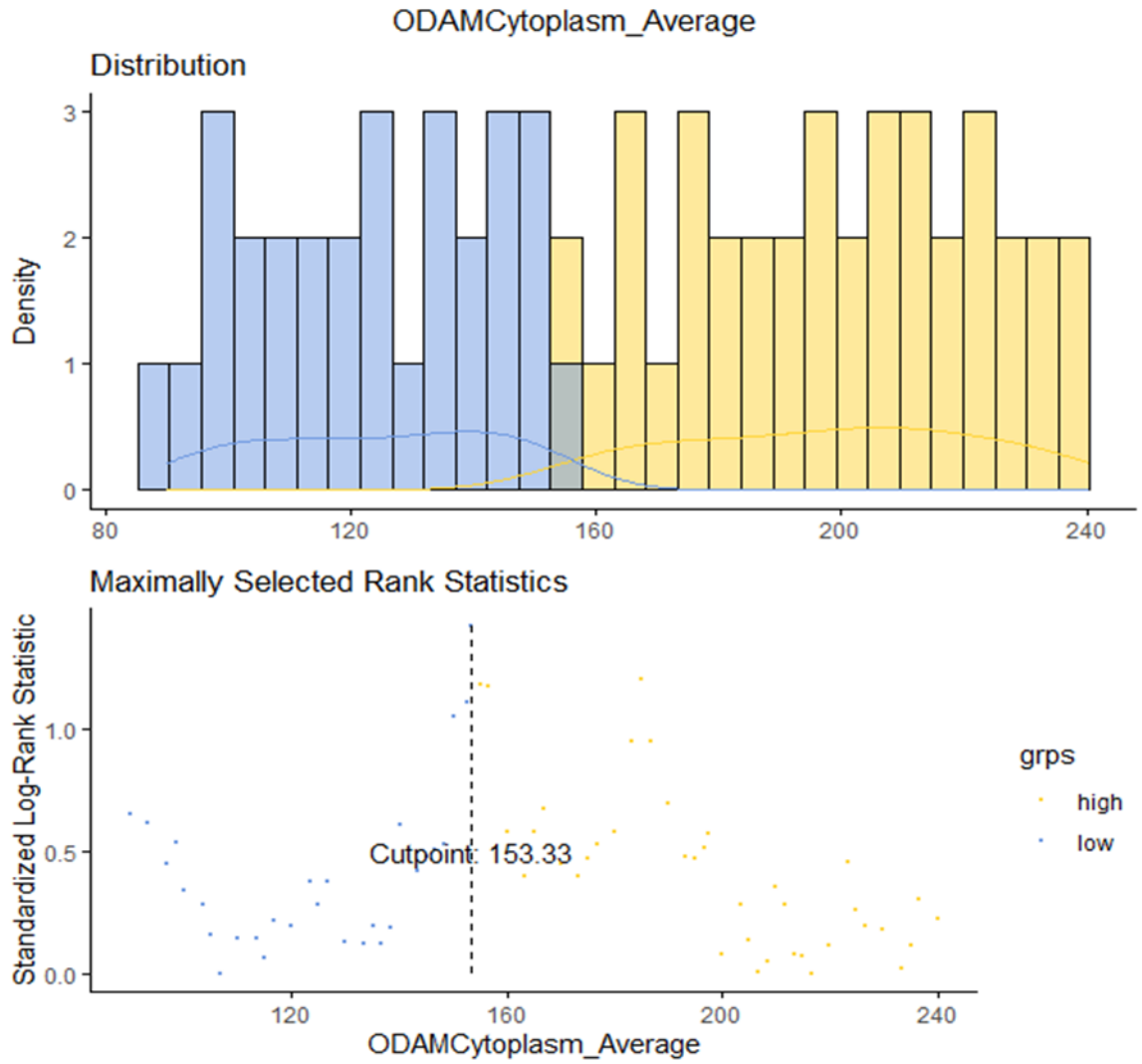

Low Expression

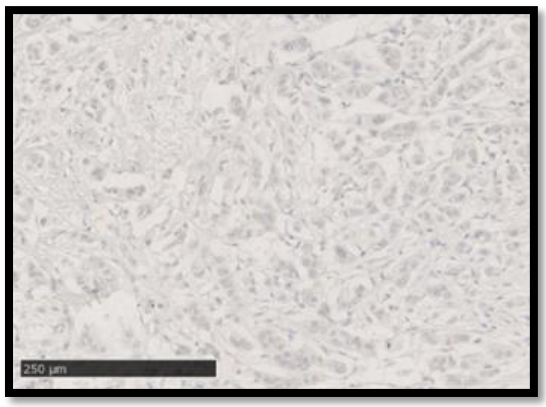

High Expression

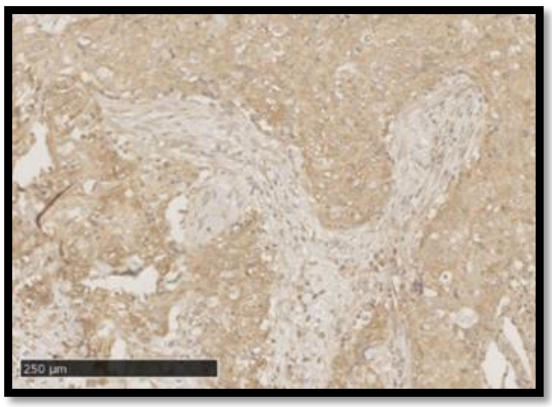

Figure 4-25 ODAM cytoplasm expression threshold for high and low expression in the Glasgow Breast Cancer Cohort. The threshold was identified as 153.33, with patients with weighted histoscores above 153.33 considered to have high ODAM cytoplasmic expression. Examples of protein expression (high/low) on breast cancer specimens are described below the graphical

representation.**Cytoplasmic ODAM and Survival in the Glasgow Breast Cancer Cohort**

850 patients had TMAs produced for the Glasgow Breast Cancer Cohort, of which 736 had ductal cancer and were included in the cohort for analysis. Of these, 722 of 736 had valid cancer-specific survival data and 414 had viable cores, leading to a final 411 patients with both viable cores and valid survival data. 159 patients had low ODAM cytoplasmic expression and had 32 events, while 252 had high expression and saw 64 events. Survival in the low ODAM group was 86% at 5 years, and 76% at 10 years, while in the high ODAM group survival was 82% at 5 years, and 69% at 10 years. Using Kaplan Meier survival analysis, mean cancer-specific survival (CSS) time for low ODAM cytoplasm expression was 155.1 months compared to high ODAM expression survival of 148.4 months, suggesting that low ODAM cytoplasm expression was associated with increased survival, although this was not statistically significant (HR 1.271, 95% C.I.; 0.831-1.943, log rank p=0.268) (*Figure 4-26*).

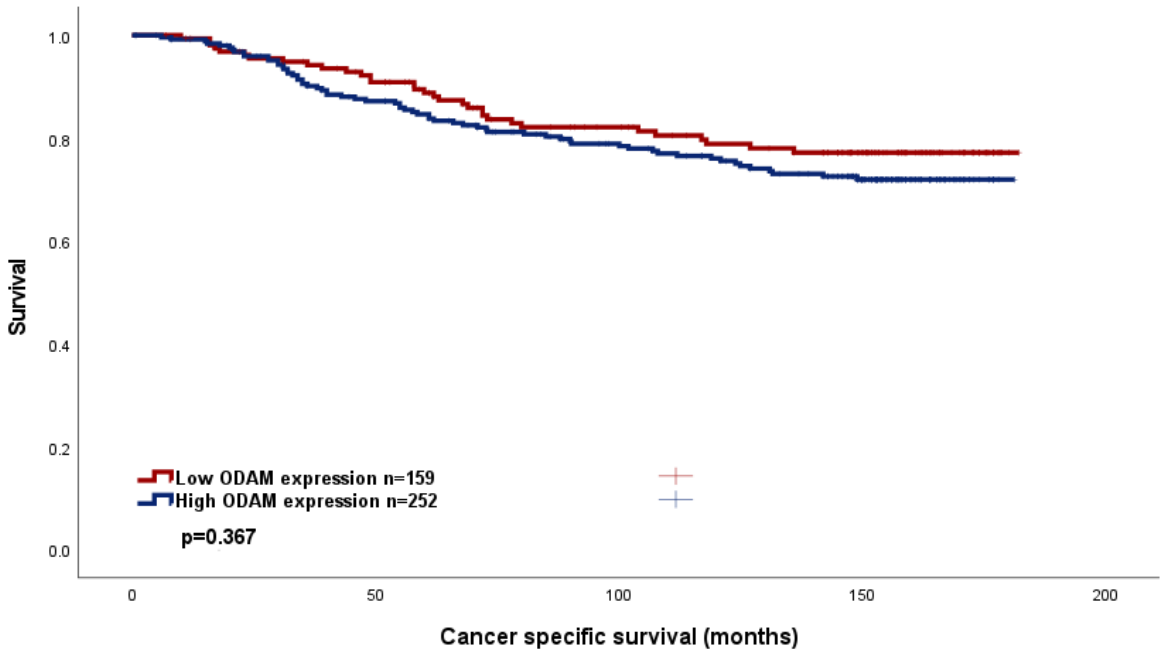

Figure 4-26 Cancer-specific survival in the Glasgow Breast Cancer Cohort according to ODAM cytoplasm expression. Kaplan Meier Curve showing the association between ODAM cytoplasm expression and survival (months). HR 1.271, 95% C.I.; 0.831-1.943, log rank p=0.268.

Within the entire Glasgow Breast Cancer Cohort, inter-factor correlation was assessed when comparing the high and low ODAM cytoplasmic expressors (*Table 4-1*). Here, necrosis was associated with ODAM cytoplasmic expression.

Table 4-1 Clinicopathological factors and their relation to ODAM cytoplasmic expression in the Glasgow Breast Cancer Cohort. Chi-squared analysis.

Clinicopathological factor	ODAM Cytoplasmic staining (%)		p
	Low	High	
Age (years)			
≤50	58(42.6)	78(57.4)	0.283
>50	102(36.7)	176(63.3)	
Tumour Size			
≤20mm	86(40)	129(60)	0.699
21-49mm	66(36.7)	114(63.3)	
≥50mm	8(44.4)	10(55.6)	
Grade			
I	20(30.3)	46(69.7)	0.206
II	65(37.8)	107(62.2)	
III	75(42.6)	101(57.4)	
Molecular Subtype			
Luminal A	59(36.2)	104(63.8)	0.542
Luminal B	37(39.4)	57(60.6)	
TNBC	38(38.8)	60(61.2))	
HER2 enriched	23(47.9)	25(52.1)	
Nodal Status			
N_0	91(36.2)	136	0.135
N_1	69(39.4)	112	
Lymphatic Invasion			
Absent	45(34.6)	85(65.4)	0.279
Present	20(27)	54(73)	
Vascular Invasion			
Absent	54(31.2)	119(68.8)	0.678
Present	11(35.5)	20(64.5)	
Necrosis			
Absent	**59(32.2)**	**124(67.8)**	**0.024**
Present	**96(43.6)**	**124(56.4)**	
Klintrup Makinen			
0	12(30.8)	27(69.2)	0.051
1	76(35.7)	137(64.3)	
2	44(39.3)	68(60.7)	
3	22(57.9)	16(42.1)	
Ki67			
Low (<15%)	99(36.8)	170(63.2)	0.126
High (>15%)	58(45)	71(55)	
Tumour Bud			
-Low	112(40)	168(60)	0.381
-High	45(35.2)	83(64.8)	
Tissue Stroma Percentage			
Low	109(38.2)	176(61.8)	0.912
High	48(39)	75(61)	

The cohort was subsequently stratified according to Oestrogen receptor status (ER-negative; ER-, and ER-positive; ER+). In the ER- group (153 patients), 64

patients had low cytoplasm ODAM and 15 events, and 89 had high ODAM, for 32 events. Within the ER- cases, 5-year survival was 82% in low ODAM cases, compared to 72% in high ODAM cases. 10-year survival was 69% in the low ODAM group compared to 59% in the high ODAM group. Mean survival for ER- patients was 147 for low cytoplasm ODAM expression, and 128.5 months for high ODAM, suggesting that in the ER- patients, low ODAM expression was protective, although this was not statistically significant (HR 1.599 95% C.I. 0.866-2.954, log rank p=0.134) (*Figure 4-27*).

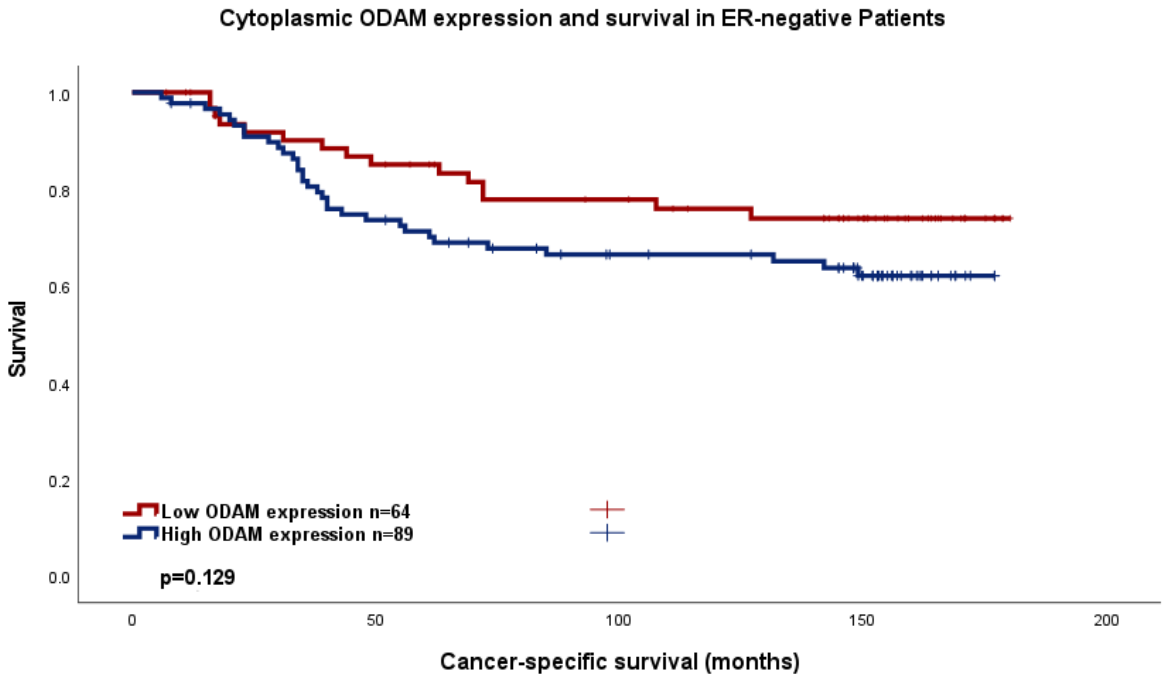

Figure 4-27 Cancer-specific survival in ER negative patients in the Glasgow Breast Cancer Cohort according to ODAM cytoplasm expression. Kaplan Meier Curve showing the association between ODAM cytoplasm expression and survival (months). HR 1.599 95% C.I. 0.866-2.954, log rank p=0.134.

Within the ER-negative group, inter-factor correlation was assessed when comparing the high and low ODAM cytoplasmic expressors (Table 4-2). Here, tumour budding, and KM score neared significance in relation to ODAM cytoplasmic expression.

Table 4-2 Clinicopathological factors and their prognostic significance within ER-negative patients in the Glasgow Breast Cancer Cohort, Chi-squared analysis.

Clinicopathological factor (ER-ve patients)	ODAM Cytoplasmic staining (%)		p
	Low	High	
Age (years)			
≤50	29(46.8)	33(53.2)	0.325

>50	36(38.7)	57(61.3)	
Tumour Size			
≤20mm	35(43.8)	45(56.3)	0.596
21-49mm	26(38.8)	41(61.2)	
≥50mm	4(57.1)	3(42.9)	
Grade			
I	1(20)	4(80)	0.583
II	16(38.8)	23(59)	
III	48(57.1)	63(56.8)	
Nodal Status			
N_0	32(38.6)	51(61.4)	0.416
N_1	33(45.8)	39(54.2)	
Lymphatic Invasion			
Absent	15(28.3)	38(71.7)	1.000
Present	9(25.7)	26(74.3)	
Vascular Invasion			
Absent	19(26)	54(74)	0.542
Present	5(33.3)	10(66.7)	
Necrosis			
Absent	15(41.7)	21(58.3)	1.000
Present	49(41.5)	69(58.5)	
Klintrup Makinen			
0	1(25)	3(75)	0.051
1	24(37.5)	40(62.5)	
2	25(38.5)	40(61.5)	
3	14(70)	6(30)	
Ki67			
Low (<15%)	36(38.3)	58(61.7)	0.083
High (>15%)	28(53.8)	24(46.2)	
Tumour Bud			
-Low	55(45.8)	65(54.2)	0.05
-High	9(26.5)	25(73.5)	
Tissue Stroma Percentage			
Low	41(39)	64(61)	0.384
High	23(46.9)	26(53.1)	

In the ER+ group (257 patients), 95 patients had low cytoplasmic ODAM with 17 events, while 162 had high cytoplasmic ODAM and 32 events. In ER+ patients, 5-year survival was 89% in low ODAM cases, and 89% in high ODAM cases, and at 10-years this reduced to 78% in low ODAM, and 74% in high ODAM expressors. In ER+ patients, survival in low cytoplasmic ODAM was 159.4 months and 157.9 for high ODAM expressing patients, suggesting similar cancer-specific survival between groups in ER+ disease (HR 1.068, 95% C.I. 0.593-1.924, log rank p=0.826), (*Figure*

4-28).

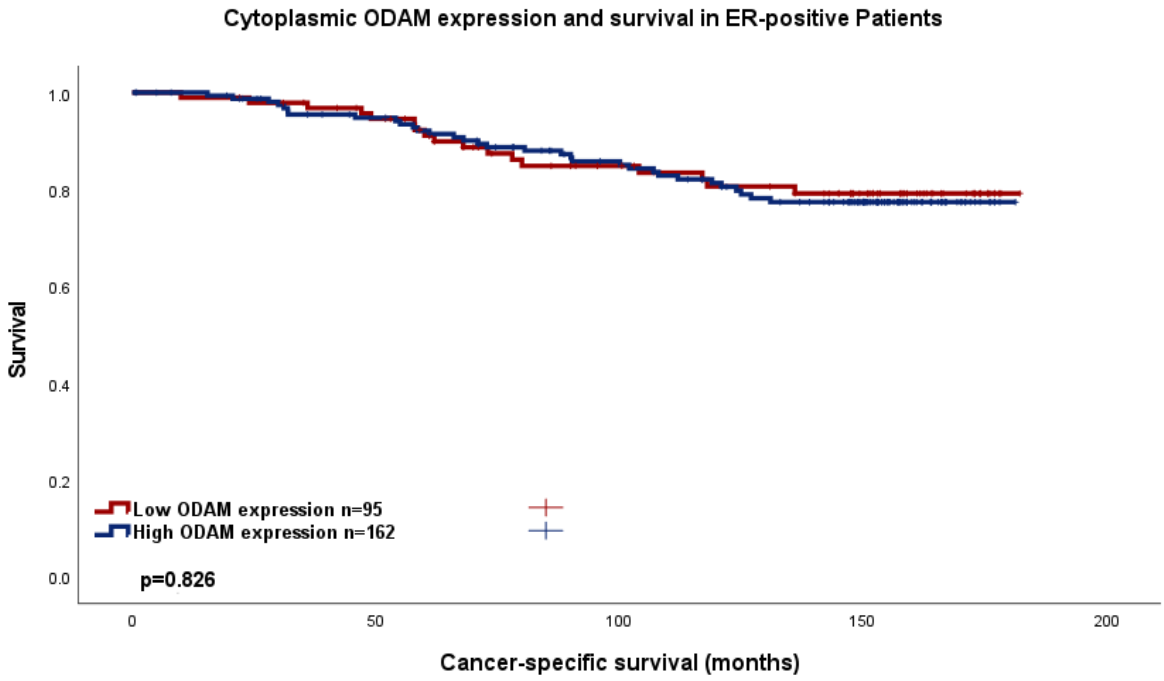

Figure 4-28 Cancer-specific survival in the ER positive patients in the Glasgow Breast Cancer Cohort according to ODAM cytoplasm expression. Kaplan Meier Curve showing the association between ODAM cytoplasm expression and survival (months). HR 1.068, 95% C.I. 0.593-1.924, log rank p=0.826.

Within the ER-positive group, inter-factor correlation was assessed when comparing the high and low ODAM cytoplasmic expressors (Table 4-3). Here, no associations were seen with ODAM cytoplasmic expression.

Table 4-3 Clinicopathological factors and their prognostic significance within ER-positive patients in the Glasgow Breast Cancer Cohort, Chi-squared analysis.

Clinicopathological factor	ODAM Cytoplasmic staining (%)		p
	Low	High	
Age (years)			
≤50	29(39.7)	44(60.3)	0.568
>50	66(35.7)	119(64.3)	
Tumour Size			
≤20mm	51(37.8)	84(62.2)	0.945
21-49mm	40(35.7)	72(64.3)	
≥50mm	4(36.4)	7(63.6)	
Grade			
I	19(31.7)	41(68.3)	0.520
II	49(36.8)	84(63.2)	
III	27(41.5)	38(58.5)	
Nodal Status			
N_0	59(41)	85(59)	0.077
N_1	36(33.3)	72(66.7)	

Lymphatic Invasion			
Absent	30(39.5)	46(60.5)	0.304
Present	11(28.2)	28(71.8)	
Vascular Invasion			
Absent	35(35.4)	64(64.6)	1.000
Present	6(37.5)	10(62.5)	
Necrosis			
Absent	44(30.1)	102(69.9)	0.011
Present	47(46.1)	55(53.9)	
Klintrup Makinen			
0	11(31.4)	24(68.6)	0.727
1	52(35.1)	96(64.9	
2	19(40.4)	28(59.6)	
3	8(50)	8(50)	
Ki67			
Low (<15%)	63(36)	112(64)	0.673
High (>15%)	30(39)	47(61)	
Tumour Bud			
-Low	57(35.8)	102(64.2)	0.787
-High	36(38.3)	58(61.7)	
Tissue Stroma Percentage			
Low	68(38)	111(62)	0.569
High	25(33.8)	49(66.2)	

Further stratification according to molecular subtype was then performed. These subtypes were divided into Luminal A, Luminal B, Triple-negative (most similar to "Basal-like" subtype) and HER-2 enriched groups. For 10 patients, molecular subgroup was not available. For the remaining patients, there were 161 Luminal A, 92 Luminal B, 95 TNBC and 48 HER-2 enriched cases. Luminal A patients had 59 low cytoplasmic ODAM expressors with 7 events, and 102 high-ODAM expressors with 17 events. Luminal B patients had 37 low ODAM expressors with 10 events, and 55 high ODAM expressors with 16 events. The TNBC patients had 38 low ODAM expressors with 11 events, and 57 patients with high ODAM with 18 events. Finally, HER-2 enriched patients consisted of 23 low ODAM cases with 4 events, and 25 high ODAM cases with 17 events. Kaplan Meier curves are shown for each subgroup below.

Luminal A patients had a 5-year survival of 90% and 85% at 10 years for low ODAM expressors, compared to 90% at 5 years and 79% at 10 years for high ODAM expressors. Mean survival was 166.8 months for low ODAM, and 158.3 months for high ODAM expressors (HR 1.332, 95% C.I. 0.552-3.214, p=0.523), (*Figure 4-29*).

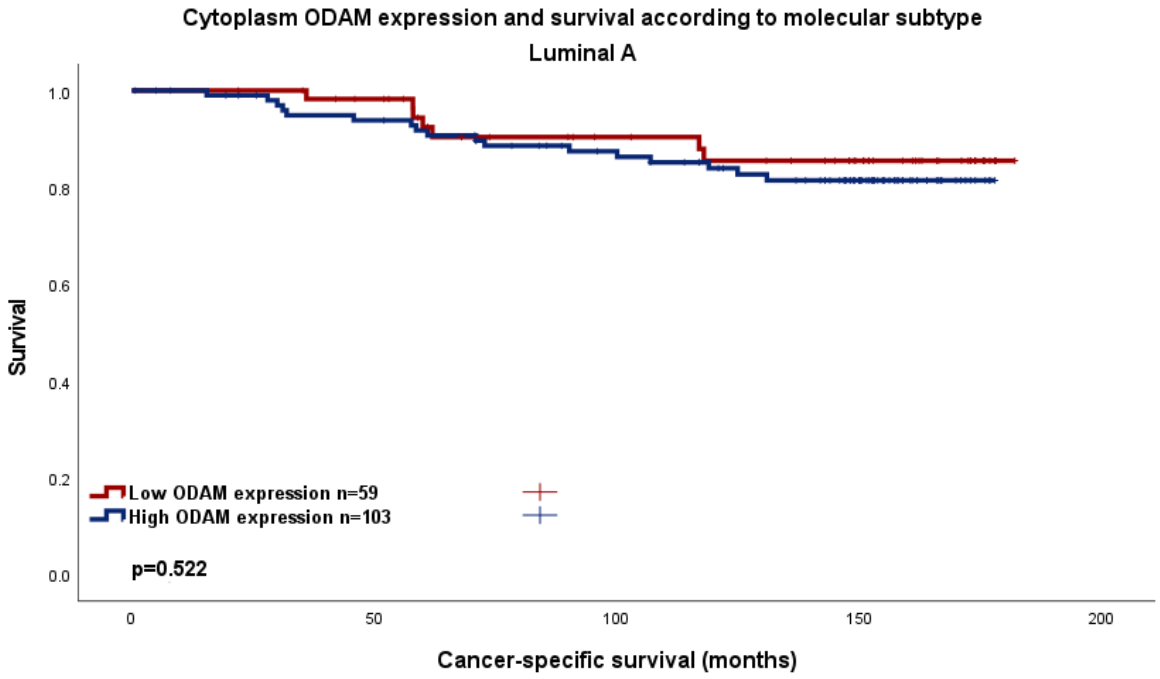

Figure 4-29 Cancer-specific survival in the Luminal A patients in the Glasgow Breast Cancer Cohort according to ODAM cytoplasm expression. Kaplan Meier Curve showing the association between ODAM cytoplasm expression and survival (months). HR 1.332, 95% C.I. 0.552--3.214, p=0.523.

Within the Luminal A group, inter-factor correlation was assessed when comparing the high and low ODAM cytoplasmic expressors (Table 4-4). Here, necrosis was associated with ODAM cytoplasmic expression.

Table 4-4 Clinicopathological factors and their relation to ODAM cytoplasmic expression in Luminal A patients in the Glasgow Breast Cancer Cohort. Chi-squared analysis

Clinicopathological factor (Luminal A)	ODAM Cytoplasmic staining (%)		p
	Low	High	
Age (years)			
≤50	18(39.1)	28(60.9)	0.718
>50	41(35)	76(65)	
Tumour Size			
≤20mm	34(39.5)	52(60.5)	0.538
21-49mm	24(33.3)	48(66.7)	
≥50mm	1(20)	4(80)	
Grade			
I	18(39.1)	28(60.9)	0.800
II	32(34)	62(66)	
III	9(39.1)	14(60.9)	
Nodal Status			
N_0	37(41.1)	53(58.9)	0.233

N_1	22(31)	49(69)	
Lymphatic Invasion			
Absent	22(35.5)	40(64.5)	0.615
Present	10(43.5)	13(56.5)	
Vascular Invasion			
Absent	28(36.8)	48(63.2)	0.723
Present	4(44.4)	5(55.6)	
Necrosis			
Absent	**30(29.4)**	**72(70.6)**	**0.023**
Present	**26(48.1)**	**28(51.9)**	
Klintrup Makinen			
0	7(33.3)	14(66.7)	0.979
1	38(36.9)	65(63.1)	
2	8(33.3)	16(66.7)	
3	2(33.3)	4(66.7)	
Ki67			
Low (<15%)	59(36.2)	104(63.8)	n/a
High (>15%)	0	0	
Tumour Bud			
-Low	35(35.4)	64(64.6)	0.736
-High	23(38.3)	37(61.7)	
Tissue Stroma Percentage			
Low	40(37)	68(63)	0.862
High	18(35.3)	33(64.7)	

Luminal B patients had a 5-year survival rate of 86% reducing to 68% at 10 years for low ODAM expressors, versus 87% 5-year survival and 61% 10-year survival in high ODAM expressors. Mean survival was 145.4months for low ODAM, and 147.9 months for high ODAM expressors (HR 1.067, 95% C.I. 484-2.352, p= 0.872), (*Figure 4-30*).

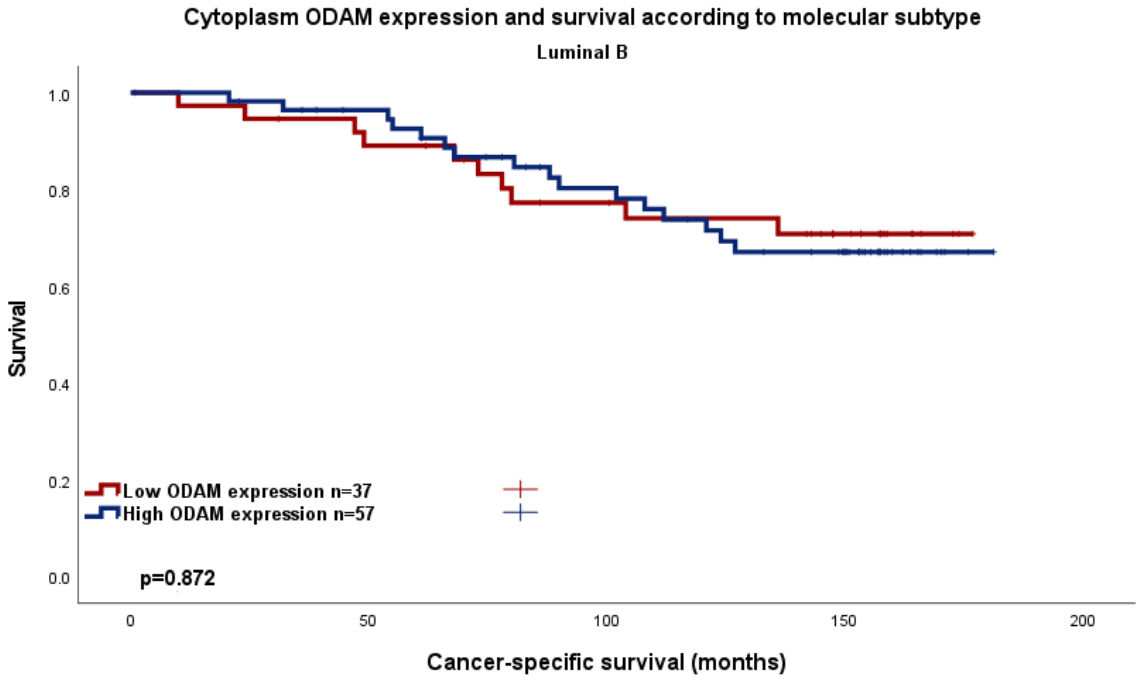

Figure 4-30 Cancer-specific survival in the Luminal B patients in the Glasgow Breast Cancer Cohort according to ODAM cytoplasm expression. Kaplan Meier Curve showing the association between ODAM cytoplasm expression and survival (months) HR 1.121, 95% C.I. 0.509-2.352, p=0.872

Within the luminal B group, inter-factor correlation was assessed when comparing the high and low ODAM cytoplasmic expressors. (Table 4-5). Here, lymphatic invasion was associated with ODAM cytoplasmic expression.

Table 4-5 Clinicopathological factors and their relation to ODAM Cytoplasmic expression in Luminal B patients in the Glasgow Breast Cancer Cohort. Chi-squared analysis.

Clinicopathological factor	ODAM Cytoplasmic staining (%)		p
	Low	High	
Age (years)			
≤50	14(42.4)	19(57.6)	0.665
>50	23(37.7)	38(62.3)	
Tumour Size			
≤20mm	16(34.8)	30(65.2)	0.495
21-49mm	17(41.5)	24(58.5)	
≥50mm	4(57.1)	3(42.9)	
Grade			
I	2(14.3)	12(85.7)	0.114
II	16(44.4)	20(55.6)	
III	19(43.2)	25(56.8)	
Nodal Status			
N_0	22(43.1)	29(56.9)	0.315
N_1	15(37.5)	25(62.5)	
Lymphatic Invasion			
Absent	**9(52.9)**	**8(47.1)**	**0.026**
Present	**2(11.8)**	**15(88.2)**	

Vascular Invasion			
Absent	9(33.3)	18(66.7)	1.000
Present	2(28.6)	5(71.4)	
Necrosis			
Absent	14(33.3)	28(66.7)	0.286
Present	23(46)	27(54)	
Klintrup Makinen			
0	4(33.3)	8(66.7)	0.528
1	15(33.3)	30(66.7)	
2	12(48)	13(52)	
3	6(50)	6(50)	
Ki67			
Low (<15%)	6(40)	9(60)	1.000
High (>15%)	31(39.2)	48(60.8)	
Tumour Bud			
-Low	24(40.7)	35(59.3)	0.828
-High	13(37.1)	22(62.9)	
Tissue Stroma Percentage			
Low	29(41.4)	41(58.6)	0.629
High	8(33.3)	16(66.7)	

TNBC patients had 5-year survival of 80% and 10-year survival of 65% in low ODAM expressors compared to 74% 5-year survival and 64% 10-year survival in high ODAM expressors. Mean survival was 141.6months for low ODAM and 134.7 months for high ODAM expressors (HR 1.069, 95% C.I.0.505-2.263, p= 0.862), (*Figure 4-31*).

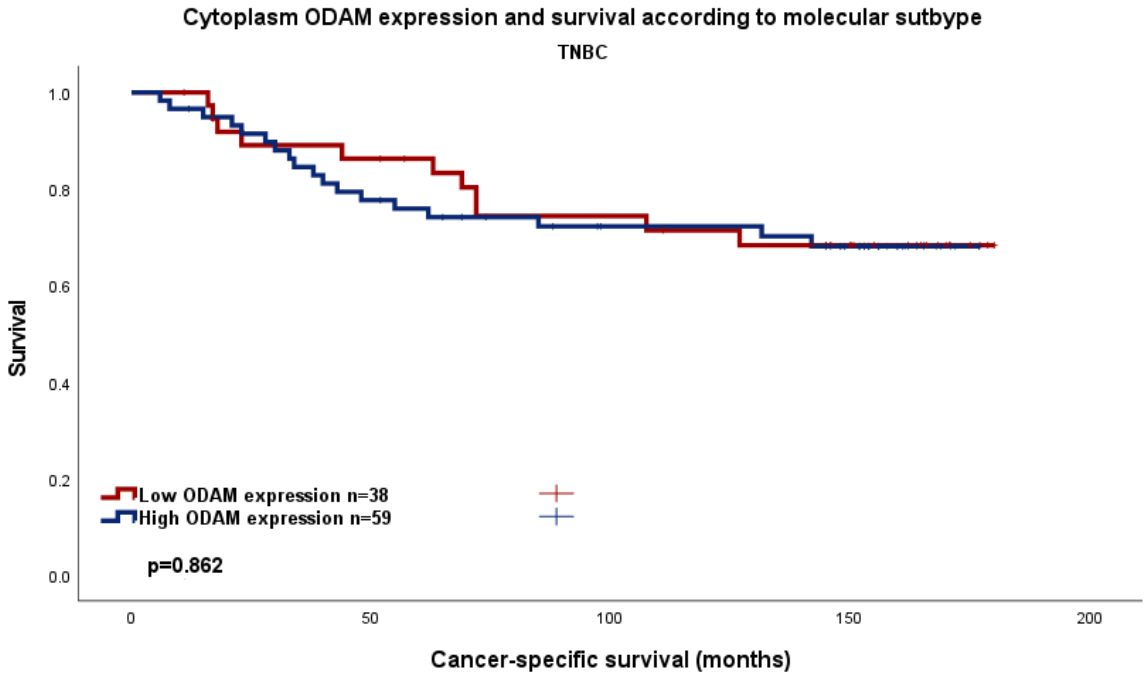

Figure 4-31 Cancer-specific survival in the Triple Negative patients in the Glasgow Breast Cancer Cohort according to ODAM cytoplasm expression. Kaplan Meier Curve showing the

association between ODAM cytoplasm expression and survival (months) HR 1.069, 95% C.I.0.505-2.263, p= 0.862.

When different clinicopathological factors were compared for inter-factor correlation within the TNBC portion of the Glasgow Breast Cancer cohort, none of the factors correlated significantly with ODAM cytoplasmic expression, (Table 4-6*)*.

Table 4-6 Clinicopathological factors and their relation to ODAM cytoplasmic expression in TNBC patients in the Glasgow Breast Cancer Cohort. Chi-squared analysis.

Clinicopathological factor	ODAM Cytoplasmic staining (%)		p
	Low	High	
Age (years)			
≤50	19(48.7)	20(51.3)	0.138
>50	19(32.2)	40(67.8)	
Tumour Size			
≤20mm	20(39.2)	31(60.8)	0.832
21-49mm	17(40.5)	25(59.5)	
≥50mm	1(25)	3(75)	
Grade			
I	0	4(100)	0.160
II	8(32)	17(68)	
III	30(43.5)	39(56.5)	
Nodal Status			
N_0	18(32)	38(67.9)	0.145
N_1	20(43.5)	22(52.4)	
Lymphatic Invasion			
Absent	10(27.8)	26(72.2)	0.339
Present	3(15)	17(85)	
Vascular Invasion			
Absent	10(21.7)	36(78.3)	0.682
Present	3(30)	7(70)	
Necrosis			
Absent	9(33.3)	18(66.7)	0.644
Present	28(40)	42(60)	
Klintrup Makinen			
0	1(25)	3(75)	0.077
1	12(29.3)	29(70.7)	
2	14(37.8)	23(62.2)	
3	10(66.7)	5(33.3)	
Ki67			
Low (<15%)	22(34.4)	42(65.6)	0.067
High (>15%)	15(55.6)	12(44.4)	
Tumour Bud			
-Low	32(42.7)	43(57.3)	0.3134
-High	5(22.7)	17(77.3)	
Tissue Stroma Percentage			
Low	27(37)	46(63)	0.809

High	10(41.7)	14(58.3)	

HER-2 enriched patients had 5-year survival rates of 81% and 10-year survival of 81% in low ODAM expressors, compared to 54% 5-year and 42% 10-year survival in high-ODAM expressors. Mean survival was 150.99 months for low ODAM, and 101.77 months for high ODAM expressors (HR 3.368, 95% C.I. 1.096-10.346, p=0.034), (*Figure 4-32*).

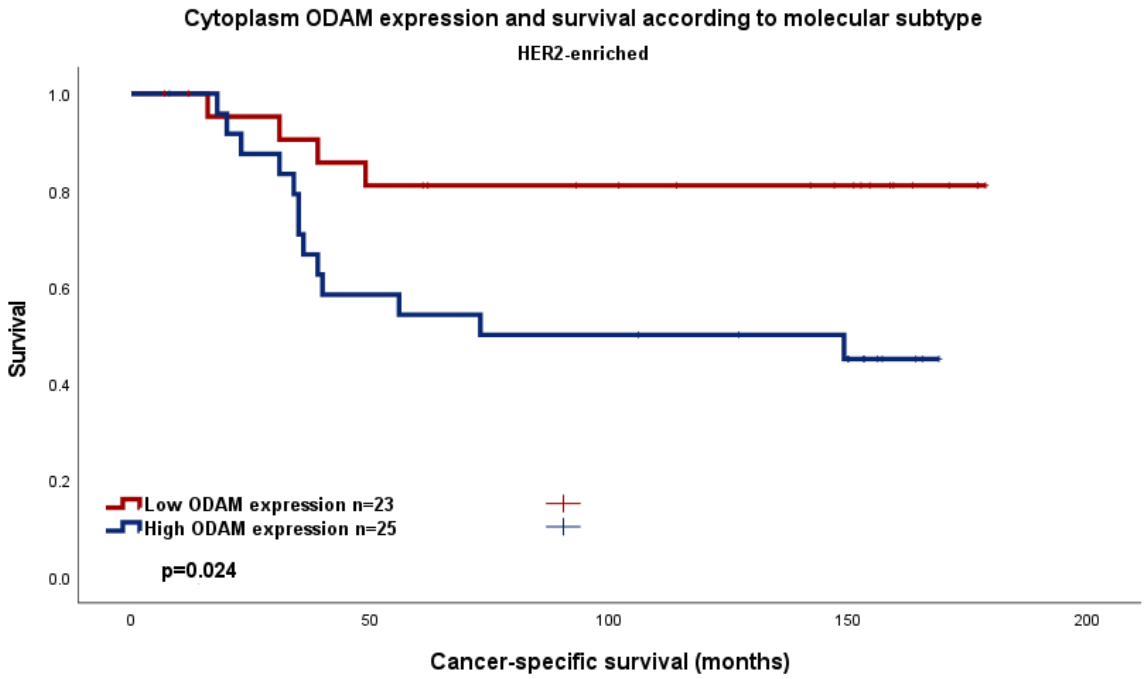

Figure 4-32 Cancer-specific survival in the HER-2 -enriched patients in the Glasgow Breast Cancer Cohort according to ODAM cytoplasm expression. Kaplan Meier Curve showing the association between ODAM cytoplasm expression and survival (month)s HR 3.368, 95% C.I. 1.096-10.346, p=0.034.

To further assess the effect of clinicopathological factors on survival in the HER2-enriched patients with the Glasgow Breast Cancer cohort, a Cox regression analysis was performed, (Table 4-7). On univariate analysis, nodal status, TSP, tumour budding and ODAM cytoplasmic expression were significantly associated with survival, but this effect was lost on multivariate analysis for all except TSP and nodal status.

Table 4-7 Clinicopathological factors and their prognostic significance within HER2-enriched patients in the Glasgow Breast Cancer Cohort. Univariate and multivariate Cox regression analysis.

Clinicopathological Factor	Univariate analysis (HR, 95% C.I.)	p	Multivariate analysis (HR, 95% C.I.)	p

Age	0.609(0.270-1.371)	0.231		
Tumour Size <20mm 20-49mm >50mm	 0.688(0.294-1.611) 2.074(0.467-9.203)	0.383 0.338 0.389 0.337		
Invasive Grade I II III	 0.704(0.263-1.886)	0.471 0.486 0.486		
Nodal Status	**2.485(1.062-5.813)**	**0.036**	**2.906(1.890-4.468)**	**<0.001**
Lymphatic Invasion	2.566(0.986-6.683)	0.054		
Vascular Invasion	0.964(0.127-7.296)	0.972		
Necrosis	1.875(0.441-7.976)	0.395		
Klintrup-Makinen 0 1 2 3	 3567.881(0-2.35^{E+96}) 3303.914(0-2.18^{E+96} 1087.661(0-7.236^{E+96}	0.501 0.731 0.940 0.941 0.949		
Ki67	1.627(0.718-3.689)	0.244		
Tumour budding	**0.537(0.358-0.805)**	**0.003**	0.999(0.640-1.558)	0.961
Tumour stroma percentage	**2.899(1.267-6.636)**	**0.012**	**1.658(1.074-2.559)**	**0.022**
ODAM cytoplasmic expression	**3.368(1.096-10.346)**	**0.034**	1.277(0.830-1.964)	0.265

Within the HER2-enriched group, inter-factor correlation was assessed when comparing the high and low ODAM cytoplasmic expression. Here, tumour size was found to be nearing significance in association with ODAM cytoplasmic expression, (*Table 4-8*).

Table 4-8 Clinicopathological factors and their relation to ODAM cytoplasmic expression in HER2-enriched patients in the Glasgow Breast Cancer Cohort. Chi-squared analysis.

Clinicopathological factor	**ODAM Cytoplasmic staining (%)**		**p**
	Low	**High**	

Age (years)			
≤50	7(43.8)	9(56.3)	0.765
>50	16(50)	16(50)	
Tumour Size			
≤20mm	14(58.3)	10(41.7)	0.064
21-49mm	7(31.8)	15(68.2)	
≥50mm	2(100)	0	
Grade			
I	0	0	0.311
II	2(33.3)	4(66.7)	
III	16(43.2)	21(56.8)	
Nodal Status			
N_0	13(54.2)	11(45.8)	0.564
N_1	10(41.7)	14(58.3)	
Lymphatic Invasion			
Absent	4(33.3)	8(66.7)	1.000
Present	4(30.8)	9(69.2)	
Vascular Invasion			
Absent	7(33.3)	14(66.7)	1.000
Present	1(25)	3(75)	
Necrosis			
Absent	4(66.7)	2(33.3)	0.407
Present	19(45.2)	23(54.8)	
Klintrup Makinen			
0	0	0	0.242
1	9(52.9)	8(47.1)	
2	10(40)	15(60)	
3	4(80)	1(20)	
Ki67			
Low (<15%)	11(47.8)	12(52.2)	1.000
High (>15%)	12(52.2)	11(47.8)	
Tumour Bud			
-Low	19(51.4)	18(48.6)	0.499
-High	4(36.4)	7(63.6)	
Tissue Stroma Percentage			
Low	12(80)	3(20)	1.000
High	11(47.8)	12(52.2)	

4.2.13 ODAM Nuclear Expression in the Glasgow Breast Cancer Cohort

Manual weighted histoscores of nuclear expression of ODAM were performed by FS. Scores varied from 0 to 195 (*Figure 4-33*).

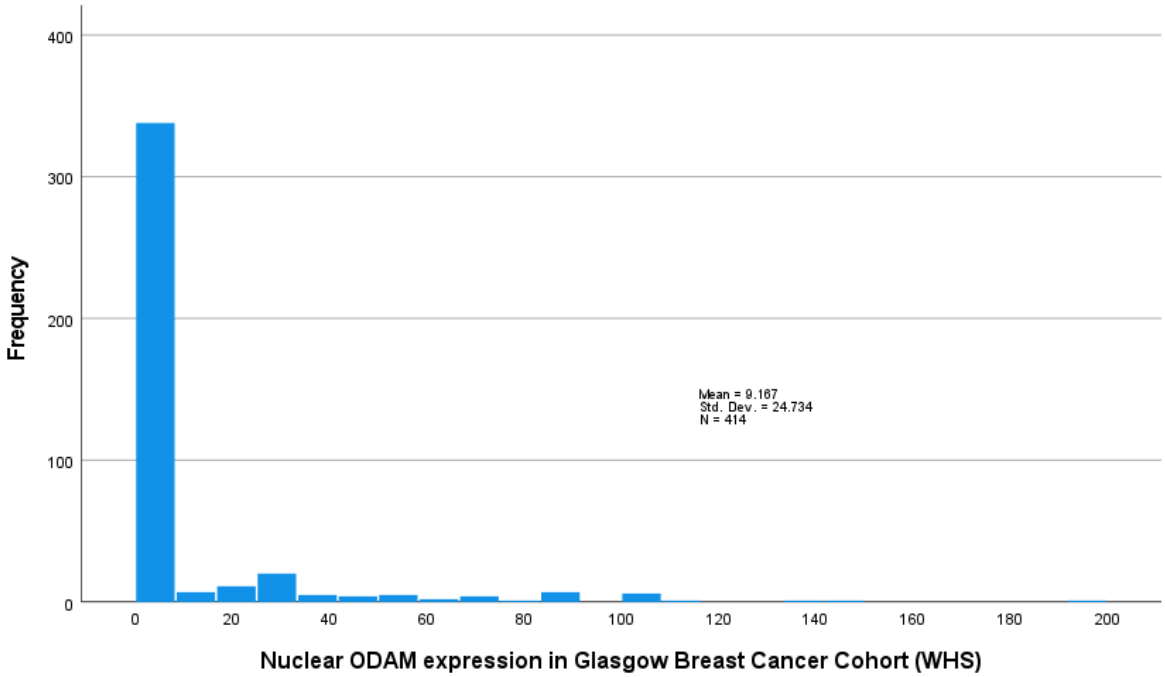

Figure 4-33 Distribution of ODAM nuclear expression (weighted histoscores) in the Glasgow Breast Cancer Cohort. Mean score 9.17, SD 24.73.

Counter-scores were performed manually by HVW for a minimum of 10% of cores, (n=90) and similarly to what was seen in FS scores, the selected sample WHS was always 0. No ICC was therefore calculated. The two scorers re-assessed a separate portion of samples informally and agreed that scores were consistent within a separate sample.

A threshold for high and low ODAM nuclear expression were delineated using R Studio to compare high versus low ODAM nuclear expression according to survival. The threshold was identified as 30 (*Figure 4-34*).

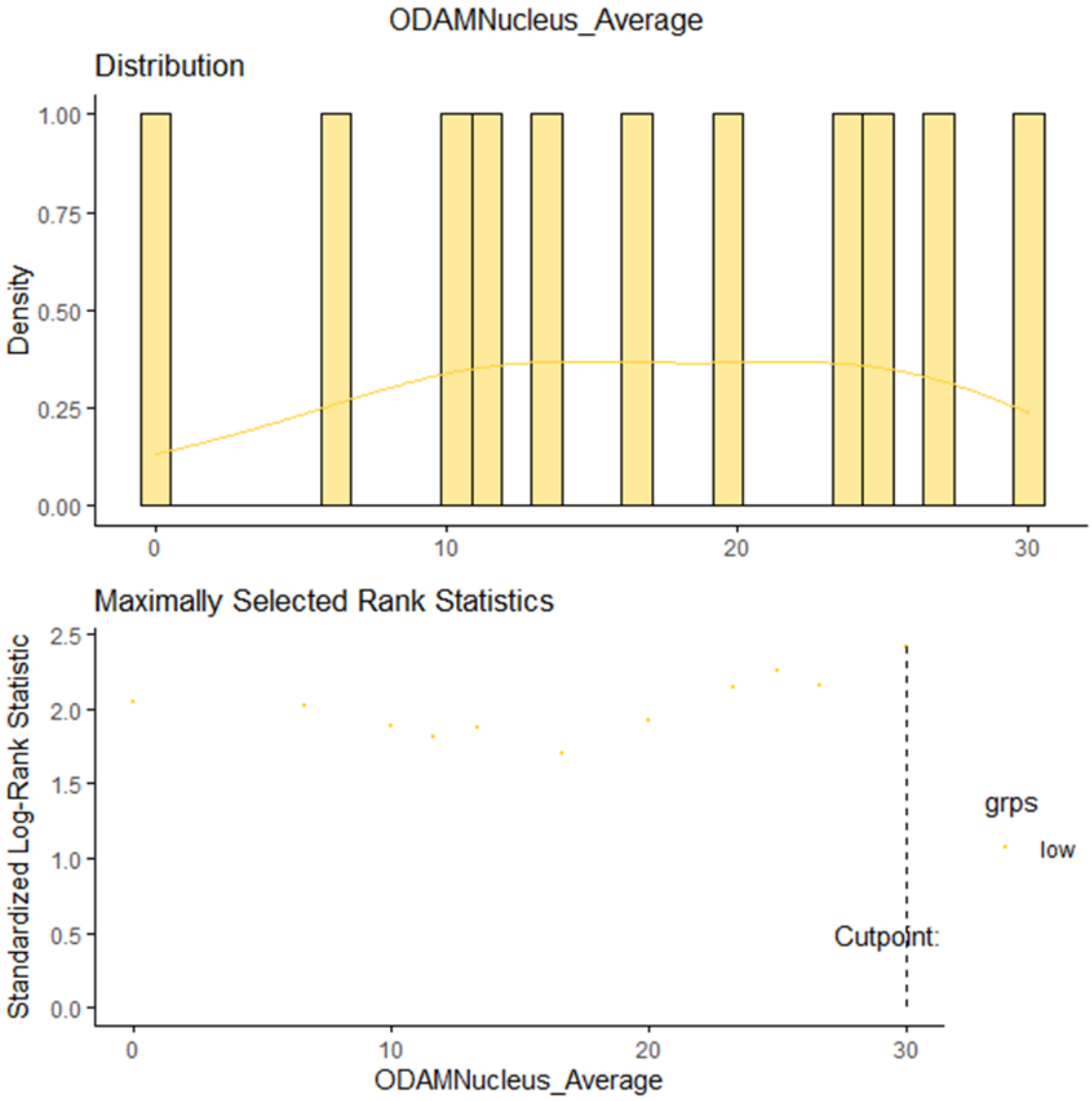

Low Expression

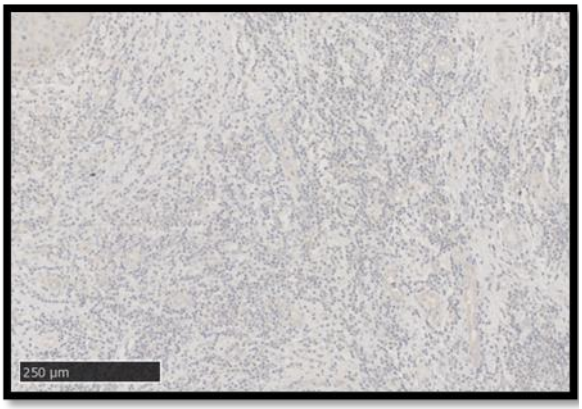

High Expression

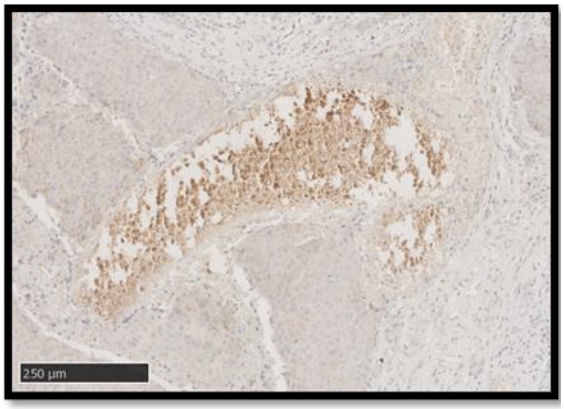

Figure 4-34 ODAM Nuclear expression - threshold for high and low expression of ODAM in the nucleus of the Glasgow Breast Cancer Cohort was identified as 30, with patients with weighted scores above 30 considered to have high ODAM nuclear expression. Examples of protein expression as seen on specimens is also described below the graphical representation.

4.2.14 Nuclear ODAM and Survival in the Glasgow Breast Cancer Cohort

850 patients had TMAs produced from the Glasgow Breast Cancer Cohort, of which 736 had ductal cancer and were included in the cohort for analysis. Of these, 722 of 736 had valid cancer-specific survival data and 414 had viable cores, leading to a final 411 patients with both viable cores and valid survival data. 362 patients had low ODAM nuclear expression and had 91 events, while 49 had high expression and 5 events. Survival in the low ODAM group was 86% at 5 years, and 76% at 10 years, while in the high ODAM group survival was 82% at 5 years, and 68% at 10 years. Using Kaplan Meier survival analysis, mean cancer-specific survival (CSS) time for low ODAM nuclear expression was 149 months compared to high ODAM expression survival of 164.9 months, suggesting that high ODAM nuclear expression was associated with increased survival (HR 0.362, 95% C.I.; 0.147-0.890, log rank p=0.027), (*Figure 4-35*).

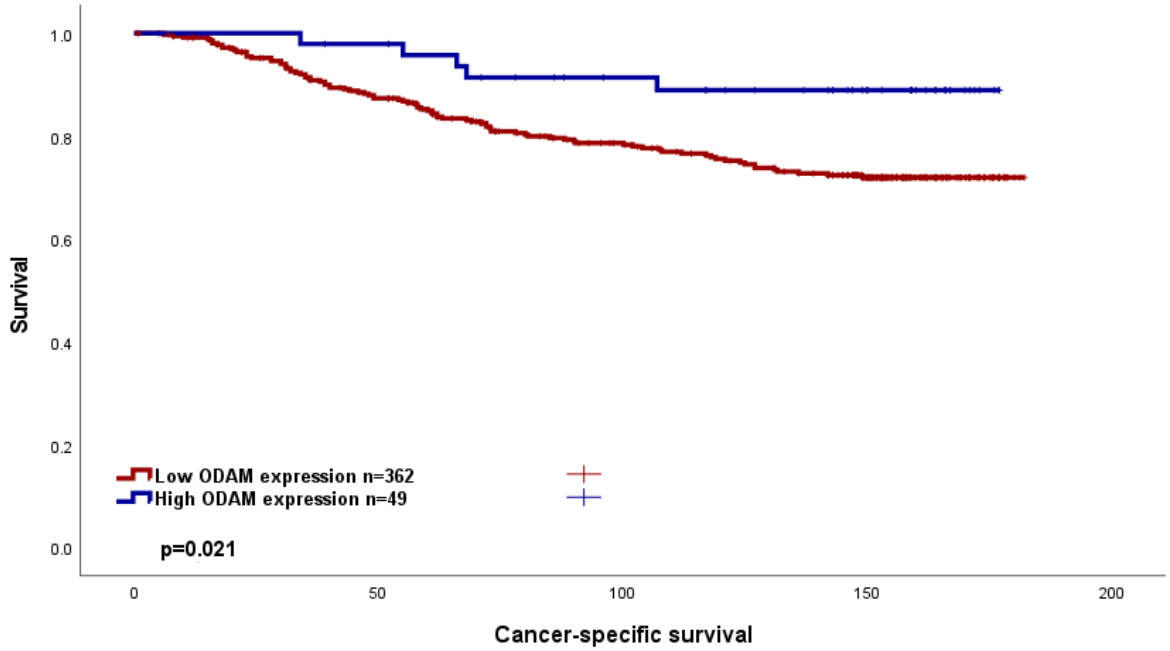

Figure 4-35 Cancer-specific survival in the Glasgow Breast Cancer Cohort according to ODAM Nuclear expression. Kaplan Meier Curve showing the association between ODAM nuclear expression and survival (months). HR 0.362, 95% C.I.;0.147-0.890, log rank p=0.027. 10-year survival noted at each key.

To further assess the effect of clinicopathological factors on survival in the Glasgow Breast Cancer cohort, a Cox regression analysis was performed. On multivariate analysis, ODAM nuclear expression retained statistical significance, together with size, molecular subtype, lymphatic invasion, vascular invasion were significant. (*Table 4-9*).

Table 4-9 Clinicopathological factors and their prognostic significance within the Glasgow Breast Cancer Cohort. Univariate and multivariate. Cox regression analysis.

Clinicopathological Factor	Univariate analysis (HR, 95% C.I.)	p	Multivariate analysis (HR, 95% C.I.)	p
Age	0.947 (0.680-1.318)	0.746		
Tumour Size		<0.001		
<20mm		<0.001		0.002
20-49mm	2.117(1.525-2.939)	<0.001	0.748(0.355-1.580)	0.447
>50mm	4.528(2.579-7.951)	<0.001	6.945(2.071-23.292)	0.002
Invasive Grade		.001		
I		.001		0.927
II	2.332(1.226-4.436)	0.010	1.300(0.348-4.851)	0.696
III	4.043(2.162-7.563)	.001	1.251(0.290-5.389)	0.764
Nodal Status	1.003(0.987-1.020)	0.694		
Molecular subtype		<0.001		
Luminal A		<0.001		0.027
Luminal B	2.343(1.525-3.599)	<0.001	1.170(0.300-4.557)	0.821
TNBC	2.710(1.779-4.128)	<0.001	4.562(1.259-16.535)	0.021
HER2-enriched	2.946(1.771-4.900)	<0.001	5.712(1.329-24.559)	0.019
Lymphatic Invasion	4.255(2.813-6.435)	<0.001	3.044(1.367-6.778)	0.006
Vascular Invasion	3.440(2.163-5.470)	<0.001	2.513(1.159-5.453)	0.020
Necrosis	3.288(2.290-4.722)	<0.001	1.686(0.635-4.475)	0.294
Klintrup-Makinen		0.033		<0.001
0		0.030		
1	0.812(0.481-1.372)	0.437	0.062(0.016-0.240)	<0.001
2	1.310(0.757-2.265)	0.334	0.048(0.009-0.251)	<0.001
3	0.621(0.277-1.395)	0.249	0.016(0.002-0.153)	<0.001
Ki67	1.658(1.199-2.294)	0.002	2.420(0.999-5.863)	0.050
Tumour budding	1.755(1.282-2.403)	<0.001	1.065(0.429-2.642)	0.893

Tumour stroma percentage	1.884(1.374-2.582)	<0.001	1.771(0.789-3.977)	0.166
ODAM nuclear expression	0.362(0.147-0.890)	0.027	0.420(0.126-1.407)	0.160

When different clinicopathological factors were compared for inter-factor correlation, grade, necrosis, and Klintrup Makinen were found to be significantly associated with ODAM nuclear expression, (*Table* 4-10).

Table 4-10 Clinicopathological factors and their relation to ODAM nuclear expression in the Glasgow Breast Cancer Cohort. Chi-squared analysis.

Clinicopathological factor	**ODAM Nuclear staining (%)**		**p**
	Low	**High**	
Age (years)			
≤50	121(88.9)	15(11.1)	0.749
>50	243(87.4)	35(12.6)	
Tumour Size			
≤20mm	189(87.9)	26(12.1)	0.991
21-49mm	158(87.8	22(12.2)	
≥50mm	16(88.9)	2(11.1)	
Grade			
I	**53(80.3)**	**13(19.7)**	**0.035**
II	**149(86.6)**	**23(13.4)**	
III	**162(94.2)**	**14(5.8)**	
Nodal Status			
N_0	199(87.7)	28(12.3)	0.657
N_1	159(87.8)	22(12.2)	
Lymphatic Invasion			
Absent	98(75.4)	32(24.6)	1.000
Present	56(75.7)	18(24.3)	
Vascular Invasion			
Absent	128(74)	45(26)	0.364
Present	26(83.9)	5(16.1)	
Necrosis			
Absent	**149(81.4)**	**34(18.6)**	**<0.001**
Present	**204(92.7)**	**16(7.3)**	
Klintrup Makinen			
0	**35(89.7)**	**4(10.3)**	**0.004**
1	**178(83.6)**	**35(16.4)**	
2	**105(93.8)**	**7(6.2)**	
3	**38(100)**	**0**	
Ki67			
Low (<15%)	231(85.9)	38(14.1)	0.142
High (>15%)	118(91.5)	11(8.5)	
Tumour Bud			
-Low	249(88.9)	31(11.1)	0.329
-High	109(85.2)	19(14.8)	
Tissue Stroma Percentage			
Low	249(87.4)	36(12.6)	0.869

High	109(88.6)	14(11.4)	

Stratification of the cohort to compare patients according to ER status was performed. 410 had valid ER-status data available. In the ER-negative patient group (n=153), 148 patients had low ODAM nuclear expression and had 461 events, while 5 had high ODAM expression and 1 event. Survival in the low ODAM group was 74% at 5 years, and 64% at 10 years, while in the high ODAM group survival was 80% at 5 and 10 years (HR 0.6 95% C.I. 0.083-4.353, p=0.614) (*Figure 4-36*).

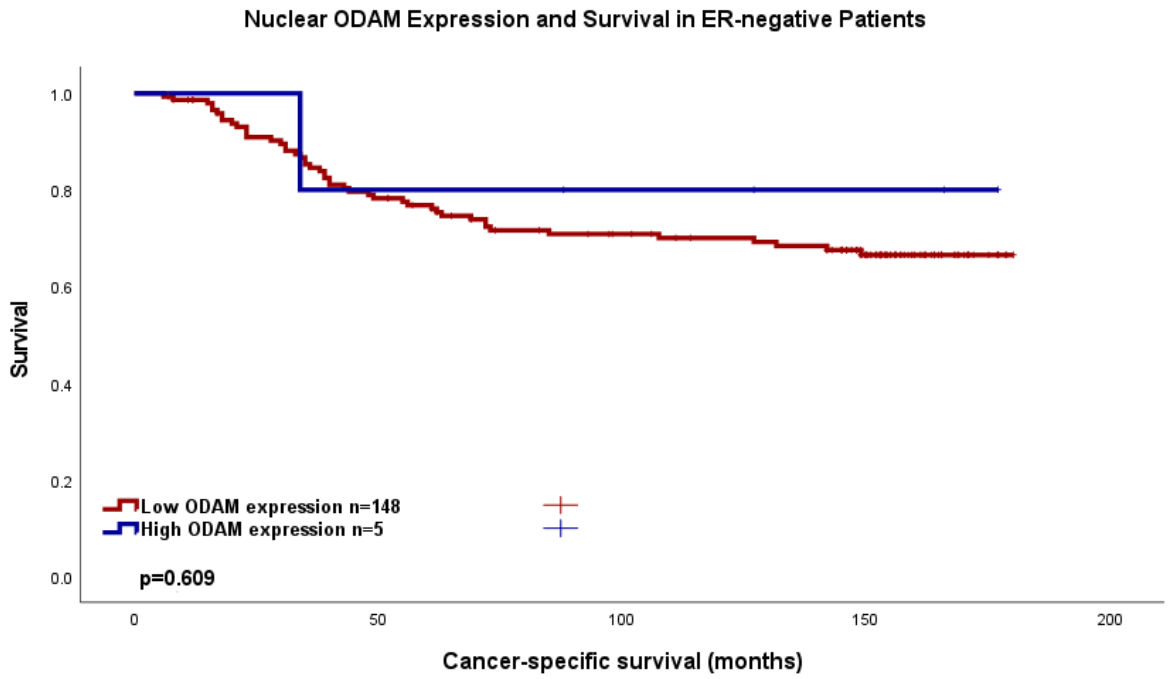

Figure 4-36 Cancer-specific survival in ER-negative patients in the Glasgow Breast Cancer Cohort according to ODAM nuclear expression. Kaplan Meier Curve showing the association between ODAM nuclear expression and survival (months). HR 0.6 95% C.I. 0.083-4.353, p=0.614

Within the ER-negative group, inter-factor correlation was assessed when comparing the high and low ODAM nuclear expressors, (*Table* 4-11*)*.

Table 4-11 Clinicopathological factors and their relation to ODAM nuclear expression in ER-negative patients in the Glasgow Breast Cancer Cohort. Chi-squared analysis.

Clinicopathological factor (ER-negative)	ODAM Nuclear staining (%)		p
	Low	High	
Age (years)	59(95.2)	3(4.8)	0.390
≤50	91(97.8)	2(2.2)	
>50			
Tumour Size			
≤20mm	76(95)	4(5)	0.433

21-49mm	66(98.5)	1(1.5)	
≥50mm	7(100)	0	
Grade			
I	5(100)	0	0.699
II	37(94.9)	2(5.1)	
III	108(97.3)	3(2.7)	
Nodal Status			
N_0	78(94)	5(6)	0.062
N_1	72(100)	0	
Lymphatic Invasion			
Absent	49(92.5)	4(7.5)	0.644
Present	34(97.1)	1(2.9)	
Vascular Invasion			
Absent	69(94.5)	4(5.5)	1.000
Present	14(93.3)	1(6.7)	
Necrosis			
Absent	33(91.7)	3(98.3)	0.084
Present	116(98.3)	2(1.7)	
Klintrup Makinen			
0	4(100)	0	0.568
1	61(95.3)	3(4.7)	
2	64(98.5)	1(1.5)	
3	20(100)	0	
Ki67			
Low (<15%)	91(96.8)	3(3.2)	1.000
High (>15%)	50(96.2)	2(3.8)	
Tumour Bud			
-Low	117(97.5)	3(2.5)	0.305
-High	32(94.1)	2(5.9)	
Tissue Stroma Percentage			
Low	100(95.2)	5(4.8)	0.179
High	49(100)	0	

In the ER-positive group (n=257), 214 had low nuclear ODAM expression, with 45 events, and 43 high ODAM expression, with 4 events. Survival in the low nuclear ODAM ER-positive group was 88% at 5 years and 79% at 10 years, and in the high ODAM group was 92% at 5 years and 90.7% at 10 years (HR 0.402 95% C.I. 0.144-1.117, p=0.081), (*Figure 4-37*).

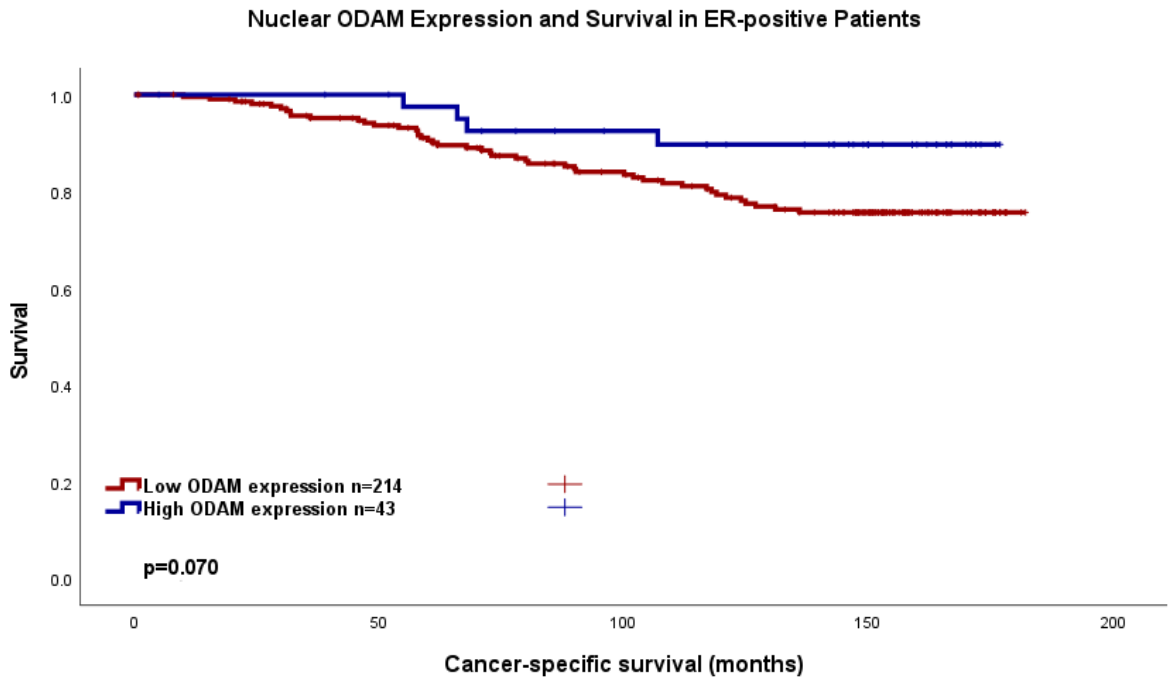

Figure 4-37 Cancer-specific survival in ER-positive patients in the Glasgow Breast Cancer Cohort according to ODAM nuclear expression. Kaplan Meier Curve showing the association between ODAM nuclear expression and survival (months). HR 0.402 95% C.I. 0.144-1.117, p=0.081

Within the ER-positive group, inter-factor correlation was assessed when comparing the high and low ODAM nuclear expressors, (Table 4-12). Here, no association with ODAM nuclear expression was seen.

Table 4-12 Clinicopathological factors and their relation to ODAM Nuclear expression in ER+ patients in the Glasgow Breast Cancer Cohort. Chi-squared analysis.

Clinicopathological factor (ER+ve patients)	ODAM Nuclear staining (%)		p
	Low	High	
Age (years)			
≤50	62(84.9)	11(15.1)	0.714
>50	152(82.2)	33(17.8)	
Tumour Size			
≤20mm	113(83.7)	22(16.3)	0.944
21-49mm	92(82.1)	20(17.9)	
≥50mm	9(81.8)	2(18.2)	
Grade			
I	48(80)	12(20)	0.771
II	112(84.2)	21(15.8)	
III	54(83.1)	11(16.9)	
Nodal Status			
N_0	121(84)	23(16)	0.409
N_1	87(80.6)	21(19.5)	
Lymphatic Invasion			
Absent	49(64.5)	27(35.5)	0.424

Present	22(56.4)	17(43.6)	
Vascular Invasion			
Absent	59(59.6)	40(40.4)	0.280
Present	12(75)	4(25)	
Necrosis			
Absent	116(76.5)	30(23.5)	0.181
Present	88(86.3)	14(13.7)	
Klintrup Makinen			
0	31(88.6)	4(11.4)	0.079
1	117(79.1)	31(20.9)	
2	41(87.2)	6(12.8)	
3	18(100)	0	
Ki67			
Low (<15%)	140(80)	35(20)	0.149
High (>15%)	68(88.3)	9(11.7)	
Tumour Bud			
-Low	132(83)	27(17)	0.864
-High	77(81.9)	17(18.1)	
Tissue Stroma Percentage			
Low	149(83.2)	30(16.8)	0.717
High	60(81.1)	14(18.9)	

Further stratification according to molecular subtype was then performed. These subtypes were divided into Luminal A, Luminal B, Triple-negative and HER-2 enriched groups. For 10 patients, molecular subgroup was not available. For the remaining patients, there were 162 Luminal A, 94 Luminal B, 97 TNBC and 48 HER-2 enriched cases. Luminal A patients had 132 low nuclear ODAM expressors with 23 events, and 30 high-ODAM expressors with 1 event. Luminal B patients had 81 low ODAM expressors with 23 events, and 13 high ODAM expressors with 3 events. The TNBC patients had 94 low ODAM expressors with 29 events, and 3 patients with high ODAM with no events. Finally, HER-2 enriched patients consisted of 46 low ODAM cases with 16 events, and 2 high ODAM cases with 1 event. Kaplan Meier curves are shown for each subgroup below.

Luminal A patients had a 5-year survival of 88% and 78% at 10 years for low ODAM expressors, compared to 100% at 5 years and 96% at 10 years for high ODAM expressors. (HR 0.164, 95% C.I. 0.022-1.214, p=0.077). When observing this using a Kaplan Meier survival curve, patients with low nuclear ODAM expression observed a survival benefit compared to low ODAM expressors (p=0.043), (*Figure 4-38*).

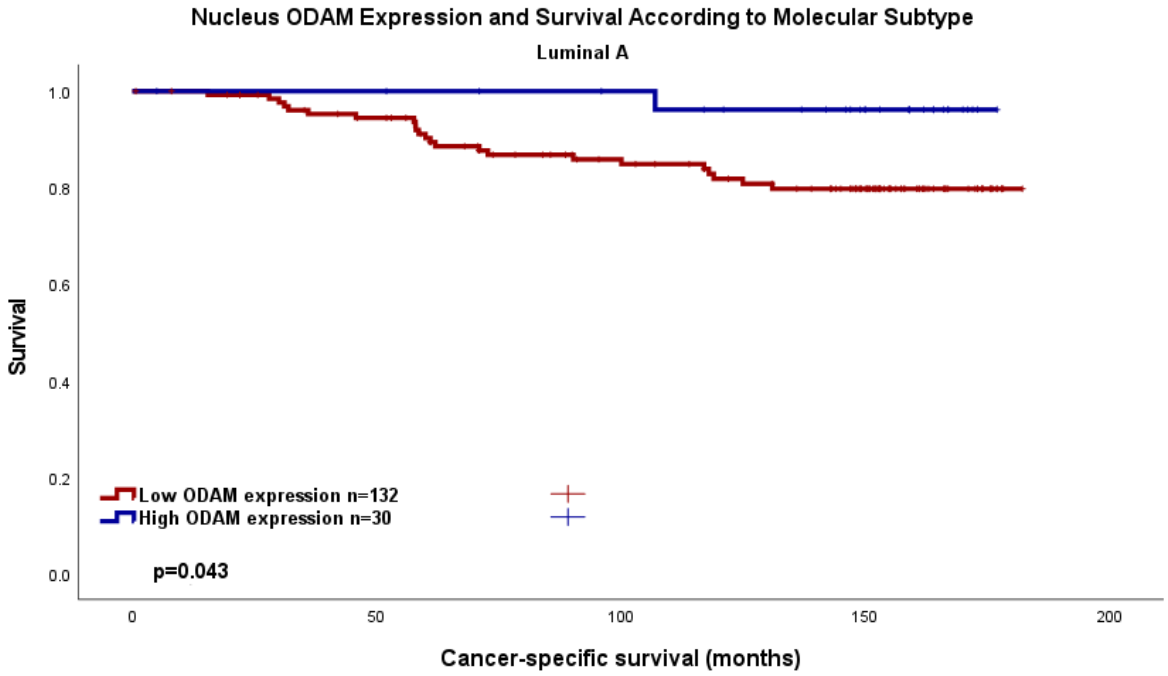

Figure 4-38 Cancer-specific survival in Luminal A patients in the Glasgow Breast Cancer Cohort according to ODAM nuclear expression. Kaplan Meier Curve showing the association between ODAM nuclear expression and survival (months). HR 0.164, 95% C.I. 0.022-1.214, p=0.077.

Despite being seen as statistically significant on Kaplan Meier survival analysis, on univariate Cox regression analysis, ODAM nuclear expression was not statistically significant, and therefore a multivariate analysis was not performed.

Within the Luminal A group, inter-factor correlation was assessed when comparing the high and low ODAM nuclear expressors, (Table 4-13). Here, tumour size and necrosis were associated with ODAM nuclear staining.

Table 4-13 Clinicopathological factors and their relation to ODAM Nuclear expression in Luminal A patients in the Glasgow Breast Cancer Cohort. Chi-squared analysis.

Clinicopathological factor	ODAM Nuclear staining (%)		p
	Low	High	
Age (years)			
≤50	39(85.3)	7(14.7)	0.512
>50	93(79.5)	24(20.5)	
Tumour Size			
≤20mm	**70(81.4)**	**16(18.6)**	**0.021**
21-49mm	**58(80.6)**	**14(19.4)**	
≥50mm	**4(80)**	**1(20)**	
Grade			
I	35(76.1)	11(23.9)	0.315
II	76(80.9)	18(19.1)	

III	21(91.3)	2(8.7)	
Nodal Status			
N_0	72(80)	18(20)	0.760
N_1	58(81.7)	13(18.3)	
Lymphatic Invasion			
Absent	39(62.9)	23(37.1)	1.000
Present	15(65.2)	8(34.8)	
Vascular Invasion			
Absent	46(60.5)	30(39.5)	0.146
Present	8(88.9)	1(11.4)	
Necrosis			
Absent	**76(74.5)**	**26(25.5)**	**0.020**
Present	**49(90.7)**	**5(9.3)**	
Klintrup Makinen			
0	18(85.7)	3(14.3)	0.088
1	79(76.7)	24(23.3)	
2	23(95.8)	1(4.2)	
3	6(100)	0	
Ki67			
Low (<15%)	132(81)	31(19)	N/A
High (>15%)	0	0	
Tumour Bud			
-Low	78(78.8)	21(21.2)	0.541
-High	50(83.3)	10(16.7)	
Tissue Stroma Percentage			
Low	88(81.5)	20(18.5)	0.672
High	40(78.4)	11(21.6)	

Luminal B patients had a 5-year survival of 88% and 63% at 10 years for low ODAM expressors, compared to 75% at both 5 and 10 years for high ODAM expressors. (HR 0.891, 95% C.I. 0.267-2.972, p=0.852), (*Figure 4-39*).

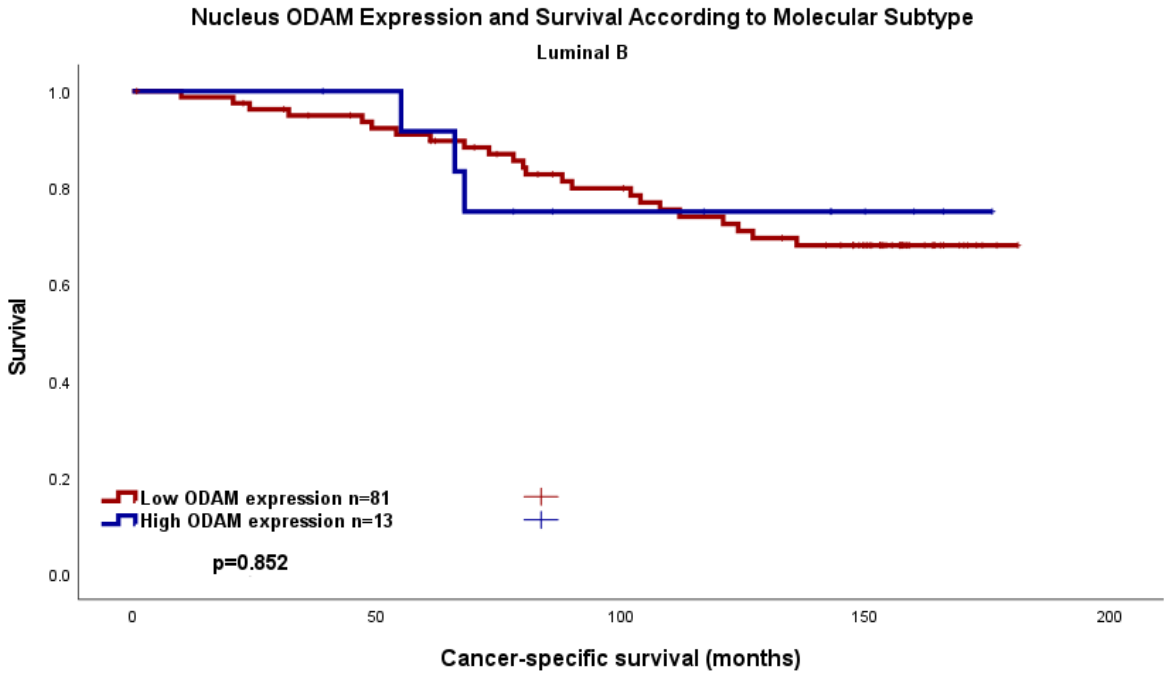

Figure 4-39 Cancer-specific survival in Luminal B patients in the Glasgow Breast Cancer Cohort according to ODAM nuclear expression. Kaplan Meier Curve showing the association between ODAM nuclear expression and survival (months). HR 0.891, 95% C.I. 0.267-2.972, p=0.852.

Within the Luminal B group, inter-factor correlation was assessed when comparing the high and low ODAM nuclear expressors, (Table 4-14). Here, no association with ODAM nuclear expression was seen.

Table 4-14 Clinicopathological factors and their relation to ODAM nuclear expression in Luminal B patients in the Glasgow Breast Cancer Cohort. Chi-squared analysis.

Clinicopathological factor	ODAM Cytoplasmic staining (%)		p
	Low	High	
Age (years)			
≤50	29(87.8)	4(12.2)	1.000
>50	52(85.2)	9(14.8)	
Tumour Size			
≤20mm	40(87)	6(13)	0.977
21-49mm	35(85.4)	6(14.6)	
≥50mm	6(85.7)	1(14.3)	
Grade			
I	13(92.9)	1(7.1)	0.217
II	33(91.7)	3(8.3)	
III	35(79.5)	9(20.5)	
Nodal Status			
N_0	46(90.1)	5(9.9)	0.293
N_1	32(80)	8(20)	
Lymphatic Invasion			

Absent	13(76.5)	4(23.5)	0.157
Present	8(47.1)	9(52.9)	
Vascular Invasion			
Absent	17(81)	4(19)	1.000
Present	4(57.1)	3(42.9)	
Necrosis			
Absent	38(90.5)	4(9.5)	0.369
Present	41(82)	9(18)	
Klintrup Makinen			
0	11(91.7)	1(8.3)	0.370
1	38(84.4)	7(15.6)	
2	20(80)	5(20)	
3	12(100)	0	
Ki67			
Low (<15%)	11(73.3)	4(26.7)	0.212
High (>15%)	70(88.6)	9(11.4)	
Tumour Bud			
-Low	53(89.8)	6(11.2)	0.222
-High	28(80)	7(20)	
Tissue Stroma Percentage			
Low	60(85.7)	10(14.3)	1.000
High	21(87.5)	3(12.5)	

Triple-negative ("basal-like) patients had a 5-year survival of 76% and 64% at 10 years for low ODAM expressors, compared to 100% at 5 and 10 years for high ODAM expressors. (HR 0.047, 95% C.I. 0-249.450, p=0.458), (*Figure 4-40*).

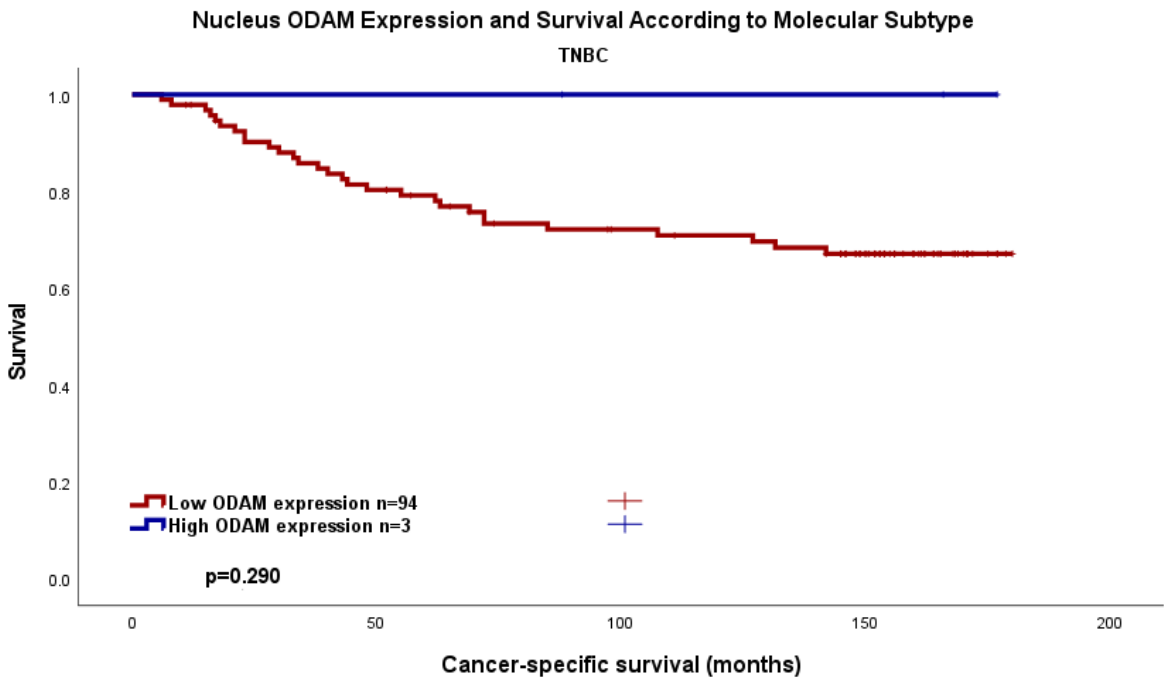

Figure 4-40 Cancer-specific survival in TNBC patients in the Glasgow Breast Cancer Cohort according to ODAM nuclear expression. Kaplan Meier Curve showing the association between ODAM nuclear expression and survival (months). HR 0.891, 95% C.I. 0.267-2.972, p=0.852. HR 0.047, 95% C.I. 0-249.450, p=0.458.

Within the TNBC group, inter-factor correlation was assessed when comparing the high and low ODAM nuclear expressors, (Table 4-15). Here, no association with ODAM nuclear expression was seen.

Table 4-15 Clinicopathological factors and their relation to ODAM nuclear expression in TNBC patients in the Glasgow Breast Cancer Cohort. Chi-squared analysis.

Clinicopathological factor	ODAM Cytoplasmic staining (%)		p
	Low	High	
Age (years)			
≤50	37(94.9)	2(5.1)	0.561
>50	58(98.3)	1(1.7)	
Tumour Size			
≤20mm	49(96.1)	2(3.9)	0.854
21-49mm	41(97.6)	1(2.4)	
≥50mm	4(80)	1(20)	
Grade			
I	4(100)	0	0.902
II	24(96)	1(4)	
III	67(97.1)	2(2.9)	
Nodal Status			
N_0	53(94.6)	3(5.4)	0.258
N_1	42(100)	0	
Lymphatic Invasion			
Absent	33(91.7)	3(8.3)	0.545
Present	20(100)	0	
Vascular Invasion			
Absent	43(93.5)	3(6.5)	1.000
Present	10(100)	0	
Necrosis			
Absent	25(92.6)	2(7.4)	0.186
Present	69(98.6)	1(1.4)	
Klintrup Makinen			
0	4(100)	0	0.238
1	38(92.7)	3(7.3)	
2	37(100)	0	
3	15(100)	0	
Ki67			
Low (<15%)	62(96.9)	2(3.1)	1.000
High (>15%)	26(96.3)	1(3.7)	
Tumour Bud			
-Low	73(97.3)	2(2.7)	0.542
-High	21(95.5)	1(4.5)	
Tissue Stroma Percentage			
Low	70(95.9)	3(4.1)	0.572
High	24(100)	0	

HER2-enriched patients had a 5-year survival of 68% and 59% at 10 years for low ODAM expressors, compared to 50% at 5 and 10 years for high ODAM expressors. (HR 1.714, 95% C.I. 0.226-13.027, =0.603), (*Figure 4-41*).

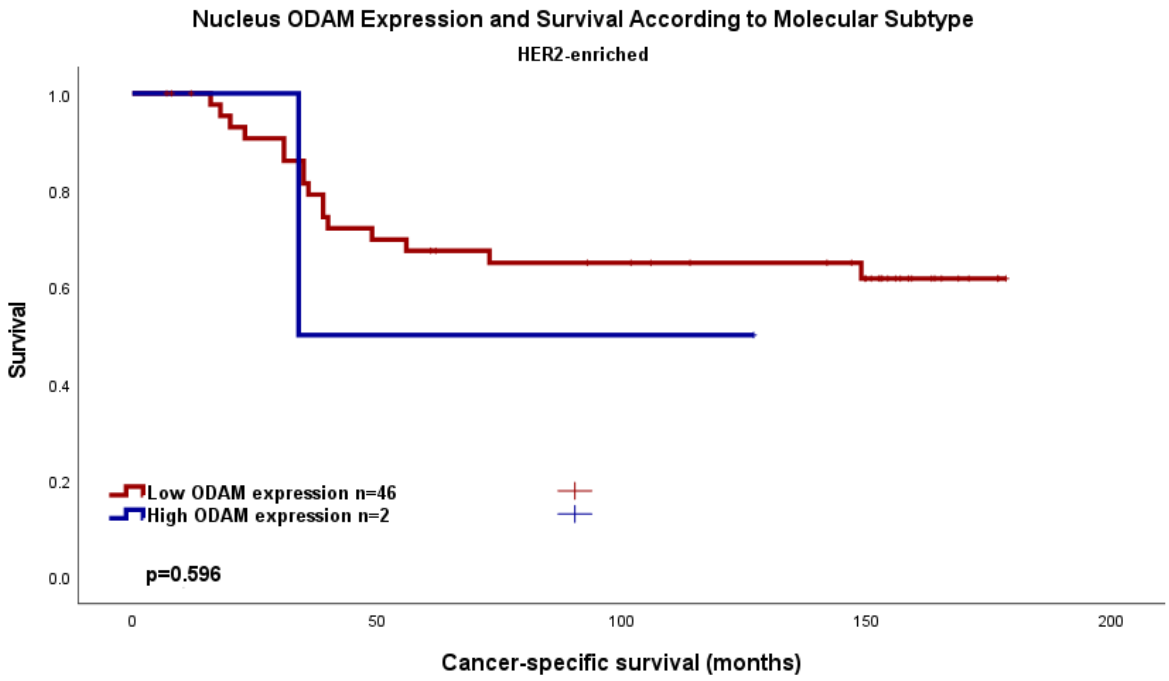

Figure 4-41 Cancer-specific survival in HER2 enriched patients in the Glasgow Breast Cancer Cohort according to ODAM nuclear expression. Kaplan Meier Curve showing the association between ODAM nuclear expression and survival (months). HR 1.714, 95% C.I. 0.226-13.02

Within the HER2-enriched group, inter-factor correlation was assessed when comparing the high and low ODAM nuclear expressors, (Table 4-16). Here, necrosis was associated with ODAM nuclear expression, and Klintrup Makinen neared significance.

Table 4-16 Clinicopathological factors and their relation to ODAM nuclear expression in HER2-enriched patients in the Glasgow Breast Cancer Cohort. Chi-squared analysis.

Clinicopathological factor	ODAM Nuclear staining (%)		p
	Low	High	
Age (years)			
≤50	39(84.8)	7(15.2)	0.512
>50	93(79.5)	24(20.5)	
Tumour Size			
≤20mm	70(81.4)	16(18.6)	0.989
21-49mm	58(80.6)	1419.4)	
≥50mm	4(80)	1(20)	
Grade			
I	35(76.1)	11(23.9)	0.315
II	76(80.9)	18(19.1)	

III	21(91.3)	2(8.7)	
Nodal Status			
N_0	72(80)	18(20)	0.760
N_1	58(81.7)	13(18.3)	
Lymphatic Invasion			
Absent	39(62.9)	23(37.1)	1.000
Present	15(65.2)	8(34.8)	
Vascular Invasion			
Absent	46(60.5)	30(39.5)	0.146
Present	8(88.9)	1(11.1)	
Necrosis			
Absent	**76(74.5)**	**26(25.5)**	**0.020**
Present	**49(90.7)**	**5(9.3)**	
Klintrup Makinen			
0	0	0	0.088
1	18(85.7)	3(14.3)	
2	79(76.7)	24(23.3)	
3	23(95.8)	1(4.2)	
Ki67			
Low (<15%)	132(81)	31(19)	
High (>15%)	0	0	
Tumour Bud			
-Low	78(78.8)	21(21.2)	0.541
-High	50(83.3)	10(16.7)	
Tissue Stroma Percentage			
Low	88(81.5)	20(18.5)	0.672
High	40(78.4)	11(21.6)	

4.2.15 ODAM Expression in the Glasgow Breast Cancer Cohort - Combined Scoring

Weighted histoscores for nuclear and cytoplasm expression of ODAM were combined to create four categories: ODAM high nuclear:high cytoplasm (HNHC, All-High), ODAM high nuclear:low cytoplasm (HNLC), ODAM low nuclear: high cytoplasm(LNHC), and ODAM low nuclear: low cytoplasm(LNLC, All-Low), to assess whether more prognostic power could be conferred to ODAM protein expression on cancer-specific survival. 411 patients had valid survival data. 45 patients had HNHC phenotype with 5 events, 4 had HNLC and 0 events, 207 had LNHC and 59 events, and 155 had LNLC and 32 events.

In the All-High group 5-year survival was 91%- and 10-year survival 88%. The LNHC group had a 5-year survival of 82%- and 10-year survival of 100%. The LNHC group had a 5-year survival of 80% and 10-year survival of 64%. The All-Low group had a 5-year survival of 85%, with 10-year survival at 75%, (*Figure 4-42*).

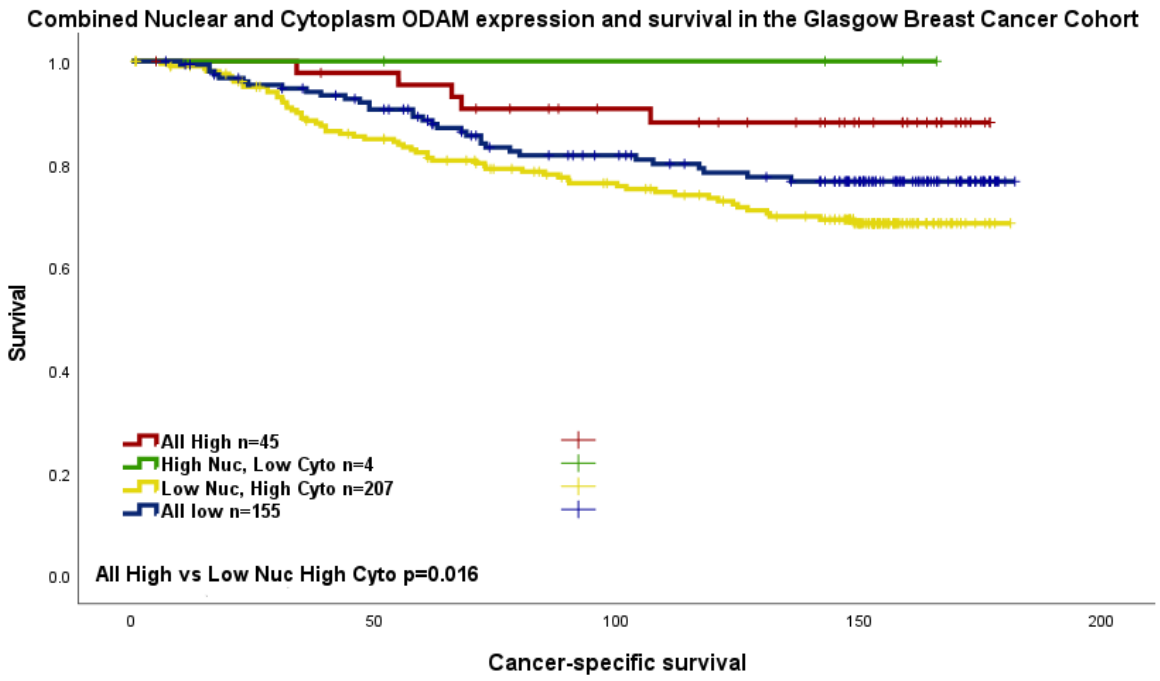

Figure 4-42 Combined Nuclear and Cytoplasm ODAM expression and survival in the Glasgow Breast Cancer Cohort. Pairwise comparisons are described in the graph.

Pairwise comparison demonstrated that LNHC had statistically significant worse survival than the All-High group, (*Table 4-17*).

Table 4-17 Pairwise comparisons on Kaplan Meier survival analysis for combined nuclear and cytoplasmic ODAM expression.

Pairwise Comparison p=	1 HNHC	2 HNLC	3 LNHC	4 LNLC
1 HNHC		0.528	**0.016**	0.121
2 HNLC	0.528		0.257	0.344
3 LNHC	**0.016**	0.257		0.107
4 LNLC	0.121	0.344	0.107	

On multivariate analysis however, ODAM combined scoring did not remain statistically significant, (*Table 4-18*).

Table 4-18 Clinicopathological factors and their prognostic significance in the Glasgow Breast Cancer Cohort with regards to combined nuclear and cytoplasmic ODAM scoring. Univariate and multivariate Cox regression analysis.

Clinicopathological Factor	**Univariate analysis (HR, 95% C.I.)**	**p**	**Multivariate analysis (HR, 95% C.I.)**	**p**
Age	0.947 (0.680-1.318)	0.746		
Tumour Size <20mm		**<0.001** **<0.001**		**0.002**

20-49mm	**2.117(1.525-2.939)**	**<0.001**	**0.936(0.420-2.089)**	**0.872**
>50mm	**4.528(2.579-7.951)**	**<0.001**	**8.321(2.396-28.900)**	**<0.001**
Invasive Grade		**<0.001**		
I				0.742
II	**2.332(1.226-4.436)**	**0.010**	1.549(0.416-5.764)	0.514
III	**4.043(2.162-7.563)**	**<0.001**	1.784(0.407-7.818)	0.443
Nodal Status	1.003(0.987-1.020)	0.694		
Molecular Subtype		**<0.001**		
Luminal A		**<0.001**		**0.087**
Luminal B	**2.343(1.525-3.599)**	**<0.001**	**1.271(0.326-4.956)**	**0.729**
TNBC	**2.710(1.779-4.128)**	**<0.001**	**3.383(0.944-12.122)**	**0.061**
HER2-enriched	**2.946(1.771-4.900)**	**<0.001**	**5.047(1.184-21.510)**	**0.029**
Lymphatic Invasion	**4.255 (2.813-6.435)**	**<0.001**	**2.641(1.169-5.965)**	**0.019**
Vascular Invasion	**3.440(2.163-5.470)**	**<0.001**	**2.462(1.120-5.413)**	**0.025**
Necrosis	**3.288(2.290-4.722)**	**<0.001**	1.496(0.551-4.063)	0.430
Klintrup-Makinen		**0.033**		
0		**0.030**		**<0.001**
1	**0.812(0.481-1.372)**	**0.437**	**0.052(0.012-0.204)**	**<0.001**
2	**1.310(0.757-2.265)**	**0.334**	**0.035(0.006-0.186)**	**<0.001**
3	**0.621(0.277-1.395)**	**0.249**	**0.013(0.001-0.132)**	**<0.001**
Ki67	**1.658(1.199-2.294)**	**0.002**	1.784(0.705-4.518)	0.222
Tumour budding	**1.755(1.282-2.403)**	**<0.001**	1.209(0.483-3.025)	0.685
Tumour stroma percentage	**1.884(1.374-2.582)**	**<0.001**	2.155(0.964 - 4.814)	0.061
ODAM combined score		**0.017**		
All High		**0.078**		0.113
All High v HNLC	**0(0-2.945^{E+2})**	**0.967**	0)0-1.06 $^{E+282}$)	0.978

All High v LNHC	**2.918(1.171-7.271**	**0.021**	3.715 (0.998-13.828)	0.050
All High v All Low	**2.053(0.800-5.270)**	**0.135**	1.300(0.327-5.177)	0.710

Examining the relationship between clinicopathological factors and patients in each subgroup, molecular subtype, Klintrup Makinen and necrosis were associated with ODAM combined score, (Table 4-19).

Table 4-19 Clinicopathological factors and their relation to ODAM combined nuclear and cytoplasmic expression in the Glasgow Breast Cancer Cohort. Chi-squared analysis.

Clinicopathological factor	**ODAM combined score (%)**				**p**
	All High	**HNLC**	**LNHC**	**All Low**	
Age (years)					
≤50	13(9.6)	2(1.5)	65(47.8)	56(41.2)	0.600
>50	33(11.9)	29(0.7)	143(51.4)	100(36)	
Tumour Size					
≤20mm	24(11.2)	2(0.9)	105(48.8)	84(39.1)	0.981
21-49mm	20(11.1)	2(1.1)	94(52.2)	64(35.6)	
≥50mm	2(11.1)	0	8(44.4)	8(44.4)	
Grade					
I	12(18.2)	1(1.5)	34(51.5)	19(28.8)	0.055
II	23(13.4)	0	84(48.8)	65(37.8)	
III	11(6.3)	3(1.7)	90(51.1)	72(40.9)	
Molecular Subtype					
Luminal A	**29(17.8)**	**2(1.2)**	**75(46)**	**57(35)**	**0.015**
Luminal B	**12(12.8)**	**1(1.1)**	**45(47.9)**	**36(38.3)**	
TNBC	**2(2)**	**1(1)**	**58(59.2)**	**37(37.8)**	
HER2-enriched	**2(4.2)**	**0**	**23(47.9)**	**23(47.9)**	
Nodal Status					
N_0	24(10.6)	4(1.8)	112(49.3)	87(38.3)	0.147
N_1	22(12.2)	0	90(49.7)	69(38.1)	
Lymphatic Invasion					
Absent	29(22.3)	3(2.3)	56(43.1)	42(32.3)	0.701
Present	17(23)	1(1.4)	37(50)	19(25.7)	
Vascular Invasion					
Absent	41(23.7)	4(2.3)	78(45.1)	50(28.9)	0.609
Present	5(16.1)	0	15(48.4)	11(48.4)	
Necrosis					
Absent	**31(16.9)**	**3(1.6)**	**93(50.8)**	**56(30.6)**	**0.002**
Present	**15(6.8)**	**1(0.5)**	**109(49.5)**	**95(43.2)**	
Klintrup Makinen					
0	**4(10.3)**	**0**	**23(59)**	**12(30.8)**	**0.024**
1	**33(15.5)**	**2(0.9)**	**104(48.8)**	**74(34.7)**	
2	**6(5.4)**	**1(0.9)**	**62(55.4)**	**43(38.4)**	
3	**0**	**0**	**64(74.4)**	**22(25.6)**	

Ki67					
Low (<15%)	34(12.6)	4(1.5)	136(50.6)	95(35.3)	0.132
High (>15%)	11(8.5)	0	60(46.5)	58(45)	
Tumour Bud					
-Low	28(10)	3(1.1)	140(50)	109(38.9)	0.602
-High	18(14.1)	1(0.8)	65(50.8)	44(34.4)	
Tissue Stroma Percentage					
Low	34(11.9)	2(0.7)	142(49.8)	107(37.5)	0.767
High	12(9.8)	2(1.6)	63(51.2)	46(37.4)	

When stratifying according to molecular subtype, Luminal A patients had a 5-year survival of 100%- and 10-year survival of 96% for the All High group, the HNLC group had 100% 5 – and 10-year survival, and the LNHC group had a 5-year survival of 86%- and 10-year survival of 73%, while the All Low group had a 5-year survival of 90% and 10-year survival of 85%, (*Figure 4-42*).

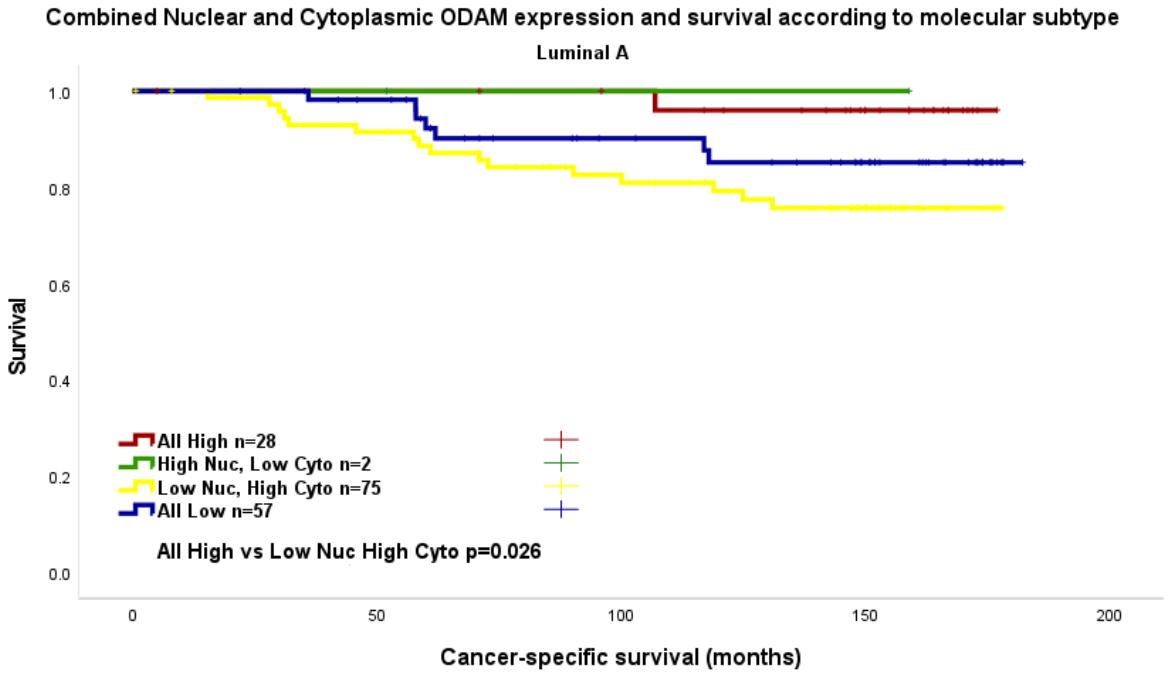

Figure 4-43 Combined nuclear and cytoplasm ODAM expression and survival in Luminal A patients in the Glasgow Breast Cancer Cohort. Pairwise comparisons are described in the graph.

Pairwise comparison demonstrated no significant difference in survival between the combined score subgroups in the luminal A patients, (*Table 4-20*Table 4-20).

Table 4-20 Pairwise comparisons on Kaplan Meier survival analysis for combined nuclear and cytoplasmic ODAM expression in Luminal A patients.

Pairwise Comparison p=	1 HNHC	2 HNLC	3 LNHC	4 LNLC

1 HNHC		0.841	**0.026**	0.146
2 HNLC	0.841		0.546	0.674
3 LNHC	**0.026**	0.546		0.202
4 LNLC	0.146	0.674	0.202	

On multivariate analysis however, ODAM combined scoring did not remain statistically significant, (*Table 4-21)*.

Table 4-21 Clinicopathological factors and their prognostic significance in the Luminal A patients within the Glasgow Breast Cancer Cohort with regards to combined nuclear and cytoplasmic ODAM scoring. Univariate and multivariate Cox regression analysis.

Clinicopathological Factor	Univariate analysis (HR, 95% C.I.)	p	Multivariate analysis (HR, 95% C.I.)	p
Age	0.891(0.443-1.790)	0.745		
Tumour Size <20mm 20-49mm >50mm	 **2.614(0.221-20.664)** **4.132(1.192-14.328)**	**0.006** **0.006** **0.004** **0.025**	 0.6570.113-3.832) 0(0)	 0.897 0.640 0.996
Invasive Grade I II III	 **2.595(0.990-6.805)** **4.311(1.470-12.642)**	**0.017** **0.029** **0.052** **0.008**	 3.699(0.436-31.404) 0(0)	 0.587 0.231 0.992
Nodal Status	**1.020(1.000-1.040)**	**0.045**	0.243(0.026-2.268)	0.214
Lymphatic Invasion	**1.020(1.000-1.040)**	**0.045**	2.543(0.366-17.652)	0.345
Vascular Invasion	**3.528(1.150-10.823)**	**0.028**	7.722(0.704-84.658)	0.094
Necrosis	**2.291(1.201-4.368)**	**0.012**	0.935(0.160-5.453)	0.940
Klintrup-Makinen 0 1 2 3	 0.552(0.246-1.235) 0.593(0.94-1.816) 0.361(0.045-2.885)	0.524 0.488 0.148 0.360 0.336		
Ki67	1.627(0.718-3.689)	0.244		
Tumour budding	1.305(0.686-2.483)	0.417		

Tumour stroma percentage	1.305(0.686-2.483)	0.417		
ODAM combined score		**0.060**		
All High		**0.198**		0.769
All High v HNLC	**0.246(0.030-2.002)**	**0.190**	0(0)	0.997
All High v LNHC	**0(0)**	**0.984**	3.605(0.310-41.970)	0.306
All High v All Low	**1.764(0.726-4.289)**	**0.211**	1.801(0.159-20.422)	0.635

Examining the relationship between clinicopathological factors and patients in the different combined score groups in the Luminal A patients, necrosis correlated with ODAM combined score, ().

Table 4-22*)*.

Table 4-22 Clinicopathological factors and their relation to ODAM combined nuclear and cytoplasmic expression in the Luminal A patients in the Glasgow Breast Cancer Cohort. Chi-squared analysis.

Clinicopathological factor	**ODAM combined score (%)**				**p**
	All High	**HNLC**	**LNHC**	**All Low**	
Age (years)					
≤50	7(15.2)	0	21(45.7)	18(39.1)	0.719
>50	22(18.8)	2(1.7)	54(46.2)	39(33.3)	
Tumour Size					
≤20mm	16(18.6)	0	36(41.9)	34(39.5)	0.590
21-49mm	12(16.7)	2(2.8)	36(50)	22(30.6)	
≥50mm	1(20)	0	3(60)	1(20)	
Grade					
I	10(21.7)	1(2.2)	18(39.1)	17(37)	0.297
II	18(191(	0	44(46.8)	32(34)	
III	1(4.3)	1(4.3)	13(56.5)	8(34.8)	
Nodal Status					
N_0	16(17.8)	2(2.2)	37(41.1))	35(38.9)	0.484
N_1	13(18.3)	0	36(50.7)	22(31)	
Lymphatic Invasion					
Absent	22(35.5)	1(1.6)	18(1.6)	21(33.9)	0.839
Present	7(30.4)	1(4.3)	6(26.1)	9(39.1)	
Vascular Invasion					
Absent	28(36.8)	2(2.6)	20(26.3)	26(34.2)	0.396
Present	1(11.1)	0	4(44.4)	4(44.4)	
Necrosis					
Absent	**24(23.5)**	**2(2)**	**48(47.1)**	**28(27.5)**	**0.024**
Present	**5(9.3)**	**0**	**23(42.6)**	**26(48.1)**	
Klintrup Makinen					

0	3(14.3)	0	11(52.4)	7(33.3)	0.509
1	23(22.3)	1(2)	42(40.8)	37(35.9)	
2	1(4.2)	0	15(62.5)	8(33.3)	
3	0	0	4(66.7)	2(33.3)	
Ki67					
Low (<15%)	29(17.8)	2(1.2)	75(46)	57(35)	n/a
High (>15%)	0	0	0	0	
Tumour Bud					
-Low	19(19.2)	2(2)	45(45.5)	33(33.3)	0.657
-High	10(16.7)	0	27(45)	23(38.3)	
Tissue Stroma Percentage					
Low	20(18.5)	0	48(44.4)	40(37)	0.202
High	9(17.6)	2(3.9)	24(47.1)	16(31.4)	

Luminal B patients had a 5-year survival of 73%- and 10-year survival of 73% for the All High group, the HNLC group had 100% 5 – and 10-year survival, and the LNHC group had a 5-year survival of 88%- and 10-year survival of 60%, while the All Low group had a 5-year survival of 86% and 10-year survival of 67%, (*Figure 4-44*).

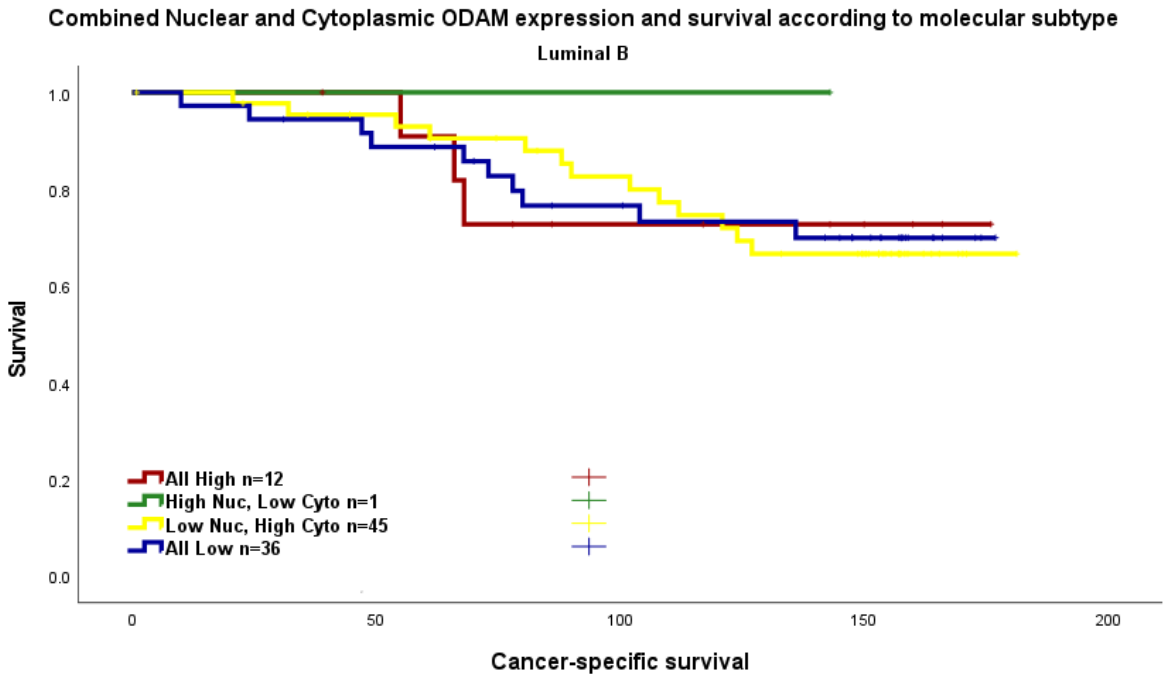

Figure 4-44 Combined nuclear and cytoplasm ODAM expression and survival in Luminal B patients in the Glasgow Breast Cancer Cohort.

Pairwise comparison demonstrated no significant difference in survival between combined ODAM score subgroups in the Luminal B patients, (*Table 4-23*).

Table 4-23 Pairwise comparisons on Kaplan Meier survival analysis for combined nuclear and cytoplasmic ODAM expression in Luminal B patients.

Pairwise Comparison p=	1 HNHC	2 HNLC	3 LNHC	4 LNLC
1 HNHC		0.583	0.977	0.976
2 HNLC	0.583		0.527	0.553
3 LNHC	0.977	0.527		0.950
4 LNLC	0.976	0.553	0.950	

Within the Luminal B group, Inter-factor correlation was assessed when comparing the combined score subgroups, (*Table* 4-24). Here, lymphatic invasion neared significance with regards to relation to ODAM combined scoring.

Table 4-24 Clinicopathological factors and their relation to ODAM combined nuclear and cytoplasmic expression in the Luminal B patients in the Glasgow Breast Cancer Cohort. Chi-squared analysis.

Clinicopathological factor	**ODAM combined score (%)**				**p**
	All High	**HNLC**	**LNHC**	**All Low**	
Age (years)					
≤50	3(9.1)	1(3)	16(48.5)	13(39.4)	0.492
>50	9(14.8)	0	29(47.5)	23(37.7)	
Tumour Size					
≤20mm	5(10.9)	1(2.2)	25(54.3)	15(32.6)	0.741
21-49mm	6(14.6)	0	18(43.9)	17(41.5)	
≥50mm	1(14.3)	0	2(28.6)	4(57.1)	
Grade					
I	1(7.1)	0	11(78.6)	2(14.3)	0.166
II	3(8.3)	0	17(47.2)	16(44.4)	
III	8(14.3)	1(2.3)	17(38.6)	18(40.9)	
Nodal Status					
N_0	4(7.8)	1(2)	25(49)	21(41.2)	0.316
N_1	8(20)	0	17(42.5)	15(37.5)	
Lymphatic Invasion					
Absent	3(17.6)	1(5.9)	5(29.4)	8(47.1)	0.053
Present	9(52.9)	0	6(35.3)	2(11.8)	
Vascular Invasion					
Absent	9(33.3)	1(3.7)	9(33.3)	8(29.6)	0.931
Present	3(42.9)	0	2(28.6)	2(28.6)	
Necrosis					
Absent	4(9.5)	0	24(57.1)	14(33.3)	0.259
Present	8(16)	1(2)	19(38)	22(44)	
Klintrup Makinen					
0	0	0	7(63.6)	4(36.4)	0.628
1	7(15.6)	0	23(51.1)	15(33.3)	
2	4(16)	1(4)	9(36)	11(44)	
3	0	0	6(50)	6(50)	
Ki67					

Low (<15%)	3(20)	1(6.7)	6(6.7)	5(33.3)	0.096
High (>15%)	9(11.4)	0	39(49.4)	31(39.2)	
Tumour Bud					
-Low	6(10.2)	0	29(49.2)	24(40.7)	0.422
-High	6(17.1)	1(2.9)	16(45.7)	12(34.3)	
Tissue Stroma Percentage					
Low	9(12.9)	1(1.4)	32(45.7)	28(40)	0.845
High	3(12.5)	0	13(54.2)	8(33.3)	

TNBC patients had a 5-year survival of 100%- and 10-year survival of 100% for the All-High group, the HNLC group had 100% 5 – and 10-year survival, and the LNHC group had a 5-year survival of 73%- and 10-year survival of 63%, while the All Low group had a 5-year survival of 80% and 10-year survival of 64%, (*Figure 4-44*).

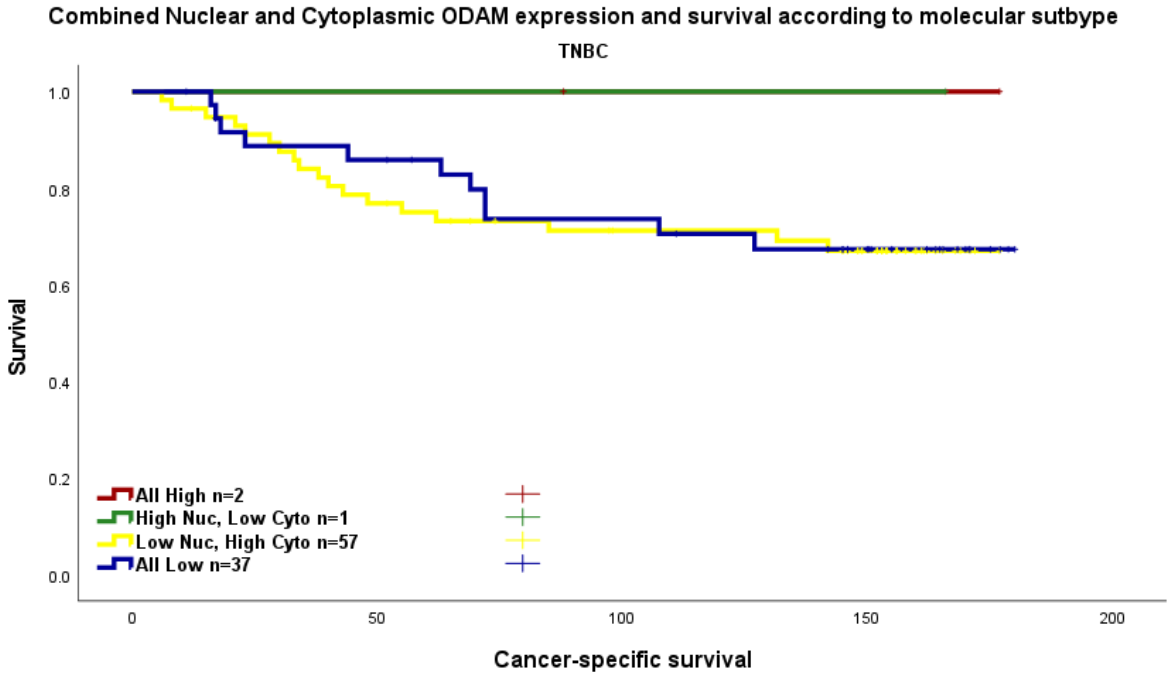

Figure 4-45 Combined nuclear and cytoplasm ODAM expression and survival in TNBC patients in the Glasgow Breast Cancer Cohort. Pairwise comparisons are described in the graph.

Pairwise comparison demonstrated no significant difference in survival according to ODAM combined score in the TNBC patients, (*Table 4-25)*.

Table 4-25 Pairwise comparisons on Kaplan Meier survival analysis for combined nuclear and cytoplasmic ODAM expression in TNBC patients.

Pairwise Comparison p=	1 HNHC	2 HNLC	3 LNHC	4 LNLC
1 HNHC		n/a	0.392	0.405
2 HNLC	n/a		0.529	0.532
3 LNHC	0.392	0.529		0.849

4 LNLC	0.405	0.532	0.849	

Within the TNBC group, inter-factor correlation was assessed when comparing the combined score subgroups. Here, no association was identified with ODAM combined score.

Table 4-26 Clinicopathological factors and their relation to ODAM combined nuclear and cytoplasmic expression in the TNBC patients in the Glasgow Breast Cancer Cohort. Chi-squared analysis.

Clinicopathological factor	**ODAM combined score (%)**				**p**
	All High	**HNLC**	**LNHC**	**All Low**	
Age (years)					
≤50	1(2.6)	1(2.6)	19(48.7)	18(46.2)	0.261
>50	1(1.7)	0	39(66.1)	19(32.2)	
Tumour Size					
≤20mm	1(2)	1(2)	30(58.8)	19(373)	0.962
21-49mm	1(2.4)	0	24(57.1)	17(40.5)	
≥50mm	0	0	3(75)	1(25)	
Grade					
I	0	0	4(100)	0	0.599
II	1(4)	0	16(64)	8(32)	
III	1(1.4)	1(1.4)	38(55.1)	29(42)	
Nodal Status					
N_0	2(3.6)	1(1.8)	36(64.3)	17(30.4)	0.194
N_1	0	0	22(52.4)	20(47.6)	
Lymphatic Invasion					
Absent	2(3.6)	1(2.8)	24(66.7)	9(25)	0.414
Present	0	0	17(85)	3(15)	
Vascular Invasion					
Absent	2(5.6)	1(2.2)	34(73.9)	9(19.6)	0.780
Present	0	0	7(70)	3(15)	
Necrosis					
Absent	1(3.7)	1(2.2)	17(63)	8(29.6)	0.295
Present	1(1.4)	0	41(58.6)	28(40)	
Klintrup Makinen					
0	0	0	3(75)	1(25)	0.265
1	2(4.9)	1(2.4)	27(65.9)	11(26.8)	
2	0	0	23(62.2)	14(37.8)	
3	0	0	5(33.3)	10(66.7)	
Ki67					
Low (<15%)	1(1.6)	1(1.6)	41(64.1)	21(32.8)	0.164
High (>15%)	1(3.7)	0	11(40.7)	15(55.6)	
Tumour Bud					
-Low	1(1.3)	1(1.3)	42(56)	31(41.3)	0.317
-High	1(4.5)	0	16(72.7)	5(22.7)	
Tissue Stroma Percentage					

Low	2(2.7)	1(1.4)	44(60.3)	26(35.6)	0.759
High	0	0	14(58.3)	10(41.7)	

The HER2-enriched patients had a 5-year survival of 50%- and 10-year survival of 50% for the All High group, the LNHC group had a 5-year survival of 55%- and 10-year survival of 45%, while the All Low group had a 5-year survival of 100% and 10-year survival of 100%, (*Figure 4-46*).

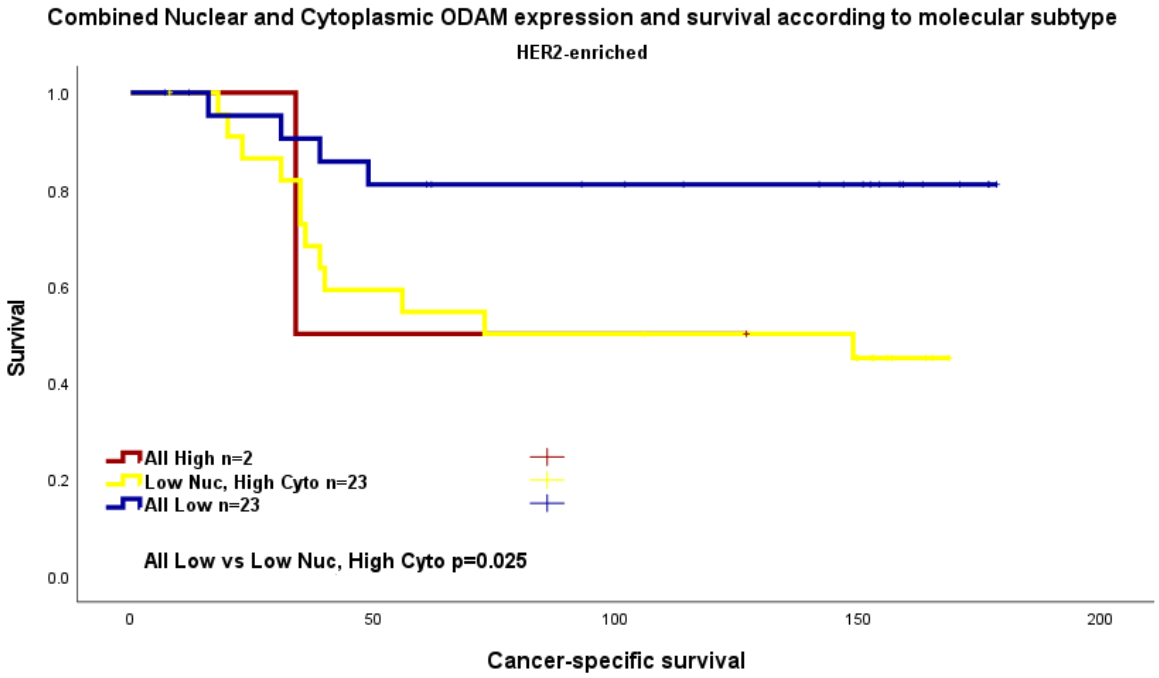

Figure 4-46 Combined nuclear and cytoplasm ODAM expression and survival in HER-2 enriched patients in the Glasgow Breast Cancer Cohort. Pairwise comparisons are described in the graph.

Pairwise comparison demonstrated that the All-Low group had significantly worse survival than the LNHC group (*Table 4-27*).

Table 4-27 Pairwise comparisons on Kaplan Meier survival analysis for combined nuclear and cytoplasmic ODAM expression in HER2-enriched patients.

Pairwise Comparison p=	1 HNHC	2 HNLC	3 LNHC	4 LNLC
1 HNHC		n/a	0.910	0.288
2 HNLC	n/a		n/a	n/a
3 LNHC	0.910	n/a		**0.025**
4 LNLC	0.288	n/a	**0.025**	

On multivariate analysis however, ODAM combined scoring did not remain statistically significant, but neared significance (p=0.060), (Table 4-28).

Table 4-28 Clinicopathological factors and their prognostic significance in the HER2-enriched patients within the Glasgow Breast Cancer Cohort with regards to combined nuclear and cytoplasmic ODAM scoring. Univariate and multivariate Cox regression analysis.

Clinicopathological Factor	**Univariate analysis (HR, 95% C.I.)**	**p**	**Multivariate analysis (HR, 95% C.I.)**	**p**
Age	0.609(0.270-1.371)	0.231		
Tumour Size <20mm 20-49mm >50mm		0.383 0.338 0.389 0.337		
Invasive Grade I II III	 0.704(0.263-1.886)	0.471 0.486 0.486		
Nodal Status	**2.485(1.062-5.813)**	**0.036**	1.204(0.321-4.514)	0.783
Molecular Subtype Luminal A Luminal B TNBC HER2-enriched	2.566(0.986-6.683)	0.054		
Lymphatic Invasion	0.964(0.127-7.296)	0.972		
Vascular Invasion	1.875(0.441-7.976)	0.395		
Necrosis	1.627(0.718-3.689	0.244		
Klintrup-Makinen 0 1 2 3	 3567.881(0-2.35^{E+96}) 3303.914(0-2.18^{E+96} 1087.661(0-7.236^{E+96}	0.501 0.731 0.940 0.941 0.949		
Ki67	**0.537(0.358-0.805)**	**0.003**	1.172(0.421-3.259)	0.761
Tumour budding	**2.899(1.267-6.636)**	**0.012**	3.124(0.925-10.551)	0.067
Tumour stroma percentage	**3.368(1.096-10.346)**	**0.034**	1.884(0.631-5.626)	0.256
ODAM combined score All Low		**0.070** **0.105**		0.135

All Low v All High		-		
All Low v HNLC	**3.629(0.402-32.723)**	**0.251**	4.876(0.394-60.367)	0.217
All Low v LNHC	**3.348(1.078-10.397)**	**0.037**	3.084(0.955-9.956)	0.060

Examining the relationship between clinicopathological factors and patients in the different combined score groups in the HER2-enriched patients, tumour size neared significance in association with combined score, (Table 4-29).

Table 4-29 Clinicopathological factors and their relation to ODAM combined nuclear and cytoplasmic expression in the HER2-enriched patients in the Glasgow Breast Cancer Cohort. Chi-squared analysis.

Clinicopathological factor	**ODAM combined score (%)**				**p**
	All High	**HNLC**	**LNHC**	**All Low**	
Age (years)					
≤50	1(6.3)	0	8(50)	7(43.8)	0.836
>50	1(3.1)	0	15(46.9)	16(50)	
Tumour Size					
≤20mm	2(8.3)	0	8(33.3)	14(58.3)	0.067
21-49mm	0	0	15(46.9)	7(31.8)	
≥50mm	0	0	0	2(100)	
Grade					
I	0	0	0	0	0.242
II	1(9.1)	0	3(27.3)	7(63.6)	
III	1(2.7)	0	20(54.1)	16(43.2)	
Nodal Status					
N_0	2(8.3)	0	9(37.5)	13(54.2)	0.176
N_1	0	0	14(58.3)	10(41.7)	
Lymphatic Invasion					
Absent	1(8.3)	0	7(58.3)	4(33.3)	0.987
Present	1(7.7)	0	8(61.5)	4(30.8)	
Vascular Invasion					
Absent	1(4.8))	0	13(61.9)	7(33.3)	0.392
Present	1(25)	0	2(50)	1(25)	
Necrosis					
Absent	1(16.7)	0	1(16.7)	4	0.107
Present	1(2.4)	0	22(52.4)	19	
Klintrup Makinen					
0	0	0	0	0	0.485
1	0	0	8(47.1)	9(52.9)	
2	1(4)	0	14(56)	10(40)	
3	0	0	1(20)	4(80)	
Ki67					
Low (<15%)	1(4.3)	0	11(47.8)	11(47.8)	0.955

High (>15%)	1(4.3)	0	10(43.5)	12(52.2)	
Tumour Bud					
-Low	1(2.7)	0	17(45.9)	19(51.4)	0.507
-High	1(9.1)	0	6(54.5)	4(36.4)	
Tissue Stroma Percentage					
Low	2(8)	0	11(44)	12(48)	0.367
High	0	0	12(52.2)	11(47.8)	

4.3 Discussion

Our understanding of the role of ODAM is most established with regards to odontogenesis. However, new evidence is emerging suggesting that its presence within normal tissues, and altered expression levels within cancers of different types may point towards a role in disease progression and metastasis. When looking specifically at 243 patients' breast cancers, Siddiqui et al. reported that ODAM was expressed strongly in benign breast structures including duct, vessel, and epithelium, but weakly expressed in the cytoplasm of malignant cells, while nuclear expression showed great variability(215). When comparing for stage, ODAM nuclear expression correlated with increasing disease stage, although no correlation was found between ODAM expression and histologic grade(215). Finally, survival was found to be greater in patients with higher ODAM nuclear staining in Stage 0-II disease (but not in later stages), and with an increase in significance of survival benefit with increasing disease stage(215).

Within our cohort, ODAM was identified to be differentially expressed using TempO-Seq in patients with high vs low budding phenotype. ODAM was expressed similarly in tumour cells as well as in peritumoural buds, which allowed higher-throughput analysis of the entire Glasgow Breast Cancer Cohort using a TMA of cores from within the tumour. Within the limitations of the available data (many cores were not valid for assessment due to the relative age of the specimens) it was possible to identify links between nuclear ODAM expression and survival, and cytoplasmic expression and survival. Membrane expression of ODAM could not be assessed in this cohort.

For cytoplasmic ODAM, WHS were normally distributed between 0-300. A threshold of 153.3 was identified and based on this, survival examined across the Glasgow Breast cancer cohort. On examining the entire cohort, it was not possible to identify a significant difference in survival between high/low ODAM cytoplasmic expressors. However, on examining the cohort grouped according to molecular subtypes, survival was seen to be significantly worse in patients with

high cytoplasmic ODAM in the HER2-enriched group (p=0.024) although this effect was lost on multivariate analysis. This may suggest that in the HER2-enriched group, ODAM may confer prognostic value, with low cytoplasmic ODAM being associated with improved survival. In the whole cohort, as well as the Luminal A patients, ODAM cytoplasmic expression was associated with necrosis, and in the luminal B, with lymphatic invasion.

Nuclear expression was less normally distributed, with more than 300 patients in the cohort having a WHS of 0. When utilising a threshold of 30, further survival analysis suggested low nuclear ODAM expression was related to worse survival across the entire cohort (p=0.027), although this effect was lost on multivariate analysis (p=0.255). An association between ODAM nuclear expression and tumour grade, necrosis and KM score was also seen. When examining molecular subgroups more closely, Luminal A patients with low ODAM expression had worse survival, and ODAM expression was associated with tumour size. In HER2-enriched patients, although no survival difference was noted, ODAM nuclear expression was associated with necrosis. It appears therefore that high cytoplasmic expression of ODAM is associated with better survival outcomes, whereas the opposite is true for nuclear ODAM expression, suggesting that location plays a role in activity of ODAM with regards to TB phenotype.

Finally, on combined nuclear and cytoplasmic scoring, the All-High score subgroups appeared to be significant associated with improved survival across the entire cohort, with the LNHC group having poorer CSS (p=0.016). This was seen in the luminal A subgroup, with the All-high ODAM expressors seeing a survival benefit compared to LNHC. Finally, in the HER2-enriched group, once again the HNLC group appeared to have poorer CSS, this time when compared to the All-Low group (p=0.025). These results may however have been impacted by being underpowered due to a paucity of cases available for analysis. It may be that the combination of low nuclear and high cytoplasmic ODAM confer a survival disadvantage, suggesting a difference in action across the tumour cell based on location.

Limitations within this cohort are that a significant proportion of TMA core subjects were not assessable, and a repeated experiment involving a larger cohort of patients may improve power and allow us to expand upon the role of ODAM in survival in breast cancer patients. However, despite these limitations,

ODAM appears to have some effect on prognosis, both at the transcriptomic and the protein expression level, and warrants further interest.

Chapter 5 RFX5

5.1 Introduction

Regulatory Factor X5 (RFX5), belonging to the RFX family, encodes transcription factors involved in encoding DNA binding protein, previously known to function as a regulator of transcription for MHCII gene, as part of the immune response(216). The RFX family is thought to include 8 members, genes for which are encoded within a highly conserved DNA binding domain(217). RFX5 has been implicated in the development of Bare Lymphocyte Syndrome, an inherited autosomal recessive disorder which leads to a MHCII related severe immunodeficiency characterised by mutations in RFX complex.(218)

5.1.1 RFX5 and Cancer

RFX family mutations have been identified in cancers including glioblastoma, large B cell lymphoma, acute myeloid leukaemia as well as solid organ cancers(219-222). The encoding genes are located in 1q21, within a region known to house other potential sites whereby chromosomal mutations can lead to preneoplastic/neoplastic outcomes and contribute to progression, including in breast cancer and glioblastoma(220, 221). However, more recent evidence suggests, particularly in cases of hepatocellular carcinoma, that RFX5 may play a role in tumour progression even in the absence of MHCII, suggesting an alternative route of action, particularly through transcriptional regulation of Tripeptidyl peptidase 1 (TPP1), which has been found to be highly expressed in some cases of hepatocellular carcinoma (HCC)(216, 223, 224). TPP1 encodes a lysosomal protease, and its role in HCC disease progression has yet to be elucidated, although higher levels of TPP1 mRNA expression have been tied to reduced survival in HCC(216). Regulatory factor X5 (RFX5) is thought to act as a transcription factor in the regulation of Immediate Early Response 3 (IER3), a family of genes which in part may act as transcription factors, and identified as prognostically important in bladder, ovarian and pancreatic cancers(225-227). RFX5 has been identified to play a potential role in HCC in regulating the cellular progress through the P53 signalling pathway and promoting tumour development in HCC through its interaction with IER3(228). One of the downstream targets of RFX5 appears to be lysine-specific demethylase 4A (KDM4A or JMJD2A), to which it binds via KDM4As promoter region(229). In HCC tumour tissue, levels of KDM4A were found to be highly expressed, and appeared to correlate with poorer prognosis. It is thought that the RFX5-KDM4A pathway promotes passage from

G0/G1 into phase S, reducing apoptosis via regulation of p53 and its downstream target(228, 229). In non-small-cell lung cancer (NSCLC) RFX5 has been shown to activate transcription of transcriptional co-activator Yes-Associated Protein (YAP), known to elicit oncogenicity in certain cancers (229). Finally, RFX5 has been found to drive development and progression of HCC by suppressing apoptosis, through transactivation of tyrosine 3-monooxygenase/tryptophan 5-monooxygenase activation protein (YWHAQ)(230). Therefore, RFX5, through possible multiple/varied pathways, may be involved in the regulation of factors which promote progression in cancer.

Guo et al. recently examined the role of RFX family members in stomach adenocarcinoma, suggesting that high RFX5 expression in adenocarcinoma cells led to improved outcomes in terms of overall survival, first progression and post-progression survival(222). Here, RFX5 expression was associated with an increase in immune cells, immune biomarkers and tumour mutational score, potentially through a role in T cell activation, antigen receptor-mediated signalling, cell adhesion molecules and Th17 cell differentiation(222).

The following chapter describes how RFX5 was identified as one of the most differentially expressed genes on TempO-Seq analysis of the Glasgow Breast Cancer Cohort surplus biorepository tissue, and how this compares to RFX5 in the same cohort using immunohistochemistry. Prior to commencing the immunohistochemistry for the Glasgow Breast Cancer Cohort, the staining protocol was optimized, and specificity analysis was performed. The cohort was initially stained in part using full section specimens to validate how expression within the tumour compared to that within the peritumoural buds, and then breast tissue microarrays were analysed to produce the results detailed in a later section. Weighted histoscores for this protein expression in the cellular, membrane and nuclear portions of breast tumour cells were manually assessed and analysed in relation to clinicopathological characteristics, including tumour budding, and cancer-specific survival. It was hypothesised that RFX5 expression may correlate inversely with survival.

5.1.2 The Study Cohorts

The following chapter describes how RFX5 was identified as one of the most differentially expressed genes using TempO-Seq RNA transcriptional analysis of the Glasgow Breast Cancer Cohort surplus biorepository tissue, and how this

compares to RFX5 expression in the same cohort using immunohistochemistry. Prior to commencing the immunohistochemistry for the Glasgow Breast Cohort, the staining protocol was optimized, and specificity analysis was performed. The process for the results therefore can be represented below, (*Figure 5-1*)

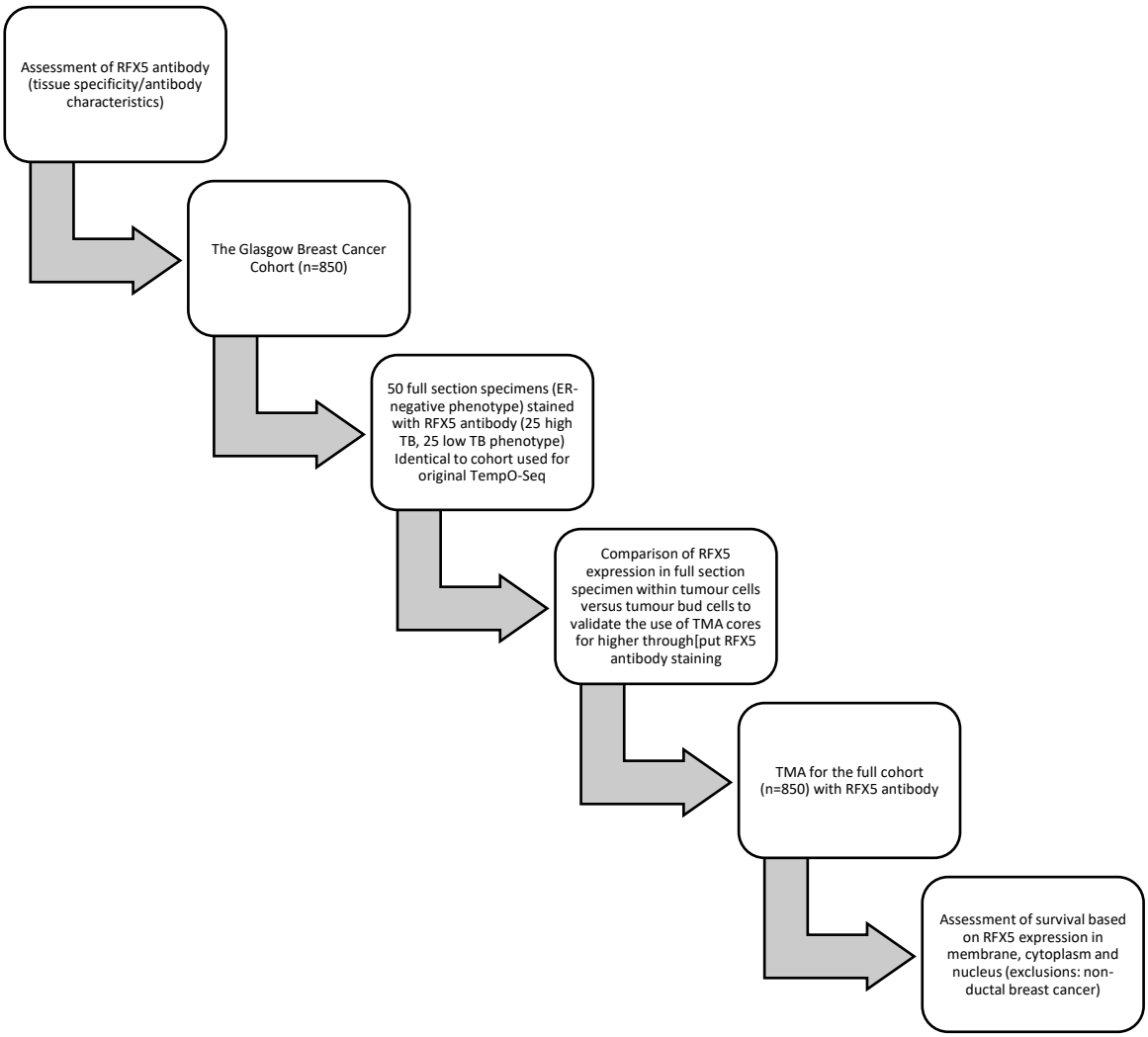

Figure 5-1 Study process flowchart for RFX5 protein expression analysis.

The cohort was initially stained in part using the 50 full section ER-negative specimens used for TempO-Seq, originally selected by virtue of being either of high tumour budding (n=25) or low tumour budding (n=25) phenotype. RFX5 expression within the tumour was compared to that within the peritumoural buds, following which breast tissue microarrays were produced from the entire Glasgow Breast Cancer Cohort were analysed to produce the results discussed later in this chapter. Weighted histoscores (WHS) for this RFX5 expression in the cellular, membrane and nuclear compartments of breast tumour cells were manually assessed and analysed in relation to clinicopathological characteristics, including tumour budding, and cancer-specific survival. It was hypothesised that

RFX5 expression may correlate inversely with survival, and that in patients with poorer prognostic indicators (higher disease stage, higher tumour budding status) this effect may be more pronounced.

5.2 Results

5.2.1 RFX5 Expression Within Cell Lineages

To identify cell lines suitable for antibody specificity, an exploratory search was performed using DEPMAP, a freely accessible cancer dependency map online database which compiles the information from genomic data and large-scale cancer cell line datasets. When a search was performed for RFX5 protein expression (versus knockdown) and compiling the cancer cell line lineage data information with regards to RFX5 expression, Breast appeared to have comparatively high transcripts per million (TPM) compared to other lineages (*Figure 5-2*).

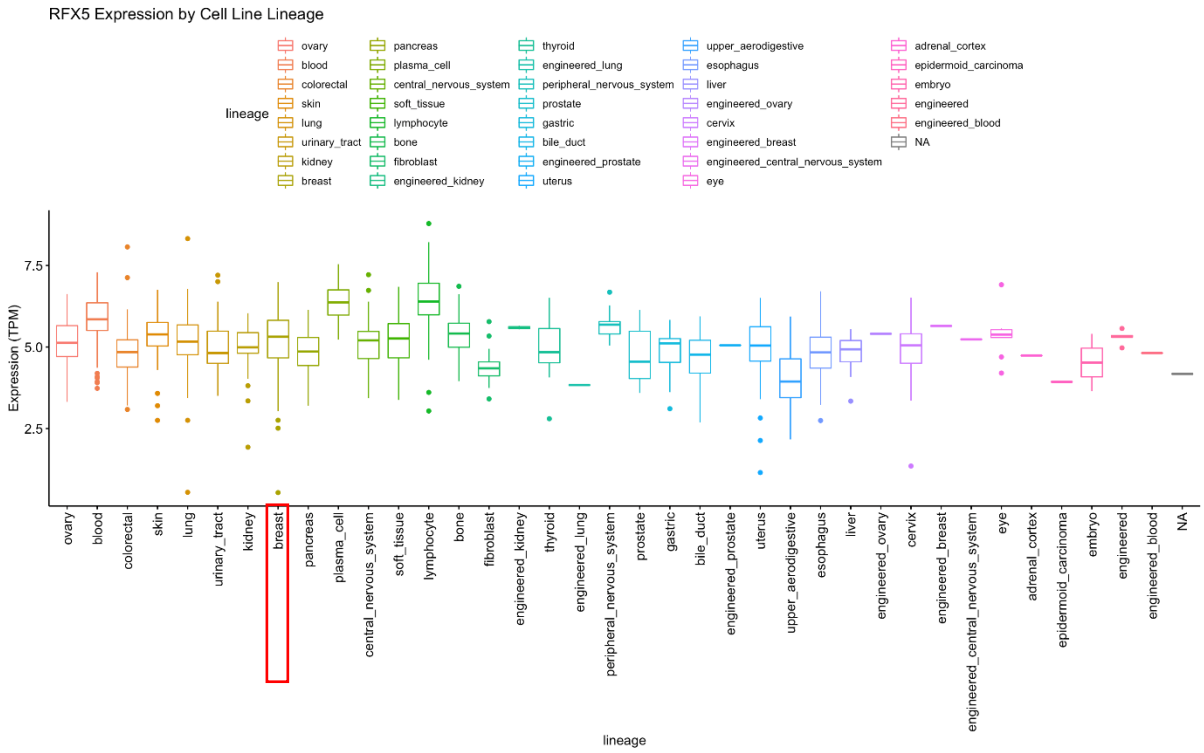

Figure 5-2 DEPMAP RFX5 expression by cell lineage (Transcripts per million, TPM: for every 1,000,000 RNA molecules in the RNA-seq sample, x came from this gene/transcript.)

When exclusively examining breast cancer cell lines known to express RFX5, there is some variability in expression, although overall expression remains beyond 2 TPM for all cell lines except one (*Figure 5-3*).

Within our laboratory, the available cell lines were MDAMB453 and MDAMB231, the former of which had expression higher than 4. However, colorectal and prostate cancer cell lines were also available for further analysis which also expressed satisfactory levels of RFX5 expression, described later in this chapter.

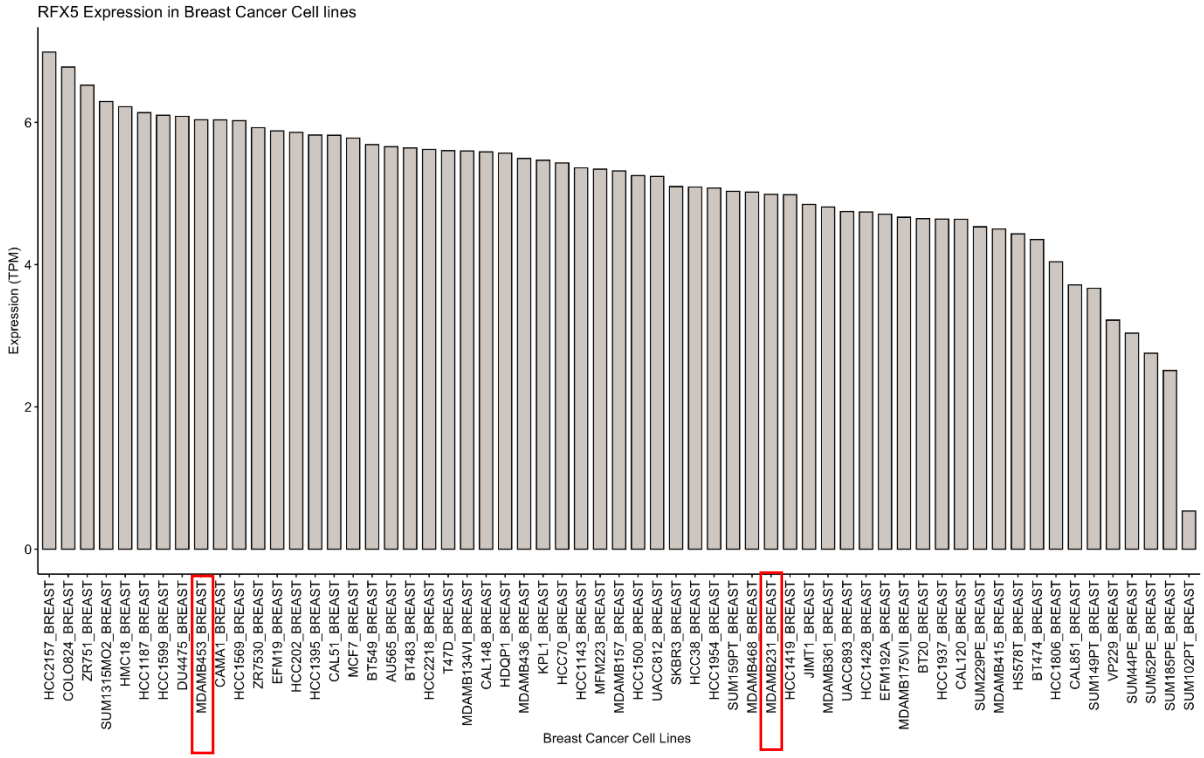

Figure 5-3 DEPMAP RFX5 Expression in Breast Cancer Cell lines (Transcripts per million, TPM: for every 1,000,000 RNA molecules in the RNA-seq sample, x came from this gene/transcript). The cell lines highlighted were utilised for specificity assays.

When DEPMAP was explored with regards to colorectal cancer cell lines, it appeared that almost 2/3 of the available cell lines on the database had some evidence of RFX5 RNA expression, of which two were available in our laboratory, namely HT29 and T84 (*Figure 5-4*).

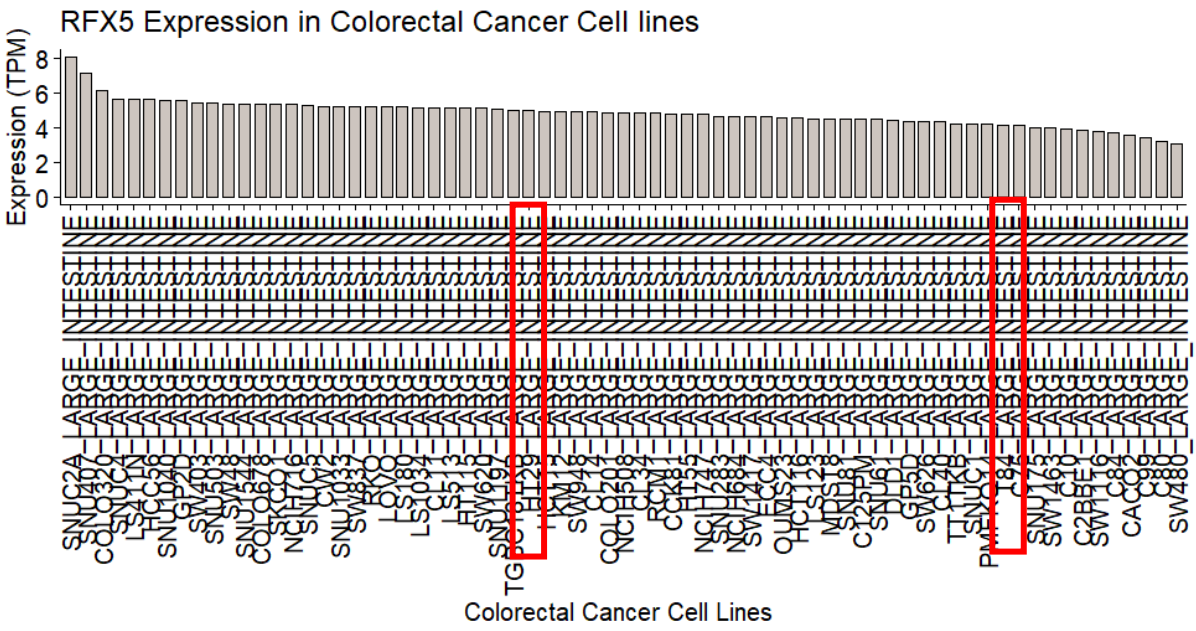

Figure 5-4 DEPMAP RFX5 Expression in Colorectal Cancer Cell lines (Transcripts per million, TPM: for every 1,000,000 RNA molecules in the RNA-seq sample, x came from this gene/transcript.)

When DEPMAP was probed for prostate cancer cell lines, fewer cell lines had available data, although LNCAP cell lines figured here, and were available within our laboratory (*Figure 5-5*).

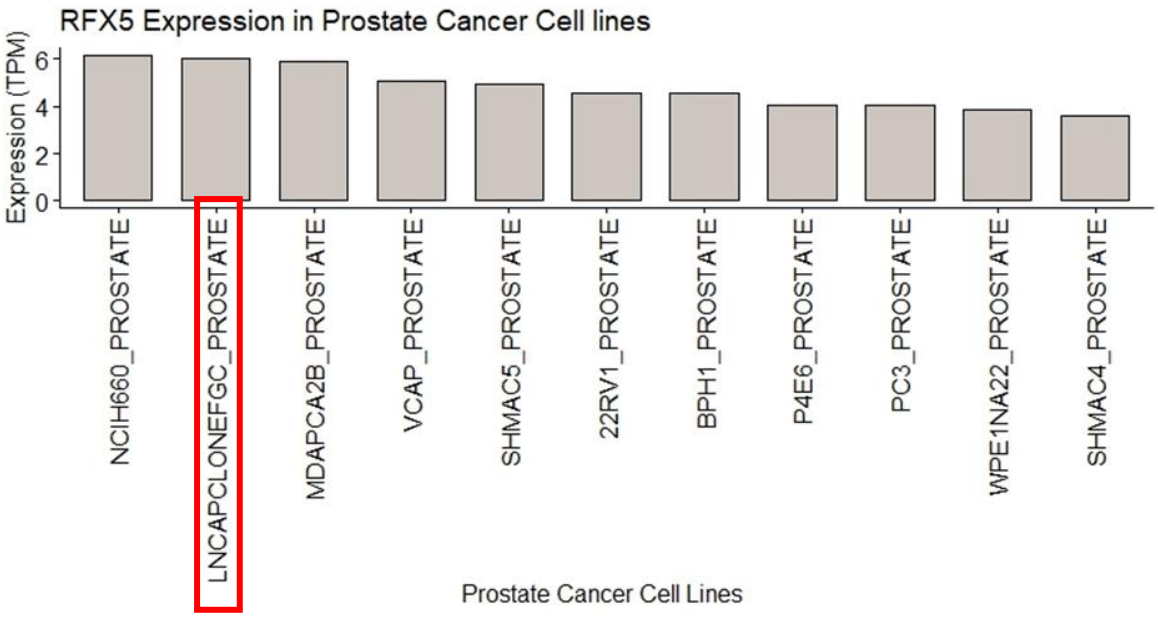

Figure 5-5 DEPMAP RFX5 Expression in Prostate Cancer Cell lines. (Transcripts per million, TPM: for every 1,000,000 RNA molecules in the RNA-seq sample, x came from this gene/transcript.)

5.2.2 RFX5 Antibody Specificity

Examples of weak, moderate, and strong staining are shown in their respective sections within this chapter, together with a true positive and negative control tissue. Antibody specificity was validated using western blotting.

A single band (reproduced in triplicate) was observed at 43kDa in HeLa, overexpressed RFX5 lysate and 231 cell lysates, and tubulin was seen at similar intensity at 52kDa (*Figure 5-6*).

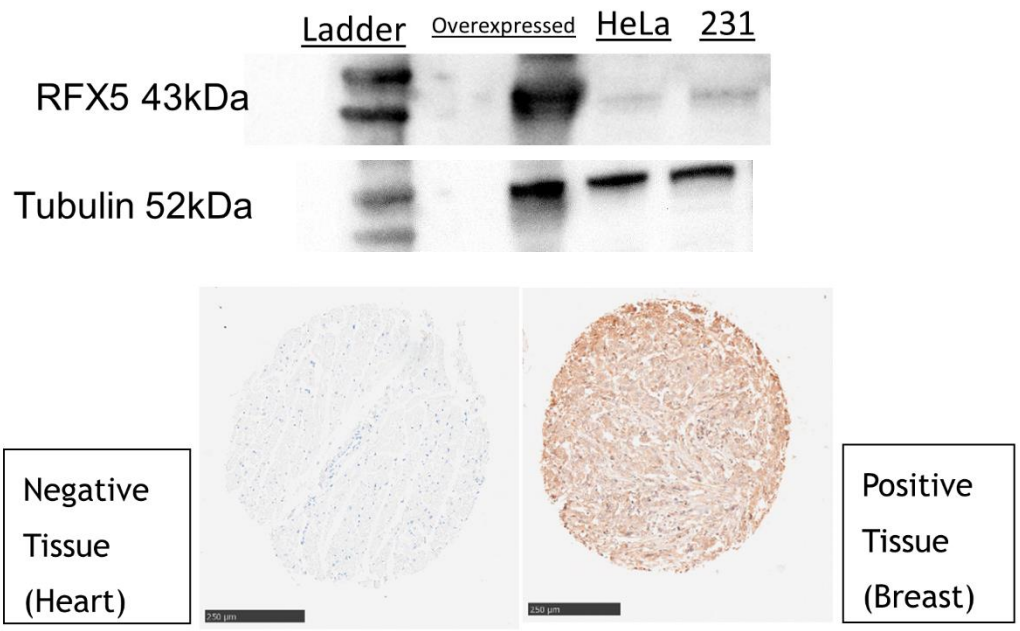

Figure 5-6 RFX5 expression and antibody specificity on Western Blotting. Examples of positive and negative tissue types used for analysis are included.

5.2.3 RFX5 Expression in Full Section Specimens

RFX5 expression was first assessed using full section breast cancer tissue in a selected cohort of the Glasgow Breast Cancer Cohort. The sub-cohort of 50 patients had previously been used for TempO-Seq analysis and allowed identification of the most differentially expressed RNA, of which RFX5 was one. As described previously, 50 patient sections with ER-negative phenotype were selected, 25 with high tumour budding and 25 with low tumour budding characteristics. These were prepared, optimised, and stained for RFX5 (see methods). Manual weighted histoscores were produced for nuclear, cytoplasmic and membrane expression of RFX5 by a single observer (FS). 42 specimens were included for analysis, as 8 patients had missing/damaged section slides. Cytoplasmic, nuclear and membrane expression of RFX5 were manually scored

for validation by Warapan Numprasit (WN) using 10% of this sub-cohort. Scores varied from 0 to 210 for membrane, 0-300 for cytoplasm and 0-90 for nucleus. Each cellular location will be discussed in turn in the subsections below.

5.2.4 Membrane RFX Expression in Full Section Specimens

RFX5 expression in membrane in the full section and then in the full Glasgow cohort was 0 in 37 of the 42 specimens assessed, therefore this portion of cellular RFX5 expression was not assessed further. However, as noted later in this chapter, seeing that cytoplasmic and nucleic WHS within tumour cells matched those within peritumoural buds, further analysis was performed on the full Glasgow Cohort, assuming the same was true for membrane expression of RFX5.

5.2.5 Cytoplasmic RFX5 Expression in Full section specimens

After selecting the original 50 patients with ductal cancer selected from the Glasgow Breast Cohort and used for TempO-Seq, these were stained using RFX5-specific antibody, weighted histoscores were generated by manual evaluation by a single observer (FS). Examples of light, moderate and strong cytoplasmic staining, together with positive and negative control tissue are shown below, (*Figure 5-7*).

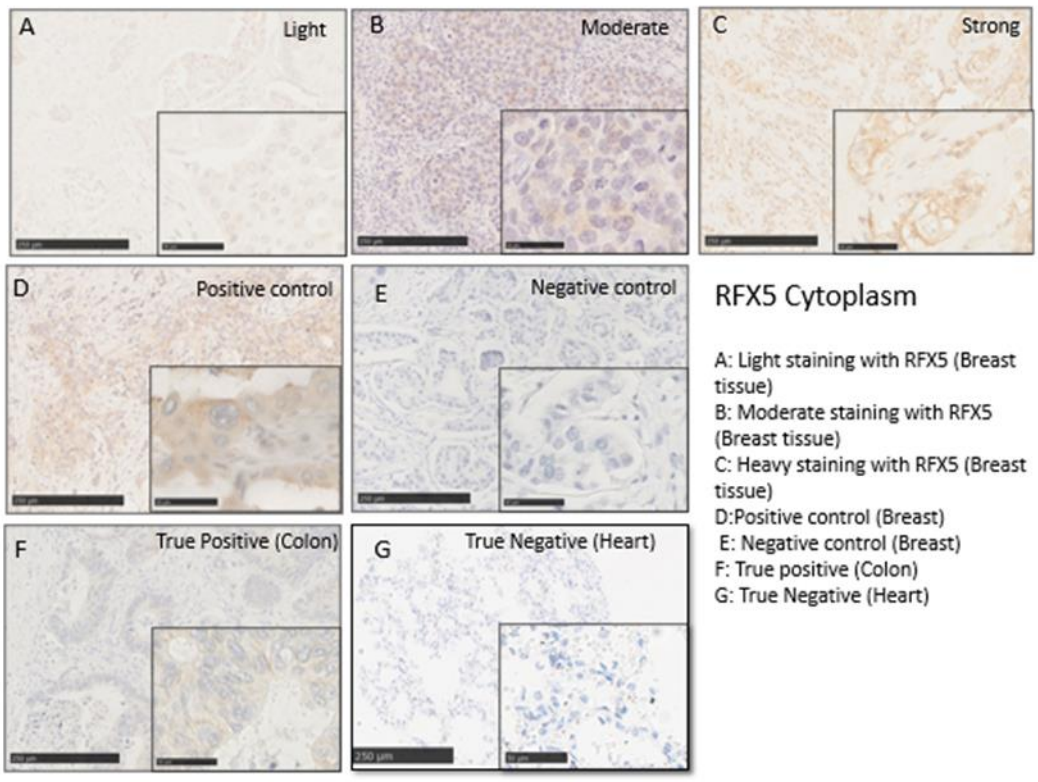

Figure 5-7 RFX5 cytoplasm staining representative images.

Cytoplasm expression of RFX5 was manually scored by a single assessor, and scores varied from 0-300, (*Figure 5-8*).

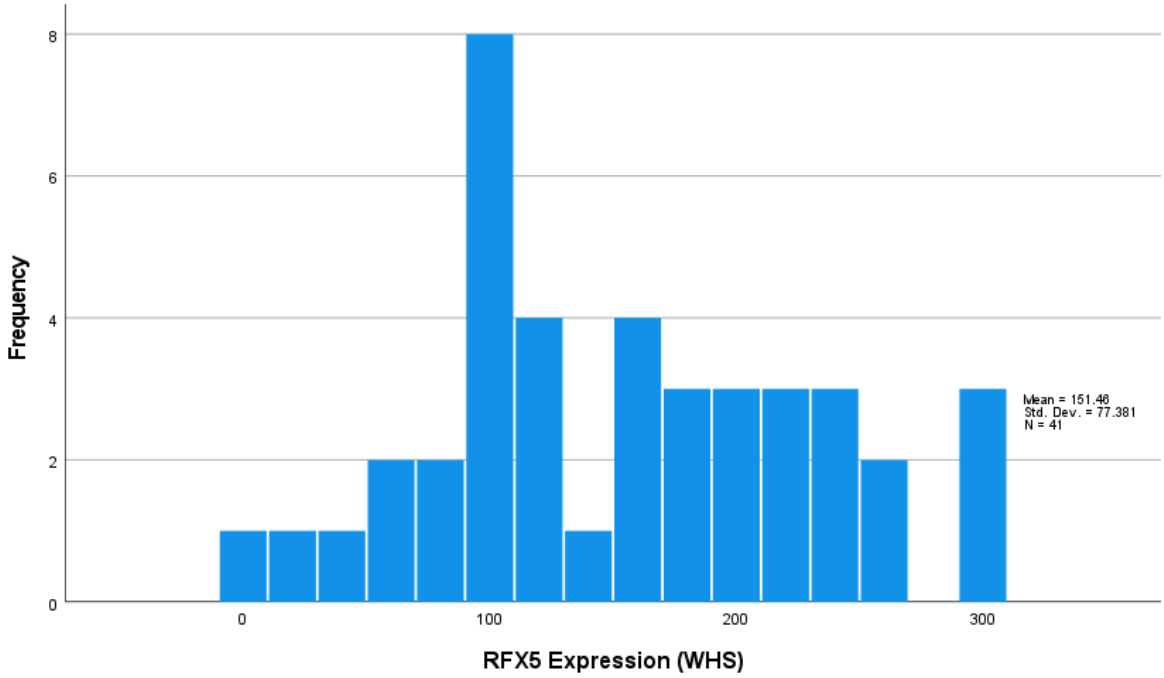

Figure 5-8 RFX5 cytoplasmic expression in full section specimens (WHS, weighted histoscores)

Manual assessment for validation by WN using 10% of this sub-cohort is described using the scatter plot, (*Figure 5-9*). An intraclass correlation coefficient (ICCC) of 0.959 suggested a strong positive correlation between validation and primary assessors' cores.

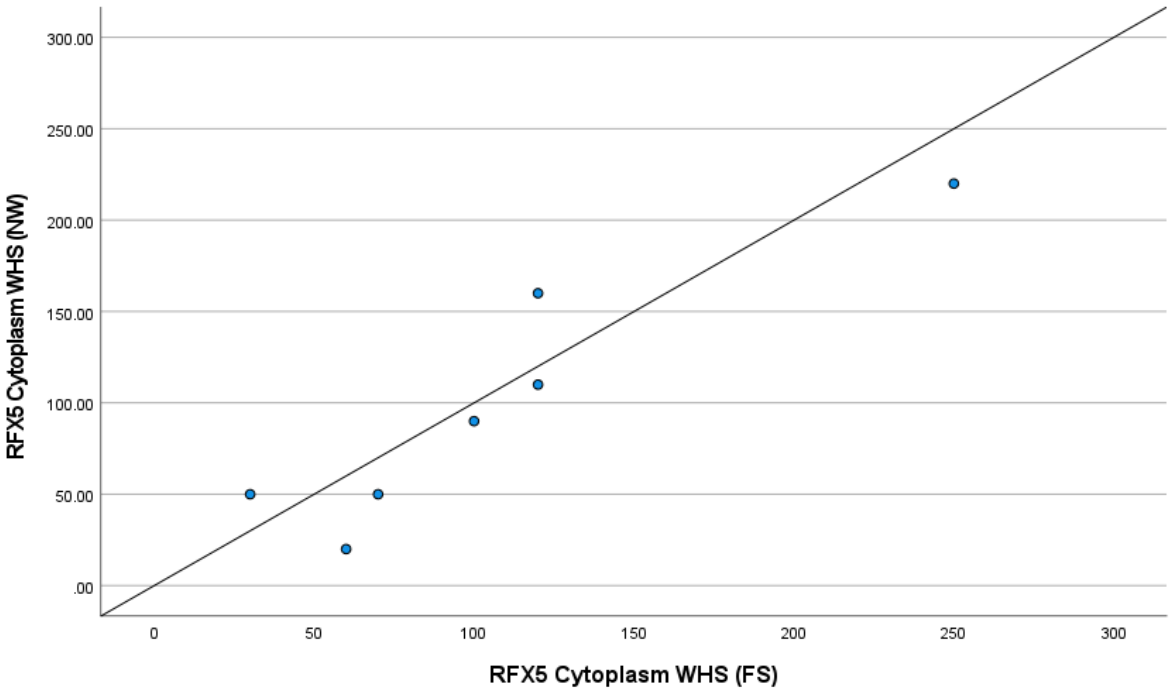

Figure 5-9 Correlation between FS and NW manual weighted histoscore (WHS) for cytoplasmic RFX5 staining. Scatter plot showing correlation between FS and NW for cytoplasmic staining. Intraclass correlation coefficient 0.959 for 10% specimens.

A subsequent comparison of averages and differences in scores was plotted as a Bland-Altman plot and demonstrated no bias between observers, (*Figure 5-10*).

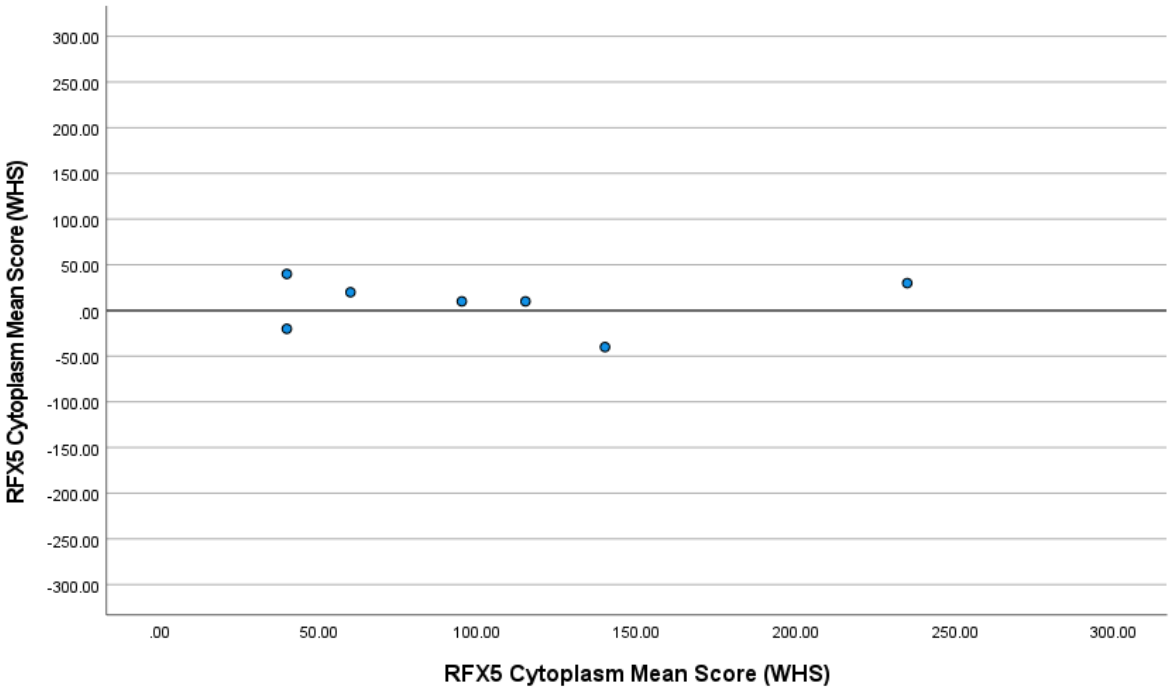

Figure 5-10 Bland Altman Plot comparing difference in scores for RFX5 expression in cytoplasm.

5.2.6 RFX5 Cytoplasmic Expression in Tumour Cells Versus Tumour Buds

RFX5 expression was compared between tumour buds (where present) and intratumoural cells. A scatter plot was used to visualise the correlation between cytoplasmic RFX5 expression in intratumoral cells and tumour buds (*Figure 5-11*). Only 24 specimens had tumour buds present, in these specimens the WHS of the buds were comparable to that of the tumour core. The intraclass correlation coefficient (ICCC) was 0.926.

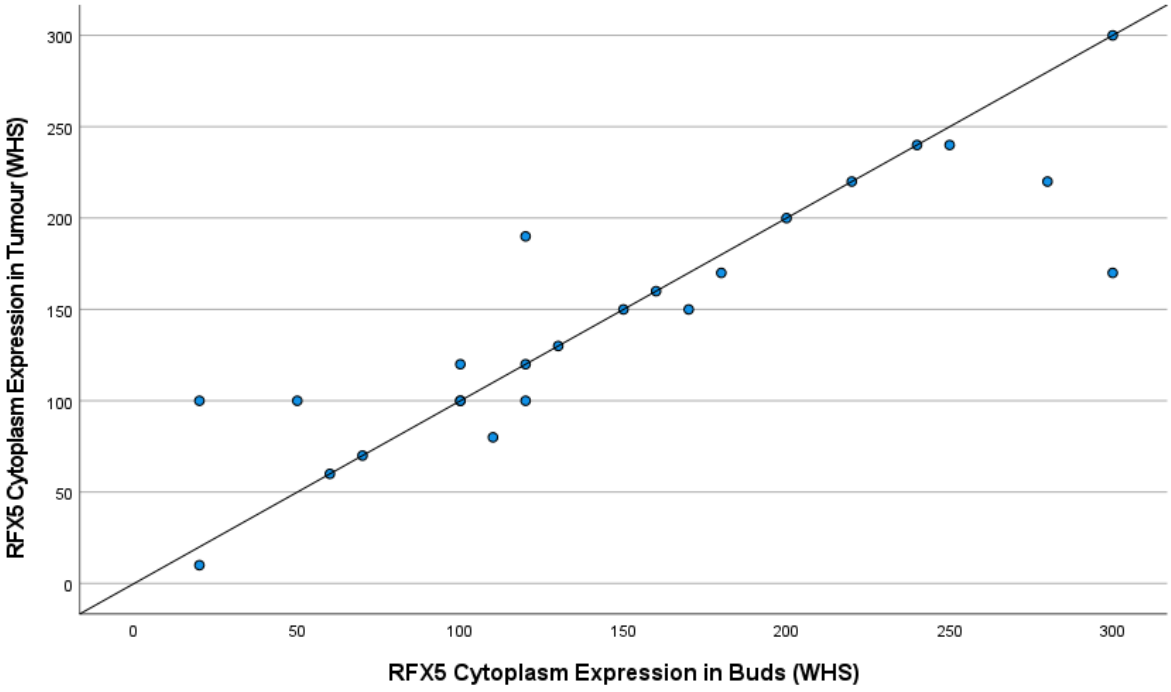

Figure 5-11 Cytoplasmic RFX5 expression in tumour versus tumour buds. ICCC 0.926

A subsequent comparison of averages and differences in scores was plotted as a Bland-Altman plot and demonstrated no bias between observers, (*Figure 5-12*).

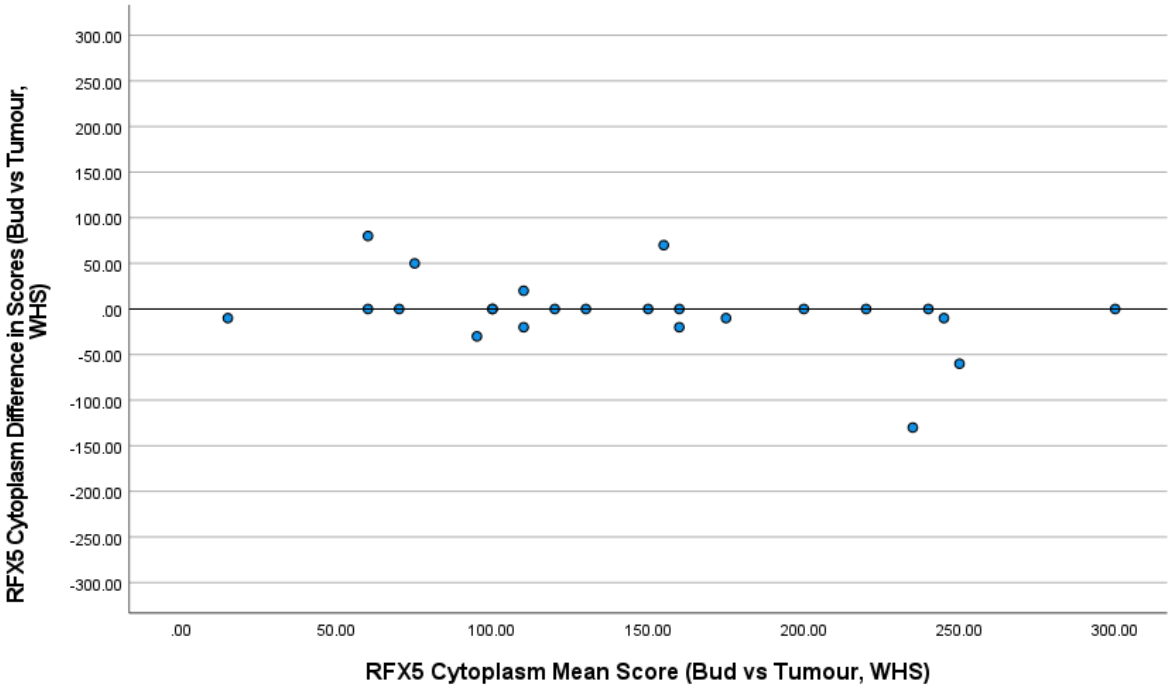

Figure 5-12 Bland Altman Plot comparing the difference in scores to mean scores for RFX5 expression in cytoplasm in buds and tumour cells.

Based on these findings, it was possible to infer that further analysis of protein expression could be expanded to the full cohort of the Glasgow Breast Cancer Cohort in the form of a tissue microarray and remain representative of expression both within the tumour buds as in within the intratumoural environment, (*Figure 5-13*).

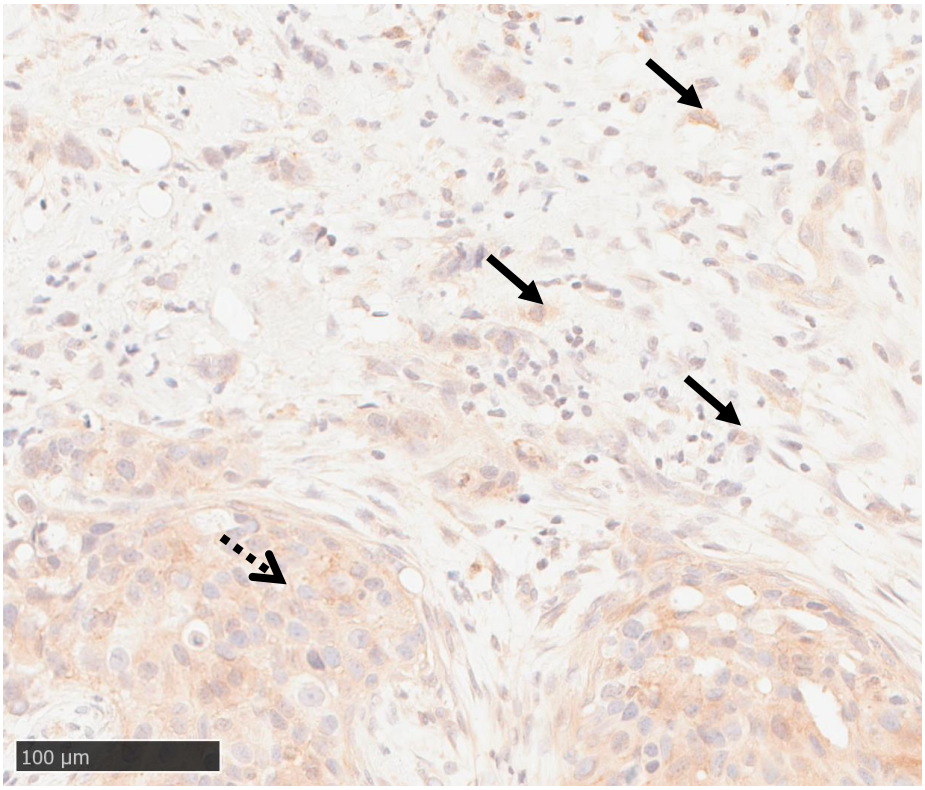

Figure 5-13 Cytoplasmic RFX5 staining in tumour mass (dotted arrow) correlated closely with staining in tumour buds (black arrow)

5.2.7 Nuclear RFX5 Expression in Full Section Specimens

Using RFX5-specific antibody, weighted histoscores were generated by manual evaluation by a single observer (FS). Examples of light, moderate and strong nuclear staining, together with positive and negative control tissue are shown below, (*Figure 5-14*).

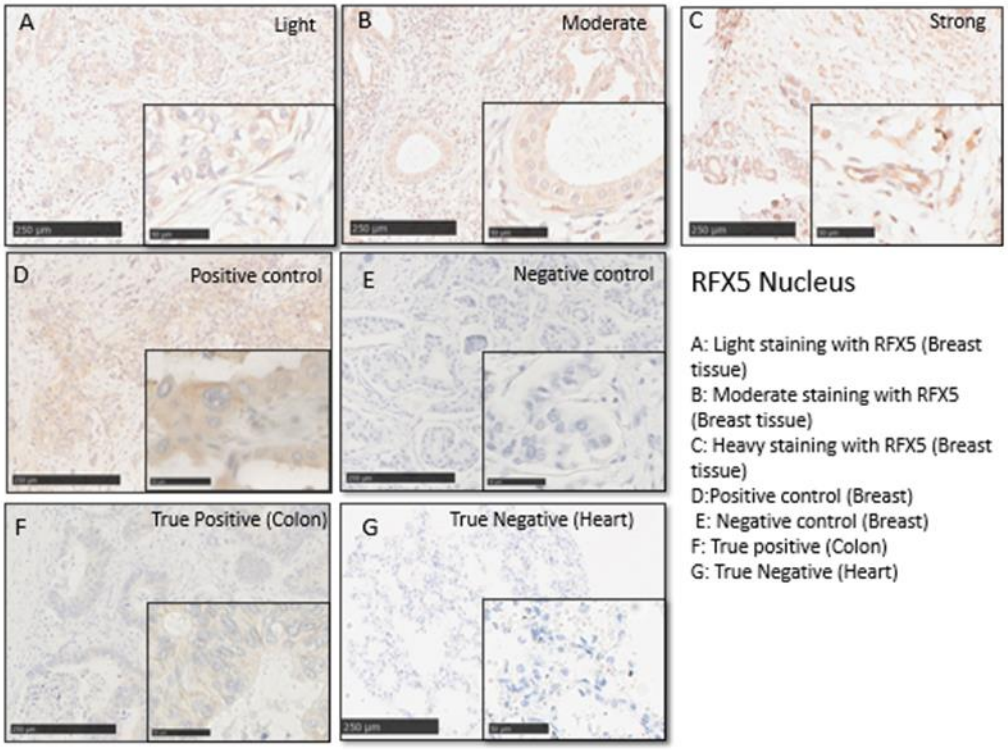

Figure 5-14 RFX5 nuclear staining representative images.

Nuclear expression of RFX5 was manually scored by a single assessor (FS), and scores varied from 0-250 (*Figure 5-15*).

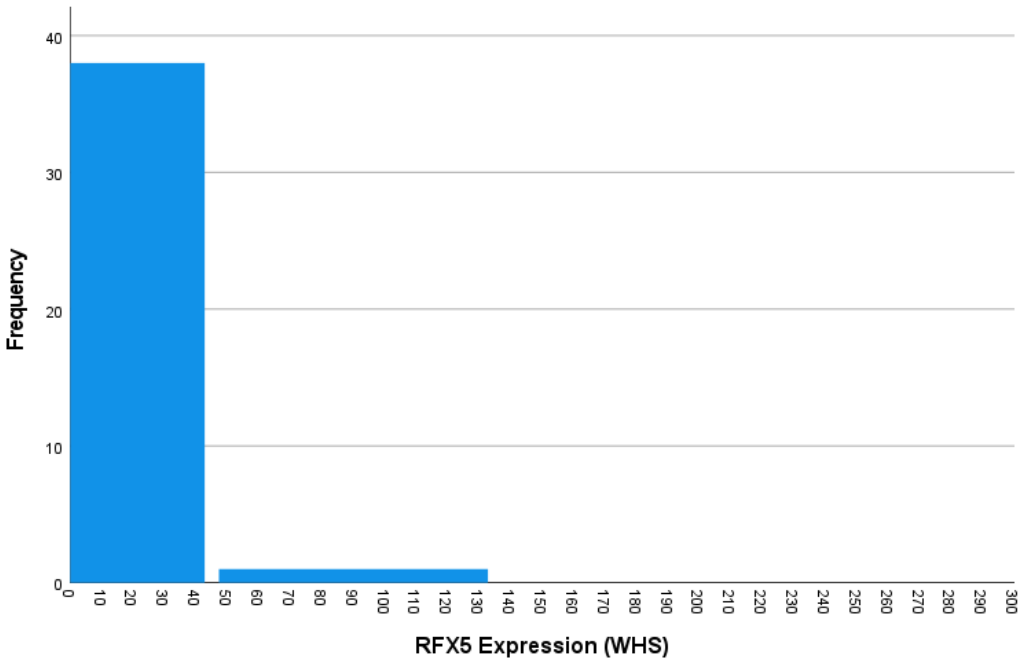

Figure 5-15 RFX5 nuclear expression. (WHS, weighted histoscores).

Manual assessment for validation by WN using 10% of this sub-cohort is described using the scatter plot below, (*Figure 5-16*). An intraclass correlation coefficient

(ICCC) of 0.977 suggesting a strong correlation between validation and primary assessors' scores.

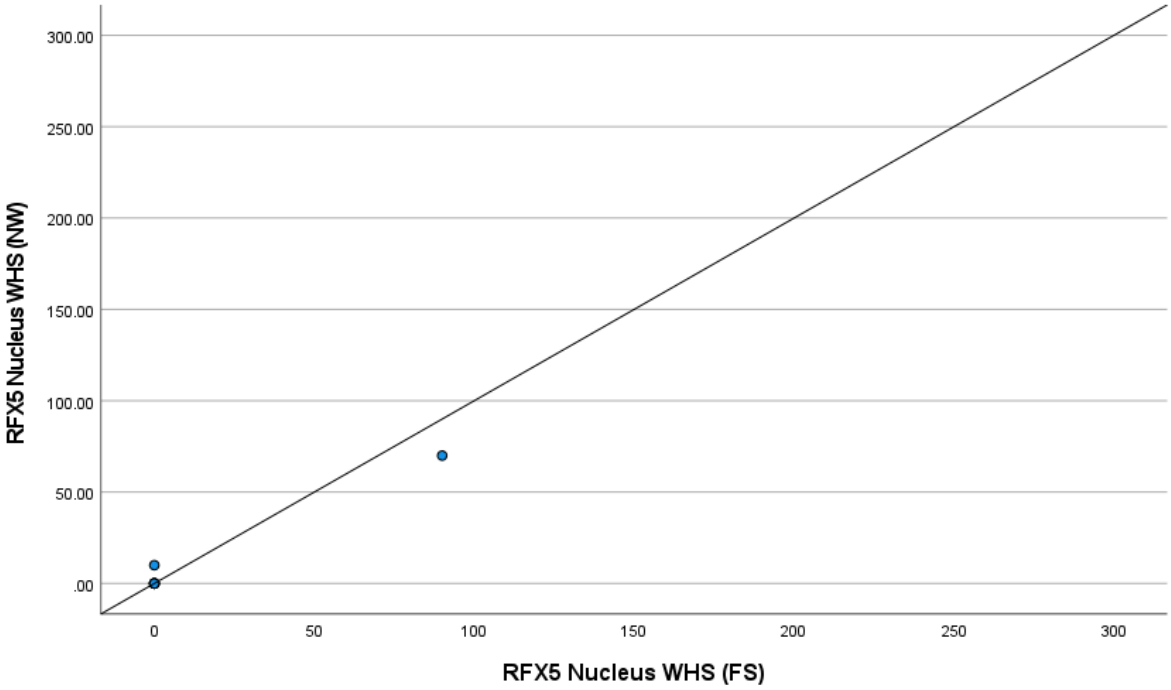

Figure 5-16 Correlation between FS and NW manual weighted histoscore (WHS) for nucleus RFX5 staining. Scatter plot showing correlation between FS and NW for nucleus staining. Intraclass correlation coefficient 0.977 for 10% specimens.

A subsequent comparison of averages and differences in scores was produced as a Bland-Altman plot suggested the scores correlated satisfactorily, (*Figure 5-17*).

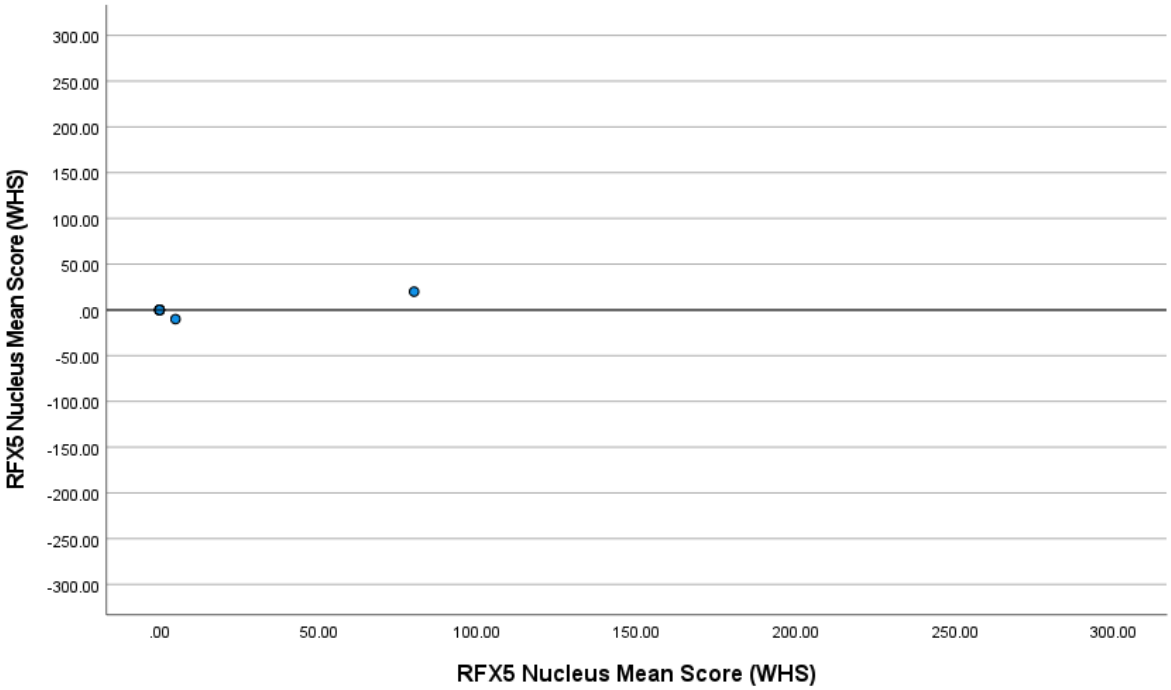

Figure 5-17 Bland Altman Plot comparing difference in scores for RFX5 expression in nucleus.

5.2.8 RFX5 Nuclear Expression in Tumour Cells Versus Tumour Buds

RFX5 nuclear expression was compared between tumour buds (where present) and intratumoural cells. A scatter plot was used to visualise the correlation between nuclear RFX5 expression in intratumoral cells and tumour buds (*Figure 5-18*). Only 24 full sections stained had tumour buds present, in these the WHS of the bud were comparable to that of the tumour core. The intraclass correlation coefficient (ICCC) was 0.968.

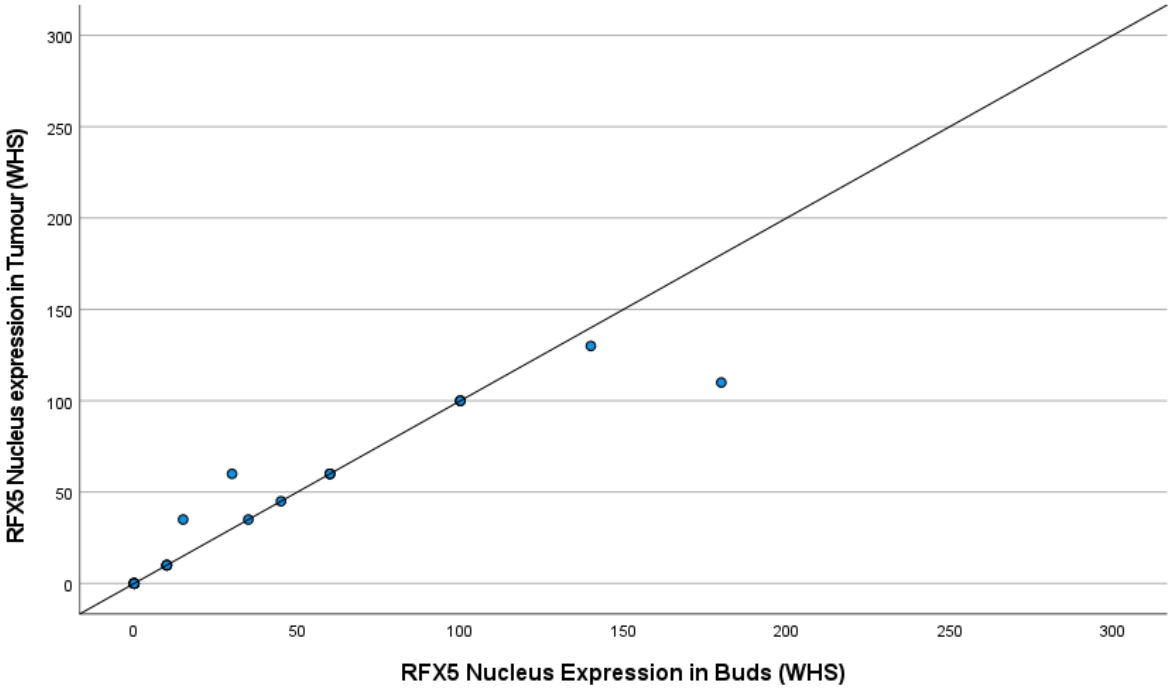

Figure 5-18 Nucleus RFX5 expression in tumour versus buds, ICCC 0.968.

A subsequent comparison of averages and differences in scores was plotted as a Bland-Altman plot and demonstrated no bias between observers, (*Figure 5-19*).

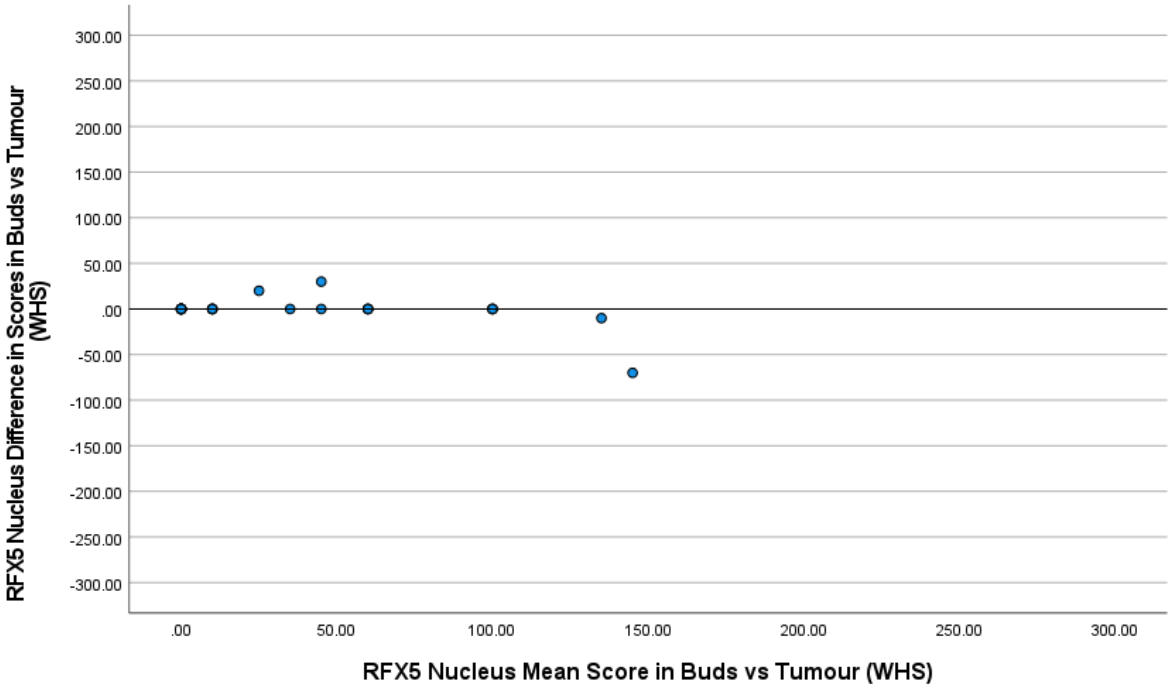

Figure 5-19 Bland Altman Plot comparing the difference in scores to mean scores for RFX5 expression in nucleus in bud vs tumour cells.

Based on these findings, it was possible to infer that further analysis of protein expression could be expanded to the full cohort of the Glasgow Breast Cancer Cohort in the form of a tissue microarray and remain representative of expression both within the tumour buds as in within the intratumoural environment, (*Figure 5-20*).

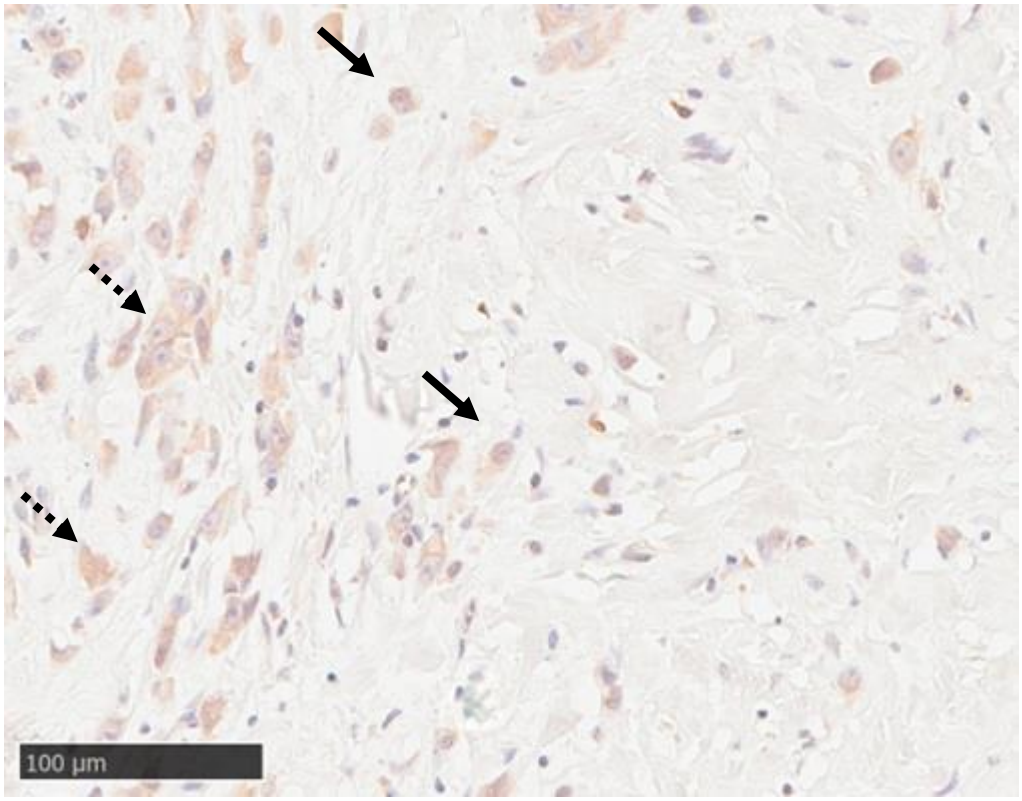

Figure 5-20 Nuclear RFX5 staining in tumour mass (dotted arrow) correlated closely with staining in tumour buds (black arrow).

5.2.9 RFX5 Expression in the Glasgow Breast Cancer Cohort

TMA slides composed of specimens from the Glasgow Breast Cancer cohort were used to assess RFX5 expression. Slides were stained with RFX5 antibody, and manually assessed to achieve a weighted histoscore. Included patients had ductal cancer only, resulting in 736 specimens being included in the overall cohort. Each specimen was assessed on 3 different TMA slides, and an average WHS was calculated, unless only one specimen was available, in which case this was used as the final WHS. 351 cases were included in the final analysis as out of the total 736 cases, 385 did not have assessable cores, (*Figure 5-21*).

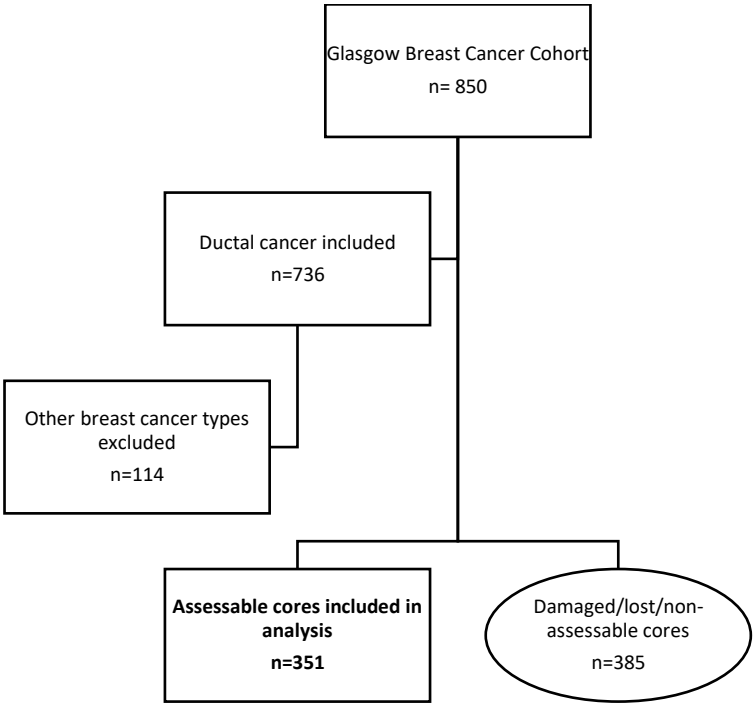

Figure 5-21 CONSORT diagram of cases included in analysis from the Glasgow Breast Cancer Cohort.

Manual weighted histoscores of RFX5 expression were performed by FS. Validation of the scores (minimum 10%) was performed by Hester van Wyk.

5.2.10 RFX5 Membrane Expression in the Glasgow Breast Cancer Cohort

Manual weighted histoscores of membrane RFX5 expression were performed by FS. Scores by FS varied between 0 and 280 (FIGURE), with a mean of 8.433, (*Figure 5-22*).

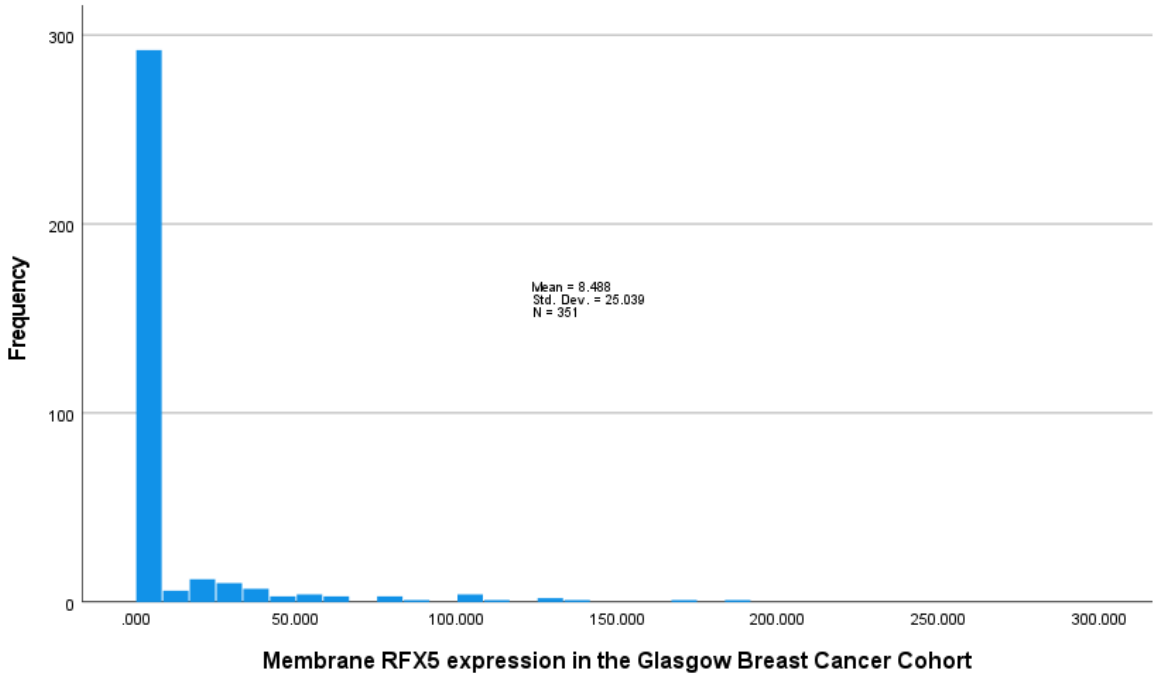

Figure 5-22 Distribution of RFX5 membrane expression (weighted histoscores) in the Glasgow Breast Cancer Cohort. Mean score 8.433, SD 25.039.

Counter-scores were performed manually by HVW for a minimum of 10% of cores, (n=63) similarly to what was seen in FS scores, the selected sample WHS was always 0. No ICC was therefore calculated. The two scorers re-assessed a separate portion of samples informally and agreed that scores were consistent within a separate sample.

A threshold for high and low RFX5 membrane expression were delineated using R Studio to compare high versus low RFX5 expression according to survival. The threshold was identified at 6.67, (*Figure 5-23*).

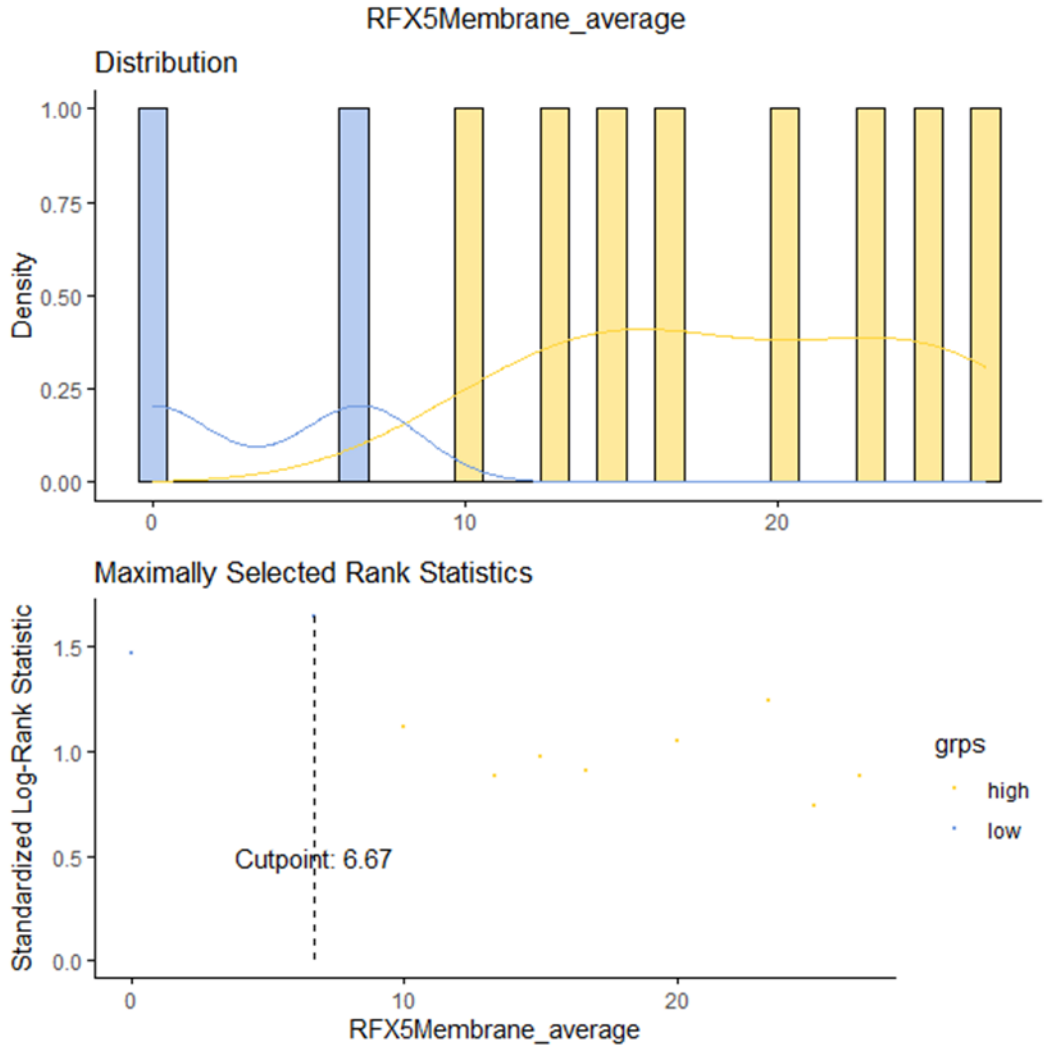

Low Expression

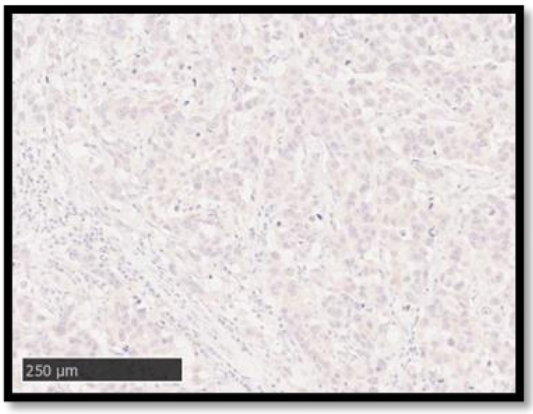

High expression

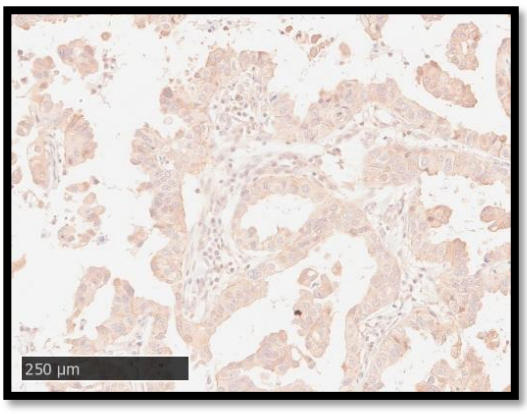

Figure 5-23 RFX5 membrane expression - threshold for high and low expression of RFX5 in the membrane of the Glasgow Breast Cancer Cohort was identified as 6.67, with patients with weighted scores above 6.67 considered to have high RFX5 membrane expression. Examples of protein expression as seen on specimens is also described below the graphical representation.

5.2.11 Membrane RFX5 and Survival in the Glasgow Breast Cancer Cohort

850 patients had TMAs produced from the Glasgow Breast Cancer Cohort, of which 736 had ductal cancers and were included in the cohort for analysis. Of these, 722 of 736 had valid cancer-specific survival data and 350 had viable cores, leading to a final 344 with assessable cores and survival data. 283 patients had low RFX5 membrane expression and had 53 events, while 61 had high expression and 16 events. Survival in the low RFX5 group was 88% at 5 years, and 76% at 10 years, while in the high RFX5 group survival was 80% at 5 years, and 70% at 10 years. Using Kaplan Meier survival analysis, mean cancer-specific survival (CSS) time for low RFX5 membrane expression was 155.3 months compared to high RFX5 expression survival of 141.3 months, (HR 1.531, 95% C.I.; 0.875-2.679, log rank p=0.135), (*Figure 5-24*).

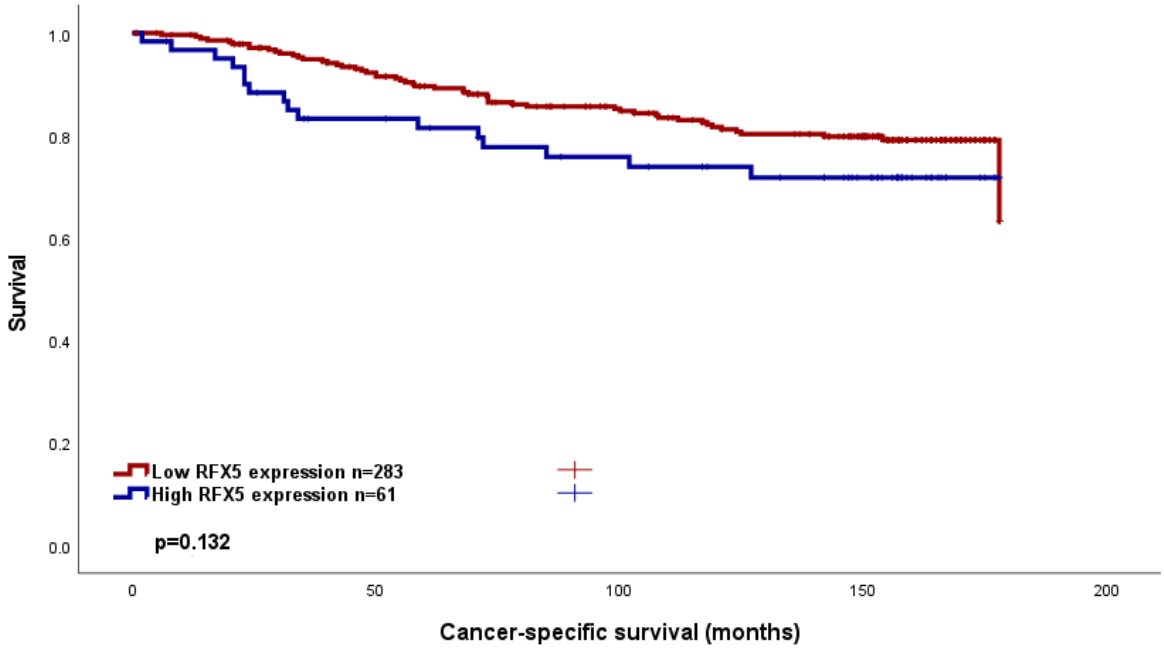

Figure 5-24 Cancer-specific survival in the Glasgow Breast Cancer Cohort according to RFX5 membrane expression. Kaplan Meier Curve showing the association between RFX5 membrane expression and survival (months). HR 1.531, 95% C.I.; 0.875-2.679, log rank p=0.135

When different clinicopathological factors were compared for inter-factor correlation, invasive grade, molecular subtype and KM score were significantly associated with RFX5 membrane expression, (Table 5-1).

Table 5-1 Clinicopathological factors and their relation to RFX5 membrane expression in the Glasgow Breast Cancer Cohort. Chi-squared analysis.

Clinicopathological factor	RFX5 membrane staining (%)		p
	Low	High	
Age (years)			
≤50	82(86.3)	13(13.7)	0.341
>50	208(81.3)	48(18.8)	
Tumour Size			
≤20mm	170(83.7)	33(16.3)	0.791
21-49mm	110(80.9)	26(19.1)	
≥50mm	10(83.3)	2(16.7)	
Grade			
I	**70(92.1)**	**6(7.9)**	**0.042**
II	**132(81)**	**31(19)**	
III	**88(78.6)**	**24(16.7)**	
Nodal Status			
N_0	167(83.9)	32(16.1)	0.754
N_1	118(80.8)	28(19.2)	
Molecular Subtype			
Luminal A	**156(88.1)**	**21(11.9)**	**0.005**
Luminal B	**80(82.5)**	**17(17.5)**	
TNBC	**31(67.4)**	**15(32.6)**	
HER2-enriched	**15(71.4)**	**6(28.6)**	
Lymphatic Invasion			
Absent	123(79.4)	32(20.6)	0.503
Present	77(83.7)	15(16.3)	
Vascular Invasion			
Absent	178(81.3)	41(18.7)	0.798
Present	22(78.6)	6(21.4)	
Necrosis			
Absent	163(85.8)	27(14.2)	0.063
Present	116(77.9)	33(21.4)	
Klintrup Makinen			
0	**37(97.4)**	**1(2.6)**	**0.006**
1	**159(80.3)**	**39(19.7)**	
2	**64(77.1)**	**19(22.9)**	
3	**20(100)**	**0**	
Ki67			
Low (<15%)	204(82.9)	42(17.1)	0.755
High (>15%)	80(81.6)	18(18.4)	
Tumour Bud			
-Low	184(82.9)	38(17.1)	0.882
-High	100(82)	22(18)	
Tissue Stroma Percentage			
Low	199(82.9)	41(17.1)	0.877
High	85(81.7)	19(18.3)	

Stratification of the cohort to compare patients according to ER status was performed. 344 had valid ER-status data available. In the ER-negative patient group (n=71), 50 patients had low RFX5 membrane expression and had 15 events, while 21 had high RFX5 expression and 7 event. Survival in the low RFX5 group

was 76% at 5 years, and 66% at 10 years, while in the high RFX5 group survival was 75% at 5 and 64% at 10 years (HR 1.258 95% C.I. 0.513-3.088, p=0.616), (*Figure 5-24*).

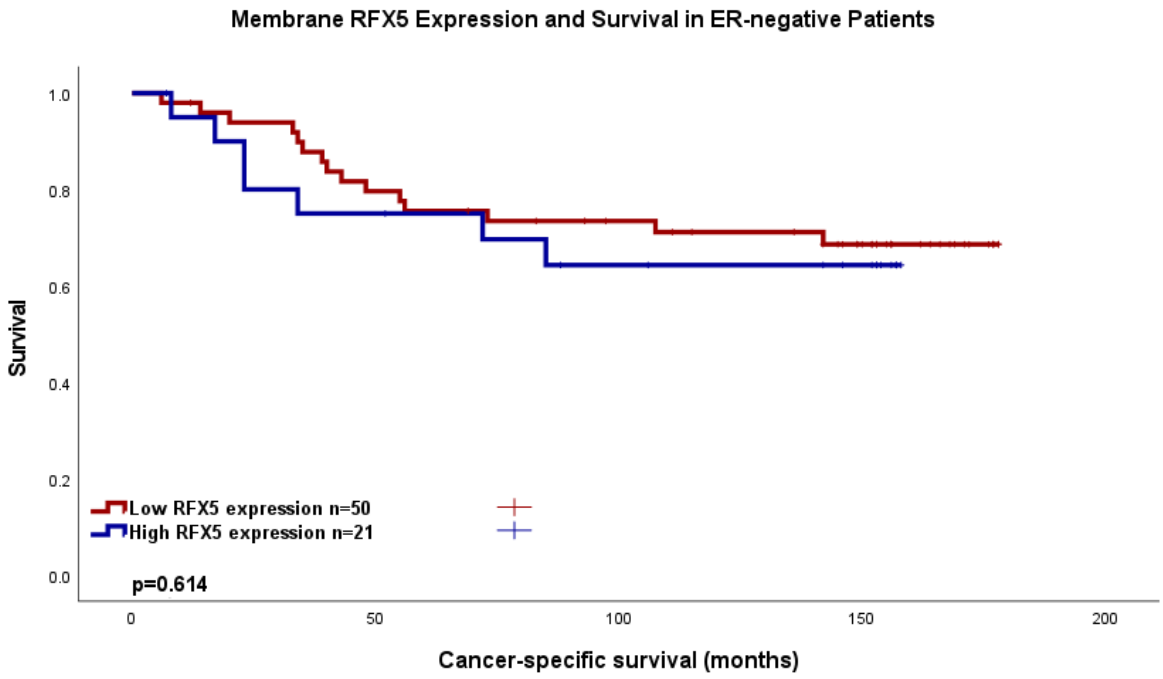

Figure 5-25 Cancer-specific survival in ER-negative patients in the Glasgow Breast Cancer Cohort according to RFX5 membrane expression. Kaplan Meier Curve showing the association between RFX5 membrane expression and survival (months). HR 1.258 95% C.I. 0.513-3.088, p=0.616.

Within the ER-negative group, inter-factor correlation was assessed when comparing the high and low RFX5 membrane expressors, (*Table 5-2*). Here, age was associated with RFX5 membrane expression.

Table 5-2 Clinicopathological factors and their relation to RFX5 membrane expression in ER-negative patients in the Glasgow Breast Cancer Cohort. Chi-squared analysis.

Clinicopathological factor	RFX5 membrane staining (%)		p
	Low	High	
Age (years)			
<50	**23(88.5)**	**3(11.5)**	**0.015**
>50	**27(60)**	**18(40)**	
Tumour Size			
<20mm	23(63.9)	13(36.1)	0.314
21-49mm	24(75)	8(25)	
>50mm	3(100)	0	
Grade			
I	2(50)	2(50)	0.239
II	16(84.2)	3(15.8)	

III	32(66.7)	16(33.3)	
Nodal Status			
N_0	26(98.4)	11(31.6)	1.000
N_1	24(72.4)	10(27.6)	
Lymphatic Invasion			
Absent	26(68.5)	12(30.5)	0.792
Present	21(75)	8(25)	
Vascular Invasion			
Absent	41(69.5)	18(30.5)	1.000
Present	6(75)	2(25)	
Necrosis			
Absent	13(72.2)	5(27.8)	1.000
Present	36(69.2)	16(30.8)	
Klintrup Makinen			
0	1(100)	0	
1	18(58.1)	13(41.9)	0.150
2	23(74.2)	8(25.8)	
3	6(100)	0	
Ki67			
Low (<15%)	39(68.4)	18(31.6)	0.741
High (>15%)	10(76.9)	3(23.1)	
Tumour Bud			
-Low	34(69.4)	15(30.6)	1.000
-High	15(71.4)	6(28.6)	
Tissue Stroma Percentage			
Low	39(75)	13(25)	0.143
High	10(55.6)	8(44.4)	

In the ER-positive group (n=273), 233 had low nuclear RFX5 expression, with 38 events, and 40 high RFX5 expression, with 9 events. Survival in the low membrane RFX5 ER-positive group was 91% at 5 years and 78% at 10 years, and in the high RFX5 group was 82% at 5 years and 73% at 10 years (HR 1.412 95% C.I. 0.682-2.924, p=0.352), (*Figure 5-26*).

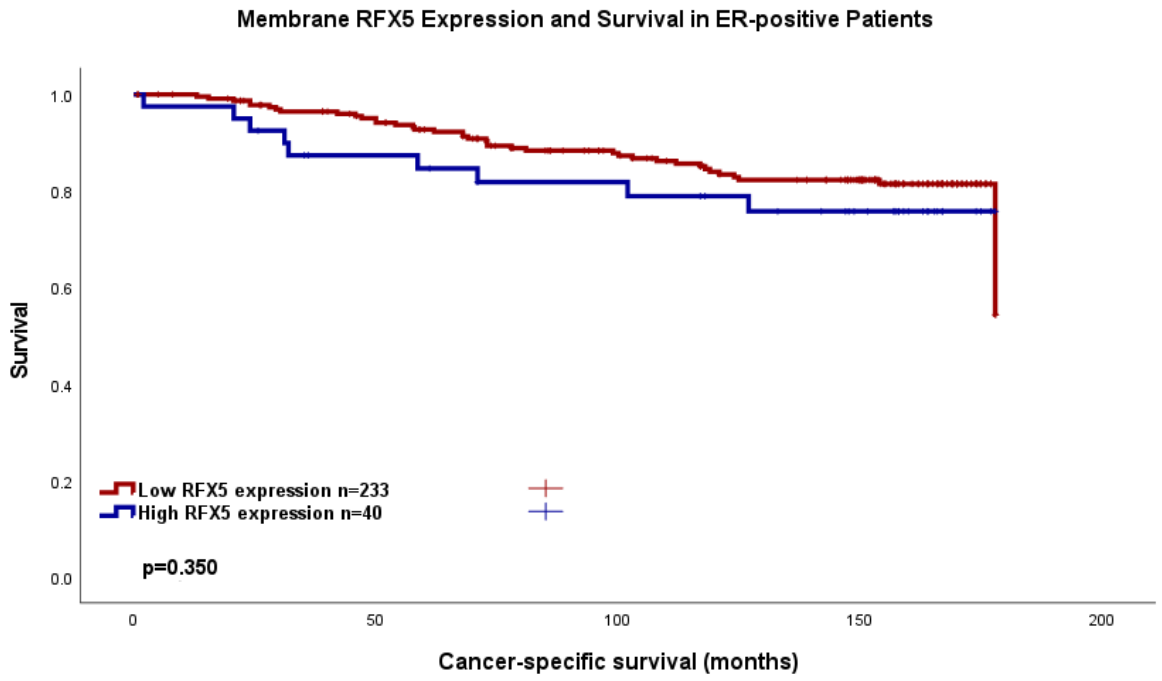

Figure 5-26 Cancer-specific survival in ER-positive patients in the Glasgow Breast Cancer Cohort according to RFX5 membrane expression. Kaplan Meier Curve showing the association between RFX5 membrane expression and survival (months). HR 1.412 95% C.I. 0.682-2.924, p=0.352.

Within the ER-positive group, inter-factor correlation was assessed when comparing the high and low RFX5 membrane expressors, (Table 5-3). Here, grade and KM score was associated with RFX5 membrane expression.

Table 5-3 Clinicopathological factors and their relation to RFX5 membrane expression in ER+ patients in the Glasgow Breast Cancer Cohort. Chi-squared analysis.

Clinicopathological factor	RFX5 membrane staining (%)		p
	Low	High	
Age (years)			
≤50	59(85.5)	10(14.5)	1.000
>50	181(85.8)	30(14.2)	
Tumour Size			
≤20mm	147(88)	20(12)	0.374
21-49mm	86(82.7)	18(17.3)	
≥50mm	7(77.8)	2(22.2)	
Grade			
I	**68(94.4)**	**4(5.6)**	**0.020**
II	**116(80.6)**	**28(19.4)**	
III	**56(87.5)**	**8(12.5)**	
Nodal Status			
N_0	141(87)	21(13)	0.759
N_1	94(83.9)	18(16.1)	
Lymphatic Invasion			

Absent	97(82.9)	20(17.1)	0.382
Present	56(88.9)	7(11.1)	
Vascular Invasion			
Absent	137(85.6)	23(14.4)	0.509
Present	16(80)	4(20)	
Necrosis			
Absent	150(87.2)	22(12.8)	0.367
Present	80(82.5)	17(17.5)	
Klintrup Makinen			
0	**36(97.3)**	**1(2.7)**	**0.033**
1	**141(84.4)**	**26(15.6)**	
2	**41(78.8)**	**11(21.2)**	
3	**14(100)**	**0**	
Ki67			
Low (<15%)	165(87.3)	24(12.7)	0.350
High (>15%)	70(82.4)	15(17.6)	
Tumour Bud			
-Low	150(86.7)	23(13.3)	0.593
-High	85(84.2)	16(15.8)	
Tissue Stroma Percentage			
Low	160(85.1)	28(14.9)	0.713
High	75(87.2)	11(12.8)	

Further stratification according to molecular subtype was then performed. These subtypes were divided into Luminal A, Luminal B, Triple-negative (most similar to "Basal-like" subtype) and HER-2 enriched groups. For 10 patients, molecular subgroup was not available. For the remaining patients, there were 171 Luminal A, 96 Luminal B, 46 TNBC and 21 HER-2 enriched cases. Luminal A patients had 150 low nuclear RFX5 expressors with 17 events, and 21 high-RFX5 expressors with 5 events. Luminal B patients had 79 low RFX5 expressors with 20 events, and 17 high RFX5 expressors with 4 events. The TNBC patients had 31 low RFX5 expressors with 7 events, and 15 patients with high RFX5 with 6 events. Finally, HER-2 enriched patients consisted of 15 low RFX5 cases with 8 events, and 6 high RFX5 cases with 1 event. Kaplan Meier curves are shown for each subgroup below.

Luminal A patients had a 5-year survival of 93% and 86% at 10 years for low RFX5 expressors, compared to 74% at 5 years and 10 years for high RFX5 expressors. (HR 2.279, 95% C.I. 0.836-6.216, p=0.108), (*Figure 5-27*).

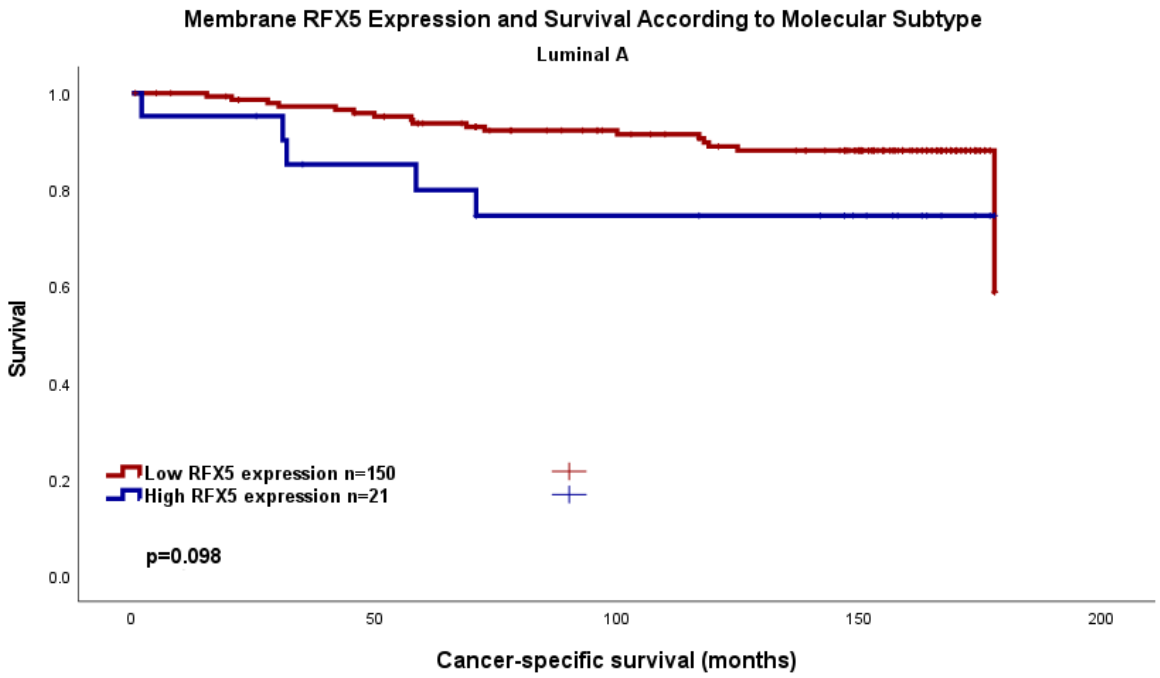

Figure 5-27 Cancer-specific survival in Luminal A patients in the Glasgow Breast Cancer Cohort according to RFX5 membrane expression. Kaplan Meier Curve showing the association between RFX5 membrane expression and survival (months). HR 2.279, 95% C.I. 0.836-6.216, p=0.108.

Within the Luminal A group, inter-factor correlation was assessed when comparing the high and low RFX5 membrane expressors, (Table 5-4). Here, no association with RFX5 membrane expression was seen.

Table 5-4 Clinicopathological factors and their relation to RFX5 membrane expression in Luminal A patients in the Glasgow Breast Cancer Cohort. Chi-squared analysis.

Clinicopathological factor	RFX5 membrane staining (%)		p
	Low	High	
Age (years)			
≤50	44(91.7)	4(8.3)	0.445
>50	112(86.8)	17(13.2)	
Tumour Size			
≤20mm	100(90.1)	11(9.9)	0.364
21-49mm	52(83.9)	10(16.1)	
≥50mm	4(100)	0	
Grade			
I	55(94.8)	3(5.2)	0.073
II	78(83)	16(17)	
III	23(92)	2(8)	
Nodal Status			
N_0	97(91.5)	9(8.5)	0.179
N_1	57(82.6)	12(17.4)	
Lymphatic Invasion			
Absent	76(89.4)	9(10.6)	0.755

Present	29(87.9)	4(12.1)	
Vascular Invasion			
Absent	94(88.7)	12(11.3)	1.000
Present	11(91.7)	1(8.3)	
Necrosis			
Absent	105(89.7)	12(10.3)	0.439
Present	44(84.6)	8(15.4)	
Klintrup Makinen			
0	24(100)	0	
1	95(86.4)	15(13.6)	0.181
2	23(85.2)	4(14.8)	
3	7(100)	0	
Ki67			
Low (<15%)	156(88.1)	21(11.9)	n/a
High (>15%)	0	0	
Tumour Bud			
-Low	97(91.5)	9(8.5)	0.141
-High	55(83.3)	11(16.7)	
Tissue Stroma Percentage			
Low	105(89.7)	12(10.3)	0.449
High	47(85.5)	8(14.5)	

Luminal B patients had a 5-year survival of 88% and 65% at 10 years for low RFX5 expressors, compared to 88% at 5 and 65% at 10 years for high RFX5 expressors. (HR 0.845, 95% C.I. 0.288-2.476, p=0.758), (*Figure 5-28*).

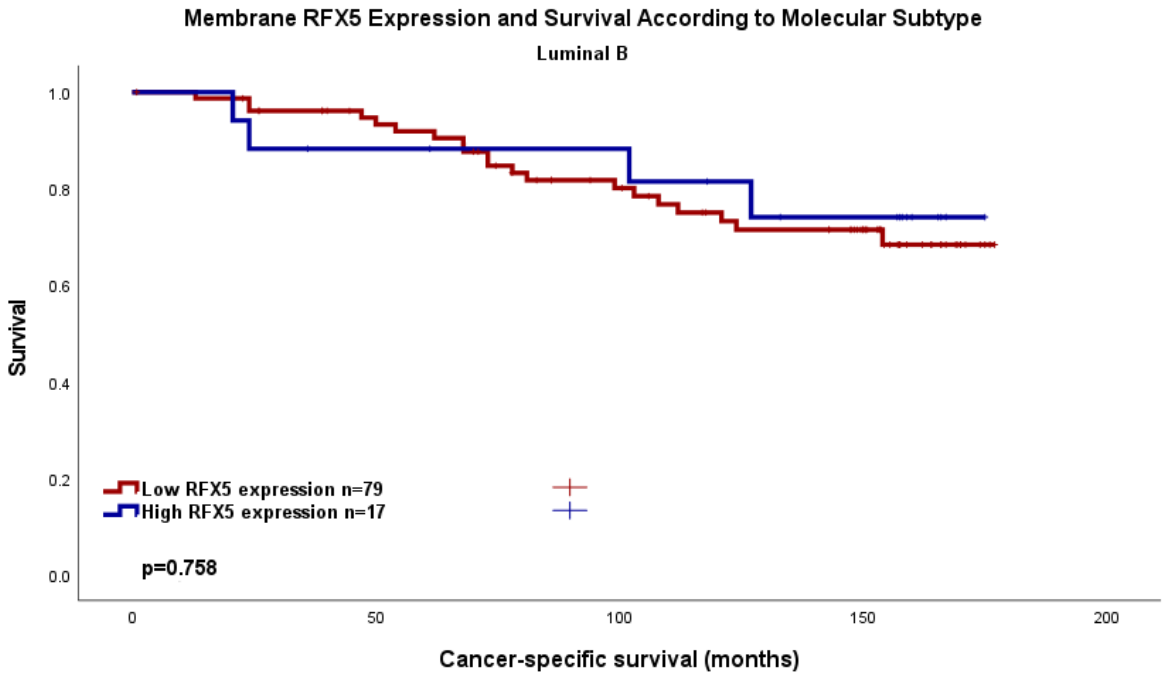

Figure 5-28 Cancer-specific survival in Luminal B patients in the Glasgow Breast Cancer Cohort according to RFX5 membrane expression. Kaplan Meier Curve showing the association between RFX5 membrane expression and survival (months). HR 0.845, 95% C.I. 0.288-2.476, p=0.758.

Within the Luminal B group, inter-factor correlation was assessed when comparing the high and low RFX5 membrane expressors, (Table 5-5). Here, lymphatic invasion neared statistically significant association with RFX5 membrane expression.

Table 5-5 Clinicopathological factors and their relation to RFX5 membrane expression in Luminal B patients in the Glasgow Breast Cancer Cohort. Chi-squared analysis.

Clinicopathological factor	**RFX5 membrane staining (%)**		**p**
	Low	**High**	
Age (years)			
≤50	17(77.3)	5(22.7)	0.526
>50	63(84)	12(16)	
Tumour Size			
≤20mm	44(86.3)	7(13.7)	0.306
21-49mm	33(80.5)	8(19.5)	
≥50mm	3(60)	2(40)	
Grade			
I	13(92.9)	1(7.1)	0.219
II	34(75.6)	11(24.4)	
III	33(86.8)	5(13.2)	
Nodal Status			
N_0	42(80.8)	10(19.2)	0.629
N_1	36(85.7)	6(14.3)	
Lymphatic Invasion			
Absent	22(68.8)	10(31.3)	0.063
Present	26(89.7)	3(10.3)	
Vascular Invasion			
Absent	43(81.1)	10(18.9)	0.350
Present	5(62.5)	3(37.5)	
Necrosis			
Absent	42(82.4)	9(17.6)	1.000
Present	36(81.8)	8(18.2)	
Klintrup Makinen			
0	11(91.7)	1(8.3)	0.395
1	43(81.1)	10(18.9)	
2	19(76)	6(24)	
3	7(100)	0	
Ki67			
Low (<15%)	11(84.6)	2(15.4)	1.000
High (>15%)	69(82.1)	15(17.9)	
Tumour Bud			
-Low	50(80.6)	12(19.4)	0.590
-High	30(85.7)	5(14.3)	
Tissue Stroma Percentage			
Low	53(79.1)	14(20.9)	0.254
High	27(90)	3(10)	

Triple-negative ("basal-like) patients had a 5-year survival of 83% and 73% at 10 years for low RFX5 expressors, compared to 73% at 5 and 58% at 10 years for high RFX5 expressors. (HR 2.084 95% C.I. 0.699-6.217, p=0.188), (*Figure* 5-29).

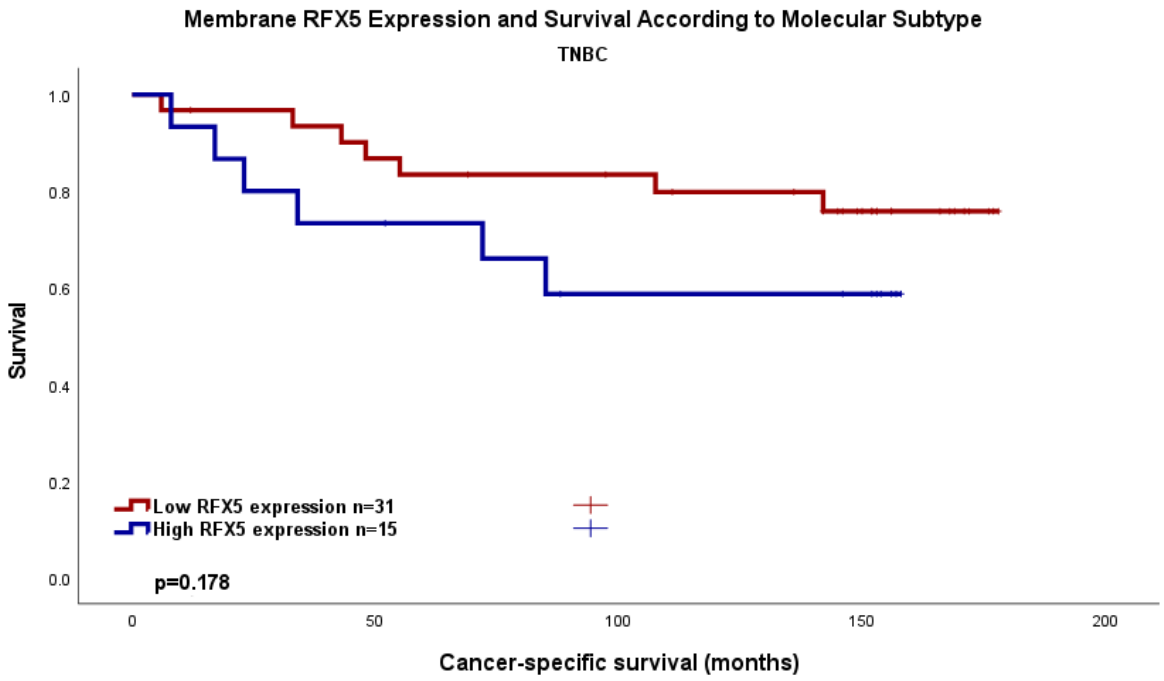

Figure 5-29 Cancer-specific survival in TNBC patients in the Glasgow Breast Cancer Cohort according to RFX5 membrane expression. Kaplan Meier Curve showing the association between RFX5 membrane expression and survival (months). HR 2.084 95% C.I. 0.699-6.217, p=0.188.

Within the TNBC group, inter-factor correlation was assessed when comparing the high and low RFX5 membrane expressors, (Table 5-6). Here, no association with RFX5 membrane expression was seen.

Table 5-6 Clinicopathological factors and their relation to RFX5 membrane expression in TNBC patients in the Glasgow Breast Cancer Cohort. Chi-squared analysis.

Clinicopathological factor	RFX5 membrane staining (%)		p
	Low	High	
Age (years)			
≤50	13(86.7)	2(13.3)	0.092
>50	18(58.1)	13(41.9)	
Tumour Size			
≤20mm	15(57.7)	11(42.3)	0.253
21-49mm	15(78.9)	4(21.1)	
≥50mm	10(100)	0	
Grade			
I	1(33.3)	2(66.7)	0.345
II	10(76.9)	3(23.1)	

III	20(66.7)	10(33.3)	
Nodal Status			
N_0	18(66.7)	9(33.3)	1.000
N_1	13(68.4)	6(28.6)	
Lymphatic Invasion			
Absent	16(66.7)	8(33.3)	1.000
Present	13(68.4)	6(31.6)	
Vascular Invasion			
Absent	24(66.7)	12(33.3)	1.000
Present	5(71.4)	2(28.6)	
Necrosis			
Absent	8(66.7)	4(33.3)	1.000
Present	22(66.7)	11(33.3)	
Klintrup Makinen			
0	1(100)	0	0.129
1	12(52.2)	11(47.8)	
2	12(75)	4(25)	
3	5(100)	0	
Ki67			
Low (<15%)	26(66.7)	13(33.3)	1.000
High (>15%)	4(66.7)	2(33.3)	
Tumour Bud			
-Low	23(69.7)	10(30.3)	0.496
-High	7(58.3)	5(41.7)	
Tissue Stroma Percentage			
Low	25(73.5)	9(26.5)	0.140
High	5(45.5)	6(54.5)	

HER2-enriched patients had a 5-year survival of 53% and 47% at 10 years for low RFX5 expressors, compared to 80% at 5 and 80% at 10 years for high RFX5 expressors. (HR 0.329, 95% C.I. 0.041-2.639, =0.296), (*Figure 5-30*).

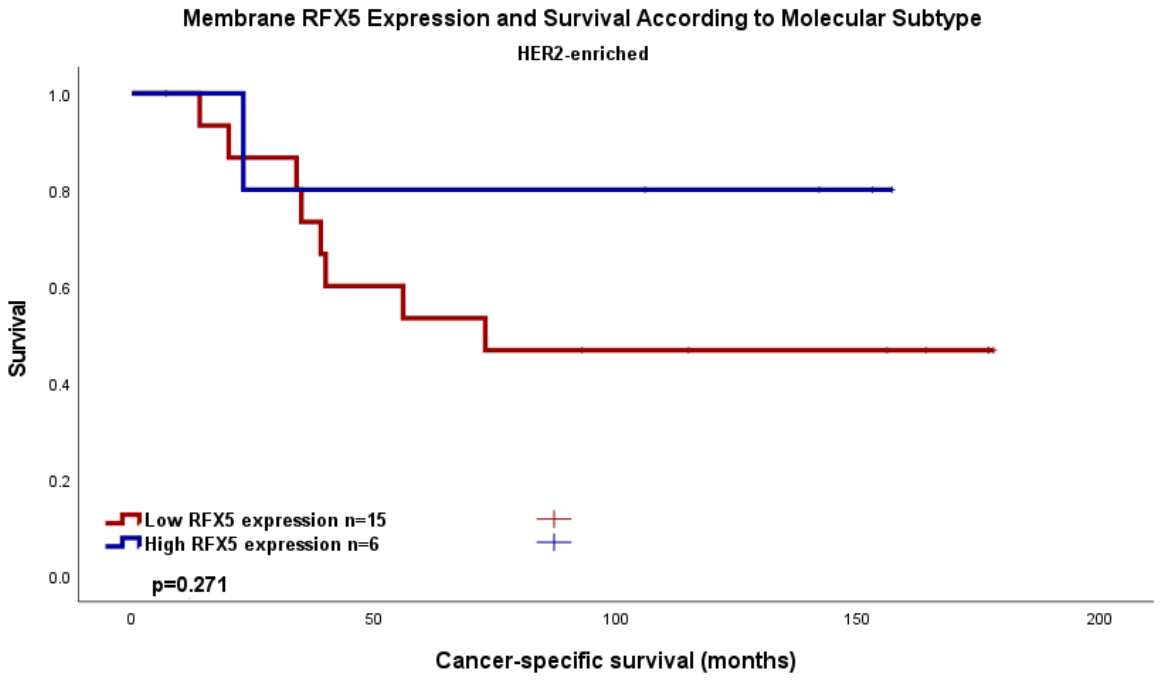

Figure 5-30 Cancer-specific survival in HER2 enriched patients in the Glasgow Breast Cancer Cohort according to RFX5 membrane expression. Kaplan Meier Curve showing the association between RFX5 membrane expression and survival (months). HR 0.329, 95% C.I. 0.041-2.639, =0.296.

Within the HER2-enriched group, inter-factor correlation was assessed when comparing the high and low RFX5 membrane expressors, (Table 5-7). Here, no association with RFX5 membrane expression was seen.

Table 5-7 Clinicopathological factors and their relation to RFX5 membrane expression in HER2-enriched patients in the Glasgow Breast Cancer Cohort. Chi-squared analysis.

Clinicopathological factor	**RFX5 membrane staining (%)**		**p**
	Low	**High**	
Age (years)			
≤50	6(85.7)	1(14.3)	0.613
>50	9(64.3)	5(35.7)	
Tumour Size			
≤20mm	5(71.4)	2(28.6)	0.627
21-49mm	8(66.7)	4(33.3)	
≥50mm	2(100)	0	
Grade			
I	0	0	0.262
II	5(100)	0	
III	10(62.5)	6(37.5)	
Nodal Status			
N_0	5(71.4)	2(28.6)	1.000
N_1	10(71.4)	4(28.6)	
Lymphatic Invasion			
Absent	6(60)	4(40)	0.628
Present	8(80)	2(20)	
Vascular Invasion			
Absent	13(68.4)	6(31.6)	1.000
Present	1(100)	0	
Necrosis			
Absent	3(75)	1(25)	1.000
Present	12(70.6)	5(29.4)	
Klintrup Makinen			
0	0	0	0.793
1	4(66.7)	2(33.3)	
2	9(69.2)	4(30.8)	
3	1(100)	0	
Ki67			
Low (<15%)	9(94.3)	5(35.7)	0.613
High (>15%)	6(85.7)	1(14.3)	
Tumour Bud			
-Low	8(61.5)	5(38.5)	0.336
-High	7(87.5)	1(12.5)	
Tissue Stroma Percentage			

Low	11(73.3)	4(26.7)	1.000
High	4(66.7)	2(33.3)	

5.2.12 RFX5 Cytoplasmic Expression in the Glasgow Breast Cancer Cohort

Manual weighted histoscores of cytoplasmic RFX5 expression were performed by FS. Scores by FS varied between 0 and 300, with a mean of 173.5, (*Figure 5-31)*.

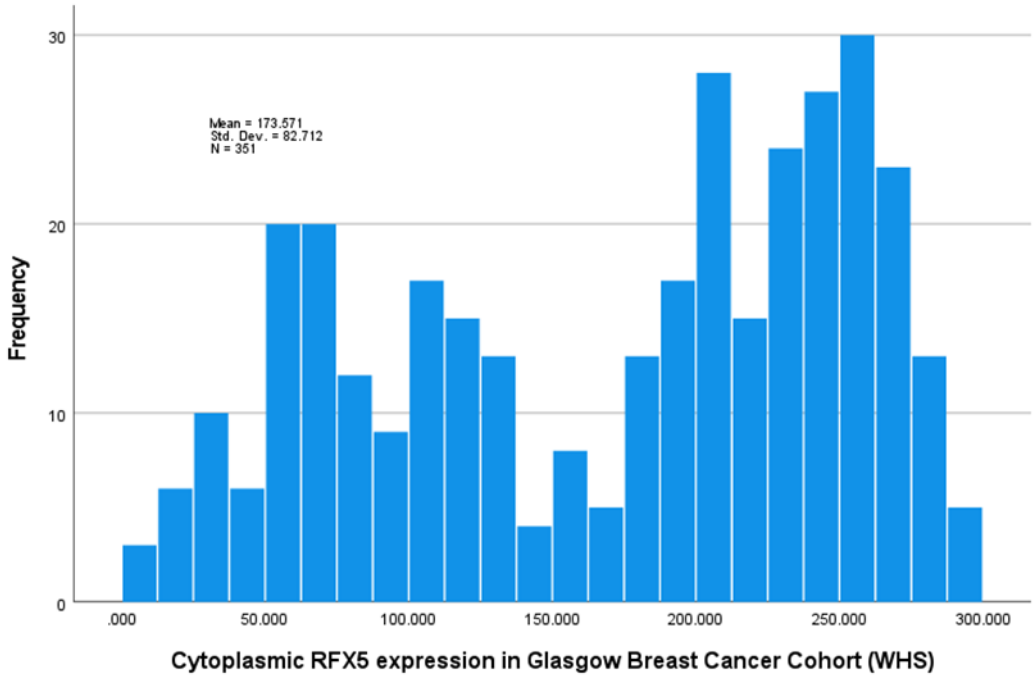

Figure 5-31 Distribution of RFX5 cytoplasmic expression in Glasgow Breast Cancer Cohort. Mean Score 173.57, SD 82.7

Counter-scores were performed manually by HVW for a minimum of 10% of cores, (n=67) and are shown below for comparison (*Figure 5-32*). WHS were reproducible between the two scorers for 67 cores. An intraclass correlation coefficient (ICCC) of 0.995 suggested a strong positive correlation between validation and primary assessor's scores.

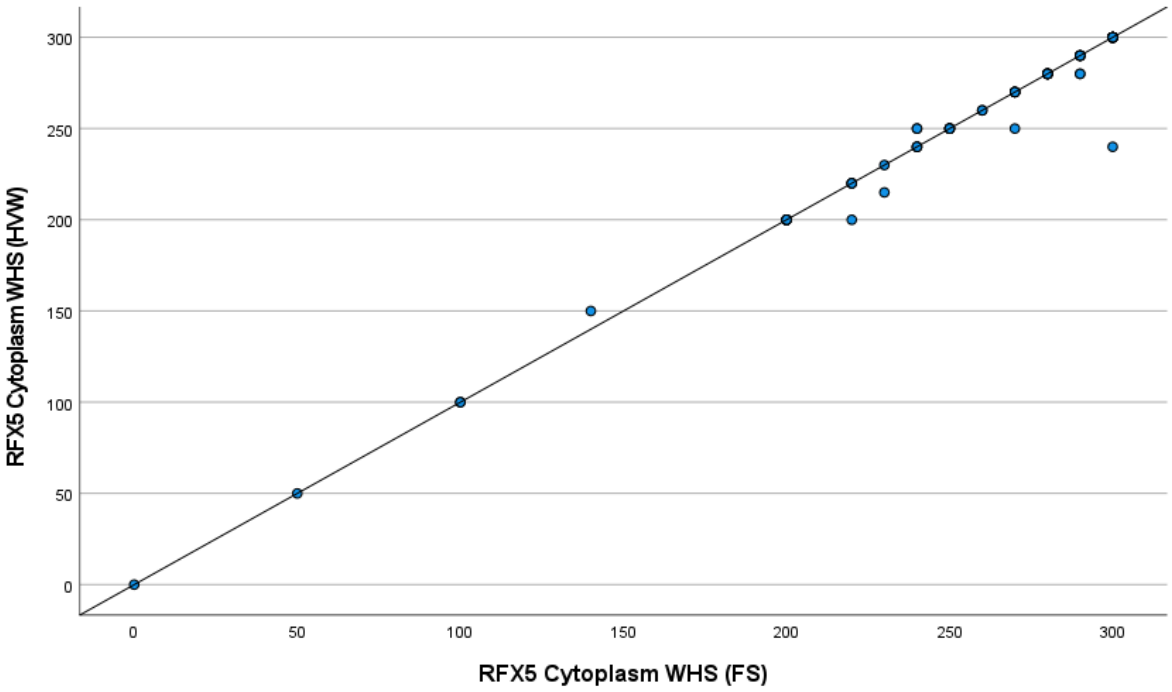

Figure 5-32 Correlation between FS and HVW manual weighted histoscore (WHS) for RFX5 cytoplasm staining. Scatter plot showing correlation between FS and HVW for cytoplasm RFX5 scores. Intraclass correlation coefficient 0.995 for 10% specimens.

A subsequent comparison of averages and differences in scores was produced as a Bland-Altman plot and suggested the scores correlated satisfactorily (*Figure 5-33*).

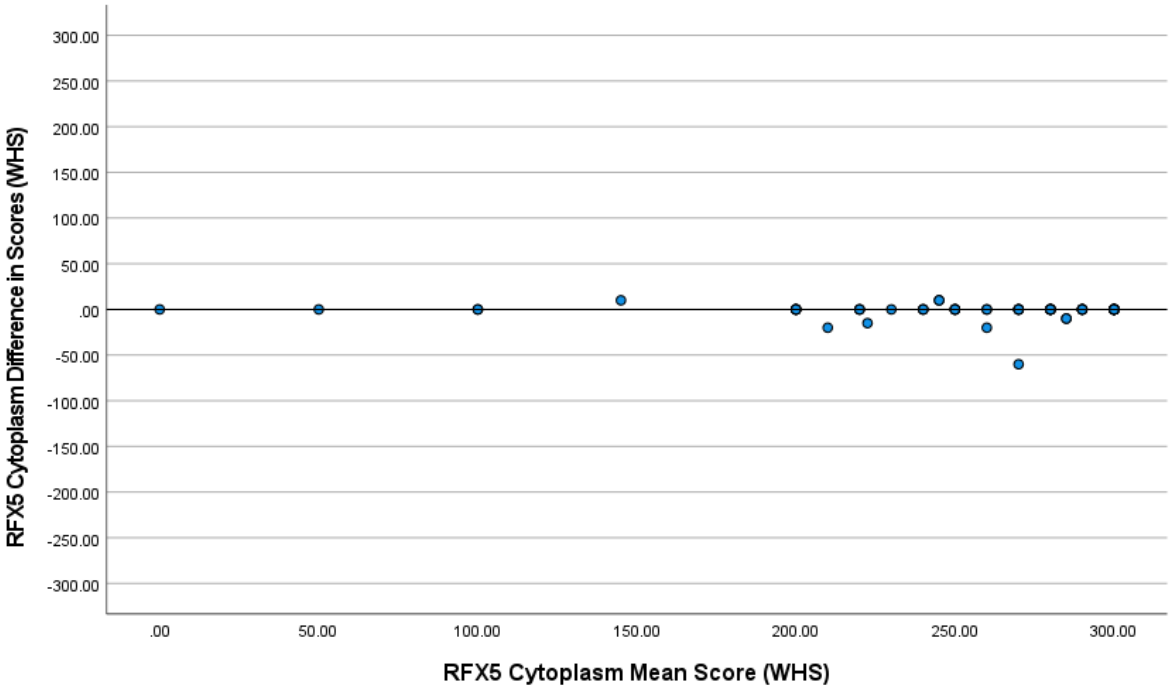

Figure 5-33 Bland-Altman Plot comparing difference in scores to mean scores for RFX5 cytoplasmic expression.

A threshold for high and low RFX5 cytoplasm expression was delineated using R Studio to compare high versus low RFX5 expression according to survival. The threshold was identified at 263.33 as described below, (*Figure 5-34*).

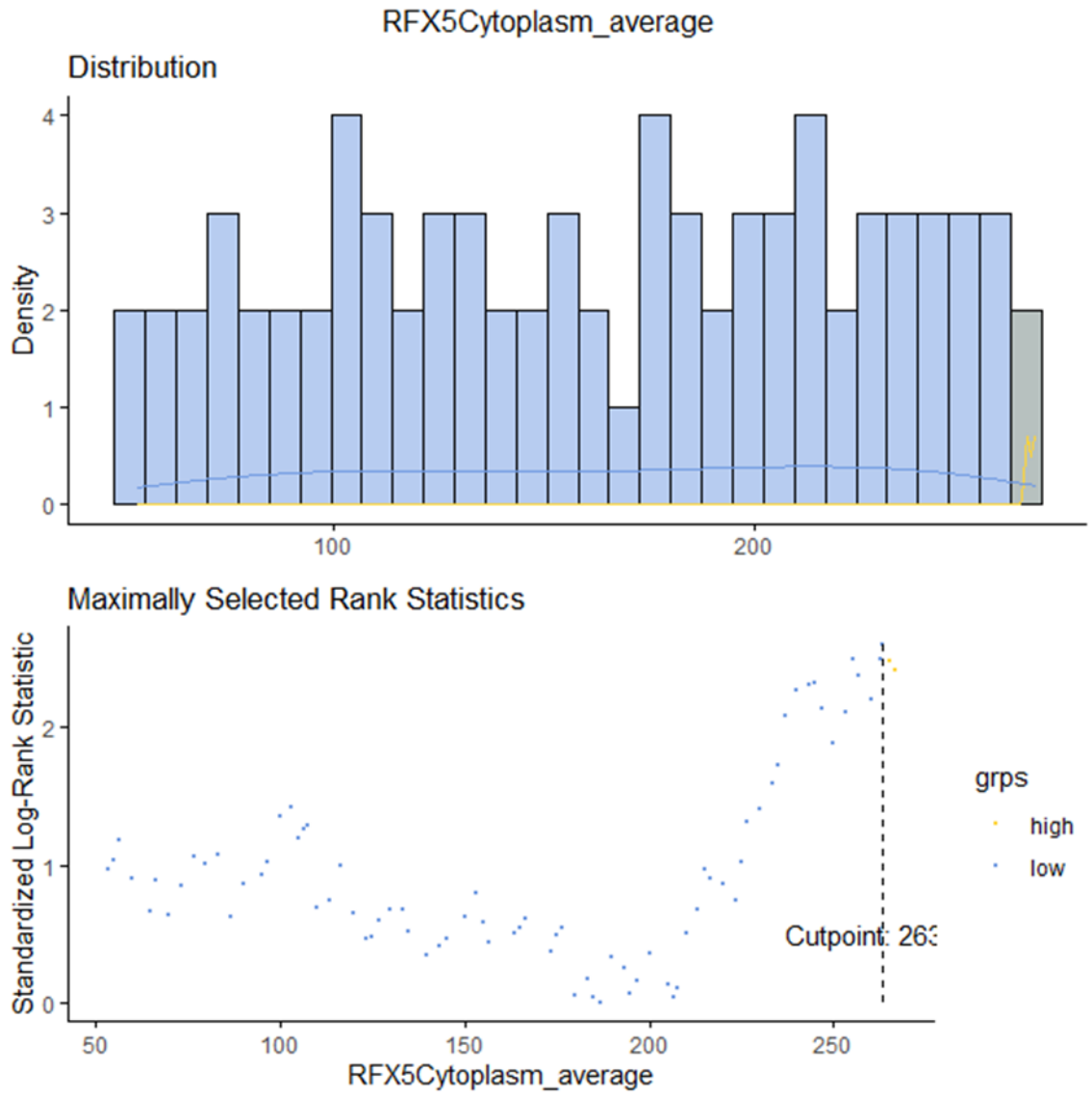

Low Expression

High Expression

Figure 5-34 RFX5 cytoplasmic expression threshold for high and low expression in the Glasgow Breast Cancer Cohort. The threshold was identified as 263.33, with patients with

weighted scores above 263.33 considered to have high RFX5 cytoplasm expression. Examples of protein expression as seen on specimens is also described below the graphical representation.

5.2.13 Cytoplasmic RFX5 and Survival in the Glasgow Breast Cancer Cohort

850 patients had TMAs produced for the Glasgow Breast Cancer Cohort, of which 736 had ductal cancer and were included in the cohort for analysis. Of these, 722 of 736 had valid cancer-specific survival data and 414 had viable cores, leading to a final 413 patients with both viable cores and valid survival data. 297 patients had low RFX5 cytoplasmic expression and had 66 events, while 47 had high expression and saw 3 events. Survival in the low RFX5 group was 85% at 5 years, and 72% at 10 years, while in the high RFX5 group survival was 96% at 5 years, and 93% at 10 years. Using Kaplan Meier survival analysis, mean cancer-specific survival (CSS) time for low RFX5 cytoplasm expression was 149.9 months compared to high RFX5 expression survival of 166.7 months, suggesting that low RFX5 cytoplasm expression was associated with increased survival, (HR 0.265, 95% C.I.; 0.083-0.843, log rank p=0.025), (*Figure 5-35*).

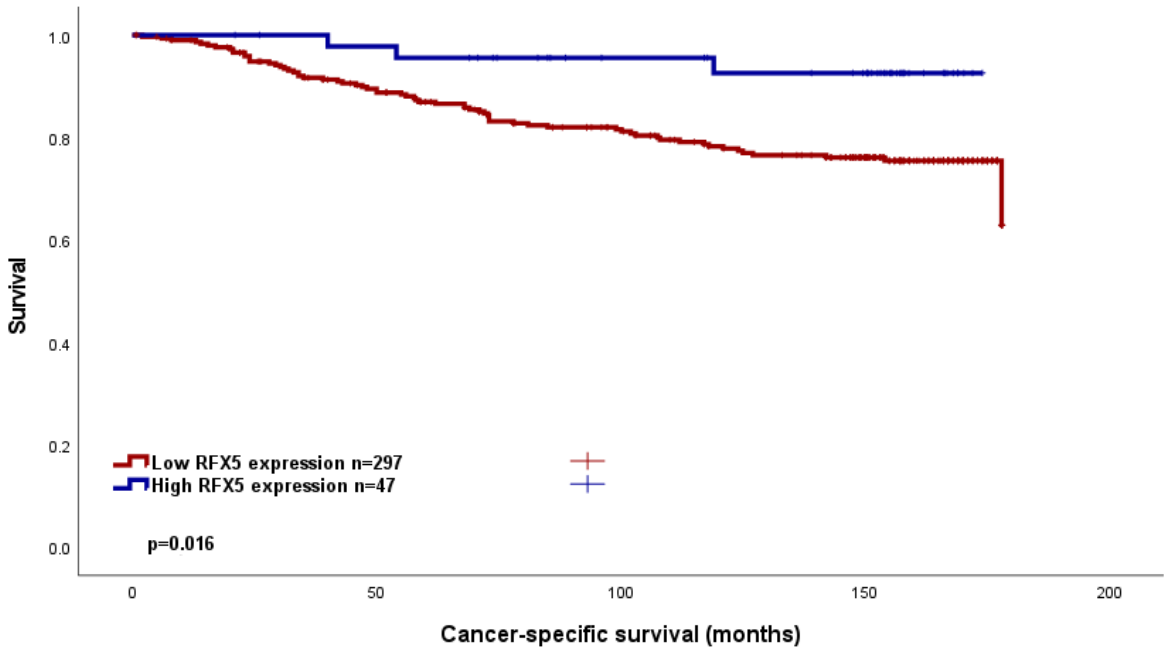

Figure 5-35 Cancer-specific survival in the Glasgow Breast Cancer Cohort according to RFX5 cytoplasm expression. Kaplan Meier Curve showing the association between RFX5 cytoplasm expression and survival (months). HR 0.265, 95% C.I.; 0.083-0.843, log rank p=0.025

To further assess the effect of clinicopathological factors on survival in the Glasgow Breast Cancer cohort, a Cox regression analysis was performed, (*Table*

5-8). On multivariate analysis, RFX5 cytoplasmic expression did not retain statistical significance, while molecular subtype, lymphatic invasion and TSP remained significant.

Table 5-8 Clinicopathological factors and their prognostic significance in the Glasgow Breast Cancer Cohort. Univariate and multivariate Cox regression analysis.

Clinicopathological Factor	Univariate analysis (HR, 95% C.I.)	p	Multivariate analysis (HR, 95% C.I.)	p
Age	0.947(0.680-1.318)	0.746		
Tumour Size		**<0.001**		
<20mm		**<0.001**		0.089
20-49mm	**2.117(1.525-2.939)**	**<0.001**	1.598(0.830-3.077)	0.161
>50mm	**4.528(2.579-7.951)**	**<0.001**	3.498(1.053-11.621)	0.041
Invasive Grade		**<0.001**		
I		**<0.001**		0.904
II	**2.332(1.226-4.436)**	**0.010**	0.791(0.249-2.515)	0.691
III	**4.043(2.162-7.563)**	**<0.001**	0.878(0.264-2.923)	0.833
Nodal Status	**3.258(2.339-4.537)**	**<0.001**	1.565(0.789-3.104)	0.200
Molecular Subtype		**<0.001**		
Luminal A				**0.010**
Luminal B		**<0.001**		
	2.343(1.525-3.599)	**<0.001**	**2.140(0.648-7.073)**	**0.212**
TNBC	**2.710(1.779-4.128)**	**<0.001**	**4.246(1.425-12.652)**	**0.009**
HER2-enriched	**2.946(1.771-4.900)**	**<0.001**	**6.433(1.830-22.618)**	**0.004**
Lymphatic Invasion	**4.255(2.813-6.435)**	**<0.001**	**2.795(1.334)**	**0.006**
Vascular Invasion	**3.440(2.163-5.470)**	**<0.001**	1.915(0.899-4.083)	0.092
Necrosis	**3.288(2.290-4.722)**	**<0.001**	1.899(0.851-4239)	0.117
Klintrup-Makinen		0.033		
0		0.030		
1	0.812(0.481-1.372)	0.437		
2	1.310(0.757-2.265)	0.334		
3	0.621(0.277-1.395)	0.249		

Ki67	**1.658(1.199-2.294)**	**0.002**	1.957(0.826-4.637)	0.127
Tumour budding	**1.755(1.282-2.403)**	**<0.001**	1.746(0.876-3.480)	0.113
Tumour stroma percentage	**1.884(1.374-2.582)**	**<0.001**	**2.178(1.136-4.176)**	**0.019**
RFX5 expression	**0.265(0.083-0.843)**	**0.025**	0.909(0.114-7.263)	0.928

Within the entire Glasgow Breast Cancer Cohort, inter-factor correlation was assessed when comparing the high and low RFX5 cytoplasmic expressors, (*Table* 5-9Table 5-9). Here, necrosis was statistically associated with RFX5 cytoplasmic expression.

Table 5-9 Clinicopathological factors and their relation to RFX5 cytoplasmic expression in the Glasgow Breast Cancer Cohort. Chi-squared analysis.

Clinicopathological factor	**RFX5 Cytoplasmic staining (%)**		**p**
	Low	**High**	
Age (years)			
≤50	82(86.3)	13(13.7)	0.523
>50	222(86.7)	34(13.3)	
Tumour Size			
≤20mm	174(85.7)	29(14.3)	0.368
21-49mm	118(68.8)	18(13.2)	
≥50mm	12(100)	0	
Grade			
I	65(85.7)	11(14.5)	0.232
II	137(84.0)	26(16.0)	
III	102(91.1)	10(8.9)	
Molecular Subtype			
Luminal A	151(85.3)	26(14.7)	0.085
Luminal B	84(86.6)	13(13.4)	
TNBC	45(97.8)	1(2.2)	
HER2 enriched	20(95.2)	1(2.2)	
Nodal Status			
N_0	168(81.6)	31(5.7)	0.350
N_1	31(93.5)	15(5.4)	
Lymphatic Invasion			
Absent	146(91.8)	9(5.7)	1.000
Present	87(93.5)	5(5.4)	
Vascular Invasion			
Absent	205(91.5)	14(6.3)	0.379
Present	28(100)	0	
Necrosis			
Absent	**160(83.3)**	**30(15.6)**	**0.045**
Present	**137(85.1)**	**12(2.5)**	
Klintrup Makinen			
0	29(76.3)	9(23.7)	0.077
1	179(90.4)	19(9.6)	

2	72(86.7)	11(13.3)	
3	16(80.0)	4(20.0)	
Ki67			
Low (<15%)	215(87.4)	31(12.6)	0.859
High (>15%)	85(86.7)	13(13.3)	
Tumour Bud			
-Low	192(86.5)	30(13.5)	0.499
-High	109(89.3)	13(10.7)	
Tissue Stroma Percentage			
Low	209(87.1)	31(12.9)	0.859
High	92(88.5)	12(11.5)	

The cohort was subsequently stratified according to Oestrogen receptor status (ER-negative; ER-, and ER-positive; ER+). In the ER- group (71 patients), 68 patients had low cytoplasm RFX5 and 21 events, and 3 had high RFX5, for 1 event. Within the ER- cases, 5-year survival was 76% in low RFX5 cases, compared to 67% in high RFX5 cases. 10-year survival was 66% in the low RFX5 group compared to 67% in the high RFX5 group at 70 months. Mean survival for ER- patients was 135.7 months for low cytoplasm RFX5 expression, and 68.66 months for high RFX5, suggesting that in the ER- patients, low RFX5 expression was associated was not associated with a significant difference in survival (HR 1.254 95% C.I. 0.167-9.416, log rank p=0.825), (*Figure 5-36*).

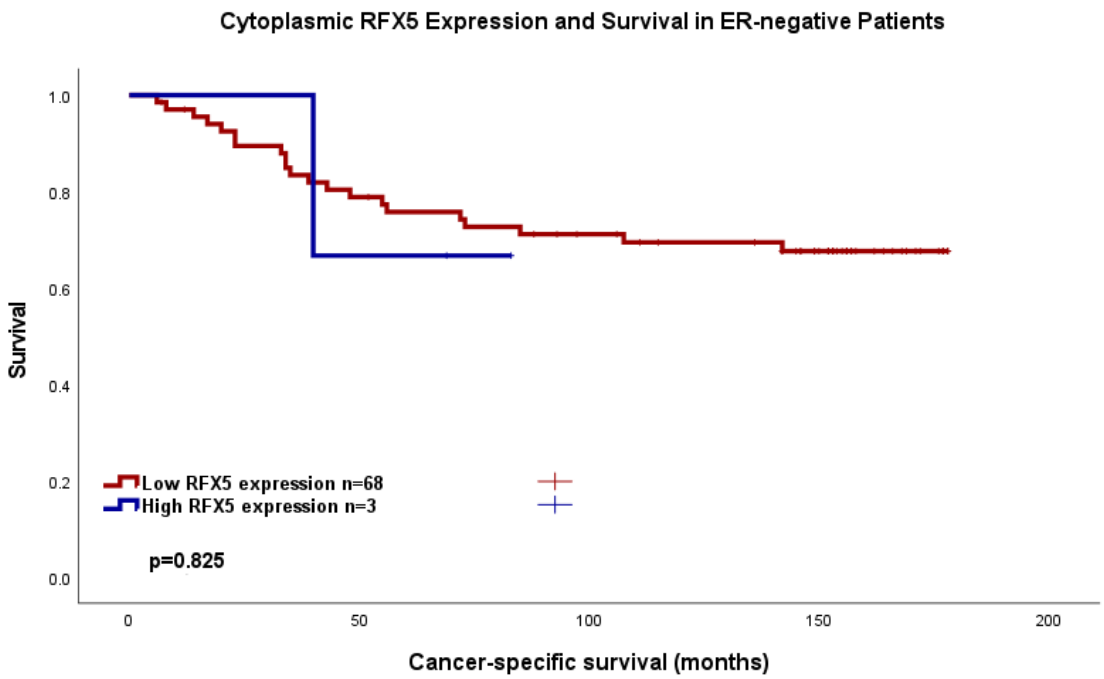

Figure 5-36 Cancer-specific survival in ER negative patients in the Glasgow Breast Cancer Cohort according to RFX5 cytoplasm expression. Kaplan Meier Curve showing the association between RFX5 cytoplasm expression and survival (months). HR 1.254 95% C.I. 0.167-9.416, log rank p=0.826.

Within the ER-negative group, inter-factor correlation was assessed when comparing the high and low RFX5 cytoplasmic expressors (Table 5-10*)*. Here, age was statistically significant in relation to RFX5 cytoplasmic expression.

Table 5-10 Clinicopathological factors and their prognostic significance within ER-negative patients in the Glasgow Breast Cancer Cohort. Chi-squared analysis.

Clinicopathological factor	**RFX5 Cytoplasmic staining (%)**		**p**
	Low	**High**	
Age (years)			
≤50	**23(88.5)**	**3(11.5)**	**0.045**
>50	**45(100)**	**0**	
Tumour Size			
≤20mm	35(97.2)	1(2.8)	0.725
21-49mm	30(93.8)	2(6.3)	
≥50mm	3(100)	0	
Grade			
I	4(100)	0	0.893
II	18(94.7)	1(5.3)	
III	46(95.8)	2(4.2)	
Nodal Status			
N_0	36(97.3)	1(2.7)	0.604
N_1	32(94.1)	2(5.9)	
Lymphatic Invasion			
Absent	37(97.4)	1(2.6)	0.574
Present	27(93.1)	2(6.9)	
Vascular Invasion			
Absent	56(94.9)	3(5.1)	1.000
Present	8(100)	0	
Necrosis			
Absent	18(100)	0	0.564
Present	49(94.2)	3(5.8)	
Klintrup Makinen			
0	1(100)	0	0.279
1	31(100)	0	
2	28(90.3)	3(9.7)	
3	6(100)	0	
Ki67			
Low (<15%)	54(94.7)	3(5.3)	1.000
High (>15%)	13(100)	0	
Tumour Bud			
-Low	46(93.9)	3(6.1)	0.549
-High	21(100)	0	
Tissue Stroma Percentage			
Low	51(98.1)	1(1.9)	0.160
High	16(88.9)	2(11.1)	

In the ER+ group (273 patients), 229 patients had low cytoplasmic RFX5 with 45 events, while 44 had high cytoplasmic RFX5 and 2 events. In ER+ patients, 5-year

survival was 88% in low RFX5 cases, and 98% in high RFX5 cases, and at 10-years this reduced to 74% in low RFX5, and 95% in high RFX5 expressors. In ER+ patients, survival in low cytoplasmic RFX5 was 154.2 months and 169.5 months for high RFX5 expressing patients, suggesting a survival benefit in high RFX5 expressors (HR 0.211, 95% C.I. 0.051-0.872, log rank p=0.032),(*Figure 5-37*).

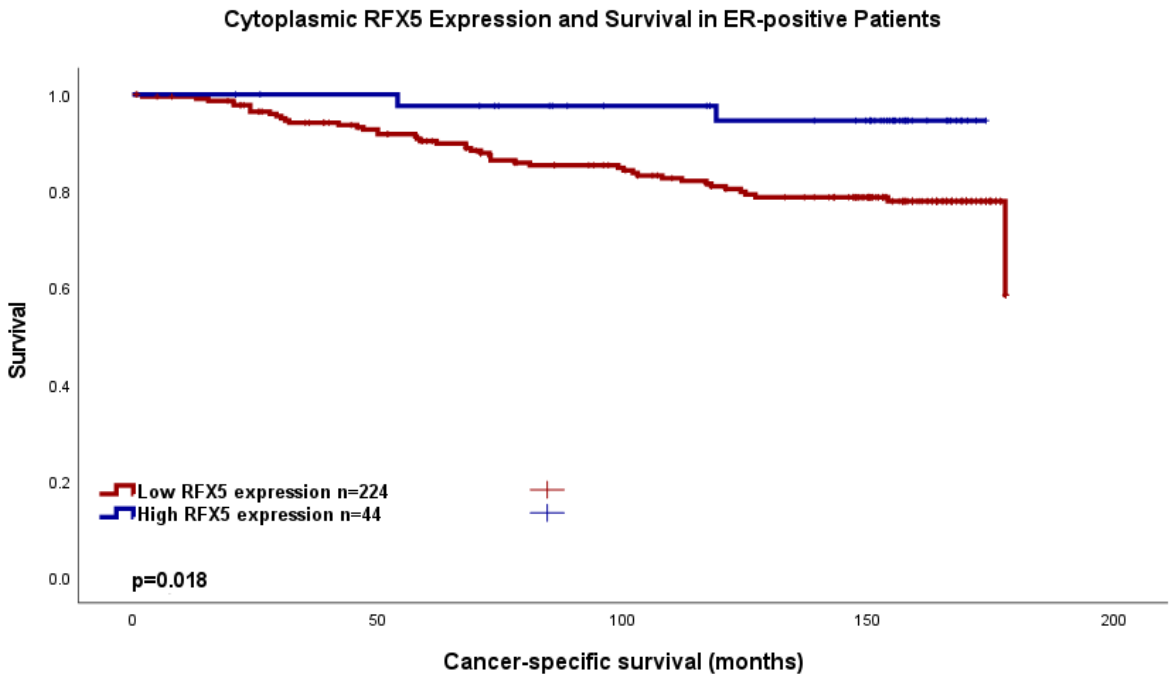

Figure 5-37 Cancer-specific survival in ER positive patients in the Glasgow Breast Cancer Cohort according to RFX5 cytoplasm expression. Kaplan Meier Curve showing the association between RFX5 cytoplasm expression and survival (months). HR 0.211, 95% C.I. 0.051-0.872, log rank p=0.032

To further assess the effect of clinicopathological factors on survival in the ER+ patients within the Glasgow Breast Cancer cohort, a Cox regression analysis was performed, (Table 5-11Table 5-8). On multivariate analysis, RFX5 cytoplasmic expression did not retain statistical significance, while Ki67 and TSP remained significant.

Table 5-11 Clinicopathological factors and their prognostic significance in the Glasgow Breast Cancer Cohort. Univariate and multivariate Cox regression analysis.

Clinicopathological Factor	Univariate analysis (HR, 95% C.I.)	p	Multivariate analysis (HR, 95% C.I.)	p
Age	0.951(0.590-1.534)	0.838		
Tumour Size		**<0.001**		

<20mm		**<0.001**		0.202
20-49mm	**2.283(1.465-3.558)**	**<0.001**	2.029(0.845-4.871)	0.113
>50mm	**4.371(1.939-9.854)**	**<0.001**	2.736(0.534-14.025)	0.228
Invasive Grade		**<0.001**		
I		**<0.001**		0.973
II	**1.762(0.907-3.423)**	**0.094**	0.903(0.276-2.951)	0.866
III	**3.383(1.709-6.697)**	**<0.001**	0.993(0.276-3.573)	0.992
Nodal Status	**3.427(2.179-5.390)**	**<0.001**	1.453(0.600-3.516)	0.408
Lymphatic Invasion	**3.331(1.872-5.926)**	**<0.001**	2.202(0.899-5.396)	0.084
Vascular Invasion	**2.599(1.292-5.228)**	**0.007**	1.106(0.392-3.126)	0.849
Necrosis	**2.720(1.754-4.216)**	**<0.001**	2.190(0.847-5.665)	0.106
Klintrup-Makinen		0.063		
0		0.066		
1	0.579(0.332-1.010)	0.054		
2	0.960(0495-1.863)	0.903		
3	0.336(0.098-1.148)	0.082		
Ki67	**2.151(1.395-3.315)**	**<0.001**	3.869(1.593-9.396)	**0.003**
Tumour budding	1.468(0.957-2.252)	0.079		
Tumour stroma percentage	**1.812(1.174-2.796)**	**0.007**	2.296(1.000-5.270)	**0.050**
RFX5 expression	**0.211(0.051-0.872)**	**0.032**	0(0)	0.978

Within the ER-positive group, inter-factor correlation was assessed when comparing the high and low RFX5 cytoplasmic expressors (*Table 5-12*). Here, no associations were seen with RFX5 cytoplasmic expression.

Table 5-12 Clinicopathological factors and their prognostic significance within ER-positive patients in the Glasgow Breast Cancer Cohort, Chi-squared analysis.

Clinicopathological factor	**RFX5 Cytoplasmic staining (%)**		**p**
	Low	**High**	
Age (years)			
≤50	59(85.5)	10(14.5)	0.850
>50	177(83.9)	34(16.1)	
Tumour Size			

≤20mm	139(83.2)	28(16.8)	0.401
21-49mm	88(84.6)	16(15.4)	
≥50mm	9(100)	0	
Grade			
I	61(84.7)	11(15.3)	0.669
II	119(82.6)	25(17.4)	
III	56(87.5)	8(12.5)	
Nodal Status			
N_0	132(81.5)	30(18.5)	0.302
N_1	99(88.4)	13(11.6)	
Lymphatic Invasion			
Absent	109(93.2)	8(6.8)	0.749
Present	60(95.2)	3(4.8)	
Vascular Invasion			
Absent	149(93.1)	11(6.9)	0.614
Present	20(100)	0	
Necrosis			
Absent	142(82.6)	30(17.4)	0.074
Present	88(90.7)	9(9.3)	
Klintrup Makinen			
0	28(75.7)	9(24.3)	0.097
1	148(88.6)	19(11.4)	
2	44(84.6)	8(15.4)	
3	10(71.4)	4(28.6)	
Ki67			
Low (<15%)	161(85.2)	28(14.8)	1.000
High (>15%)	72(84.7)	13(15.3)	
Tumour Bud			
-Low	146(84.4)	27(15.6)	0.598
-High	88(87.1)	13(12.9)	
Tissue Stroma Percentage			
Low	158(84.0)	30(16.0)	0.461
High	76(88.4)	10(11.6)	

Further stratification according to molecular subtype was then performed. These subtypes were divided into Luminal A, Luminal B, Triple-negative (most similar to “Basal-like” subtype) and HER-2 enriched groups. For 10 patients, molecular subgroup was not available. For the remaining patients, there were 171 Luminal A, 96 Luminal B, 46 TNBC and 21 HER-2 enriched cases. Luminal A patients had 145 low cytoplasmic RFX5 expressors with 21 events, and 26 high-RFX5 expressors with 1 event. Luminal B patients had 83 low RFX5 expressors with 23 events, and 13 high RFX5 expressors with 1 event. The TNBC patients had 45 low RFX5 expressors with 13 events, and 1 patient with high RFX5 with 0 events. Finally, HER-2 enriched patients consisted of 20 low RFX5 cases with 8 events, and 1 high RFX5 cases with 1 event. Kaplan Meier curves are shown for each subgroup in Figures 16-19.

Luminal A patients had a 5-year survival of 89% and 82% at 10 years for low RFX5 expressors, compared to 100% at 5 years and 95% at 10 years for high RFX5 expressors. Mean survival was 160 months for low RFX5, and 171.3 months for high RFX5 expressors (HR 0.0248, 95% C.I. 0.033-1.849, log rank p=0.174), (*Figure 5-38*).

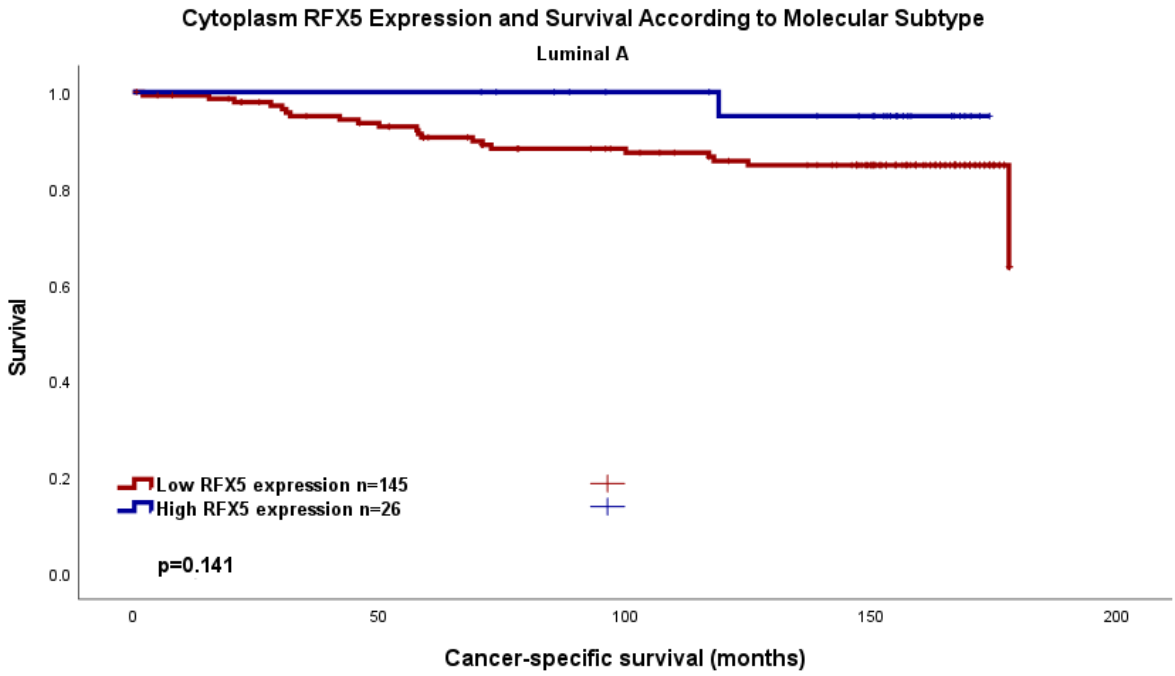

Figure 5-38 Cancer-specific survival in the Luminal A patients in the Glasgow Breast Cancer Cohort according to RFX5 cytoplasm expression. Kaplan Meier Curve showing the association between RFX5 cytoplasm expression and survival (months). HR 0.0248, 95% C.I. 0.033-1.849, log rank p=0.174.

Within the Luminal A group, inter-factor correlation was assessed when comparing the high and low RFX5 cytoplasmic expressors, (Table 5-13*)*. Here, no association with RFX5 cytoplasmic expression was seen.

Table 5-13 Clinicopathological factors and their relation to RFX5 cytoplasmic expression in Luminal A patients in the Glasgow Breast Cancer Cohort. Chi-squared analysis

Clinicopathological factor	RFX5 Cytoplasmic staining (%)		p
	Low	High	
Age (years)			
≤50	44(91.7)	4(8.3)	0.231
>50	107(82.9)	22(17.1)	
Tumour Size			
≤20mm	97(87.4)	14(12.6)	0.342
21-49mm	50(80.6)	12(19.4)	
≥50mm	4(100)	0	
Grade			

I	49(84.5)	9(15.5)	0.914
II	80(85.1)	14(14.9)	
III	22(88)	3(12.0)	
Nodal Status			
N_0	88(83.0)	18(17.0)	0.518
N_1	61(88.4)	8(11.6)	
Lymphatic Invasion			
Absent	81(95.3)	4(4.7)	1.000
Present	32(100)	1	
Vascular Invasion			
Absent	101(95.3)	5(4.7)	1.000
Present	12(100)	0	
Necrosis			
Absent	98(83.8)	19(16.2)	0.153
Present	48(92.3)	4(7.7)	
Klintrup Makinen			
0	18(75)	6(25)	0.157
1	99(90.0)	11(10.0)	
2	23(85.2)	4(14.8)	
3	5(71.4)	2(28.6)	
Ki67			
Low (<15%)	151(85.3)	26(14.7)	n/a
High (>15%)	0	0	
Tumour Bud			
-Low	93(87.7)	13(12.3)	0.648
-High	56(84.8)	10(15.2)	
Tissue Stroma Percentage			
Low	100(85.5)	17(14.5)	0.634
High	49(89.1)	6(10.9)	

Luminal B patients had a 5-year survival rate of 87% reducing to 62% at 10 years for low RFX5 expressors, versus 92% 5-year survival and 92% 10-year survival in high RFX5 expressors. Mean survival was 145 months for low RFX5, and 156.7 months for high RFX5 expressors (HR 0.248, 95% C.I. 0.033-1.849, log rank p= 0.174), (*Figure 5-39*).

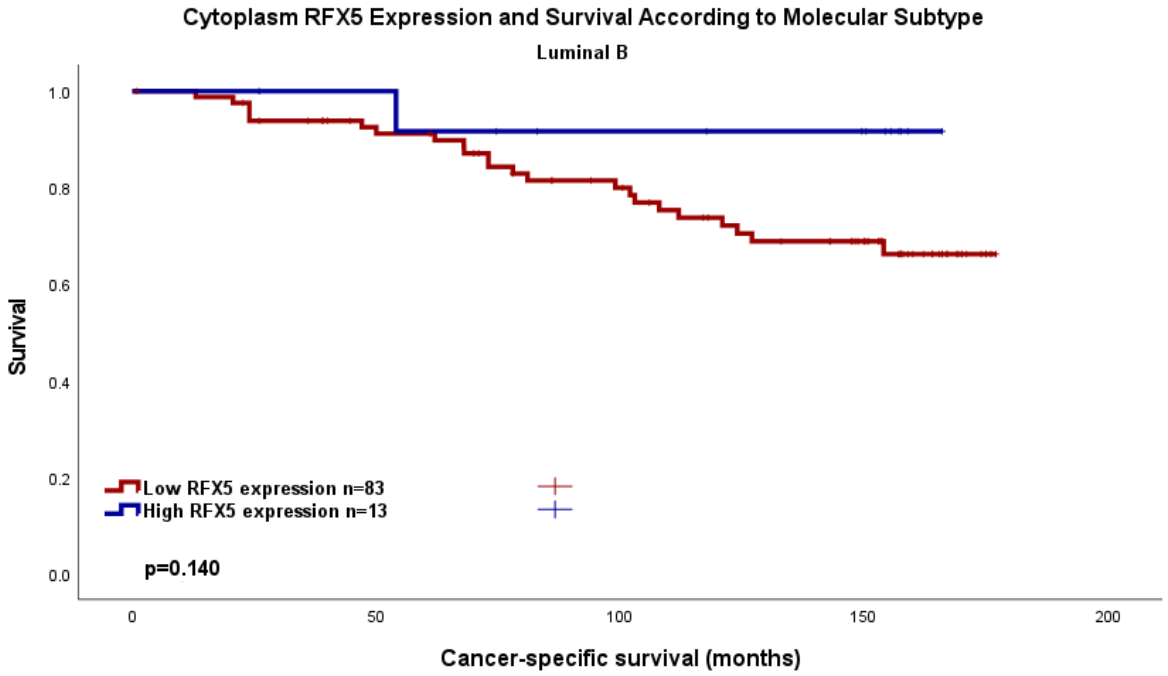

Figure 5-39 Cancer-specific survival in the Luminal B patients in the Glasgow Breast Cancer Cohort according to RFX5 cytoplasm expression. Kaplan Meier Curve showing the association between RFX5 cytoplasm expression and survival (months) HR 0.248, 95% C.I. 0.033-1.849, log rank p= 0.174.

Within the luminal B group, inter-factor correlation was assessed when comparing the high and low RFX5 cytoplasmic expressors, (Table 5-14). Here, no association with RFX5 cytoplasmic expression was seen.

Table 5-14 Clinicopathological factors and their relation to RFX5 Cytoplasmic expression in Luminal B patients in the Glasgow Breast Cancer Cohort. Chi-squared analysis.

Clinicopathological factor	RFX5 Cytoplasmic staining (%)		p
	Low	High	
Age (years)			
≤50	17(77.3)	5(22.7)	0.163
>50	67(89.3)	8(10.7)	
Tumour Size			
≤20mm	41(80.4)	10(19.6)	0.152
21-49mm	38(92.7)	3(7.3)	
≥50mm	5(100)	0	
Grade			
I	12(85.7)	2(14.3)	0.795
II	38(84.4)	7(15.6)	
III	34(89.5)	4(10.5)	
Nodal Status			
N_0	44(84.6)	8(15.4)	0.417
N_1	38(90.5)	4(9.5)	
Lymphatic Invasion			

Absent	30(93.8)	2(5.7)	1.000
Present	28(96.6)	1(3.4)	
Vascular Invasion			
Absent	50(94.3)	3(5.7)	1.000
Present	8(100)	0	
Necrosis			
Absent	43(84.3)	8(15.7)	0.373
Present	40(90.9)	4(9.1)	
Klintrup Makinen			
0	9(75)	3(25)	0.213
1	49(92.5)	4(7.5)	
2	21(84.0)	4(16.0)	
3	5(71.4)	2(28.6)	
Ki67			
Low (<15%)	12(92.3)	1(7.7)	1.000
High (>15%)	72(85.7)	12(14.3)	
Tumour Bud			
-Low	51(82.3)	11(17.7)	0.126
-High	33(94.3)	2(5.7)	
Tissue Stroma Percentage			
Low	56(83.6)	11(16.4)	0.333
High	28(93.3)	2(6.7)	

TNBC patients had 5-year survival of 80%- and 10-year survival of 67% in low RFX5 expressors compared to 100% 5-year survival (End of follow up). Mean survival could not be estimated due to lack of follow up (HR 0.048, 95% C.I. 0.00-7460011.628, log rank p= 0.752), (*Figure 5-40*).

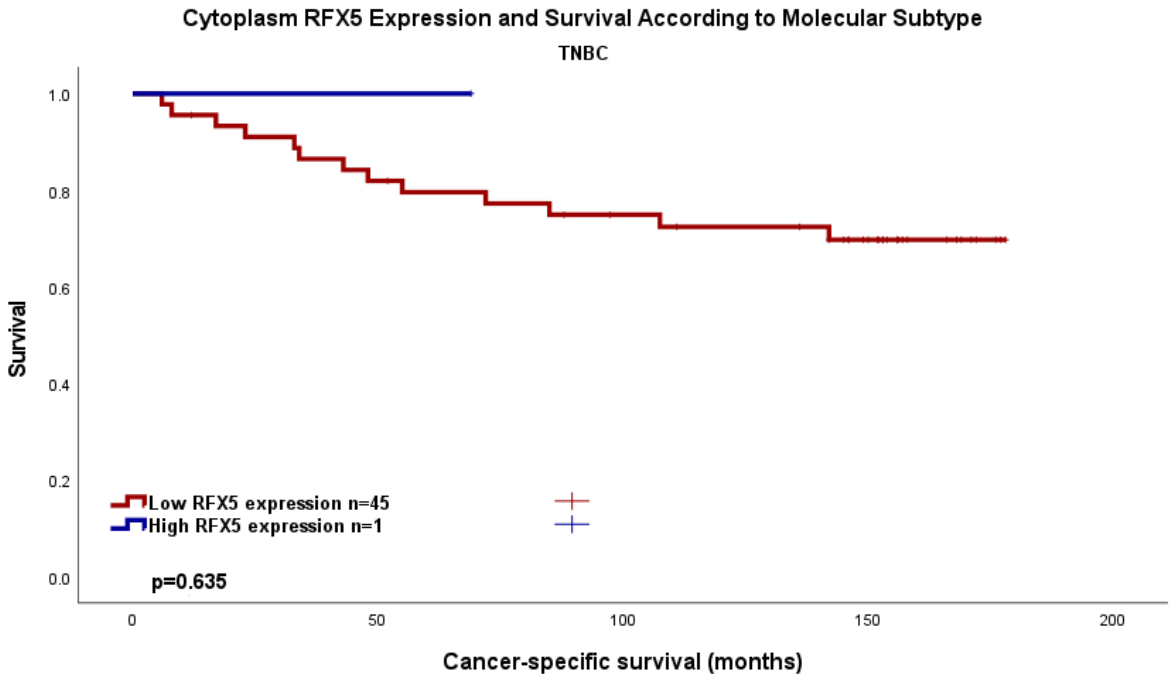

Figure 5-40 Cancer-specific survival in the TNBC patients in the Glasgow Breast Cancer Cohort according to RFX5 cytoplasm expression. Kaplan Meier Curve showing the association

between RFX5 cytoplasm expression and survival (months) HR 0.048, 95% C.I. 0.00-7460011.628, log rank p= 0.725.

Within the TNBC group, inter-factor correlation was assessed when comparing the high and low RFX5 cytoplasmic expressors, (Table 5-15). Here, no association with RFX5 cytoplasmic expression was seen.

Table 5-15 Clinicopathological factors and their relation to RFX5 Cytoplasmic expression in TNBC patients in the Glasgow Breast Cancer Cohort. Chi-squared analysis.

Clinicopathological factor	**RFX5 Cytoplasmic staining (%)**		**p**
	Low	**High**	
Age (years)			
≤50	14(93.3)	1(6.7)	0.326
>50	31(100)	0	
Tumour Size			
≤20mm	25(96.2)	1(3.8)	0.675
21-49mm	19(100)	0	
≥50mm	1(100)	0	
Grade			
I	3(100)	0	0.273
II	12(92.3)	1(7.7)	
III	30(100)	0	
Nodal Status			
N_0	26(96.3)	1(3.7)	1.000
N_1	19(100)	0	
Lymphatic Invasion			
Absent	24(100)	0	0.442
Present	18(94.7)	1(5.3)	
Vascular Invasion			
Absent	35(97.2)	1(2.8)	1.000
Present	7(100)	0	
Necrosis			
Absent	12(100)	0	1.000
Present	32(97.0)	1(3.0)	
Klintrup Makinen			
0	1(100)	0	
1	23(100)	0	0.603
2	15(93.8)	1(6.3)	
3	5(100)	0	
Ki67			
Low (<15%)	38(97.4)	1(2.6)	1.000
High (>15%)	6(100)	0	
Tumour Bud			
-Low	32(97.0)	1(3.0)	1.000
-High	12(100)	0	
Tissue Stroma Percentage			
Low	34(100)	0	0.244
High	10(90.9)	1(9.1)	

HER-2 enriched patients had 5-year survival rates of 63% and 10-year survival of 58% in low RFX5 expressors, compared to 0% at 36 months in high-RFX5 expressors. Mean survival was 118.5 months or low RFX5, and 40 months for high RFX5 expressors (HR 2.631, 95% C.I. 0.316-21.896, log rank p=0.371), (*Figure 5-41*).

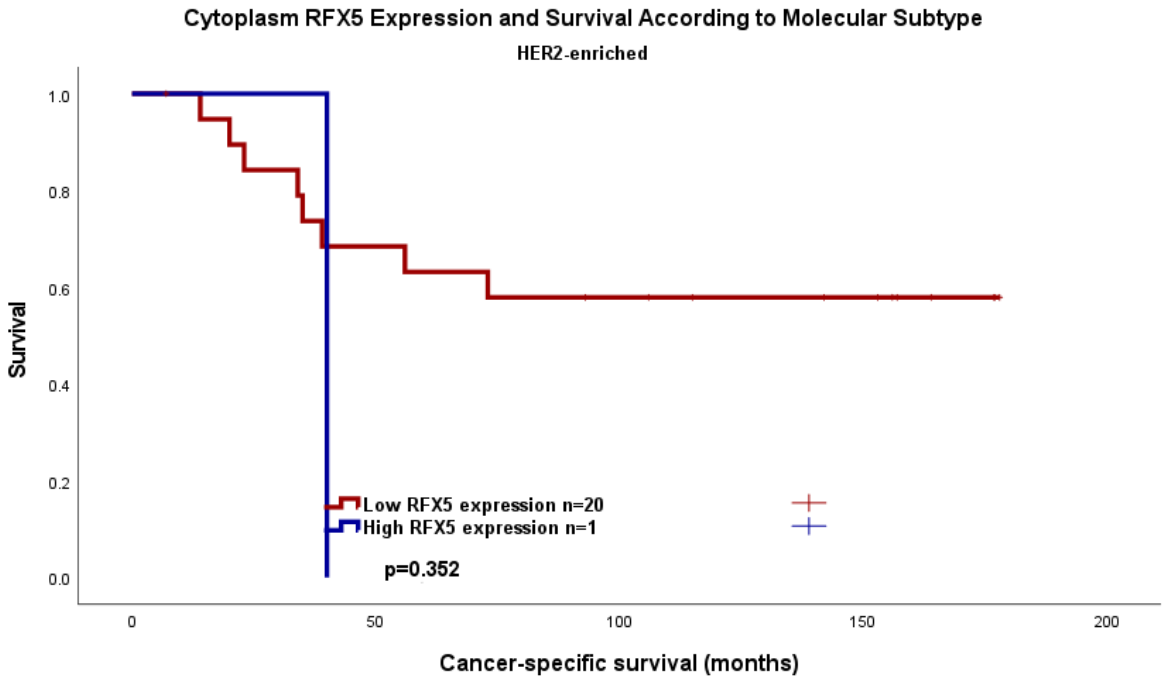

Figure 5-41 Cancer-specific survival in the HER2=enriched patients in the Glasgow Breast Cancer Cohort according to RFX5 cytoplasm expression. Kaplan Meier Curve showing the association between RFX5 cytoplasm expression and survival (months) HR 2.631, 95% C.I. 0.316-21.896, log rank p=0.371

Within the HER2-enriched group, inter-factor correlation was assessed when comparing the high and low RFX5 cytoplasmic expressors, (Table 5-16). Here, no association was seen with RFX5 cytoplasmic expression.

Table 5-16 Clinicopathological factors and their relation to RFX5 Cytoplasmic expression in HER2-enriched patients in the Glasgow Breast Cancer Cohort. Chi-squared analysis.

Clinicopathological factor	RFX5 Cytoplasmic staining (%)		p
	Low	High	
Age (years)			
≤50	6(85.7)	1(14.3)	0.333
>50	14(100)	0	
Tumour Size			
≤20mm	7(100)	0	0.675
21-49mm	11(91.7)	1(8.3)	
≥50mm	2(100)	0	
Grade			

I	0	0	1.000
II	5(100)	0	
III	15(93.8)	1(6.3)	
Nodal Status			
N_0	7(100)	0	1.000
N_1	13(92.9)	1(7.1)	
Lymphatic Invasion			
Absent	10(100)	0	1.000
Present	9(90.0)	1(10.0)	
Vascular Invasion			
Absent	18(94.7)	1(5.3)	1.000
Present	1(100)	0	
Necrosis			
Absent	4(100)	0	1.000
Present	16(64.1)	1(5.9)	
Klintrup Makinen			
0	0	0	0.753
1	6(100)	0	
2	12(92.3)	1(7.7)	
3	1(100)	0	
Ki67			
Low (<15%)	13(92.9)	1(7.1)	1.000
High (>15%)	7(100)	0	
Tumour Bud			
-Low	12(92.3)	1(7.7)	1.00
-High	8(100)	0	
Tissue Stroma Percentage			
Low	15(100)	0	0.286
High	5(83.3)	1(16.7)	

5.2.14 RFX5 Nuclear Expression in the Glasgow Breast Cancer Cohort

Manual weighted histoscores of nuclear expression of RFX5 were performed by FS. Scores varied from 0 to 150, (*Figure 5-42*).

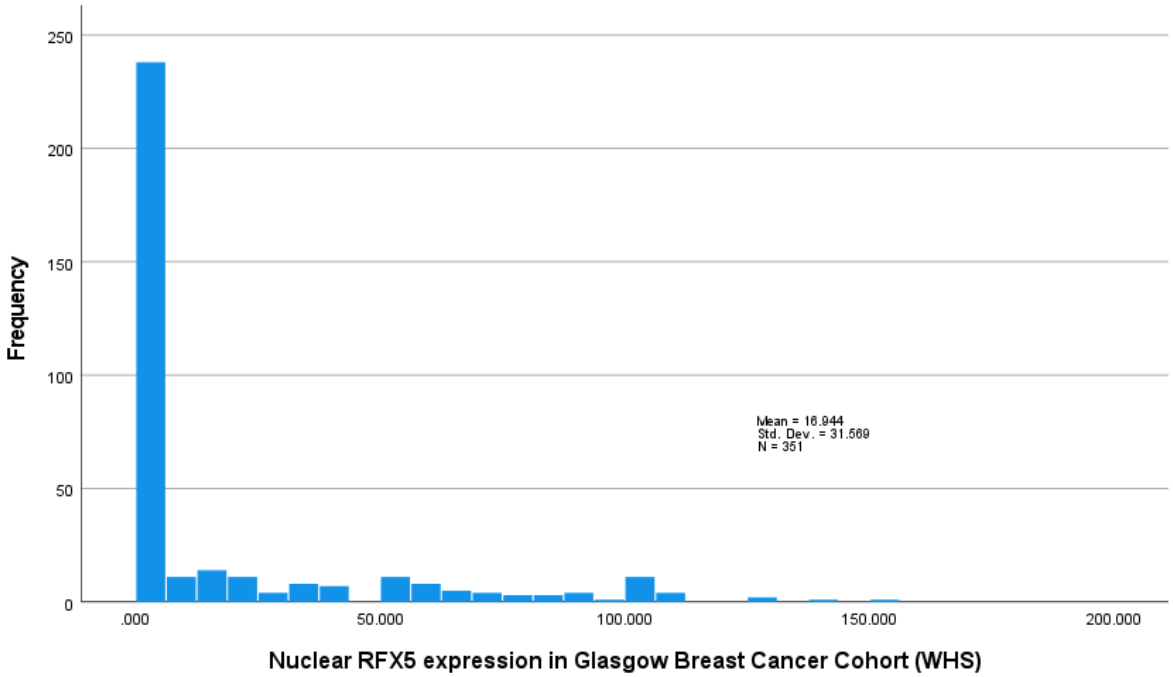

Figure 5-42 Distribution of RFX5 nuclear expression (weighted histoscores) in the Glasgow Breast Cancer Cohort. Mean score 16.94, SD 31.56.

Counter scores were performed by HVW for a minimum of 10% cores (n=67) and similarly to what was seen in FS scores, the selected sample WHS was always 0. No ICC was therefore calculated. The two scorers re-assessed a separate portion of samples informally and agreed that scores were consistent within a separate sample.

A threshold for high and low RFX5 nuclear expression was delineated using R Studio to compare high versus low RFX5 nuclear expression according to survival. The threshold was identified as 60, (*Figure 5-43*)

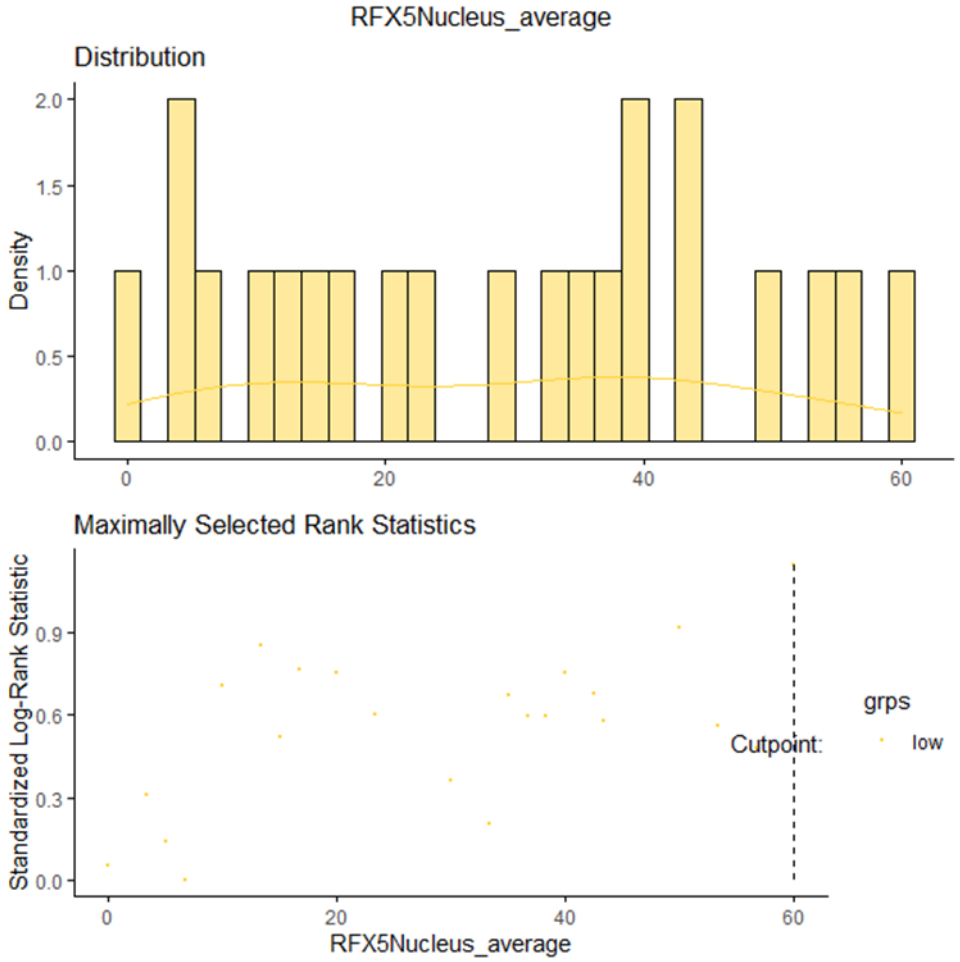

Low Expression

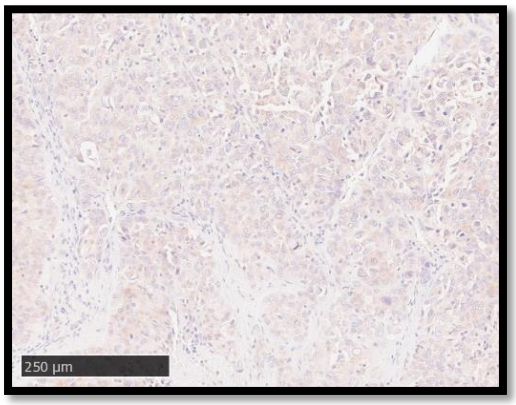

High Expression

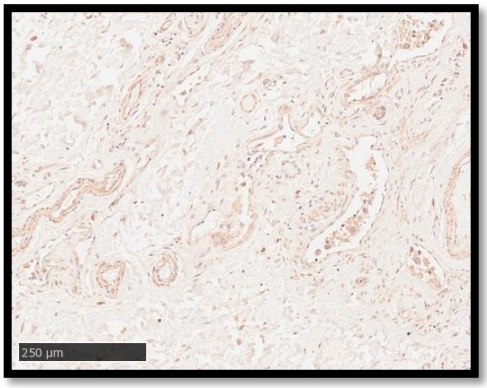

Figure 5-43 RFX5 Nuclear expression - threshold for high and low expression of RFX5 in the Glasgow Breast Cancer Cohort The threshold was identified as 60, with patients with weighted scores above 60 considered to have high RFX5 nuclear expression. Examples of protein expression as seen on specimens is also described below the graphical representation.

5.2.15 Nuclear RFX5 and Survival in the Glasgow Breast Cancer Cohort

Within the Glasgow Breast Cancer Cohort, 351 had valid cores and 344 had both WHS and cancer-specific survival data available. 299 patients had low RFX5 nuclear expression and had 61 events, while 45 had high expression and 8

events. Survival in the low RFX5 group was 87% at 5 years, and 74% at 10 years, while in the high RFX5 group survival was 86% at 5 years, and 81% at 10 years. Using Kaplan Meier survival analysis, mean cancer-specific survival (CSS) time for low RFX5 nuclear expression was 152.3 months compared to high RFX5 expression survival of 155.2 months, (HR 838, 95% C.I.; 0.401-1.752, log rank p=0.639), (*Figure 5-44*).

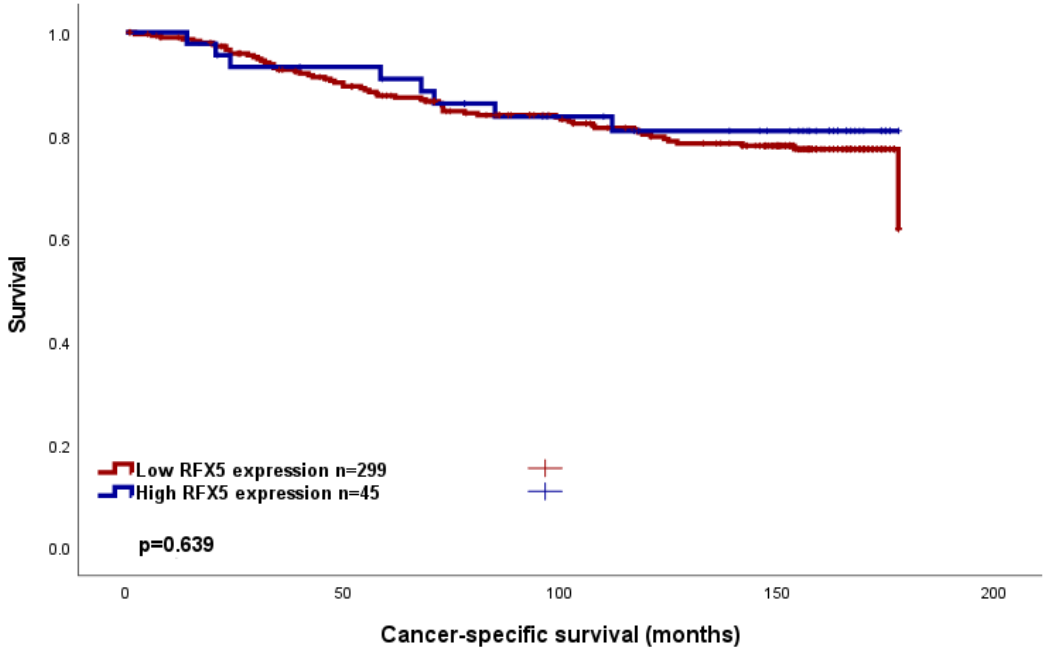

Figure 5-44 Cancer-specific survival in the Glasgow Breast Cancer Cohort according to RFX5 nuclear expression. Kaplan Meier Curve showing the association between RFX5 nuclear expression and survival (months). HR 838, 95% C.I.; 0.401-1.752, log rank p=0.639.

Within the entire Glasgow Breast Cancer Cohort, inter-factor correlation was assessed when comparing the high and low RFX5 nuclear expressors, (*Table* 5-17). Here, Ki67 was associated with RFX5 nuclear expression.

Table 5-17 Clinicopathological factors and their relation to RFX5 nuclear expression in the Glasgow Breast Cancer Cohort. Chi-squared analysis.

Clinicopathological factor	RFX5 nuclear staining (%)		p
	Low	High	
Age (years)			
≤50	81(85.3)	14(14.7)	0.595
>50	224(87.5)	32(12.5)	
Tumour Size			
≤20mm	174(85.7)	29(14.3)	0.639
21-49mm	121(89)	15(11)	
≥50mm	10(83.3)	2(16.7)	

Grade			
I	67(88.2)	9(11.8)	0.866
II	140(85.9)	23(14.1)	
III	98(87.5)	14(12.5)	
Nodal Status			
N_0	174(87.4)	25(12.6)	0.558
N_1	125(85.6)	21(14.4)	
Molecular Subtype			
Luminal A	157(88.7)	20(11.3)	0.485
Luminal B	81(83.5)	16(16.5)	
TNBC	42(91.3)	4(8.7)	
HER2-enriched	19(90.5)	2(9.5)	
Lymphatic Invasion			
Absent	129(88.7)	26(16.8)	1.000
Present	76(82.6)	16(17.4)	
Vascular Invasion			
Absent	180(82.2)	39(17.8)	0.434
Present	25(89.3)	3(10.7)	
Necrosis			
Absent	161(84.7)	29(15.3)	0.260
Present	133(89.3)	16(10.7)	
Klintrup Makinen			
0	32(84.2)	6(15.8)	0.398
1	168(84.8)	30(15.2)	
2	75(90.4)	8(9.6)	
3	19(95)	1(5)	
Ki67			
Low (<15%)	**221(89.8)**	**25(10.2)**	**0.031**
High (>15%)	**79(80.6)**	**19(19.4)**	
Tumour Bud			
-Low	195(87.8)	27(12.2)	0.507
-High	104(85.2)	18(14.8)	
Tissue Stroma Percentage			
Low	211(87.9)	29(12.1)	0.391
High	88(84.6)	16(15.4)	

Stratification of the cohort to compare patients according to ER status was performed. In the ER-negative patient group (n=71), 64 patients had low RFX5 nuclear expression and had 20 events, while 7 had high RFX5 expression and 1 event. Survival in the low RFX5 group was 74% at 5 years, and 65% at 10 years, while in the high RFX5 group survival was 86% at 5 and 71% at 10 years (HR 0.838 95% C.I. 0.196-3.589, p=0.812). Mean survival was 134.7 months for low RFX5, and 141.3 months for high RFX5 expressors, (*Figure 5-45*)

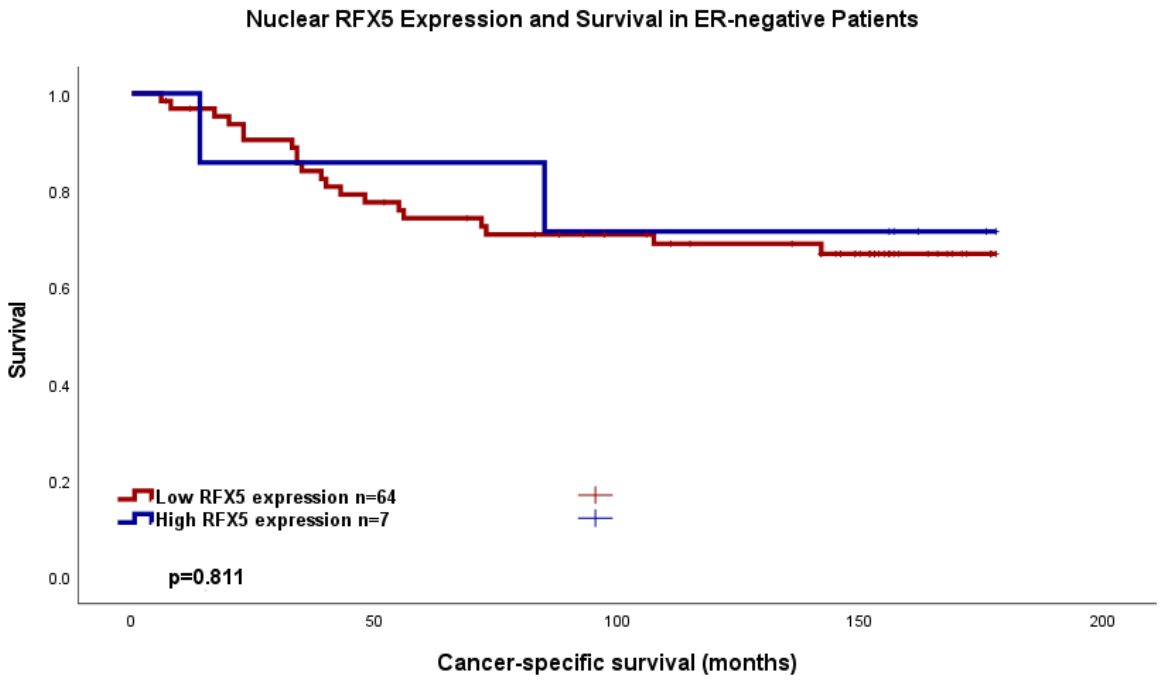

Figure 5-45 Cancer-specific survival in the ER-negative patients within the Glasgow Breast Cancer Cohort according to RFX5 Nuclear expression. Kaplan Meier Curve showing the association between RFX5 nuclear expression and survival (months). HR 0.838 95% C.I. 0.196-3.589, p=0.812. 10-year survival noted at each key.

Within the ER-negative group, inter-factor correlation was assessed when comparing the high and low RFX5 nuclear expressors, (Table 5-18). Here, an association was seen between tumour budding and RFX5 nuclear expression.

Table 5-18 Clinicopathological factors and their relation to RFX5 nuclear expression in ER-negative patients in the Glasgow Breast Cancer Cohort. Chi-squared analysis.

Clinicopathological factor	RFX5 nuclear staining (%)		p
	Low	High	
Age (years)			
≤50	24(92.3)	2(7.7)	1.000
>50	40(88.9)	5(11.1)	
Tumour Size			
≤20mm	31(86.1)	5(13.9)	0.126
21-49mm	31(96.9)	1(3.1)	
≥50mm	2(66.7)	1(33.3)	
Grade			
I	4(100)	0	0.531
II	18(94.7)	1(5.3)	
III	42(87.5)	6(12.5)	
Nodal Status			
N_0	33(89.2)	4(10.8)	1.000
N_1	31(91.2)	3(8.8)	
Lymphatic Invasion			

Absent	34(89.5)	4(10.5)	1.000
Present	26(89.7)	3(10.3)	
Vascular Invasion			
Absent	52(88.1)	7(11.9)	0.586
Present	8(100)	0	
Necrosis			
Absent	14(77.8)	4(22.2)	0.067
Present	49(94.2)	3(5.8)	
Klintrup Makinen			
0	1(100)	0	0.356
1	26(83.9)	5(16.1)	
2	3(96.8)	1(3.2)	
3	5(83.3)	1(16.7)	
Ki67			
Low (<15%)	53(93)	4(7)	0.113
High (>15%)	10(76.9)	3(23.1)	
Tumour Bud			
-Low	**47(95.9)**	**2(4.1)**	**0.022**
-High	**16(76.2)**	**5(23.8)**	
Tissue Stroma Percentage			
Low	46(88.5)	6(11.5)	0.668
High	17(94.4)	1(5.6)	

In the ER-positive group (n=273), 235 had low nuclear RFX5 expression, with 41 events, and 38 high RFX5 expression, with 6 events. Survival in the low nuclear RFX5 ER-positive group was 90% at 5 years and 77% at 10 years, and in the high RFX5 group was 86% at 5 years and 83% at 10 years (HR 0.925 95% C.I. 0.392-2.181, p=0.858), (*Figure 5-46*).

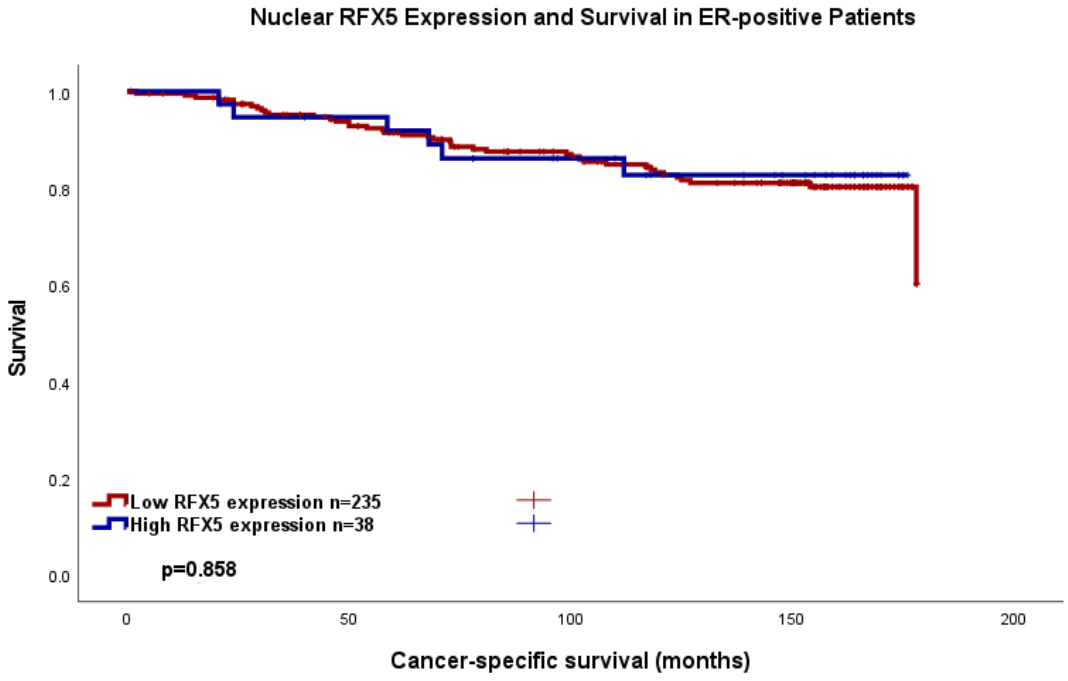

Figure 5-46 Cancer-specific survival in the ER-positive patients within the Glasgow Breast Cancer Cohort according to RFX5 Nuclear expression. Kaplan Meier Curve showing the

association between RFX5 nuclear expression and survival (months). HR 0.925 95% C.I. 0.392-2.181, p=0.858. 10-year survival noted at each key.

Within the ER-positive group, inter-factor correlation was assessed when comparing the high and low RFX5 nuclear expressors, (Table 5-19). Here, no association with RFX5 nuclear expression was seen.

Table 5-19 Clinicopathological factors and their relation to RFX5 Nuclear expression in ER+ patients in the Glasgow Breast Cancer Cohort. Chi-squared analysis.

Clinicopathological factor	RFX5 Nuclear staining (%)		p
	Low	High	
Age (years)			
≤50	57(82.6)	12(17.4)	0.325
>50	184(87.2)	27(12.8)	
Tumour Size			
≤20mm	143(85.6)	24(14.4)	0.948
21-49mm	90(86.5)	14(13.5)	
≥50mm	8(88.9)	1(11.1)	
Grade			
I	63(87.5)	9(12.5)	0.798
II	122(84.7)	22(15.3)	
III	56(87.5)	8(12.5)	
Nodal Status			
N_0	141(87)	21(13)	0.466
N_1	94(83.9)	18(16.1)	
Lymphatic Invasion			
Absent	95(81.2)	22(18.8)	0.844
Present	50(79.4)	13(20.6)	
Vascular Invasion			
Absent	128(80)	32(20)	0.769
Present	17(85)	3(15)	
Necrosis			
Absent	147(85.5)	25(14.5)	0.857
Present	84(86.6)	13(13.4)	
Klintrup Makinen			
0	31(83.8)	6(16.2)	0.464
1	142(85)	25(15)	
2	45(86.5)	7(13.5)	
3	14(100)	0	
Ki67			
Low (<15%)	168(88.9)	21(11.1)	0.089
High (>15%)	69(81.2)	16(18.8)	
Tumour Bud			
-Low	148(85.5)	25(14.5)	0.857
-High	88(87.1)	13(12.9)	
Tissue Stroma Percentage			
Low	165(87.8)	23(12.2)	0.262
High	71(82.6)	15(17.4)	

Further stratification according to molecular subtype was then performed. These subtypes were divided into Luminal A, Luminal B, Triple-negative (most similar to "Basal-like" subtype) and HER-2 enriched groups. For 10 patients, molecular subgroup was not available. For the remaining patients, there were 171 Luminal A, 96 Luminal B, 46 TNBC and 21 HER-2 enriched cases.

Luminal A patients had 152 low nuclear RFX5 expressors with 20 events, and 19 high-RFX5 expressors with 2 events. Luminal B patients had 80 low RFX5 expressors with 20 events, and 16 high RFX5 expressors with 4 events. The TNBC patients had 42 low RFX5 expressors with 12 events, and 4 patients with high RFX5 with 1 event. Finally, HER-2 enriched patients consisted of 19 low RFX5 cases with 8 events, and 2 high RFX5 cases with 1 event. Kaplan Meier curves are shown for each subgroup below.

Luminal A patients had a 5-year survival of 91% and 84% at 10 years for low RFX5 expressors, compared to 89% at 5 years and 89% at 10 years for high RFX5 expressors. (HR 0.805, 95% C.I. 0.187-3.458, p=0.771), (*Figure 5-47*).

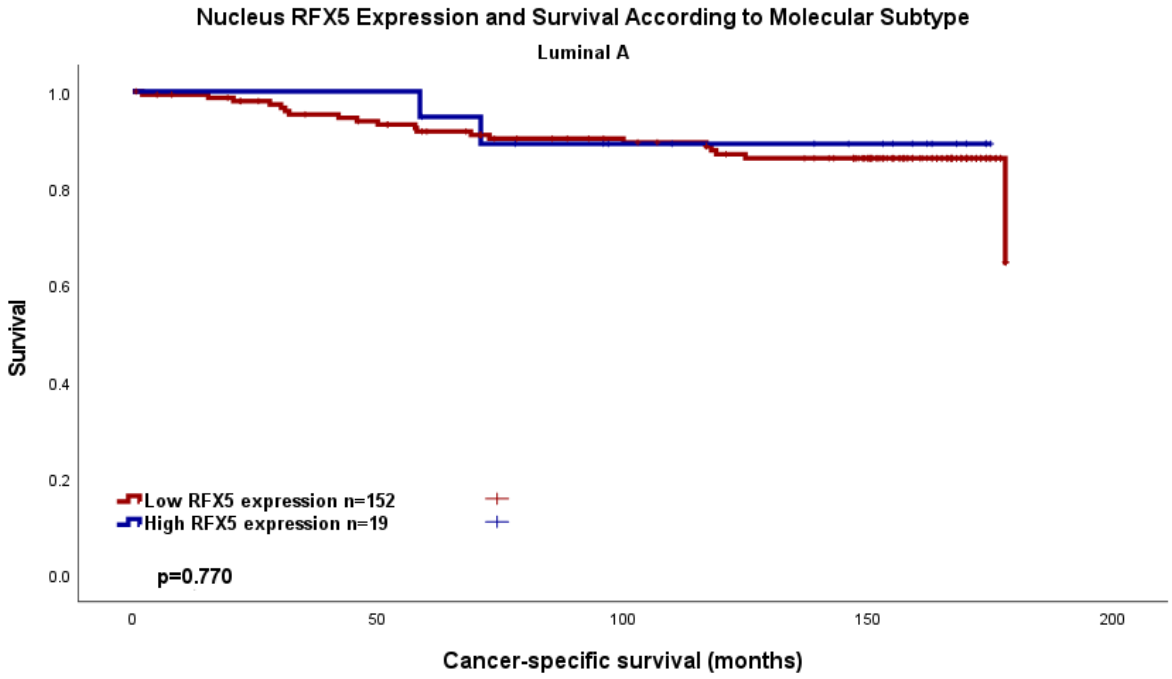

Figure 5-47 Cancer-specific survival in the Luminal A patients within the Glasgow Breast Cancer Cohort according to RFX5 Nuclear expression. Kaplan Meier Curve showing the association between RFX5 nuclear expression and survival (months). HR 0.805, 95% C.I. 0.187-3.458, p=0.771. 10-year survival noted at each key.

Within the Luminal A group, inter-factor correlation was assessed when comparing the high and low RFX5 nuclear expressors, (Table 5-20). Here, no association with RFX5 nuclear expression was seen.

Table 5-20 Clinicopathological factors and their relation to RFX5 Nuclear expression in Luminal A patients in the Glasgow Breast Cancer Cohort. Chi-squared analysis.

Clinicopathological factor	**RFX5 Nuclear staining (%)**		**p**
	Low	**High**	
Age (years)			
≤50	41(85.4)	7(14.6)	0.427
>50	116(89.9)	13(10.1)	
Tumour Size			
≤20mm	95(85.6)	16(14.4)	0.219
21-49mm	58(93.5)	4(6.5)	
≥50mm	4(100)	0	
Grade			
I	53(91.4)	5(8.6)	0.228
II	80(85.1)	14(14.9)	
III	24(96)	1(4)	
Nodal Status			
N_0	96(90.6)	10(9.4)	0.516
N_1	59(85.5)	10(14.5)	
Lymphatic Invasion			
Absent	73(85.9)	12(14.1)	0.405
Present	26(78.8)	7(21.2)	
Vascular Invasion			
Absent	88(83)	18(17)	0.688
Present	11(91.7)	1(8.3)	
Necrosis			
Absent	103(88)	14(12)	0.795
Present	47(90.4)	5(9.6)	
Klintrup Makinen			
0	19(79.2)	5(20.8)	0.081
1	96(87.3)	14(12.7)	
2	27(100)	0	
3	7(100)	0	
Ki67			
Low (<15%)	157(88.7)	20(11.3)	n/a
High (>15%)	0	0	
Tumour Bud			
-Low	96(90.6)	10(9.4)	0.456
-High	57(86.4)	9(13.6)	
Tissue Stroma Percentage			
Low	108(92.3)	9(7.7)	0.065
High	45(81.8)	10(18.2)	

Luminal B patients had a 5-year survival of 89% and 64% at 10 years for low RFX5 expressors, compared to 81% at both 5 and 73% at 10 years for high RFX5 expressors. (HR 0.968, 95% C.I. 0.330-2.835, p=0.952), (*Figure 5-48*).

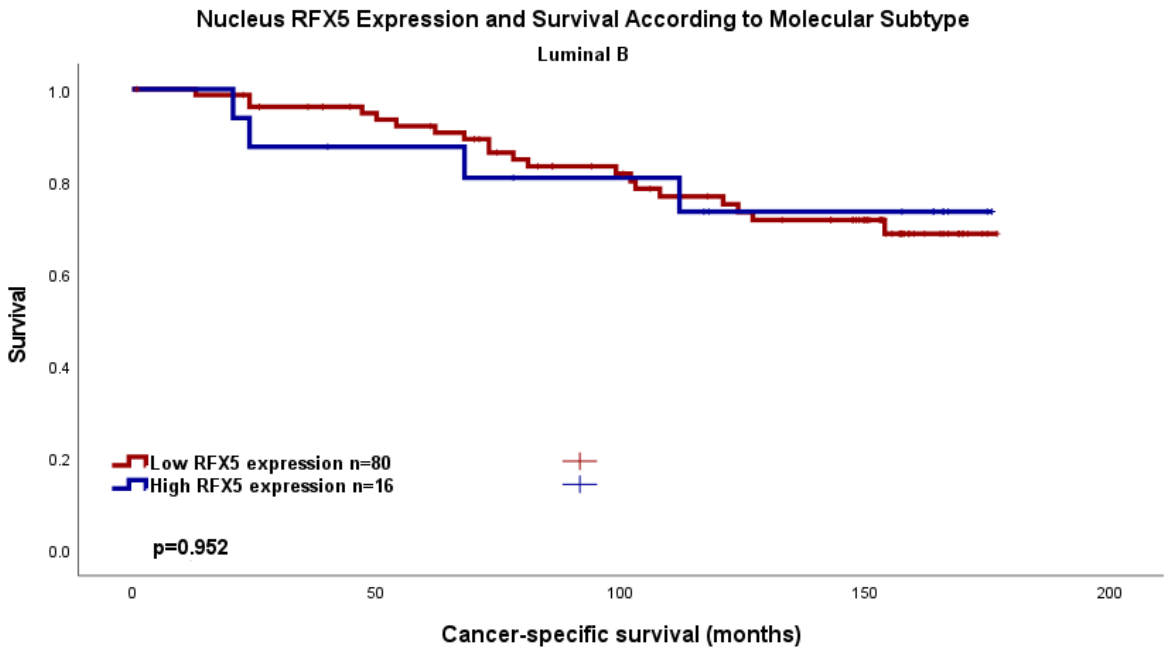

Figure 5-48 Cancer-specific survival in the Luminal B patients within the Glasgow Breast Cancer Cohort according to RFX5 nuclear expression. Kaplan Meier Curve showing the association between RFX5 nuclear expression and survival (months). HR 0.968, 95% C.I. 0.330-2.835, p=0.952. 10-year survival noted at each key.

Within the Luminal B group, inter-factor correlation was assessed when comparing the high and low RFX5 nuclear expressors, (Table 5-21). Here, no statistically significant association was seen.

Table 5-21 Clinicopathological factors and their relation to RFX5 nuclear expression in Luminal B patients in the Glasgow Breast Cancer Cohort. Chi-squared analysis.

Clinicopathological factor	RFX5 Cytoplasmic staining (%)		p
	Low	High	
Age (years)			
≤50	17(77.3)	5(22.7)	0.350
>50	64(85.3)	11(14.7)	
Tumour Size			
≤20mm	45(88.2)	6(11.8)	0.415
21-49mm	32(78)	9(22)	
≥50mm	4(80)	1(20)	
Grade			
I	10(71.4)	4(28.6)	0.284
II	37(82.2)	8(17.8)	

III	34(89.5)	4(10.5)	
Nodal Status			
N_0	43(82.7)	9(17.3)	0.734
N_1	35(83.3)	7(16.7)	
Lymphatic Invasion			
Absent	23(71.9)	9(17.3)	0.372
Present	24(82.8)	5(16.7)	
Vascular Invasion			
Absent	41(77.4)	12(22.6)	1.000
Present	6(86.4)	2(25)	
Necrosis			
Absent	41(80.4)	10(19.6)	0.584
Present	38(86.4)	6(13.6)	
Klintrup Makinen			
0	11(91.7)	1(8.3)	0.493
1	43(81.1)	10(18.9)	
2	20(80)	5(20)	
3	7(100)	0	
Ki67			
Low (<15%)	12(92.3)	1(7.7)	0.688
High (>15%)	69(82.1)	15(17.9)	
Tumour Bud			
-Low	51(82.3)	11(17.7)	0.780
-High	30(85.7)	5(14.3)	
Tissue Stroma Percentage			
Low	55(82.1)	12(17.9)	0.769
High	26(86.7)	4(13.3)	

Triple-negative (“basal-like) patients had a 5-year survival of 78% and 67% at 10 years for low RFX5 expressors, compared to 100% at 5 and 75% at 10 years for high RFX5 expressors. (HR 0.731, 95% C.I. 0.095-5.624, p=0.763), (*Figure 5-49)*.

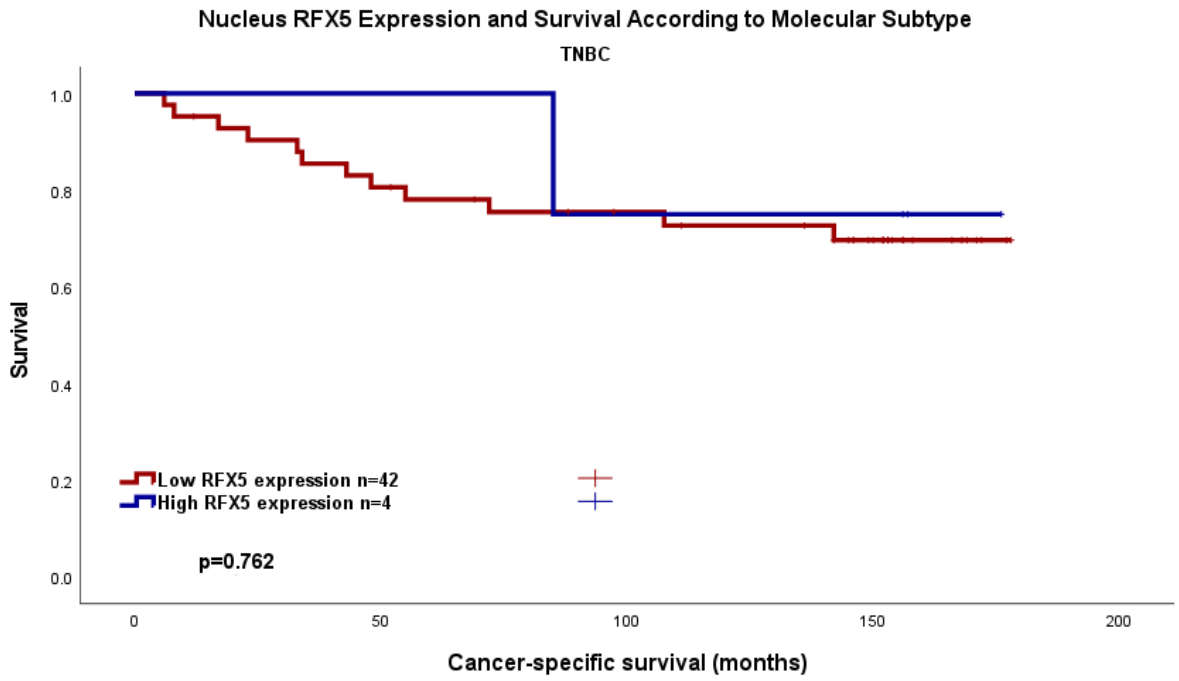

Figure 5-49 Cancer-specific survival in the TNBC patients within the Glasgow Breast Cancer Cohort according to RFX5 Nuclear expression. Kaplan Meier Curve showing the association between RFX5 nuclear expression and survival (months). HR 0.731, 95% C.I. 0.095-5.624, p=0.763. 10-year survival noted at each key.

Within the TNBC group, inter-factor correlation was assessed when comparing the high and low RFX5 nuclear expressors, (Table 5-22). Here, no association was seen.

Table 5-22 Clinicopathological factors and their relation to RFX5 nuclear expression in TNBC patients in the Glasgow Breast Cancer Cohort. Chi-squared analysis.

Clinicopathological factor	RFX5 Cytoplasmic staining (%)		p
	Low	High	
Age (years)			
≤50	14(93.3)	1(6.7)	1.000
>50	28(90.3)	3(9.7)	
Tumour Size			
≤20mm	22(84.6)	4(15.4)	0.185
21-49mm	19(100)	0	
≥50mm	1(100)	0	
Grade			
I	3(100)	0	0.311
II	13(100)	0	
III	26(86.7)	4(13.3)	
Nodal Status			
N_0	25(92.6)	2(7.4)	1.000
N_1	17(89.5)	2(10.5)	
Lymphatic Invasion			

Absent	22(91.7)	2(8.3)	1.000
Present	17(89.5)	2(10.5)	
Vascular Invasion			
Absent	32(88.9)	4(11.1)	1.000
Present	7(100)	0	
Necrosis			
Absent	10(83.3)	2(16.7)	0.286
Present	31(93.9)	2(6.1)	
Klintrup Makinen			
0	1(100)	0	0.241
1	19(82.6)	4(17.4)	
2	16(100)	0	
3	5(100)	0	
Ki67			
Low (<15%)	37(94.9)	2(5.1)	0.080
High (>15%)	4(66.7)	2(33.3)	
Tumour Bud			
-Low	32(97)	1(3)	0.052
-High	9(75)	3(25)	
Tissue Stroma Percentage			
Low	30(97)	4(11.8)	0.558
High	11975)	0	

HER2-enriched patients had a 5-year survival of 61% and 56% at 10 years for low RFX5 expressors, compared to 50% at 5 and 10 years for high RFX5 expressors. (HR 1.670, 95% C.I. 0.208-13.419, p=0.630), (*Figure 5-50)*.

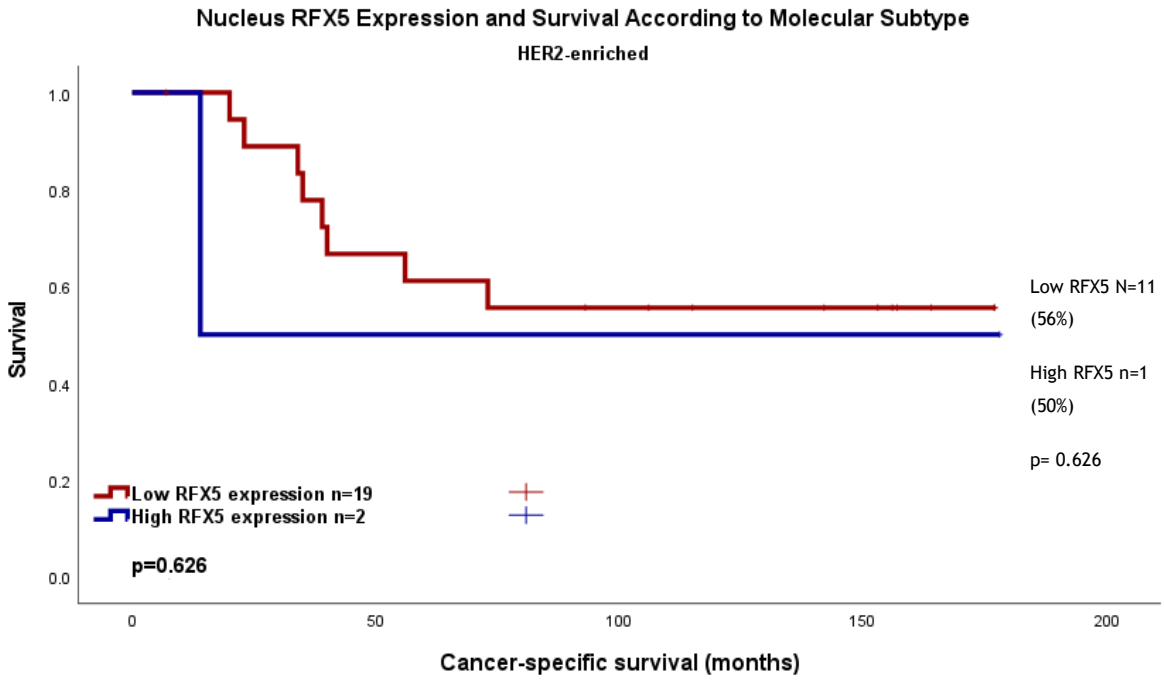

Figure 5-50 Cancer-specific survival in the HER2-enriched patients within the Glasgow Breast Cancer Cohort according to RFX5 nuclear expression. Kaplan Meier Curve showing the association between RFX5 nuclear expression and survival (months). HR 1.670, 95% C.I. 0.208-13.419, p=0.630. 10-year survival noted at each key.

Within the HER2-enriched group, inter-factor correlation was assessed when comparing the high and low RFX5 nuclear expressors, (Table 5-23). Here an association between KM score and RFX5 nuclear expression was seen.

Table 5-23 Clinicopathological factors and their relation to RFX5 nuclear expression in HER2-enriched patients in the Glasgow Breast Cancer Cohort. Chi-squared analysis.

Clinicopathological factor	**RFX5 Cytoplasmic staining (%)**		**p**
	Low	**High**	
Age (years)			
≤50	7(100)	0	0.533
>50	12(85.7)	2(14.3)	
Tumour Size			
≤20mm	7(100)	0	0.102
21-49mm	11(91.7)	1(8.3)	
≥50mm	1(50)	1(50)	
Grade			
I	0	0	1.000
II	5(26.3)	14(73.7)	
III	14(87.5)	2(12.5)	
Nodal Status			
N_0	6(85.7)	1(14.3)	1.000
N_1	13(92.9)	1(7.1)	
Lymphatic Invasion			
Absent	9(90)	1(10)	1.000
Present	9(90)	1(10)	
Vascular Invasion			
Absent	17(89.5)	2(10.5)	1.000
Present	1(100)	0	
Necrosis			
Absent	3(75)	1(25)	0.352
Present	16(94.1)	1(5.9)	
Klintrup Makinen			
0	**0**	**0**	**0.008**
1	**6(100)**	**0**	
2	**12(92.3)**	**1(7.7)**	
3	**0**	**1(100)**	
Ki67			
Low (<15%)	13(92.9)	1(7.1)	1.000
High (>15%)	6(85.7)	1(14.3)	
Tumour Bud			
-Low	12(92.3)	1(7.7)	1.000
-High	7(87.5)	1(12.5)	
Tissue Stroma Percentage			
Low	14(93.3)	1(6.7)	0.500
High	5(83.3)	1(16.7)	

5.2.16 RFX5 Expression in the Glasgow Breast Cancer Cohort - Combined Scoring

Weighted histoscores for membrane, cytoplasm, and nuclear expression of RFX5 were combined to create 4 categories (each a combination of high vs low membrane, cytoplasm and nuclear score) to assess whether more prognostic power could be conferred to RFX5 protein expression on cancer-specific survival. 344 patients had valid survival data and scores for each cellular location which allowed for a combined score.

The 4 categories were grouped into “all high” (high membrane, cytoplasm, nucleus expression of RFX5), “two high” (two of either membrane, cytoplasm, or nucleus high, one low), “two low” (two of either membrane cytoplasm or nucleus low, one high) and “all low”.

Amongst the entire Glasgow Breast Cancer Cohort, there were 8 cases with “All High” (AH) score and 4 events, 65 with “Two High and One Low” (2H1L) with 12 events, 217 “Two Low and One High” (2L1H) with 45 events, and 54 “All Low” (AL) with 8 events.

The AH group had a 5-year survival of 63% and 10-year survival of 50%, the 2H1L group had a 5-year survival of 87% and 10-year survival of 78%. The 2L1H group had a 5-year survival of 87% and 10-year survival of 74%, while the AL group had a 5-year survival of 88% and 10-year survival of 82%, (*Figure 5-51*).

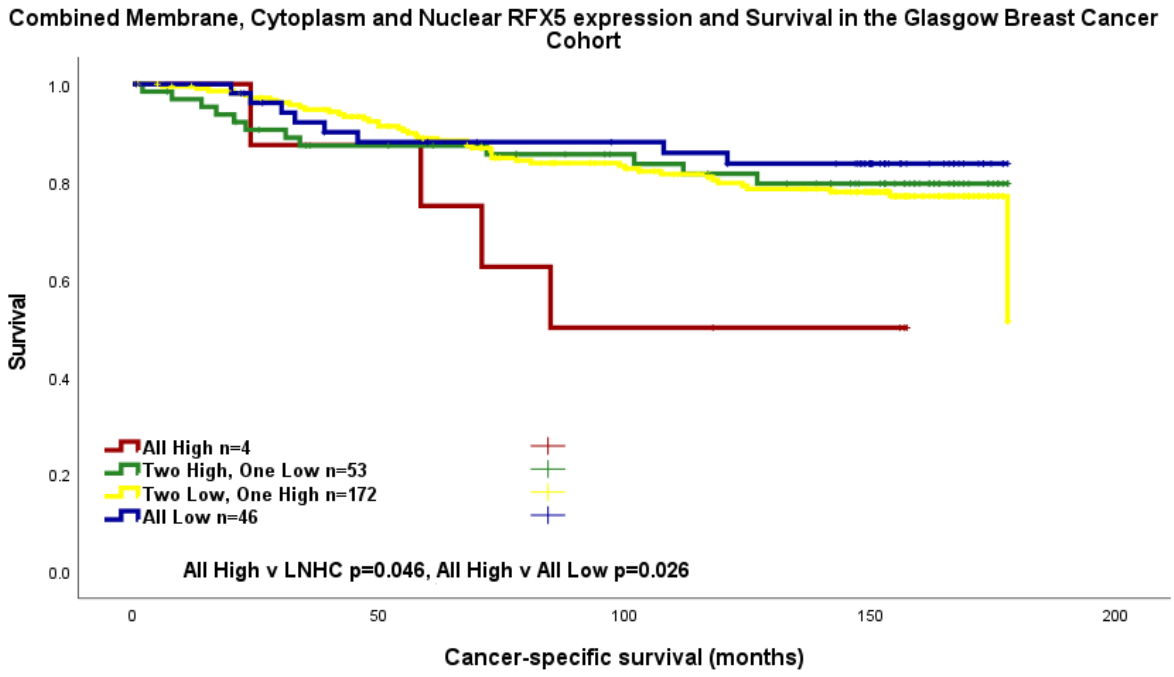

Figure 5-51 Combined membrane, cytoplasmic and nuclear RFX5 expression and survival in the Glasgow Breast Cancer Cohort. Pairwise comparisons are described in the graph.

Pairwise comparison demonstrated that the AH group had significantly worse survival than the TL1H and AL groups, (Table *5-24*).

Table 5-24 Pairwise comparisons on Kaplan Meier survival analysis for combined membrane, nuclear and cytoplasmic RFX5 expression.

Pairwise Comparison p=	All High	Two High, One Low	Two Low, One High	All Low
All High		0.062	**0.046**	**0.026**
Two high, one low	0.062		0.784	0.549
Two low, one high	**0.046**	0.784		0.378
All Low	**0.026**	0.549	0.378	

On multivariate analysis RFX5 combined score remained statistically significant, with the AH group showing the worst survival (Table 5-25).

Table 5-25 Clinicopathological factors and their prognostic significance in the Glasgow Breast Cancer Cohort with regards to combined nuclear and cytoplasmic RFX5 scoring. Univariate and multivariate Cox regression analysis.

Clinicopathological Factor	**Univariate analysis (HR, 95% C.I.)**	**p**	**Multivariate analysis (HR, 95% C.I.)**	**p**
Age	0.947(0.680-1.318)	0.746		

Tumour Size		**<0.001**		
<20mm		**<0.001**		0.051
20-49mm	**2.117(1.525-2.939)**	**<0.001**	1.856(0.924-3.728)	0.082
>50mm	**4.528(2.579-7.951)**	**<0.001**	3.894(1.140-13.301)	0.030
Invasive Grade		**<0.001**		
I		**<0.001**		0.697
II	**2.332(1.226-4.436)**	**0.010**	0.592(0.173-2.028)	0.404
III	**4.043(2.162-7.563)**	**<0.001**	0.679(0.195-2.365)	0.543
Nodal Status	**3.258(2.339-4.537)**	**<0.001**	1.445(0.723-2.887)	0.298
Molecular Subtype		**<0.001**		
Luminal A				
Luminal B	**2.343(1.525-3.599)**	**<0.001**	**2.216(0.669-7.338)**	**0.020** **0.193**
TNBC	**2.710(1.779-4.128)**	**<0.001**	**3.424(1.111-10.552)**	**0.032**
HER2-enriched	**2.946(1.771-4.900)**	**<0.001**	**6.623(1.856-23.631)**	**0.004**
Lymphatic Invasion	**4.255(2.813-6.435)**	**<0.001**	**3.229(1.511-6.900)**	**0.002**
Vascular Invasion	**3.440(2.163-5.470)**	**<0.001**	2.091(0.967-4.522)	0.061
Necrosis	**3.288(2.290-4.722)**	**<0.001**	2.184(0.963-4.949)	0.061
Klintrup-Makinen		0.033		
0		0.030		
1	0.812(0.481-1.372)	0.437		
2	1.310(0.757-2.265)	0.334		
3	0.621(0.277-1.395)	0.249		
Ki67	**1.658(1.199-2.294)**	**0.002**	1.880(0.799-4.423)	0.148
Tumour budding	**1.755(1.282-2.403)**	**<0.001**	1.594(0.800-3.176)	0.185
Tumour stroma percentage	**1.884(1.374-2.582)**	**<0.001**	**2.437(1.254-4.735)**	**0.009**
RFX5 combined score		**0.269**		
All high*		**0.181**		**0.117**
Two high, one low	**0343(0.110-1.065)**	**0.064**	**0.158(0.032-0.777)**	**0.023**
Two low, one high	**0.373(0.134-1.039)**	**0.059**	**0.201(0.046-0.885)**	**0.034**

All low	**0.266(0.080-0.885)**	**0.031**	**0.131(0.023-0.749)**	**0.022**

Within the Glasgow Breast Cancer Cohort, inter-factor correlation was assessed when comparing the combined score subgroups, (Table 5-26). Here, KM score was associated with RFX5 combined score.

Table 5-26 Clinicopathological factors and their relation to RFX combined membrane, nuclear and cytoplasmic expression in the Glasgow Breast Cancer Cohort. Chi-squared analysis.

Clinicopathological factor	**RFX5 combined score (%)**				**p value**
	All high	**Two high, one low**	**Two low, one high**	**All low**	
Age (years)					
<50	1(1.2)	14(16.5)	50(58.8)	20(23.5)	0.263
>50	7(2.7)	51(19.9)	162(63.3)	36(14.1)	
Tumour Size					
<20mm	6(3)	34(16.7)	129(63.5)	34(16.7)	0.860
21-49mm	2(1.5)	28(20.6)	85(62.5)	21(15.4)	
>50mm	0	3(25)	8(66.7)	1(8.3)	
Grade					
I	1(1.3)	11(14.5)	46(60.5)	18(23.7)	0.436
II	4(2.5)	30(18.4)	108(66.3)	21(12.9)	
III	3(2.7)	24(21.4)	68(60.7)	17(15.2)	
Nodal Status					
N_0	3(1.5)	37(18.6)	127(63.8)	32(16.1)	0.706
N_1	5(3.4)	27(18.5)	92(63)	22(15.1)	
Molecular Subtype					
Luminal A	2(1.1)	27(15.3)	120(67.8)	28(15.8)	0.194
Luminal B	3(3.1)	15(15.5)	62(63.9)	17(17.5)	
TNBC	3(6.5)	11(23.9)	24(52.2)	8(17.4)	
HER2-enriched	0	7(33.3)	12(57.1)	2(9.5)	
Lymphatic Invasion					
Absent	5(3.2)	34(21.9)	93(60)	23(14.8)	0.609
Present	1(1.1)	25(27.2)	53(57.6)	13(14.1)	
Vascular Invasion					
Absent	6(2.7)	54(24.7)	127(58)	32(14.6)	0.646
Present	0	5(17.9)	19(67.9)	4(14.3)	
Necrosis					
Absent	3(1.6)	36(18.9)	116(61.1)	35(18.4)	0.584
Present	4(2.7)	29(19.5)	96(64.4)	20(13.4)	
Klintrup Makinen					
0	**1(3.7)**	**2(7.4)**	**24(88.9)**	**0**	**0.025**
1	**6(3.6)**	**45(26.9)**	**115(68.9)**	**1(0.6)**	
2	**0**	**16(18)**	**59(66.3)**	**14(15.7)**	
3	**0**	**1(5)**	**14(70)**	**5(25)**	
Ki67					
Low (<15%)	4(1.6)	44(17.9)	158(64.2)	40(16.3)	0.564
High (>15%)	4(4.1)	19(19.4)	60(61.2)	15(15.3)	

Tumour Bud					
-Low	3(1.4)	42(18.9)	136(61.3)	41(18.5)	0.319
-High	4(3.3)	23(18.9)	80(65.6)	15(12.3)	
Tissue Stroma Percentage					
Low	5(2.1)	41(17.1)	158(65.8)	36(15)	0.340
High	2(1.9)	24(23.1)	58(55.8)	20(19.2)	

When stratifying according to molecular subtype, within the Luminal A patients of the Glasgow Breast Cancer Cohort, the AH group had two patients with 2 events, two 2H1L group had 27 patients with 2 events, the 2L1H group had 116 patients with 16 events, and the AL group had 26 patients with 2 events.

For the AH group the 5-year survival was 0%, for the 2H1L group the 5-year survival was 92% and 10-year survival was 92% , for the 2L1H group the 5-year survival was 92% and 10-year survival was 82% and for the AL group the 5-year survival and 10-year survival was 92%, (*Figure 5-52)*.

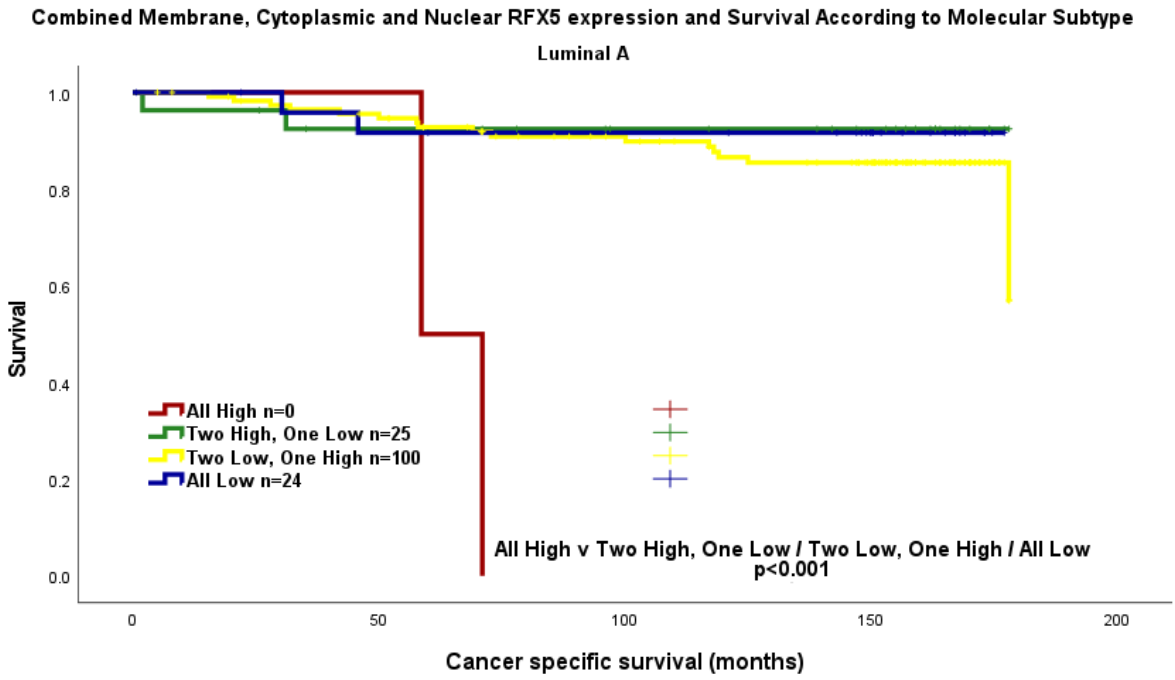

Figure 5-52 Combined membrane, cytoplasm and nuclear RFX5 expression and survival in the Luminal A patients in the Glasgow Breast Cancer Cohort.

Pairwise comparison demonstrated worse survival in the AH group compared to all other subgroups in the Luminal A patients, (Table 5-27).

Table 5-27 Pairwise comparisons on Kaplan Meier survival analysis for combined membrane, nuclear and cytoplasmic RFX5 expression in Luminal A patients.

Pairwise Comparison p=	All High	Two High, One Low	Two Low, One High	All Low
All High		**<0.001**	**<0.001**	**<.001**
Two high, one low	**<0.001**		0.404	0.960
Two low, one high	**<0.001**	0.404		0.474
All Low	**<0.001**	0.960	0.474	

On multivariate analysis however, RFX5 combined score did not retain statistical significance, (Table 5-28).

Table 5-28 Clinicopathological factors and their prognostic significance in the Luminal A patients within the Glasgow Breast Cancer Cohort with regards to combined membrane, nuclear and cytoplasmic RFX5 scoring. Univariate and multivariate Cox regression analysis.

Clinicopathological Factor	**Univariate analysis (HR, 95% C.I.)**	**p**	**Multivariate analysis (HR, 95% C.I.)**	**p**
Age	0.891(0.443-1.790)	0.745		
Tumour Size <20mm 20-49mm >50mm	 **2.614(1.351-5.055)** **4.132(1.192-14.328)**	**0.006** **0.004** **0.025**	 11.731(1.270-108.324) 0(0)	0.095 **0.030** 0.996
Invasive Grade I II III	 **2.595(0.990-6.805)** **4.311(1.470-12.642)**	**0.017** **0.052** **0.008**	 2.179(0.276-17.219) 2.986(0.156-57.225)	0.709 0.460 0.468
Nodal Status	**3.871(1.918-7.813)**	**<0.001**	1.615(0.277-9.431)	0.594
Lymphatic Invasion	1.811(0.670-4.899)	0.242		
Vascular Invasion	**3.528(1.150-10.823)**	**0.028**	2.956(0.383-22.841)	0.299
Necrosis	**2.291(1.201-4.368)**	**0.012**	**30.546(2.155-432.868)**	**0.011**
Klintrup-Makinen 0 1 2 3	 0.552(0.246-1.2365) 0.593(0.194-1.816)	0.524 0.488 0.148 0.360 0.336		

	0.361(0.045-2.885)			
Ki67	**n/a**			
Tumour budding	1.305(0.686-2.483)	0.417		
Tumour stroma percentage	**2.168(1.145-4.107)**	**0.018**	1.859(0.259-13.348)	0.538
RFX5 combined score		**0.059**		
All high*		**0.007**		0.288
Two high, one low	**0.049(0.007-0.357)**	**0.003**	0.028(0.001-1.072)	0.055
Two low, one high	**0.090(0.020-0.408)**	**0.002**	0.067(0.003-1.751)	0.104
All low	**0.053(0.007-0.387)**	**0.004**	0(0)	0.971

Within the Luminal A group, inter-factor correlation was assessed when comparing the combined score subgroups, (Table 5-29*)*. Here, TSP was associated with RFX5 combined score.

Table 5-29 Clinicopathological factors and their relation to RFX5 combined membrane, nuclear and cytoplasmic expression in the Luminal A patients in the Glasgow Breast Cancer Cohort. Chi-squared analysis.

Clinicopathological factor	**RFX5 combined score (%)**				**P value**
	All high	**Two high, one low**	**Two low, one high**	**All low**	
Age (years)					
<50	0	5(10.)	33(68.8)	10(20.8)	0.422
>50	2(1.6)	22(17.1)	87(67.4)	18(14)	
Tumour Size					
<20mm	2(1.8)	15(13.5)	76(68.5)	18(16.2)	0.667
21-49mm	0	12(19.4)	40(64.5)	10(16.1)	
>50mm	0	0	4(100)	0	
Grade					
I	0	8(13.8)	40(69)	10(17.2)	0.370
II	2(2.1)	18(19.1)	59(62.8)	15(16)	
III	0	1(4)	21(4)	3(12)	
Nodal Status					
N_0	1(0.9)	14(13.2)	75(70.8)	16(15.1)	0.736
N_1	1(1.4)	13(18.8)	44(63.8)	11(15.9)	
Lymphatic Invasion					
Absent	1(1.2)	13(15.3)	56(65.9)	15(65.9)	0.167
Present	0	11(33.3)	17(8)	5(15.2)	
Vascular Invasion					
Absent	1(0.9)	22(20.8)	65(61.3)	18(17)	0.969
Present	0	2(16.7)	8(66.7)	2(13.5)	
Necrosis					

Absent	0	19(16.2)	78(66.7)	20(17.1)	0.458
Present	1(1.9)	8(15.4)	36(69.2)	7(13.5)	
Klintrup Makinen					
0	0	2(8.3)	16(66.7)	6(25)	0.789
1	1(0.9)	21(19.1)	71(64.5)	17(15.5)	
2	0	3(11.1)	20(74.1)	4(14.8)	
3	0	0	6(85.7)	1(14.3)	
Ki67					
Low (<15%)	2(1.1)	27(15.3)	120(67.8)	28(15.8)	n/a
High (>15%)	0	0	0	0	
Tumour Bud					
-Low	0	13(12.3)	72(67.9)	21(19.8)	0.121
-High	1(1.5)	14(21.2)	44(66.7)	7(10.6)	
Tissue Stroma Percentage					
Low	**0**	**15(12.8)**	**88(75.2)**	**14(12)**	**0.009**
High	**1(1.8)**	**12(21.8)**	**28(50.9)**	**14(25.5)**	

Amongst the Luminal B patients of the Glasgow Breast Cancer Cohort, the AH group had three patients with 1 event, the 2H1L group had 15 patients with 4 events, the 2L1H group had 61 patients with 16 events, and the AL group had 17 patients with 3 events.

For the AH group the 5-year survival and 10-year survival was 67%, for the 2H1L group the 5-year survival was 93% and 10-year survival was 61%, for the 2L1H group the 5-year survival was 86% and 10-year survival was 65% and for the AL group the 5-year survival was 94% and 10-year survival was 73%, (*Figure 5-53*).

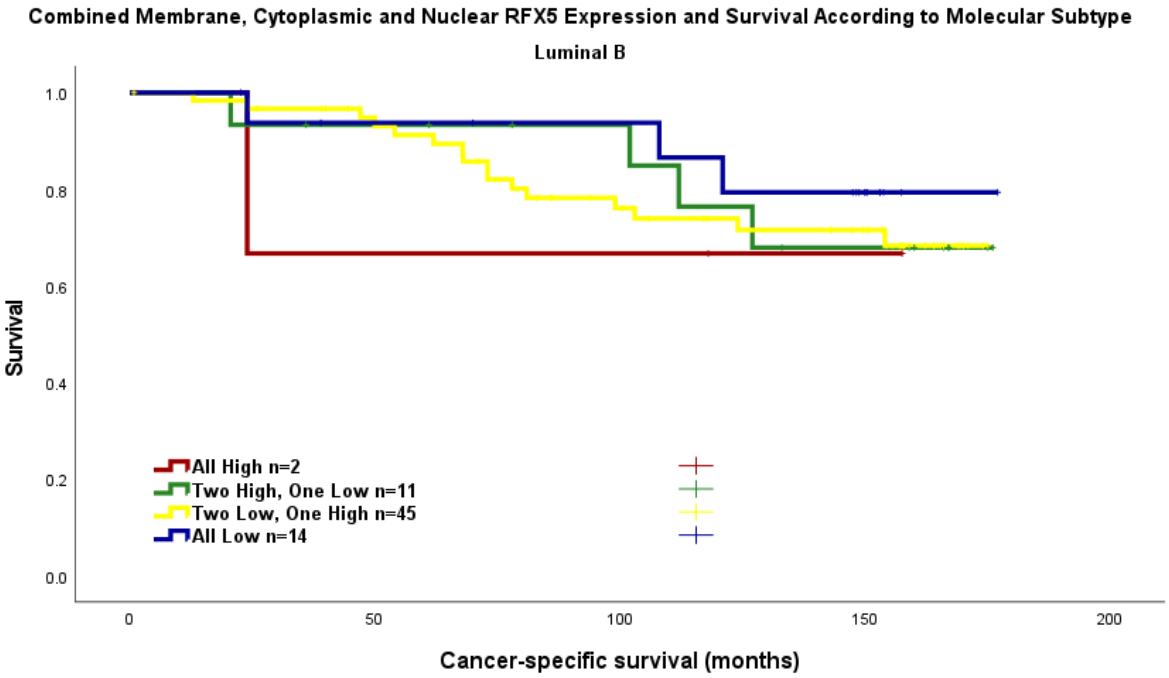

Figure 5-53 Combined membrane, cytoplasm and nuclear RFX5 expression and survival in the Luminal B patients in the Glasgow Breast Cancer Cohort.

Pairwise comparison demonstrated no significant difference in survival between combined RFX5 subgroups in the Luminal B patients, (*Table 5-30*).

Table 5-30 Pairwise comparisons on Kaplan Meier survival analysis for combined membrane nuclear and cytoplasmic RFX5 expression in Luminal B patients.

Pairwise Comparison p=	All High	Two High, One Low	Two Low, One High	All Low
All High		0.768	0.742	0.474
Two high, one low	0.768		0.893	0.524
Two low, one high	0.742	0.893		0.474
All Low	0.474	0.524	0.474	

Within the Luminal B group, inter-factor correlation was assessed when comparing the combined score subgroups, (Table 5-31). Here, grade was associated with RFX5 combined score.

Table 5-31 Clinicopathological factors and their relation to RFX5 combined membrane, nuclear and cytoplasmic expression in the Luminal B patients in the Glasgow Breast Cancer Cohort. Chi-squared analysis.

Clinicopathological factor	**RFX5 combined score (%)**				**P value**
	All high	**Two high, one low**	**Two low, one high**	**All low**	
Age (years)					
<50	1(4.5)	4(18.2)	13(59.1)	4(18.2)	0.932
>50	2(2.7)	11(14.7)	49(65.3)	13(17.3)	
Tumour Size					
<20mm	1(2)	6(11.8)	33(64.7)	11(21.6)	0.558
21-49mm	2(4.9)	7(17.1)	27(65.9)	5(12.2)	
>50mm	0	2(40)	2(40)	1(20)	
Grade					
I	**1(7.1)**	**2(14.3)**	**4(28.6)**	**7(50)**	**0.013**
II	**2(4.4)**	**8(17.8)**	**31(68.9)**	**4(8.9)**	
III	**0**	**5(13.2)**	**27(71.1)**	**6(15.8)**	
Nodal Status					
N_0	1(1.9)	8(15.4)	34(65.4)	9(17.3)	0.876
N_1	2(4.8)	6(14.3)	26(61.9)	8(19)	
Lymphatic Invasion					
Absent	2(6.3)	8(25)	20(62.5)	2(6.3)	0.276
Present	0	5(17.2)	19(65.5)	5(17.2)	
Vascular Invasion					
Absent	2(3.8)	11(20.8)	34(64.2)	6(11.3)	0.946
Present	0	2(25)	5(62.5)	1(12.5)	
Necrosis					

Absent	2(3.9)	9(17.6)	28(54.9)	12(23.5)	0.310
Present	1(2.3)	6(13.6)	32(72.7)	5(11.4)	
Klintrup Makinen					
0	1(8.3)	0	8(66.7)	3(25)	0.298
1	2(3.8)	10(18.9)	30(56.6)	11(20.8)	
2	0	5(20)	19(76)	1(4)	
3	0	0	5(71.4)	2(28.6)	
Ki67					
Low (<15%)	0	1(7.7)	9(69.2)	3(23.1)	0.710
High (>15%)	3(3.6)	14(16.7)	53(63.1)	14(16.7)	
Tumour Bud					
-Low	2(3.2)	11(17.7)	38(61.3)	11(17.7)	0.855
-High	1(2.9)	4(11.4)	24(68.6)	6(17.1)	
Tissue Stroma Percentage					
Low	2(3)	12(17.9)	42(62.47)	11(16.4)	0.789
High	1(3.3)	3(10)	20(66.7)	6(20)	

Amongst the TNBC patients of the Glasgow Breast Cancer Cohort, the AH group had three patients with 1 event, the 2H1L group had 11 patients with 4 events, the 2L1H group had 24 patients with 7 events, and the AL group had 8 patients with 1 event.

For the AH group the 5-year survival was 100% and 10-year survival was 67%, for the 2H1L group the 5-year survival was 73% and 10-year survival was 62% , for the 2L1H group the 5-year survival was 75% and 10-year survival was 65% and for the AL group the 5-year survival and 10-year survival was 88%, (*Figure 5-54*).

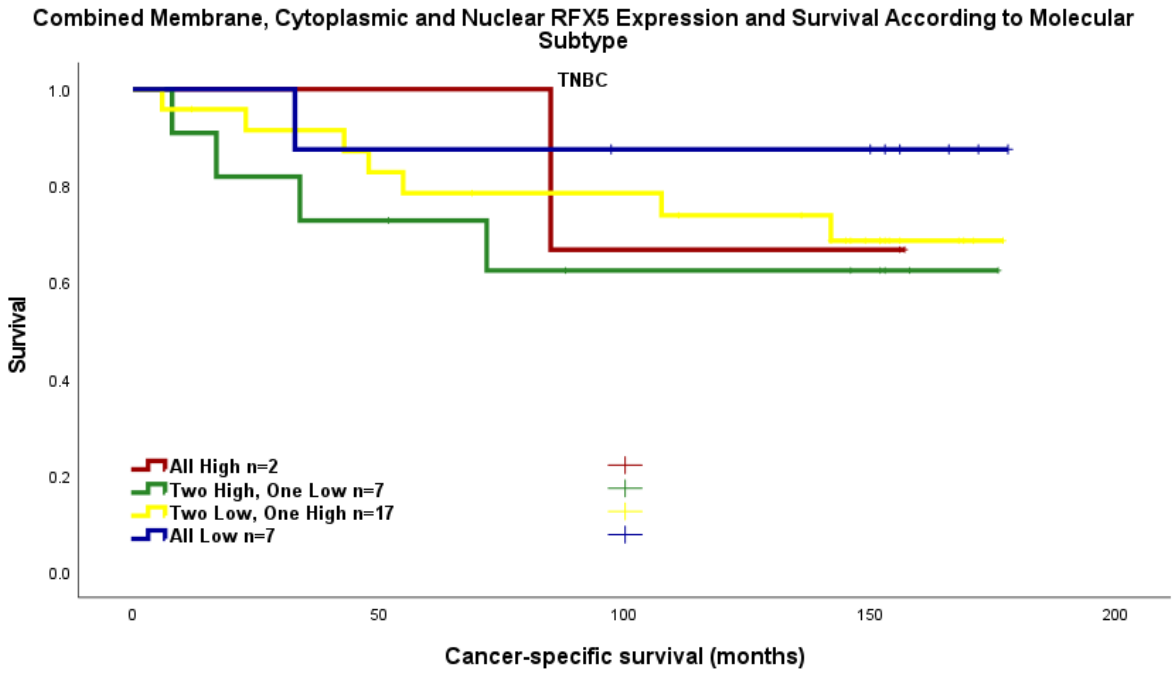

Figure 5-54 Combined membrane, cytoplasm and nuclear RFX5 expression and survival in the TNBC patients in the Glasgow Breast Cancer Cohort

Pairwise comparison demonstrated no significant difference in survival according to RFX5 combined score in TNBC patients, (*Table 5-32*).

Table 5-32 Pairwise comparisons on Kaplan Meier survival analysis for combined membrane, nuclear and cytoplasmic RFX5 expression in TNBC patients.

Pairwise Comparison p=	All High	Two High, One Low	Two Low, One High	All Low
All High		0.738	0.997	0.504
Two high, one low	0.738		0.572	0.252
Two low, one high	0.997	0.572		0.365
All Low	0.447	0.252	0.365	

Within the TNBC group, inter-factor correlation was assessed when comparing the combined score subgroups, (Table 5-33). Here, KM score was associated with combined RFX5 score.

Table 5-33 Clinicopathological factors and their relation to RFX5 combined membrane, nuclear and cytoplasmic expression in the TNBC patients in the Glasgow Breast Cancer Cohort. Chi-squared analysis.

Clinicopathological factor	RFX5 combined score (%)	P value

	All high	Two high, one low	Two low, one high	All low	
Age (years)					
<50	0	2(13.3)	9(60)	4(26.7)	0.277
>50	3(9.7)	9(29)	15(48.4)	4(12.9)	
Tumour Size					
<20mm	3(11.5)	7(26.9)	13(50)	3(11.5)	0.579
21-49mm	0	4(21.1)	10(52.6)	5(26.3)	
>50mm	0	0	1(100)	0	
Grade					
I	0	1(33.3)	2(66.7)	0	0.654
II	2(13.3)	2(13.3)	9(60)	2(13.3)	
III	3(10)	8(26.7)	13(43.3)	6(20)	
Nodal Status					
N_0	1(3.7)	8(29.6)	12(44.4)	6(22.2)	0.346
N_1	2(10.5)	3(15.8)	12(63.2)	2(10.5)	
Lymphatic Invasion					
Absent	2(8.3)	6(25)	10(41.7)	6(25)	0.302
Present	1(5.3)	5(26.3)	12(63.2)	1(5.3)	
Vascular Invasion					
Absent	3(8.3)	10(27.8)	17(47.2)	6(16.7)	0.639
Present	0	1(14.3)	5(71.4)	1(14.3)	
Necrosis					
Absent	1(8.3)	3(25)	6(50)	2(16.7)	0.994
Present	2(6.1)	8(24.2)	17(51.5)	6(18.2)	
Klintrup Makinen					
0	**0**	**0**	**0**	**1(100)**	**0.025**
1	**3(13)**	**9(39.1)**	**7(30.4)**	**4(17.4)**	
2	**0**	**2(12.5)**	**13(81.3)**	**1(6.3)**	
3	**0**	**0**	**3(60)**	**2(40)**	
Ki67					
Low (<15%)	2(5.1)	9(23.1)	20(51.3)	8(20.5)	0.476
High (>15%)	1(16.7)	2(33.3)	3(50)	0	
Tumour Bud					
-Low	1(3)	8(24.2)	17(51.5)	7(21.2)	0.350
-High	2(16.7)	3(25)	6(50)	1(8.3)	
Tissue Stroma Percentage					
Low	3(8.8)	6(17.6)	17(50)	8(23.5)	0.101
High	0	5(45.5)	6(54.5)	0	

Amongst the HER2-enriched patients of the Glasgow Breast Cancer Cohort, the AH group had seven patients with 2 events, the 2H1L group had 12 patients with 5 events, the 2L1H group had 2 patients with 2 events, and the AL group had 21 patients with 9 events.

There were no AH group cases. For the 2H1L group the 5-year survival was 67% and 10-year survival was 67% , for the 2L1H group the 5-year survival was 67%

and 10-year survival was 58% and for the AL group the 5-year survival and 10-year survival was 0%. Survival was significantly lower for the AL group compared to 2H1L group, (p=0.007), (HR 0.160(95%C.I. 0.027-0.945) p=0.043), (*Figure 5-55*).

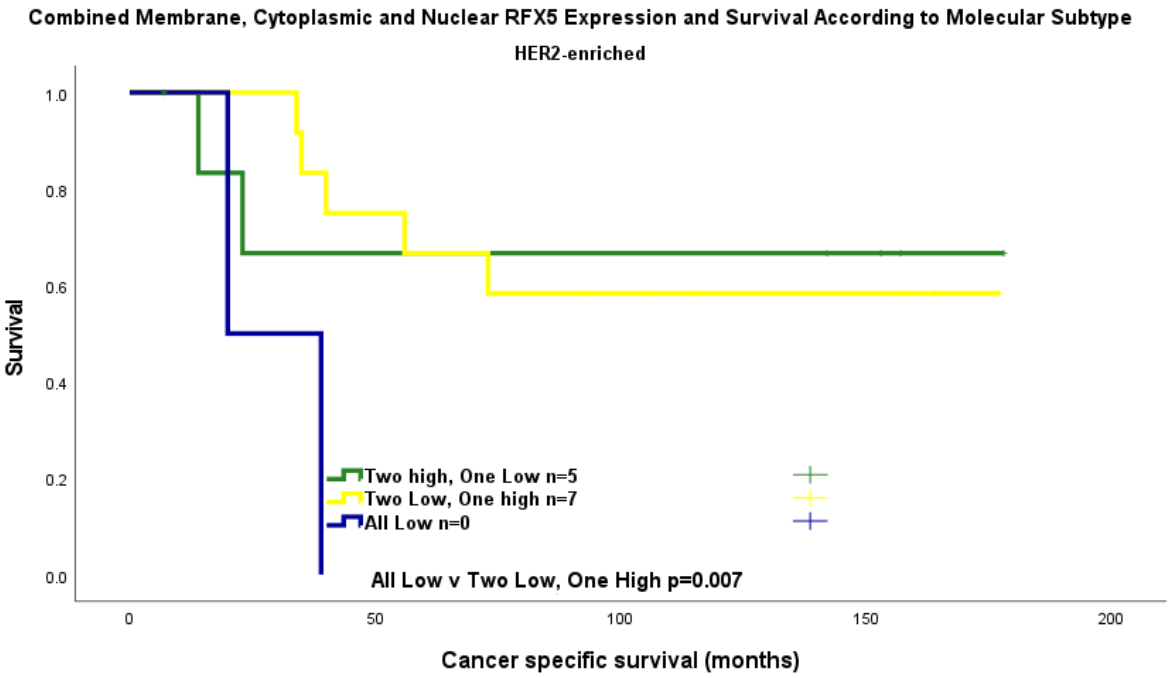

Figure 5-55 Combined membrane, cytoplasm and nuclear RFX5 expression and survival in the HER2-enriched patients in the Glasgow Breast Cancer Cohort. Pairwise comparisons are described in the graph.

Pairwise comparison demonstrated that the AL group had significantly worse survival than the 2L1H group, (Table 5-34).

Table 5-34, Pairwise comparisons on Kaplan Meier survival analysis for combined membrane, nuclear and cytoplasmic RFX5 expression in HER2-enriched patients.

Pairwise Comparison p=	All High	Two High, One Low	Two Low, One High	All Low
All High				
Two high, one low			0.953	0.187
Two low, one high		0.953		**0.007**
All Low		0.187	**0.007**	

On multivariate analysis however, RFX5 combined scoring did not remain statistically significant, (Table 5-35).

Table 5-35 Clinicopathological factors and their prognostic significance in the HER2-enriched patients within the Glasgow Breast Cancer Cohort with regards to combined membrane, nuclear and cytoplasmic RFX5 scoring. Univariate and multivariate Cox regression analysis.

Clinicopathological Factor	Univariate analysis (HR, 95% C.I.)	p	Multivariate analysis (HR, 95% C.I.)	p
Age	0.609(0.270-1.371)	0.231		
Tumour Size		0.383		
<20mm		0.338		
20-49mm	0.688(0.294-1.611)	0.389		
>50mm	2.074(0.467-9.203)	0.337		
Invasive Grade		0.519		
I		0.486		
II	0.704(0.263-1.886)	0.486		
III	-	-		
Nodal Status	**2.485(1.062-5.813)**	**0.036**	0.507(0.041-6.293)	0.597
Lymphatic Invasion	2.566(0.986-6.683)	0.054		
Vascular Invasion	0.964(0.127-7.296)	0.972		
Necrosis	1.875(0.441-7.946)	0.395		
Klintrup-Makinen		0.501		
0		0.731		
1	3567.881(0-2.354^{E+96})	0.940		
2	3303.914(0-2.180^{E+96})	0.941		
3	1087.661(0-7.236^{E+95})	0.949		
Ki67	1.627(0.718-3.689)	0.244		
Tumour budding	**3.466(1.543-7.786)**	**0.003**	**17.511(1.062-288.644)**	**0.045**
Tumour stroma percentage	**2.899(1.267-6.636)**	**0.012**	2.962(0.616-14.240)	0.175
RFX5 combined score		**0.183**		0.181
All high (None)				
Two high, one low*		**0.108**		
Two low, one high	**0.153(0.019-1.226)**	**0.077**	0.354(0.019-6.595)	0.487
All low				

	0.160(0.027-0.945)	**0.043**	0.166(0.023-1.204)	0.076

Examining the relationship between clinicopathological factors and patients in the different combined score subgroups in the HER2-enriched patients, no association with RFX5 combined score was seen (*Table 5-36*).

Table 5-36 Clinicopathological factors and their relation to RFX5 combined membrane nuclear and cytoplasmic expression in the HER2-enriched patients in the Glasgow Breast Cancer Cohort. Chi-squared analysis.

Clinicopathological factor	**RFX5 combined score (%)**				**P value**
	All high	**Two high, one low**	**Two low, one high**	**All low**	
Age (years)					
<50	0	1(14.3)	4(57.1)	2(28.6)	0.076
>50	0	6(42.9)	8(57.1)	0	
Tumour Size					
<20mm	0	2(28.6)	4(57.1)	1(14.3)	0.962
21-49mm	0	4(33.3)	7(58.3)	1(8.3)	
>50mm	0	1(50)	1(50)	0	
Grade					
I	0	0	0	0	
II	0	0	5(100)	0	0.085
III	0	7(43.8)	7(43.8)	2(12.5)	
Nodal Status					
N_0	0	3(42.9)	3(42.9)	1(14.3)	0.634
N_1	0	4(28.6)	9(64.3)	1(7.1)	
Lymphatic Invasion					
Absent	0	4(40)	6(60)	0	0.327
Present	0	3(30)	5(50)	2(20)	
Vascular Invasion					
Absent	0	7(36.8)	10(52.6)	2(10.5)	0.650
Present	0	0	1(100)	0	
Necrosis					
Absent	0	2(50)	2(50)	0	0.629
Present	0	15(55.6)	10(37)	2(7.4)	
Klintrup Makinen					
0	0	0	0	0	0.548
1	0	2(33.3)	4(66.7)	0	
2	0	4(30.8)	7(53.8)	2(15.4)	
3	0	1(100)	0	0	
Ki67					
Low (<15%)	0	5(35.7)	8(57.1)	1(7.1)	0.852
High (>15%)	0	2(28.6)	4(57.1)	1(14.3)	
Tumour Bud					
-Low	0	5(38.5)	7(53.8)	1(7.7)	0.797

-High	0	2(25)	5(62.5)	1(12.5)	
Tissue Stroma Percentage					
Low	0	4(26.7)	9(60)	2(13.3)	0.455
High	0	3(50)	3(50)	0	

5.3 DISCUSSION

Recent work by Hou et al. has demonstrated the role of Long Noncoding RNA 00504 gene (LINC00504) in induction of tumour development in breast cancer through inhibition of miR-140-5p-VEGFA pathway(227). RFX5 has been identified as the primary transcription factor for LINC00504, and that high RFX5 expression is associated with respectively high expression of LINC00504, which in turn was found to be upregulated in breast cancer, and played a critical role in proliferation, migration and invasion of breast cancer cells(227). Therefore, RFX5 may play multiple roles in breast cancer tumorigenesis and disease progression and may be a valuable target for further study.

Within our cohort, RFX5 was identified to be differentially expressed using TempO-Seq in patients with a high vs low tumour budding phenotype. RFX5 was expressed similarly in tumour cells as well as in peritumoural buds, allowing higher-throughput analysis of the entire Glasgow Breast Cancer Cohort using a TMA of cores from within the tumour. Despite the limitation of the available data (many cores were not valid for assessment due to the relative age of the specimens), it was possible to identify links between membrane, cytoplasmic and nuclear RFX5 expression and survival.

When examining each cellular compartment with regards to RFX5 staining and prognostic relevance, membrane scores varied from 0-280 (mean 8.4). Membrane RFX5 WHS did not predict survival across the cohort, but correlated with age (ER- patients), grade (ER+ patients) molecular subtype (all patients) and Klintrup Makinen (ER+ patients).

When examining cytoplasmic RFX5 WHS and survival, scores varied between 0-300 (mean 173.5). Across the cohort, low RFX5 was associated with reduced CSS (HR 0.265 (95%C.I. 0.083-0.843) p=0.025). The same was seen in the ER+ portion of the cohort, but not across the different molecular subgroups. It is possible that under-powering due to lack of patient numbers in some molecular subgroups may have failed to highlight any differences in survival between high and low RFX5 cytoplasmic expression groups.

For nuclear RFX5 scores and survival, scores varied between 0-150 (mean 16.9) but no significant difference in CSS was identified either within the cohort as a whole, or within the subgroup analysis for molecular subgroups. Some association between nuclear RFX5 and ki67(whole cohort), and KM (HER2-enriched) was seen, however.

When scores were combined, having “All-high” expression was found to be associated with worse prognosis, including after multivariate analysis. KM score appeared to be significantly associated with combined subgroup, an effect which was seen again in the TNBC group. Again, due to patient numbers being low in some molecular subgroups, this may have explained why the effect on survival was not seen in one particular molecular subgroup over another. In fact the HER2-enriched group, the opposite effect was seen, with “All-low” RFX5 score being associated with worse prognosis, although this effect was lost on multivariate analysis. TSP (Luminal A), Grade (Luminal B) and KM were associated with combined RFX5 score, however.

Finally, it appears that low cytoplasmic RFX5 may be associated with poorer CSS for patients with breast cancer, and that conversely, combined subgrouping into “all high” RFX5 expression may be associated with reduced survival. When comparing the results of this study to the literature(229), the latter suggests that expression does not correlate directly with improved or worsened prognosis, in turn suggesting that the effect may be regulatory in processes involved in tumorigenesis, proliferation and advancement of disease, with effects being more pronounced in certain disease subgroups. This may also suggest that the cellular location determines where the oncogenic properties of RFX5 are most significant, although further analysis and localisation studies will be required to elucidate this.

Chapter 6 TBX22

6.1 Introduction

T-Box Transcription Factor 22 (TBX22) belongs to a family of genes encoding transcription factors known as the T-box genes. TBX22, a protein-coding gene, has a well-documented role in the formation of the human palate (palatogenesis), and mutations and loss of function of the gene are associated with cleft palate, ankyloglossia, and other disorders of the formation of the components of the palate(231, 232). Changes in expression of T-box family genes have been associated in the inherited, and spontaneous disorders of organ development, although more recent work suggests a role may also exist for T-box genes in tumorigenesis and cancer progression(233, 234).

6.1.1 TBX22 and Cancer

T-box transcription regulator 2 (TBX2) has been associated with development and progression of childhood neuroblastomas(235), while TBX1 has been demonstrated to function as a tumour suppressor in papillary thyroid cancer (PTC)(236).

The role of TBX22 has not been documented in breast cancers, although recent work has suggested a role in papillary thyroid cancer (PTC) when over-expression of TBX22 was shown to have a tumour-suppressor role, inhibiting proliferation, invasion and migration in PTC cells(237). In addition, a role for TBX22 has been suggested in anticancer immunity, through a role in recruitment of anticancer CD8+ cells, T-helper cells, T-regulatory cells and Natural killer (NK) cells(237). Other T-box transcription regulators such as TBX2 and TBX3 have been shown to participate in EMT-related gene expression, such as SLUG and TWIST1, in breast cancers(234). TBX3 was shown to be highly expressed in low grade lesions compared to high grade breast cancers, particularly through the promotion of invasive behaviour and progression in DCIS and early-stage cancer(234). TBX2 was demonstrated to promote proliferation of breast cancer cells, through a role partnered with Early Growth Response 1 (EGR-1) to repress EGR-1-target genes, responsible for growth control mechanisms(233). It is therefore likely that other members of the T-box regulatory gene family may also play a part in tumour formation, progression and invasiveness, and TBX22 may represent a potential biomarker for breast cancer prognostication.

6.1.2 The Study Cohorts

The following chapter describes how TBX22 was identified as one of the most differentially expressed genes using TempO-Seq RNA transcriptional analysis of the Glasgow Breast Cancer Cohort surplus biorepository tissue and how this compares to TBX22 expression in the same cohort using immunohistochemistry. Prior to commencing the immunohistochemistry for the Glasgow Breast Cohort, the staining protocol was optimized, and specificity analysis was performed.

The process for the results therefore can be represented below, (*Figure 6-1*).

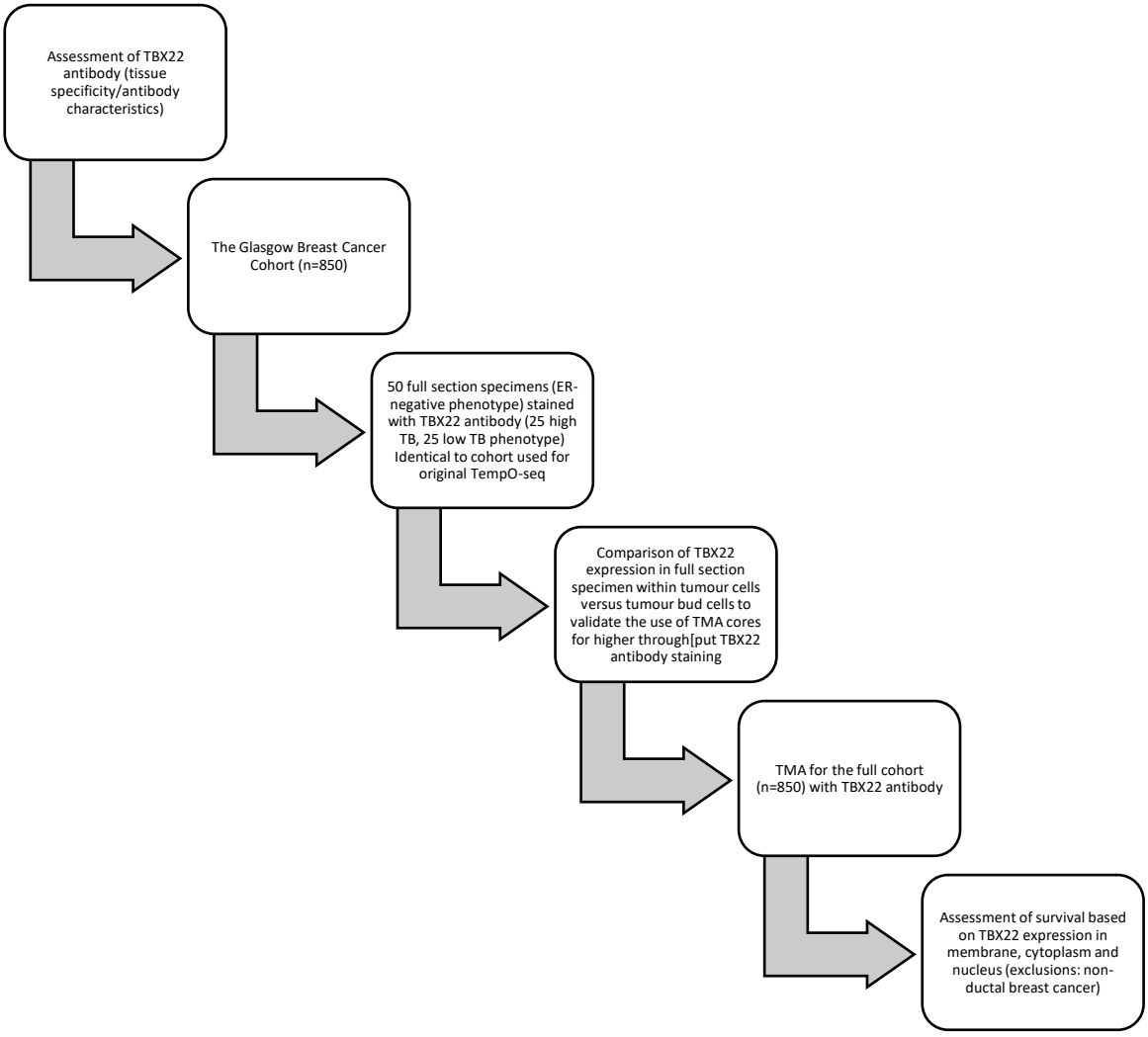

Figure 6-1 Study process flowchart for TBX22 protein expression analysis

The cohort was initially stained in part using the 50 full section ER-negative specimens used for TempO-Seq, originally selected by virtue of being either of high tumour budding (n=25) or low tumour budding (n=25) phenotype. TBX22 expression within the tumour was compared to that within the peritumoural buds, following which breast tissue microarrays for the entire Glasgow Breast Cancer Cohort were analysed to produce the results discussed later in this chapter.

Weighted histoscores (WHS) for this TBX22 expression in the cellular, membrane and nuclear compartments of breast tumour cells were manually assessed and analysed in relation to clinicopathological characteristics, including tumour budding, and cancer-specific survival. It was hypothesised that TBX22 expression may correlate inversely with survival and be more pronounced in patients with poorer prognostic indicators (higher disease stage, higher tumour budding status).

6.2 Results

6.2.1 TBX22 Expression Within Cell Lineages

To identify cell lines suitable for antibody specificity, an exploratory search was performed using DEPMAP, a freely accessible cancer dependency map online database which compiles the information from genomic data and large-scale cancer cell line datasets. When a search was performed for TBX22 protein expression (versus knockdown) and compiling the cancer cell line lineage data information with regards to TBX22 expression, Breast appeared to have transcripts per million (TPM) consistent with other cell cancer lineages, (*Figure 6-2*).

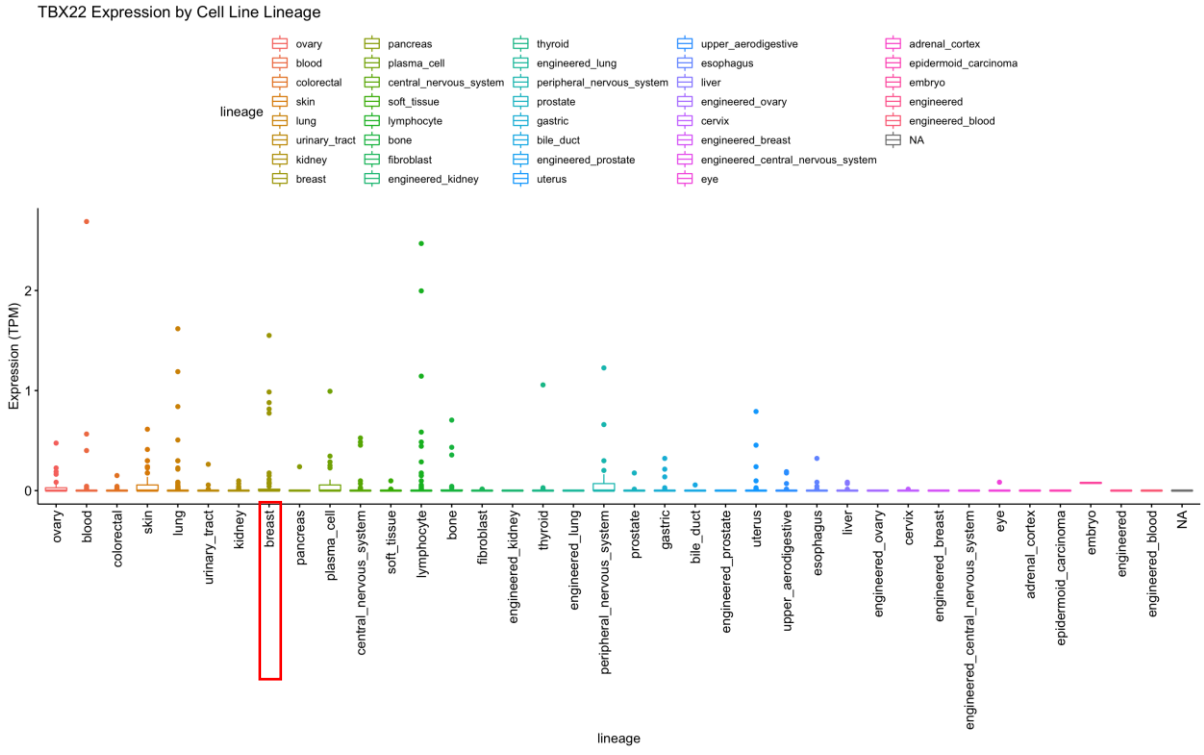

Figure 6-2 DEPMAP TBX22 expression by cell lineage (Transcripts per million, TPM: for every 1,000,000 RNA molecules in the RNA-seq sample, x came from this gene/transcript.)

When exclusively examining breast cancer cell lines known to express TBX22, there is considerable variability in expression, with low levels of expression in more than half of the overall lines for which information is available. Within our

laboratory, the available cell lines were MDAMB453 and MDAMB231, both of which were shown to have low expression of TBX22, (*Figure 6-3*). Due to this, it was not possible to produce satisfactory antibody specificity testing within this portion of the study. The same process was repeated for colorectal and prostate cancer cell lines, as these were the other available tissue types within our laboratory.

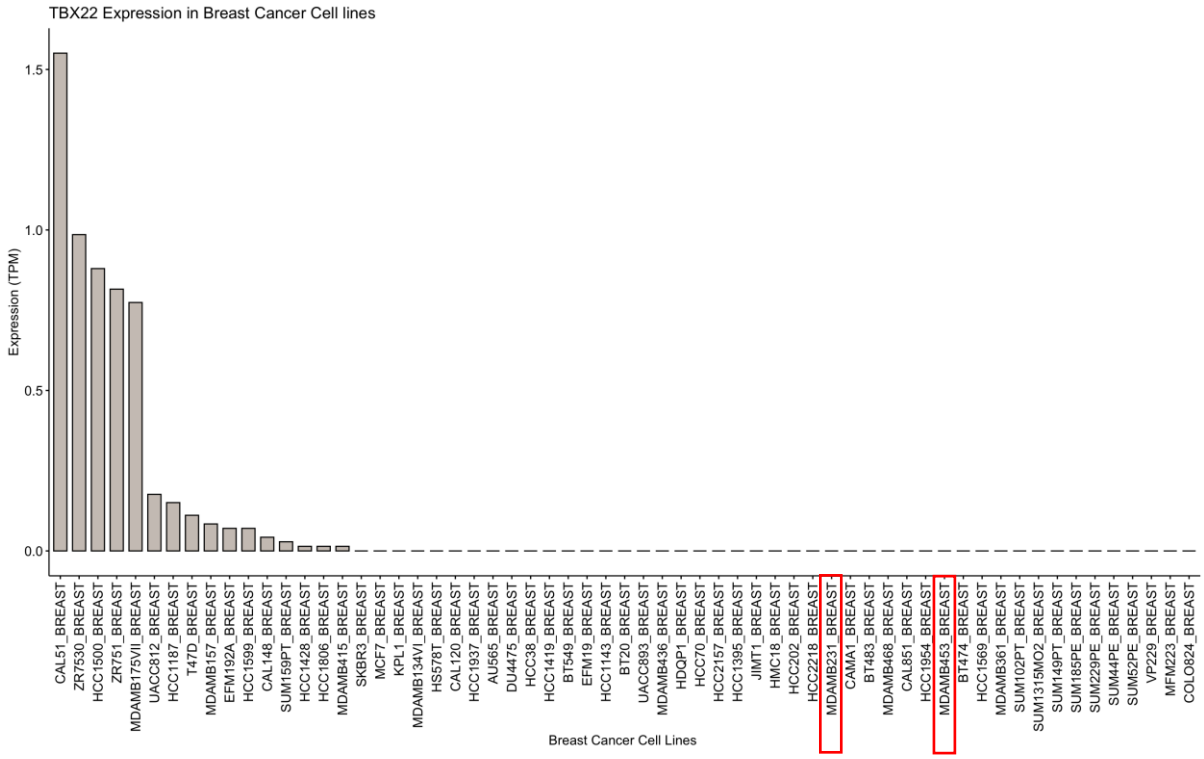

Figure 6-3 DEPMAP TBX22 Expression in Breast Cancer Cell lines (Transcripts per million, TPM: for every 1,000,000 RNA molecules in the RNA-seq sample, x came from this gene/transcript).

When DEPMAP was explored with regards to colorectal cancer cell lines, it appeared that most cell lines had some limited TBX22 RNA expression, of which two were available in our laboratory =, namely HT29 and T84 (*Figure 6-4*Figure 6-5). Despite relatively low expression levels noted, these two lines were selected for further analysis due to availability.

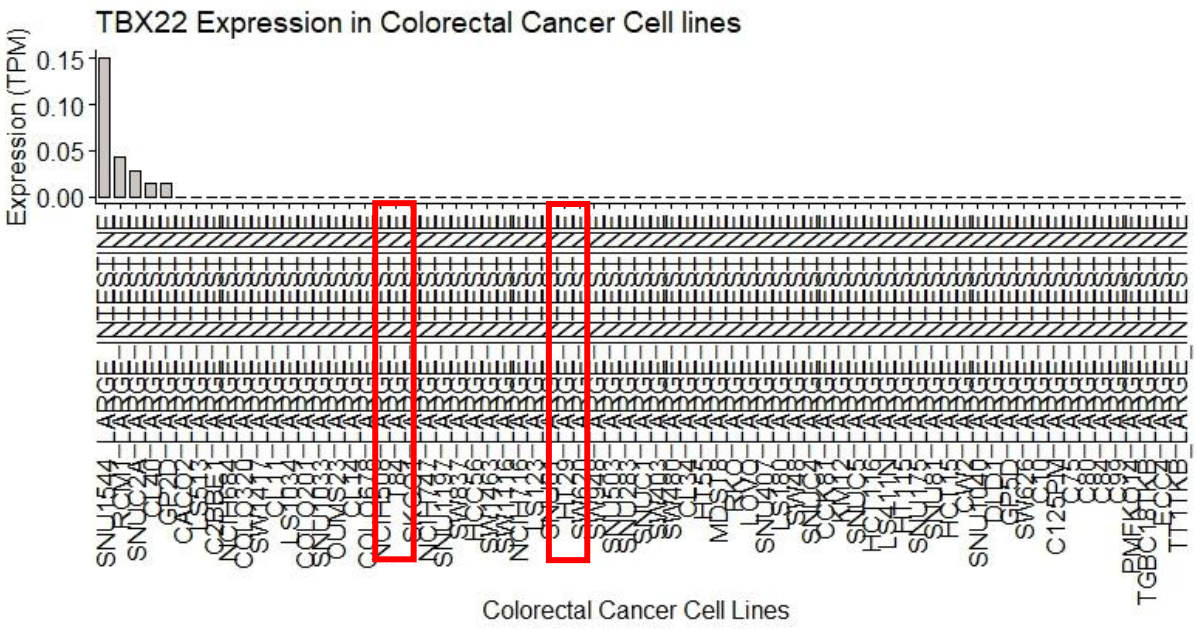

Figure 6-4 DEPMAP TBX22 Expression in Colorectal Cancer Cell lines (Transcripts per million, TPM: for every 1,000,000 RNA molecules in the RNA-seq sample, x came from this gene/transcript.)

When DEPMAP was probed for prostate cancer cell lines, fewer cell lines (11) had available data, although LNCAP cell lines figured here, and were available within our laboratory, although once again with minimal expression of TBX22 (*Figure 6-5*).

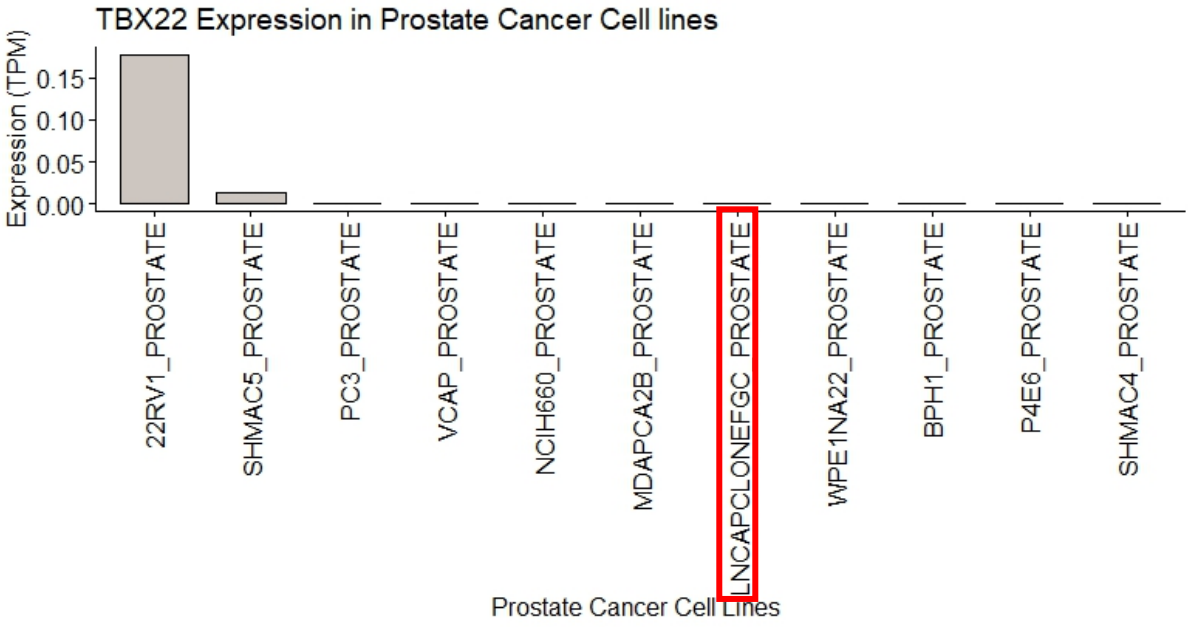

Figure 6-5 TBX22 Expression in Prostate Cancer Cell lines (Transcripts per million, TPM: for every 1,000,000 RNA molecules in the RNA-seq sample, x came from this gene/transcript.)

1.1. TBX22 antibody specificity

Examples of weak, moderate, and strong staining are shown in their respective sections within this chapter, together with a true positive and negative control tissue. Initial attempts to complete antibody specificity assays using Western Blotting were unsuccessful due to non-availability of cell lines with sufficient TBX22 expression. However, expression was identified on subsequent staining of breast specimens, and therefore analysis was performed on the Glasgow Breast Cancer Cohort.

6.2.2 TBX22 Expression in Full Section Specimens

TBX22 expression was first assessed using full section breast cancer tissue in a selected cohort of the Glasgow Breast Cancer Cohort. The sub-cohort of 50 patients had previously been used for TempO-Seq analysis and allowed identification of the most differentially expressed RNA, of which TBX22 was one. As described previously, 50 patient sections with ER-negative phenotype were selected, 25 with high tumour budding and 25 with low tumour budding characteristics. These were stained by stained for TBX22 (see methods). Manual weighted histoscores were produced for nuclear, cytoplasmic and membrane expression of TBX22 by a single observer (FS). 41 specimens were included for analysis, as 9 patients had missing/damaged section slides. Cytoplasmic, nuclear and membrane expression of TBX22 were manually scored for validation by Alan Whittingham using 10% of this sub-cohort. Scores varied from 0 to 130 for membrane, 0-210 for cytoplasm and 0-110 for nucleus. Each cellular location will be discussed in turn in the subsections below (Figure 5).

6.2.3 Membrane TBX22 Expression in Full Section Specimens

After selecting the original 50 patients with ductal cancer selected from the Glasgow Breast Cohort and used for TempO-Seq, these were stained using TBX22-specific antibody, weighted histoscores were generated by manual evaluation by a single observer (FS). Examples of light, moderate and strong membrane staining, together with positive and negative control tissue are shown below, (*Figure 6-6*).

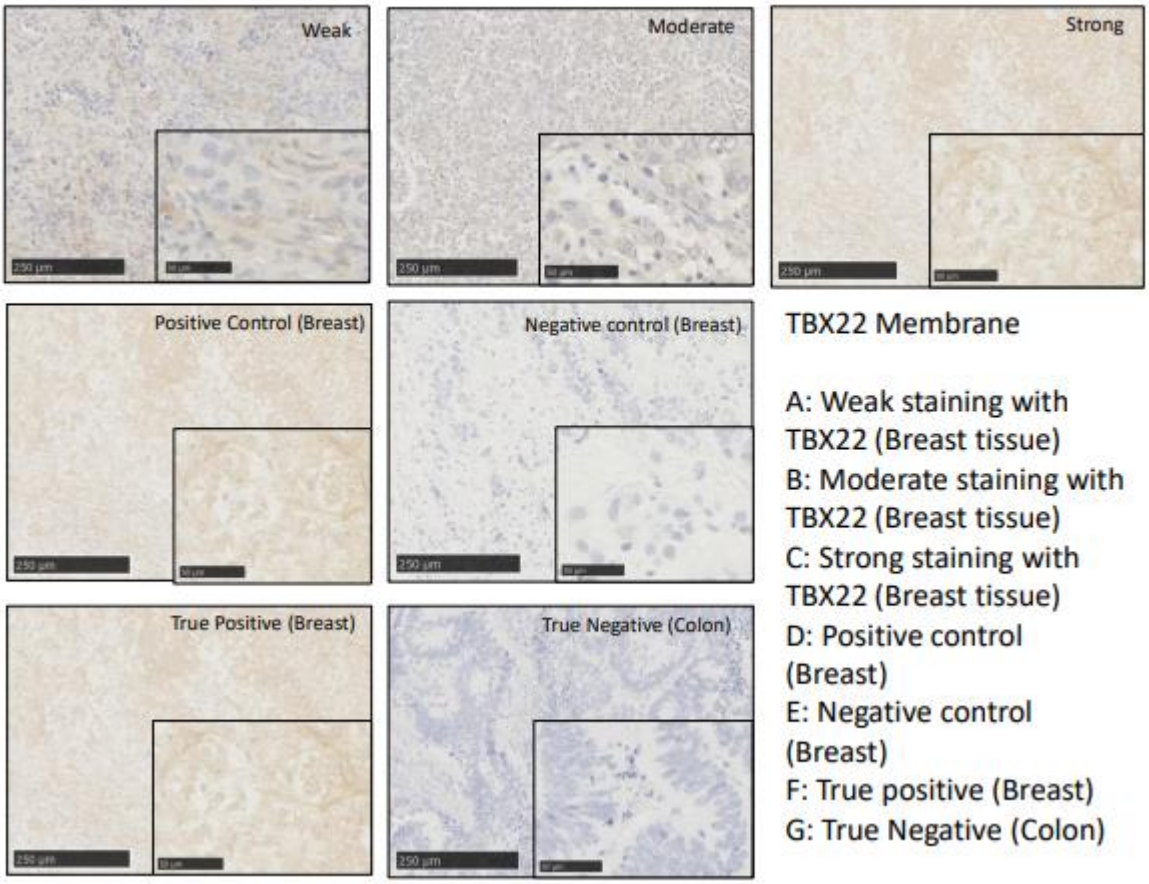

Figure 6-6 TBX22 membrane staining representative images.

Membrane expression of TBX22 was manually scored by a single assessor (FS), and scores varied from 0-60 (Figure 7). However, only 2 specimens had scores above 0. No further analysis was therefore performed for membrane TBX22 expression.

6.2.4 Cytoplasmic TBX22 Expression in Full section specimens

After selecting the original 50 patients with ductal cancer selected from the Glasgow Breast Cohort and used for TempO-Seq, these were stained using TBX22-specific antibody, weighted histoscores were generated by manual evaluation by a single observer (FS). Examples of light, moderate and strong cytoplasmic staining, together with positive and negative control tissue are shown below, (*Figure 6-7*).

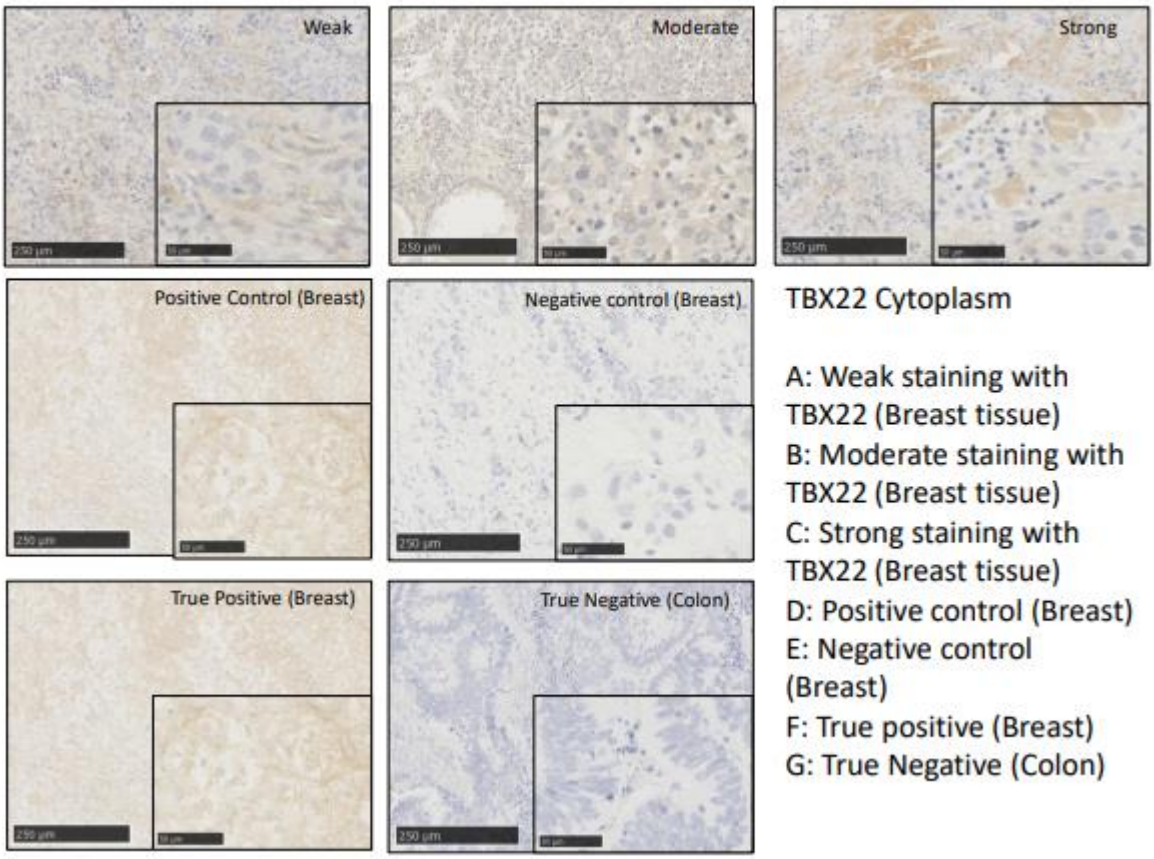

Figure 6-7 TBX22 cytoplasm staining representative images

Cytoplasmic expression of TBX22 was manually scored by a single assessor (FS), and scores varied from 0-300, (*Figure 6-8*).

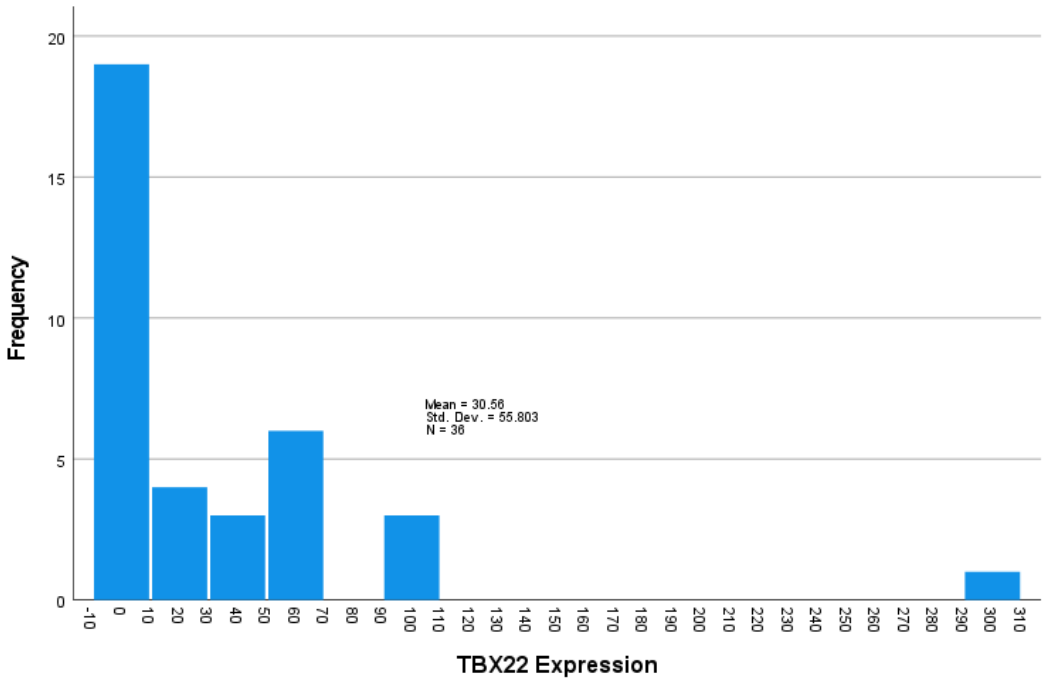

Figure 6-8 TBX22 cytoplasm expression (WHS, weighted histoscore)

Manual assessment for validation by AW using 10% of this sub-cohort is described using the scatter plot below, (*Figure 6-9*). An intraclass correlation coefficient

(ICCC) of 0.994 suggested a strong positive correlation between validation and primary assessors' scores.

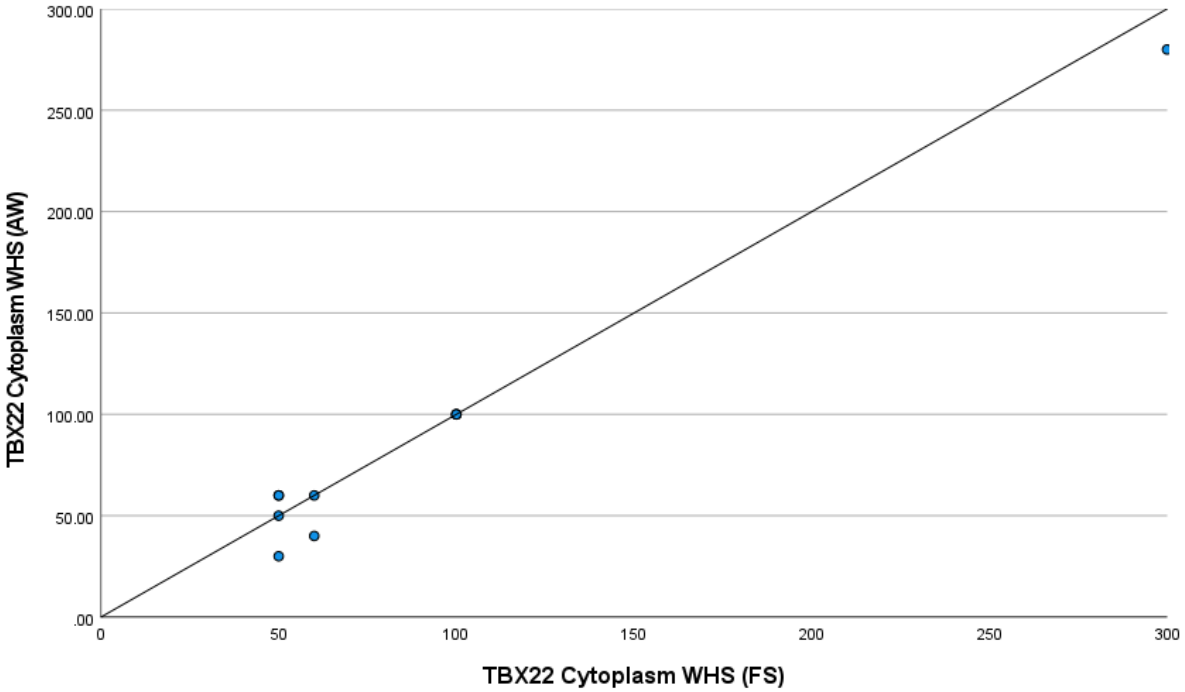

Figure 6-9 Correlation between FS and AW manual weighted histoscore (WHS) for TBX22 cytoplasm staining. Scatter plot showing correlation between FS and AW for cytoplasm TBX22 scores. Intraclass correlation coefficient of 0.933 for 10% specimens.

A subsequent comparison of averages and differences in scores was plotted as a Bland-Altman plot and demonstrated no bias between observers, (*Figure 6-10*).

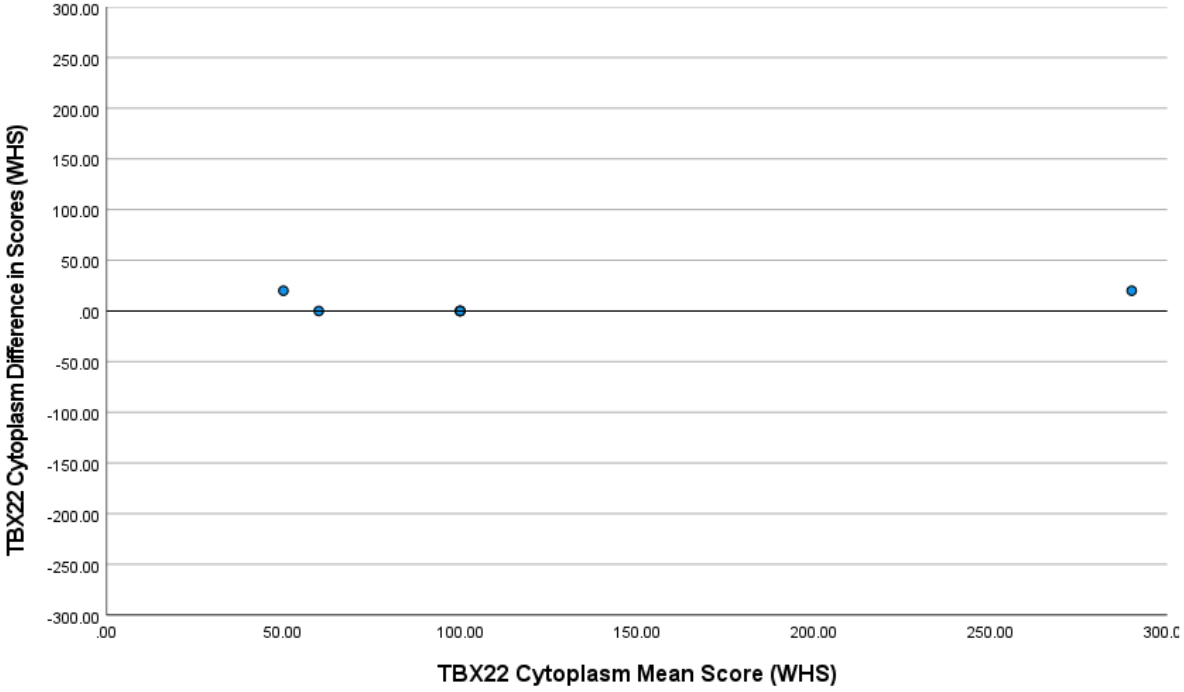

Figure 6-10 Bland-Altman Plot comparing difference in scores to mean scores for TBX22 expression in cytoplasm.

6.2.5 TBX22 Cytoplasmic Expression in Tumour Cells Versus Tumour Buds

TBX22 expression was compared between tumour buds (where present) and intratumoural cells. A scatter plot was used to visualise the correlation between cytoplasmic TBX22 expression in intratumoral cells and tumour buds, (*Figure 6-11*). Only 17 specimens had tumour buds present, in these specimens the WHS of the buds were comparable to that of the tumour core. The intraclass correlation coefficient (ICCC) was 0.988.

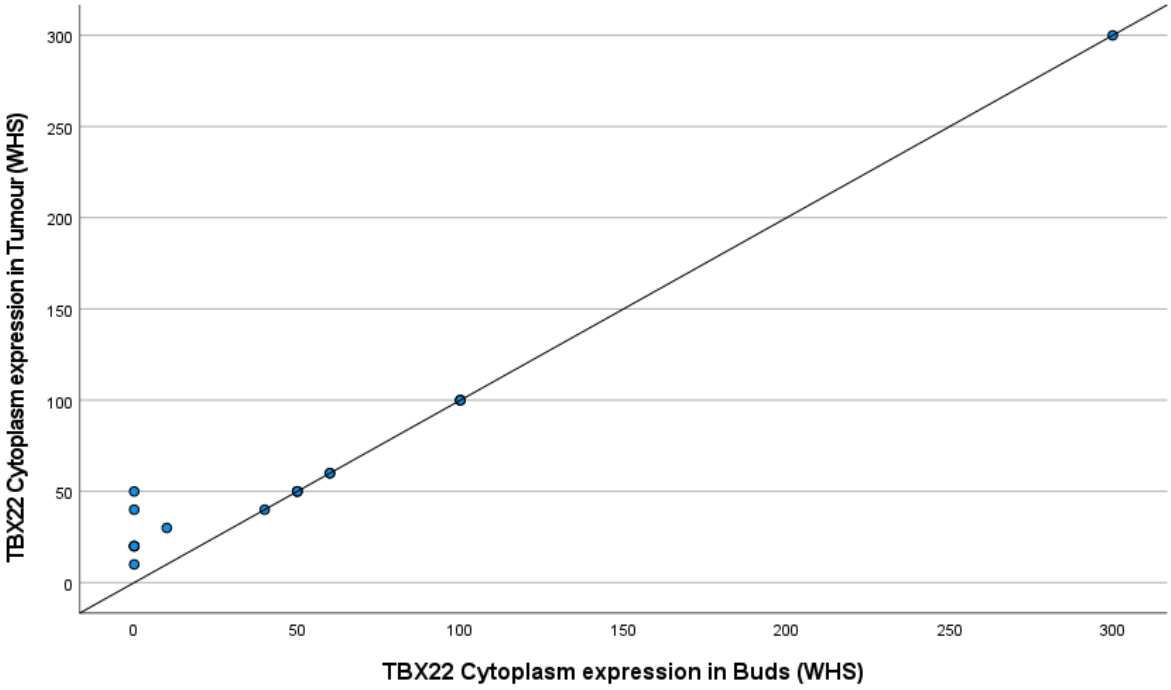

Figure 6-11 Cytoplasm TBX22 expression in tumour versus buds (WHS)

A subsequent comparison of averages and differences in scores was plotted as a Bland-Altman plot and demonstrated no bias between observers, (*Figure 6-12*Figure 5-12).

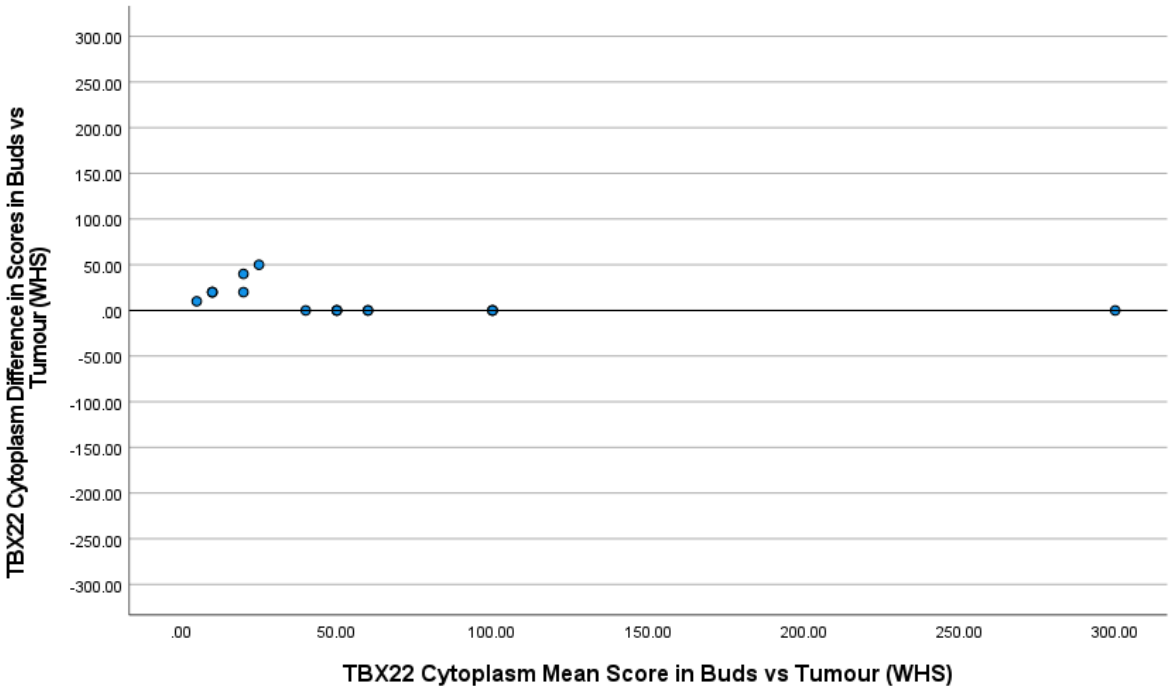

Figure 6-12 Bland-Altman Plot comparing the difference in scores to mean scores for TBX22 expression in cytoplasm in bud vs tumour cells.

Based on these findings, it was possible to infer that further analysis of protein expression could be expanded to the full cohort of the Glasgow Breast Cancer

Cohort in the form of a tissue microarray and remain representative of expression both within the tumour buds as in within the intratumoural environment, (*Figure 6-13*).

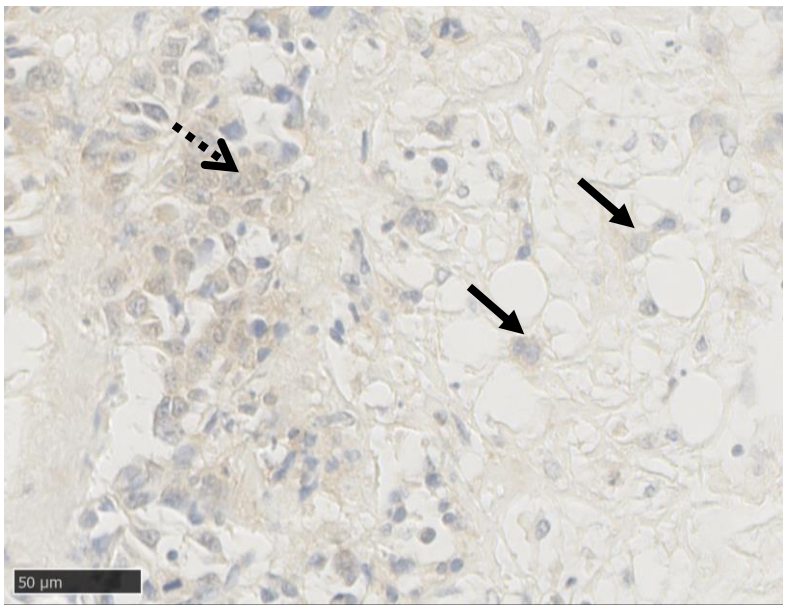

Figure 6-13 Cytoplasmic TBX22 staining in tumour mass (dotted arrow) correlated closely with staining in tumour buds (black arrow)

6.2.6 Nuclear TBX22 Expression in Full Section Specimens

Using TBX22-specific antibody, weighted histoscores were generated by manual evaluation by a single observer (FS). Examples of light, moderate and strong nuclear staining, together with positive and negative control tissue are shown below, (*Figure 6-14*).

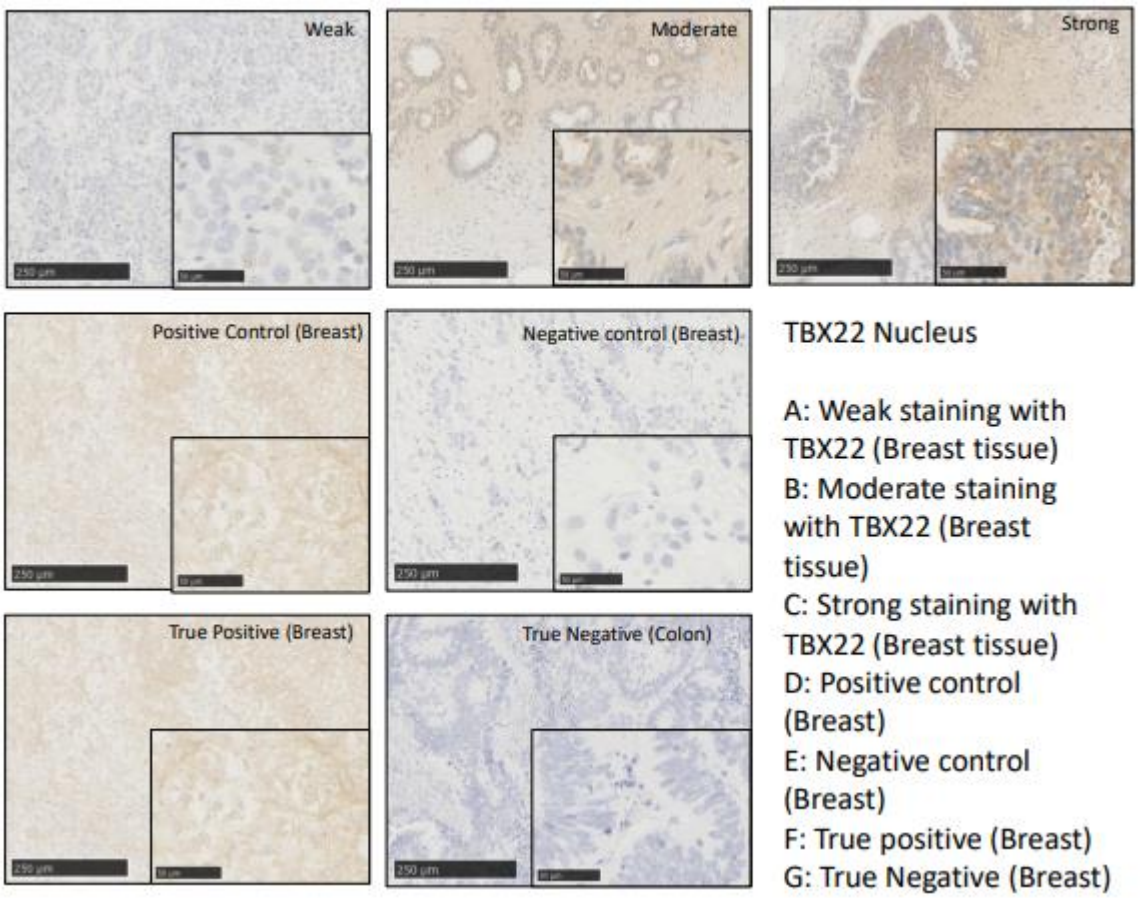

Figure 6-14 TBX22 Nucleus staining representative images.

Nuclear expression of TBX22 was manually scored by a single assessor (FS), and scores varied from 0-130 (*Figure 6-15)*.

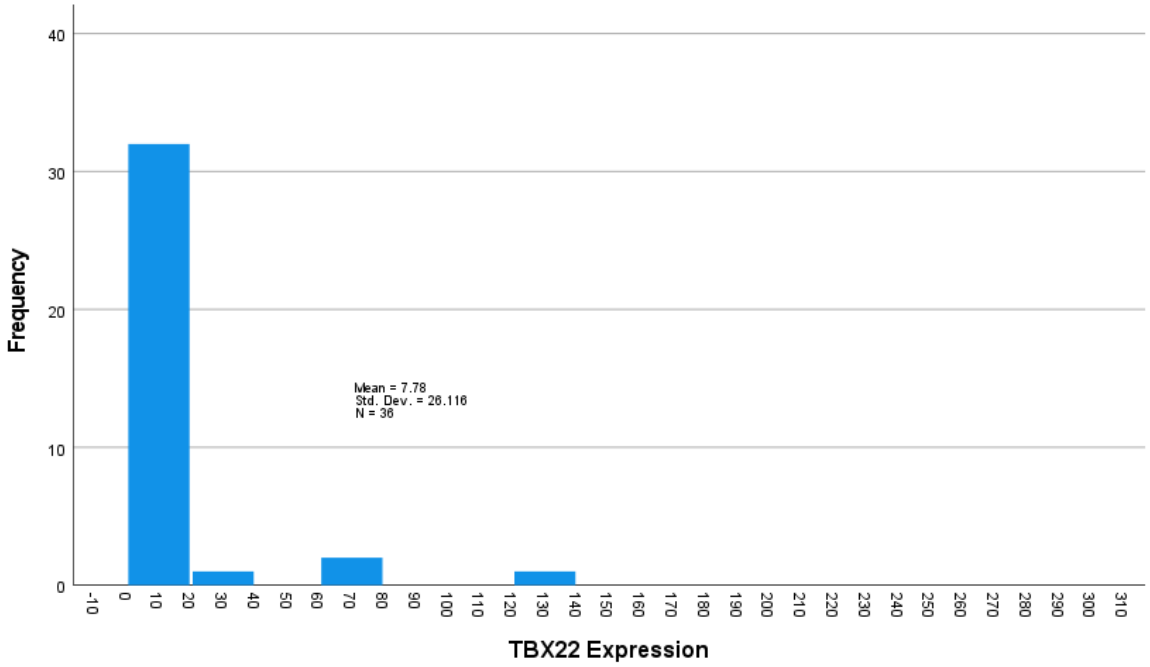

Figure 6-15 TBX22 nuclear expression (WHS, weighted histoscore)

Manual assessment for validation by AW using 10% of this sub-cohort is described using the scatter plot below (*Figure 6-16*). An intraclass correlation coefficient (ICCC) of 0.994 suggested a strong positive correlation between validation and primary assessors' scores.

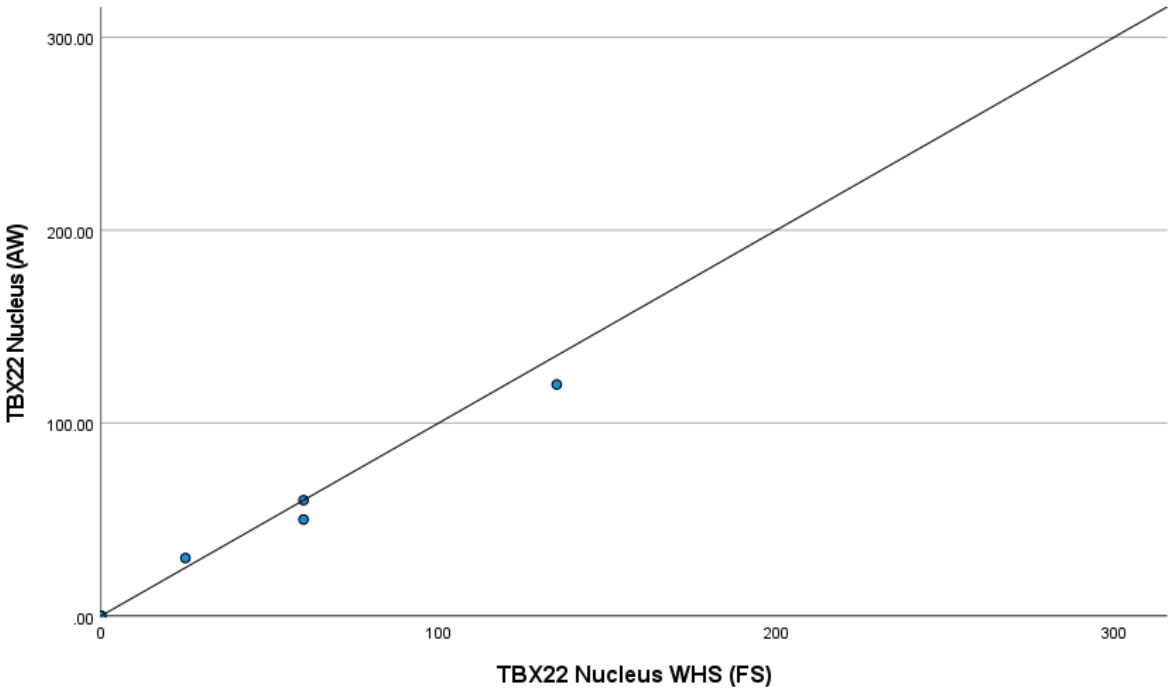

Figure 6-16 Correlation between FS and AW manual weighted histoscore (WHS) for TBX22 nucleus staining. Scatter plot showing correlation between FS and AW for nucleus TBX22 scores. Intraclass correlation coefficient of 0.933 for 10% specimens.

A subsequent comparison of averages and differences in scores was plotted as a Bland-Altman plot and demonstrated no bias between observers, (*Figure 6-17*).

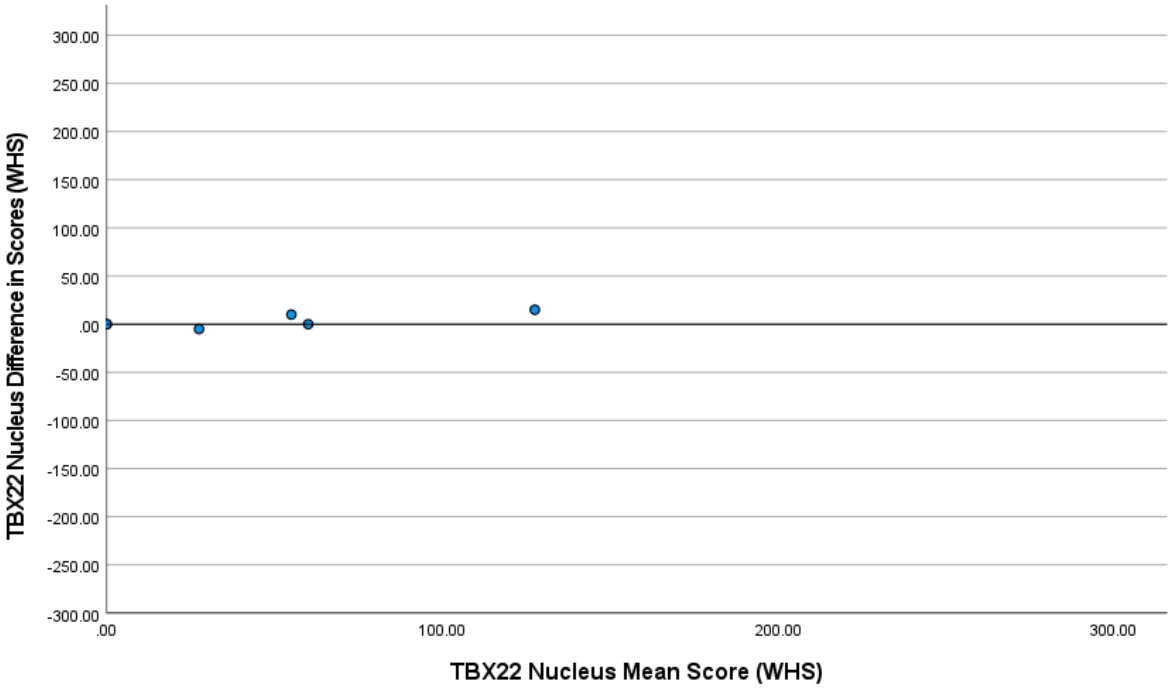

Figure 6-17 Bland-Altman Plot comparing difference in scores to mean scores for TBX22 expression in nucleus.

6.2.7 TBX22 Nuclear Expression in Tumour Cells Versus Tumour Buds

TBX22 expression was compared between tumour buds (where present) and intratumoural cells. A scatter plot was used to visualise the correlation between nuclear TBX22 expression in intratumoral cells and tumour buds (*Figure 6-18*). Only 17 full sections stained had tumour buds present, in these the WHS of the bud were comparable to that of the tumour core. The intraclass correlation coefficient (ICCC) was 0.993.

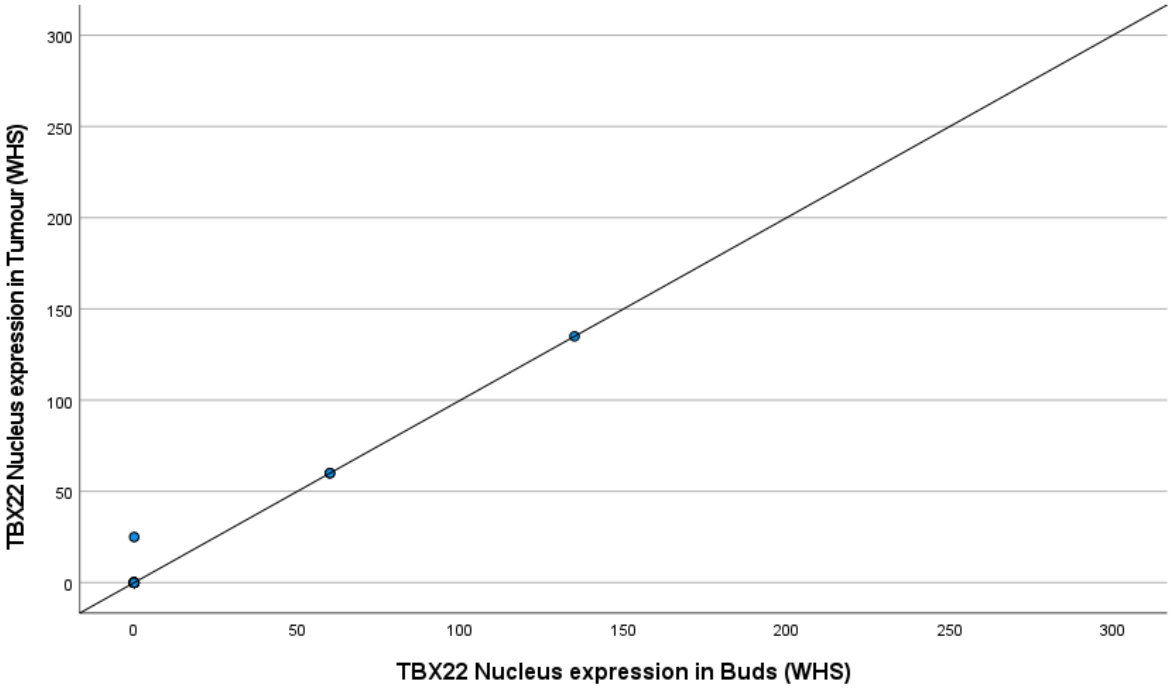

Figure 6-18 Nucleus TBX22 expression in tumour versus buds (WHS)

A subsequent comparison of averages and differences in scores was plotted as a Bland-Altman plot and demonstrated no bias between observers, (*Figure 6-19)*.

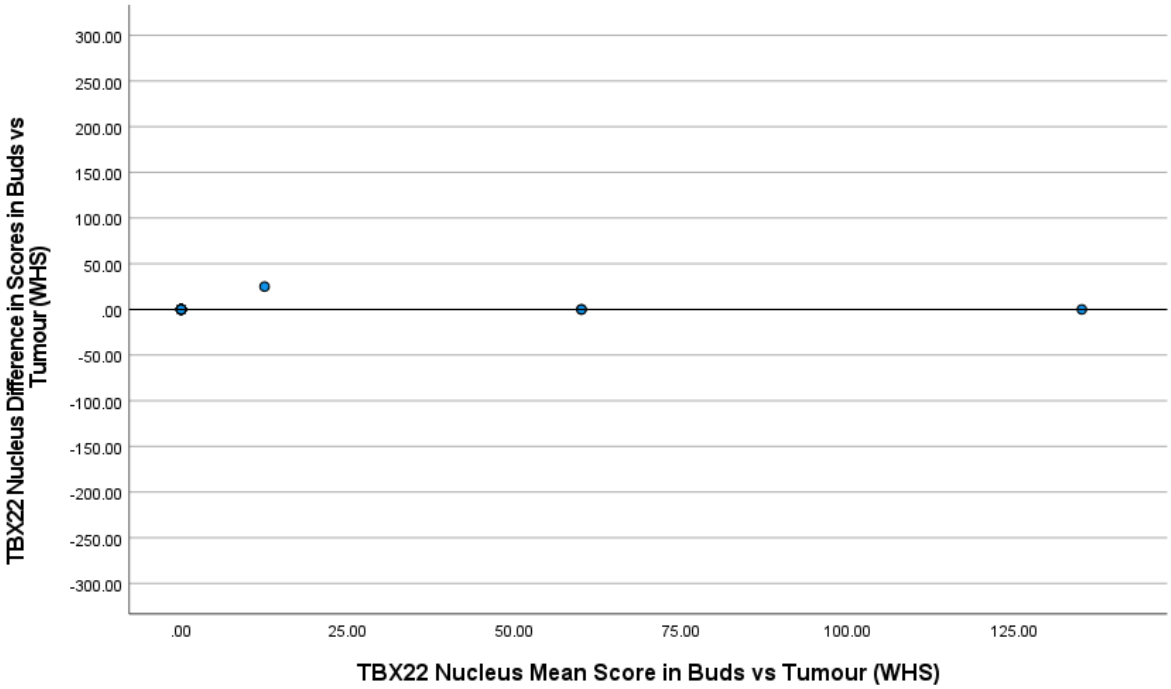

Figure 6-19 Bland-Altman Plot comparing the difference in scores to mean scores for TBX22 expression in nucleus in bud vs tumour cells.

Based on these findings, it was possible to infer that further analysis of protein expression could be expanded to the full cohort of the Glasgow Breast Cancer Cohort in the form of a tissue microarray and remain representative of

expression both within the tumour buds as in within the intratumoural environment, (*Figure 6-20*).

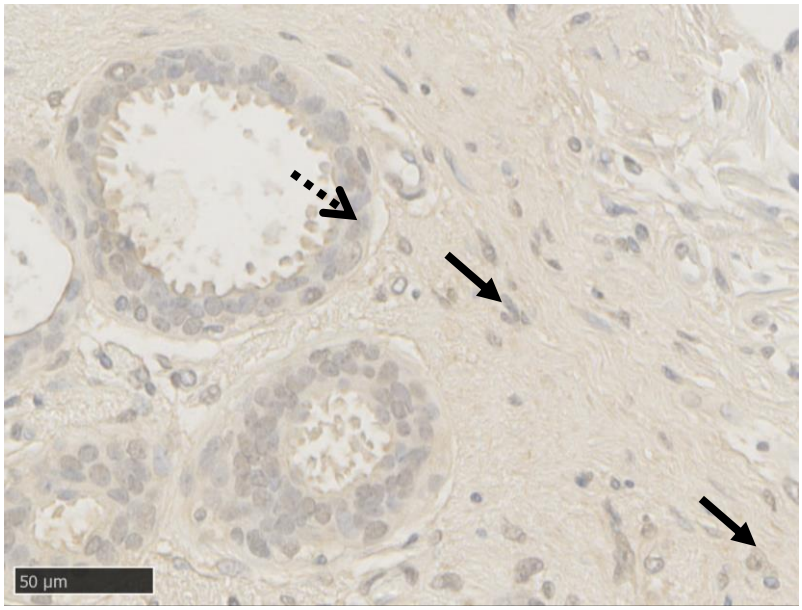

Figure 6-20 Nuclear TBX22 staining in tumour mass (dotted arrow) correlated closely with staining in tumour buds (black arrow)

6.2.8 TBX22 Expression in the Glasgow Breast Cancer Cohort

TMA slides composed of specimens from the Glasgow Breast Cancer cohort were used to assess TBX22 expression. Slides were stained with TBX22 antibody, and manually assessed to achieve a weighted histoscore. Included patients had ductal cancer only, resulting in 736 specimens being included in the overall cohort. Each specimen was assessed on 3 different TMA slides, and an average WHS was calculated, unless only one specimen was available, in which case this was used as the final 476 cases were included in the final analysis as out of the total 722 cases, 260 did not have assessable cores, (*Figure 6-21*)

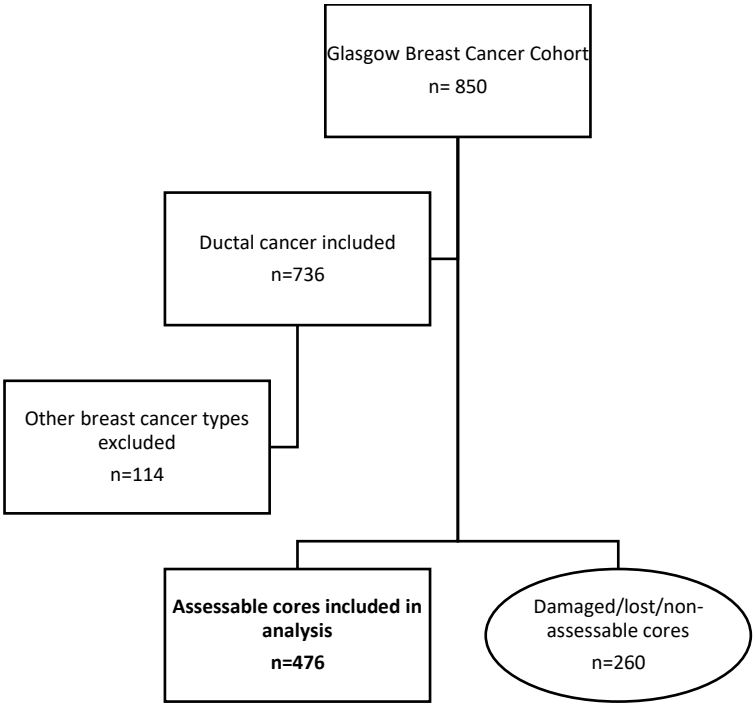

Figure 6-21 CONSORT diagram of cases included in analysis from the Glasgow Breast Cancer Cohort.

Manual weighted histoscores of cytoplasmic TBX22 expression were performed by FS. Validation of the scores was performed by Alan Whittingham.

6.2.9 TBX22 Membrane Expression in the Glasgow Breast Cancer Cohort

Manual weighted histoscores of membrane TBX22 expression were performed by FS. Scores by FS varied between 0 and 125, with a mean of 2.502 with only 22 cases scoring above 0, (*Figure 6-22*).

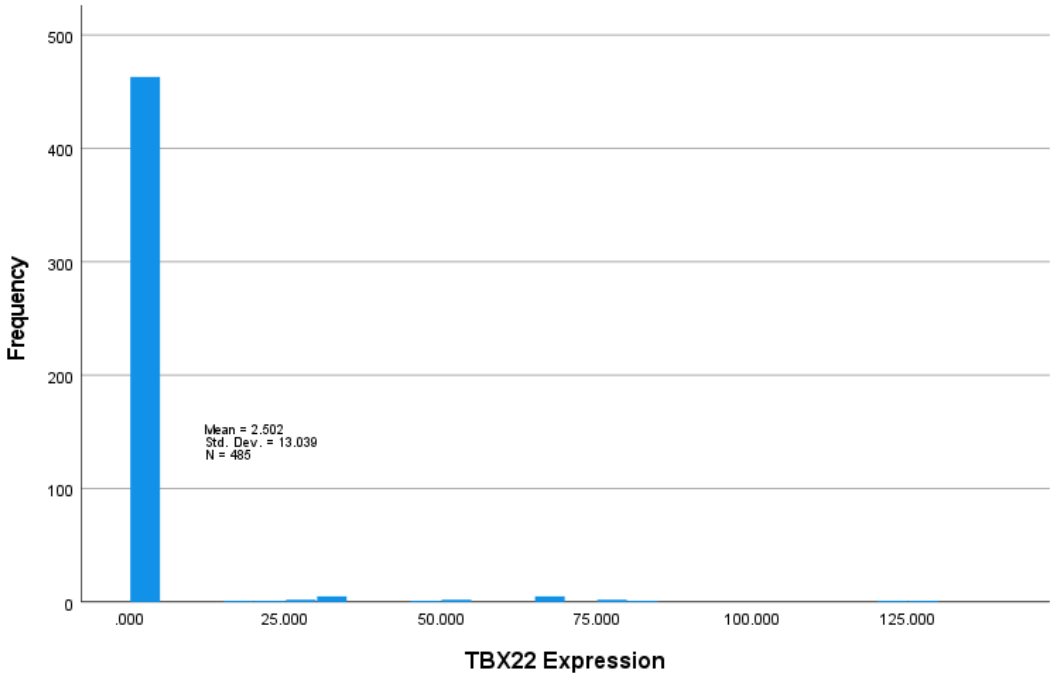

Figure 6-22 Distribution of TBX22 membrane expression (weighted histoscores) in the Glasgow Breast Cancer Cohort. Mean score 2.502, SD 13.039.

Due to the small number of cases with scores above 0, it was not possible to obtain a threshold for high vs low expression of TBX22 in the membrane. Therefore, no further counter-scoring or analysis was produced.

6.2.10 TBX22 Cytoplasmic Expression in the Glasgow Breast Cancer Cohort

Manual weighted histoscores of membrane TBX22 expression were performed by FS. Scores by FS varied between 0 and 256, with a mean of 88.585, (*Figure 6-23*).

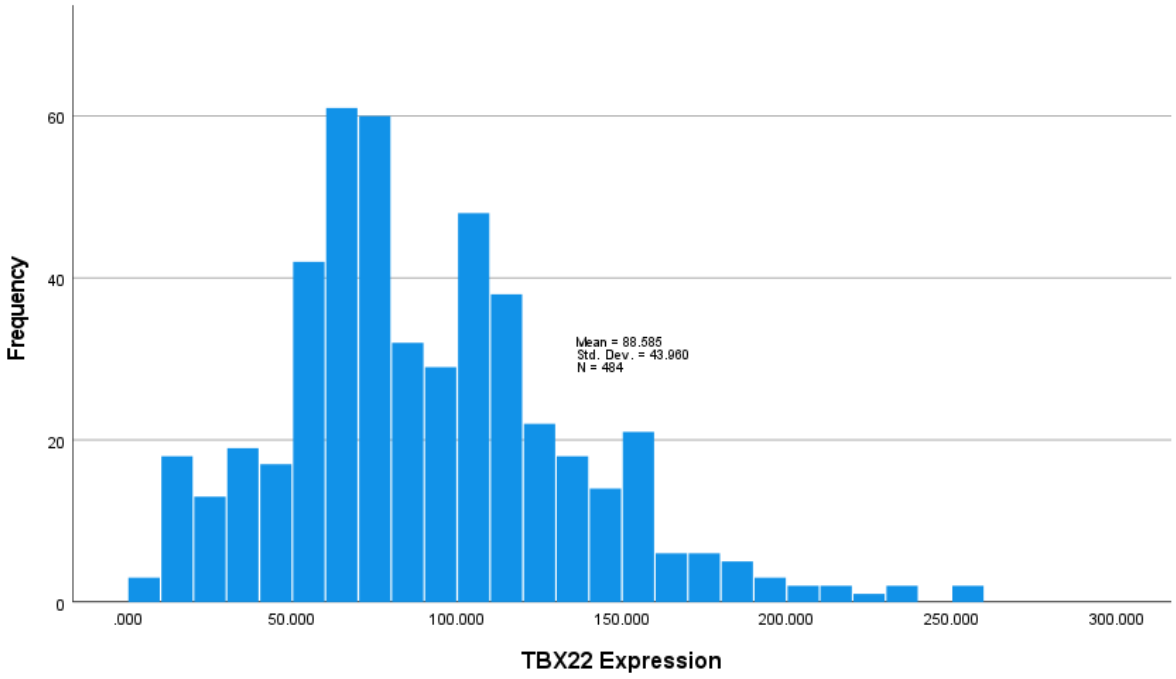

Figure 6-23 Distribution of TBX22 cytoplasmic expression in Glasgow Breast Cancer Cohort. Mean Score 88.585, SD 43.960.

Counter-scores were performed manually by AW for a minimum of 10% of cores, (n=49) and are shown below for comparison, (*Figure 6-24*). WHS were reproducible between the two scorers for 49 cores. An intraclass correlation coefficient (ICCC) of 0.894 suggested a strong positive correlation between validation and primary assessor's scores.

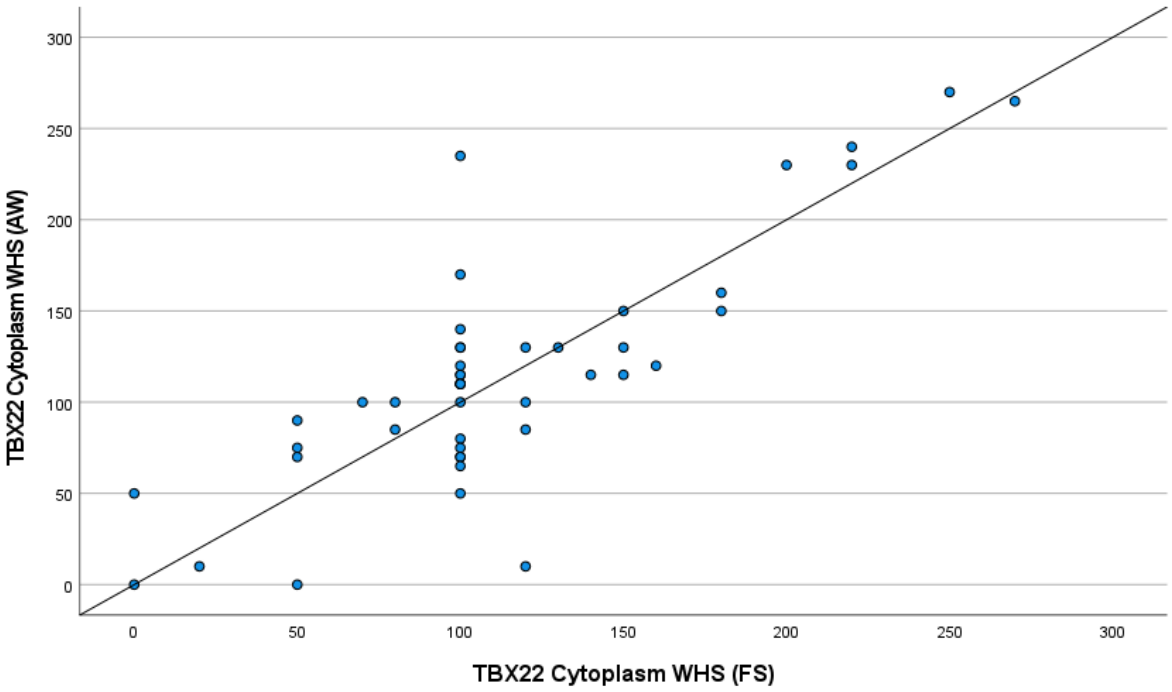

Figure 6-24 Correlation between FS and AW manual weighted histoscore (WHS) for TBX22 cytoplasm staining. Scatter plot showing correlation between FS and AW for cytoplasm TBX22 scores. Intraclass correlation coefficient 0.9894 for 10% specimens.

A subsequent comparison of averages and differences in scores was plotted as a Bland-Altman plot and demonstrated no bias between observers, (*Figure 6-25*).

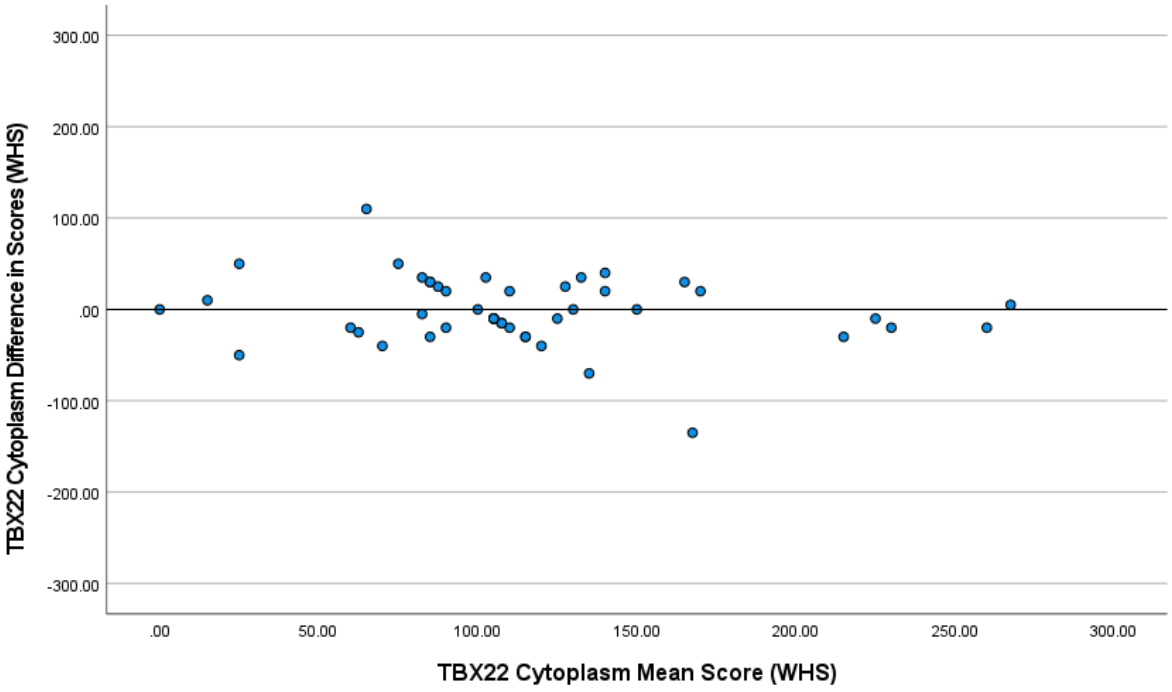

Figure 6-25 Bland-Altman Plot comparing difference in scores to mean scores for TBX22 cytoplasmic expression.

A threshold for high and low TBX22 cytoplasm expression was delineated using R Studio to compare high versus low TBX22 cytoplasmic expression according to survival. The threshold was identified as 46.67 as described below, (*Figure 6-26*).

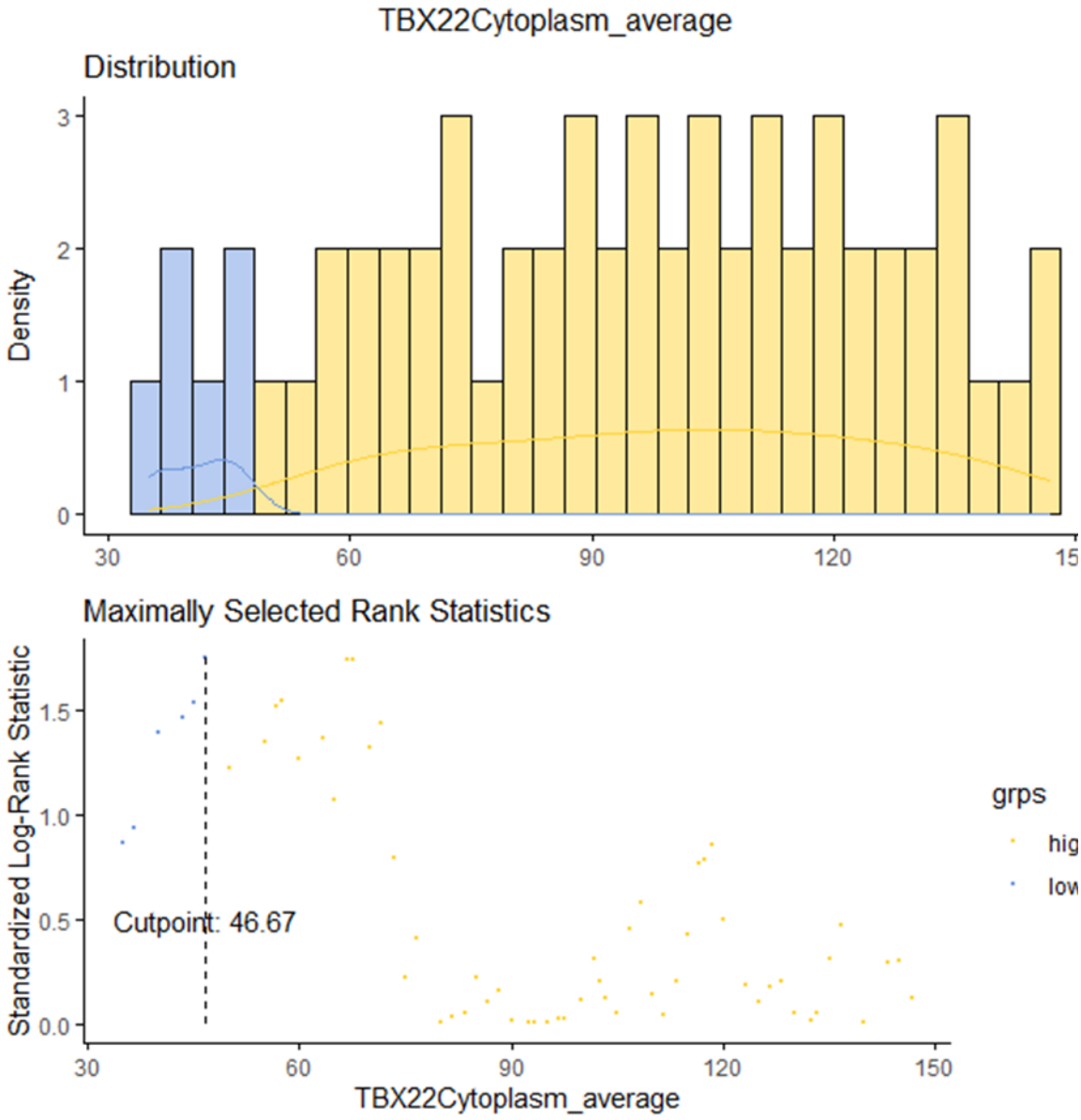

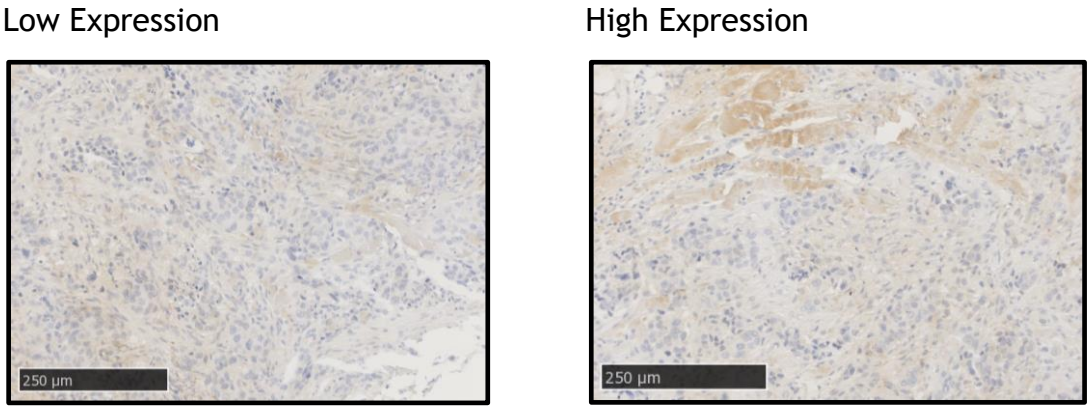

Figure 6-26 TBX22 cytoplasmic expression threshold for high and low expression in the cytoplasm of the Glasgow Breast Cancer Cohort. The threshold was identified as 46.67, with patients with weighted scores above 46.67 considered to have high TBX22 cytoplasm

expression. Examples of protein expression as seen on specimens is also described below the graphical representation.

6.2.11 Cytoplasmic TBX22 and Survival in the Glasgow Breast Cancer Cohort

850 patients had TMAs produced for the Glasgow Breast Cancer Cohort, of which 736 had ductal cancer and were included in the cohort for analysis. Of these, 722 of 736 had valid cancer-specific survival data and 484 had viable cores, leading to a final 476 patients with both viable cores and valid survival data. 66 patients had low TBX22 cytoplasmic expression and had 10 events, while 410 had high expression and saw 98 events. Survival in the low TBX22 group was 90% at 5 years, and 83% at 10 years, while in the high TBX22 group survival was 83% at 5 years, and 71% at 10 years. Using Kaplan Meier survival analysis, mean cancer-specific survival (CSS) time for low TBX22 cytoplasm expression was 158.5 months compared to high TBX22 expression survival of 149.8 months, suggesting that low TBX22 cytoplasm expression was associated with increased survival, although this was not statistically significant (HR 1.642, 95% C.I.; 0.856-3.147, log rank p=0.135), (*Figure 6-27*).

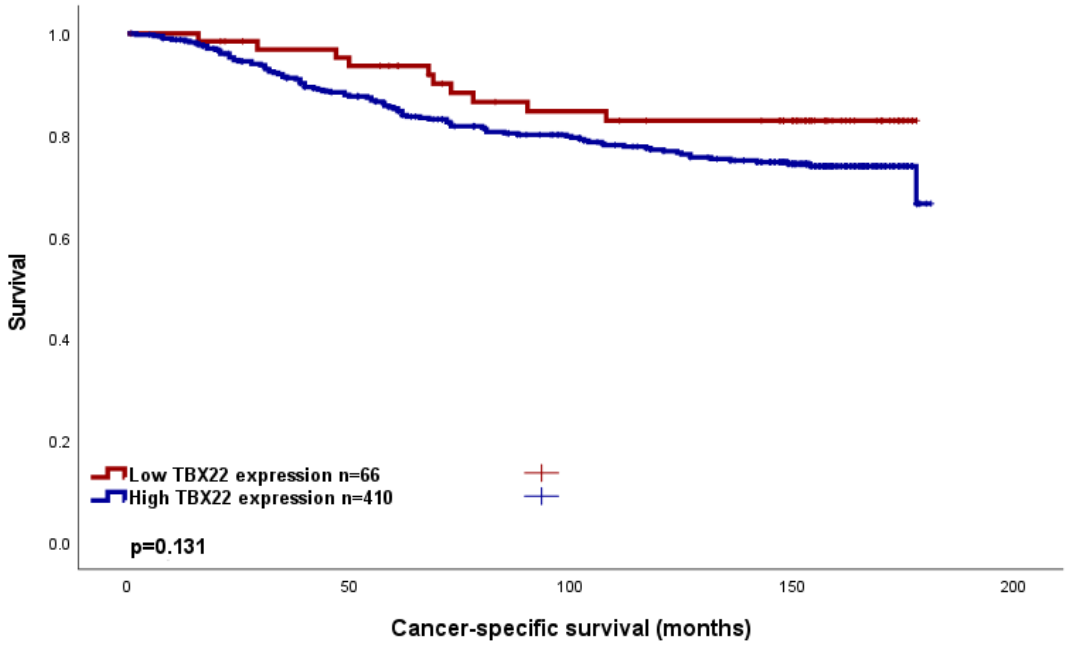

Figure 6-27 Cancer-specific survival in the Glasgow Breast Cancer Cohort according to TBX22 cytoplasm expression. Kaplan Meier Curve showing the association between TBX22 cytoplasm expression and survival (months). HR 1.642, 95% C.I.; 0.856-3.147, log rank p=0.135

Within the entire Glasgow Breast Cancer Cohort, inter-factor correlation was assessed when comparing the high and low TBX22 cytoplasmic expressors, (*Table*

6-1). Here, an association between molecular subtype and TBX22 cytoplasmic expression was seen.

Table 6-1 Clinicopathological factors and their relation to TBX22 cytoplasmic expression in the Glasgow Breast Cancer Cohort. Chi-squared analysis.

Clinicopathological factor	**TBX22 Cytoplasmic staining (%)**		**p**
	Low	**High**	
Age (years)			
<50	20(12.7)	137(87.3)	0.778
>50	46(14.1)	281(85.9)	
Tumour Size			
<20mm	37(14.1)	226(85.9)	0.808
21-49mm	27(13.6)	171(86.4)	
>50mm	2(9.1)	20(90.9)	
Grade			
I	12(13.8)	75(86.2)	0.966
II	27(13.2)	178(86.8)	
III	27(14.1)	165(85.9)	
Molecular Subtype			
Luminal A	**30(14.4)**	**179(85.6)**	**0.05**
Luminal B	**18(14.8)**	**104(85.2)**	
TNBC	**12(12.6)**	**83(87.5)**	
HER2 enriched	**0**	**47(100)**	
Nodal Status			
N0	35(12.9)	236(87.1)	0.553
N1	30(14.3)	180(85.7)	
Lymphatic Invasion			
Absent	33(18.1)	149(81.9)	0.168
Present	11(11.2)	87(88.8)	
Vascular Invasion			
Absent	41(16.7)	205(83.3)	0.318
Present	3(8.8)	31(91.2)	
Necrosis			
Absent	33(14.8)	190(85.2)	0690
Present	33(13.1)	218(86.9)	
Klintrup Makinen			
0	612.8)	41(87.2)	0.529
1	42(15.9)	222(84.1)	
2	13(10.4)	112(89.6)	
3	5(13.5)	32(86.5)	
Ki67			
Low (<15%)	42(13.7)	265(86.3)	0.665
High (>15%)	19(11.9)	141(88.1)	
Tumour Bud			
-Low	46(14.3)	276(85.7)	0.675
-High	20(12.7)	137(87.3)	
Tissue Stroma Percentage			
Low	50(15)	283(85)	0.253

High	16(11)	130(89)	

The cohort was subsequently stratified according to Oestrogen receptor status (ER-negative; ER-, and ER-positive; ER+). In the ER- group (149 patients), 14 patients had low cytoplasm TBX22 and 2 events, and 135 had high TBX22, for 44 events. Within the ER- cases, 5-year survival was 85% in low TBX22 cases, compared to 73% in high TBX22 cases. 10-year survival was 85% in the low TBX22 group compared to 62% in the high TBX22 group. Mean survival for ER- patients was 157.3 for low cytoplasm TBX22 expression, and 135.2 months for high TBX22 (HR 2.543 95% C.I. 0.617-10.493, log rank p=0.197), (*Figure 6-28*).

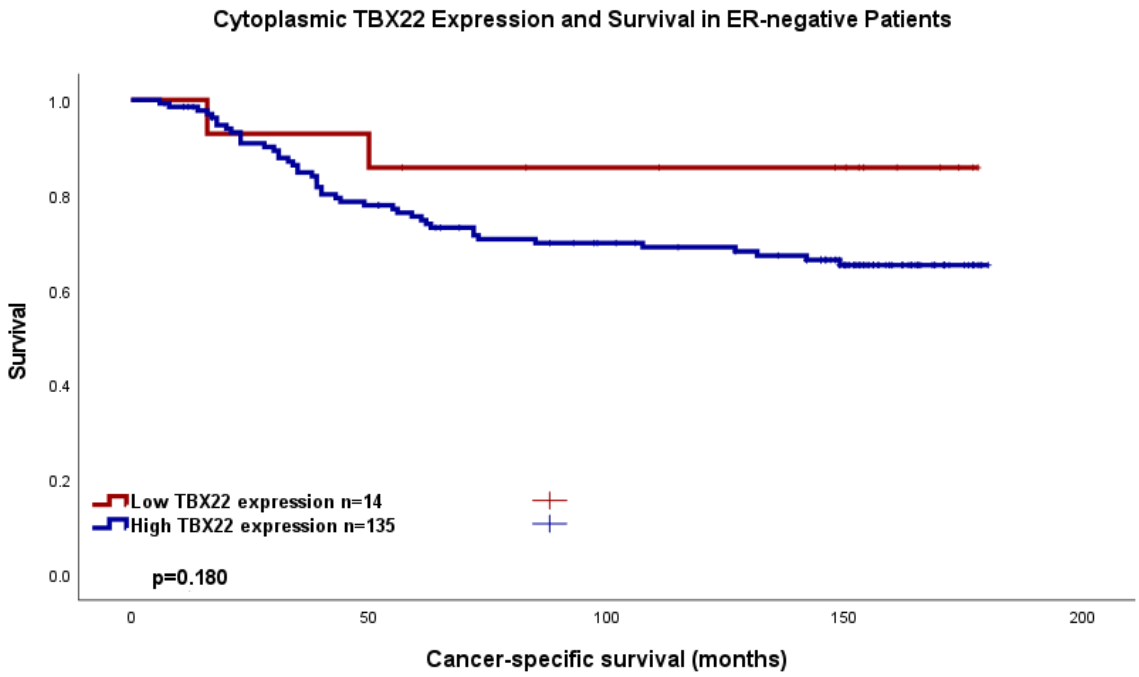

Figure 6-28 Cancer-specific survival in ER negative patients in the Glasgow Breast Cancer Cohort according to TBX22 cytoplasm expression. Kaplan Meier Curve showing the association between TBX22 cytoplasm expression and survival (months). HR 2.543 95% C.I. 0.617-10.493, log rank p=0.197.

Within the ER-negative group, inter-factor correlation was assessed when comparing the high and low TBX22 cytoplasmic expressors, (Table 6-2). Here, age and lymphatic invasion were associated with TBX22 cytoplasmic expression.

Table 6-2 Clinicopathological factors and their relation to TBX22 cytoplasmic expression in the ER-negative patients within the Glasgow Breast Cancer Cohort. Chi-squared analysis

Clinicopathological factor	**TBX22 Cytoplasmic staining (%)**		**p**
	Low	**High**	
Age (years)			
≤50	**11(17.7)**	**51(82.3)**	**0.004**
>50	**3(3.4)**	**84(96.6)**	

Tumour Size			
≤20mm	5(6.8)	69(93.2)	0.245
21-49mm	9(13.6)	57(86.4)	
≥50mm	0	8(100)	
Grade			
I	1(20)	4(80)	0.711
II	3(9.1)	30(90.9)	
III	10(9)	101(91)	
Nodal Status			
N_0	8(9.9)	73(90.1)	1.000
N_1	9(12.7)	62(87.3)	
Lymphatic Invasion			
Absent	**9(17.6)**	**42(82.4)**	**0.023**
Present	**0**	**30(100)**	
Vascular Invasion			
Absent	9(12.9)	61(87.1)	0.349
Present	0	11(100)	
Necrosis			
Absent	3(8.8)	31(91.2)	1.000
Present	11	103(90.4)	
Klintrup Makinen			
0	0	4(100)	0.918
1	6(10.3)	52(89.7)	
2	6(9.1)	60(90.9)	
3	12(41.4)	17(58.6)	
Ki67			
Low (<15%)	9(10.7)	75(89.3)	0.364
High (>15%)	3(5.5)	52(94.5)	
Tumour Bud			
-Low	10(8.6)	106(91.4)	0.503
-High	4(12.5)	28(87.5)	
Tissue Stroma Percentage			
Low	10(9.3)	97(90.7)	1.000
High	4(9.8)	37(90.2)	

In the ER+ group (327), 52 patients had low cytoplasm TBX22 and 8 events, and 275 had high TBX22, for 54 events. Within the ER+ cases, 5-year survival was 91% in low TBX22 cases, compared to 88% in high TBX22 cases. 10-year survival was 82% in the low TBX22 group compared to 75% in the high TBX22 group. Mean survival for ER- patients was 157.9 for low cytoplasm TBX22 expression, and 156.5 months for high TBX22 (HR 1.261 95% C.I. 0.599-2.651, log rank p=0.541) (*Figure 6-29*).

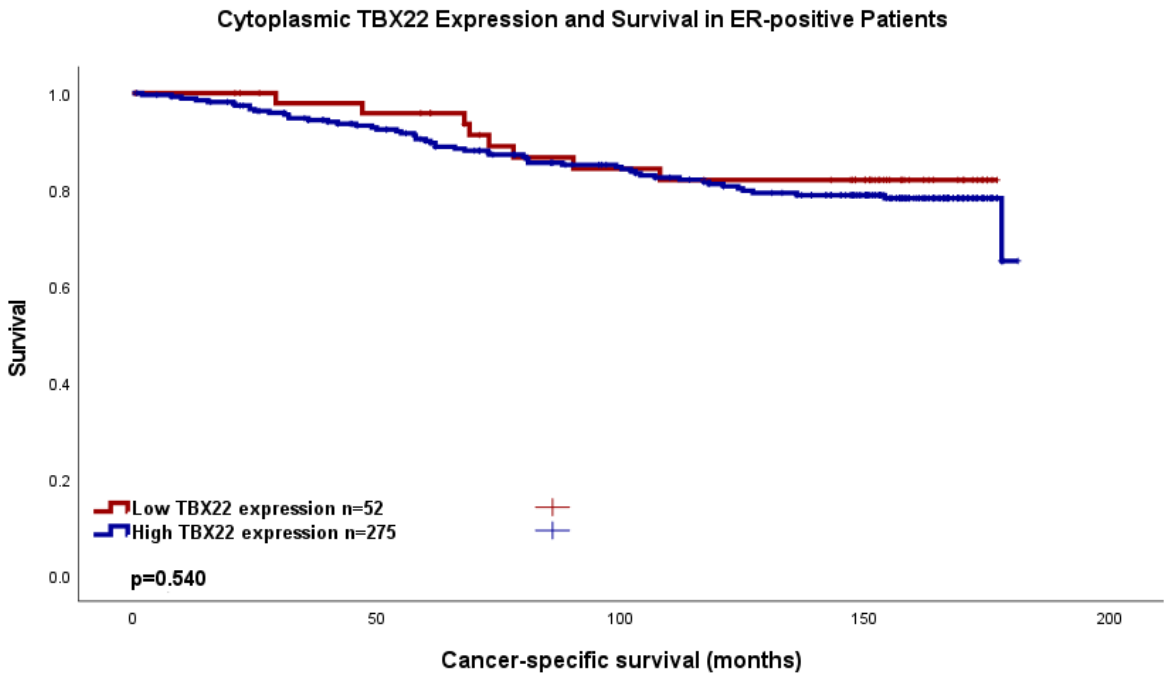

Figure 6-29 Cancer-specific survival in ER negative patients in the Glasgow Breast Cancer Cohort according to TBX22 cytoplasm expression. Kaplan Meier Curve showing the association between TBX22 cytoplasm expression and survival (months). HR 1.261 95% C.I. 0.599-2.651, log rank p=0.541.

Within the ER-positive group, inter-factor correlation was assessed when comparing the high and low TBX22 cytoplasmic expressors, (Table 6-3). Here, age neared statistical significance in association with TBX22 cytoplasmic expression.

Table 6-3 Clinicopathological factors and their relation to TBX22 cytoplasmic expression in the ER-positive patients the Glasgow Breast Cancer Cohort. Chi-squared analysis

Clinicopathological factor	TBX22 Cytoplasmic staining (%)		p
	Low	High	
Age (years)			
≤50	9(9.5)	86(90.5)	0.065
>50	43(17.9)	197(82.1)	
Tumour Size			
≤20mm	32(16.9)	157(83.1)	0.719
21-49mm	18(13.6)	114(86.4)	
≥50mm	2(14.3)	12(85.7)	
Grade			
I	11(13.4)	71(86.6)	0.294
II	24(14)	148(86)	
III	17(21)	64(79)	
Nodal Status			
N_0	27(14.2)	163(85.8)	0.554
N_1	24(16.9)	118(83.1)	
Lymphatic Invasion			

Absent	24(183)	107(81.7)	0.845
Present	11(16.2)	57(83.1)	
Vascular Invasion			
Absent	32(18.2)	144(81.8)	0.772
Present	3(13)	20(87)	
Necrosis			
Absent	30(15.9)	159(84.1)	1.000
Present	22(16.1)	115(83.9)	
Klintrup Makinen			
0	6(14)	37(86)	0.747
1	36(17.5)	170(82.5)	
2	7(11.9)	52(88.1)	
3	3(16.7)	15(83.3)	
Ki67			
Low (<15%)	33(14.8)	190(85.2)	1.000
High (>15%)	16(15.2)	89(84.8)	
Tumour Bud			
-Low	36(17.5)	170(82.5)	0.279
-High	16(12.8)	109(87.2)	
Tissue Stroma Percentage			
Low	40(17.7)	186(82.3)	0.194
High	12(11.4)	93(88.6)	

Further stratification according to molecular subtype was then performed. These subtypes were divided into Luminal A, Luminal B, Triple-negative (most similar to "Basal-like" subtype) and HER-2 enriched groups. For 11 patients, molecular subgroup was not available. For the remaining patients, there were 202 Luminal A, 121 Luminal B, 95 TNBC and 47 HER-2 enriched cases. Luminal A patients had 30 low cytoplasmic TBX22 expressors with 2 events, and 172 high-TBX22 expressors with 22 events. Luminal B patients had 18 low TBX22 expressors with 5 events, and 103 high TBX22 expressors with 33 events. The TNBC patients had 12 low TBX22 expressors with 2 events, and 83 patients with high TBX22 with 26 events. Finally, HER-2 enriched patients consisted of 47 high TBX22 cases with 17 events, while no cases had low TBX22 cytoplasmic expression. Kaplan Meier curves are shown for each subgroup below.

Luminal A patients had a 5-year survival of 96% and 92% at 10 years for low TBX22 expressors, compared to 91% at 5 years and 84% at 10 years for high TBX22 expressors. Mean survival was 167.8 months for low TBX22, and 162.6 months for high TBX22 expressors (HR 1.841, 95% C.I. 0.432-7.853, log rank p=0.410), (*Figure 6-30*).

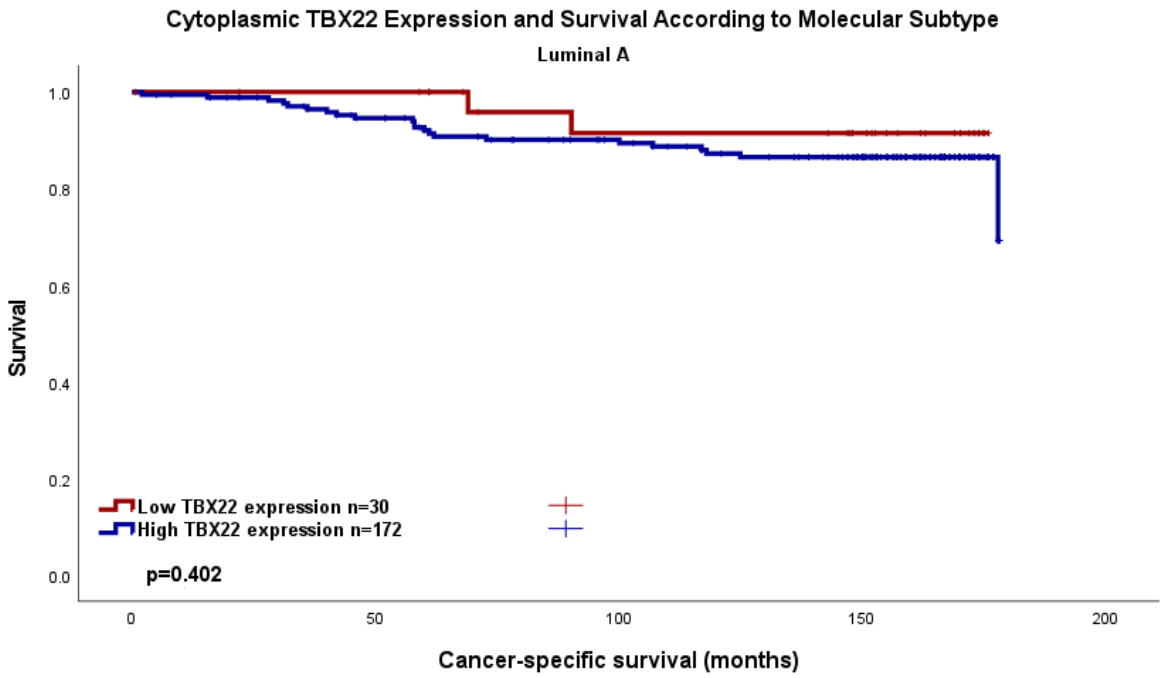

Figure 6-30 Cancer-specific survival in the Luminal A patients in the Glasgow Breast Cancer Cohort according to TBX22 cytoplasm expression. Kaplan Meier Curve showing the association between TBX22 cytoplasm expression and survival (months) HR 1.841, 95% C.I. 0.432-7.853, log rank p=0.410

Within the Luminal A group, inter-factor correlation was assessed when comparing the high and low TBX22 cytoplasmic expressors, (Table 6-4Table 5-13*)*. Here, an association between nodal status and TBX22 cytoplasmic expression was identified.

Table 6-4 Clinicopathological factors and their relation to TBX22 cytoplasmic expression in Luminal A patients in the Glasgow Breast Cancer Cohort. Chi-squared analysis

Clinicopathological factor	TBX22 Cytoplasmic staining (%)		p
	Low	High	
Age (years)			
≤50	7(11.7)	53(88.3)	0.663
>50	23(15.4)	126(84.6)	
Tumour Size			
≤20mm	22(17.6)	103(82.4)	0.190
21-49mm	8(10.5)	68(89.5)	
≥50mm	0	8(100)	
Grade			
I	8(11.9)	59(88.1)	0.775
II	17(15.2)	95(84.8)	
III	5(16.7)	25(83.3)	
Nodal Status			
N_0	**13(10.6)**	**110(89.4)**	**0.012**
N_1	**16(18.8)**	**69(81.2)**	
Lymphatic Invasion			

Absent	17(17.5)	80(82.5)	1.000
Present	6(16.2)	31(83.8)	
Vascular Invasion			
Absent	21(17.5)	99(82.5)	1.000
Present	2(14.3)	12(83.8)	
Necrosis			
Absent	19(14.3)	114(85.7)	0.836
Present	11(15.7)	59(84.3)	
Klintrup Makinen			
0	3(11.1)	24(88.9)	0.415
1	22(16.2)	114(83.8)	
2	3(9.4)	29(90.6)	
3	2(33.3)	4(66.7)	
Ki67			
Low (<15%)	30(14.4)	179(85.6)	n/a
High (>15%)	0	0	
Tumour Bud			
-Low	20(15.7)	107(84.3)	0.685
-High	10(12.7)	69(87.3)	
Tissue Stroma Percentage			
Low	22(16.3)	113(83.7)	0.408
High	8(11.3)	63(88.7)	

Luminal B patients had a 5-year survival of 88% and 69% at 10 years for low TBX22 expressors, compared to 82% at 5 years and 52% at 10 years for high TBX22 expressors. Mean survival was 146.6 months for low TBX22, and 141.6 months for high TBX22 expressors (HR 1.248, 95% C.I. 0.487-3.198, log rank p=0.644), (*Figure 6-31*).

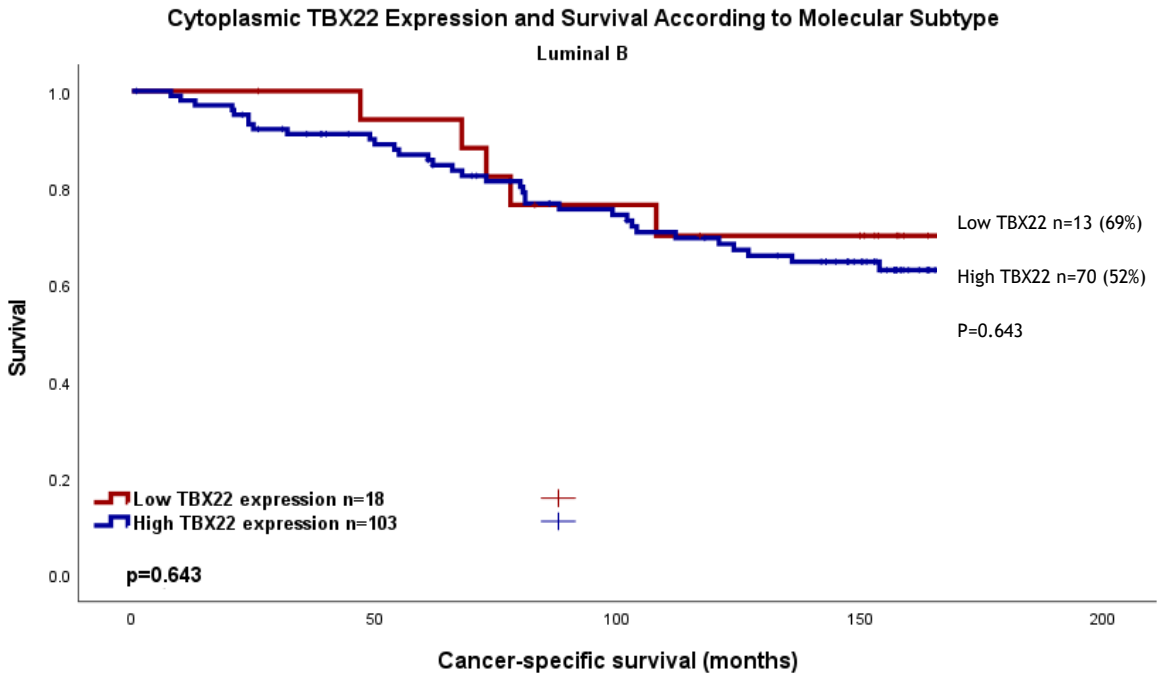

Figure 6-31 Cancer-specific survival in the Luminal B patients in the Glasgow Breast Cancer Cohort according to TBX22 cytoplasm expression. Kaplan Meier Curve showing the

association between TBX22 cytoplasm expression and survival (months) HR 1.248, 95% C.I. 0.487-3.198, log rank p=0.644

Within the luminal B group, inter-factor correlation was assessed when comparing the high and low TBX22 cytoplasmic expressors, (Table 6-5Table 5-14). Here, no association with TBX22 cytoplasmic expression was seen.

Table 6-5 Clinicopathological factors and their relation to TBX22 Cytoplasmic expression in Luminal B patients in the Glasgow Breast Cancer Cohort. Chi-squared analysis.

Clinicopathological factor	TBX22 Cytoplasmic staining (%)		p
	Low	High	
Age (years)			
≤50	3(7.7)	36(92.3)	0.175
>50	15(18.1)	68(81.9)	
Tumour Size			
≤20mm	7(11.7)	53(88.3)	0.443
21-49mm	9(16.4)	46(83.6)	
≥50mm	2(28.6)	5(71.4)	
Grade			
I	3(18.8)	13(81.3)	0.122
II	4(7.4)	50(92.6)	
III	11(21.2)	41(78.8)	
Nodal Status			
N_0	10(16.1)	52(83.9)	0.786
N_1	8(13.8)	50(86.2)	
Lymphatic Invasion			
Absent	6(17.6)	28(82.4)	1.000
Present	5(16.1)	26(83.9)	
Vascular Invasion			
Absent	10(17.9)	46(82.1)	1.000
Present	1(11.1)	8(88.9)	
Necrosis			
Absent	8(15.1)	45(84.9)	1.000
Present	10(14.9)	57(85.1)	
Klintrup Makinen			
0	2(13.3)	13(86.7)	0.903
1	11(16.4)	56(83.6)	
2	4(14.3)	24(85.7)	
3	1(8.3)	11(91.7)	
Ki67			
Low (<15%)	3(18.8)	13(81.3)	0.705
High (>15%)	15(14.2)	91(85.8)	
Tumour Bud			
-Low	12(16)	63(84)	0.794
-High	6(12.8)	41(87.2)	
Tissue Stroma Percentage			
Low	14(15.9)	74(84.1)	0.777
High	4(11.8)	30(88.2)	

TNBC patients had a 5-year survival of 83% and 83% at 10 years for low TBX22 expressors, compared to 76% at 5 years and 63% at 10 years for high TBX22 expressors. Mean survival was 153.8 months for low TBX22, and 138.1 months for high TBX22 expressors (HR 2.030, 95% C.I. 0.482-8.554, log rank p=0.335), (*Figure 6-32*).

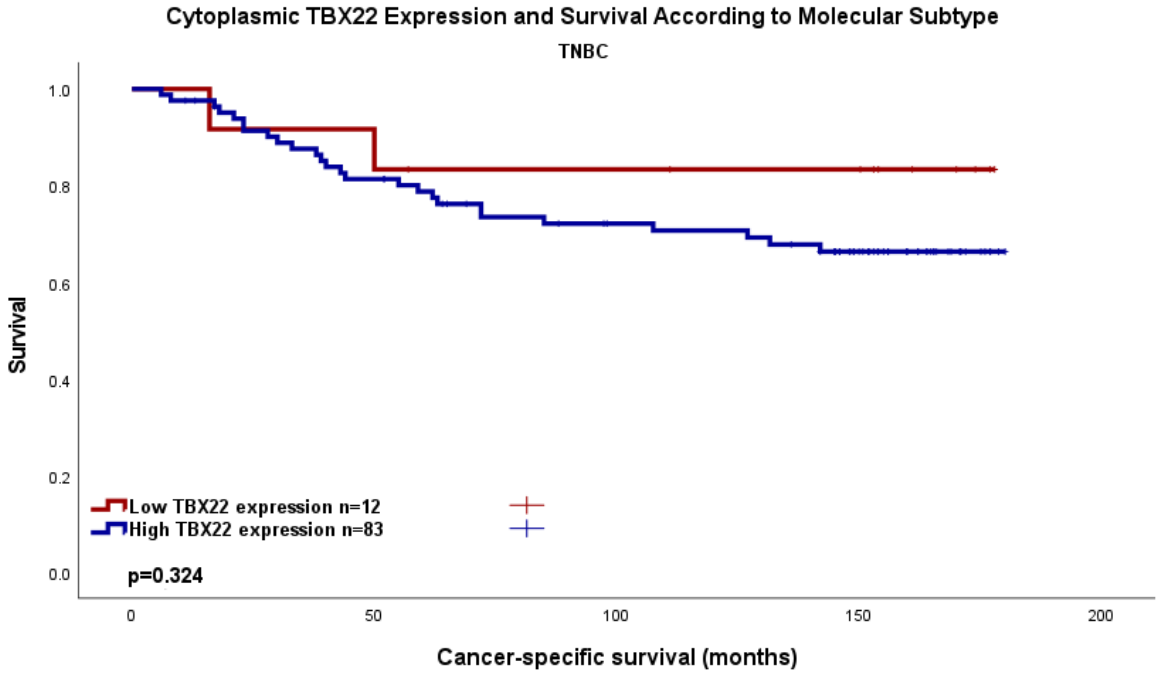

Figure 6-32 Cancer-specific survival in the TNBC patients in the Glasgow Breast Cancer Cohort according to TBX22 cytoplasm expression. Kaplan Meier Curve showing the association between TBX22 cytoplasm expression and survival (months) HR 2.030, 95% C.I. 0.482-8.554, log rank p=0.335

Within the TNBC group, inter-factor correlation was assessed when comparing the high and low TBX22 cytoplasmic expressors, (Table 6-6). Here, an association between age and lymphatic invasion and TBX22 cytoplasmic expression was seen.

Table 6-6 Clinicopathological factors and their relation to TBX22 Cytoplasmic expression in TNBC patients in the Glasgow Breast Cancer Cohort. Chi-squared analysis.

Clinicopathological factor	TBX22 Cytoplasmic staining (%)		p
	Low	High	
Age (years)			
<50	**10(25)**	**30(75)**	**0.003**
>50	**2(3.6)**	**53(96.4)**	
Tumour Size			
<20mm	4(8.7)	42(91.3)	0.297
21-49mm	8(18.2)	36(81.8)	
>50mm	0	4(100)	

Grade			
I	1(25)	3(75)	0.712
II	2(10)	18(90)	
III	9(12.7)	62(87.3)	
Nodal Status			
N_0	8(14.5)	47(85.5)	0.756
N_1	4(10)	36(90)	
Lymphatic Invasion			
Absent	**7(20.6)**	**27(79.4)**	**0.041**
Present	**0**	**19(100)**	
Vascular Invasion			
Absent	7(15.9)	37(84.1)	0.334
Present	0	9(100)	
Necrosis			
Absent	3(11.5)	23(88.5)	1.000
Present	9(13.2)	59(86.8)	
Klintrup Makinen			
0	0	4(100)	0.876
1	5(12.5)	35(87.5)	
2	5(13.5)	32(86.5)	
3	2(15.4)	11(84.6)	
Ki67			
Low (<15%)	7(11.9)	52(88.1)	1.000
High (>15%)	3(10.7)	25(81.8)	
Tumour Bud			
-Low	8(11.1)	64(88.9)	0.466
-High	4(18.2)	18(81.8)	
Tissue Stroma Percentage			
Low	8(10.7)	67(89.3)	0.253
High	4(21.1)	15(78.9)	

HER2-enriched patients had a 5-year survival of 67% and 60% at 10 years for high (all) TBX22 expressors. Mean survival was 126.5 months for high TBX22 expressors. As there were no low TBX22 cytoplasmic expressors, therefore no comparison was possible.

6.2.12 TBX22 Nuclear expression in the Glasgow Breast Cancer Cohort

Manual weighted histoscores of nuclear TBX22 expression were performed by FS. Scores by FS varied between 0 and 300, with a mean of 67.860, (*Figure 6-33)*.

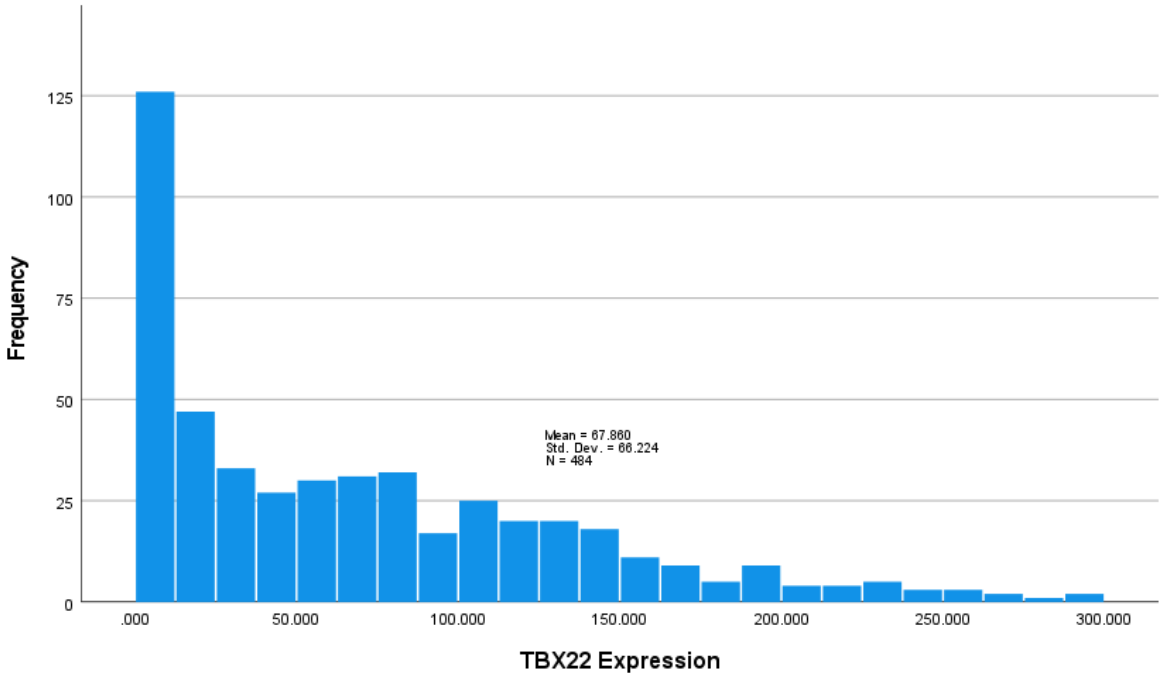

Figure 6-33 Distribution of TBX22 nuclear expression (weighted histoscores) in the Glasgow Breast Cancer Cohort. Mean score 67.860, SD 66.224.

Counter-scores were performed manually by Warapan Numprasit for a minimum of 10% of cores, (n=57) and are shown below for comparison, (*Figure 6-34*). WHS were reproducible between the two scorers for 49 cores. An intraclass correlation coefficient (ICCC) of 0.985 suggested a strong positive correlation between validation and primary assessor's scores.

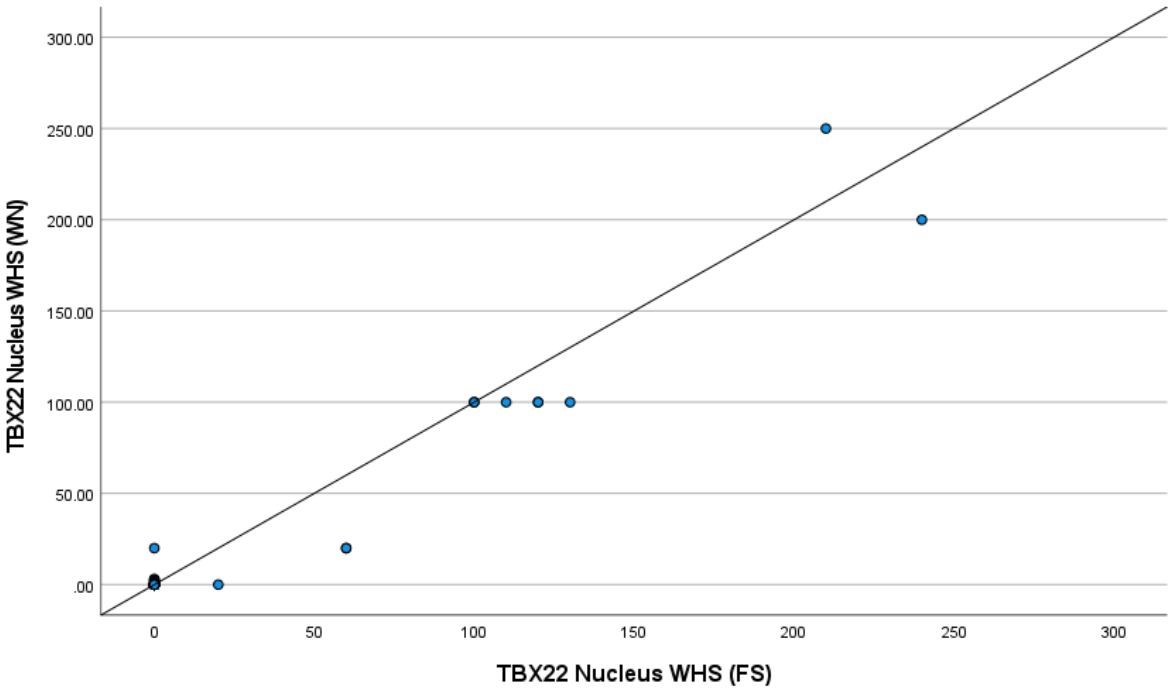

Figure 6-34 Correlation between FS and WN manual weighted histoscore (WHS) for TBX22 nucleus staining. Scatter plot showing correlation between FS and NW for cytoplasm TBX22 scores. Intraclass correlation coefficient 0.985 for 10% specimens.

A subsequent comparison of averages and differences in scores was produced as a Bland-Altman plot and suggested the scores correlated satisfactorily (*Figure 6-35*Figure 5-33).

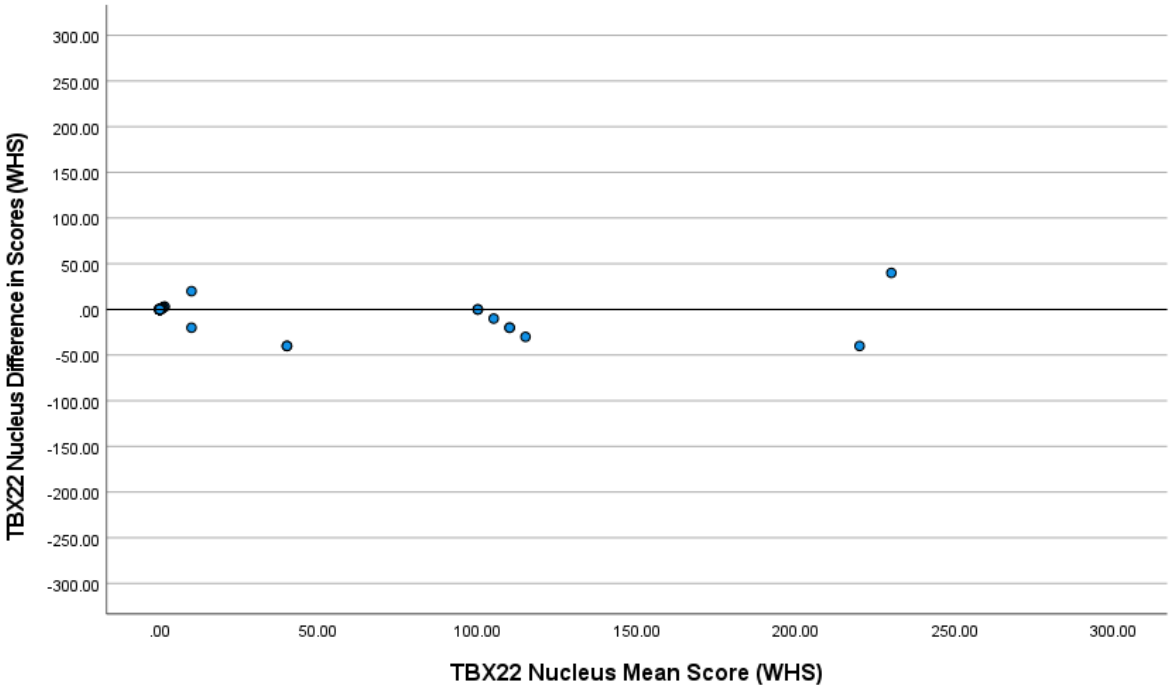

Figure 6-35 Bland-Altman Plot comparing difference in scores to mean scores for TBX22 nucleus expression.

A threshold for high and low TBX22 nuclear expression was delineated using R Studio to compare high versus low RFX5 nuclear expression according to survival. The threshold was identified as 5, (*Figure 6-36*).

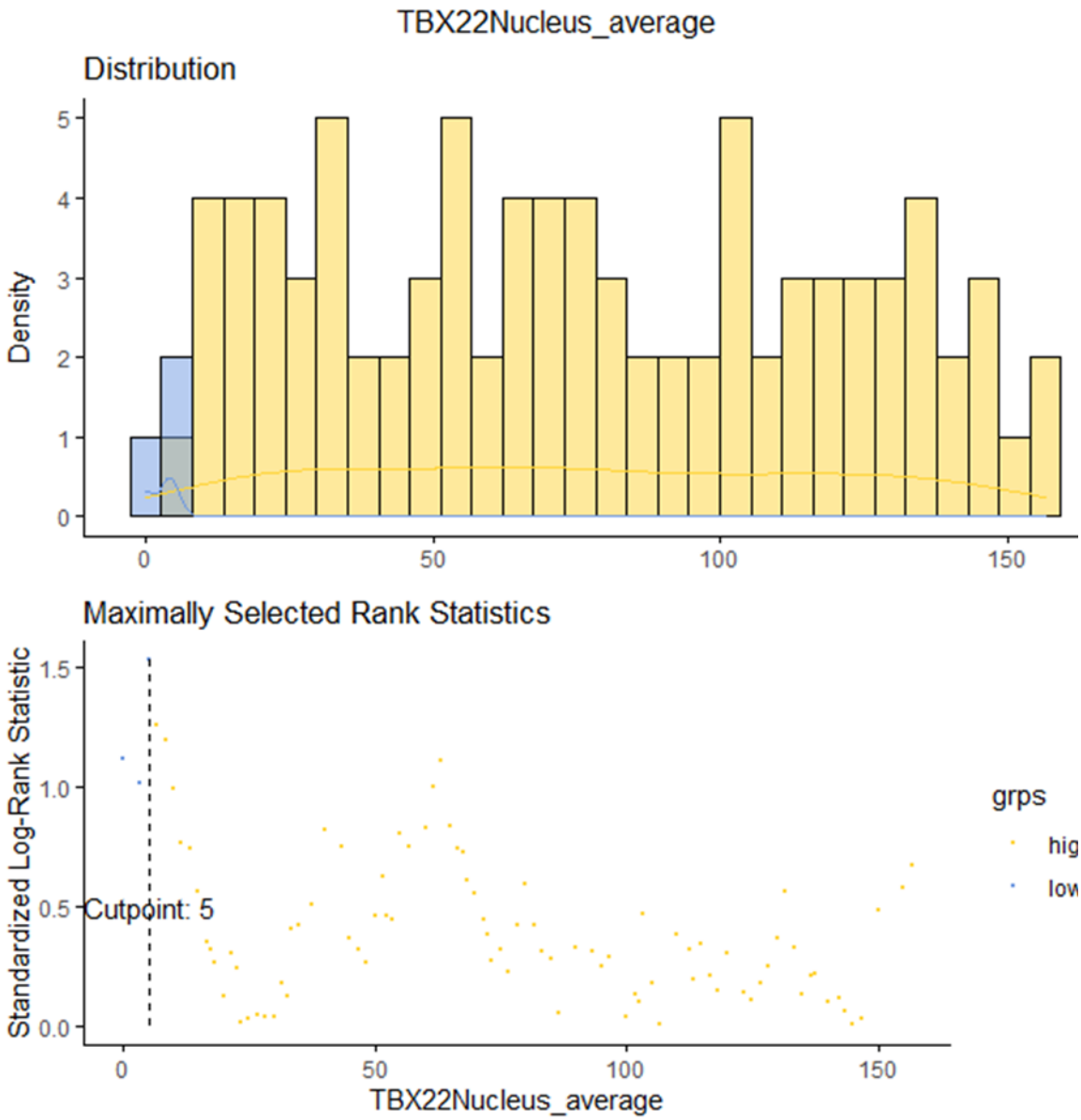

Low Expression

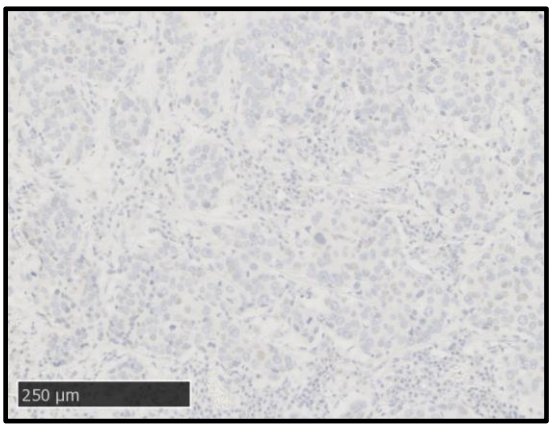

High Expression

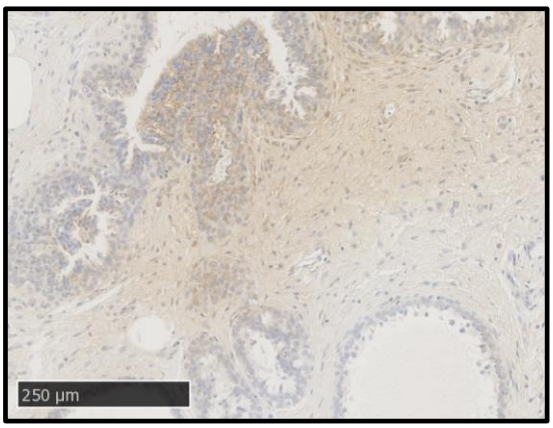

Figure 6-36 TBX22 Nuclear expression threshold for high and low expression of TBX22 in the Glasgow Breast Cancer Cohort. The threshold was identified as 5, with patients with weighted scores above 60 considered to have high TBX22 nuclear expression. Examples of protein expression as seen on specimens is also described below the graphical representation.

Nuclear TBX22 and Survival in the Glasgow Breast Cancer Cohort

Within the Glasgow Breast Cancer Cohort,479 patients had both viable cores and cancer specific survival data available. 102 patients had low TBX22 nuclear expression and had 26 events, while 374 had high expression and saw 82 events. Survival in the low TBX22 group was 78% at 5 years, and 71% at 10 years, while in the high TBX22 group survival was 86% at 5 years, and 73% at 10 years. Using Kaplan Meier survival analysis, mean cancer-specific survival (CSS) time for low TBX22 nuclear expression was 142 months compared to high TBX22 expression survival of 153.3 months (HR 0.792, 95% C.I.; 0.509-1.231, log rank p=0.300), (*Figure 6-37*).

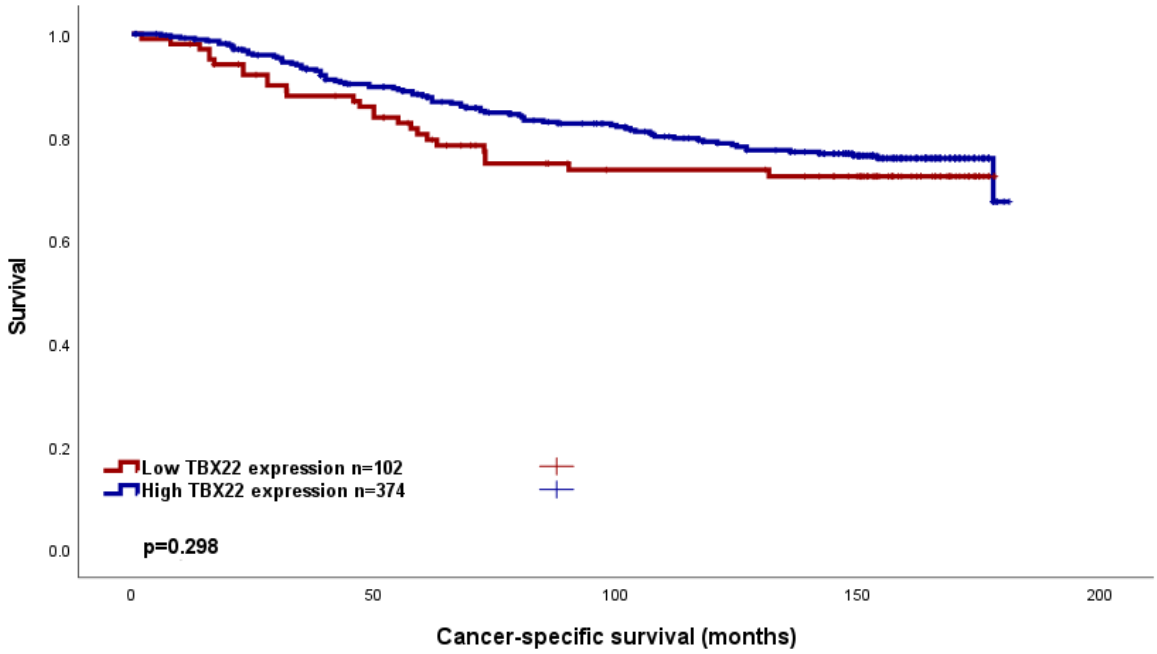

Figure 6-37 Cancer-specific survival in the Glasgow Breast Cancer Cohort according to TBX22 nuclear expression. Kaplan Meier Curve showing the association between TBX22 nuclear expression and survival (months). HR 0.792, 95% C.I.; 0.509-1.231, log rank p=0.300.

Within the entire Glasgow Breast Cancer Cohort, inter-factor correlation was assessed when comparing the high and low TBX22 nuclear expressors, (Table 6-7). Here, no association with TBX22 nuclear staining was seen.

Table 6-7 Clinicopathological factors and their relation to TBX22 nuclear expression in the Glasgow Breast Cancer Cohort. Chi-squared analysis.

Clinicopathological factor	TBX22 nuclear staining (%)		p
	Low	High	
Age (years)			
≤50	26(16.6)	131(83.4)	0.097
>50	76(23.2)	251(76.8)	
Tumour Size			
≤20mm	49(18.6)	214(81.4)	0.265
21-49mm	49(24.7)	149(75.3)	
≥50mm	4(18.2)	18(81.8)	
Grade			
I	12(13.8)	75(86.2)	0.052
II	40(19.5)	165(80.5)	
III	50(26)	142(74)	
Molecular Subtype			
Luminal A	41(19.6)	168(80.4)	0.164
Luminal B	23(18.9)	99(81.1)	
TNBC	28(29.5)	67(70.5)	
HER2 enriched	8(17)	39(83)	
Nodal Status			
N_0	59(21.8)	212(78.2)	0.630
N_1	43(20.5)	167(79.5)	
Lymphatic Invasion			
Absent	34(18.7)	148(81.3)	0.180
Present	12(12.2)	86(87.8)	
Vascular Invasion			
Absent	40(16.3)	206(83.7)	0.807
Present	6(17.6)	28(82.4)	
Necrosis			
Absent	42(18.8)	181(81.2)	0.262
Present	58(23.1)	193(76.9)	
Klintrup Makinen			
0	8(17)	39(83)	0.107
1	48(18.2)	216(81.8)	
2	35(28)	90(72)	
3	10(27)	27(73)	
Ki67			
Low (<15%)	69(22.5)	238(77.5)	0.284
High (>15%)	29(18.1)	131(81.9)	
Tumour Bud			
-Low	73(22.7)	249(77.3)	0.342
-High	29(18.5)	128(81.5)	
Tissue Stroma Percentage			
Low	75(22.5)	258(77.5)	0.335
High	27(27)	119(81.5)	

Stratification of the cohort to compare patients according to ER status was performed. 476 had valid ER-status data available. In the ER-negative patient group (n=149), 37 patients had low TBX22 nuclear expression and had 13 events, while 112 had high TBX22 expression and 33 event. Survival in the low TBX22

group was 68% at 5 years, and 59% at 10 years, while in the high TBX22 group survival was 76% at 5 and 66% 10 years (HR 0.747 95% C.I. 0.393-1.419, p=0.373), (*Figure 6-38*).

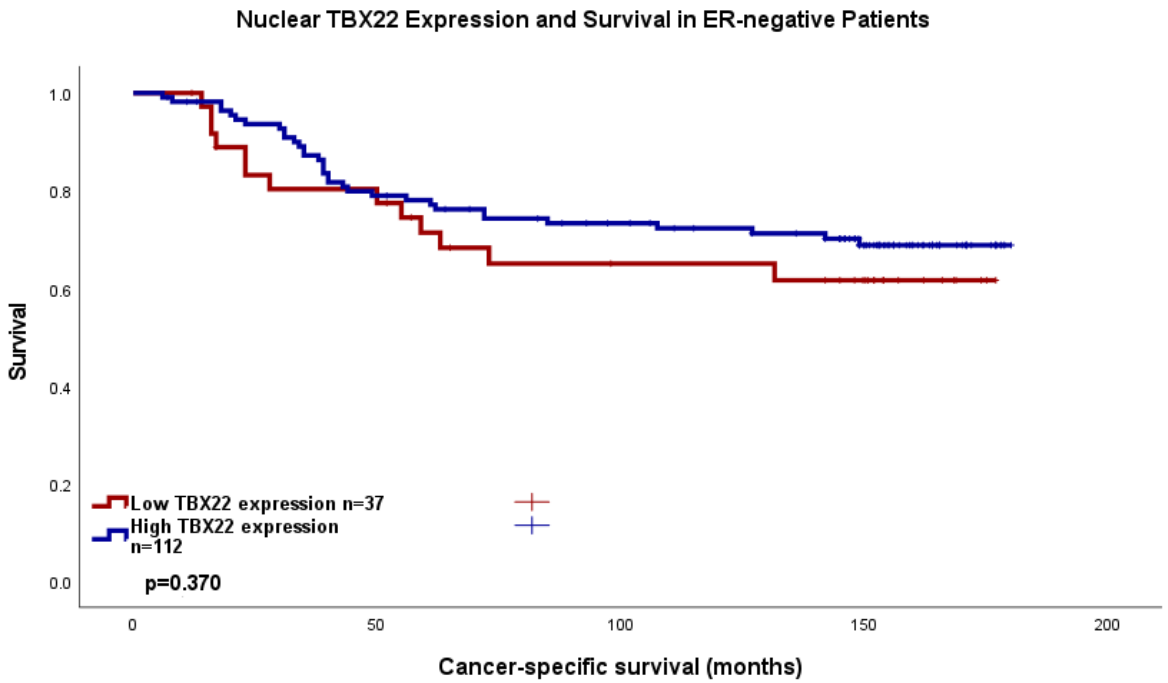

Figure 6-38 Cancer-specific survival in ER-negative patients in the Glasgow Breast Cancer Cohort according to TBX22 nuclear expression. Kaplan Meier Curve showing the association between TBX22 nuclear expression and survival (months). HR 0.747 95% C.I. 0.393-1.419, p=0.373.

Within the ER-negative group, inter-factor correlation was assessed when comparing the high and low TBX22 nuclear expressors, (Table 6-8). Here, no association with TBX22 nuclear expression was seen.

Table 6-8 Clinicopathological factors and their relation to TBX22 nuclear expression in ER-negative patients in the Glasgow Breast Cancer Cohort. Chi-squared analysis.

Clinicopathological factor	TBX22 nuclear staining (%)		p
	Low	High	
Age (years)			
≤50	14(22.6)	48(77.4)	0.701
>50	23(26.4)	64(73.6)	
Tumour Size			
≤20mm	17(23)	57(77)	0.654
21-49mm	17(25.8)	49(74.2)	
≥50mm	3(37.5)	5(62.5)	
Grade			
I	1(20)	4(80)	0.568
II	6(25.8)	27(81.8)	
III	30(37.5)	81(73)	

Nodal Status			
N_0	20(25.5)	61(75.3)	1.000
N_1	17(16.7)	51(75)	
Lymphatic Invasion			
Absent	13(25.5)	38(74.5)	0.418
Present	5(16.7)	25(83.3)	
Vascular Invasion			
Absent	16(22.9)	54(77.1)	1.000
Present	2(18.2)	9(81.8)	
Necrosis			
Absent	5(14.7)	29(85.3)	0.174
Present	32(28.1)	82(71.9)	
Klintrup Makinen			
0	1(25)	3(75)	0.779
1	12(20.7)	46(79.3)	
2	19(28.8)	47(71.2)	
3	5(26.3)	14(73.7)	
Ki67			
Low (<15%)	24(28.6)	60(71.4)	0.226
High (>15%)	10(18.2)	45(78.1)	
Tumour Bud			
-Low	30(259)	86(74.1)	0.818
-High	7(21.9)	25(78.1)	
Tissue Stroma Percentage			
Low	25(23.4)	82(76.6)	0.526
High	12(29.3)	29(70.7)	

In the ER-positive patient group (n=327), 65 patients had low TBX22 nuclear expression and had 13 events, while 262 had high TBX22 expression and 49 events. Survival in the low TBX22 group was 84% at 5 years, and 78% at 10 years, while in the high TBX22 group survival was 90% at 5 and 76% at 10 years (HR

0.893 95% C.I. 0.484-1.648, p=0.718), (*Figure 6-39*)

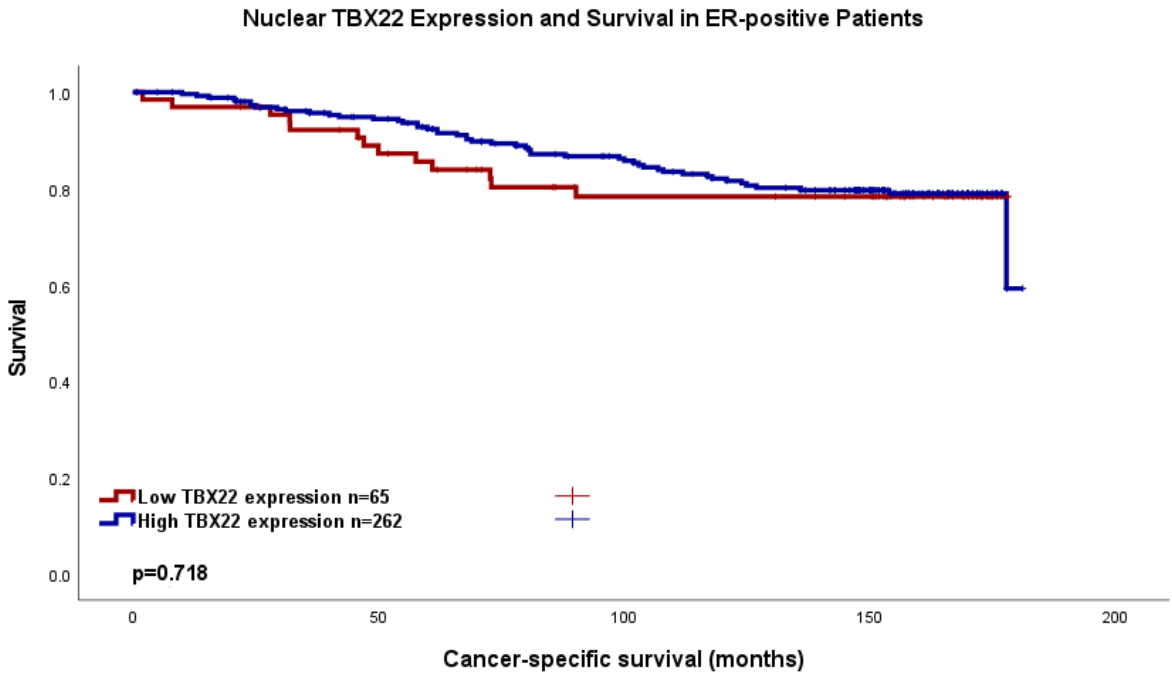

Figure 6-39 Cancer-specific survival in ER-positive patients in the Glasgow Breast Cancer Cohort according to TBX22 nuclear expression. Kaplan Meier Curve showing the association between TBX22 nuclear expression and survival (months). HR 0.893 95% C.I. 0.484-1.648, p=0.718.

Within the ER-positive group, inter-factor correlation was assessed when comparing the high and low TBX22 nuclear expressor, (Table 6-9). Here, age neared statistically significant association with TBX22 nuclear staining.

Table 6-9 Clinicopathological factors and their relation to TBX22 Nuclear expression in ER+ patients in the Glasgow Breast Cancer Cohort. Chi-squared analysis.

Clinicopathological factor	TBX22 nuclear staining (%)		p
	Low	High	
Age (years)			
≤50	12(12.6)	83(87.4)	0.065
>50	53(22.1)	187(77.9)	
Tumour Size			
≤20mm	32(16.9)	157(83.1)	0.131
21-49mm	32(24.2)	100(75.8)	
≥50mm	1(7.1)	13(92.9)	
Grade			
I	11(13.4)	71(86.6)	0.188
II	34(19.8)	138(80.2)	
III	20(24.7)	61(75.3)	
Nodal Status			
N_0	39(20.5)	151(79.5)	0.611
N_1	26(18.3)	116(81.7)	

Lymphatic Invasion			
Absent	21(16)	110(84)	0.390
Present	7(10.3)	61(89.7)	
Vascular Invasion			
Absent	24(13.6)	152(86.4)	0.540
Present	4(17.4)	19(82.6)	
Necrosis			
Absent	37(19.6)	152(80.4)	1.000
Present	26(19)	111(81)	
Klintrup Makinen			
0	7(16.3)	36(83.7)	0.288
1	36(17.5)	170(82.5)	
2	16(27.1)	43(72.9)	
3	5(27.8)	13(72.2)	
Ki67			
Low (<15%)	45(20.2)	178(79.8)	0.765
High (>15%)	19(18.1)	86(81.9)	
Tumour Bud			
-Low	43(20.9)	163(79.1)	0.568
-High	22(17.6)	103(82.4)	
Tissue Stroma Percentage			
Low	50(22.1)	176(77.9)	0.104
High	15(14.3)	90(85.7)	

Further stratification according to molecular subtype was then performed. These subtypes were divided into Luminal A, Luminal B, Triple-negative (most similar to "Basal-like" subtype) and HER-2 enriched groups. For 11 patients, molecular subgroup was not available. For the remaining patients, there were 202 Luminal A, 121 Luminal B, 95 TNBC and 47 HER-2 enriched cases. Luminal A patients had 71 low nuclear TBX22 expressors with 8 events, and 161 high-TBX22 expressors with 16 events. Luminal B patients had 23 low TBX22 expressors with 5 events, and 98 high TBX22 expressors with 33 events. The TNBC patients had 28 low TBX22 expressors with 10 events, and 67 patients with high TBX22 with 18 events. Finally, HER-2 enriched patients consisted of 8 low TBX22 cases with 3 events, and 39 high TBX22 cases with 14 events. Kaplan Meier curves are shown for each subgroup below.

Luminal A patients had a 5-year survival of 84% and 78% at 10 years for low TBX22 expressors, compared to 93% at 5 years and 87% at 10 years for high TBX22 expressors. (HR 0.467, 95% C.I. 0.199-1.098, p=0.081). When observing this using a Kaplan Meier survival curve, patients with low nuclear TBX22 expression observed a survival benefit compared to low TBX22 expressors (p=0.043), (*Figure 6-40*).

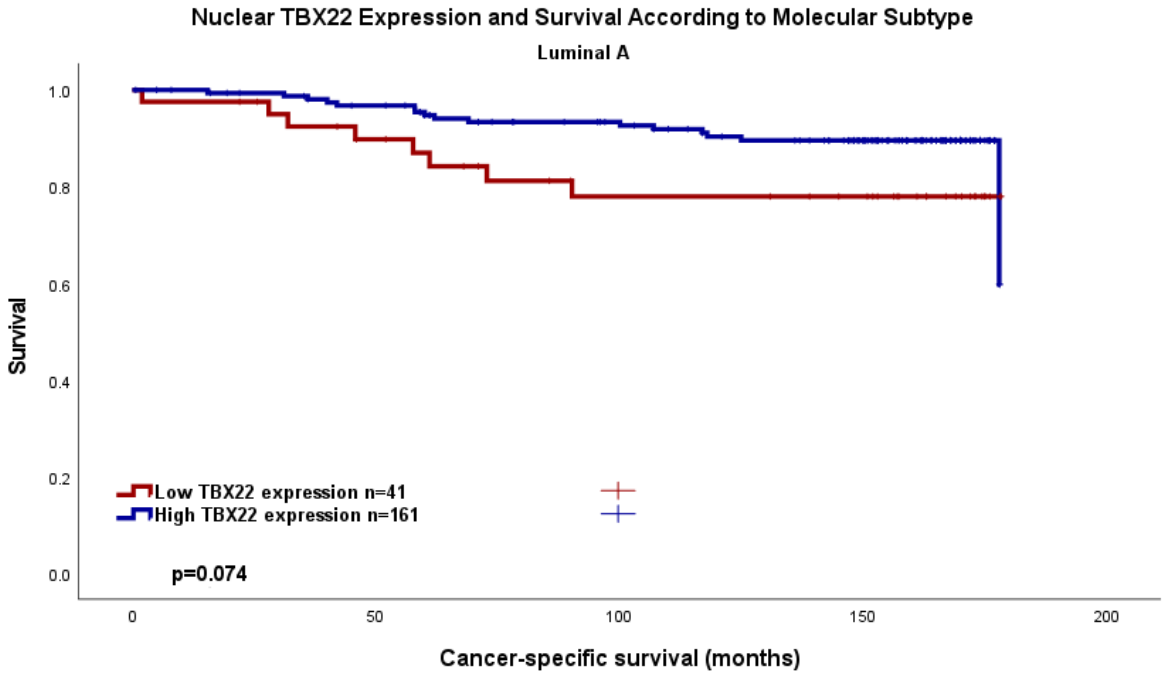

Figure 6-40 Cancer-specific survival in Luminal A patients in the Glasgow Breast Cancer Cohort according to TBX22 nuclear expression. Kaplan Meier Curve showing the association between TBX22 nuclear expression and survival (months). HR 0.467, 95% C.I. 0.199-1.098, p=0.081.

Within the Luminal A group, inter-factor correlation was assessed when comparing the high and low TBX22 nuclear expressors, (Table 6-10). Here, TSP neared statistically significant association with TBX22 nuclear expression.

Table 6-10 Clinicopathological factors and their relation to TBX22 Nuclear expression in Luminal A patients in the Glasgow Breast Cancer Cohort. Chi-squared analysis.

Clinicopathological factor	TBX22 nuclear staining (%)		p
	Low	High	
Age (years)			
≤50	7(11.7)	53(88.3)	0.083
>50	34(22.8)	115(77.2)	
Tumour Size			
≤20mm	22(17.6)	103(82.4)	0.502
21-49mm	18(23.7)	58(76.3)	
≥50mm	1(12.5)	7(87.5)	
Grade			
I	8(11.9)	59(88.1)	0.091
II	24(21.4)	88(78.6)	
III	9(30)	21(70)	
Nodal Status			
N_0	25(20.3)	98(79.7)	0.853
N_1	16(18.8)	69(81.2)	
Lymphatic Invasion			
Absent	17(17.5)	80(82.5)	0.097

Present	2(5.4)	35(94.6)	
Vascular Invasion			
Absent	17(14.2)	103(85.8)	1.000
Present	2(14.3)	12(85.7)	
Necrosis			
Absent	25(18.8)	108(81.2)	0.712
Present	15(21.4)	55(78.6)	
Klintrup Makinen			
0	4(14.8)	23(85.2)	0.108
1	23(16.9)	113(83.1)	
2	11(34.4)	21(65.6)	
3	2(33.3)	4(66.7)	
Ki67			
Low (<15%)	41(19.6)	168(80.4)	n/a
High (>15%)	0	0	
Tumour Bud			
-Low	28(22)	99(78)	0.373
-High	13(16.5)	66(83.5)	
Tissue Stroma Percentage			
Low	32(23.7)	103(76.3)	0.068
High	9(12.7)	62(87.3)	

Luminal B patients had a 5-year survival of 83% and 78% at 10 years for low TBX22 expressors, compared to 83% at both 5 and 56% at 10 years for high TBX22 expressors. (HR 1.665, 95% C.I. 0.650-4.268, p=0.288), (*Figure 6-41*).

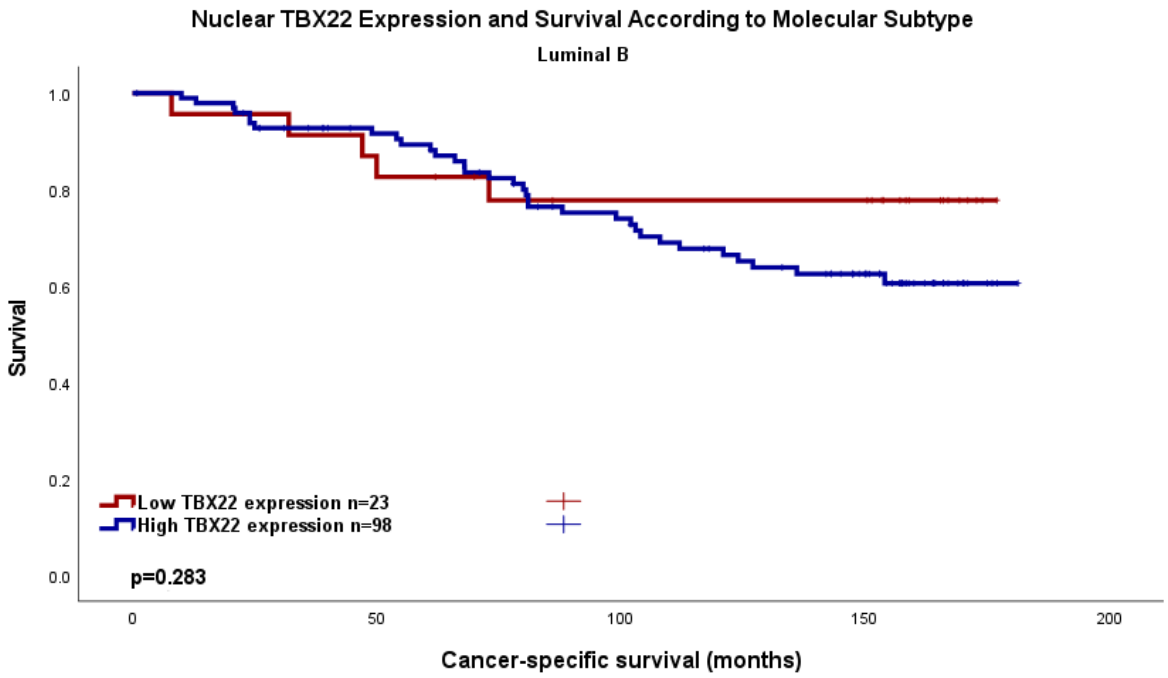

Figure 6-41 Cancer-specific survival in Luminal B patients in the Glasgow Breast Cancer Cohort according to TBX22 nuclear expression. Kaplan Meier Curve showing the association between TBX22 nuclear expression and survival (months). HR 1.665, 95% C.I. 0.650-4.268, p=0.288

Within the Luminal B group, inter-factor correlation was assessed when comparing the high and low TBX22 nuclear expressors, (Table 6-11). Here, no association with TBX22 nuclear staining was seen.

Table 6-11 Clinicopathological factors and their relation to TBX22 nuclear expression in Luminal B patients in the Glasgow Breast Cancer Cohort. Chi-squared analysis.

Clinicopathological factor	**TBX22 nuclear staining (%)**		**p**
	Low	**High**	
Age (years)			
≤50	5(12.8)	34(87.2)	0.323
>50	18(21.7)	65(78.3)	
Tumour Size			
≤20mm	9(15)	51(85)	0.151
21-49mm	14(25.5)	41(74.5)	
≥50mm	0	7(100)	
Grade			
I	3(18.8)	13(81.3)	0.996
II	10(18.5)	44(81.5)	
III	10(19.2)	42(80.8)	
Nodal Status			
N_0	13(21)	49(79)	0.689
N_1	10(17.2)	48(82.8)	
Lymphatic Invasion			
Absent	4(11.8)	30(88.2)	0.726
Present	5(16.1)	26(83.9)	
Vascular Invasion			
Absent	7(12.5)	49(87.5)	0.600
Present	2(22.2)	7(77.8)	
Necrosis			
Absent	11(20.8)	42(79.2)	0.637
Present	11(16.4)	56(83.6)	
Klintrup Makinen			
0	2(13.3)	13(86.7)	0.890
1	13(19.4)	54(80.6)	
2	5(17.9)	23(82.1)	
3	3(25)	9(75)	
Ki67			
Low (<15%)	4(25)	12(75)	0.500
High (>15%)	19(17.9)	87(82.1)	
Tumour Bud			
-Low	14(18.7)	61(81.3)	1.000
-High	9(19.1)	38(80.9)	
Tissue Stroma Percentage			
Low	17(19.3)	71(80.7)	1.000
High	6(17.6)	28(82.4)	

Triple-negative ("basal-like) patients had a 5-year survival of 66% and 57% at 10 years for low TBX22 expressors, compared to 82% at 5 and 68% at 10 years for high TBX22 expressors. (HR 0.662, 95% C.I. 0.305-1.435, p=0.296), (*Figure 6-42*).

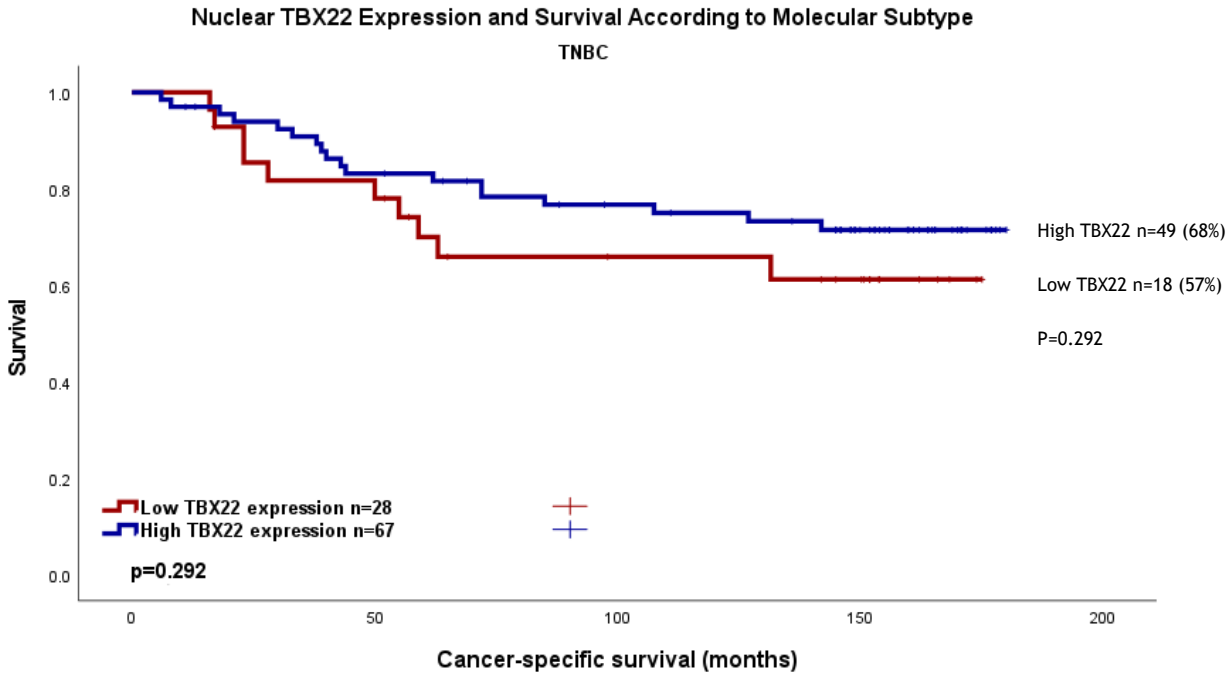

Figure 6-42 Cancer-specific survival in TNBC patients in the Glasgow Breast Cancer Cohort according to TBX22 nuclear expression. Kaplan Meier Curve showing the association between TBX22 nuclear expression and survival (months). HR 0.662, 95% C.I. 0.305-1.435, p=0.296.

Within the TNBC group, inter-factor correlation was assessed when comparing the high and low TBX22 nuclear expressors, (Table 6-12). Here, no association with TBX22 nuclear expression was seen.

Table 6-12 Clinicopathological factors and their relation to TBX22 nuclear expression in TNBC patients in the Glasgow Breast Cancer Cohort. Chi-squared analysis.

Clinicopathological factor	TBX22 nuclear staining (%)		p
	Low	High	
Age (years)			
≤50	13(32.5)	27(67.5)	0.651
>50	15(27.3)	40(72.7)	
Tumour Size			
≤20mm	14(30.4)	32(69.6)	0.973
21-49mm	13(29.5)	31(70.5)	
≥50mm	1(25)	3(75)	
Grade			
I	1(25)	3(75)	0.857
II	5(25)	15(75)	
III	22(31)	49(69)	

Nodal Status			
N_0	17(30.9)	38(69.1)	0.821
N_1	11(27.5)	29(72.5)	
Lymphatic Invasion			
Absent	10(29.4)	24(70.6)	0.334
Present	3(15.8)	16(72.5)	
Vascular Invasion			
Absent	11(25)	33(75)	1.000
Present	2(22.2)	7(77.8)	
Necrosis			
Absent	5(19.2)	21(80.8)	0.212
Present	23(33.8)	45(66.2)	
Klintrup Makinen			
0	1(25)	3(75)	0.803
1	10(25)	30(75)	
2	13(35.1)	24(64.9)	
3	4(30.8)	9(69.2)	
Ki67			
Low (<15%)	18)30.5)	41(69.5)	0.800
High (>15%)	7(25)	21(75)	
Tumour Bud			
-Low	24(33.3)	48(66.7)	0.197
-High	4(18.2)	18(81.8)	
Tissue Stroma Percentage			
Low	21(28)	54(72)	0.575
High	7(36.8)	12(63.2)	

HER2-enriched patients had a 5-year survival of 73% and 59% at 10 years for low TBX22 expressors, compared to 66% at 5 and 60% at 10 years for high TBX22 expressors. (HR 28.393, 95% C.I. 0-4.$^{022E+10}$, =0.756), (*Figure 6-43*).

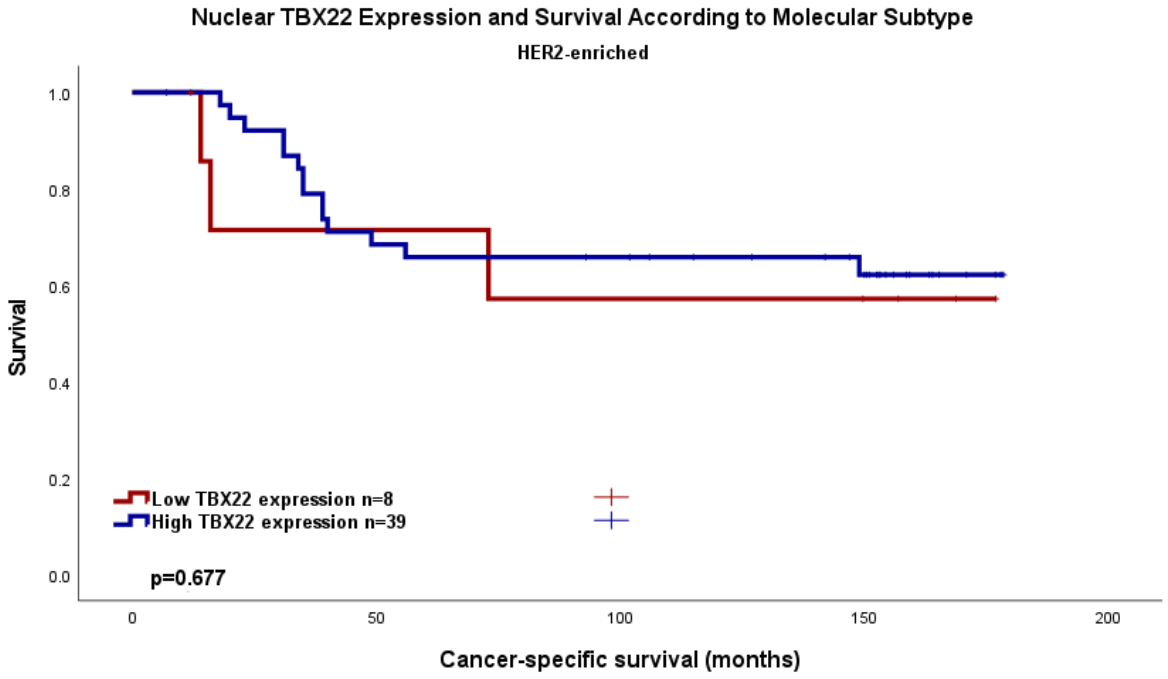

Figure 6-43 Cancer-specific survival in HER2 enriched patients in the Glasgow Breast Cancer Cohort according to TBX22 nuclear expression. Kaplan Meier Curve showing the association between TBX22 nuclear expression and survival (months). HR 28.393, 95% C.I. 0-4.$^{022E+10}$, =0.756

Within the HER2-enriched group, inter-factor correlation was assessed when comparing the high and low TBX22 nuclear expressors, (Table 6-13). Here, tumour size was associated with TBX22 nuclear expression.

Table 6-13 Clinicopathological factors and their relation to TBX22 nuclear expression in HER2-enriched patients in the Glasgow Breast Cancer Cohort. Chi-squared analysis.

Clinicopathological factor	TBX22 nuclear staining (%)		p
	Low	High	
Age (years)			
≤50	1(6.3)	15(93.8)	0.234
>50	7(22.6)	24(77.4)	
Tumour Size			
≤20mm	**2(8.7)**	**21(91.3)**	**0.040**
21-49mm	**4(19)**	**17(81)**	
≥50mm	**2(66.7)**	**1(33.3)**	
Grade			
I	0	0	0.170
II	0	11(100)	
III	8(22.2)	28(77.8)	
Nodal Status			
N_0	3(13)	20(87)	0.701
N_1	5(20.8)	19(79.2)	
Lymphatic Invasion			
Absent	2(16.7)	10(83.3)	1.000

Present	2(18.2)	9(81.8)	
Vascular Invasion			
Absent	4(19)	17(81)	1.000
Present	0	2(100)	
Necrosis			
Absent	0	6(100)	0.571
Present	8(19.5)	33(80.5)	
Klintrup Makinen			
0	0	0	0.447
1	1(7.1)	13(92.9)	
2	6(23.1)	20976.9)	
3	1(16.7)	5(83.3)	
Ki67			
Low (<15%)	5(25)	15(75)	0.435
High (>15%)	3(12)	22(88)	
Tumour Bud			
-Low	5(13.2)	33(86.8)	0.167
-High	3(33.3)	6(66.7)	
Tissue Stroma Percentage			
Low	3(11.5)	23(88.5)	0.437
High	5(23.8)	16(76.2)	

6.2.14 TBX22 Expression in the Glasgow Breast Cancer Cohort - Combined Scoring

Weighted histoscores for nuclear and cytoplasm expression of TBX22 were combined to create four categories: TBX22 high nuclear: high cytoplasm (All-High), TBX22 high nuclear: low cytoplasm (HNLC), TBX22 low nuclear: high cytoplasm (LNHC), and TBX22 low nuclear: low cytoplasm (All-Low), to assess whether more prognostic power could be conferred to TBX22 protein expression on cancer-specific survival. 476 patients had valid survival data. 329 (69.1%) patients had All-High phenotype with 77 events, 45 (9.5%) had HNLC and 5 events, 81 (17%) had LNHC and 21 events, and 21 (4.4%) had All-Low and 5 events.

In the All-High group (n=329) 5-year survival was 85%- and 10-year survival 71%. The HNLC group had a 5-year survival of 92%- and 10-year survival of 87%. LNHC group had a 5-year survival of 76%- and 10-year survival of 70%. The All-Low group had a 5-year survival of 86%, with 10-year survival of 75%, (*Figure 6-44*).

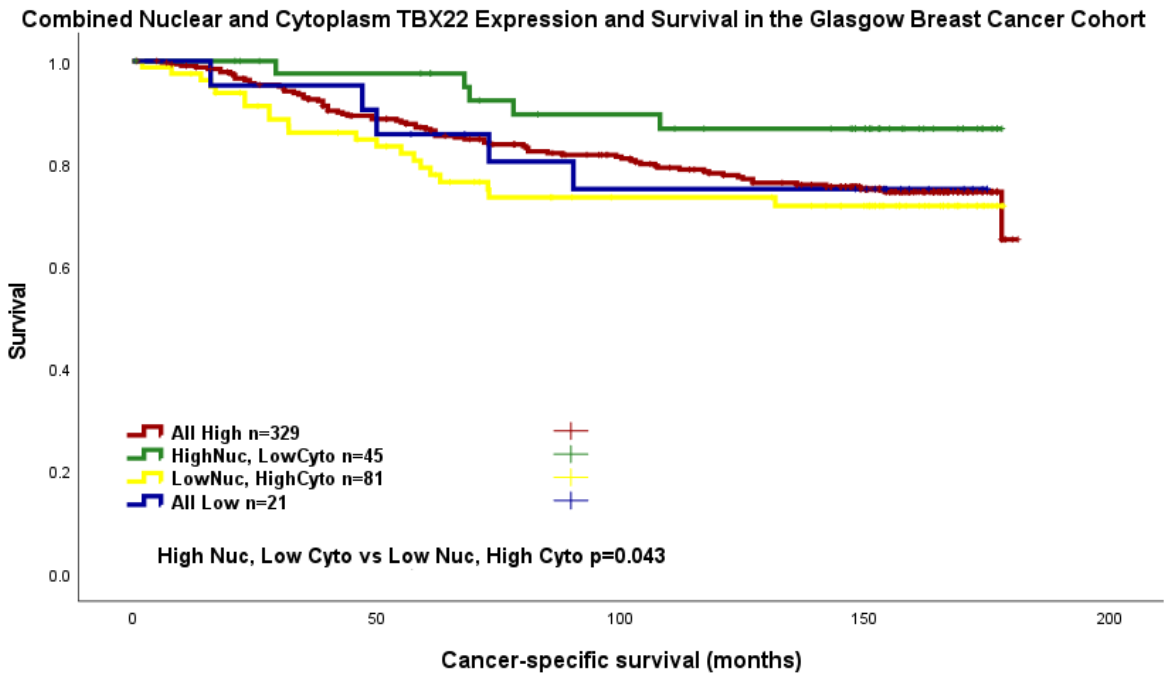

Figure 6-44 Combined Nuclear and Cytoplasm TBX22 expression and survival in the Glasgow Breast Cancer Cohort. Pairwise comparisons are described in the graph.

Pairwise comparison demonstrated that the LNHC group had significantly worse survival than the HNLC group (*Table 6-14*).

Table 6-14 Pairwise comparisons on Kaplan Meier survival analysis for combined nuclear and cytoplasmic TBX22 expression.

Pairwise Comparison p=	1 All-High	2 HNLC	3 LNHC	4 All-Low
1 All-High		0.091	0.398	0.995
2 HNLC	0.091		**0.043**	0.216
3 LNHC	0.398	**0.043**		0.675
4 All-Low	0.995	0.216	0.675	

On multivariate analysis TBX22 however this difference did not remain statistically significant, (Table 6-15).

Table 6-15 Clinicopathological factors and their prognostic significance in the Glasgow Breast Cancer Cohort with regards to combined nuclear and cytoplasmic TBX22 scoring. Univariate and multivariate Cox regression analysis.

Clinicopathological Factor	**Univariate analysis (HR, 95% C.I.)**	**p**	**Multivariate analysis (HR, 95% C.I.)**	**p**
Age	0.947(0.680-1.318)	0.746		
Tumour Size <20mm		**<0.001** **<0.001**		**0.004**

20-49mm	**2.117(1.525-2.939)**	**<0.001**	1.717	0.093
>50mm	**4.528(2.579-7.951)**	**<0.001**	**6.695**	**<0.001**
Invasive Grade		**<0.001**		0.696
I		**<0.001**		
II	**2.332(1.226-4.436)**	**0.010**		
III	**4.043(2.162-7.563)**	**<0.001**		
Nodal Status	**3.258(2.339-4.537)**	**<0.001**	**2.080(1.017-4.253)**	**0.045**
Molecular Subtype		**<0.001**		**0.004**
Luminal A				
Luminal B	**2.343(1.525-3.599)**	**<0.001**		0.074
TNBC	**2.710(1.779-4.128)**	**<0.001**	8.122(2.465-26.759)	**<0.001**
HER2-enriched	**2.946(1.771-4.900)**	**<0.001**	8.695(2.131-35.482)	**0.003**
Lymphatic Invasion	**4.255(2.813-6.435)**	**<0.001**	2.866(1.373-5.982)	**0.0005**
Vascular Invasion	**3.440(2.163-5.470)**	**<0.001**	1.463(0.705-3.036)	0.307
Necrosis	**3.288(2.290-4.722)**	**<0.001**	2.318(1.001-5.369)	**0.050**
Klintrup-Makinen		**0.033**		**<0.001**
0				
1	**1.609(0.717-3.613)**	**0.249**	**0.049(0.016-0.147)**	**<0.001**
2	**1.308(0.656-2.605)**	**0.446**	**0.034(0.009-0.128)**	**<0.001**
3	**2.108(1.038-4.279)**	**0.039**	**0.020(0.003-0.129)**	**<0.001**
Ki67	**1.658(1.199-2.294)**	**0.002**	2.168(0.917-5.129)	0.078
Tumour budding	**1.755(1.282-2.403)**	**<0.001**	**2.146(1.065-4.326)**	**0.033**
Tumour stroma percentage	**1.884(1.374-2.582)**	**<0.001**	**2.313(1.190-4.498)**	**0.013**
TBX22 combined score		**0.198**		0.257
HNLC v All high	**0.810(0.5-1.312)**	**0.0391**	0.464(0.208-1.034)	0.060
HNLC v LNHC	**0.377(0.142-1.001)**	**0.050**	0.338(0.083-1.372)	0.129
HNLC v All low	**0.806(0.304-2.139)**	**0.666**	0.464(0.051-4.187)	0.494

Within the Luminal A group, inter-factor correlation was assessed when comparing the combined score subgroups, (Table 6-16). Here, no association with combined score was seen.

Table 6-16 Clinicopathological factors and their relation to TBX22 combined nuclear and cytoplasmic expression in the Glasgow Breast Cancer Cohort. Chi-squared analysis.

Clinicopathological factor	**TBX22 combined score (%)**				**p**
	All-High	**HNLC**	**LNHC**	**All-Low**	
Age (years)					
≤50	117(74.5)	14(8.9)	20(12.7)	6(3.8)	0.362
>50	220(67.3)	31(9.5)	61(18.7)	15(4.6)	
Tumour Size					
≤20mm	188(815)	26(9.9)	38(9.9)	11(4.2)	0.718
21-49mm	132(66.7)	17(8.6)	39(8.6)	10(5.1)	
≥50mm	16(72.7)	2(9.1)	4(18.2)	0	
Grade					
I	66(75.9)	9(10.3)	9(10.3)	3(3.4)	0.384
II	145(70.7)	20(9.8)	33(16.1)	7(3.4)	
III	126(65.6)	16(8.3)	39(20.3)	11(5.7)	
Molecular Subtype					
Luminal A	147(70.3)	21(10)	32(15.3)	9(4.3)	0.131
Luminal B	85(69.7)	14(11.5)	19(15.6)	4(3.3)	
TNBC	6164.3)	6(6.3)	22(23.2)	6(6.3)	
HER2 enriched	39(83)	0	8(17)	0	
Nodal Status					
N_0	190(70.1)	22(8.1)	46(17)	13(4.8)	0.742
N_1	145(69)	22(10.5)	35(16.7)	8(3.8)	
Lymphatic Invasion					
Absent	124(68.1)	24(13.2)	25(13.7)	9(4.9)	0.229
Present	76(77.6)	10(10.2)	11(11.2)	1(1)	
Vascular Invasion					
Absent	175(71.1)	31(12.6)	30(12.2)	10(4.1)	0.485
Present	25(73.5)	3(8.8)	6(17.6)	0	
Necrosis					
Absent	156(70)	25(11.2)	34(15.2)	8(3.6)	0.473
Present	173(68.9)	20(8)	45(17.9)	13(5.2)	
Klintrup Makinen					
0	36(76.6)	3(6.4)	5(10.6)	3(6.4)	0.155
1	183(69.3)	33(12.5)	39(14.8)	9(3.4)	
2	83(66.4)	7(5.6)	29(23.2)	6(4.8)	
3	25(67.6)	2(5.4)	7(18.9)	3(8.1)	
Ki67					
Low (<15%)	208(67.8)	30(9.8)	57(18.6)	12(3.9)	0.585
High (>15%)	118(73.8)	13(8.1)	23(14.4)	6(3.8)	
Tumour Bud					
-Low	220(68.3)	29(9)	56(17.4)	17(5.3)	0.527
-High	112(71.3)	16(10.2)	25(15.9)	4(2.5)	

Tissue Stroma Percentage					
Low	223(67)	35(10.5)	60(18)	15(4.5)	0.370
High	109(74.7)	10(6.8)	21(14.4)	6(4.1)	

When stratifying according to molecular subtype, Luminal A patients in the ALL-HIGH group had a 5-year survival of 93% and 10-year survival of 86%, in the HNLC group had 5-year survival of 94% and 10-year survival of 94%. The LNHC group had 5-year survival of 79% and 10-year survival of 75%, and the ALL-LOW group had a 5-year survival of 100% and 10-year survival of 88%, (*Figure 6-45)*.

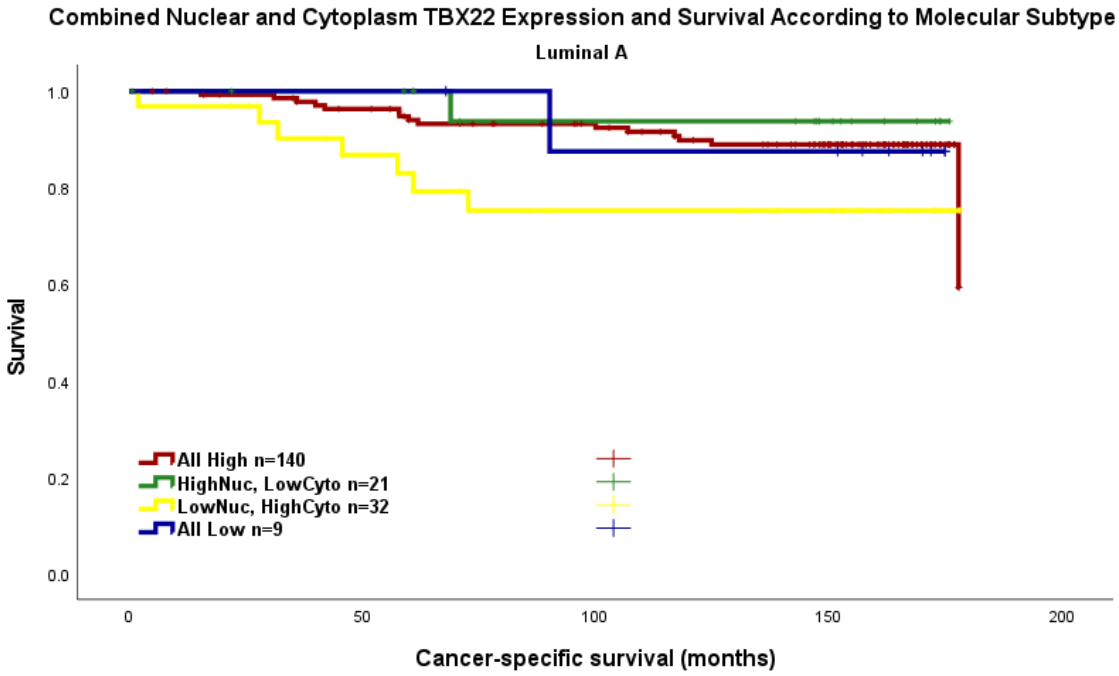

Figure 6-45 Combined nuclear and cytoplasm TBX22 expression and survival in Luminal A patients in the Glasgow Breast Cancer Cohort.

Pairwise failed to demonstrate a statistically significant difference in survival in the Luminal A patients, (Table 6-17Table 5-27).

Table 6-17 Pairwise comparisons on Kaplan Meier survival analysis for combined nuclear and cytoplasmic TBX22 expression in Luminal A patients.

Pairwise Comparison p=	1 All-High	2 HNLC	3 LNHC	4 All-Low
1 All-High		0.270	0.107	0.283
2 HNLC	0.270		0.765	0.219
3 LNHC	0.107	0.765		0.184
4 All-Low	0.283	0.219	0.184	

Within the Luminal A group, inter-factor correlation was assessed when comparing the combined score subgroups, (*Table* 6-18). Here, KM score was associated with TBX22 combined score.

Table 6-18 Clinicopathological factors and their relation to TBX22 combined nuclear and cytoplasmic expression in the Luminal A patients in the Glasgow Breast Cancer Cohort. Chi-squared analysis.

Clinicopathological factor	**TBX22 combined score (%)**				**p**
	All-High	**HNLC**	**LNHC**	**All-Low**	
Age (years)					
≤50	47(78.3)	6(10)	6(10)	1(1.7)	0.298
>50	100(67.1)	15(10.1)	26(17.4)	8(5.4)	
Tumour Size					
≤20mm	87(69.6)	16(12.8)	16(12.8)	6(4.8_	0.548
21-49mm	53(69.7)	5(6.6)	15(19.7)	3(3.9)	
≥50mm	7(87.5)	0	1(12.5)	0	
Grade					
I	53(79.1)	6(9)	6(9)	2(3)	0.327
II	77(69.8)	11(9.8)	18(16.1)	6(5.4)	
III	17(56.7)	4(13.3)	8(26.7)	1(3.3)	
Nodal Status					
N_0	90(73.2)	8(6.5)	20(16.3)	5(4.1)	0.054
N_1	57(67.1)	12(14.1)	12(14.1)	4(14.1)	
Lymphatic Invasion					
Absent	68(70.1)	12(12.4)	12(12.4)	5(5.2)	0.296
Present	29(78.4)	6(16.2)	2(5.4)	0	
Vascular Invasion					
Absent	87(72.5)	16(13.3)	12(10)	5(4.2)	0.846
Present	10(71.4)	2(14.3)	2(14.3)	0	
Necrosis					
Absent	94(70.7)	14(13.3)	20(15)	5(3.8)	0.930
Present	48(68.6)	7(10)	11(15.7)	4(5.7)	
Klintrup Makinen					
0	21(77.8)	2(7.4)	3(11.1)	1(3.7)	0.012
1	96(70.6)	17(12.5)	18(13.2)	5(3.7)	
2	19(59.4)	2(6.3)	10(31.3)	1(3.1)	
3	4(66.7)	0	0	2(33.3)	
Ki67					
Low (<15%)	147(70.3)	21(10)	32(15.3)	9(4.3)	n/a
High (>15%)	0	0	0	0	
Tumour Bud					
-Low	87(68.5)	12(9.4)	20(15.7)	8(6.3)	0.375
-High	57(72.2)	9(11.4)	12(15.2)	1(1.3)	
Tissue Stroma Percentage					
Low	88(65.2)	15(11.1)	25(18.5)	7(5.2)	0.220
High	56(78.9)	6(8.5)	7(9.9)	2(2.8)	

Amongst the Luminal B patients in the Glasgow Breast Cancer Cohort, the All-High group had a 5-year survival of 82% and 10-year survival of 53%, in the HNLC group had 5-year survival of 92% and 10-year survival of 75%. The LNHC group had 5-year survival of 84% and 10-year survival of 84%, and the All-Low group had a 5-year survival of 75% and 10-year survival of 50%, (*Figure 6-46*).

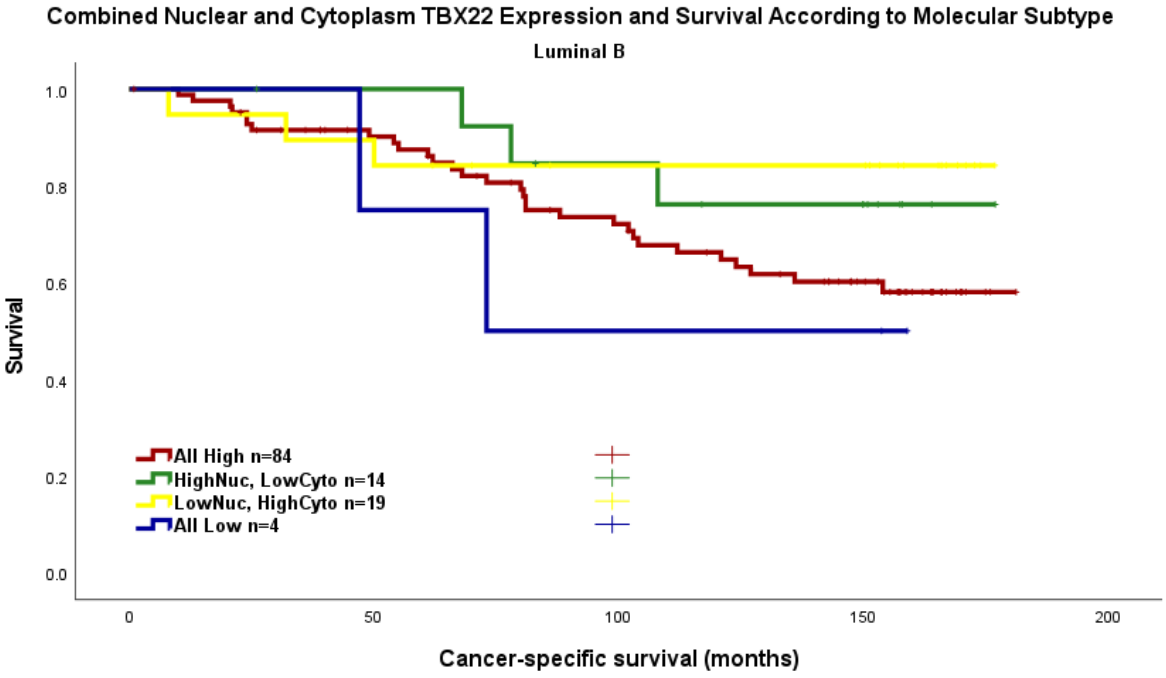

Figure 6-46 Combined nuclear and cytoplasm TBX22 expression and survival in Luminal B patients in the Glasgow Breast Cancer Cohort.

Pairwise comparison demonstrated no significant difference in survival between combined TBX22 score subgroups in the Luminal B patients, (*Table 6-19*).

Table 6-19 Pairwise comparisons on Kaplan Meier survival analysis for combined nuclear and cytoplasmic TBX22 expression in Luminal B patients.

Pairwise Comparison p=	1 All-High	2 HNLC	3 LNHC	4 All-Low
1 All-High		0.270	0.107	0.283
2 HNLC	0.270		0.756	0.219
3 LNHC	0.107	0.756		0.184
4 All-Low	0.283	0.219	0.184	

Within the Luminal B group, inter-factor correlation was assessed when comparing the combined score subgroups, (Table 6-20). Here, grade was associated with TBX22 combined score.

Table 6-20 Clinicopathological factors and their relation to TBX22 combined nuclear and cytoplasmic expression in the Luminal B patients in the Glasgow Breast Cancer Cohort. Chi-squared analysis.

Clinicopathological factor	TBX22 combined score (%)				p
	All-High	HNLC	LNHC	All-Low	
Age (years)					
≤50	31(79.5)	3(7.7)	5(12.8)	0	0.300
>50	54(65.1)	11(13.3)	14(16.9)	4(4.8)	
Tumour Size					
≤20mm	46(76.7)	5(8.3)	7(11.7)	2(3.3)	0.360
21-49mm	34(61.8)	7(12.7)	12(21.8)	2(3.6)	
≥50mm	5(71.4)	2(28.6)	0	0	
Grade					
I	11(68.8)	2(12.5)	2(12.5)	1(6.3)	0.481
II	40(74.1)	4(7.4)	10(18.5)	0	
III	34(65.4)	8(15.4)	7(13.5)	3(5.8)	
Nodal Status					
N_0	42(67.7)	7(11.3)	10(16.1)	3(4.8)	0.934
N_1	41(707)	7(12.1)	9(15.5)	1(1.7)	
Lymphatic Invasion					
Absent	25(73.5)	5(14.7)	3(8.8)	1(2.9)	0.959
Present	22(71)	4(12.9)	4(12.9)	1(3.2)	
Vascular Invasion					
Absent	41(73.2)	8(14.3)	5(8.9)	2(3.6)	0.638
Present	6(66.7)	1(11.1)	2(22.2)	0	
Necrosis					
Absent	36(67.9)	6(11.3)	9(17)	2(3.8)	0.946
Present	48(71.6)	8(11.9)	9(13.4)	2(3)	
Klintrup Makinen					
0	12(80)	1(6.7)	1(6.7)	1(6.7)	0.946
1	45(66.2)	9(13.2)	11(16.2)	3(4.4)	
2	20(71.4)	3(10.7)	4(14.3)	1(3.6)	
3	8(66.7)	1(8.3)	3(25)	0	
Ki67					
Low (<15%)	9(56.3)	3(18.8)	4(25)	0	0.395
High (>15%)	76(71.7)	11(10.4)	15(14.2)	4(3.8)	
Tumour Bud					
-Low	51(68)	10(13.3)	12(16)	2(2.7)	0.823
-High	34(72.3)	4(8.5)	7(14.9)	2(4.3)	
Tissue Stroma Percentage					
Low	59(67)	12(13.6)	15(17)	2(2.3)	0.390
High	26(76.5)	2(5.9)	4(11.8)	2(5.9)	

TNBC patients in the ALL-HIGH group had a 5-year survival of 80% and 10-year survival of 65%, in the HNLC group had 5-year survival of 100% and 10-year survival of 100%. The LNHC group had 5-year survival of 66% and 10-year survival

of 55%, and the ALL-LOW group had a 5-year survival of 65% and 10-year survival of 65%, (*Figure 6-47*).

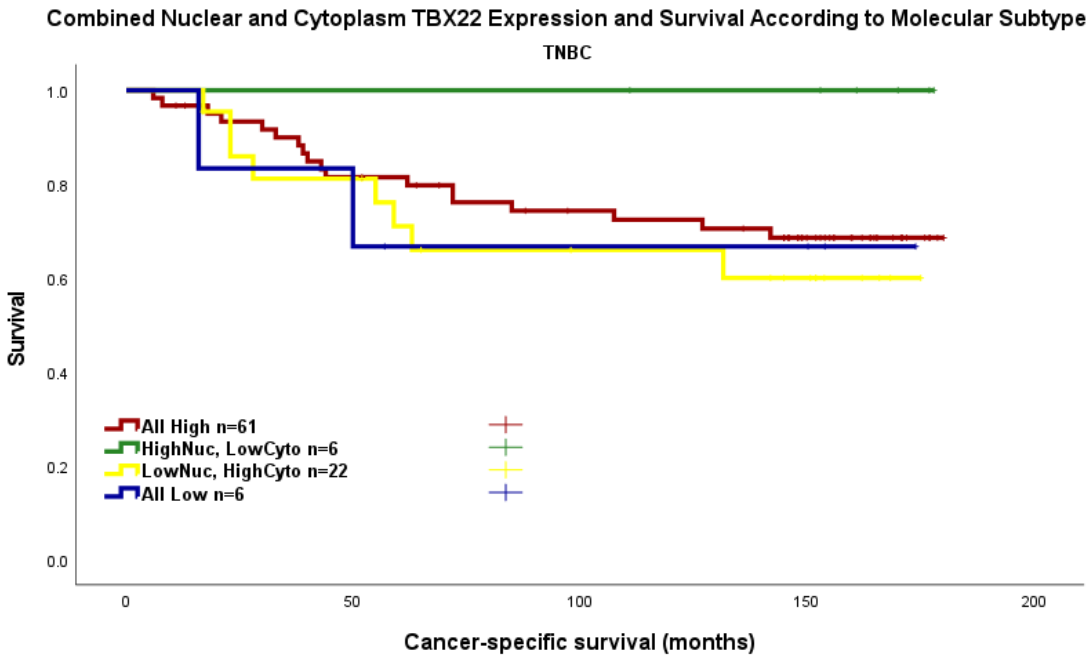

Figure 6-47 Combined nuclear and cytoplasm TBX22 expression and survival in TNBC patients in the Glasgow Breast Cancer Cohort.

Pairwise comparison demonstrated no significant difference in survival according to TBX22 combined score in the TNBC patients, (*Table 6-21*).

Table 6-21 Pairwise comparisons on Kaplan Meier survival analysis for combined membrane, nuclear and cytoplasmic TBX22 expression in TNBC patients.

Pairwise Comparison p=	1 All-High	2 HNLC	3 LNHC	4 All-Low
1 All-High		0.139	0.448	0.757
2 HNLC	0.139		0.089	0.138
3 LNHC	0.448	0.089		0.999
4 All-Low	0.757	0.138	0.999	

Within the TNBC group, Inter-factor correlation was assessed when comparing the combined score subgroups, (Table 6-22). Here, age was associated with combined TBX22 score.

Table 6-22 Clinicopathological factors and their relation to TBX22 combined membrane, nuclear and cytoplasmic expression in the TNBC patients in the Glasgow Breast Cancer Cohort. Chi-squared analysis.

Clinicopathological factor	**TBX22 combined score (%)**	**p**

	All-High	HNLC	LNHC	All-Low	
Age (years)					
≤50	22(55)	5(12.5)	8(20)	5(12.5)	0.023
>50	39(70.9)	1(1.8)	14(25.5)	1(1.8)	
Tumour Size					
≤20mm	29(63)	3(6.5)	13(28.3)	1(2.2)	0.599
21-49mm	28(63.6)	3(6.8)	8(18.2)	5(11.4)	
≥50mm	3(75)	0	1(25)	0	
Grade					
I	2(50)	1(25)	1(25)	0	0.501
II	13(65)	2(10)	5(25)	0	
III	46(64.8)	3(4.2)	16(22.5)	6(8.5)	
Nodal Status					
N_0	34(61.8)	4(7.3)	13(23.6)	4(7.3)	0.917
N_1	27(67.5)	2(5)	9(22.5)	2(5)	
Lymphatic Invasion					
Absent	19(55.9)	5(14.7)	8(23.5)	2(5.9)	0.125
Present	16(84.2)	0	3(15.8)	0	
Vascular Invasion					
Absent	28(63.6)	5(11.4)	9(20.5)	2(4.5)	0.644
Present	7(77.8)	0	2(22.2)	0	
Necrosis					
Absent	18(69.2)	3(11.5)	5(19.2)	0	0.238
Present	42(61.8)	3(4.4)	17(25)	6(8.8)	
Klintrup Makinen					
0	3(75)	0	1(25)	0	0.882
1	26(65)	4(10)	9(22.5)	1(2.5)	
2	23(62.2)	1(2.7)	9(24.3)	4(10.8)	
3	8(61.5)	1(7.7)	3(23.1)	1(7.7)	
Ki67					
Low (<15%)	36(61)	5(8.5)	16(27.1)	2(3.4)	0.524
High (>15%)	20(71.4)	1(3.6)	5(17.9)	2(7.1)	
Tumour Bud					
-Low	45(62.5)	3(4.2)	19(26.4)	5(6.9)	0.287
-High	15(68.2)	3(13.6)	3(13.6)	1(4.5)	
Tissue Stroma Percentage					
Low	50(66.7)	4(5.3)	17(22.7)	4(5.3)	0.607
High	10(52.6)	2(10.5)	5(26.3)	2(10.5)	

HER2-enriched patients in the All-High group had a 5-year survival of 66% and 10-year survival of 60% and the LNHC group had 5-year survival of 73% and 10-year survival of 59% (HR 1.141 95% C.I. 0.611-2.130, p=0.679). There were no cases from the HNLC or All-Low group. There was no significant difference between CSS in the two remaining score subgroups, All high vs LNHC groups (HR 1.302 95%C.I. 0.373-4.539, p=0.679), (*Figure 6-48*).

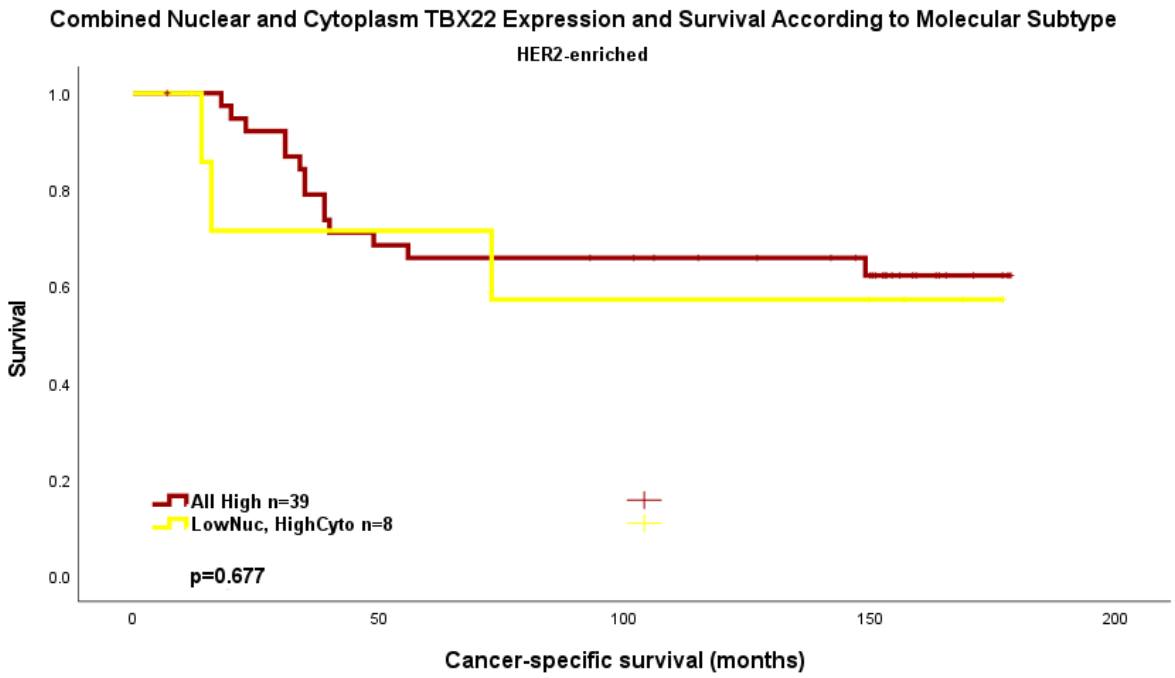

Figure 6-48 Combined nuclear and cytoplasm TBX22 expression and survival in HER2-enriched patients in the Glasgow Breast Cancer Cohort. Pairwise comparison is described in the graph.

Within the HER-2 enriched group, inter-factor correlation was assessed when comparing the combined score subgroups to other clinicopathological factors, (Table 6-23). Here, an association between size and combined TBX22 score subgroup was seen.

Table 6-23 Clinicopathological factors and their prognostic significance in the HER2-enriched patients within the Glasgow Breast Cancer Cohort with regards to combined membrane, nuclear and cytoplasmic TBX22 scoring. Univariate and multivariate Cox regression analysis.

Clinicopathological factor	TBX22 combined score (%)				p
	All-High	HNLC	LNHC	All-Low	
Age (years)					
≤50	15(93.8)	0	1(6.3)	0	0.234
>50	24(77.4)	0	7(22.6)	0	
Tumour Size					
≤20mm	**21(91.3)**	**0**	**2(8.7)**	**0**	**0.040**
21-49mm	**17(81)**	**0**	**4(19)**	**0**	
≥50mm	**1(33.3)**	**0**	**2(66.7)**	**0**	
Grade					
I	0	0	0	0	
II	11(100)	0	0	0	0.170
III	28(77.8)	0	8(22.2)	0	
Nodal Status					
N_0	20(87)	0	3(16.7)	0	0.701

N_1	19(81.8)	0	5(18.2)	0	
Lymphatic Invasion					
Absent	10(83.3)	0	2(16.7)	0	1.000
Present	9(81.8)	0	2(18.2)	0	
Vascular Invasion					
Absent	17(81)	0	4(19)	0	1.000
Present	2(100)	0	0	0	
Necrosis					
Absent	6(100)	0	0	0	0.571
Present	33(80.5)	0	8(19.5)	0	
Klintrup Makinen					
0	0	0	0	0	0.447
1	13(92.9)	0	1(7.1)	0	
2	20(76.9)	0	6(23.1)	0	
3	5(83.3)	0	1(16.7)	0	
Ki67					
Low (<15%)	15(75)	0	5(25)	0	0.435
High (>15%)	22(88)	0	3(12)	0	
Tumour Bud					
-Low	33(86.8)	0	5(13.2)	0	0.167
-High	6(66.7)	0	3(33.3)	0	
Tissue Stroma Percentage					
Low	23(88.5)	0	3(11.5)	0	0.437
High	16(76.2)	0	5(23.8)	0	

6.3 Discussion

Currently, our knowledge of the role of TBX22 in cancer remains limited. However, previous work by Ashktorab et al., comparing a mostly Caucasian cohort of colorectal patient tumours to a second cohort of African American colorectal cancer patients suggests that in the latter, deletions in the TBX22 gene was found to be amongst the most common differences in genomic expression(238). This cohort of patients had mostly (90%) stage IV cancers, which may indicate a role in cancer progression, or in prognosis with regards to TBX22 deletion(238).

During this analysis, membrane expression was minimal in both full section and TMA specimens, precluding any further analysis of prognostic significance.

Cytoplasmic expression of TBX22 was found to be comparable in tumour mass compared to tumour buds, and TMA analysis was therefore possible. Within the Glasgow Breast Cancer Cohort, 476 cases had cores available for analysis, and with survival data. A threshold between low and high TBX22 cytoplasmic expression was identified at 46.67, and an analysis of survival performed. There was no significant difference in survival between high and low TBX22

cytoplasmic expressor cases, including when the cohort was examined according to ER status or molecular subgroup. However, a relationship was identified between TBX22 cytoplasmic expression and molecular subtype, as well as age (in the case of ER-negative and TNBC groups) and all HER2-enriched cases had high TBX22 cytoplasmic expression, suggesting that there may be a relationship between TBX22 and this molecular subgroup.

Nuclear TBX22 expression was analysed for the Glasgow Breast Cancer cohort, and a threshold of 5 was identified to be associated with difference in survival. However, on further analysis, no survival benefit was identified between high/low TBX22 nuclear expression within the cohort, or within the ER status/molecular subtype groups. However, in the Luminal A group some evidence of low TBX22 being associated with poor survival was seen, although this failed to reach statistical significance ($p=0.07$). Some association was seen with tumour size (HER2-enriched), but overall, the scores may have been too low over the entire cohort to allow any further conclusions to be made.

Further classification of the cohort depending on combined nuclear and cytoplasmic scoring was performed, and here again, some groups (HER2-enriched in particular) did not have sufficient cases in each subgroup to allow any effects to be seen, and overall, no survival difference was noted according to combined nuclear and cytoplasmic TBX22 score.

Limitations within this portion of this study may relate to the findings suggested by DEPMAP and our antibody specificity studies, that TBX22 expression is often seen in very low levels in breast cancer tissues (as well as others). In addition, a portion of the specimens in the Glasgow Breast Cancer Cohort were lost/damaged during processing, partly due to the age of the specimens, and partly due to some of the processes involved in their conservation during the coronavirus 19 (COVID-19) pandemic (storage in paraffin-wax), which required de-waxing to be performed prior to their use. Therefore, any small effect on survival may have been too subtle to pick up in the remaining specimens, and repeating these efforts in a newer cohort may provide different results.

Overall, TBX22 has been identified to have some role in cancer progression in other types of cancers and suggests that with further insight into its cellular location, role in cell function and a greater understanding of expression changes

in normal versus cancer tissue, further evidence of its role may become of prognostic value.

Chapter 7 The role of hypoxia, apoptosis, and tumour-infiltrating lymphocyte markers in predicting survival in patients with triple negative breast cancer

7.1 Introduction

Triple negative breast cancers are a subgroup of breast cancer lacking the expression of oestrogen, progesterone and HER2 receptors, hence denoting their "triple negative" receptor status. There is considerable overlap in TNBC and the molecular subgroup basal-like breast cancers (80%) therefore, these are often used interchangeably within the literature(239, 240). Basal-like breast cancers are described to have low ER expression, absent HER2 overexpression, and a phenotype suggestive of basal or myoepithelial origin within the normal breast (239, 241).

Approximately 15% of all breast cancer fall into the TNBC category, but represent a considerably poor prognostic group (241, 242). Found to be more common in ethnic groups belonging to Black and Hispanic women, as well as in carriers of the BRCA1 gene mutation, these cancers often develop in young patients and are subsequently found to have higher invasive grade and larger tumour size at diagnosis, with reduced survival outcomes(241-244). Interestingly, survival for TNBC cancer patients differs from ER-positive patients, with the first 5 years from diagnosis representing the most at-risk period of relapse, after which, at 10-years post-diagnosis, disease recurrence is more common in the ER-positive group(5, 240, 243, 245, 246).

Due to the lack of surface and nuclear receptors, TNBC patients have a scarcity of known targets for endocrine or chemotherapy, although patients who respond well to neoadjuvant chemotherapy have a tendency to improved overall survival(247). It is therefore of paramount importance, that for patients with poorer prognostic scores at diagnosis, new targets for chemotherapy are identified, and a clear understanding of the factors involved in prognostic determination is achieved.

In this study, the GeoMx Digital Spatial Profiler (DSP) was utilised to further characterise the tumour and microenvironment in TNBC patients. Based on previous work by Morrow et al(2), it was suggested that tumour budding correlates with poor outcome in this group. By establishing the differences in the transcriptional landscape of TNBC this study set out to evaluate the differences between the high tumour budding and low tumour budding phenotype TNBCs.

7.1.1 The Cohort

As described in more detail in Chapter 2 Materials & Methods, the Triple Negative Breast Cancer (TNBC) cohort, consisting of 207 patients with TNBC cancer who underwent surgical resection for primary operable invasive breast cancer at two Glasgow Hospitals between 2011 and 2019 were included. Clinicopathological characteristics including age, nodal status, invasive grade, and overall and disease-free survival were collected prospectively, (*Table 7-1)*.

Table 7-1 Clinicopathological characteristics of the TNBC cohort. (n=157 unless indicated otherwise)

Clinicopathological Characteristics	Patients n (%)
Age (n=157)	
≤50	37 (23.6)
>50	120 (76.4)
Tumour Size (n=154)	
<20mm	66 (42.9)
20-49mm	79 (51.3)
>50mm	9 (5.8)
Invasive Grade (n=154)	
I	1(0.6)
II	8(5.2)
III	145(94.2)
Nodal Status (n=154)	
Negative	122(65)
Positive	32(35)
Received adjuvant (n=157)	
Chemotherapy	102(65)
Radiotherapy	55(35)
Identified via (n=157)	
Screening	38(24.2)
Symptomatic	117(74.5)
At surgery	2(1.3)
Re-excision required after primary surgery (n=157)	
No	146(93)
Yes	11(7)

Outcome data was confirmed for all cases on 31 March 2022, with recurrence, or death by cancer/any cause documented. Median follow up was 73 months, (mean 75.8 months) with a minimum of 35 months and maximum of 125 months. TMA microarray was constructed by the GTRF, and sections supplied for digital spatial profiling. Data analysis was performed after patients who received neoadjuvant chemotherapy were excluded (n=50)(*Figure 7-1*).

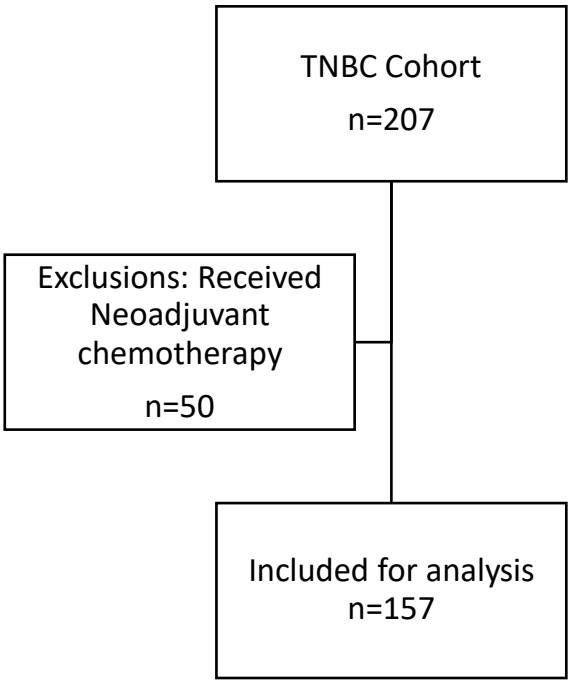

Figure 7-1 CONSORT diagram describing the TNBC Cohort.

7.1.2 GeoMx Digital Spatial Profiler

GeoMx digital spatial profiling (DSP) is a technology by which the role of potential biomarkers in the TNBC cohort could be explored. As described in Chapter 2 Materials & Methods, specimens from the TNBC cohort were processed and sections used as part of a TMA series. Following the processes described in Chapter 2, the slides were stained with fluorescently labelled antibodies to Pancytokeratin (anti-PanCK) and CD45 (anti-CD45), to allow identification of tumour cells and immune cells. Following successful 3-plex immunofluorescence staining, regions of interest (ROIs) were manually selected using the GeoMx platform, which then was utilised to collect information regarding RNA expression of 84 genes. Differential gene expression was assessed and a comparison between high TB, and low TB tumour samples was made. Differentially expressed genes with a log2 fold change ≥ 1 and $p<0.05$ were considered statistically significant. Following this analysis, Volcano plots were created to visualise the relationship between differential gene expression and tumour budding, as described later in this chapter.

7.1.3 IHC for Protein Expression Validation and Scoring

To validate the findings from GeoMx DSP, TMA specimens from the TNBC Cohort were stained using immunohistochemistry for 4 proteins: HIF-1alpha, CAIX, BCL2 and CD3. Details of the IHC process are described in more detail in Chapter 2 Materials & Methods. A negative control slide was performed each time the process was repeated to check for non-specific staining. Each protein was

manually scored by SS to reach a WHS, and counter scores for 10% of each protein specimen series performed by independent scorer (Joanne Edwards, JE) to validate the WHS before use for further analysis. An ICCC value of >0.7 was considered satisfactory evidence of reliability.

7.2 Results

A comparison was made between high TB (≥28) and low TB (TB <28) cases within 52 TMA samples from the TNBC cohort. The tumour buds were scored by FS as described in Materials & Methods,(Chapter 2). Previously described (for the Glasgow Breast Cancer Cohort) as a threshold of 20 by Gujam et al., survival data was analysed using RStudio and a new threshold identified as 28 for the TNBC cohort(10). The threshold of 28 was utilised, with 28+ denoting a "high tumour budding" phenotype as described in Chapter 1(*Figure 7-2)*.

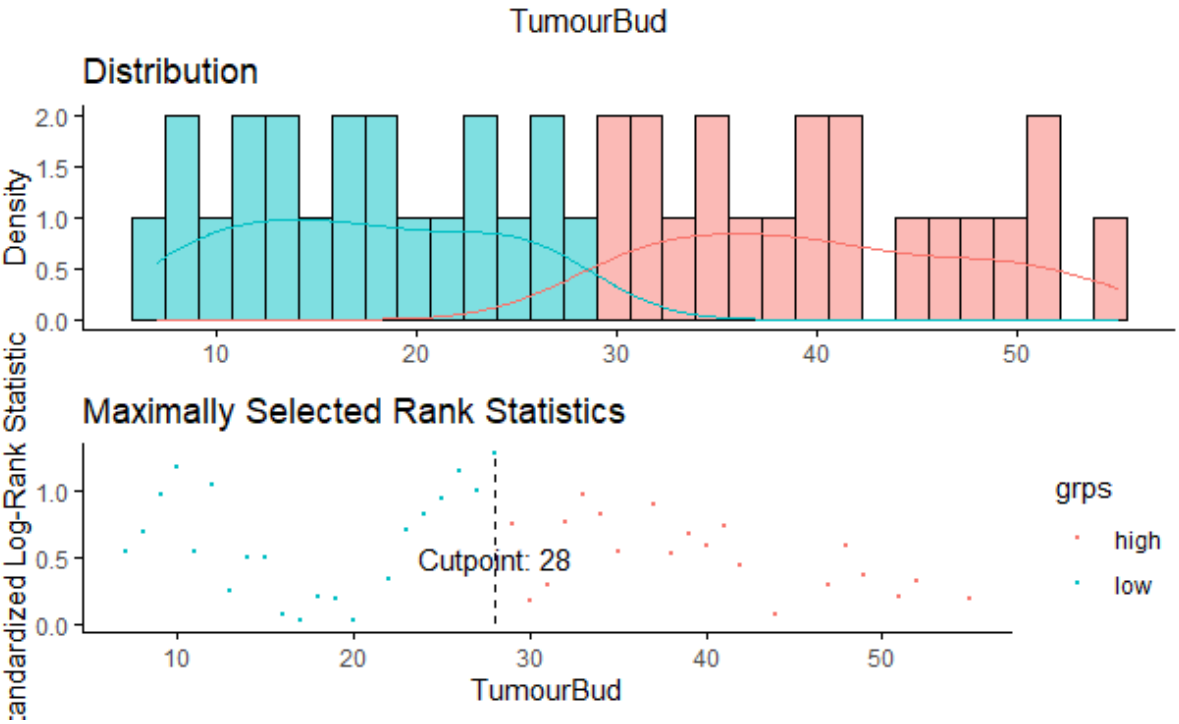

Figure 7-2 Threshold calculation for TNBC Cohort Tumour Budding denoting a threshold of 28 to denote high TB vs low TB. Scores of 28 TB or above were considered "high TB" phenotype.

7.2.1 GeoMX DSP for Assessment of Tumour and Microenvironment

The GeoMx DSP platform was utilised, as described earlier in this chapter, to compare RNA expression of 84 genes, and allowed for identification of differences between PanCK-positive (considered tumour-rich) areas, and PanCK-negative (stroma-rich) areas. Differentially expressed genes with a log2 fold

change ≥1 and p=0.05 were considered statistically significant. Volcano plots were created using Nanostring plug in described in Chapter 2, and are shown below.

Within the ROIs identified during processing, a Volcano plot was created for the regions with high anti-PanCK fluorescent antibody, considered to represent the tumour-rich portion of the ROI, (*Figure 7-3)*. In the PanCK-positive areas, 9 genes were found to be highly expressed in low tumour budding specimens compared to high tumour budding specimens. These included VEGFA, FOXP3, CD4, LAG3, IDO1, HIF1alpha, AKT1, pan-melanocyte and TIGIT. Stat3, IFNAR1 and PDCD1 neared significance.

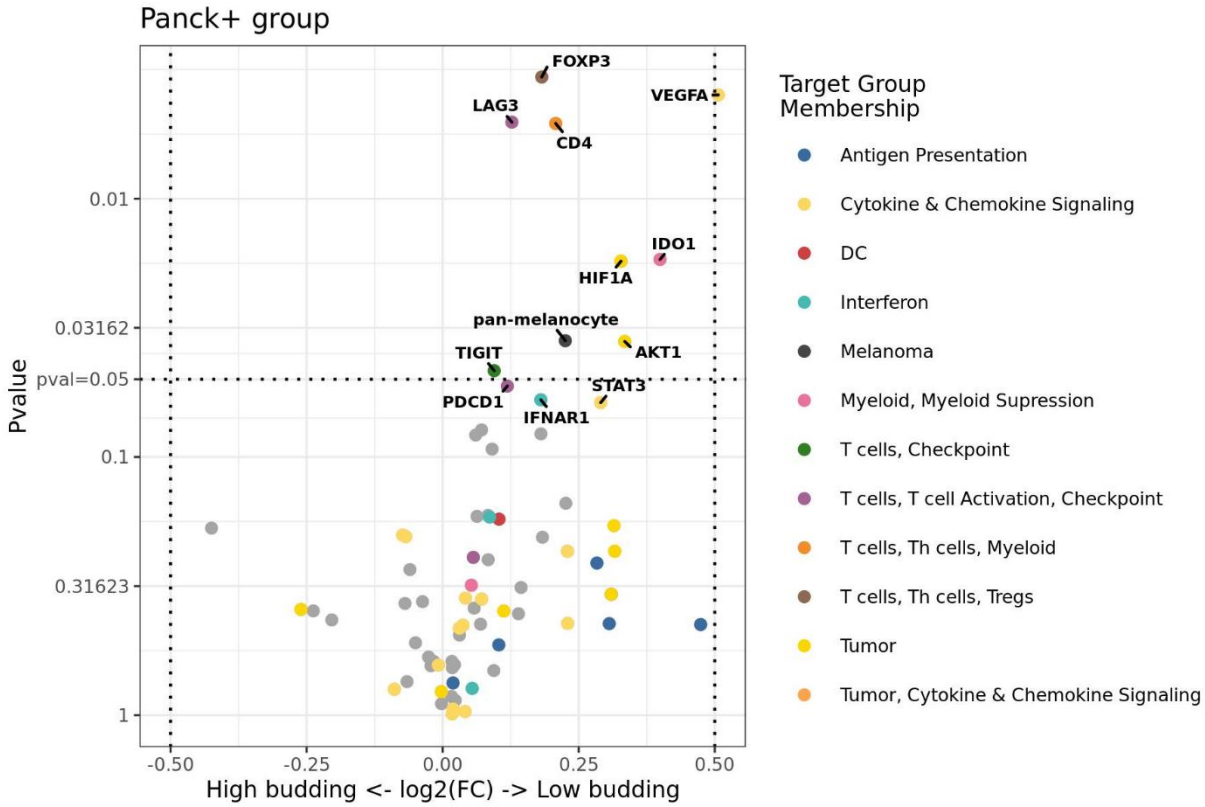

Figure 7-3 Volcano Plot depicting the most differentially expressed genes within the PanCK+ / Tumour rich areas within the selected TNBC cohort according to tumour budding phenotype.

In the cells with low/no PanCK expression, (considered stroma-rich areas), VEGFA and BATF3 were highly differently expressed in low budding cases, whereas PSMB10, BLC2 and CMKLR1 were highly differentially expressed in high budding tumours(*Figure 7-4)*.

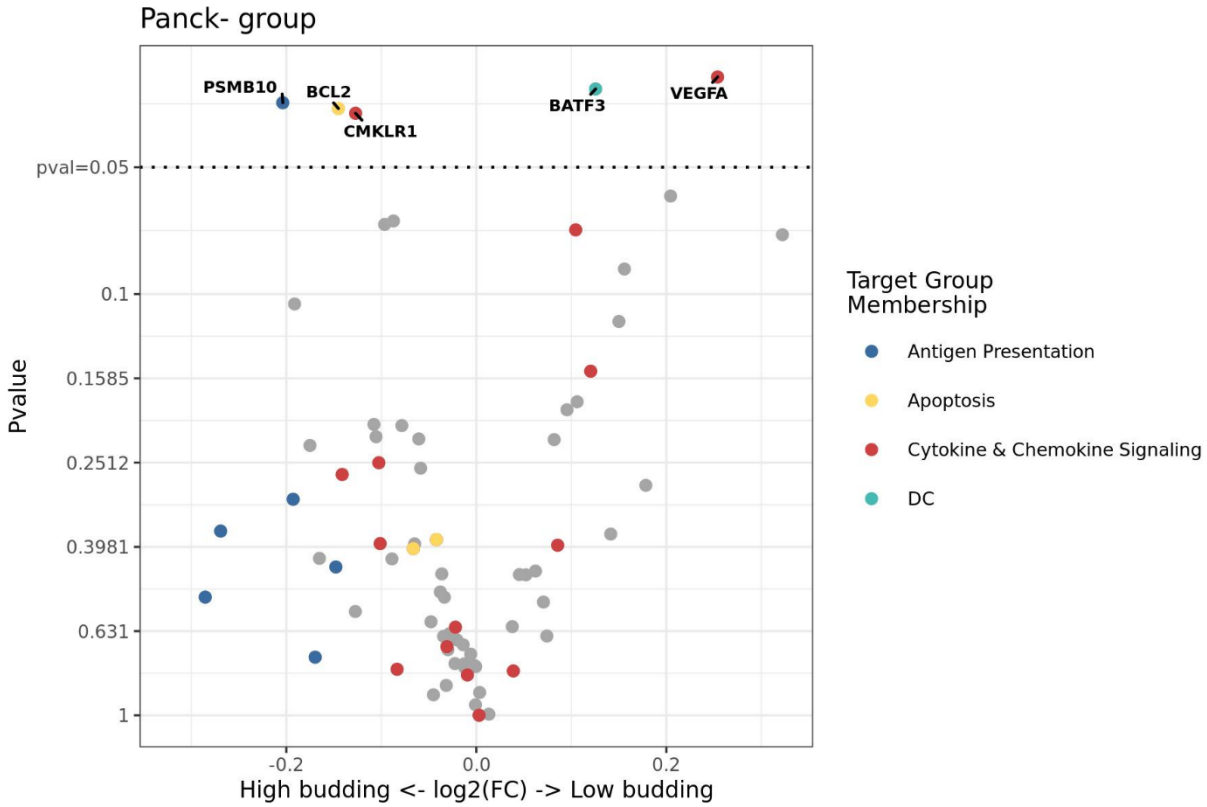

Figure 7-4 Volcano Plot depicting the most differentially expressed genes within the PanCK-/Stroma rich areas within the selected TNBC cohort according to tumour budding phenotype.

Based on these results, further analysis was conducted looking at the following protein expression: HIF-1alpha and CD3 (considered as surrogate for and closely related to CD4) identified as significantly differentially expressed gene in tumour-rich regions in low-tumour budding specimens. In addition, BCL2 was selected as a differentially expressed gene in the stroma-rich microenvironment in high budding tumours. Finally, as an additional marker of cellular hypoxia, CAIX (known to have a more stable half-life versus HIF-1α during immunohistochemistry) was also available for analysis within our laboratory, and included in the results of this study.

7.2.2 HIF-1α

Hypoxia-inducible factor 1α (HIF-1α) is one of two subunits (the other being HIF-1β) which composes the heterodimer family HIF-1, HIF-2 and HIF-3 involved in regulation of a cell's response to hypoxia. HIF activity is regulated through oxygen (0_2), and plays a key role in cancer development and progression, particularly due to the relative hypoxia related to rapid cellular growth and abnormalities in vascular development seen within a tumour mass, and in some cases, as a result of the hypoxia, which drives disease progression (248-250). The activity of HIFs has been described to be primarily through the hydroxylation of

proline and asparagine, which initiates a process by which the final outcome is increased transcriptional activity in the context of low O_2 levels within the cell with an effect on more than 100 target genes(248, 251, 252). This relatively vast input into multiple transcriptional processes across the genome, and the inherent importance of hypoxia in cancer biology, suggest a significant role for HIF across multiple types of cancers as well as normal human cellular processes. Cancers of the breast, ovaries, bladder, uterus, colon, brain, pancreas, renal tract and prostate have all been demonstrated to have overexpressed levels of HIF-1(248) In fact, HIFs are described in roles relating to angiogenesis, growth factor signalling, epithelial-mesenchymal transition (EMT), invasion, metastasis and in development of resistance to adjuvant therapies amongst other roles in cancers (253-261). Some effects of HIFs regulate the transcription of genes such as VEGF, also identified in our study to be differentially expressed when comparing high to low tumour budding TNBCs(248). HIF-1α is commonly associated with cancer suggesting that this may be a valuable biomarker to examine with regards to tumour budding(262). Thanks to work by Li et al. the primary activity of HIF-1alpha has been localised to the cellular cytoplasm, which accumulates in response to hypoxia, and subsequently dimerises with HIF-1ß within the nucleus proceeds to bind to the hypoxia-response element (HRE) of target genes leading to transcriptional activity(263).

The role of HIF-1α in breast cancer prognosis has been well documented, and recently been the subject of a systematic review and meta-analysis by Shamis et al(264). High levels of HIF-1α are associated with poor outcomes, particularly in the TNBC cases(265-269). More recently, Guindy et al. have demonstrated that high levels of HIF-1α, amongst other biomarkers including Bcl-2, as associated with reduced survival in TNBC(270). BCL-2 is discussed in further detail later in this chapter. HIF-1α scoring was performed by SS based on IHC examination of the membrane and cytoplasm expression of anti-HIF-1α protein antibody, as described in Chapter 2 materials and methods.

7.2.3 CAIX

Carbonic anhydrase IX (CAIX), a transmembrane metalloenzyme, is considered a marker of endogenous hypoxia, has been associated with reduced prognosis in many cancers, including TNBC(271, 272). There has been evidence of the role of CAIX and hypoxia in promoting BRCA1 and BRCA2 mutation carriers towards

carcinogenesis, including at the DCIS stage(273, 274). Recently, a systematic review and meta-analysis by Numprasit et al. demonstrated that high levels of CAIX expression are associated with reduced survival in all subtypes of breast cancer, including TNBC, with recent work by Shamis et al. supporting these findings (275-277). As one of the genes for which HIF-1α is known to activate transcription, CAIX has been demonstrated to maintain acid-base balance within the cellular microenvironment, by promoting an acidic extracellular pH (278). Through this role, and through effects mediated by hypoxia itself, CAIX expression therefore mediates downstream effects on cancer cell growth, suppression of anti-tumour immune response, promoting EMT, and invasion, therefore promoting cancer disease progression(279-281). In addition, a role for CAIX has been identified in basal-like cell cancers in promoting resistance to chemotherapy(275, 282, 283). More recent work by Twomey et al. has established the role of CAIX suppression on reduction of in vitro models of circulating tumour cells (CTCs), suggesting that CAIX may not only provide a serum biomarker for micrometastatic disease, but also as a potential therapeutic target, although evidence remains to be fully supported by the literature, with contrasting findings suggesting a lack of role for serum CAIX (284-286). Finally, some evidence suggest a role for CAIX as a prognostic indicator of complete pathological response to neoadjuvant chemotherapy in breast cancers, as well as in predicting response to radiotherapy, suggests a more complex role for this protein (287, 288). Jin et al. have proposed a role in combined HIF-1α and CAIX in predicting response to adjuvant therapies(289). CAIX scoring was performed by SS based on IHC examination of the membrane and cytoplasm expression of anti-CAIX protein antibody, as described in Chapter 2.

7.2.4 BCL2

B-cell lymphoma 2 (Bcl-2) is a membrane-bound protein from the anti-apoptotic Bcl-2 family with more than 20 described members, and high levels of expression have been associated with favourable outcomes in breast cancer(290, 291). Bcl-2 has been identified in normal breast tissue and is associated with markers of differentiation including lower cancer histology grade, low proliferative status, and ER-negative status(290). Their role has been described as “pro-apoptotic scavengers” which, in response to apoptotic signals, facilitate the mediation of apoptosis as part of the intrinsic apoptotic pathway, through a mechanism which has been proposed to involve mitochondrial membrane targets (292-294).

Approximately 75% of primary breast cancer, and particularly ER-positive phenotype tumours (85% have Bcl-2 over-expression), are thought to express Bcl-2(295). The role of Bcl-2 on breast cancer progression has been suggested to vary depending on tumour type and stage. For example, there is evidence that in metastatic breast cancer, lower Bcl-2 expression was associated with poorer prognosis, in contrast to previously found in ER-positive, early tumours, where Bcl-2 may offer a protective role(296). This is thought to be consistent with the role of Bcl-2 in mediating apoptosis, particularly in the context of promoting survival of tumour cells when present in conjunction with other abnormalities in normal signalling within the cell cycle(297, 298). The role of Bcl-2 in breast cancers has raised interest in the field of development of adjuvant therapies, particularly after some encouraging results in Phase 1 trials in other types of cancer including lymphoma using BH3-mimetic agents, but also when outcomes appeared to be improved when Bcl-2 inhibiting agents were used in conjunction with therapies including tamoxifen and doxorubicin *in vitro(299-302)*. Approximately 41% of TNBCs and 19% of Basal-type tumours have been demonstrated to have high levels of Bcl-2(295). In TNBC, Bcl-2 was identified as a predictor of poor outcome for patients treated with anthracycline-based adjuvant chemotherapy, suggesting a role in Bcl-2 as a prognostic predictor and potentially an aid in clinical decision-making for patients in this subgroup(303).

7.2.5 CD3

Tumour-infiltrating lymphocytes (TILs) have been identified to have an important role in breast cancer in general, and particularly in HER2-enriched TNBCs, with higher levels of TILs being associated with improved response to neoadjuvant chemotherapy(304-309). As CD4 was identified to be one of the most differentially expressed genes in the low budding, tumour rich regions of interest, this suggests that other TILs may also be involved in prognosis and act as a biomarker. Parallel work within our laboratory looking at CD3 expression allowed immunohistochemical staining and score results to be readily available, and hence this study focused on CD3 expression as a surrogate marker of TILs within our cohort and explore the relationship between CD3 expression and survival.

In summary, as part of this study, HIF-1α and CAIX were considered indicators of hypoxia, while Bcl-2 was considered a marker of apoptosis, and CD3 as a marker

of TILs within the tumour microenvironment. Recurrence-free survival (RFS) and Cancer-specific survival (CSS) were used as primary end-points and are indicated in the results. RFS was utilised to allow capture of recurrence in this cohort, which had a relatively shorter follow-up period (median 73months), as discussed later in this chapter.

7.2.6 Thresholds for Protein Expression

Thresholds for high/low expression of each protein were established using R studio (RStudio, Boston, MA, USA), as performed by S Shamis (SS) using survminer and maxstat packages, based on OS as the outcome. This allowed each protein expression to be classified into “low” and “high” expression. The thresholds were identified as shown below,(Table 7-2*)*.

Table 7-2 Thresholds established using R Studio for HIF-1alpha, CAIX, Bcl2 and CD3. Any expression with a weighted histoscore (WHS) at or over the threshold was considered "high expression".

Marker	Threshold
Cytoplasmic CAIX	27
Membranous CAIX	30
Cytoplasmic BCL2	47
Cytoplasmic HIF-1a	180
Nuclear HIF-1a	150
Tumour CD3	0.26
Stromal CD3	2
Combined CD3	0.9

Using these thresholds, using SPSS (IBM SPSS, SPSS Inc. Chicago, IL, USA), statistical analysis was performed. Kaplan-Meier’s survival plot, log rank test were used to calculate RFS and CSS. Univariate Cox regression survival analysis was used to create a HR and 95% C.I., and perform multivariate Cox regression survival analysis using a backward conditional model when HR was statistically significant ($p<0.05$).

7.2.7 Protein Expression and Survival in the TNBC cohort

7.2.8 HIF-Alpha

HIF-1α WHS were scored and based on two cellular locations: cytoplasm HIF-1α (cytHIF-1α) expression, and nuclear HIF-1α (nucHIF-1α).

7.2.9 Cytoplasmic HIF-1a

Cytoplasmic HIF-1α (cytHIF-1α) was scored and thresholds considered as a WHS of 180. Recurrence-free survival was calculated for the low versus high expression groups in the TNBC cohort. In the low cytHIF-1α group 91 cases had 7 events, while in the high cytHIF-1α group 16 cases had 4 events. Mean RFS was 92.3 months for the low cytHIF-1α group, with a 5-year RFS of 92%, and the high cytHIF-1α group had a mean RFS of 76.3 months and a 5-year RFS of 54% (p=0.018), HR 3.960 (95% C.I. 1.151-13.632) p=0.029, (*Figure 7-5*).

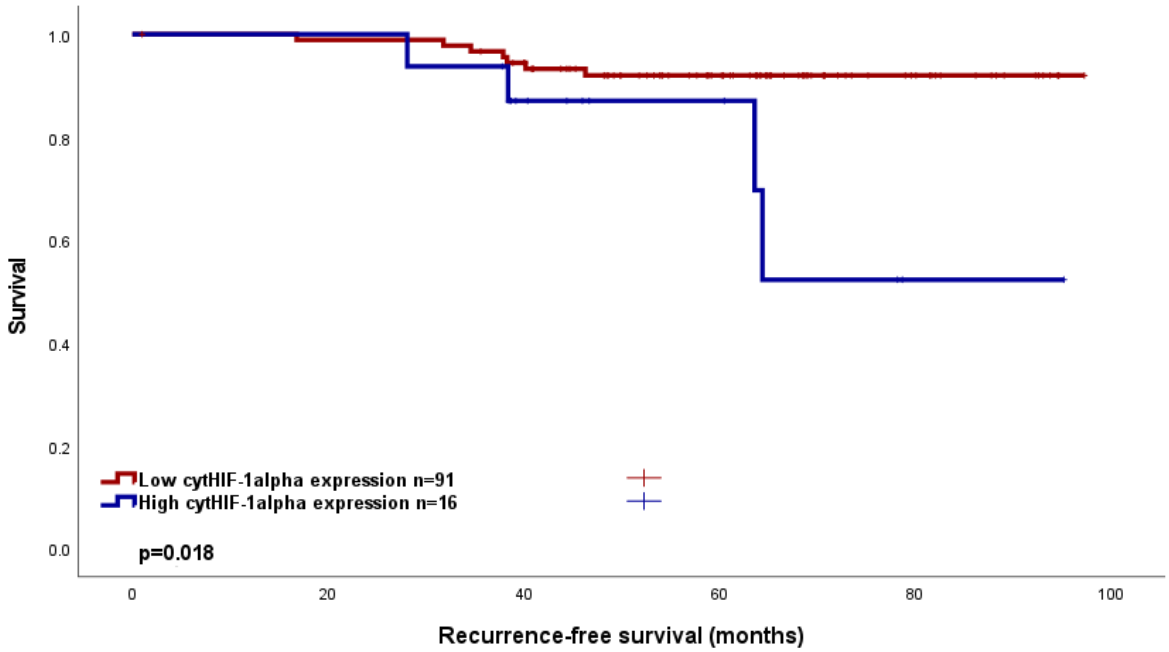

Figure 7-5 Kaplan Meier curve describing RFS and cytoplasmic HIF-1alpha expression in TNBC. HR 3.960 (95% C.I. 1.151-13.632) p=0.029.

Clinicopathological factors were examined using Cox univariate and multivariate regression analysis. This suggested that cytHIF-1α was statistically significant on multivariate analysis (HR 4.738 (95% C.I. 1.142-19.650) p=0.032, (*Table 7-3*).

Table 7-3 Cox Univariate and Multivariate regression analysis of clinicopathological findings associated with RFS compared with cytHIF-1α expression.

Clinicopathological Factor	Univariate analysis (HR, 95% C.I.)	p	Multivariate analysis (HR, 95% C.I.)	p
Age	4.000(0.510-31.360)	0.187		
Tumour Size <20mm 20-49mm	 **4.039(0.839-19.456)**	**0.070** **0.086** **0.082**	 **3.327(0.637-17.391)**	 **0.067** **0.154**

>50mm	**12.748(1.139-142.684)**	**0.039**	**4.738(1.142-19.650)**	**0.022**
Invasive Grade I II III	 **0.088(0.005-1.543)** **0.036(0.004-0.324)**	**0.084** **0.011** **0.096** **0.003**	 0.136(0.014-1.276)	 0.081
Nodal Status	2.997(0.875-10.270)	0.081		
Lymphatic Invasion	23.768(0.003-198847.255)	0.492		
Vascular Invasion	1.157(0.306-4.369)	0.830		
Necrosis	0.644(0.186-2.227)	0.487		
Klintrup-Makinen 0 1 2 3	 0.422(0.113-1.573) 0.137(0.015-1.232) 0(0)	0.042 0.297 0.422 0.137 0.973		
Tumour budding	0.629(0.166-2.374)	0.494		
Tumour stroma percentage	2.431(0.702-8.416)	0.161		
CytHIF-1α	**3.960(1.151-13.632)**	**0.029**	**4.738(1.142-19.650)**	**0.032**

Cancer-specific survival was assessed with regards to cytHIF-1α expression. In the low cytHIF-1α group 124 cases had 30 events, while in the high cytHIF-1α group 23 cases had 6 events. Mean CSS was 90.6 months for the low cytHIF-1α group, with a 5-year CSS of 74%, and the high cytHIF-1α group had a mean CSS of 77.5 months and a 5-year CSS of 74% (p=0.678), HR 1.204 (95% C.I. 0.500-2.897) p=0.679(*Figure 7-6*).

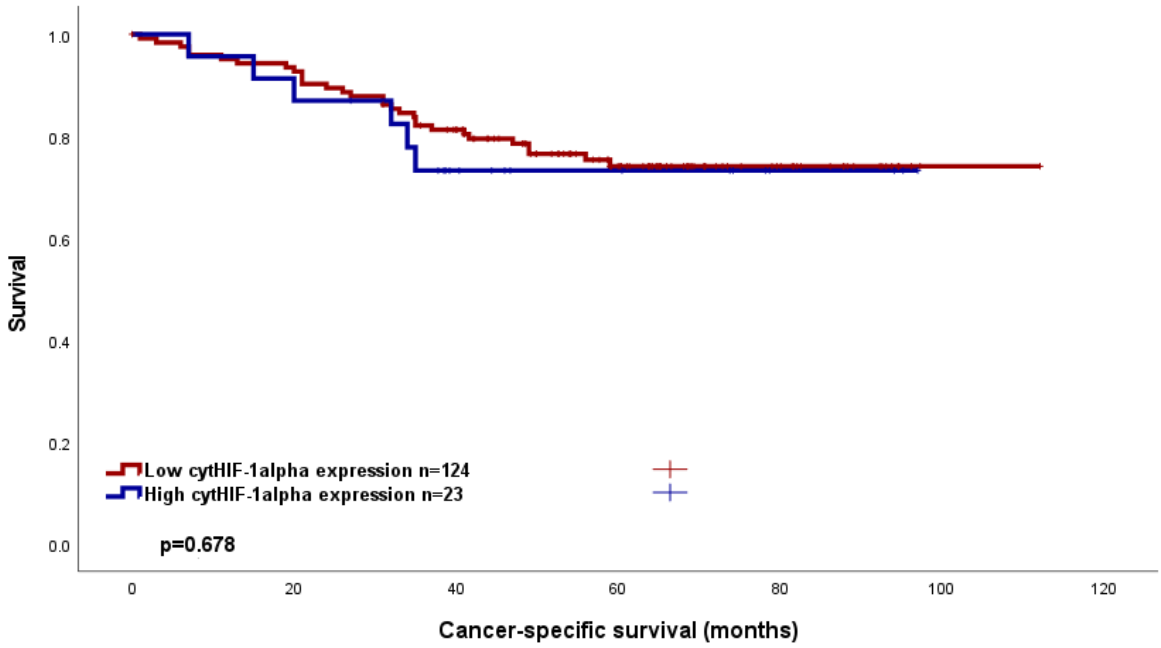

Figure 7-6 Kaplan Meier curve describing CSS and cytoplasmic HIF-1alpha expression in TNBC. HR 1.204 (95% C.I. 0.500-2.897) p=0.679.

Clinicopathological factors were assessed with regards to their association with cytHIF-1α expression. No statistically significant association was identified on Chi-squared analysis, although LVI neared significance (p=0.072), (*Table 7-4*)

Table 7-4 Comparison of clinicopathological findings and their relation to cytHIF-1alpha expression using Chi-squared analysis.

Clinicopathological factor	cytHIF-1α expression (%)		p
	Low	High	
Age (years)			
≤50	33(91.7)	3(8.3)	0.197
>50	91(82)	20(18)	
Tumour Size			
≤20mm	54(88.5)	7(11.5)	0.156
21-49mm	60(78.9)	16(21.1)	
≥50mm	7(100)	0	
Grade			
I	1(100)	0	0.552
II	5(100)	0	
III	115(83.3)	23(16.7)	
Nodal Status			
N_0	98(85.2)	17(14.8)	0.410
N_1	23(79.3)	6(20.7)	
Lymphovascular Invasion (LVI)			
Absent	10(66.7)	5(33.3)	0.072
Present	108(85.7)	18(14.3)	
Vascular Invasion			
Absent	83(83)	17(17)	0.633
Present	39(86.7)	6(13.3)	
Necrosis			
Absent	57(85.1)	10(14.9)	0.821
Present	62(82.7)	13(17.3)	
Klintrup Makinen			
0	15(78.9)	4(21.1)	0.788
1	48(84.2)	9(15.8)	
2	35(81.4)	8(18.6)	
3	18(90)	2(100	
Tumour Bud			
-Low	71(88.8)	9(11.3)	0.100
-High	45(77.6)	13(22.4)	
Tissue Stroma Percentage			
Low	83(85.6)	14(144)	0.461
High	35(79.5)	9(20.5)	

7.2.10 Nuclear HIF-1a

Nuclear HIF-1α (nucHIF-1α) was scored and thresholds considered as a WHS of 150. Recurrence-free survival was calculated for the low versus high expression groups in the TNBC cohort. In the low nucHIF-1α group 32 cases had 2 events, while in the high nucHIF-1α group 75 cases had 9 events. Mean RFS was 93.2 months for the low nucHIF-1α group, with a 5-year RFS of 94%, and the high nucHIF-1α group had a mean RFS of 87.3 months and a 5-year RFS of 84% (p=0.443), HR 1.807 (95% C.I. 0.390-8.369) p=0.449, (*Figure 7-7*).

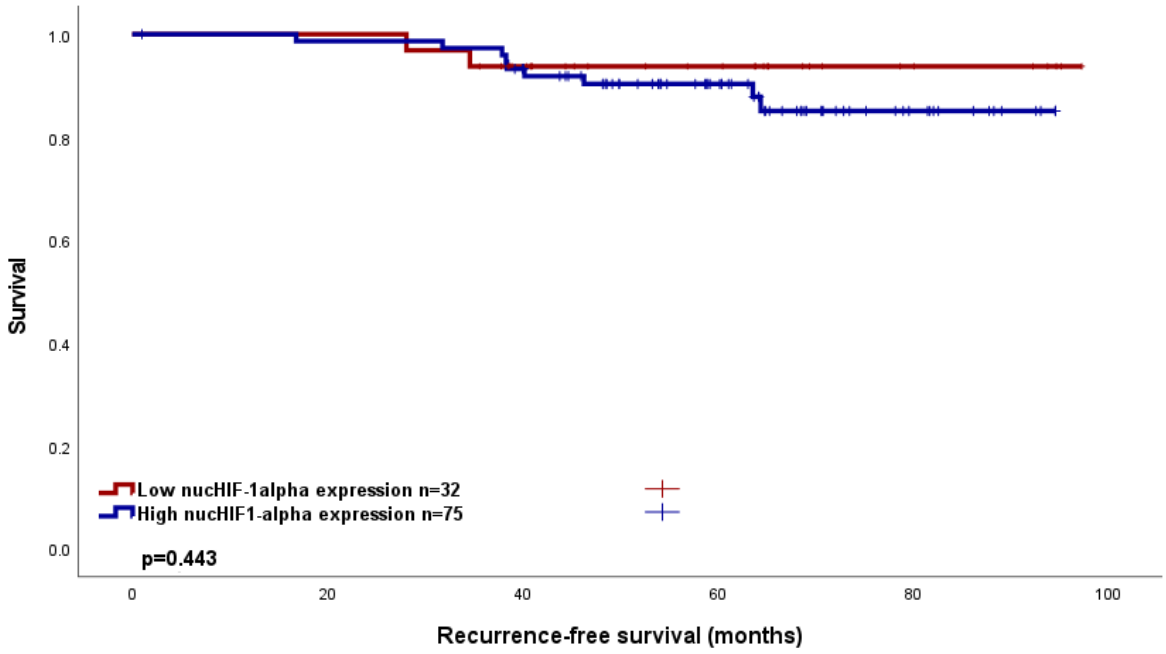

Figure 7-7 Kaplan Meier curve describing RFS and nuclear HIF-1alpha expression in TNBC. HR 1.807 (95% C.I. 0.390-8.369) p=0.449.

Cancer-specific survival was assessed with regards to nucHIF-1α expression. In the low nucHIF-1α group 36 cases had 6 events, while in the high nucHIF-1α group 111 cases had 30 events. Mean CSS was 84.6 months for the low nucHIF-1α group, with a 5-year CSS of 81%, and the high nucHIF-1α group had a mean CSS of 88.0 months and a 5-year CSS of 71% (p=0.231), HR 1.696 (95% C.I. 0.705-4.076) p=0.238, (*Figure 7-8*).

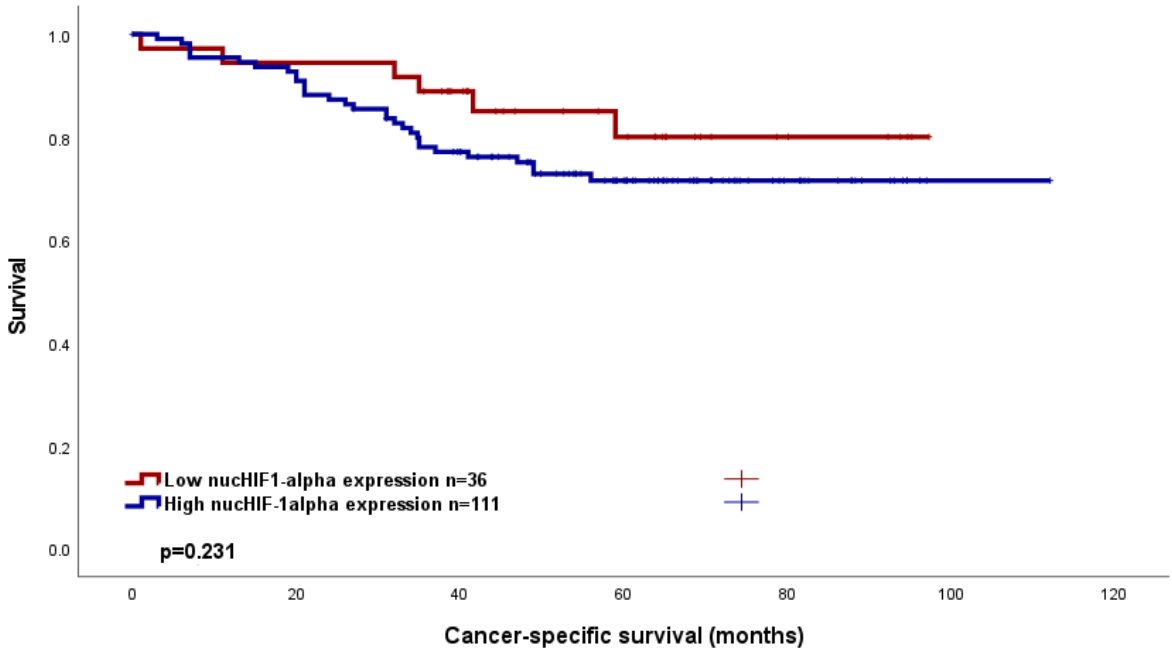

Figure 7-8 Kaplan Meier curve describing CSS and nuclear HIF-1alpha expression in TNBC. HR 1.696 (95% C.I. 0.705-4.076) p=0.238.

Clinicopathological factors were assessed with regards to their association with nucHIF-1α expression. Nodal status (p=0.031) and necrosis (p=0.033) appeared statistically significant on Chi-squared analysis in association with nucHIF-1α expression, (*Table 7-5*).

Table 7-5 Comparison of clinicopathological findings and their relation to nucHIF-1α expression using Chi-squared analysis.

Clinicopathological factor	**nucHIF-1α expression (%)**		**p**
	Low	**High**	
Age (years)			
≤50	9(25)	27(75)	1.000
>50	27(24.3)	84(75.7)	
Tumour Size			
≤20mm	14(23)	47(77)	0.500
21-49mm	18(23.7)	58(76.3)	
≥50mm	3(42.9)	4(57.1)	
Grade			
I	0	1(100)	0.624
II	2(40)	3(76.3)	
III	34(24.6)	104(75.4)	
Nodal Status			
N_0	**24(20.9)**	**91(79.1)**	**0.031**
N_1	**12(41.4)**	**17(58.6)**	
Lymphovascular Invasion (LVI)			
Absent	3(20)	12(80)	0.762

Present	32(25.4)	94(74.6)	
Vascular Invasion			
Absent	26(26)	74(74)	0.683
Present	10(22.2)	35(77.8)	
Necrosis			
Absent	**11(16.4)**	**56(83.6)**	**0.033**
Present	**25(33.3)**	**50(66.7)**	
Klintrup Makinen			
0	4(21.1)	15(78.9)	0.845
1	12(21.1)	45(78.9)	
2	11(25.6)	32(74.4)	
3	6(30)	14(70)	
Tumour Bud			
-Low	19(23.8)	61(76.3)	0.837
-High	12(20.7)	46(79.3)	
Tissue Stroma Percentage			
Low	28(28.9)	69(71.1)	0.140
High	7(15.9)	37(84.1)	

7.2.11 CAIX

CAIX expression was assessed in two cellular compartments, membrane (memCAIX) and cytoplasm (cytCAIX), for which WHS were manually scored and used for analysis.

7.2.12 Membrane CAIX

Membrane CAIX (memCAIX) was scored and threshold considered as a WHS of 30. Recurrence-free survival was calculated for the low versus high expression groups in the TNBC cohort. In the low cytCAIX group 77 cases had 6 events, while in the high cytCAIX group 30 cases had 5 events. Mean RFS was 90 months for the low cytCAIX group, with a 5-year RFS of 90%, and the high cytCAIX group had a mean RFS of 85.6 months and a 5-year RFS of 78% (p=0.146), HR 2.350(95% C.I. 0.717-7.709) p=0.158, (*Figure 7-9*).

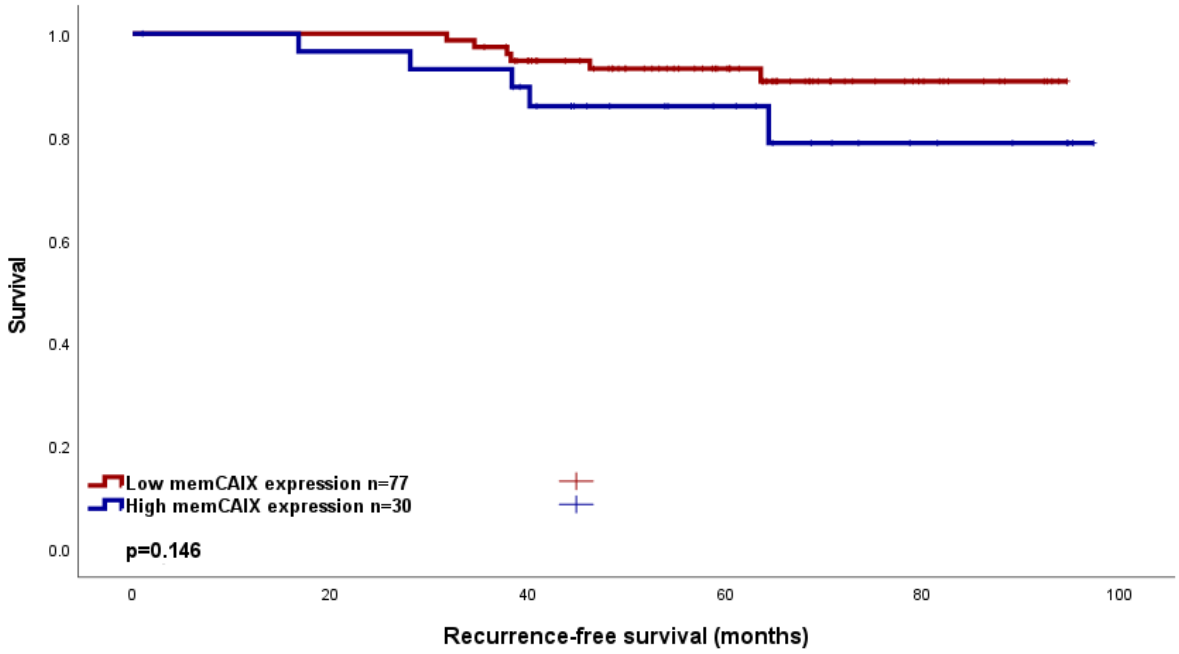

Figure 7-9 Kaplan Meier curve describing RFS and memCAIX expression in TNBC. HR 2.350(95% C.I. 0.717-7.709) p=0.158.

Cancer-specific survival was then assessed for memCAIX expression. In the low cytCAIX group 108 cases had 29 events, while in the high cytCAIX group 41 cases had 8 events. Mean CSS was 76.7 months for the low cytCAIX group, with a 5-year CSS of 72%, and the high cytCAIX group had a mean CSS of 94.3 months and a 5-year CSS of 80% (p=0.445), HR 0.458(95% C.I. 0.339-1.628) p=0.458, (*Figure 7-10*)

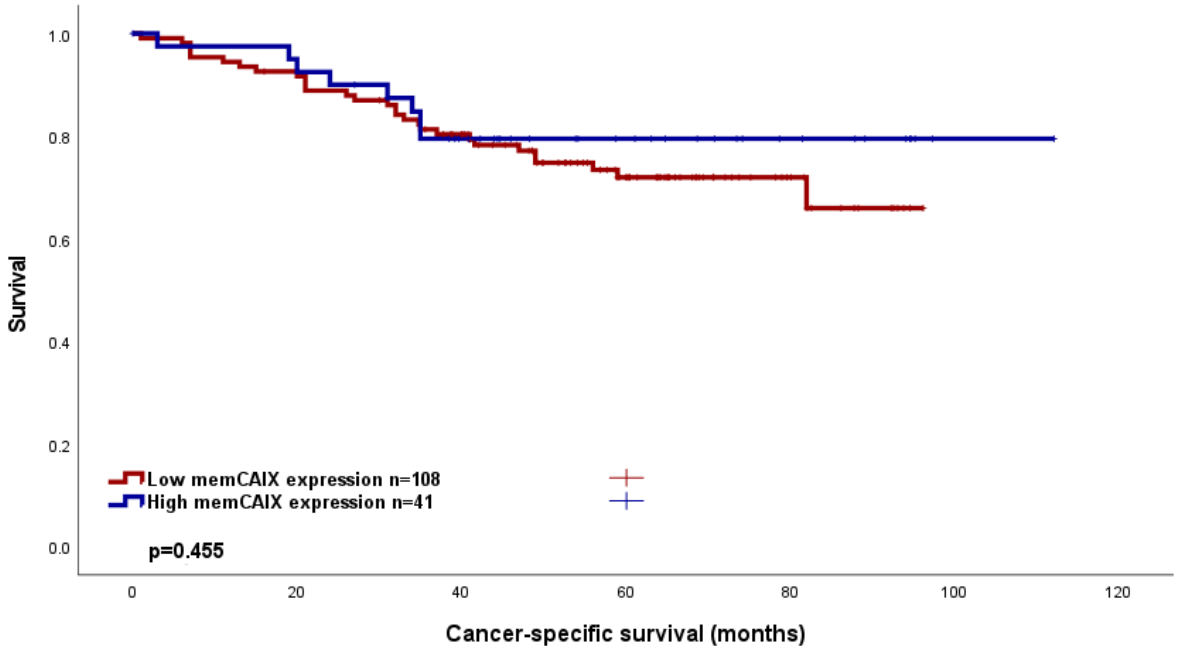

Figure 7-10 Kaplan Meier curve describing CSS and memCAIX expression in TNBC. HR 0.458(95% C.I. 0.339-1.628) p=0.458.

Clinicopathological factors were assessed with regards to their association with memCAIX expression. No statistically significant association was identified on Chi-squared analysis, (*Table 7-6*).

Table 7-6 Comparison of clinicopathological findings and their relation to memCAIX expression using Chi-squared analysis.

Clinicopathological factor	**memCAIX expression (%)**		**p**
	Low	**High**	
Age (years)			
<50	27(73)	10(27)	1.000
>50	81(72.3)	31(27.7)	
Tumour Size			
<20mm	46(75.4)	15(24.6)	0.507
21-49mm	54(70.1)	23(29.9)	
>50mm	7(87.5)	1(12.5)	
Grade			
I	1(100)	0	0.253
II	6(100)	0	
III	100(71.4)	40(28.6)	
Nodal Status			
N0	83(72.2)	32(27.8)	1.000
N1	22(71)	9(29)	
Lymphovascular Invasion (LVI)			
Absent	10(66.7)	5(33.3)	0.534
Present	97(75.2)	32(32)	

Vascular Invasion			
Absent	71(70.3)	30(29.7)	0.554
Present	35(76.1)	11(23.9)	
Necrosis			
Absent	52(75.4)	17(24.6)	0.851
Present	56(73.7)	20(26.3)	
Klintrup Makinen			
0	15(78.9)	4(21.1)	0.777
1	41(70.7)	17(29.3)	
2	32(74.4)	11(25.6)	
3	17(81)	4(19)	
Tumour Bud			
-Low	60(73.2)	22(26.8)	0.845
-High	44(74.6)	15(25.4)	
Tissue Stroma Percentage			
Low	72(73.5)	26(26.5)	0.839
High	35(76.1)	11(23.9)	

7.2.13 Cytoplasmic CAIX

Cytoplasmic CAIX (cytCAIX) was scored, and thresholds considered as a WHS of 27. Recurrence-free survival was calculated for the low versus high expression groups in the TNBC cohort. In the low cytCAIX group 79 cases had 5 events, while in the high cytCAIX group 28 cases had 6 events. Mean RFS was 93.3 months for the low cytCAIX group, with a 5-year RFS of 92%, and the high cytCAIX group had a mean RFS of 80.8 months and a 5-year RFS of 72% (p=0.019), HR 3.755 (95% C.I. 1.145-12.314) p=0.029, (*Figure 7-11*).

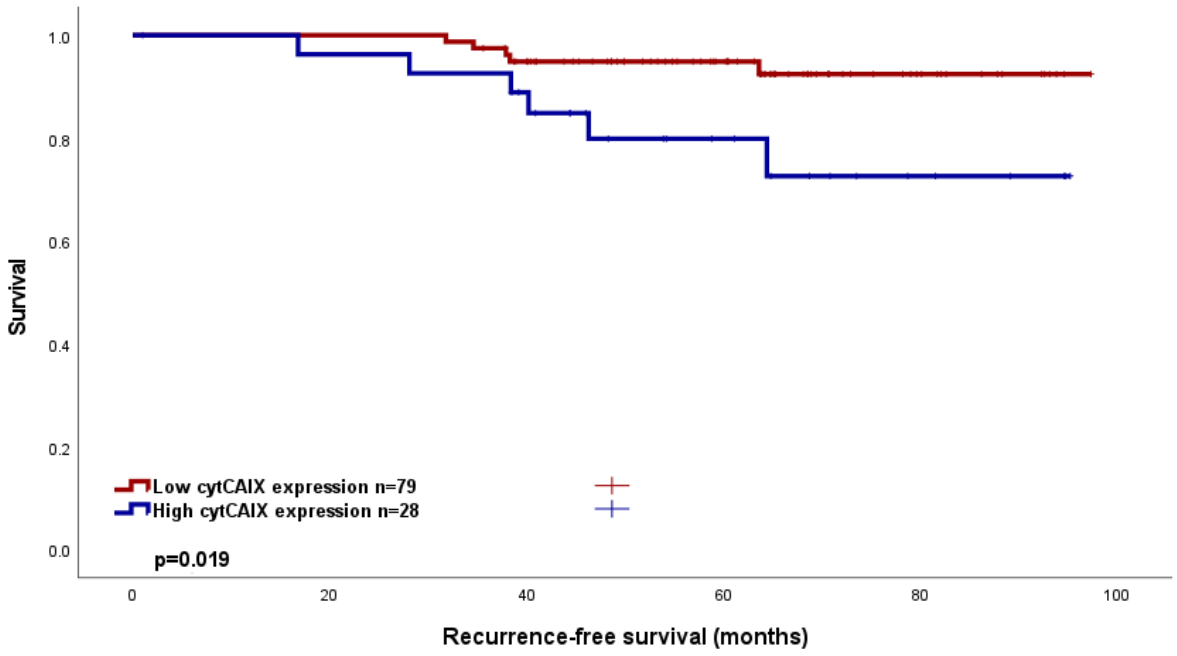

Figure 7-11 Kaplan Meier curve describing RFS and cytCAIX expression in TNBC. HR 3.755 (95% C.I. 1.145-12.314) p=0.029. Pairwise comparison and numbers in each expression subgroup are described.

Clinicopathological factors were examined using Cox univariate and multivariate regression analysis. This suggested that cytCAIX was statistically significant on multivariate analysis (HR 5.333 (95% C.I. 1.311-21.695) p=0.019), (*Table 7-7*).

Table 7-7 Cox Univariate and Multivariate regression analysis of clinicopathological findings associated with RFS compared with cytCAIX expression.

Clinicopathological Factor	Univariate analysis (HR, 95% C.I.)	p	Multivariate analysis (HR, 95% C.I.)	p
Age	4.000(0.510-31.360)	0.187		
Tumour Size		0.070		
<20mm		0.086		0.052
20-49mm	4.039(0.839-19.456)	0.082	2.939(0.598-14.441)	0.184
>50mm	12.748(1.139-142.684)	0.039	22.649(1.796-285.614)	0.016
Invasive Grade		0.084		
I		0.011		
II	0.088(0.005-1.543)	0.096		
III	0.036(0.004-0.324)	0.003	0.371(0.045-3.059)	0.357
Nodal Status	2.997(0.875-10.270)	0.081		
Lymphatic Invasion	23.768(0.003-198847.255)	0.492		
Vascular Invasion	1.157(0.306-4.369)	0.830		
Necrosis	0.644(0.186-2.227)	0.487		
Klintrup-Makinen		0.042		
0		0.297		
1	0.422(0.113-1.573)	0.422		
2	0.137(0.015-1.232)	0.137		
3	0(0)	0.973		
Tumour budding	0.629(0.166-2.374)	0.494		
Tumour stroma percentage	2.431(0.702-8.416)	0.161		
CytCAIX	3.755(1.145-12.314)	0.029	5.333(1.311-21.695)	0.019

Cancer-specific survival was calculated with regards to cytCAIX expression. In the low cytCAIX group 112 cases had 30 events, while in the high cytCAIX group 37 cases had 7 events. Mean CSS was 77.5 months for the low cytCAIX group,

with a 5-year CSS of 72%, and the high cytCAIX group had a mean CSS of 94.6 months and a 5-year CSS of 80% (p=0.441), HR 0.725 (95% C.I. 0.318-1.652) p=0.444,(*Figure 7-12*).

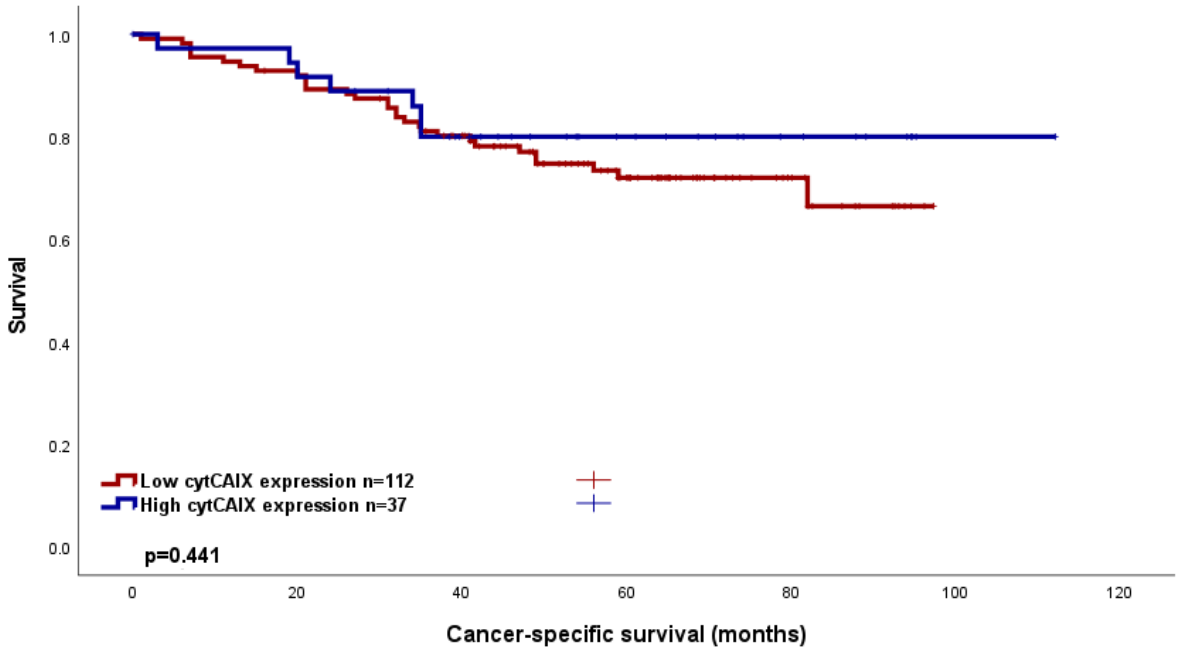

Figure 7-12 Kaplan Meier curve describing CSS and cytCAIX expression in TNBC. HR 0.725 (95% C.I. 0.318-1.652) p=0.444. Pairwise comparison and numbers in each expression subgroup are described.

Clinicopathological factors were assessed with regards to their association with cytCAIX expression. No statistically significant association was identified on Chi-squared analysis,(*Table 7-8*).

Table 7-8 Comparison of clinicopathological findings and their relation to cytCAIX expression using Chi-squared analysis.

Clinicopathological factor	**cytCAIX expression (%)**		**p**
	Low	High	
Age (years)			
≤50	29(78.4)	8(21.6)	0.667
>50	83(74.1)	29(25.9)	
Tumour Size			
≤20mm	49(80.3)	12(19.7)	0.075
21-49mm	53(68.8)	24(31.2)	
≥50mm	8(100)	0	
Grade			
I	1(100)	0	0.762
II	5(83.3)	1(16.7)	
III	105(75)	35(25)	
Nodal Status			

N_0	86(74.8)	29(25.2)	1.000
N_1	23(74.2)	8(25.8)	
Lymphovascular Invasion (LVI)			
Absent	11(73.3)	4(26.7)	0.753
Present	99(76.7)	30(23.3)	
Vascular Invasion			
Absent	72(71.3)	29(28.7)	0.158
Present	38(82.6)	8(17.4)	
Necrosis			
Absent	53(76.8)	16(23.2)	1.000
Present	58(76.3)	18(23.7)	
Klintrup Makinen			
0	14(73.7)	5(26.3)	0.739
1	43(74.1)	15(25.9)	
2	33(76.7)	10(23.3)	
3	18(85.7)	3(14.3)	
Tumour Bud			
-Low	63(76.8)	19(23.2)	1.000
-High	45(77.6)	13(22.4)	
Tissue Stroma Percentage			
Low	75(76.5)	23(23.5)	1.000
High	35(76.1)	11(23.9)	

7.2.14 Bcl-2

Overall expression of Bcl-2 was scored and thresholds considered as a WHS of 47. Recurrence-free survival was calculated for the low versus high expression groups in the TNBC cohort. In the low Bcl-2 group 19 cases had 5 events, while in the high Bcl-2 group 88 cases had 6 events. Mean RFS was 68.1 months for the low Bcl-2 group, with a 5-year RFS of 64%, and the high Bcl-2 group had a mean RFS of 92.9 months and a 5-year RFS of 91% (p=0.011), HR 0.240(95% C.I. 0.073-0.788) p=0.019, (*Figure 7-13*).

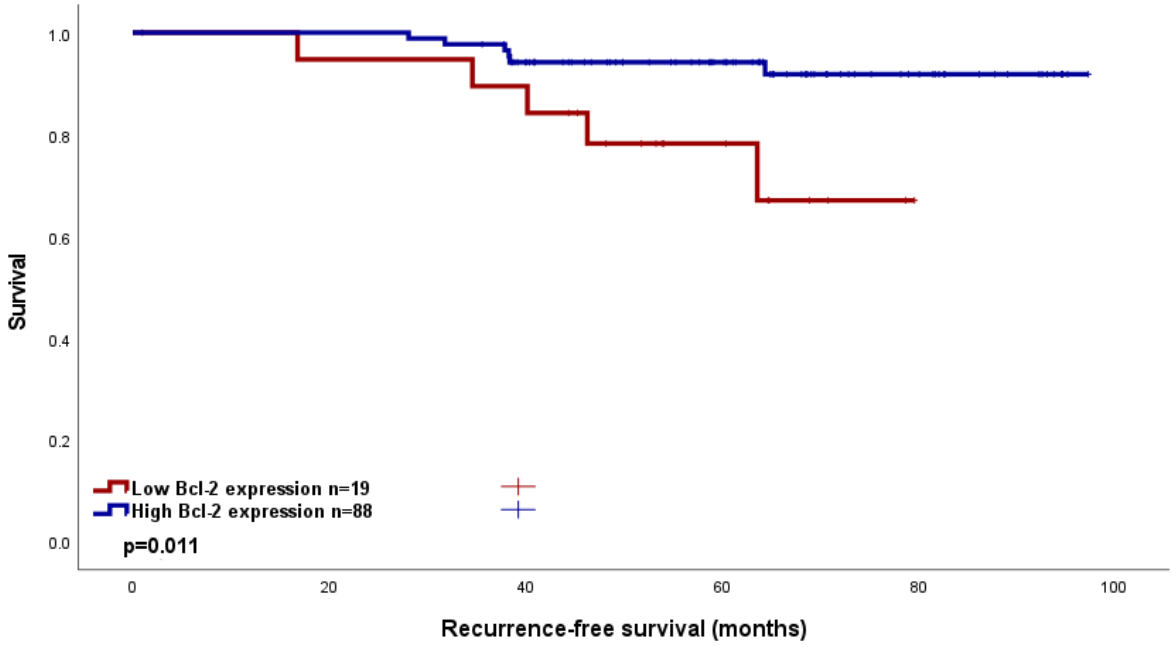

Figure 7-13 Kaplan Meier curve describing RFS and Bcl-2 expression in TNBC. HR 0.240(95% C.I. 0.073-0.788) p=0.019.

Clinicopathological factors were examined using Cox univariate and multivariate regression analysis. This suggested that Bcl-2 expression was statistically significant on multivariate analysis (HR 0.190 (95% C.I. 0.050-0.723) p=0.015), (*Table 7-9*).

Table 7-9 Cox Univariate and Multivariate regression analysis of clinicopathological findings associated with RFS compared with Bcl-2 expression.

Clinicopathological Factor	Univariate analysis (HR, 95% C.I.)	p	Multivariate analysis (HR, 95% C.I.)	p
Age	4.000(0.510-31.360)	0.187		
Tumour Size <20mm 20-49mm >50mm	 **4.039(0.839-19.456)** **12.748(1.139-142.684)**	**0.070** **0.086** **0.082** **0.039**	 **3.399(0.697-16.569)** **21.084(1.695-262.316)**	 **0.052** **0.184** **0.018**
Invasive Grade I II III	 **0.088(0.005-1.543)** **0.036(0.004-0.324)**	**0.084** **0.011** **0.096** **0.003**	 0.427(0.051-3.582)	 0.433
Nodal Status	2.997(0.875-10.270)	0.081		

Lymphatic Invasion	23.768(0.003-198847.255)	0.492		
Vascular Invasion	1.157(0.306-4.369)	0.830		
Necrosis	0.644(0.186-2.227)	0.487		
Klintrup-Makinen 0 1 2 3	 0.422(0.113-1.573) 0.137(0.015-1.232) 0(0)	0.042 0.297 0.422 0.137 0.973		
Tumour budding	0.629(0.166-2.374)	0.494		
Tumour stroma percentage	2.431(0.702-8.416)	0.161		
Bcl-2	**0.240(0.073-0.788)**	**0.019**	**0.190(0.050-0.723)**	**0.015**

Cancer-specific survival was assessed with regards to Bcl-2 expression. In the low Bcl-2 group 31 cases had 9 events, while in the high Bcl-2 group 116 cases had 27 events. Mean CSS was 84.2 months for the low Bcl2 group, with a 5-year CSS of 68%, and the high Bcl-2 group had a mean CSS of 80.4 months and a 5-year CSS of 76% (p=0.359), HR 0.704(95% C.I. 0.331-1.499), p=0.363, (*Figure 7-14*).

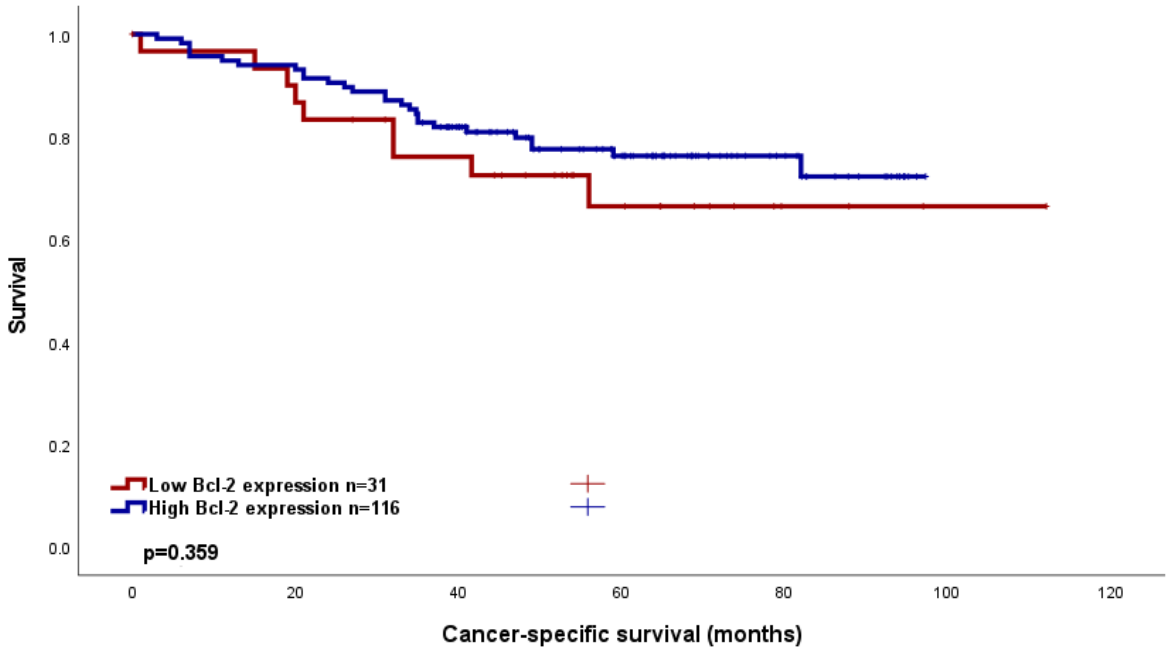

Figure 7-14 Kaplan Meier curve describing CSS and Bcl-2 expression in TNBC. HR 0.704(95% C.I. 0.331-1.499) p=0.363.

Clinicopathological factors were assessed with regards to their association with Bcl-2 expression. Nodal status appeared statistically associated to Bcl-2 expression (p=0.026), (*Table 7-10*).

Table 7-10 Comparison of clinicopathological findings and their relation to Bcl-2 expression using Chi-squared analysis.

Clinicopathological factor	**Bcl-2 expression (%)**		**p**
	Low	**High**	
Age (years)			
≤50	6(16.2)	31(83.8)	0.489
>50	25(22.7)	85(77.3)	
Tumour Size			
≤20mm	11(18.3)	49(81.7)	0.696
21-49mm	18(23.4)	59(76.6)	
≥50mm	2(28.6)	5(71.4)	
Grade			
I	0	1(100)	0.859
II	1(25)	3(75)	
III	30(21.6)	109(78.4)	
Nodal Status			
N_0	**29(25.4)**	**85(74.6)**	**0.026**
N_1	**2(6.7)**	**28(93.3)**	
Lymphovascular Invasion (LVI)			
Absent	5(31.3)	11(68.8)	0.349
Present	26(21)	98(79)	
Vascular Invasion			
Absent	22(21.6)	80(78.4)	1.000
Present	9(20.9)	34(79.1)	
Necrosis			
Absent	19(27.9)	49(72.1)	0.108
Present	12(16.4)	61(83.6)	
Klintrup Makinen			
0	7(33.3)	14(66.7)	0.389
1	12(21.8)	43(78.2)	
2	10(23.8)	32(76.2)	
3	2(10.5)	17(89.5)	
Tumour Bud			
-Low	14(17.5)	66(82.5)	0.210
-High	16(27.6)	42(72.4)	
Tissue Stroma Percentage			
Low	19(19.8)	77(80.2)	0.382
High	12(27.3)	32(72.7)	

7.2.15 CD3

CD3 was assessed and considered a marker of TILs. WHS were scored for CD3 expression in tumour (tumCD3), stroma (stromaCD3) and then combined (combined CD3) within the specimen.

7.2.16 CD3 in Tumour

CD3 in tumour cells (tumCD3) was scored and thresholds considered as a WHS of 0.26. Recurrence-free survival was calculated for the low versus high expression groups in the TNBC cohort. In the low tumCD3 group 16 cases had 5 events, while in the high tumCD3 group 94 cases had 6 events. Mean RFS was 76.9 months for the low tumCD3 group, with a 5-year RFS of 62%, and the high tumCD3 group had a mean RFS of 93 months and a 5-year RFS of 92% (p=0.002), HR 0.183 (95% C.I. 0.056-0.602) p=0.005, (*Figure 7-15*).

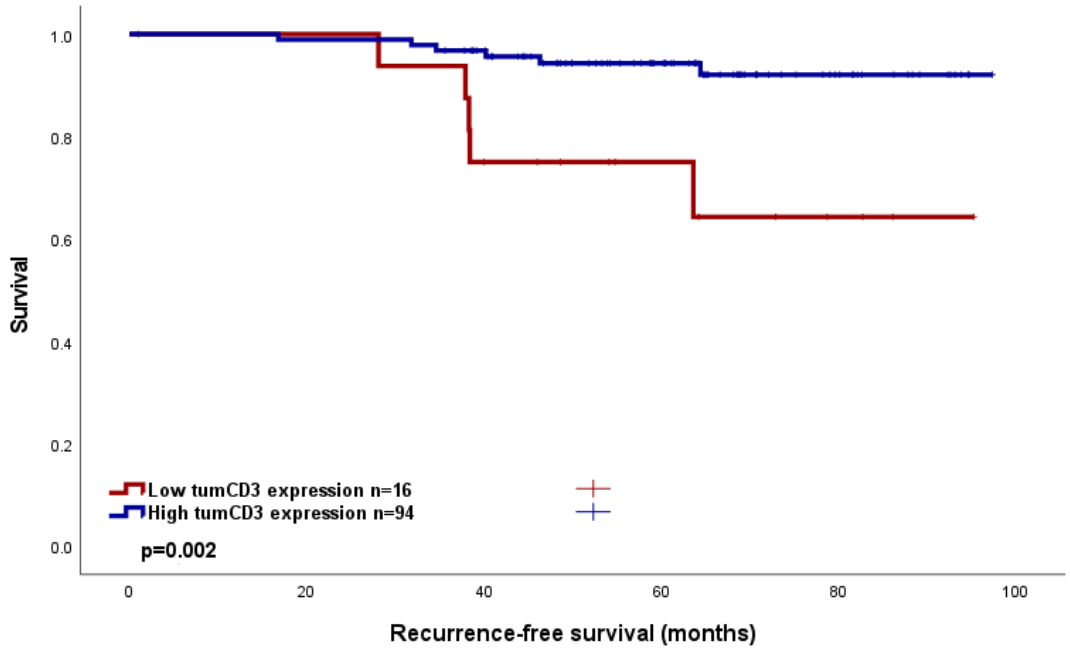

Figure 7-15 Kaplan Meier curve describing RFS and tumCD3 expression in TNBC. HR 0.183 (95% C.I. 0.056-0.602) p=0.005.

Clinicopathological factors were examined using Cox univariate and multivariate regression analysis. This suggested that tumCD3 expression was statistically significant on multivariate analysis (HR 0.195 (95% C.I. 0.052-0.734) p=0.016), (*Table 7-11*).

Table 7-11 Cox Univariate and Multivariate regression analysis of clinicopathological findings associated with RFS compared with tumCD3 expression.

Clinicopathological Factor	Univariate analysis (HR, 95% C.I.)	p	Multivariate analysis (HR, 95% C.I.)	p
Age	4.000(0.510-31.360)	0.187		
Tumour Size <20mm		**0.070** **0.086**		**0.046**

20-49mm >50mm	**4.039(0.839-19.456)** **12.748(1.139-142.684)**	**0.082** **0.039**	**4.391(0.877-21.993)** **23.308(1.782-304.941)**	**0.072** **0.016**
Invasive Grade I II III	 **0.088(0.005-1.543)** **0.036(0.004-0.324)**	**0.084** **0.011** **0.096** **0.003**	 0.269(0.031-2.341)	 0.234
Nodal Status	2.997(0.875-10.270)	0.081		
Lymphatic Invasion	23.768(0.003-198847.255)	0.492		
Vascular Invasion	1.157(0.306-4.369)	0.830		
Necrosis	0.644(0.186-2.227)	0.487		
Klintrup-Makinen 0 1 2 3	 0.422(0.113-1.573) 0.137(0.015-1.232) 0(0)	0.042 0.297 0.422 0.137 0.973		
Tumour budding	0.629(0.166-2.374)	0.494		
Tumour stroma percentage	2.431(0.702-8.416)	0.161		
TumCD3 expression	**0.183(0.056-0.602)**	**0.005**	**0.195(0.052-0.734)**	**0.016**

Cancer-specific survival was assessed with regards to tumCD3 expression. In the low tumCD3 group 19 cases had 4 events, while in the high tumCD3 group 135 cases had 35 events. Mean CSS was 82.6 months for the low tumCD3 group, with a 5-year DFS of 76%, and the high tumCD3 group had a mean CSS of 87.7 months and a 5-year DFS of 74% (p=0.516), HR 1.406 (95% C.I. 0.499-3.960) p=0.519, (*Figure 7-16*).

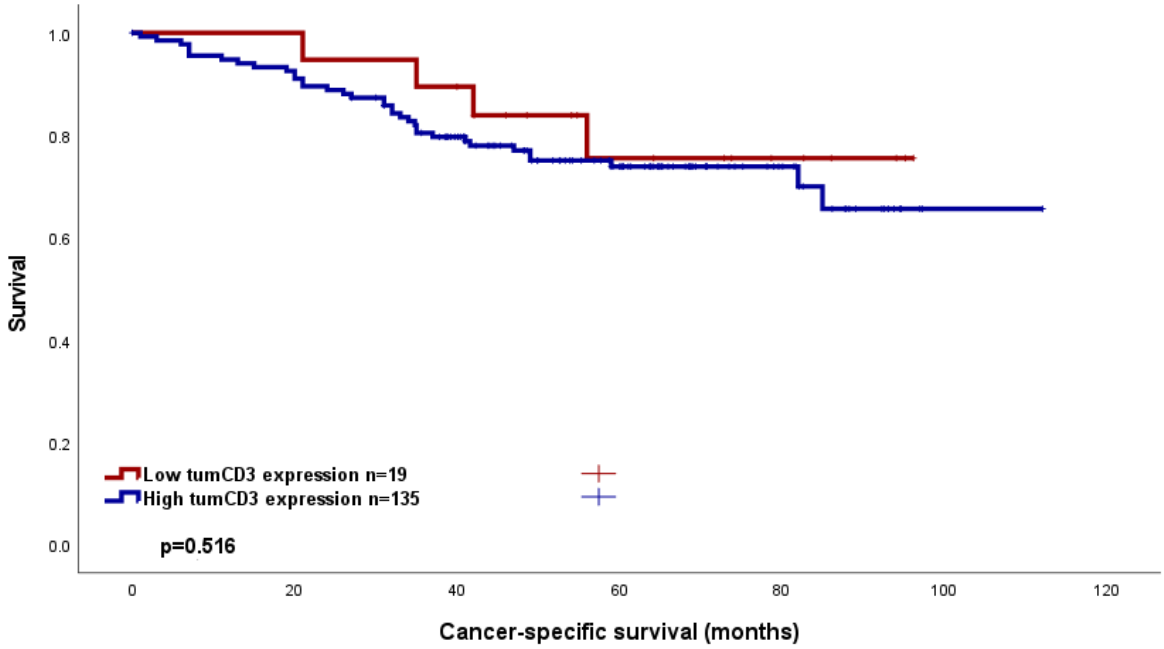

Figure 7-16 Kaplan Meier curve describing CSS and tumCD3 expression in TNBC. HR 1.406 (95% C.I. 0.499-3.960) p=0.519.

Clinicopathological factors were assessed with regards to their association with tumCD3 expression. Age (p=0.045), Grade (p=0.030)and Klintrup-Makinen (p=0.003) score appeared significantly associated with tumCD3 expression, (*Table 7-12*).

Table 7-12 Comparison of clinicopathological findings and their relation to tumCD3 expression using Chi-squared analysis

Clinicopathological factor	**TumCD3 expression (%)**		**p**
	Low	**High**	
Age (years)			
≤50	**1(2.7)**	**36(97.3)**	**0.045**
>50	**18(15.4)**	**99(84.6)**	
Tumour Size			
≤20mm	7(11.1)	56(88.9)	0.459
21-49mm	11(13.9)	68(86.1)	
≥50mm	0	9(100)	
Grade			
I	**1(100)**	**0**	**0.030**
II	**1(14.3)**	**6(85.7)**	
III	**17(11.9)**	**126(88.1)**	
Nodal Status			
N_0	17(14.3)	102(85.7)	0.367
N_1	2(6.3)	30(93.8)	
Lymphovascular Invasion (LVI)			
Absent	1(6.3)	15(93.8)	0.694
Present	17(13)	114(87)	

Vascular Invasion			
Absent	12(11.5)	92(88.5)	0.605
Present	7(14.6)	41(85.4)	
Necrosis			
Absent	8(11.6)	61(88.4)	1.000
Present	10(12.7)	69(87.3)	
Klintrup Makinen			
0	**8(34.8)**	**15(65.2)**	**0.003**
1	**5(8.6)**	**53(91.4)**	
2	**5(11.6)**	**38(88.4)**	
3	**0**	**20(100)**	
Tumour Bud			
-Low	10(12)	73(88)	1.000
-High	7(11.9)	52(88.1)	
Tissue Stroma Percentage			
Low	12(12)	88(88)	1.000
High	6(12.8)	41(87.2)	

7.2.17 CD3 in Stroma

CD3 in stroma (stromaCD3) was scored and threshold considered as a WHS of 2. Recurrence-free survival was calculated for the low versus high expression groups in the TNBC cohort. In the low stromaCD3 group 22 cases had 7 events, while in the high stromaCD3 group 88 cases had 4 events. Mean RFS was 77.9 months for the low stromaCD3 group, with a 5-year RFS of 63%, and the high stromaCD3 group had a mean RFS of 91.9 months and a 5-year RFS of 95% ($p<0.001$), HR 0.138 (95% C.I. 0.040-0.471) p=0.002, (*Figure 7-17*).

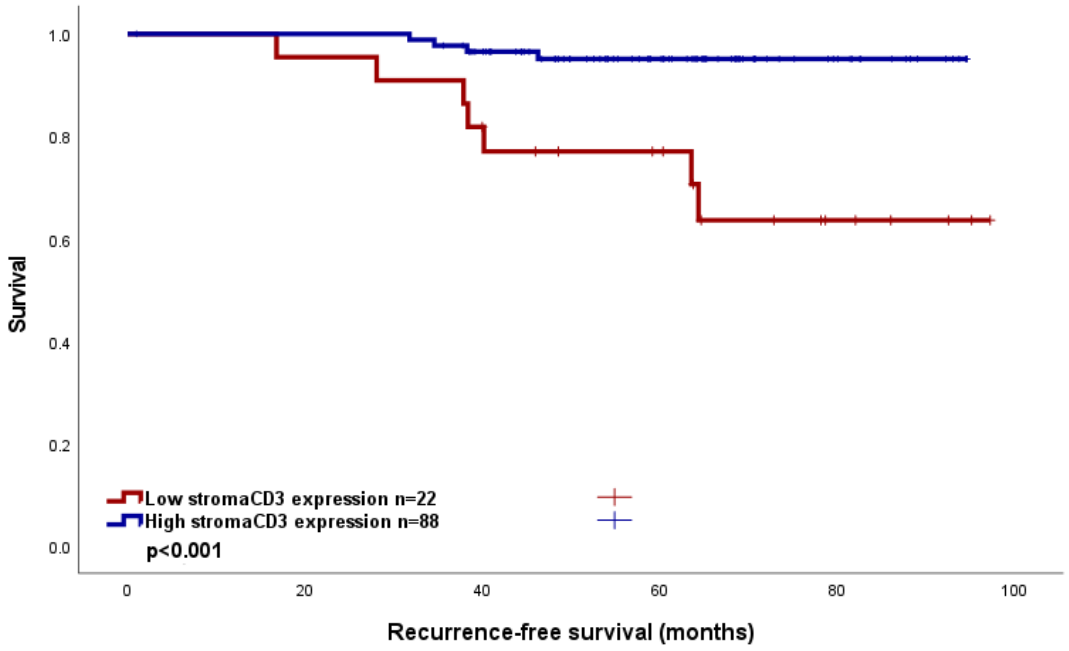

Figure 7-17 Kaplan Meier curve describing RFS and stromaCD3 expression in TNBC. HR 0.138 (95% C.I. 0.040-0.471) p=0.002. Pairwise comparison and numbers in each expression subgroup are described.

Clinicopathological factors were examined using Cox univariate and multivariate regression analysis. This suggested that stromaCD3 expression was statistically significant on multivariate analysis (HR 0.097 (95% C.I. 0.019-0.482) p=0.004), (*Table 7-13*).

Table 7-13 Cox Univariate and Multivariate regression analysis of clinicopathological findings associated with RFS compared with stromaCD3 expression.

Clinicopathological Factor	Univariate analysis (HR, 95% C.I.)	p	Multivariate analysis (HR, 95% C.I.)	p
Age	4.000(0.510-31.360)	0.187		
Tumour Size		0.070		
<20mm				0.031
20-49mm	4.039(0.839-19.456)	0.086	3.261(0.666-15.956)	0.142
>50mm	12.748(1.139-142.684)	0.082 0.039	35.351(2.424-515.549)	0.009
Invasive Grade		0.084		
I		0.011		
II	0.088(0.005-1.543)	0.096		
III	0.036(0.004-0.324)	0.003	0.109(0.010-1.217)	0.072

Nodal Status	2.997(0.875-10.270)	0.081		
Lymphatic Invasion	23.768(0.003-198847.255)	0.492		
Vascular Invasion	1.157(0.306-4.369)	0.830		
Necrosis	0.644(0.186-2.227)	0.487		
Klintrup-Makinen 0 1 2 3	 0.422(0.113-1.573) 0.137(0.015-1.232) 0(0)	0.042 0.297 0.422 0.137 0.973		
Tumour budding	0.629(0.166-2.374)	0.494		
Tumour stroma percentage	2.431(0.702-8.416)	0.161		
StromaCD3 expression	0.138(0.040-0.471)	0.002	0.097(0.019-0.482)	0.004

Cancer-specific survival was assessed with regards to stromaCD3. In the low stromaCD3 group 29 cases had 7 events, while in the high stromaCD3 group 125 cases had 32 events. Mean CSS was 93.4 months for the low stromaCD3 group, with a 5-year DFS of 83%, and the high stromaCD3 group had a mean CSS of 76.3 months and a 5-year CSS of 72% (p=0.519), HR 1.312 (95% C.I. 0.573-3.003) p=0.521, (*Figure 7-18*).

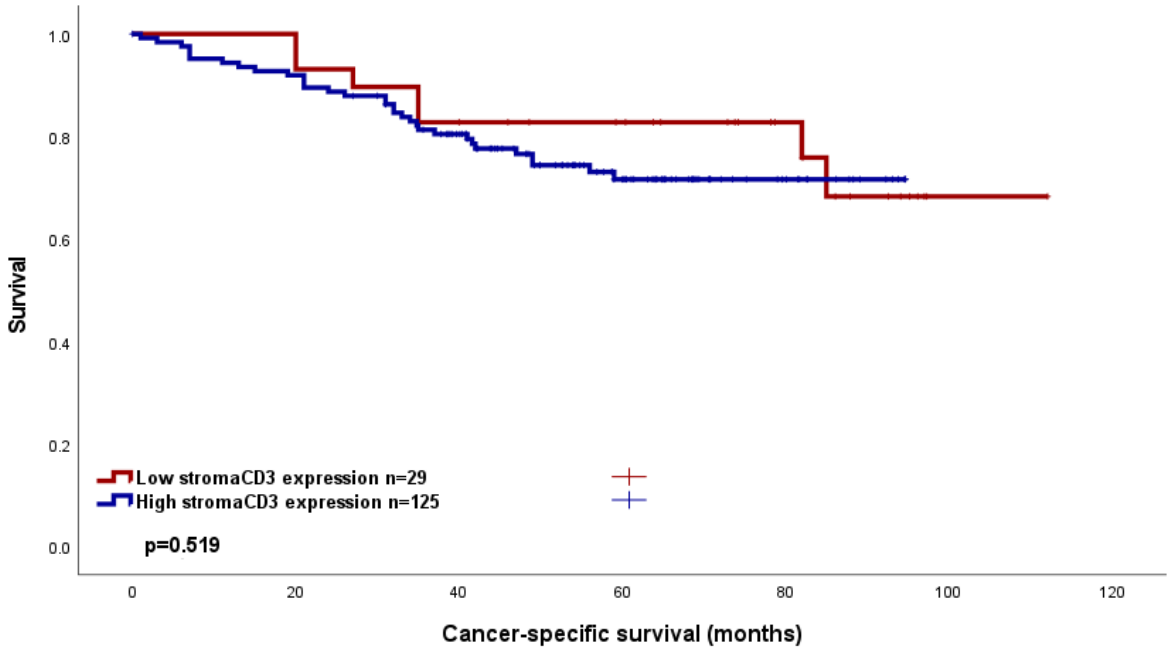

Figure 7-18 Kaplan Meier curve describing CSS and stromaCD3 expression in TNBC. HR 1.312 (95% C.I. 0.573-3.003) p=0.521. Pairwise comparison and numbers in each expression subgroup are described.

Clinicopathological factors were assessed with regards to their association with stromaCD3 expression. Klintrup-Makinen score was significantly associated with stromaCD3 expression (p=0.003), (Table 7-14).

Table 7-14 Comparison of clinicopathological findings and their relation to stromaCD3 expression using Chi-squared analysis.

Clinicopathological factor	StromaCD3 expression (%)		p
	Low	High	
Age (years)			
≤50	5(13.5)	32(86.5)	0.470
>50	24(20.5)	93(79.5)	
Tumour Size			
≤20mm	8(12.7)	55(87.3)	0.256
21-49mm	18(22.8)	61(77.2)	
≥50mm	1(11.1)	8(88.9)	
Grade			
I	1(100)	0	0.115
II	1(14.3)	6(85.7)	
III	27(18.9)	116(81.1)	
Nodal Status			
N_0	22(18.5)	97(81.5)	0.623
N_1	7(21.9)	25(78.1)	
Lymphovascular Invasion (LVI)			

Absent	3(18.8)	13(81.3)	1.000
Present	25(19.1)	106(80.9)	
Vascular Invasion			
Absent	21(20.2)	83(79.8)	0.664
Present	8(16.7)	40(83.3)	
Necrosis			
Absent	13(18.8)	56(81.2)	1.000
Present	15(19)	64(81)	
Klintrup Makinen			
0	**9(39.1)**	**14(60.9)**	**0.003**
1	**15(25.9)**	**43(74.1)**	
2	**3(7)**	**40(93)**	
3	**1(5)**	**19(95)**	
Tumour Bud			
-Low	14(16.9)	69(83.1)	0.825
-High	11(18.6)	48(81.4)	
Tissue Stroma Percentage			
Low	17(17)	83(83)	0.374
High	11(23.4)	36(76.6)	

7.2.18 Combined CD3

Combined stroma and tumour CD3 was scored and thresholds considered as a WHS of 0.9. Recurrence-free survival was calculated for the low versus high expression groups in the TNBC cohort. In the low combined CD3 group 16 cases had 5 events, while in the high combined CD3 group 94 cases had 6 events. Mean RFS was 76.9 months for the low combined CD3 group, with a 5-year RFS of 67%, and the high combined CD3 group had a mean RFS of 90.8 months and a 5-year RFS of 91% ($p<0.001$), HR 0.166 (95% C.I. 0.051-0.546) p=0.003, (*Figure 7-19*).

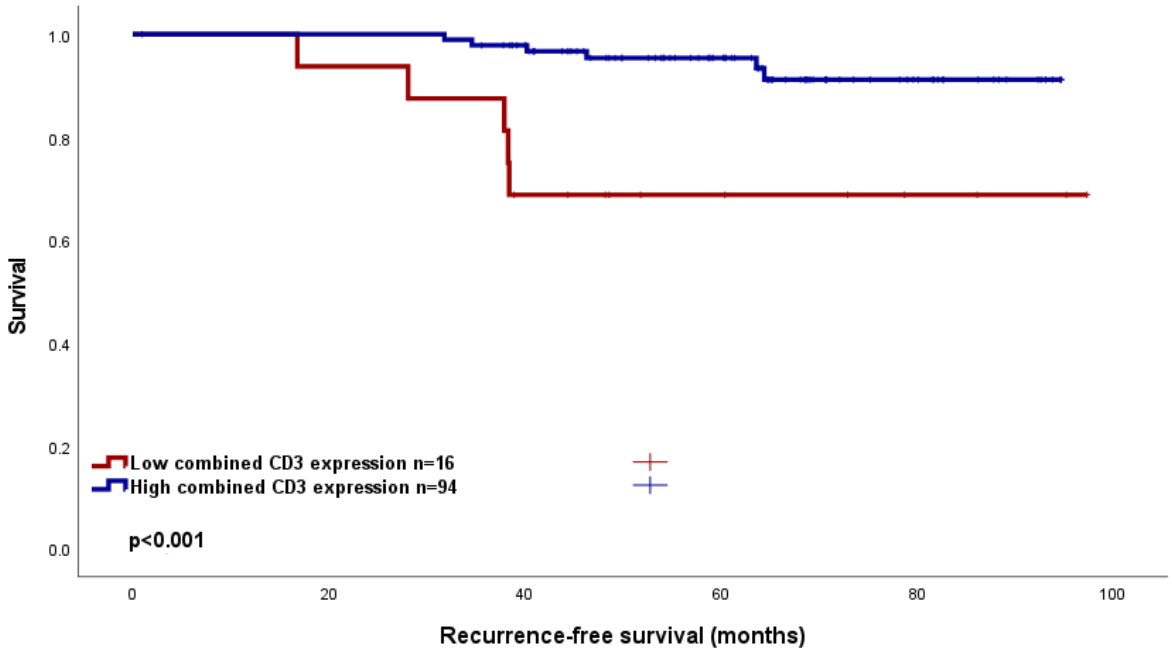

Figure 7-19 Kaplan Meier curve describing RFS and combined CD3 expression in TNBC. HR 0.166 (95% C.I. 0.051-0.546) p=0.003. Pairwise comparison and numbers in each expression subgroup are described.

Clinicopathological factors were examined using Cox univariate and multivariate regression analysis. This suggested that Bcl-2 expression was statistically significant on multivariate analysis (HR 0.169 (95% C.I. 0.041-0.700) p=0.014), (*Table 7-15*)

Table 7-15 Cox Univariate and Multivariate regression analysis of clinicopathological findings associated with RFS compared to combined CD3 expression.

Clinicopathological Factor	Univariate analysis (HR, 95% C.I.)	p	Multivariate analysis (HR, 95% C.I.)	p
Age	4.000(0.510-31.360)	0.187		
Tumour Size		**0.070**		
<20mm		**0.086**		**0.065**
20-49mm	**4.039(0.839-19.456)**	**0.082**	**3.096(0.613-15.627)**	**0.171**
>50mm	**12.748(1.139-142.684)**	**0.039**	**19.330(1.578-236.827)**	**0.021**
Invasive Grade		**0.084**		
I		**0.011**		
II	**0.088(0.005-1.543)**	**0.096**		
III	**0.036(0.004-0.324)**	**0.003**	0.190(0.021-1.748)	0.142

Nodal Status	2.997(0.875-10.270)	0.081		
Lymphatic Invasion	23.768(0.003-198847.255)	0.492		
Vascular Invasion	1.157(0.306-4.369)	0.830		
Necrosis	0.644(0.186-2.227)	0.487		
Klintrup-Makinen 0 1 2 3	 0.422(0.113-1.573) 0.137(0.015-1.232) 0(0)	0.042 0.297 0.422 0.137 0.973		
Tumour budding	0.629(0.166-2.374)	0.494		
Tumour stroma percentage	2.431(0.702-8.416)	0.161		
Combined CD3 expression	**0.166(0.051-0.546)**	**0.003**	**0.169(0.041-0.700)**	**0.014**

Cancer-specific survival was assessed with regards to combined CD3 expression. In the low combined CD3 group 20 cases had 5 events, while in the high combined CD3 group 134 cases had 34 events. Mean CSS was 89.7 months for the low combined CD3 group, with a 5-year DFS of 75%, and the high combined CD3 group had a mean CSS of 78.4 months and a 5-year CSS of 74% (p=0.894), HR 1.066 (95% C.I. 0.415-2.738) p=0.894, (*Figure 7-20*).

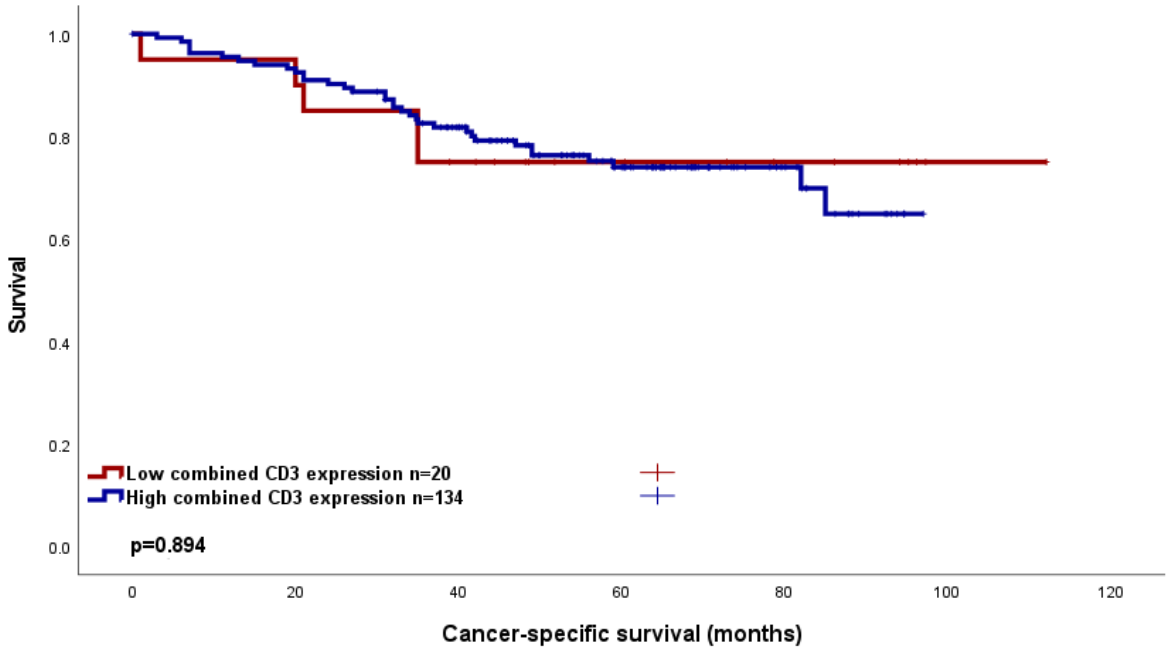

Figure 7-20 Kaplan Meier curve describing CSS and combined CD3 expression in TNBC. HR 1.066 (95% C.I. 0.415-2.738) p=0.894. Pairwise comparison and numbers in each expression subgroup are described.

Clinicopathological factors were assessed with regards to their association with combined CD3 expression. Grade was significantly associated with combined CD3 expression (p=0.022), (*Table 7-16*).

Table 7-16 Comparison of clinicopathological findings and their relation to combined CD3 expression using Chi-squared analysis.

Clinicopathological factor	Combined CD3 expression (%)		p
	Low	High	
Age (years)			
≤50	5(13.5)	32(86.5)	1.000
>50	15(12.8)	102(87.2)	
Tumour Size			
≤20mm	3(4.8)	60(95.2)	0.060
21-49mm	14(17.7)	65(82.3)	
≥50mm	1(11.1)	8(88.9)	
Grade			
I	**1(100)**	**0**	**0.022**
II	**0**	**7(100)**	
III	**19(13.3)**	**124(86.7)**	
Nodal Status			
N_0	15(12.6)	104(87.5)	0.769
N_1	5(15.6)	27(87)	
Lymphovascular Invasion (LVI)			

Absent	2(12.5)	14(87.5)	1.000
Present	17(13)	114(87)	
Vascular Invasion			
Absent	14(13.5)	90(86.5)	1.000
Present	6(12.5)	42(87.5)	
Necrosis			
Absent	10(14.5)	59(85.5)	0.628
Present	9(11.4)	70(88.6)	
Klintrup Makinen			
0	6(26.1)	17(73.9)	0.198
1	7(12.1)	51(87.9)	
2	5(11.6)	38(88.4)	
3	1(5)	19(95)	
Tumour Bud			
-Low	11(13.3)	72(86.7)	1.000
-High	7(11.9)	52(88.1)	
Tissue Stroma Percentage			
Low	12(12)	88(88)	0.609
High	7(14.9)	40(85.1)	

7.3 Discussion

Following DSP analysis with GeoMX, four proteins allowed an evaluation of the tumour microenvironment to be made and their effect on survival to be assessed. Tumour budding was associated with differential expression of hypoxia marker HIF-1α and CD4 (considered a marker of TILs, for which a surrogate in the form of CD3 was assessed) within the tumour-rich ROIs in low budding phenotype tumours, and Bcl-2 in the high budding phenotype TNBCs. CAIX was added to the analysis as a more stable marker of hypoxia. All four proteins appeared to have an association with survival, with variations noted depending on the cellular compartment in which their expression was scored.

High HIF-1α expression within the cytoplasm appeared to be associated with poorer RFS, whereas this was not seen on assessment of nuclear HIF-1α. However, there was a trend towards poorer prognosis with high levels of nuclear expression, and an associated identified with necrosis and nodal status, suggesting that with longer follow up, there may be evidence of prognostic value within this cellular compartment. When examining the literature, however, the varied and far-reaching effect of HIFs in cancer and normal human biology make this a complex field in which to identify targets for therapy. The role of HIFs may therefore pose a more attractive prognostic indicator rather than a target for adjuvant/neoadjuvant therapy. HIF-1α is less stable on immunohistochemistry, and therefore, to validate findings with regards to the role of hypoxia in

prognosis, we included analysis for CAIX, which has a more stable half-life and is more resistant to degradation in the presence of oxygen and withstands the immunohistochemistry process more robustly, and has been shown to be a robust prognostic indicator in other breast cancer types(276, 310).

CAIX expression in the membrane trended towards significance on Kaplan-Meier survival analysis only. However, on cytoplasmic CAIX expression, RFS was poorer for high expression. This supports the findings seen with HIF-1α which suggests that high levels of hypoxia markers are associated with poorer prognosis in the TNBC cohort. In this study however, no statistically significant association was noted with regards to other clinicopathological factors, although this may be related to other influences that CAIX may have, namely with regards to response to adjuvant therapies, or neoadjuvant therapies, which were not assessed in this work.

In TNBC, Bcl-2 was identified as a predictor of poor outcome for patients treated with anthracycline-based adjuvant chemotherapy, suggesting a role in Bcl-2 as a prognostic predictor and an aid in clinical decision making for patients in this subgroup(303). Within this study, low Bcl-2 expression was associated with poor RFS and associated with nodal status. Overall, it is safe to suggest that Bcl-2 may propose an attractive and valuable candidate in the chemotherapeutic arsenal, particularly in cases where chemotherapeutic resistance or overall poor prognosis is expected, and that together with tumour budding, this biomarker may be an attractive prognostic indicator(295).

Recent work by Mutka et al. demonstrated that CD4+ cell numbers did not reduce in recurrent cancer specimens compared to a relative reduction in CD3+ (amongst others) in recurrences versus primary tumours. This may indicate that CD4+ cells in particular may hold an important role in the progression of metastatic disease and encourages further review of CD4 expression to be pursued in future study(311). Within this study, low CD3 expression in all regions, both tumour and stromal, as well as combined, was associated with poorer RFS. In tumour cells, CD3 expression appeared associated with age, invasive grade and Klintrup-Makinen status, whereas in stroma, only KM was statistically significant in its association. In the combined CD3 expression analysis, invasive grade was associated with CD3 expression. Previous work in colorectal cancers, has suggested that loss of MHC class I expression may provide an indication of

poor prognosis in different molecular subgroups(312). Our findings would be in-keeping with this, and the assumption that the innate immune system may provide an anti-tumour budding action, whereas adaptive responses may have permissive or promoting factors for metastatic spread(159). In fact, CD8+ T cells, FOXP3 T cells and CD68+ T macrophages have been closely associated with tumour budding in colorectal cancer, suggesting that a closer examination of the immune landscape within the TME of cancers with TB phenotype may be of value in providing prognostic information for breast cancers as well(312).

Where in previous chapters, CSS has been used as the primary measure of outcome, the TNBC cohort has a relatively shorter follow up (median follow up 73 months), albeit with robust recurrence data available. This led to the decision to include measures of RFS as well as CSS to allow any granularity in the results to come forward. It may be possible in future to identify similar statistically significant outcomes in CSS when longer follow up becomes possible in the fullness of time, particularly when backed up by robust, prospective follow up. As noted previously, TNBC cancer patients differs from ER-positive patients, with the first 5 years from diagnosis representing the most at-risk period of relapse, suggesting that our data may still be of value for stratification of high-risk cases following initial treatment with curative intent (5, 240, 243, 245, 246).

In summary, the use of DSP proposes a valuable tool in furthering our understanding of how the tumour and microenvironment may work in tandem to create conditions which have prognostic importance in cancers. It remains unclear at present whether factors of hypoxia, apoptosis or TIL activity are responsible for, or a result of, the tumour budding process. However, these results may be re-examined using reproducible methods such as immunohistochemistry to validate the findings at the histopathological level, and relate these to clinicopathological outcomes in the hope of clarifying this further.

Chapter 8 General Discussion

8.1 General Discussion and Future Work

Breast cancer is the most common type of malignancy in the UK and is now understood to be extremely heterogeneous in its natural history, molecular and pathological characteristics. As such, it has become clear that “one size fits all” treatment cannot be sufficient to tackle the challenges of diagnosis, surgical therapy, and adjuvant options available to people who are diagnosed with this cancer every year. This thesis aims to explore the transcriptomic landscape of breast cancer in a cohort of retrospectively assembled breast cancers, with particular interest in the most differentially expressed genes according to bulk RNA-seq using TempO-seq analysis and relate protein expression to prognosis. Using tumour budding to stratify prognosis, this study allowed four proteins, JUNB, ODAM, RFX5 and TBX22 to be evaluated with regards to their clinicopathological significance, survival characteristics, and how they vary amongst the four main molecular subgroups of breast cancer. Finally, in an independent cohort of triple negative cancer patients, the transcriptomic landscape according to tumour budding phenotype was examined using digital spatial profiling, allowing the identification of differentially expressed genes, and explore how their expression varies between the TME and tumour epithelia, and their subsequent expression and significance for survival. These experiments were performed with aim of exploring how different transcriptomic analyses may help evaluate the biological study of breast cancer subtypes, and may identify targets for therapy, or risk stratification biomarkers to guide clinical decision-making. Acting as a form of “introductory exploration”, this study has, through two methods of transcriptomic analysis, allowed us to gain further understanding of potential targets for further study.

8.2 Tumour budding

Tumour budding and scoring protocols have been most thoroughly examined and established in colorectal cancer, where the most recent International Tumour Budding Consensus Conference (2017) has recommended that TB is used in daily practice as a risk stratification tool(6). Within colorectal cancers, the role of both PTB and ITB has been established. The former relies on analysis of histopathological resection specimens, while the latter is possible on diagnostic biopsy specimens. The consensus has been reached on 10 points within this meeting, including the fact that TB is an independent predictor of lymph node

metastasis in Pt1 CRC, and a predictor of survival in stage II CRC(6). The possibility of assessing TB on H&E provides an easily reproducible and low -cost method, without additional laboratory investment, to include this in the pathological assessment of cancer patients, therefore proposing an attractive solution when considering this additional approach to staging for patients with cancer.

It is therefore an attractive solution to prognosis/staging in breast cancers, where tissue biopsy underlies one third of the “triple assessment” method adopted as the Gold Standard diagnostic technique, and in which the role of neoadjuvant therapy is becoming more common, following which surgery (and a final pathological specimen being available) may be a secondary therapeutic option. The current challenges against the use of TB in breast cancer lie in the lack of a consensus on the method of assessment of TB, the lack of information on the difference in role between PTB and ITB, and the heterogeneity of the disease pathology itself.

During the course of this study, it became apparent that TB scoring was more challenging on H&E slides, unless this was after the addition of pancytokeratin staining(155). This method has been described by Salhia et al. and should be considered as a valid step in specimen immunohistochemical analysis(155). Other limitations to our use of TB as a risk stratification tool would be to examine the role of ITB, which was not considered in this thesis. However, an encouraging finding is the comparison between tumour budding protein expression in TB versus tumour mass cells, suggesting that these correlate closely, allowing the use TMA slides to establish higher throughout examination during this study. The close relationship in protein expression between tumour and TB may provide basic evidence that core biopsies may provide sufficient information to allow prognostication, even without using TBs as the primary source of biomarker scoring but requires further validation with regards to ITB.

During this thesis, immunohistochemical analysis relied on manual scoring for the majority of the results, and these were validated by double scores. A smaller subset of results, namely those in the TNBC cohort, relied on artificial intelligence (AI)-supported techniques, such as is described using QuPath. Manual validation of these scores suggest that these are reliable and may provide another method of analysing specimens at core biopsy or following

surgical resection, without the additional burden of clinical work on a pathologist. Other methods of AI-facilitated analysis are currently being examined in our laboratory, including methods of computer deep-learning software, as seen in some recently published work looking at tumour budding using comprehensive multi-modal analysis including DSP, 3D immunofluorescence, multiplex immunofluorescence, transmission electron microscopy and immunohistochemistry, which when combined may provide an additional tool for analysis of specimens(313).

Different methods of transcriptional analysis are also available, which have progressed from bulk RNA-seq, and may provide myriad more information about how tumour mass and TME differ in gene expression. The TempO-seq results which led to this study provide a useful tool in validating how protein expression may differ between different prognostic groups (high budding versus low budding phenotype) while DSP may be a more specific way of answering how expression relates to the tumour versus TME. Temp0-seq, although having the benefit of having a wide range of available genes to examine, may however not reveal the difference in expression amongst different tumour and stromal components. It is this difference in particular which may be of further interest, and future study using DSP to identify the four genes of JUNB, ODAM, RFX5 and TBX22 may become possible in future and help elucidate their role within the tumour versus the TME.

8.3 Immunohistochemical analysis – JUNB, ODAM, RFX5 and TBX22 Expression in the Glasgow Breast Cancer Cohort

High expression of JUNB mRNA has been associated with improved survival, when compared to JUNB expression in non-tumour tissues(314). Within this study, JUNB cytoplasmic expression appeared to correlate with this finding, although our population may have been underpowered to allow this to be seen on multivariate Cox regression analysis. Interestingly, this was particularly seen in the ER- portion of the Glasgow Breast Cancer Cohort, suggesting that this protein may be a valuable biomarker in hormone-receptor-negative group, who are already associated with a survival disadvantage compared to the hormone positive counterparts. The location of JUNB expression however also appears to be of significance, as the opposite was seen with high nuclear JUNB resulting in poorer prognosis. During this study, scores from different cell regions

(membrane/cytoplasm/nucleus) were combined to allow results to capture the total expression of each protein, and assess whether this affected survival results, potentiated links to clinicopathological factors, or uncovered other effects unrelated to position. Combining scores, HNHC had greater survival than HNLC suggesting that the “protective” role of JUNB may be most important within the cytoplasmic region. This may be in-keeping with suggested signalling of JUNB after activation by fibroblast growth factor receptor 2 (FGFR2) involvement in ER and PR related transcription of genes relating to poorer prognosis in patients by abolishing inhibitory cell growth signalling, suggesting that once JUNB is at the nucleus, anti-cancer effects are lost(184). Localisation of JUNB and clearer information of how this relates to ER+/- status therefore may provide a promising area of study.

ODAM has been identified in multiple tissues, beyond those relating to odontogenesis(315). In this study, low cytoplasmic ODAM was associated with improved survival in the HER2-enriched portion of patients in the Glasgow Breast Cancer Cohort. Low ODAM nuclear expression on the other hand, was seen to result in worse survival in the cohort, particularly in the ER- cases. However, these effects were lost on multivariate analysis. Interestingly, the LNHC ODAM expressors had poor CSS across the cohort, although in the HER2 enriched group, HNLC ODAM expression appeared to be worse for survival. This suggests that further study of the cellular biology of ODAM expression, as well as the variations between molecular subgroup may reveal further information about the significance of ODAM in the context of breast cancer.

RFX5 expression within the membrane appeared to correlate to grade, subtype and Klintrup-Makinen score, but did not correlate with survival. On cytoplasmic expression analysis however, low RFX5 expression was associated with poorer CSS across the Glasgow Breast Cancer Cohort, although this effect was not identified when examining nuclear RFX5 expression. On combined scoring however, the “All low” RFX expression group appeared to have worse survival (on univariate analysis) suggesting that although RFX expression does seem to pose a prognostic indication, further understanding of the effect of RFX5 as a regulatory protein is required.

TBX22 expression in high levels appeared to be associated with HER2-enriched cancer in the Glasgow Breast Cancer Cohort but was not found to have

significance with regards to survival, until combined scoring was used. Here, HNLC TBX22 was seen to have improved CSS compared with LNHC expressors. Our understanding of TBX22 and its role in cell function and a greater understanding of expression changes in normal versus cancer tissue, further evidence of its role may become of prognostic value. Examining the literature, there is a relative paucity of data with regards to the role of TBX22 in cancers, but some emerging evidence of the role of TBX22 in anti-cancer immunity and in genes relating to EMT, highlighting TBX22 and associated T-box genes as a potential area of interest in cancer, and in relation to tumour budding(316).

Interestingly, for the most part the relationship between tumour budding and protein expression was not seen, suggesting that there is still more to be uncovered with regards to tumour budding and the role of these proteins in development of the phenotype. It is unclear whether one precedes the other, and therefore temporal analysis (i.e., comparing core biopsies to tumour specimens) may reveal further information regarding the relationship between budding and these proteins. Extending transcriptomic analysis to other histological types of cancer, such as lobular cancer, may also open other avenues of interest.

8.4 Digital Spatial Profiling – Transcriptomic Analysis in the TNBC Cohort

Digital spatial profiling is a useful tool in examining the difference between the tumour and TME, as well as giving more in-depth information regarding molecular subtyping, allowing comparison between transcriptomic and proteomic expression within different regions of specimens. In our TNBC cohort, this allowed a comparison between differential gene expression in the stroma versus tumour cells, and further categorisation according to tumour budding. This allowed the identification of differential expression of HIF-1alpha and CD3 in tumour cells (higher expression in low TB patients), with the Bcl2 expression being higher in the stroma of high TB patients. CAIX was included in further analysis, to further inform our understanding of the role of hypoxia in prognosis in TNBC, in the context of TB. GeoMX DSP offers an additional tool compared to bulk RNA-seq in establishing how transcriptomic expression varies within individual specimens. More work is in progress to use this technique for other

subtypes of breast cancer, including lobular cancers, and may yield further insights.

8.5 HIF-1alpha, CAIX, Bcl2 and CD3 Expression and Survival in TNBC

HIF-1α has a well-established role in hypoxia and cancer-related progression of disease. Interestingly, it was in our low TB subset that the highest differential expression was noted to be, suggesting that further understanding of the role of HIF-1α and the relation to TB may be necessary. Within this study, high cytHIF-1α expression correlated with significantly poorer RFS, and a trend towards similar findings for nucHIF-1α albeit not reaching statistical significance. The limitations of a shorter follow up may, in the fullness of time, allow further conclusions to be made regarding HIF-1α and prognosis. To further delineate the role of hypoxia in TNBC, CAIX was examined. This was in part due to the finding that HIF-1α was more easily degraded in laboratory conditions on FFPE specimens, due to the relatively shorter half-life (15min) compared to CAIX (16 hours).

CAIX, a downstream element in hypoxia has also been associated with worse prognosis in breast cancers, particularly in Basal-type cancers where CAIX levels and their relation to resistance to chemotherapy has been noted, and TNBC cancers, with some degree of prognostic value for response to neoadjuvant chemotherapy being attributed to CAIX(275-277, 283, 287). High CytCAIX expression was identified to result in poorer RFS, supporting the idea that hypoxia plays a role in reduced survival in TNBCs.

In his most recent edition of “Hallmarks of Cancer”, Hanahan re-iterates the eight hallmarks of cancer biology, and introduces the emerging hallmarks and enabling characteristics of cancer cell behaviour. One such emerging hallmark is “non-mutational epigenetic reprogramming”, of which the reaction to hypoxia is used as an example(16). There is evidence that hypoxia can both drive the growth of abnormal cells, but also induce steps leading to EMT, leading to distant spread(16, 317-320). Although these examples are more generalised or within cancers beyond the breast, these are examples of how hypoxia is likely to contribute to disease progression in any context. Examining the well-established hallmarks of cancer, the ability to resist cell death, is another hallmark of interest following the results of this research thesis(16). Apoptosis, or programmed cell death, therefore, is another mechanism by which cancer cells

may promote their own success and evade destruction. In the 2011 edition of their review, Hanahan et al. details the role of Bcl-2 in preventing apoptosis, and introduces the mechanisms by which Bcl-2 and similar proteins may contribute to the evasion of cancer cells from this physiological protective mechanism(321-323).

Bcl2, an indicator of antiapoptotic activity, is highly expressed in approximately 75% of breast cancers, and 41% of TNBC cancers(295). Its role appears to be protective in early stage cancer, with reduced levels of Bcl-2 correlating with poorer outcomes in metastatic disease, and leading to the development of Bcl-2 inhibiting agents being assessed with regards to breast cancer survival (300, 324-326). This echoes the results detailed within this thesis, suggesting that low Bcl2 levels correlated with worse RFS. Further pharmaceutical trials looking at harnessing Bcl-2 activity may pose attractive options for adjunctive therapies in certain breast cancer subsets.

The immune response and how this is particularly altered in TNBC cancers has raised interest in recent years, particularly thanks to the findings that this molecular subgroup has highly immunogenic potential (77-79). Tumour-infiltrating lymphocytes, part of the innate immune system, have been associated with improved response to neoadjuvant chemotherapy which therefore proposes that TILs may be a valuable risk stratification tool for TNBC to identify those who will benefit the most (308, 309, 327). Within this study, low CD3 expression was associated with poorer RFS, regardless of the location (stroma versus tumour), supporting the idea that disease progression relies on the “dampening” of innate immunity, and once again, relating to higher TB phenotype being related to a loss of the innate response to cancer(328). The role of immunotherapy in TNBC may therefore provide an attractive pathway for treatment for this poor prognostic subgroup and encourage deeper understanding of this element of cancer biology as a way to bypass our current lack of targeted therapies.

8.6 Future Perspectives

Limitations of the TNBC cohort include the relatively shorter follow up available which most likely underpowers the findings of CSS not having statistical significance. However, having a relatively new cohort, with prospectively collected data, will improve the quality of the results which will become

available. With the fullness of time, further follow up data may provide evidence for nuclear HIF-1α as a prognostic marker or unearth further relationships between biomarkers and clinicopathological findings. Introducing the role of other biomarkers, such as those indicating lymphovascular invasion and other markers of immune response may be of particular interest in helping clarify which biomarkers will help stratify those who are likely to respond (or not) to treatment, and merit alterations in follow up, or more aggressive therapy. For some of these markers, particularly TBX22 and RFX5, there is very little data available with regards to their role in breast cancer, and therefore further validation of immunohistochemistry techniques should be undertaken to improve the quality of data available for analysis. This may relate to why no prognostic effect was noted when examining protein expression, following transcriptomic analysis identifying these genes as significantly different between high and low TB groups.

This study was aimed at providing an exploration of the transcriptomic landscape of ER negative breast cancers, within the context of tumour budding. In future, combining the work seen from the cohorts and looking at expression of JUNB,ODAM, RFX5, TBX22 in the TNBC cohort, or vice versa with results pertaining to expression of tumour microenvironment markers may lead to increased understanding and characterisation of the potential for their use as biomarkers. What may be a limitation of this study in the presence of multiple hypotheses, should instead pose as an invitation for further study, strengthened by well-tested protocols for immunohistochemical analysis.

Thanks to the longer follow up period for the Glasgow Breast cancer cohort, and the relative size of the population under study, a general overview of protein expression was possible. However, due to the passage of time and loss of core quality, a significant proportion of the cohort was lost. Some of the results may therefore be of additional value in a newer cohort, prospectively collected and examined for clinicopathological findings, and including those who now would be eligible for neoadjuvant and adjuvant therapies. In an era where genotyping is more readily available, it may be possible to stratify a cohort further into molecular subtypes according to more strict phenotypic criteria, again improving the value of the analyses with regards to prognostic planning. With some of the cancer within this cohort predating a number of adjuvant therapeutic advances,

we may also find that the effects of these proteins are more (or less) significant in prognostication than before.

The role of ITB and PTB should be compared in further studies, and the potential use of core biopsies may therefore be examined as a prognostic indicator in all subtypes, but particularly in TNBC or HER2-enriched cancers. These are often the recipients of neoadjuvant chemotherapy prior to surgical specimens being excised and therefore becoming available, and if the relation between ITB and PTB is known, these characteristics may become useful markers of pathological response to therapy and allow follow up to be tailored to each patient based on their recurrence risk.

Cell culture and organoid work or single-cell transcriptomic analysis such as CosmX (NanoString), (using cells derived from surplus cancer specimens, particularly tumour buds) may allow a more granular insight into the role of each protein in the progression of breast cancer, and in tumour buds themselves and allow for selection of specific molecular subgroup characteristics to be matched to certain subsets of breast cancer with worse prognosis. In a more controlled environment, this may reveal further information about the four proteins, JUNB, ODAM, RFX5 and TBX22 and their effect on different stages of the cell and tumour behaviour.

Finally, the emerging role of AI in the study and quantification of biomarker expression may provide additional options for higher-throughput and rapid examination of specimens, while reducing the inter-examiner variability of results. Preliminary results from this study, namely in the scoring of protein expression in the TNBC cohort, support this effort being of value.

From a clinical perspective, there is a distinct need for a standardised method of processing samples, analysing and scoring tumour buds in order for this to translate to practical, daily clinical risk stratification. The fact that this has been possible with colorectal cancer is indication that this should be the case in breast cancer. As research continues, identifying the gene signatures associated with tumour budding phenotype may in turn, advance our options for adjuvant therapies for all types of solid cancers.

8.7 Conclusion

The hypothesis of this study was that tumour budding could act as the basis for differential transcriptomic analysis in the context of breast cancer. This revealed that JUNB, ODAM, RFX5 and TBX22 were differentially expressed in high versus low tumour budding phenotype ER- cancers, and that this translated to variation in prognosis amongst the subgroups within the Glasgow Breast Cancer Cohort. This was particularly the case for JUNB, where high expression correlated to improved survival. ODAM appeared to have a negative impact on prognosis, with low levels correlating with improved CSS in ER- cancers. RFX5 was associated with improved survival when highly expressed, whereas TBX22 revealed itself to be more equivocal in its relationship to prognosis in all subsets of breast cancer. Preliminary results across a relatively large cohort of all subtypes of breast cancer reveals promising results in how prognosis relates to expression, but further information is required with regards to the proteins themselves, their role in normal cellular biology, and how this might be affected in cancer cells. Finally, thanks to DSP, a spatial examination of differential gene expression was possible, and offered valuable insights into how the TME and Tumour transcriptomic landscape differ in the context of TB. With early results suggesting an effect of hypoxia, apoptosis, and immune infiltrate on survival, it remains to be seen if longer follow up will provide additional information of how markers of how these elements are affected, or in turn affect, tumour budding phenotype.

Appendices

Publications by author during the course of this research:

Shamis, Suad & Savioli, Francesca & Ammar, Aula & Al-Badran, Sara & Hatthakarnkul, Phimmada & Leslie, Holly & Mallon, Elizabeth & Jamieson, Nigel & Mcmillan, Donald & Edwards, Joanne. (2023). Spatial transcriptomic analysis of tumour with high and low CAIX expression in TNBC tissue samples using GeoMx™ RNA assay. Histology and histopathology. 18655. 10.14670/HH-18-655.

Savioli, Francesca & Morrow, Elizabeth & Dolan, Ross & Romics, Laszlo & Lannigan, Alison & Edwards, Joanne & Mcmillan, Donald. (2022). Prognostic role of preoperative circulating systemic inflammatory response markers in primary breast cancer: meta-analysis. The British journal of surgery. 109. 10.1093/bjs/znac319.

Stallard, Sheila & Savioli, Francesca & McConnachie, Alex & Norrie, John & Dudman, Katie & Morrow, Elizabeth & Romics, Laszlo. (2022). Antibiotic prophylaxis in breast cancer surgery (PAUS trial): randomised clinical double-blind parallel-group multicentre superiority trial. The British journal of surgery. 109. 10.1093/bjs/znac280.

Savioli, Francesca & Morrow, Elizabeth & Cheung, Lok Ka & Stallard, Sheila & Doughty, Julia & Romics, Laszlo. (2022). Routine four-quadrant cavity shaving at the time of wide local excision for breast cancer reduces re-excision rate. Annals of The Royal College of Surgeons of England. 10.1308/rcsann.2021.0285.

Savioli, Francesca & Seth, Subodh & Morrow, Elizabeth & Doughty, Julie & Stallard, Sheila & Malyon, Andy & Romics, Laszlo. (2021). Extreme Oncoplasty: Breast Conservation in Patients with Large, Multifocal, and Multicentric Breast Cancer. Breast Cancer: Targets and Therapy. Volume 13. 353-359. 10.2147/BCTT.S296242.

Romics, Laszlo & Doughty, Julie & Stallard, Sheila & Mansell, James & Blackhall, Vivienne & Lannigan, Alison & Elgammal, Suzanne & Reid, Judith & McGuigan, Marie-Claire & Savioli, Francesca & Tovey, Sian & Murphy, Dermott & Reid, Iona & Malyon, Andy & McIlhenny, Jennifer & Wilson, Christopher. (2021). A prospective cohort study of the safety of breast cancer surgery during COVID-19 pandemic in the West of Scotland. The Breast. 55. 1-6. 10.1016/j.breast.2020.11.015.

Edwards, Joanne & Mcmillan, Donald & Stallard, Sheila & Doughty, J. & Romics, Laszlo & Savioli, F. (2020). The effect of postoperative complications on survival and recurrence after surgery for breast cancer: A systematic review and meta-analysis. European Journal of Cancer. 138. S108. 10.1016/S0959-8049(20)30826-1.

List of References

1. UK CR. What is Breast Cancer? : Cancer Research UK; 2022 [Available from: https://www.cancerresearchuk.org/about-cancer/breast-cancer/about.
2. Morrow E. The role of systemic and local inflammation, the tumour microenvironment and the IL6/JAK/STAT3 pathway in primary operable breast cancer. Glasgow, United Kingdom: University of Glasgow; 2021.
3. Lyons TG. Targeted Therapies for Triple-Negative Breast Cancer. Curr Treat Options Oncol. 2019;20(11):82.
4. Prat A, Pineda E, Adamo B, Galván P, Fernández A, Gaba L, et al. Clinical implications of the intrinsic molecular subtypes of breast cancer. The Breast. 2015;24:S26-S35.
5. Dent R, Trudeau M, Pritchard KI, Hanna WM, Kahn HK, Sawka CA, et al. Triple-negative breast cancer: clinical features and patterns of recurrence. Clinical cancer research. 2007;13(15):4429-34.
6. Lugli A, Kirsch R, Ajioka Y, Bosman F, Cathomas G, Dawson H, et al. Recommendations for reporting tumor budding in colorectal cancer based on the International Tumor Budding Consensus Conference (ITBCC) 2016. Mod Pathol. 2017;30(9):1299-311.
7. Lugli A, Zlobec I, Berger MD, Kirsch R, Nagtegaal ID. Tumour budding in solid cancers. Nat Rev Clin Oncol. 2021;18(2):101-15.
8. Studer L, Blank A, Bokhorst JM, Nagtegaal ID, Zlobec I, Lugli A, et al. Taking tumour budding to the next frontier - a post International Tumour Budding Consensus Conference (ITBCC) 2016 review. Histopathology. 2021;78(4):476-84.
9. Ueno H, Price AB, Wilkinson KH, Jass JR, Mochizuki H, Talbot IC. A new prognostic staging system for rectal cancer. Ann Surg. 2004;240(5):832-9.
10. Gujam FJ, McMillan DC, Mohammed ZM, Edwards J, Going JJ. The relationship between tumour budding, the tumour microenvironment and survival in patients with invasive ductal breast cancer. Br J Cancer. 2015;113(7):1066-74.
11. Sun Y, Liang F, Cao W, Wang K, He J, Wang H, et al. Prognostic value of poorly differentiated clusters in invasive breast cancer. World Journal of Surgical Oncology. 2014;12(1):310.
12. Liang F, Cao W, Wang Y, Li L, Zhang G, Wang Z. The prognostic value of tumor budding in invasive breast cancer. Pathol Res Pract. 2013;209(5):269-75.
13. Salhia B, Trippel M, Pfaltz K, Cihoric N, Grogg A, Lädrach C, et al. High tumor budding stratifies breast cancer with metastatic properties. Breast Cancer Res Treat. 2015;150(2):363-71.
14. Kalluri R, Weinberg RA. The basics of epithelial-mesenchymal transition. The Journal of Clinical Investigation. 2009;119(6):1420-8.
15. Sakorafas GH, Safioleas M. Breast cancer surgery: an historical narrative. Part III. From the sunset of the 19th to the dawn of the 21st century. Eur J Cancer Care (Engl). 2010;19(2):145-66.
16. Hanahan D. Hallmarks of Cancer: New Dimensions. Cancer Discov. 2022;12(1):31-46.
17. Veronesi U, Boyle P, Goldhirsch A, Orecchia R, Viale G. Breast cancer. The Lancet. 2005;365(9472):1727-41.
18. Teichgraeber DC, Guirguis MS, Whitman GJ. Breast Cancer Staging: Updates in the AJCC Cancer Staging Manual, 8th Edition, and Current Challenges for Radiologists, From the AJR Special Series on Cancer Staging. AJR Am J Roentgenol. 2021;217(2):278-90.

19. Giuliano AE, Connolly JL, Edge SB, Mittendorf EA, Rugo HS, Solin LJ, et al. Breast Cancer-Major changes in the American Joint Committee on Cancer eighth edition cancer staging manual. CA Cancer J Clin. 2017;67(4):290-303.
20. Syed YY. Oncotype DX Breast Recurrence Score(®): A Review of its Use in Early-Stage Breast Cancer. Mol Diagn Ther. 2020;24(5):621-32.
21. Kwa M, Makris A, Esteva FJ. Clinical utility of gene-expression signatures in early stage breast cancer. Nature reviews Clinical oncology. 2017;14(10):595-610.
22. Bogaerts J, Cardoso F, Buyse M, Braga S, Loi S, Harrison JA, et al. Gene signature evaluation as a prognostic tool: challenges in the design of the MINDACT trial. Nature clinical practice Oncology. 2006;3(10):540-51.
23. Cardoso F, van't Veer LJ, Bogaerts J, Slaets L, Viale G, Delaloge S, et al. 70-gene signature as an aid to treatment decisions in early-stage breast cancer. New England Journal of Medicine. 2016;375(8):717-29.
24. Lee AH, Ellis IO. The Nottingham prognostic index for invasive carcinoma of the breast. Pathol Oncol Res. 2008;14(2):113-5.
25. Veronesi U, Stafyla V, Luini A, Veronesi P. Breast cancer: from "maximum tolerable" to "minimum effective" treatment. Front Oncol. 2012;2:125.
26. Veronesi U, Viale G, Paganelli G, Zurrida S, Luini A, Galimberti V, et al. Sentinel lymph node biopsy in breast cancer: ten-year results of a randomized controlled study. Ann Surg. 2010;251(4):595-600.
27. Rietjens M, Urban C, Rey P, Mazzarol G, Maisonneuve P, Garusi C, et al. Long-term oncological results of breast conservative treatment with oncoplastic surgery. The Breast. 2007;16(4):387-95.
28. Giuliano AE, Hunt KK, Ballman KV, Beitsch PD, Whitworth PW, Blumencranz PW, et al. Axillary dissection vs no axillary dissection in women with invasive breast cancer and sentinel node metastasis: a randomized clinical trial. Jama. 2011;305(6):569-75.
29. Donker M, van Tienhoven G, Straver ME, Meijnen P, van de Velde CJ, Mansel RE, et al. Radiotherapy or surgery of the axilla after a positive sentinel node in breast cancer (EORTC 10981-22023 AMAROS): a randomised, multicentre, open-label, phase 3 non-inferiority trial. The lancet oncology. 2014;15(12):1303-10.
30. Goyal A, Mann GB, Fallowfield L, Duley L, Reed M, Dodwell D, et al. POSNOC-POsitive Sentinel NOde: adjuvant therapy alone versus adjuvant therapy plus Clearance or axillary radiotherapy: a randomised controlled trial of axillary treatment in women with early-stage breast cancer who have metastases in one or two sentinel nodes. BMJ Open. 2021;11(12):e054365.
31. Pondé NF, Zardavas D, Piccart M. Progress in adjuvant systemic therapy for breast cancer. Nat Rev Clin Oncol. 2019;16(1):27-44.
32. Jazieh K, Bell R, Agarwal N, Abraham J. Novel targeted therapies for metastatic breast cancer. Ann Transl Med. 2020;8(14):907.
33. Bonadonna G, Brusamolino E, Valagussa P, Rossi A, Brugnatelli L, Brambilla C, et al. Combination chemotherapy as an adjuvant treatment in operable breast cancer. New England Journal of Medicine. 1976;294(8):405-10.
34. Baum M. Controlled trial of tamoxifen as single adjuvant agent in the management of early breast cancer: analysis at six years by Nolvadex Adjuvant Trial Organization. Cancer. 1985;1:836-9.
35. Pan H, Gray R, Braybrooke J, Davies C, Taylor C, McGale P, et al. 20-year risks of breast-cancer recurrence after stopping endocrine therapy at 5 years. New England Journal of Medicine. 2017;377(19):1836-46.

36. Group EBCTC. Effects of chemotherapy and hormonal therapy for early breast cancer on recurrence and 15-year survival: an overview of the randomised trials. The Lancet. 2005;365(9472):1687-717.
37. Group EBCTC. Comparisons between different polychemotherapy regimens for early breast cancer: meta-analyses of long-term outcome among 100 000 women in 123 randomised trials. The Lancet. 2012;379(9814):432-44.
38. Cardinale D, Colombo A, Lamantia G, Colombo N, Civelli M, De Giacomi G, et al. Anthracycline-induced cardiomyopathy: clinical relevance and response to pharmacologic therapy. Journal of the American College of Cardiology. 2010;55(3):213-20.
39. Blum JL, Flynn PJ, Yothers G, Asmar L, Geyer Jr CE, Jacobs SA, et al. Anthracyclines in early breast cancer: The abc trials—usor 06-090, nsabp b-46-i/usor 07132, and nsabp b-49 (nrg oncology). Journal of clinical oncology. 2017;35(23):2647.
40. Gray R, Bradley R, Braybrooke J, Davies C, Pan H, Peto R, et al. Abstract GS1-01: increasing the dose density of adjuvant chemotherapy by shortening intervals between courses or by sequential drug administration significantly reduces both disease recurrence and breast cancer mortality: an EBCTCG meta-analysis of 21,000 women in 16 randomised trials. Cancer Research. 2018;78(4_Supplement):GS1-01-GS1-.
41. Curigliano G, Burstein HJ, Winer EP, Gnant M, Dubsky P, Loibl S, et al. De-escalating and escalating treatments for early-stage breast cancer: the St. Gallen International Expert Consensus Conference on the Primary Therapy of Early Breast Cancer 2017. Annals of Oncology. 2017;28(8):1700-12.
42. Reeder-Hayes KE, Meyer AM, Hinton SP, Meng K, Carey LA, Dusetzina SB. Comparative toxicity and effectiveness of trastuzumab-based chemotherapy regimens in older women with early-stage breast cancer. Journal of Clinical Oncology. 2017;35(29):3298.
43. Tolaney SM, Barry WT, Dang CT, Yardley DA, Moy B, Marcom PK, et al. Adjuvant paclitaxel and trastuzumab for node-negative, HER2-positive breast cancer. New England Journal of Medicine. 2015;372(2):134-41.
44. Masuda N, Lee S-J, Ohtani S, Im Y-H, Lee E-S, Yokota I, et al. Adjuvant capecitabine for breast cancer after preoperative chemotherapy. New England Journal of Medicine. 2017;376(22):2147-59.
45. Denduluri N, Chavez-MacGregor M, Telli ML, Eisen A, Graff SL, Hassett MJ, et al. Selection of optimal adjuvant chemotherapy and targeted therapy for early breast cancer: ASCO clinical practice guideline focused update. Journal of Clinical Oncology. 2018;36(23):2433-43.
46. Eisen A, Somerfield MR, Accordino MK, Blanchette PS, Clemons MJ, Dhesy-Thind S, et al. Use of Adjuvant Bisphosphonates and Other Bone-Modifying Agents in Breast Cancer: ASCO-OH (CCO) Guideline Update. J Clin Oncol. 2022;40(7):787-800.
47. Piccart-Gebhart MJ, Procter M, Leyland-Jones B, Goldhirsch A, Untch M, Smith I, et al. Trastuzumab after adjuvant chemotherapy in HER2-positive breast cancer. New England Journal of Medicine. 2005;353(16):1659-72.
48. Von Minckwitz G, Procter M, De Azambuja E, Zardavas D, Benyunes M, Viale G, et al. Adjuvant pertuzumab and trastuzumab in early HER2-positive breast cancer. New England Journal of Medicine. 2017;377(2):122-31.
49. Chan A, Delaloge S, Holmes FA, Moy B, Iwata H, Harvey VJ, et al. Neratinib after trastuzumab-based adjuvant therapy in patients with HER2-positive breast cancer (ExteNET): a multicentre, randomised, double-blind, placebo-controlled, phase 3 trial. The Lancet Oncology. 2016;17(3):367-77.

50. Sestak I, Buus R, Cuzick J, Dubsky P, Kronenwett R, Denkert C, et al. Comparison of the performance of 6 prognostic signatures for estrogen receptor–positive breast cancer: a secondary analysis of a randomized clinical trial. JAMA oncology. 2018;4(4):545-53.
51. Glassman D, Hignett S, Rehman S, Linforth R, Salhab M. Adjuvant endocrine therapy for hormone-positive breast cancer, focusing on ovarian suppression and extended treatment: an update. Anticancer research. 2017;37(10):5329-41.
52. Partridge AH, Niman SM, Ruggeri M, Peccatori FA, Azim HA, Colleoni M, et al. Interrupting Endocrine Therapy to Attempt Pregnancy after Breast Cancer. New England Journal of Medicine. 2023;388(18):1645-56.
53. Musgrove EA, Sutherland RL. Biological determinants of endocrine resistance in breast cancer. Nature Reviews Cancer. 2009;9(9):631-43.
54. LoRusso PM. Inhibition of the PI3K/AKT/mTOR pathway in solid tumors. Journal of clinical oncology. 2016;34(31):3803.
55. Lim W, Mayer B, Pawson T. Cell signaling: Taylor & Francis; 2014.
56. Miricescu D, Totan A, Stanescu S, II, Badoiu SC, Stefani C, Greabu M. PI3K/AKT/mTOR Signaling Pathway in Breast Cancer: From Molecular Landscape to Clinical Aspects. Int J Mol Sci. 2020;22(1).
57. Berchtold D, Walther TC. TORC2 plasma membrane localization is essential for cell viability and restricted to a distinct domain. Molecular biology of the cell. 2009;20(5):1565-75.
58. Maiese K. Forkhead transcription factors: formulating a FOXO target for cognitive loss. Current neurovascular research. 2017;14(4):415-20.
59. Cretella D, Digiacomo G, Giovannetti E, Cavazzoni A. PTEN alterations as a potential mechanism for tumor cell escape from PD-1/PD-L1 inhibition. Cancers. 2019;11(9):1318.
60. Luongo F, Colonna F, Calapà F, Vitale S, Fiori ME, De Maria R. PTEN tumor-suppressor: the dam of stemness in cancer. Cancers. 2019;11(8):1076.
61. Naderali E, Khaki AA, Rad JS, Ali-Hemmati A, Rahmati M, Charoudeh HN. Regulation and modulation of PTEN activity. Molecular biology reports. 2018;45:2869-81.
62. Miller TW, Rexer BN, Garrett JT, Arteaga CL. Mutations in the phosphatidylinositol 3-kinase pathway: role in tumor progression and therapeutic implications in breast cancer. Breast cancer research. 2011;13:1-12.
63. Maehama T, Taylor GS, Dixon JE. PTEN and myotubularin: novel phosphoinositide phosphatases. Annual review of biochemistry. 2001;70(1):247-79.
64. Xing Y, Lin NU, Maurer MA, Chen H, Mahvash A, Sahin A, et al. Phase II trial of AKT inhibitor MK-2206 in patients with advanced breast cancer who have tumors with PIK3CA or AKT mutations, and/or PTEN loss/PTEN mutation. Breast Cancer Res. 2019;21(1):78.
65. Li SY, Rong M, Grieu F, Iacopetta B. PIK3CA mutations in breast cancer are associated with poor outcome. Breast Cancer Res Treat. 2006;96(1):91-5.
66. Lehmann BD, Bauer JA, Schafer JM, Pendleton CS, Tang L, Johnson KC, et al. PIK3CA mutations in androgen receptor-positive triple negative breast cancer confer sensitivity to the combination of PI3K and androgen receptor inhibitors. Breast Cancer Res. 2014;16(4):406.
67. Toss A, Cristofanilli M. Molecular characterization and targeted therapeutic approaches in breast cancer. Breast Cancer Res. 2015;17(1):60.
68. Anestis A, Zoi I, Papavassiliou AG, Karamouzis MV. Androgen Receptor in Breast Cancer—Clinical and Preclinical Research Insights. Molecules. 2020;25(2):358.

69. Collins LC, Cole KS, Marotti JD, Hu R, Schnitt SJ, Tamimi RM. Androgen receptor expression in breast cancer in relation to molecular phenotype: results from the Nurses' Health Study. Mod Pathol. 2011;24(7):924-31.
70. Sarker D, Reid AHM, Yap TA, de Bono JS. Targeting the PI3K/AKT Pathway for the Treatment of Prostate Cancer. Clinical Cancer Research. 2009;15(15):4799-805.
71. Elebro K, Borgquist S, Simonsson M, Markkula A, Jirström K, Ingvar C, et al. Combined Androgen and Estrogen Receptor Status in Breast Cancer: Treatment Prediction and Prognosis in a Population-Based Prospective Cohort. Clinical Cancer Research. 2015;21(16):3640-50.
72. Park S, Koo JS, Kim MS, Park HS, Lee JS, Lee JS, et al. Androgen receptor expression is significantly associated with better outcomes in estrogen receptor-positive breast cancers. Annals of Oncology. 2011;22(8):1755-62.
73. Hu R, Dawood S, Holmes MD, Collins LC, Schnitt SJ, Cole K, et al. Androgen Receptor Expression and Breast Cancer Survival in Postmenopausal Women. Clinical Cancer Research. 2011;17(7):1867-74.
74. Vera-Badillo FE, Templeton AJ, de Gouveia P, Diaz-Padilla I, Bedard PL, Al-Mubarak M, et al. Androgen Receptor Expression and Outcomes in Early Breast Cancer: A Systematic Review and Meta-Analysis. JNCI: Journal of the National Cancer Institute. 2014;106(1):djt319.
75. Astvatsaturyan K, Yue Y, Walts AE, Bose S. Androgen receptor positive triple negative breast cancer: Clinicopathologic, prognostic, and predictive features. PLoS One. 2018;13(6):e0197827.
76. Tutt ANJ, Garber JE, Kaufman B, Viale G, Fumagalli D, Rastogi P, et al. Adjuvant Olaparib for Patients with BRCA1- or BRCA2-Mutated Breast Cancer. New England Journal of Medicine. 2021;384(25):2394-405.
77. Katz H, Alsharedi M. Immunotherapy in triple-negative breast cancer. Medical oncology. 2018;35:1-9.
78. Mahoney KM, Sun H, Liao X, Hua P, Callea M, Greenfield EA, et al. PD-L1 antibodies to its cytoplasmic domain most clearly delineate cell membranes in immunohistochemical staining of tumor cells. Cancer immunology research. 2015;3(12):1308-15.
79. Teng MW, Ngiow SF, Ribas A, Smyth MJ. Classifying cancers based on T-cell infiltration and PD-L1. Cancer research. 2015;75(11):2139-45.
80. Saji S, McArthur HL, Ignatiadis M, Bailey A, El-Abed S, Brandao M, et al. ALEXANDRA/IMpassion030: A phase 3 study of standard adjuvant chemotherapy with or without atezolizumab in patients with early-stage triple-negative breast cancer. Journal of Clinical Oncology. 2021;39(15_suppl):TPS597-TPS.
81. Goodman AM, Kato S, Bazhenova L, Patel SP, Frampton GM, Miller V, et al. Tumor mutational burden as an independent predictor of response to immunotherapy in diverse cancers. Molecular cancer therapeutics. 2017;16(11):2598-608.
82. Domchek SM, Postel-Vinay S, Bang Y-J, Park YH, Alexandre J, Delord J-P, et al. Abstract PD6-11: An open-label, multitumor, phase II basket study of olaparib and durvalumab (MEDIOLA): Results in germline BRCA-mutated (g BRCA m) HER2-negative metastatic breast cancer (MBC). Cancer Research. 2018;78(4_Supplement):PD6-11-PD6-.
83. Li CI, Anderson BO, Daling JR, Moe RE. Trends in incidence rates of invasive lobular and ductal breast carcinoma. Jama. 2003;289(11):1421-4.
84. Ellis I, Carder P, Hales S, Lee AHS et al. . Pathology reporting of breast disease in surgical excision specimens incorporating the dataset for histological reporting of breast cancer. In: Pathologists TRCo, editor. 4th Floor, 21 Prescot Street, London, E1 8BB: The Royal College of Pathologists; 2016.

85. Waks AG, Winer EP. Breast Cancer Treatment: A Review. Jama. 2019;321(3):288-300.
86. Burstein HJ, Curigliano G, Thürlimann B, Weber WP, Poortmans P, Regan MM, et al. Customizing local and systemic therapies for women with early breast cancer: the St. Gallen International Consensus Guidelines for treatment of early breast cancer 2021. Ann Oncol. 2021;32(10):1216-35.
87. Eroles P, Bosch A, Pérez-Fidalgo JA, Lluch A. Molecular biology in breast cancer: intrinsic subtypes and signaling pathways. Cancer Treat Rev. 2012;38(6):698-707.
88. Perou CM, Sørlie T, Eisen MB, van de Rijn M, Jeffrey SS, Rees CA, et al. Molecular portraits of human breast tumours. Nature. 2000;406(6797):747-52.
89. Cheang MCU, Chia SK, Voduc D, Gao D, Leung S, Snider J, et al. Ki67 Index, HER2 Status, and Prognosis of Patients With Luminal B Breast Cancer. JNCI: Journal of the National Cancer Institute. 2009;101(10):736-50.
90. Kennecke H, Yerushalmi R, Woods R, Cheang MCU, Voduc D, Speers CH, et al. Metastatic Behavior of Breast Cancer Subtypes. Journal of Clinical Oncology. 2010;28(20):3271-7.
91. Goldhirsch A, Wood WC, Coates AS, Gelber RD, Thürlimann B, Senn HJ. Strategies for subtypes—dealing with the diversity of breast cancer: highlights of the St Gallen International Expert Consensus on the Primary Therapy of Early Breast Cancer 2011. Annals of Oncology. 2011;22(8):1736-47.
92. Parker JS, Mullins M, Cheang MC, Leung S, Voduc D, Vickery T, et al. Supervised risk predictor of breast cancer based on intrinsic subtypes. J Clin Oncol. 2009;27(8):1160-7.
93. Staaf J, Ringnér M, Vallon-Christersson J, Jönsson G, Bendahl P-O, Holm K, et al. Identification of Subtypes in Human Epidermal Growth Factor Receptor 2–Positive Breast Cancer Reveals a Gene Signature Prognostic of Outcome. Journal of Clinical Oncology. 2010;28(11):1813-20.
94. Bosch A, Eroles P, Zaragoza R, Viña JR, Lluch A. Triple-negative breast cancer: Molecular features, pathogenesis, treatment and current lines of research. Cancer Treatment Reviews. 2010;36(3):206-15.
95. Livasy CA, Karaca G, Nanda R, Tretiakova MS, Olopade OI, Moore DT, et al. Phenotypic evaluation of the basal-like subtype of invasive breast carcinoma. Modern Pathology. 2006;19(2):264-71.
96. Won KA, Spruck C. Triple-negative breast cancer therapy: Current and future perspectives (Review). Int J Oncol. 2020;57(6):1245-61.
97. Bonotto M, Gerratana L, Poletto E, Driol P, Giangreco M, Russo S, et al. Measures of outcome in metastatic breast cancer: insights from a real-world scenario. Oncologist. 2014;19(6):608-15.
98. Kohler BA, Sherman RL, Howlader N, Jemal A, Ryerson AB, Henry KA, et al. Annual Report to the Nation on the Status of Cancer, 1975-2011, Featuring Incidence of Breast Cancer Subtypes by Race/Ethnicity, Poverty, and State. J Natl Cancer Inst. 2015;107(6):djv048.
99. Fisher B, Redmond C, Legault-Poisson S, Dimitrov NV, Brown AM, Wickerham DL, et al. Postoperative chemotherapy and tamoxifen compared with tamoxifen alone in the treatment of positive-node breast cancer patients aged 50 years and older with tumors responsive to tamoxifen: results from the National Surgical Adjuvant Breast and Bowel Project B-16. J Clin Oncol. 1990;8(6):1005-18.
100. Fong PC, Boss DS, Yap TA, Tutt A, Wu P, Mergui-Roelvink M, et al. Inhibition of Poly(ADP-Ribose) Polymerase in Tumors from BRCA Mutation Carriers. New England Journal of Medicine. 2009;361(2):123-34.

101. Weigelt B, Mackay A, A'Hern R, Natrajan R, Tan DSP, Dowsett M, et al. Breast cancer molecular profiling with single sample predictors: a retrospective analysis. The Lancet Oncology. 2010;11(4):339-49.
102. Herschkowitz JI, Simin K, Weigman VJ, Mikaelian I, Usary J, Hu Z, et al. Identification of conserved gene expression features between murine mammary carcinoma models and human breast tumors. Genome Biology. 2007;8(5):R76.
103. Goldhirsch A, Winer EP, Coates AS, Gelber RD, Piccart-Gebhart M, Thürlimann B, et al. Personalizing the treatment of women with early breast cancer: highlights of the St Gallen International Expert Consensus on the Primary Therapy of Early Breast Cancer 2013. Ann Oncol. 2013;24(9):2206-23.
104. Scholzen T, Gerdes J. The Ki-67 protein: From the known and the unknown. Journal of Cellular Physiology. 2000;182(3):311-22.
105. Li LT, Jiang G, Chen Q, Zheng JN. Ki67 is a promising molecular target in the diagnosis of cancer (review). Mol Med Rep. 2015;11(3):1566-72.
106. Nakano T, Ohno T, Ishikawa H, Suzuki Y, Takahashi T. Current advancement in radiation therapy for uterine cervical cancer. J Radiat Res. 2010;51(1):1-8.
107. Probert J, Dodwell D, Broggio J, Charman J, Dowsett M, Kerr A, et al. Ki67 and breast cancer mortality in women with invasive breast cancer. JNCI Cancer Spectrum. 2023;7(5).
108. Dowsett M, Smith IE, Ebbs SR, Dixon JM, Skene A, Griffith C, et al. Short-Term Changes in Ki-67 during Neoadjuvant Treatment of Primary Breast Cancer with Anastrozole or Tamoxifen Alone or Combined Correlate with Recurrence-Free Survival. Clinical Cancer Research. 2009;11(2):951s-8s.
109. Ellis MJ, Coop A, Singh B, Tao Y, Llombart-Cussac A, Jänicke F, et al. Letrozole Inhibits Tumor Proliferation More Effectively than Tamoxifen Independent of HER1/2 Expression Status1. Cancer Research. 2003;63(19):6523-31.
110. Ellis MJ, Suman VJ, Hoog J, Lin L, Snider J, Prat A, et al. Randomized phase II neoadjuvant comparison between letrozole, anastrozole, and exemestane for postmenopausal women with estrogen receptor-rich stage 2 to 3 breast cancer: clinical and biomarker outcomes and predictive value of the baseline PAM50-based intrinsic subtype--ACOSOG Z1031. J Clin Oncol. 2011;29(17):2342-9.
111. Laplane L, Duluc D, Bikfalvi A, Larmonier N, Pradeu T. Beyond the tumour microenvironment. Int J Cancer. 2019;145(10):2611-8.
112. Diakos CI, Charles KA, McMillan DC, Clarke SJ. Cancer-related inflammation and treatment effectiveness. The Lancet Oncology. 2014;15(11):e493-e503.
113. Savioli F, Morrow ES, Dolan RD, Romics L, Lannigan A, Edwards J, et al. Prognostic role of preoperative circulating systemic inflammatory response markers in primary breast cancer: meta-analysis. Br J Surg. 2022;109(12):1206-15.
114. Savioli F, Edwards J, McMillan D, Stallard S, Doughty J, Romics L. The effect of postoperative complications on survival and recurrence after surgery for breast cancer: A systematic review and meta-analysis. Crit Rev Oncol Hematol. 2020;155:103075.
115. Roxburgh C, McDonald A, Salmond J, Oien K, Anderson J, McKee R, et al. Adjuvant chemotherapy for resected colon cancer: comparison of the prognostic value of tumour and patient related factors. International journal of colorectal disease. 2011;26:483-92.
116. McMillan DC. The systemic inflammation-based Glasgow Prognostic Score: a decade of experience in patients with cancer. Cancer Treat Rev. 2013;39(5):534-40.

117. Leitch E, Chakrabarti M, Crozier J, McKee R, Anderson J, Horgan P, et al. Comparison of the prognostic value of selected markers of the systemic inflammatory response in patients with colorectal cancer. British journal of cancer. 2007;97(9):1266-70.
118. Proctor MJ, Morrison DS, Talwar D, Balmer SM, Fletcher CD, O'Reilly DSJ, et al. A comparison of inflammation-based prognostic scores in patients with cancer. A Glasgow Inflammation Outcome Study. European journal of cancer. 2011;47(17):2633-41.
119. Bissell MJ, Radisky D. Putting tumours in context. Nat Rev Cancer. 2001;1(1):46-54.
120. Witz IP. The tumor microenvironment: the making of a paradigm. Cancer Microenviron. 2009;2 Suppl 1(Suppl 1):9-17.
121. Richards CH, Mohammed Z, Qayyum T, Horgan PG, McMillan DC. The prognostic value of histological tumor necrosis in solid organ malignant disease: a systematic review. Future Oncology. 2011;7(10):1223-35.
122. Fisher ER, Palekar AS, Gregorio RM, Redmond C, Fisher B. Pathological findings from the national surgical adjuvant breast project (Protocol No. 4). IV. Significance of tumor necrosis. Human pathology. 1978;9(5):523-30.
123. Gujam FJ, Edwards J, Mohammed ZM, Going JJ, McMillan DC. The relationship between the tumour stroma percentage, clinicopathological characteristics and outcome in patients with operable ductal breast cancer. Br J Cancer. 2014;111(1):157-65.
124. Gujam FJA, Edwards J, Mohammed ZMA, Going JJ, McMillan DC. The relationship between the tumour stroma percentage, clinicopathological characteristics and outcome in patients with operable ductal breast cancer. British Journal of Cancer. 2014;111(1):157-65.
125. Andisha NM, McMillan DC, Gujam FJA, Roseweir A, Edwards J. The relationship between phosphorylation status of focal adhesion kinases, molecular subtypes, tumour microenvironment and survival in patients with primary operable ductal breast cancer. Cellular Signalling. 2019;60:91-9.
126. de Kruijf EM, van Nes JG, van de Velde CJ, Putter H, Smit VT, Liefers GJ, et al. Tumor–stroma ratio in the primary tumor is a prognostic factor in early breast cancer patients, especially in triple-negative carcinoma patients. Breast cancer research and treatment. 2011;125:687-96.
127. Engels B, Rowley DA, Schreiber H. Targeting stroma to treat cancers. Semin Cancer Biol. 2012;22(1):41-9.
128. Klintrup K, Mäkinen JM, Kauppila S, Väre PO, Melkko J, Tuominen H, et al. Inflammation and prognosis in colorectal cancer. European journal of cancer. 2005;41(17):2645-54.
129. Klintrup K, Mäkinen JM, Kauppila S, Väre PO, Melkko J, Tuominen H, et al. Inflammation and prognosis in colorectal cancer. Eur J Cancer. 2005;41(17):2645-54.
130. Moore Jr OS, Foote Jr FW. The relatively favorable prognosis of medullary carcinoma of the breast. Cancer. 1949;2(4):635-42.
131. Matsumoto H, Koo S-l, Dent R, Tan PH, Iqbal J. Role of inflammatory infiltrates in triple negative breast cancer. Journal of Clinical Pathology. 2015;68(7):506-10.
132. Hiraoka K, Miyamoto M, Cho Y, Suzuoki M, Oshikiri T, Nakakubo Y, et al. Concurrent infiltration by CD8+ T cells and CD4+ T cells is a favourable prognostic factor in non-small-cell lung carcinoma. British journal of cancer. 2006;94(2):275-80.

133. Tanchot C, Terme M, Pere H, Tran T, Benhamouda N, Strioga M, et al. Tumor-infiltrating regulatory T cells: phenotype, role, mechanism of expansion in situ and clinical significance. Cancer Microenvironment. 2013;6:147-57.
134. Curiel TJ, Coukos G, Zou L, Alvarez X, Cheng P, Mottram P, et al. Specific recruitment of regulatory T cells in ovarian carcinoma fosters immune privilege and predicts reduced survival. Nature medicine. 2004;10(9):942-9.
135. Bron L, Jandus C, Andrejevic-Blant S, Speiser DE, Monnier P, Romero P, et al. Prognostic value of arginase-II expression and regulatory T-cell infiltration in head and neck squamous cell carcinoma. International journal of cancer. 2013;132(3):E85-E93.
136. Allavena P, Mantovani A. Immunology in the clinic review series; focus on cancer: tumour-associated macrophages: undisputed stars of the inflammatory tumour microenvironment. Clinical & Experimental Immunology. 2012;167(2):195-205.
137. Mohammed Z, Going J, Edwards J, Elsberger B, Doughty J, McMillan D. The relationship between components of tumour inflammatory cell infiltrate and clinicopathological factors and survival in patients with primary operable invasive ductal breast cancer. British journal of cancer. 2012;107(5):864-73.
138. Richards C, Flegg K, SD Roxburgh C, Going J, Mohammed Z, Horgan P, et al. The relationships between cellular components of the peritumoural inflammatory response, clinicopathological characteristics and survival in patients with primary operable colorectal cancer. British journal of cancer. 2012;106(12):2010-5.
139. Michael-Robinson J, Biemer-Hüttmann A, Purdie D, Walsh M, Simms L, Biden K, et al. Tumour infiltrating lymphocytes and apoptosis are independent features in colorectal cancer stratified according to microsatellite instability status. Gut. 2001;48(3):360-6.
140. Richards C, Roxburgh C, Anderson J, McKee R, Foulis A, Horgan P, et al. Prognostic value of tumour necrosis and host inflammatory responses in colorectal cancer. Journal of British Surgery. 2012;99(2):287-94.
141. Terlizzi M, Casolaro V, Pinto A, Sorrentino R. Inflammasome: cancer's friend or foe? Pharmacology & therapeutics. 2014;143(1):24-33.
142. Guthrie GJ, Roxburgh CS, Horgan PG, McMillan DC. Does interleukin-6 link explain the link between tumour necrosis, local and systemic inflammatory responses and outcome in patients with colorectal cancer? Cancer treatment reviews. 2013;39(1):89-96.
143. Morishima T, Watanabe Ki, Niwa A, Fujino H, Matsubara H, Adachi S, et al. Neutrophil differentiation from human-induced pluripotent stem cells. Journal of cellular physiology. 2011;226(5):1283-91.
144. Mitchell S, Vargas J, Hoffmann A. Signaling via the NFκB system. Wiley Interdiscip Rev Syst Biol Med. 2016;8(3):227-41.
145. Khongthong P, Roseweir AK, Edwards J. The NF-KB pathway and endocrine therapy resistance in breast cancer. Endocr Relat Cancer. 2019;26(6):R369-r80.
146. Radisky D, Muschler J, Bissell MJ. Order and disorder: the role of extracellular matrix in epithelial cancer. Cancer investigation. 2002;20(1):139-53.
147. Perl A-K, Wilgenbus P, Dahl U, Semb H, Christofori G. A causal role for E-cadherin in the transition from adenoma to carcinoma. Nature. 1998;392(6672):190-3.
148. Yamada N, Sugai T, Eizuka M, Tsuchida K, Sugimoto R, Mue Y, et al. Tumor budding at the invasive front of colorectal cancer may not be associated with the epithelial-mesenchymal transition. Hum Pathol. 2017;60:151-9.

149. Lugli A, Zlobec I, Berger MD, Kirsch R, Nagtegaal ID. Tumour budding in solid cancers. Nature Reviews Clinical Oncology. 2021;18(2):101-15.
150. Liang F, Cao W, Wang Y, Li L, Zhang G, Wang Z. The prognostic value of tumor budding in invasive breast cancer. Pathology-Research and Practice. 2013;209(5):269-75.
151. Ueno H, Murphy J, Jass JR, Mochizuki H, Talbot IC. Tumour `budding' as an index to estimate the potential of aggressiveness in rectal cancer. Histopathology. 2002;40(2):127-32.
152. Laedrach C, Salhia B, Cihoric N, Zlobec I, Tapia C. Immunophenotypic profile of tumor buds in breast cancer. Pathol Res Pract. 2018;214(1):25-9.
153. Kevans D, Wang LM, Sheahan K, Hyland J, O'Donoghue D, Mulcahy H, et al. Epithelial-mesenchymal transition (EMT) protein expression in a cohort of stage II colorectal cancer patients with characterized tumor budding and mismatch repair protein status. International journal of surgical pathology. 2011;19(6):751-60.
154. Maffeis V, Cappellesso R, Galuppini F, Guzzardo V, Zanon A, Cazzador D, et al. Tumor budding is an adverse prognostic marker in intestinal-type sinonasal adenocarcinoma and seems to be unrelated to epithelial-mesenchymal transition. Virchows Archiv. 2020;477:241-8.
155. Salhia B, Trippel M, Pfaltz K, Cihoric N, Grogg A, Lädrach C, et al. High tumor budding stratifies breast cancer with metastatic properties. Breast cancer research and treatment. 2015;150:363-71.
156. Guinney J, Dienstmann R, Wang X, De Reynies A, Schlicker A, Soneson C, et al. The consensus molecular subtypes of colorectal cancer. Nature medicine. 2015;21(11):1350-6.
157. Trinh A, Lädrach C, Dawson HE, Ten Hoorn S, Kuppen PJ, Reimers MS, et al. Tumour budding is associated with the mesenchymal colon cancer subtype and RAS/RAF mutations: a study of 1320 colorectal cancers with Consensus Molecular Subgroup (CMS) data. British journal of cancer. 2018;119(10):1244-51.
158. Møller T, James JP, Holmstrøm K, Sørensen FB, Lindebjerg J, Nielsen BS. Co-detection of miR-21 and TNF-α mRNA in budding cancer cells in colorectal cancer. International Journal of Molecular Sciences. 2019;20(8):1907.
159. Koelzer VH, Dawson H, Andersson E, Karamitopoulou E, Masucci GV, Lugli A, et al. Active immunosurveillance in the tumor microenvironment of colorectal cancer is associated with low frequency tumor budding and improved outcome. Translational Research. 2015;166(2):207-17.
160. Shamis SAK. The Relationship Between Hypoxia, Hypoxia Gene Signature and Survival in Patients with Triple Negative Breast Cancer. Glasgow, United Kingdom: University of Glasgow; 2023.
161. Sundqvist A, Zieba A, Vasilaki E, Herrera Hidalgo C, Söderberg O, Koinuma D, et al. Specific interactions between Smad proteins and AP-1 components determine TGFß-induced breast cancer cell invasion. Oncogene. 2013;32(31):3606-15.
162. Zhao C, Qiao Y, Jonsson P, Wang J, Xu L, Rouhi P, et al. Genome-wide profiling of AP-1-regulated transcription provides insights into the invasiveness of triple-negative breast cancer. Cancer Res. 2014;74(14):3983-94.
163. Selvamurugan N, Kwok S, Partridge NC. Smad3 Interacts with JunB and Cbfa1/Runx2 for Transforming Growth Factor-ß1-stimulated Collagenase-3 Expression in Human Breast Cancer Cells*. Journal of Biological Chemistry. 2004;279(26):27764-73.
164. Yoshitomi Y, Ikeda T, Saito-Takatsuji H, Yonekura H. Emerging Role of AP-1 Transcription Factor JunB in Angiogenesis and Vascular Development. Int J Mol Sci. 2021;22(6).

165. Eferl R, Wagner EF. AP-1: a double-edged sword in tumorigenesis. Nat Rev Cancer. 2003;3(11):859-68.
166. Hai TW, Liu F, Coukos WJ, Green MR. Transcription factor ATF cDNA clones: an extensive family of leucine zipper proteins able to selectively form DNA-binding heterodimers. Genes Dev. 1989;3(12b):2083-90.
167. Wutschka J, Kast B, Sator-Schmitt M, Appak-Baskoy S, Hess J, Sinn HP, et al. JUNB suppresses distant metastasis by influencing the initial metastatic stage. Clin Exp Metastasis. 2021;38(4):411-23.
168. Ozanne BW, Spence HJ, McGarry LC, Hennigan RF. Transcription factors control invasion: AP-1 the first among equals. Oncogene. 2007;26(1):1-10.
169. Hsieh T, Sasaki D, Taira N, Chien H, Sarkar S, Seto Y, et al. JunB Is Critical for Survival of T Helper Cells. Front Immunol. 2022;13:901030.
170. Yanagida K, Engelbrecht E, Niaudet C, Jung B, Gaengel K, Holton K, et al. Sphingosine 1-Phosphate Receptor Signaling Establishes AP-1 Gradients to Allow for Retinal Endothelial Cell Specialization. Dev Cell. 2020;52(6):779-93.e7.
171. Bakiri L, Lallemand D, Bossy-Wetzel E, Yaniv M. Cell cycle-dependent variations in c-Jun and JunB phosphorylation: a role in the control of cyclin D1 expression. Embo j. 2000;19(9):2056-68.
172. Li B, Tournier C, Davis RJ, Flavell RA. Regulation of IL-4 expression by the transcription factor JunB during T helper cell differentiation. Embo j. 1999;18(2):420-32.
173. Licht AH, Pein OT, Florin L, Hartenstein B, Reuter H, Arnold B, et al. JunB is required for endothelial cell morphogenesis by regulating core-binding factor beta. J Cell Biol. 2006;175(6):981-91.
174. Schmidt D, Textor B, Pein OT, Licht AH, Andrecht S, Sator-Schmitt M, et al. Critical role for NF-kappaB-induced JunB in VEGF regulation and tumor angiogenesis. Embo j. 2007;26(3):710-9.
175. Schorpp-Kistner M, Wang ZQ, Angel P, Wagner EF. JunB is essential for mammalian placentation. Embo j. 1999;18(4):934-48.
176. Kumar R, Mani AM, Singh NK, Rao GN. PKCθ-JunB axis via upregulation of VEGFR3 expression mediates hypoxia-induced pathological retinal neovascularization. Cell Death Dis. 2020;11(5):325.
177. Kiesow K, Bennewitz K, Miranda LG, Stoll SJ, Hartenstein B, Angel P, et al. Junb controls lymphatic vascular development in zebrafish via miR-182. Sci Rep. 2015;5:15007.
178. Kallergi G, Hoffmann O, Bittner AK, Papadimitriou L, Katsarou SD, Zacharopoulou N, et al. CXCR4 and JUNB double-positive disseminated tumor cells are detected frequently in breast cancer patients at primary diagnosis. Ther Adv Med Oncol. 2020;12:1758835919895754.
179. Pérez-Benavente B, Fathinajafabadi A, de la Fuente L, Gandía C, Martínez-Férriz A, Pardo-Sánchez JM, et al. New roles for AP-1/JUNB in cell cycle control and tumorigenic cell invasion via regulation of cyclin E1 and TGF-β2. Genome Biol. 2022;23(1):252.
180. Hyakusoku H, Sano D, Takahashi H, Hatano T, Isono Y, Shimada S, et al. JunB promotes cell invasion, migration and distant metastasis of head and neck squamous cell carcinoma. J Exp Clin Cancer Res. 2016;35:6.
181. Lian S, Shao Y, Liu H, He J, Lu W, Zhang Y, et al. PDK1 induces JunB, EMT, cell migration and invasion in human gallbladder cancer. Oncotarget. 2015;6(30):29076-86.
182. Thomsen MK, Bakiri L, Hasenfuss SC, Wu H, Morente M, Wagner EF. Loss of JUNB/AP-1 promotes invasive prostate cancer. Cell Death Differ. 2015;22(4):574-82.

183. Hu YF, Li R. JunB potentiates function of BRCA1 activation domain 1 (AD1) through a coiled-coil-mediated interaction. Genes Dev. 2002;16(12):1509-17.
184. Mieczkowski K, Kitowska K, Braun M, Galikowska-Bogut B, Gorska-Arcisz M, Piasecka D, et al. FGF7/FGFR2-JunB signalling counteracts the effect of progesterone in luminal breast cancer. Mol Oncol. 2022;16(15):2823-42.
185. Ikushima H, Miyazono K. TGFβ signalling: a complex web in cancer progression. Nature Reviews Cancer. 2010;10(6):415-24.
186. Sundqvist A, Morikawa M, Ren J, Vasilaki E, Kawasaki N, Kobayashi M, et al. JUNB governs a feed-forward network of TGFβ signaling that aggravates breast cancer invasion. Nucleic Acids Res. 2018;46(3):1180-95.
187. Avgustinova A, Iravani M, Robertson D, Fearns A, Gao Q, Klingbeil P, et al. Tumour cell-derived Wnt7a recruits and activates fibroblasts to promote tumour aggressiveness. Nature Communications. 2016;7(1):10305.
188. Thiery JP, Acloque H, Huang RYJ, Nieto MA. Epithelial-Mesenchymal Transitions in Development and Disease. Cell. 2009;139(5):871-90.
189. Hicks M, Hu Q, Macrae ER, Dewille JW. JUNB promotes the survival of Flavopiridol treated human breast cancer cells. Biochemical and biophysical research communications. 2014;450 1:19-24.
190. Kallergi G, Tsintari V, Sfakianakis S, Bei E, Lagoudaki E, Koutsopoulos A, et al. The prognostic value of JUNB-positive CTCs in metastatic breast cancer: from bioinformatics to phenotypic characterization. Breast Cancer Res. 2019;21(1):86.
191. Kharman-Biz A, Gao H, Ghiasvand R, Zhao C, Zendehdel K, Dahlman-Wright K. Expression of activator protein-1 (AP-1) family members in breast cancer. BMC Cancer. 2013;13:441.
192. Lee HK, Choung HW, Yang YI, Yoon HJ, Park IA, Park JC. ODAM inhibits RhoA-dependent invasion in breast cancer. Cell Biochem Funct. 2015;33(7):451-61.
193. Moffatt P, Smith CE, Sooknanan R, St-Arnaud R, Nanci A. Identification of secreted and membrane proteins in the rat incisor enamel organ using a signal-trap screening approach. Eur J Oral Sci. 2006;114 Suppl 1:139-46; discussion 64-5, 380-1.
194. Kawasaki K, Weiss KM. Mineralized tissue and vertebrate evolution: the secretory calcium-binding phosphoprotein gene cluster. Proc Natl Acad Sci U S A. 2003;100(7):4060-5.
195. Lee HK, Lee DS, Ryoo HM, Park JT, Park SJ, Bae HS, et al. The odontogenic ameloblast-associated protein (ODAM) cooperates with RUNX2 and modulates enamel mineralization via regulation of MMP-20. J Cell Biochem. 2010;111(3):755-67.
196. Moffatt P, Smith CE, St-Arnaud R, Nanci A. Characterization of Apin, a secreted protein highly expressed in tooth-associated epithelia. J Cell Biochem. 2008;103(3):941-56.
197. Kestler DP, Foster JS, Bruker CT, Prenshaw JW, Kennel SJ, Wall JS, et al. ODAM Expression Inhibits Human Breast Cancer Tumorigenesis. Breast Cancer (Auckl). 2011;5:73-85.
198. Dos Santos Neves J, Wazen RM, Kuroda S, Francis Zalzal S, Moffatt P, Nanci A. Odontogenic ameloblast-associated and amelotin are novel basal lamina components. Histochem Cell Biol. 2012;137(3):329-38.
199. Sugano S SY, Ota T, et al. . Hypothetical protein FLJ20513 (FLJ20513 mRNA). 2000.
200. Crivelini MM, Felipini RC, Miyahara GI, de Sousa SC. Expression of odontogenic ameloblast-associated protein, amelotin, ameloblastin, and amelogenin in odontogenic tumors: immunohistochemical analysis and pathogenetic considerations. J Oral Pathol Med. 2012;41(3):272-80.

201. Park JC, Park JT, Son HH, Kim HJ, Jeong MJ, Lee CS, et al. The amyloid protein APin is highly expressed during enamel mineralization and maturation in rat incisors. Eur J Oral Sci. 2007;115(2):153-60.
202. Nishio C, Wazen R, Kuroda S, Moffatt P, Nanci A. Disruption of periodontal integrity induces expression of apin by epithelial cell rests of Malassez. J Periodontal Res. 2010;45(6):709-13.
203. Nishio C, Wazen R, Kuroda S, Moffatt P, Nanci A. Expression pattern of odontogenic ameloblast-associated and amelotin during formation and regeneration of the junctional epithelium. Eur Cell Mater. 2010;20:393-402.
204. Lee HK, Park SJ, Oh HJ, Kim JW, Bae HS, Park JC. Expression pattern, subcellular localization, and functional implications of ODAM in ameloblasts, odontoblasts, osteoblasts, and various cancer cells. Gene Expr Patterns. 2012;12(3-4):102-8.
205. Solomon A, Murphy CL, Weaver K, Weiss DT, Hrncic R, Eulitz M, et al. Calcifying epithelial odontogenic (Pindborg) tumor-associated amyloid consists of a novel human protein. J Lab Clin Med. 2003;142(5):348-55.
206. Aung PP, Oue N, Mitani Y, Nakayama H, Yoshida K, Noguchi T, et al. Systematic search for gastric cancer-specific genes based on SAGE data: melanoma inhibitory activity and matrix metalloproteinase-10 are novel prognostic factors in patients with gastric cancer. Oncogene. 2006;25(17):2546-57.
207. Kestler DP, Foster JS, Macy SD, Murphy CL, Weiss DT, Solomon A. Expression of odontogenic ameloblast-associated protein (ODAM) in dental and other epithelial neoplasms. Mol Med. 2008;14(5-6):318-26.
208. Foster JS, Fish LM, Phipps JE, Bruker CT, Lewis JM, Bell JL, et al. Odontogenic ameloblast-associated protein (ODAM) inhibits growth and migration of human melanoma cells and elicits PTEN elevation and inactivation of PI3K/AKT signaling. BMC Cancer. 2013;13:227.
209. Yuan DF, Wang HR, Wang ZF, Liang GH, Xing WQ, Qin JJ. CircRNA CircZMYM4 inhibits the growth and metastasis of lung adenocarcinoma via the miR-587/ODAM pathway. Biochemical and Biophysical Research Communications. 2021;580:100-6.
210. Pratap J, Imbalzano KM, Underwood JM, Cohet N, Gokul K, Akech J, et al. Ectopic runx2 expression in mammary epithelial cells disrupts formation of normal acini structure: implications for breast cancer progression. Cancer Res. 2009;69(17):6807-14.
211. Leong DT, Lim J, Goh X, Pratap J, Pereira BP, Kwok HS, et al. Cancer-related ectopic expression of the bone-related transcription factor RUNX2 in non-osseous metastatic tumor cells is linked to cell proliferation and motility. Breast Cancer Res. 2010;12(5):R89.
212. Hegedus L, Cho H, Xie X, Eliceiri GL. Additional MDA-MB-231 breast cancer cell matrix metalloproteinases promote invasiveness. J Cell Physiol. 2008;216(2):480-5.
213. Vaananen A, Srinivas R, Parikka M, Palosaari H, Bartlett JD, Iwata K, et al. Expression and regulation of MMP-20 in human tongue carcinoma cells. J Dent Res. 2001;80(10):1884-9.
214. Luo Y, Wu JY, Hou GL, Lu MH, Shi Z, Di JM. ODAM is a predictor for biomedical recurrence and inhibits the migration and invasion of prostate cancer. Am J Transl Res. 2016;8(2):670-9.
215. Siddiqui S, Bruker CT, Kestler DP, Foster JS, Gray KD, Solomon A, et al. Odontogenic Ameloblast Associated Protein as a Novel Biomarker for Human Breast Cancer. Am Surgeon. 2009;75(9):769-75.

216. Zhao Y, Xie X, Liao W, Zhang H, Cao H, Fei R, et al. The transcription factor RFX5 is a transcriptional activator of the TPP1 gene in hepatocellular carcinoma. Oncol Rep. 2017;37(1):289-96.
217. Harris HK, Nakayama T, Lai J, Zhao B, Argyrou N, Gubbels CS, et al. Disruption of RFX family transcription factors causes autism, attention-deficit/hyperactivity disorder, intellectual disability, and dysregulated behavior. Genet Med. 2021;23(6):1028-40.
218. Clausen BE, Waldburger JM, Schwenk F, Barras E, Mach B, Rajewsky K, et al. Residual MHC class II expression on mature dendritic cells and activated B cells in RFX5-deficient mice. Immunity. 1998;8(2):143-55.
219. Coronel L, Riege K, Schwab K, Förste S, Häckes D, Semerau L, et al. Transcription factor RFX7 governs a tumor suppressor network in response to p53 and stress. Nucleic Acids Res. 2021;49(13):7437-56.
220. Villard J, Reith W, Barras E, Gos A, Morris MA, Antonarakis SE, et al. Analysis of mutations and chromosomal localisation of the gene encoding RFX5, a novel transcription factor affected in major histocompatibility complex class II deficiency. Hum Mutat. 1997;10(6):430-5.
221. Jeong HY, Kim HJ, Kim CE, Lee S, Choi MC, Kim SH. High expression of RFX4 is associated with tumor progression and poor prognosis in patients with glioblastoma. Int J Neurosci. 2021;131(1):7-14.
222. Guo L, Liu D. Identification of RFX5 as prognostic biomarker and associated with immune infiltration in stomach adenocarcinoma. Eur J Med Res. 2022;27(1):164.
223. Gobin SJ, Peijnenburg A, van Eggermond M, van Zutphen M, van den Berg R, van den Elsen PJ. The RFX complex is crucial for the constitutive and CIITA-mediated transactivation of MHC class I and beta2-microglobulin genes. Immunity. 1998;9(4):531-41.
224. Sengupta PK, Fargo J, Smith BD. The RFX family interacts at the collagen (COL1A2) start site and represses transcription. J Biol Chem. 2002;277(28):24926-37.
225. Ye J, Zhang Y, Cai Z, Jiang M, Li B, Chen G, et al. Increased expression of immediate early response gene 3 protein promotes aggressive progression and predicts poor prognosis in human bladder cancer. BMC Urology. 2018;18(1):82.
226. Han L, Geng L, Liu X, Shi H, He W, Wu MX. Clinical Significance of IEX-1 Expression in Ovarian Carcinoma. Ultrastructural Pathology. 2011;35(6):260-6.
227. Hou T, Ye L, Wu S. Knockdown of LINC00504 Inhibits the Proliferation and Invasion of Breast Cancer via the Downregulation of miR-140-5p. Onco Targets Ther. 2021;14:3991-4003.
228. He FY, Chen G, He RQ, Huang ZG, Li JD, Wu WZ, et al. Expression of IER3 in hepatocellular carcinoma: clinicopathology, prognosis, and potential regulatory pathways. PeerJ. 2022;10:e12944.
229. Chen DB, Xie XW, Zhao YJ, Wang XY, Liao WJ, Chen P, et al. RFX5 promotes the progression of hepatocellular carcinoma through transcriptional activation of KDM4A. Sci Rep. 2020;10(1):14538.
230. Chen DB, Zhao YJ, Wang XY, Liao WJ, Chen P, Deng KJ, et al. Regulatory factor X5 promotes hepatocellular carcinoma progression by transactivating tyrosine 3-monooxygenase/tryptophan 5-monooxygenase activation protein theta and suppressing apoptosis. Chin Med J (Engl). 2019;132(13):1572-81.
231. Braybrook C, Doudney K, Marçano AC, Arnason A, Bjornsson A, Patton MA, et al. The T-box transcription factor gene TBX22 is mutated in X-linked cleft palate and ankyloglossia. Nat Genet. 2001;29(2):179-83.

232. Kantaputra PN, Paramee M, Kaewkhampa A, Hoshino A, Lees M, McEntagart M, et al. Cleft lip with cleft palate, ankyloglossia, and hypodontia are associated with TBX22 mutations. J Dent Res. 2011;90(4):450-5.
233. Crawford NT, McIntyre AJ, McCormick A, D'Costa ZC, Buckley NE, Mullan PB. TBX2 interacts with heterochromatin protein 1 to recruit a novel repression complex to EGR1-targeted promoters to drive the proliferation of breast cancer cells. Oncogene. 2019;38(31):5971-86.
234. Krstic M, Kolendowski B, Cecchini MJ, Postenka CO, Hassan HM, Andrews J, et al. TBX3 promotes progression of pre-invasive breast cancer cells by inducing EMT and directly up-regulating SLUG. J Pathol. 2019;248(2):191-203.
235. Durbin AD, Zimmerman MW, Dharia NV, Abraham BJ, Iniguez AB, Weichert-Leahey N, et al. Selective gene dependencies in MYCN-amplified neuroblastoma include the core transcriptional regulatory circuitry. Nat Genet. 2018;50(9):1240-6.
236. Wang N, Li Y, Wei J, Pu J, Liu R, Yang Q, et al. TBX1 functions as a tumor suppressor in thyroid cancer through inhibiting the activities of the PI3K/AKT and MAPK/ERK pathways. Thyroid. 2019;29(3):378-94.
237. Dong X, Song J, Hu J, Zheng C, Zhang X, Liu H. T-Box Transcription Factor 22 Is an Immune Microenvironment-Related Biomarker Associated With the BRAF (V600E) Mutation in Papillary Thyroid Carcinoma. Front Cell Dev Biol. 2020;8:590898.
238. Ashktorab H, Schäffer AA, Daremipouran M, Smoot DT, Lee E, Brim H. Distinct genetic alterations in colorectal cancer. PLoS One. 2010;5(1):e8879.
239. Perou CM, Sørlie T, Eisen MB, Van De Rijn M, Jeffrey SS, Rees CA, et al. Molecular portraits of human breast tumours. nature. 2000;406(6797):747-52.
240. Foulkes WD, Smith IE, Reis-Filho JS. Triple-negative breast cancer. N Engl J Med. 2010;363(20):1938-48.
241. Rakha EA, Reis-Filho JS, Ellis IO. Basal-like breast cancer: a critical review. Journal of clinical oncology. 2008;26(15):2568-81.
242. Reis-Filho J, Tutt A. Triple negative tumours: a critical review. Histopathology. 2008;52(1):108-18.
243. Cheang MC, Voduc D, Bajdik C, Leung S, McKinney S, Chia SK, et al. Basal-like breast cancer defined by five biomarkers has superior prognostic value than triple-negative phenotype. Clinical cancer research. 2008;14(5):1368-76.
244. Li X, Yang J, Peng L, Sahin AA, Huo L, Ward KC, et al. Triple-negative breast cancer has worse overall survival and cause-specific survival than non-triple-negative breast cancer. Breast Cancer Res Treat. 2017;161(2):279-87.
245. Tischkowitz M, Brunet J-S, Bégin LR, Huntsman DG, Cheang MC, Akslen LA, et al. Use of immunohistochemical markers can refine prognosis in triple negative breast cancer. BMC cancer. 2007;7:1-11.
246. Liedtke C, Mazouni C, Hess KR, André F, Tordai A, Mejia JA, et al. Response to neoadjuvant therapy and long-term survival in patients with triple-negative breast cancer. Journal of clinical oncology. 2008;26(8):1275-81.
247. Colleoni M, Cole BF, Viale G, Regan MM, Price KN, Maiorano E, et al. Classical cyclophosphamide, methotrexate, and fluorouracil chemotherapy is more effective in triple-negative, node-negative breast cancer: results from two randomized trials of adjuvant chemoendocrine therapy for node-negative breast cancer. Journal of clinical oncology. 2010;28(18):2966.
248. Semenza GL. Hypoxia-inducible factors: mediators of cancer progression and targets for cancer therapy. Trends in Pharmacological Sciences. 2012;33(4):207-14.
249. Vaupel P, Mayer A, Höckel M. Tumor hypoxia and malignant progression. Methods in enzymology. 381: Elsevier; 2004. p. 335-54.

250. Hanahan D. Hallmarks of cancer: new dimensions. Cancer discovery. 2022;12(1):31-46.
251. Xia X, Lemieux ME, Li W, Carroll JS, Brown M, Liu XS, et al. Integrative analysis of HIF binding and transactivation reveals its role in maintaining histone methylation homeostasis. Proceedings of the National Academy of Sciences. 2009;106(11):4260-5.
252. Schödel J, Oikonomopoulos S, Ragoussis J, Pugh CW, Ratcliffe PJ, Mole DR. High-resolution genome-wide mapping of HIF-binding sites by ChIP-seq. Blood, The Journal of the American Society of Hematology. 2011;117(23):e207-e17.
253. Rohwer N, Cramer T. Hypoxia-mediated drug resistance: novel insights on the functional interaction of HIFs and cell death pathways. Drug Resistance Updates. 2011;14(3):191-201.
254. Liao D, Johnson RS. Hypoxia: a key regulator of angiogenesis in cancer. Cancer and Metastasis Reviews. 2007;26:281-90.
255. Franovic A, Gunaratnam L, Smith K, Robert I, Patten D, Lee S. Translational up-regulation of the EGFR by tumor hypoxia provides a nonmutational explanation for its overexpression in human cancer. Proceedings of the National Academy of Sciences. 2007;104(32):13092-7.
256. Wu M-Z, Tsai Y-P, Yang M-H, Huang C-H, Chang S-Y, Chang C-C, et al. Interplay between HDAC3 and WDR5 is essential for hypoxia-induced epithelial-mesenchymal transition. Molecular cell. 2011;43(5):811-22.
257. Esteban MA, Tran MG, Harten SK, Hill P, Castellanos MC, Chandra A, et al. Regulation of E-cadherin expression by VHL and hypoxia-inducible factor. Cancer research. 2006;66(7):3567-75.
258. Krishnamachary B, Zagzag D, Nagasawa H, Rainey K, Okuyama H, Baek JH, et al. Hypoxia-inducible factor-1-dependent repression of E-cadherin in von Hippel-Lindau tumor suppressor–null renal cell carcinoma mediated by TCF3, ZFHX1A, and ZFHX1B. Cancer research. 2006;66(5):2725-31.
259. Wong CC-L, Gilkes DM, Zhang H, Chen J, Wei H, Chaturvedi P, et al. Hypoxia-inducible factor 1 is a master regulator of breast cancer metastatic niche formation. Proceedings of the National Academy of Sciences. 2011;108(39):16369-74.
260. Zhang H, Wong C, Wei H, Gilkes D, Korangath P, Chaturvedi P, et al. HIF-1-dependent expression of angiopoietin-like 4 and L1CAM mediates vascular metastasis of hypoxic breast cancer cells to the lungs. Oncogene. 2012;31(14):1757-70.
261. Moeller BJ, Richardson RA, Dewhirst MW. Hypoxia and radiotherapy: opportunities for improved outcomes in cancer treatment. Cancer and Metastasis Reviews. 2007;26:241-8.
262. Li X, Wei B, Sonmez C, Li Z, Peng L. High tumor budding count is associated with adverse clinicopathologic features and poor prognosis in breast carcinoma. Hum Pathol. 2017;66:222-9.
263. Liu ZJ, Semenza GL, Zhang HF. Hypoxia-inducible factor 1 and breast cancer metastasis. J Zhejiang Univ Sci B. 2015;16(1):32-43.
264. Shamis SA, McMillan DC, Edwards J. The relationship between hypoxia-inducible factor 1α (HIF-1α) and patient survival in breast cancer: Systematic review and meta-analysis. Critical reviews in oncology/hematology. 2021;159:103231.
265. Zhong H, De Marzo AM, Laughner E, Lim M, Hilton DA, Zagzag D, et al. Overexpression of hypoxia-inducible factor 1α in common human cancers and their metastases. Cancer research. 1999;59(22):5830-5.

266. Brigham, Hospital Ws, 13 HMSCLPPJKR, 25 GdaBCoMCCJDLA, Ilya IfSBRSKRBBBBRETLJTVZWS. Comprehensive molecular portraits of human breast tumours. Nature. 2012;490(7418):61-70.
267. Bos R, Van der Groep P, Greijer AE, Shvarts A, Meijer S, Pinedo HM, et al. Levels of hypoxia-inducible factor-1α independently predict prognosis in patients with lymph node negative breast carcinoma. Cancer: Interdisciplinary International Journal of the American Cancer Society. 2003;97(6):1573-81.
268. Gruber G, Greiner RH, Hlushchuk R, Aebersold DM, Altermatt HJ, Berclaz G, et al. Hypoxia-inducible factor 1 alpha in high-risk breast cancer: an independent prognostic parameter? Breast Cancer Research. 2004;6:1-8.
269. Generali D, Berruti A, Brizzi MP, Campo L, Bonardi S, Wigfield S, et al. Hypoxia-inducible factor-1α expression predicts a poor response to primary chemoendocrine therapy and disease-free survival in primary human breast cancer. Clinical Cancer Research. 2006;12(15):4562-8.
270. El-Guindy DM, Ibrahim FM, Ali DA, El-Horany HE, Sabry NM, Elkholy RA, et al. Hypoxia-induced autophagy in triple negative breast cancer: association with prognostic variables, patients' survival and response to neoadjuvant chemotherapy. Virchows Arch. 2023;482(5):823-37.
271. Ong CHC, Lee DY, Lee B, Li H, Lim JCT, Lim JX, et al. Hypoxia-regulated carbonic anhydrase IX (CAIX) protein is an independent prognostic indicator in triple negative breast cancer. Breast Cancer Res. 2022;24(1):38.
272. Aldera AP, Govender D. Carbonic anhydrase IX: a regulator of pH and participant in carcinogenesis. J Clin Pathol. 2021.
273. van der Groep P, van Diest PJ, Smolders YH, Ausems MG, van der Luijt RB, Menko FH, et al. HIF-1α overexpression in ductal carcinoma in situ of the breast in BRCA1 and BRCA2 mutation carriers. PLoS One. 2013;8(2):e56055.
274. Neumeister VM, Sullivan CA, Lindner R, Lezon-Geyda K, Li J, Zavada J, et al. Hypoxia-induced protein CAIX is associated with somatic loss of BRCA1 protein and pathway activity in triple negative breast cancer. Breast Cancer Res Treat. 2012;136(1):67-75.
275. Numprasit W, Yangngam S, Prasopsiri J, Quinn JA, Edwards J, Thuwajit C. Carbonic anhydrase IX-related tumoral hypoxia predicts worse prognosis in breast cancer: A systematic review and meta-analysis. Front Med (Lausanne). 2023;10:1087270.
276. Shamis SAK, Edwards J, McMillan DC. The relationship between carbonic anhydrase IX (CAIX) and patient survival in breast cancer: systematic review and meta-analysis. Diagn Pathol. 2023;18(1):46.
277. Shamis SAK, Quinn J, Mallon EEA, Edwards J, McMillan DC. The Relationship Between the Tumor Cell Expression of Hypoxic Markers and Survival in Patients With ER-positive Invasive Ductal Breast Cancer. J Histochem Cytochem. 2022;70(7):479-94.
278. Wykoff CC, Beasley NJ, Watson PH, Turner KJ, Pastorek J, Sibtain A, et al. Hypoxia-inducible expression of tumor-associated carbonic anhydrases. Cancer research. 2000;60(24):7075-83.
279. Becker HM. Carbonic anhydrase IX and acid transport in cancer. British journal of cancer. 2020;122(2):157-67.
280. Huber V, Camisaschi C, Berzi A, Ferro S, Lugini L, Triulzi T, et al. Cancer acidity: An ultimate frontier of tumor immune escape and a novel target of immunomodulation. Seminars in Cancer Biology. 2017;43:74-89.
281. Boedtkjer E, Pedersen SF. The acidic tumor microenvironment as a driver of cancer. Annual review of physiology. 2020;82:103-26.

282. Tan E, Yan M, Campo L, Han C, Takano E, Turley H, et al. The key hypoxia regulated gene CAIX is upregulated in basal-like breast tumours and is associated with resistance to chemotherapy. British journal of cancer. 2009;100(2):405-11.
283. Tan EY, Yan M, Campo L, Han C, Takano E, Turley H, et al. The key hypoxia regulated gene CAIX is upregulated in basal-like breast tumours and is associated with resistance to chemotherapy. Br J Cancer. 2009;100(2):405-11.
284. Twomey JD, Zhang B. Exploring the Role of Hypoxia-Inducible Carbonic Anhydrase IX (CAIX) in Circulating Tumor Cells (CTCs) of Breast Cancer. Biomedicines. 2023;11(3).
285. Hedlund EE, McDonald PC, Nemirovsky O, Awrey S, Jensen LDE, Dedhar S. Harnessing Induced Essentiality: Targeting Carbonic Anhydrase IX and Angiogenesis Reduces Lung Metastasis of Triple Negative Breast Cancer Xenografts. Cancers (Basel). 2019;11(7).
286. Schütze D, Milde-Langosch K, Witzel I, Rody A, Karn T, Schmidt M, et al. Relevance of cellular and serum carbonic anhydrase IX in primary breast cancer. J Cancer Res Clin Oncol. 2013;139(5):747-54.
287. Alves W, Bonatelli M, Dufloth R, Kerr LM, Carrara GFA, da Costa RFA, et al. CAIX is a predictor of pathological complete response and is associated with higher survival in locally advanced breast cancer submitted to neoadjuvant chemotherapy. BMC Cancer. 2019;19(1):1173.
288. Güttler A, Theuerkorn K, Riemann A, Wichmann H, Kessler J, Thews O, et al. Cellular and radiobiological effects of carbonic anhydrase IX in human breast cancer cells. Oncol Rep. 2019;41(4):2585-94.
289. Jin MS, Lee H, Park IA, Chung YR, Im SA, Lee KH, et al. Overexpression of HIF1α and CAXI predicts poor outcome in early-stage triple negative breast cancer. Virchows Arch. 2016;469(2):183-90.
290. Callagy GM, Webber MJ, Pharoah PD, Caldas C. Meta-analysis confirms BCL2 is an independent prognostic marker in breast cancer. BMC cancer. 2008;8:1-10.
291. Al-Alem U, Rauscher GH, Alem QA, Kajdacsy-Balla A, Mahmoud AM. Prognostic Value of SGK1 and Bcl-2 in Invasive Breast Cancer. Cancers (Basel). 2023;15(12).
292. Borner C. The Bcl-2 protein family: sensors and checkpoints for life-or-death decisions. Molecular immunology. 2003;39(11):615-47.
293. Cheng EH-Y, Kirsch DG, Clem RJ, Ravi R, Kastan MB, Bedi A, et al. Conversion of Bcl-2 to a Bax-like death effector by caspases. Science. 1997;278(5345):1966-8.
294. Czabotar PE, Lessene G, Strasser A, Adams JM. Control of apoptosis by the BCL-2 protein family: implications for physiology and therapy. Nature reviews Molecular cell biology. 2014;15(1):49-63.
295. Merino D, Lok SW, Visvader JE, Lindeman GJ. Targeting BCL-2 to enhance vulnerability to therapy in estrogen receptor-positive breast cancer. Oncogene. 2016;35(15):1877-87.
296. Chang J, Clark GM, Allred DC, Mohsin S, Chamness G, Elledge RM. Survival of patients with metastatic breast carcinoma: importance of prognostic markers of the primary tumor. Cancer: Interdisciplinary International Journal of the American Cancer Society. 2003;97(3):545-53.
297. Hanahan D, Weinberg RA. The hallmarks of cancer. cell. 2000;100(1):57-70.
298. Kirkin V, Joos S, Zörnig M. The role of Bcl-2 family members in tumorigenesis. Biochim Biophys Acta. 2004;1644(2-3):229-49.

299. Teixeira C, Reed JC, Pratt MAC. Estrogen Promotes Chemotherapeutic Drug Resistance by a Mechanism Involving Bcl-2 Proto-Oncogene Expression in Human Breast Cancer Cells1. Cancer Research. 1995;55(17):3902-7.
300. Dowsett M, Smith IE, Ebbs SR, Dixon JM, Skene A, Griffith C, et al. Short-term changes in Ki-67 during neoadjuvant treatment of primary breast cancer with anastrozole or tamoxifen alone or combined correlate with recurrence-free survival. Clin Cancer Res. 2005;11(2 Pt 2):951s-8s.
301. Vaillant F, Merino D, Lee L, Breslin K, Pal B, Ritchie ME, et al. Targeting BCL-2 with the BH3 mimetic ABT-199 in estrogen receptor-positive breast cancer. Cancer Cell. 2013;24(1):120-9.
302. Martin L-A, Dowsett M. BCL-2: a new therapeutic target in estrogen receptor-positive breast cancer? Cancer cell. 2013;24(1):7-9.
303. Bouchalova K, Svoboda M, Kharaishvili G, Vrbkova J, Bouchal J, Trojanec R, et al. BCL2 is an independent predictor of outcome in basal-like triple-negative breast cancers treated with adjuvant anthracycline-based chemotherapy. Tumour Biol. 2015;36(6):4243-52.
304. Denkert C, von Minckwitz G, Darb-Esfahani S, Lederer B, Heppner BI, Weber KE, et al. Tumour-infiltrating lymphocytes and prognosis in different subtypes of breast cancer: a pooled analysis of 3771 patients treated with neoadjuvant therapy. The lancet oncology. 2018;19(1):40-50.
305. Pruneri G, Vingiani A, Denkert C. Tumor infiltrating lymphocytes in early breast cancer. The Breast. 2018;37:207-14.
306. Gao Z-h, Li C-x, Liu M, Jiang J-y. Predictive and prognostic role of tumour-infiltrating lymphocytes in breast cancer patients with different molecular subtypes: a meta-analysis. BMC cancer. 2020;20(1):1-14.
307. He L, Wang Y, Wu Q, Song Y, Ma X, Zhang B, et al. Association between levels of tumor-infiltrating lymphocytes in different subtypes of primary breast tumors and prognostic outcomes: a meta-analysis. BMC Women's Health. 2020;20:1-11.
308. He L, Wang Y, Wu Q, Song Y, Ma X, Zhang B, et al. Association between levels of tumor-infiltrating lymphocytes in different subtypes of primary breast tumors and prognostic outcomes: a meta-analysis. BMC Womens Health. 2020;20(1):194.
309. Gao ZH, Li CX, Liu M, Jiang JY. Predictive and prognostic role of tumour-infiltrating lymphocytes in breast cancer patients with different molecular subtypes: a meta-analysis. BMC Cancer. 2020;20(1):1150.
310. Rafajová M, Zatovicová M, Kettmann R, Pastorek J, Pastoreková S. Induction by hypoxia combined with low glucose or low bicarbonate and high posttranslational stability upon reoxygenation contribute to carbonic anhydrase IX expression in cancer cells. Int J Oncol. 2004;24(4):995-1004.
311. Mutka M, Joensuu K, Eray M, Heikkilä P. Quantities of CD3+, CD8+ and CD56+ lymphocytes decline in breast cancer recurrences while CD4+ remain similar. Diagn Pathol. 2023;18(1):3.
312. Zlobec I, Minoo P, Terracciano L, Baker K, Lugli A. Characterization of the immunological microenvironment of tumour buds and its impact on prognosis in mismatch repair-proficient and-deficient colorectal cancers. Histopathology. 2011;59(3):482-95.
313. Haddad TS, van den Dobbelsteen L, Öztürk SK, Geene R, Nijman IJ, Verrijp K, et al. Pseudobudding: ruptured glands do not represent true tumor buds. The Journal of Pathology. 2023;261(1):19-27.
314. Kharman-Biz A, Gao H, Ghiasvand R, Zhao C, Zendehdel K, Dahlman-Wright K. Expression of activator protein-1 (AP-1) family members in breast cancer. BMC Cancer. 2013;13(1):441.

315. Siddiqui SM, Bruker CT, Kestler DP, Foster JS, Gray KD, Solomon A, et al. Odontogenic Ameloblast Associated Protein as a Novel Biomarker for Human Breast Cancer. The American Surgeon. 2009;75:769 - 75.
316. Krstic M, Kolendowski B, Cecchini MJ, Postenka CO, Hassan HM, Andrews JD, et al. TBX3 promotes progression of pre-invasive breast cancer cells by inducing EMT and directly up-regulating SLUG. The Journal of Pathology. 2019;248:191 - 203.
317. Lin GL, Monje M. Understanding the Deadly Silence of Posterior Fossa A Ependymoma. Mol Cell. 2020;78(6):999-1001.
318. Michealraj KA, Kumar SA, Kim LJY, Cavalli FMG, Przelicki D, Wojcik JB, et al. Metabolic Regulation of the Epigenome Drives Lethal Infantile Ependymoma. Cell. 2020;181(6):1329-45.e24.
319. Serrano-Gomez SJ, Maziveyi M, Alahari SK. Regulation of epithelial-mesenchymal transition through epigenetic and post-translational modifications. Mol Cancer. 2016;15:18.
320. Skrypek N, Goossens S, De Smedt E, Vandamme N, Berx G. Epithelial-to-Mesenchymal Transition: Epigenetic Reprogramming Driving Cellular Plasticity. Trends Genet. 2017;33(12):943-59.
321. Hanahan D, Weinberg RA. Hallmarks of cancer: the next generation. Cell. 2011;144(5):646-74.
322. Willis SN, Adams JM. Life in the balance: how BH3-only proteins induce apoptosis. Current opinion in cell biology. 2005;17(6):617-25.
323. Adams JM, Cory S. The Bcl-2 apoptotic switch in cancer development and therapy. Oncogene. 2007;26(9):1324-37.
324. Teixeira C, Reed JC, Pratt MA. Estrogen promotes chemotherapeutic drug resistance by a mechanism involving Bcl-2 proto-oncogene expression in human breast cancer cells. Cancer Res. 1995;55(17):3902-7.
325. Merino D, Lok SW, Visvader JE, Lindeman GJ. Targeting BCL-2 to enhance vulnerability to therapy in estrogen receptor-positive breast cancer. Oncogene. 2016;35(15):1877-87.
326. Martin LA, Dowsett M. BCL-2: a new therapeutic target in estrogen receptor-positive breast cancer? Cancer Cell. 2013;24(1):7-9.
327. Denkert C, von Minckwitz G, Darb-Esfahani S, Lederer B, Heppner BI, Weber KE, et al. Tumour-infiltrating lymphocytes and prognosis in different subtypes of breast cancer: a pooled analysis of 3771 patients treated with neoadjuvant therapy. Lancet Oncol. 2018;19(1):40-50.
328. Zlobec I, Minoo P, Terracciano L, Baker K, Lugli A. Characterization of the immunological microenvironment of tumour buds and its impact on prognosis in mismatch repair-proficient and -deficient colorectal cancers. Histopathology. 2011;59(3):482-95.